

APPROVED FOR PUBLIC RELEASE  
DISTRIBUTION IS UNLIMITED

NEBR Technical Report TR 89-0

NAVY TACTICAL APPLICATIONS GUIDE

VOLUME 8  
PART 1

ARCTIC

Greenland/Norwegian/Barents Seas

WEATHER ANALYSIS

and

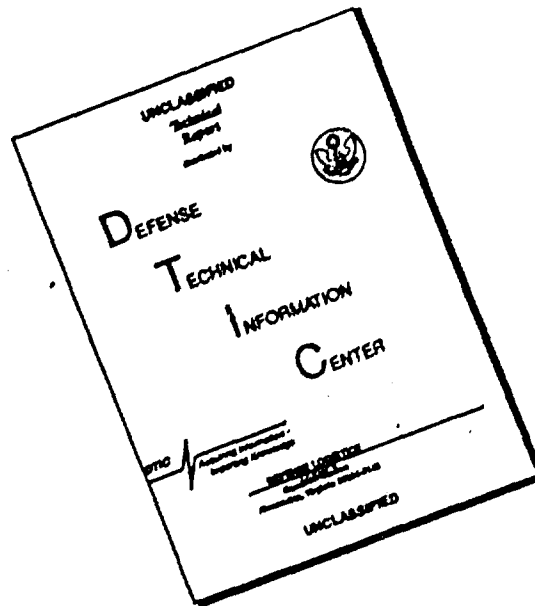
FORECAST APPLICATIONS

METEOROLOGICAL  
SATELLITE  
SYSTEMS

AD-A230 720

For full text, color  
reproduction,  
contact the author and  
publisher.

# DISCLAIMER NOTICE



THIS DOCUMENT IS BEST QUALITY AVAILABLE. THE COPY FURNISHED TO DTIC CONTAINED A SIGNIFICANT NUMBER OF PAGES WHICH DO NOT REPRODUCE LEGIBLY.



UNCLASSIFIED

SECURITY CLASSIFICATION OF THIS PAGE

## REPORT DOCUMENTATION PAGE

1a. REPORT SECURITY CLASSIFICATION <b>UNCLASSIFIED</b>		1b. RESTRICTIVE MARKINGS	
2a. SECURITY CLASSIFICATION AUTHORITY		3. DISTRIBUTION/AVAILABILITY OF REPORT <b>Approved for Public Release Distribution is Unlimited</b>	
2b. DECLASSIFICATION/DOWNGRADING SCHEDULE		4. PERFORMING ORGANIZATION REPORT NUMBER(S)	
5. MONITORING ORGANIZATION REPORT NUMBER(S) <b>TR 89-07</b>		6a. NAME OF PERFORMING ORGANIZATION <b>Science and Technology Corp.</b>	
6b. OFFICE SYMBOL (If applicable)		7a. NAME OF MONITORING ORGANIZATION <b>Naval Environmental Prediction Research Facility</b>	
6c. ADDRESS (City, State, and ZIP Code) <b>101 Research Drive Hampton, VA 23666</b>		7b. ADDRESS (City, State, and ZIP Code) <b>Monterey, CA 93943-5006</b>	
8a. NAME OF FUNDING /SPONSORING ORGANIZATION <b>Space and Naval Warfare Systems Command</b>		8b. OFFICE SYMBOL (If applicable) <b>PMW-141</b>	
9. PROCUREMENT INSTRUMENT IDENTIFICATION NUMBER <b>N00014-85-C-2404</b>		10. SOURCE OF FUNDING NUMBERS	
8c. ADDRESS (City, State, and ZIP Code) <b>Department of the Navy Washington, D.C. 20361-5100</b>		PROGRAM ELEMENT NO. <b>63704N</b>	PROJECT NO. <b>X1596</b>
		TASK NO.	WORK UNIT ACCESSION NO. <b>DN657752</b>
11. TITLE (Include Security Classification) <b>Navy Tactical Applications Guide, Volume 8, Part 1 Arctic Weather Analysis and Forecast Applications (U)</b>			
12. PERSONAL AUTHOR(S) <b>Felt, Robert W.</b>			
13a. TYPE OF REPORT <b>Applications Guide</b>	13b. TIME COVERED FROM <b>4/87</b> TO <b>9/89</b>	14. DATE OF REPORT (Year, Month, Day) <b>1989, September</b>	15. PAGE COUNT <b>364</b>
16. SUPPLEMENTARY NOTATION			
17. COSATI CODES		18. SUBJECT TERMS (Continue on reverse if necessary and identify by block number)	
FIELD <b>04</b>	GROUP <b>02</b>	SUB-GROUP	
		Meteorological Satellite Systems Analysis and Forecast Applications Arctic	
		Wind Direction Streamline Analysis Wind Flow Patterns (see also reverse)	
19. ABSTRACT (Continue on reverse if necessary and identify by block number)  Environmentally the north polar region is one of the most active regions on the earth, and for ships and seamen, one of the most dangerous due to the combined effects of wind, sea state, and structural icing. It is also the region most neglected and difficult to analyze or forecast because of the sparsity of surface, upper-air, and ocean observations, and less than adequate numerical models. This volume illustrates, with high resolution satellite data and supplementary conventional surface and upper-air analyses, some of the significant recurring patterns of weather and oceanographic phenomena in the Arctic. This volume is dedicated to weather and oceanographic phenomena in the regions surrounding Greenland, and in the Norwegian and Barents Seas. Its purpose is to document Arctic weather phenomena as observed by satellite, and in so doing, assist meteorologists in the development of satellite interpretation skills. <i>Key words: Weather, Forecast, Arctic, Meteorological, Phenomena, Wind Direction, Streamline Analysis, Wind Flow Patterns, Satellite Data, Polar Regions, Barents Seas, Greenland.</i>			
20. DISTRIBUTION/AVAILABILITY OF ABSTRACT <input checked="" type="checkbox"/> UNCLASSIFIED/UNLIMITED <input type="checkbox"/> SAME AS RPT <input type="checkbox"/> DTIC USERS		21. ABSTRACT SECURITY CLASSIFICATION <b>UNCLASSIFIED</b>	
22a. NAME OF RESPONSIBLE INDIVIDUAL <b>Robert W. Felt</b>		22b. TELEPHONE (Include Area Code) <b>(408) 647-4728</b>	22c. OFFICE SYMBOL <b>NEPRF WU 6.3-9</b>

DD FORM 1473, 84 MAR

83 APR edition may be used until exhausted  
All other editions are obsolete

SECURITY CLASSIFICATION OF THIS PAGE

UNCLASSIFIED

NAVY TACTICAL APPLICATIONS GUIDE

VOLUME 8

PART 1

ARCTIC

GREENLAND/NORWEGIAN/BARENTS SEAS

WEATHER ANALYSIS

AND FORECAST APPLICATIONS

METEOROLOGICAL SATELLITE SYSTEMS

*Prepared under the direction of*

Robert W. Fett

TACTICAL APPLICATIONS DEPARTMENT

Naval Environmental Prediction

Research Facility

Monterey, California 93943-5006

1989



Accession For	
NTIS CRASH	<input checked="" type="checkbox"/>
DIC TAG	<input type="checkbox"/>
Unpublished	<input type="checkbox"/>
Justification	
By	
Distribution	
Availability Codes	
Dist	Availability
A-1	Special

SCIENCE AND TECHNOLOGY CORPORATION

101 RESEARCH DRIVE  
HAMPTON, VIRGINIA 23666

91 1 02 104  
~~90 12 31 086~~



## *Foreword*

The Navy Tactical Applications Guide (NTAG), Volume 8, is devoted to regional analysis and forecast applications of environmental satellite data in the Arctic. Part 1 deals with operationally significant phenomena and effects in the waters surrounding Greenland, and in the Norwegian and Barents Seas. Part 2, to be published at a later date, relates to similar phenomena in the Bering, Chukchi, and Beaufort Seas region.

The volumes are organized into four sections: Section 1 provides examples of large-scale atmospheric phenomena and effects; Section 2 concerns the polar low phenomena; Section 3 focuses on local-scale atmospheric phenomena and effects; and Section 4 is devoted to a discussion of oceanographic phenomena and effects in the arctic region. A number of new analysis and prediction techniques, based primarily on satellite data, are described. These techniques should, at the very least, prove useful to Navy forecasters aboard ships operating in arctic waters.

Navy forecasters in the Arctic may have the opportunity to occasionally document additional phenomena or provide new insight into the phenomena described. It is desirable to update the NTAG on a periodic basis. Forecasters are encouraged to submit their contributions to assist in this purpose.

W.L. SHUTT  
Commander U.S. Navy  
Commanding Officer, NEPRF

## *Acknowledgments*

This volume could not have been published without the devoted effort of the NEPRF Meteorological Laboratory personnel and other members of the NEPRF Forecast Guidance Department including Dr. Frank Sechrist, Ron Miller, and Roland Picard, who obtained required documentation, offered constructive guidance, and spent many hours on the computer terminal entering information for the analyses utilized in the studies. Directed by Mr. Picard, AG1 John Coleman, AG2 Tamara Davis, and AG3 Peter Hoffman did an outstanding job in supporting the work effort required for this volume.

PH1 Kenneth Bolden processed many of the original photos utilized. The correlative meteorological data were provided by the Fleet Numerical Oceanography Center, Monterey, California.

Additional satellite imagery were supplied by the NOAA National Snow and Ice Data Center, Boulder, Colorado, Air Force Global Weather Center, Offutt AFB, New England, the Air Force readout site at Croughton, England, and the Tromsø, Norway Satellite Station, where NOAA HRPT data were collected.

A special thanks is offered to Norwegian forecasters at the Northern Norway Forecast Center, Tromsø, Norway, who assisted the author in every possible way to help understand their perception of weather in the Arctic.

## Contents

<i>Foreword</i> .....	iii
<i>Acknowledgments</i> .....	iv
<i>Introduction</i> .....	v

### Section 1

#### *Large-Scale Atmospheric Phenomena and Effects*

1A Streamline Analysis .....	1A-1
1B Fog and Stratus Formation .....	1B-1
1C Sunlint .....	1C-1
1D Arctic Fronts .....	1D-1
1E The Fleur-De-Lis Cloud System Pattern .....	1E-1

### Section 2

#### *Polar lows*

2A Polar Lows .....	2A-1
---------------------	------

### Section 3

#### *Local-Scale Atmospheric Phenomena and Effects*

3A Anomalous Cloud Lines .....	3A-1
3B Jet Streams and Mountain Waves .....	3B-1
3C Boundary Layer Fronts .....	3C-1

### Section 4 (Under Development)

#### *Oceanographic Phenomena and Effects*



## *Introduction*

Strategic interest in the Arctic has increased significantly over the past several years with the realization that more than 50% of the world's petroleum lies north of the Arctic Circle. U.S. Naval Forces are expanding their efforts to include operations further and further north so that, in the event of hostilities in arctic waters, the Fleet has experience and competence to safely and effectively conduct operations in those areas.

The north polar region is the shortest route the Soviet Union could take to the United States in the event of war. This is the region where the next generation of sensors will be developed for the "Strategic Defense Initiative," and where Soviet and American surface and subsurface ships would be forced to maneuver under the most arduous conditions for attack or counter-attack purposes, and for the gathering of required intelligence. It is, environmentally, one of the most active regions on the Earth and, for ships and seamen, one of the most dangerous in war or peacetime operations. Every year several vessels are lost in the Arctic due to combined effects of wind, sea state, and structural icing. It is also the region most neglected and difficult to analyze or forecast because of the sparsity of surface, upper-air, and ocean observations, and the less than adequate numerical models that have often been found to fail to respond realistically to arctic conditions. Hope for improvement lies in employing new high-resolution numerical models with better planetary boundary layer (PBL) and ocean and ice parameterizations, and exploiting the full range of satellite sensors now available for use in the development of new analysis and forecast techniques, specifically adapted to this region.

This volume has been developed to illustrate, with high resolution satellite data and supplementary conventional surface and upper-air analyses, some of the significant recurring patterns of weather and oceanographic phenomena in the Arctic. Volume 8, Part 1, is dedicated to weather and oceanographic phenomena in the region surrounding Greenland, and in the Norwegian and Barents Seas. Volume 8, Part 2, is dedicated to a depiction of similar phenomena in the Bering, Chukchi, and Beaufort Seas regions.

The meteorologist well-versed in the art of satellite interpretation can very rapidly become a confident analyst and forecaster, even in unfamiliar areas of the world. It is the purpose of this volume to assist in the development of such skills.

# Section 1

## *Large-Scale Atmospheric Phenomena and Effects*

### *1A Streamline Analysis*

Streamline Analysis in the Arctic .....	1A-1
---	------

#### *Case Studies*

1 <i>Complicated Flow Patterns of a Summer Regime Greenland/Norwegian Seas (8 July 1988) .....</i>	1A-2
2 <i>Identification of Cols, High Pressure Centers, and Ridge Lines Greenland/Norwegian Seas (9-10 July 1984) .....</i>	1A-6

### *1B Fog and Stratus Formation*

Fog and Stratus Formation Over the Greenland/Norwegian/ Barents Seas and Marginal Ice Zone .....	1B-1
---	------

#### *Case Studies*

1 <i>Fog Formation Over the Greenland/Norwegian Seas During a Period of Blocking (5-9 June 1984) ....</i>	1B-2
2 <i>Fog Formation Over the Greenland Marginal Ice Zone (3 April 1987 and 7, 14, and 19 June 1984) ....</i>	1B-25

### *1C Sunglint*

Sunglint Analysis in the Arctic .....	1C-1
---------------------------------------	------

#### *Case Studies*

1 <i>Detection of Ridge Lines in the Greenland/ North Seas .....</i>	1C-2
2 <i>Detection of High Pressure Centers and Ridge Lines in the Arctic .....</i>	1C-4

<b>1D</b>	<b>Arctic Fronts</b>	
	Characteristics of Arctic Fronts .....	1D-1
	<i>Case Studies</i>	
	1 Satellite Detection of a Southward-Moving Front Barents Sea (7-8 April 1987) .....	1D-2
	2 Southward Movement of the Barents Sea Ice Edge Following Arctic Frontal Passage (7-12 April 1987) .....	1D-16
	3 Off-Ice Flow From the Greenland Marginal Ice Zone .....	1D-26
<b>1E</b>	<b>The Fleur-De-Lis Cloud System Pattern</b>	
	Deformation Zone Analysis .....	1E-1
	<i>Case Studies</i>	
	1 A Summer Fleur-De-Lis Cloud System Pattern Norwegian/Barents Seas .....	1E-2

## *Case 1 Complicated Flow Patterns of a Summer Regime Greenland/Norwegian Seas*

8 July 1984

DMSP visible (LS) data acquired on this date at 0701 GMT (Fig. 1A-2a) show the area between Greenland and Novaya Zemlya and passing over Norway, Sweden, and Finland. Numbers with nearby arrows superimposed over Fig. 1A-2a denote probable wind direction based on implications of the satellite data.

Off-ice flow over the marginal ice zone (MIZ) is suggested at 1 because of clear conditions at that location (no fog). However, on-ice flow, a short-distance away is suggested at 2, where fog has obscured the MIZ. Note that individual ice floes can be seen through the thin obscuration.

At 3, 4, and 5 cold off-ice flow is again indicated as plumes of stratus are generated when cold air moves over open leads and polynya (open lake-like areas of water). Under stable, strong inversion conditions over the MIZ moisture spreads out laterally, rather than in a single plume, noted under more unstable conditions. Note the V-shaped plume at 5 that appears to have been generated from a single source, above which slightly diverging conditions produce the V-pattern.

At 6 sky conditions change from overcast stratus to open-celled stratocumulus, indicating a change from anticyclonic to cyclonic flow.

At 7 a small eddy in the fog or stratus provides the clue to cyclonic flow. This eddy is seen with greater clarity in Fig. 1A-3a, another DMSP visible (LS) depiction acquired at 1024 GMT.

At 8 a large synoptic-scale cyclonic vortex appears while another trough or vortex is suggested at 9 and also at 10.

Finally fog over cold coastal waters surrounding the southern tip of Sweden near point 11 requires anticyclonic flow.

All of these implications are considered and incorporated in the streamline analysis superimposed over the DMSP data shown in Fig. 1A-4a, which also combines available surface observations.

The analysis, in general, agrees quite well with the Fleet Numerical Oceanography Center (FNOC) surface analysis for 0600 GMT (Fig. 1A-5a). Ridging and anticyclonic flow is shown over southern Sweden where numerous reports of fog are evident; a high is shown over the Jan Mayen area with a ridge line extending westward toward Scoresby Sund (Sound) and southeastward toward central Norway and Sweden; and a general trough area extends southward from the low just northeast of Svalbard.

The main area of disagreement is the ridge line, shown extending northward in the streamline analysis over a clear slot from the Jan Mayen area (Fig. 1A-4a). The surface analysis (Fig. 1A-5a) suggests that the low northeast of Svalbard has a circulation producing strong northeast winds that extend all the way to Greenland. However, the 0900 GMT surface data superimposed on Fig. 1A-4a over northeast Greenland show light southerly winds turning cyclonically to light southeasterly near 83°N 33°W.

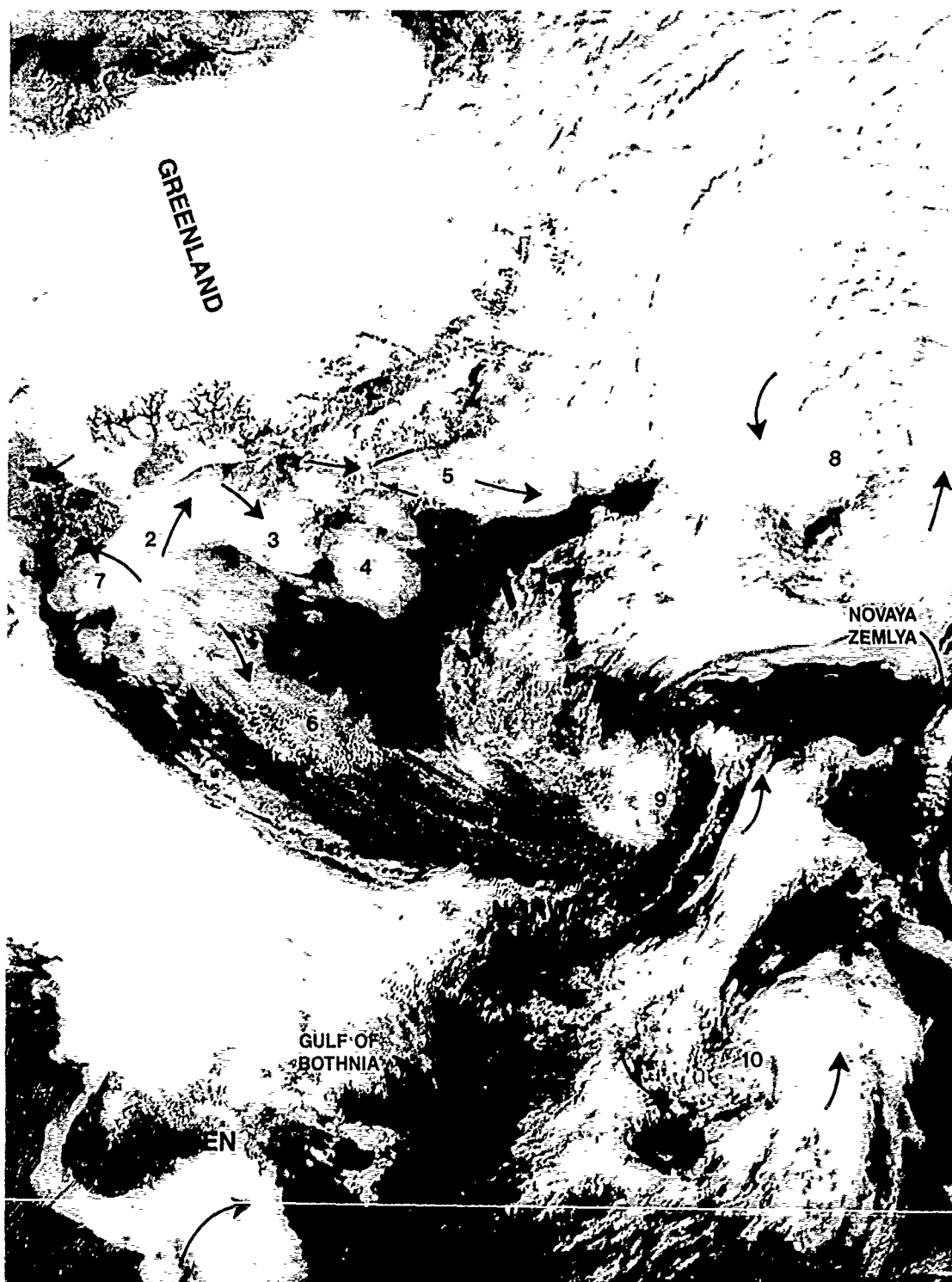
## *1A Streamline Analysis*

### *Streamline Analysis in the Arctic*

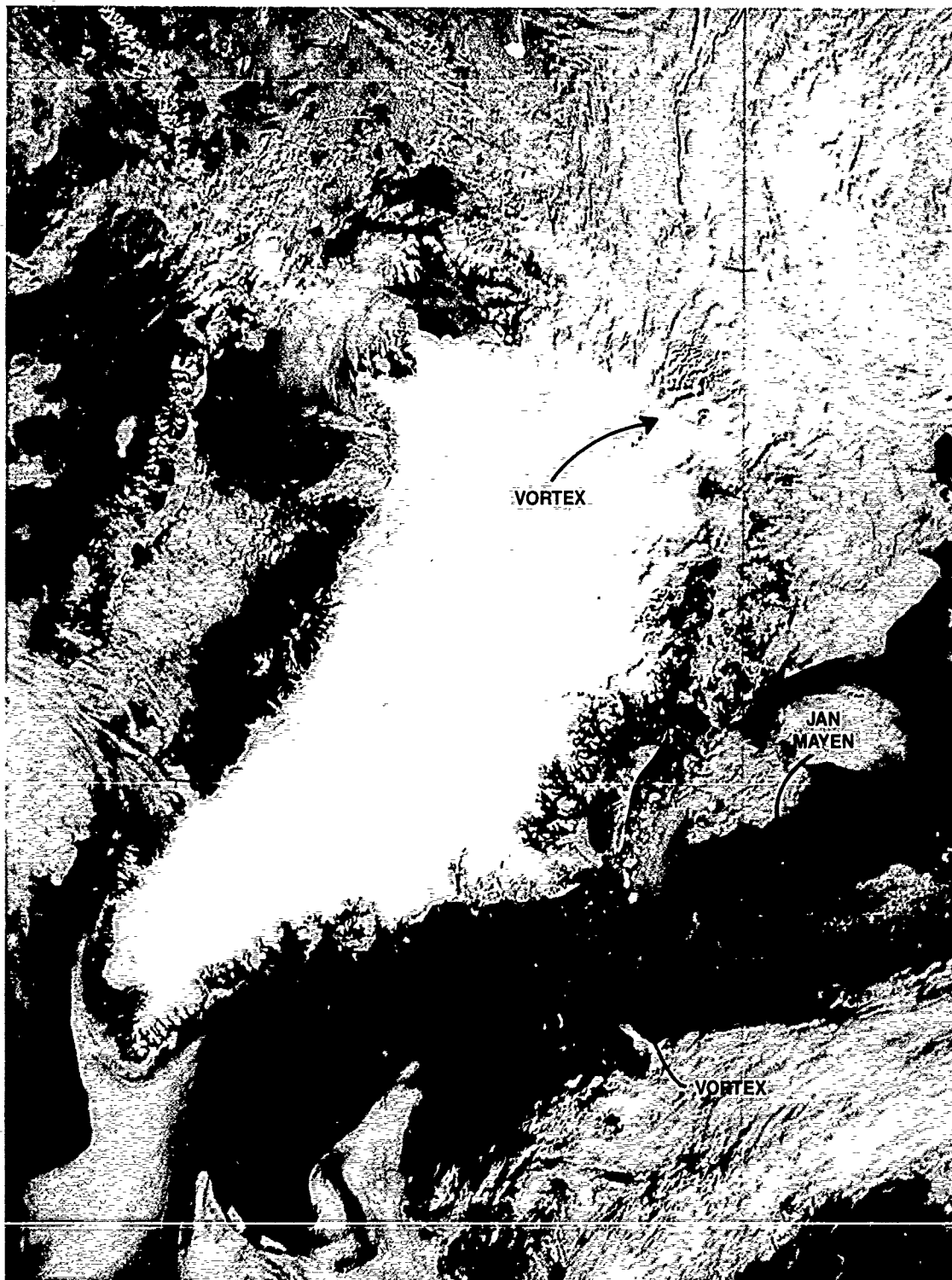
One of the most important parameters that a forecaster in the Arctic must deal with is wind direction. Streamline analysis is a useful tool to accurately assess present flow conditions by overlaying wind reports on satellite data and then using other clues from the satellite data to assess probable flow direction.

Probable speed can be gleaned from a combination of existing surface observations and judgments of intensity from satellite appearance.

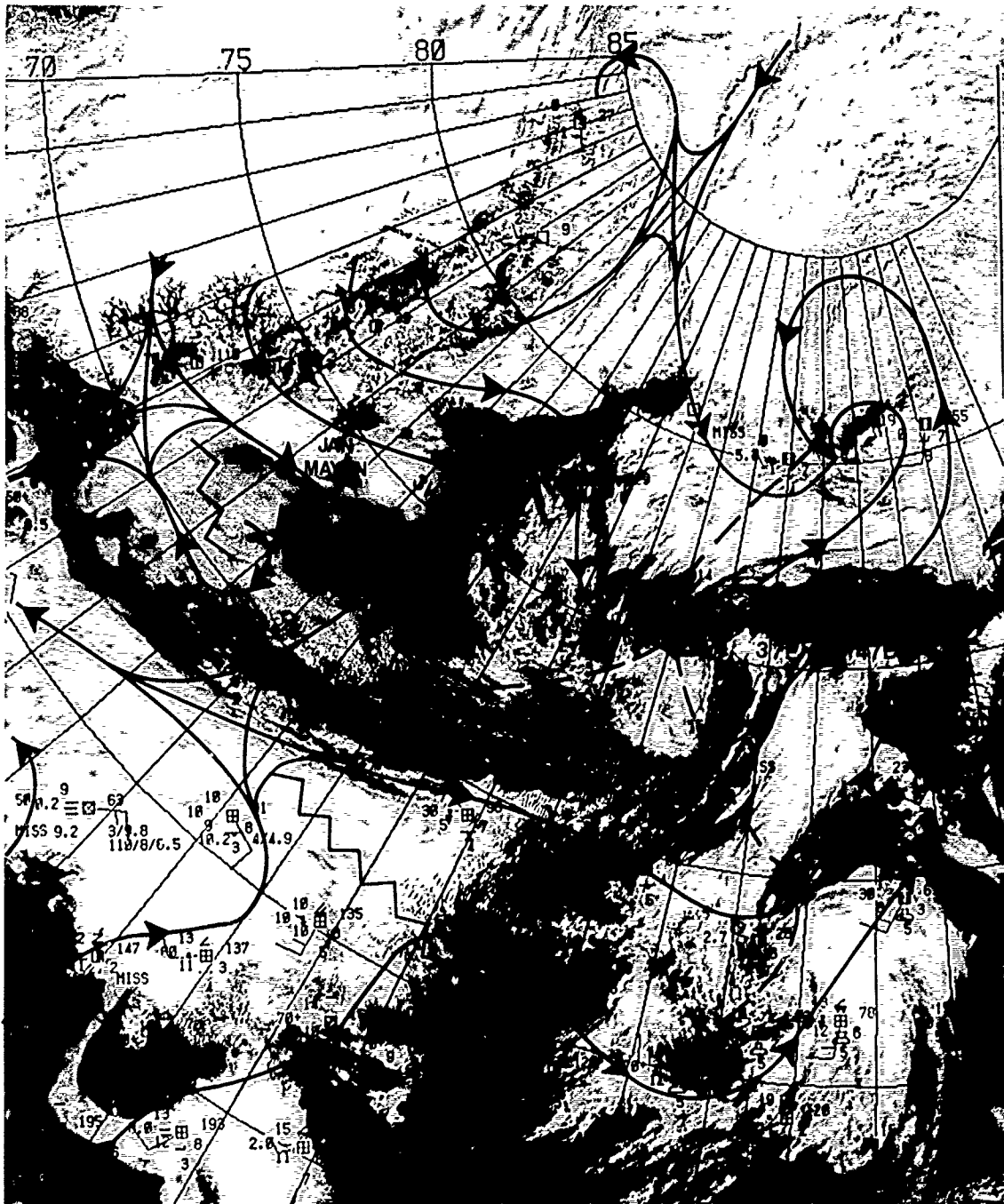




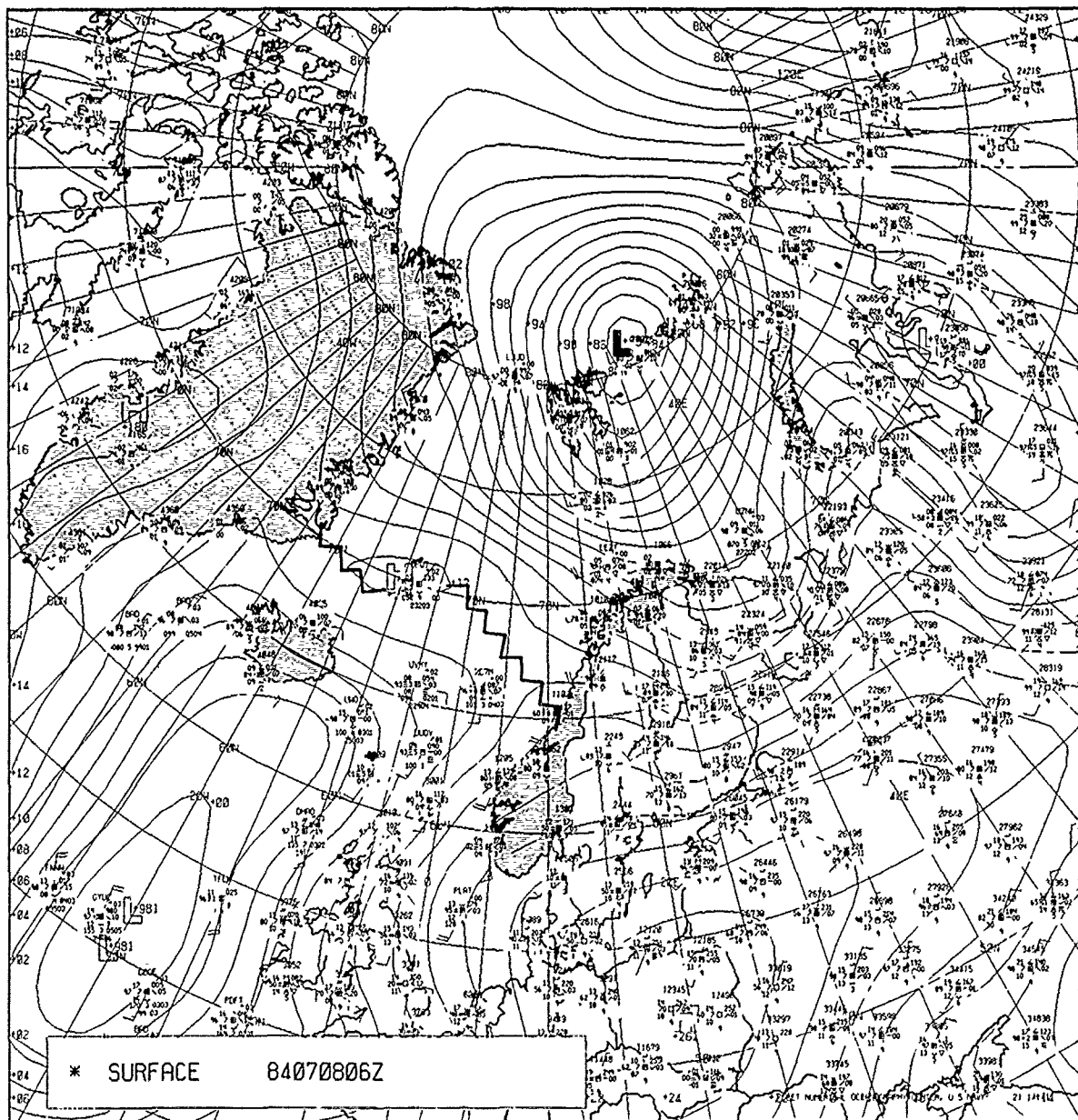
1A-2a. DMSP Visible (LS) Data. 0701 GMT 8 July 1984.



1A-3a. DMSP Visible (LS) Data. 1024 GMT 8 July 1984.



1A-4a DMSP Visible (LS) Data and Streamline Analysis/Surface Observations (0600 GMT), 1024 GMT 8 July 1984.



1A-5a. FNOC Surface Analysis. 0600 GMT 8 July 1984.

*Case 2 Identification of Cols, High Pressure Centers, and Ridge Lines  
Greenland/Norwegian Seas (9-10 July 1984)*

*Use of Cloud Patterns to Define High Pressure Centers and  
Ridge Line Locations*

High pressure centers and ridge lines emanating from these centers are regions of strongest subsidence and weakest winds. Skies tend to be clearest near the high center and along the ridge line under conditions of a surface-based or very low inversion. Flow will tend to be more cyclonic where cloud lines or rows are evident and more anticyclonic under areas of overcast stratus or stratocumulus. Transitions between such conditions often indicate a change from anticyclonic to cyclonic flow or vice versa.

Col regions are areas where the curvature of the wind changes drastically over relatively small distances. Since cloud patterns such as "closed-cell" or "open-cell" are strongly influenced by curvature effects one might anticipate the existence of a col near areas where cloud forms change in such a manner.



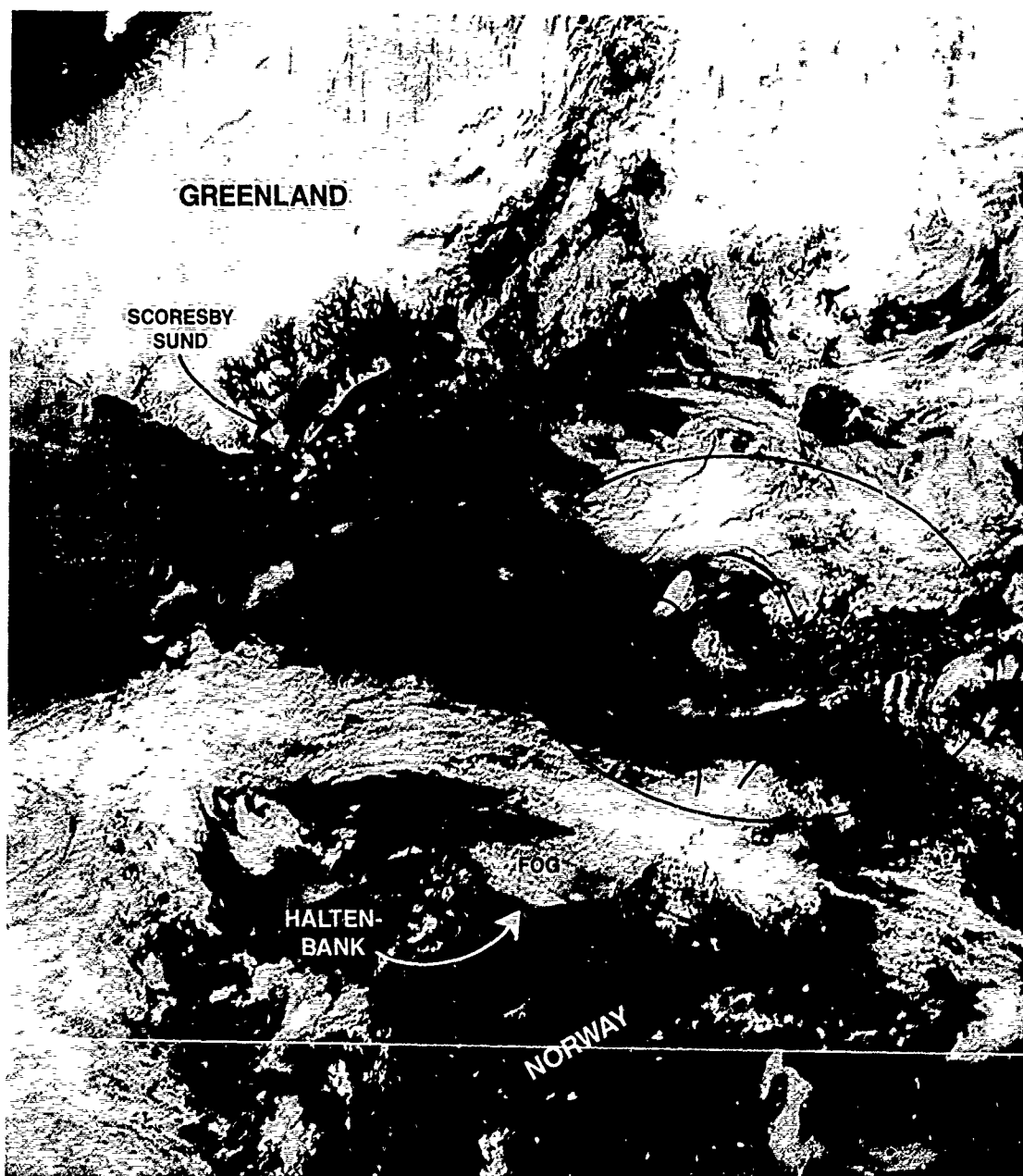
In the DMSP visible image acquired at 1024 GMT (Fig. 1A-3a) cyclonic cloud streaks in the same region imply a small vortex in that area, in agreement with the streamline analysis. Additionally, such strong northeasterly flow implied by the surface analysis (Fig. 1A-5a) would have resulted in a cold surge with cloud lines clearly in evidence over the Fram Strait. These do not appear. It seems therefore that the streamline analysis (Fig. 1A-4a) gives a more accurate representation of what was happening in that region. The streamline analysis shown is probably not definitive but is an attempt to suggest ways of using the satellite data in conjunction with conventional reports for the most reasonable analysis.

#### Important Conclusions

1. Superimposing surface reports over satellite imagery is an excellent way to derive a more accurate surface streamline analysis of the region.
2. Off-ice flow can be expected over clear or non-foggy regions of the MIZ; on-ice flow can be expected for the reverse.
3. Low overcast stratocumulus or stratus areas are normally associated with anticyclonic flow; ridge lines are frequently found as clear slots or very suppressed, thin fog areas, emanating from the anticyclonic center.
4. Open-celled stratocumulus clouds are associated with straight or cyclonic flow.
5. Anticyclonic flow can be expected over foggy areas.
6. Cloud plumes over the MIZ frequently occur as cold off-ice flow encounters the open water of leads or polyni. The plumes may spread laterally under stable, strong, low inversion conditions. Under more unstable conditions a single elongated plume is more commonly observed.

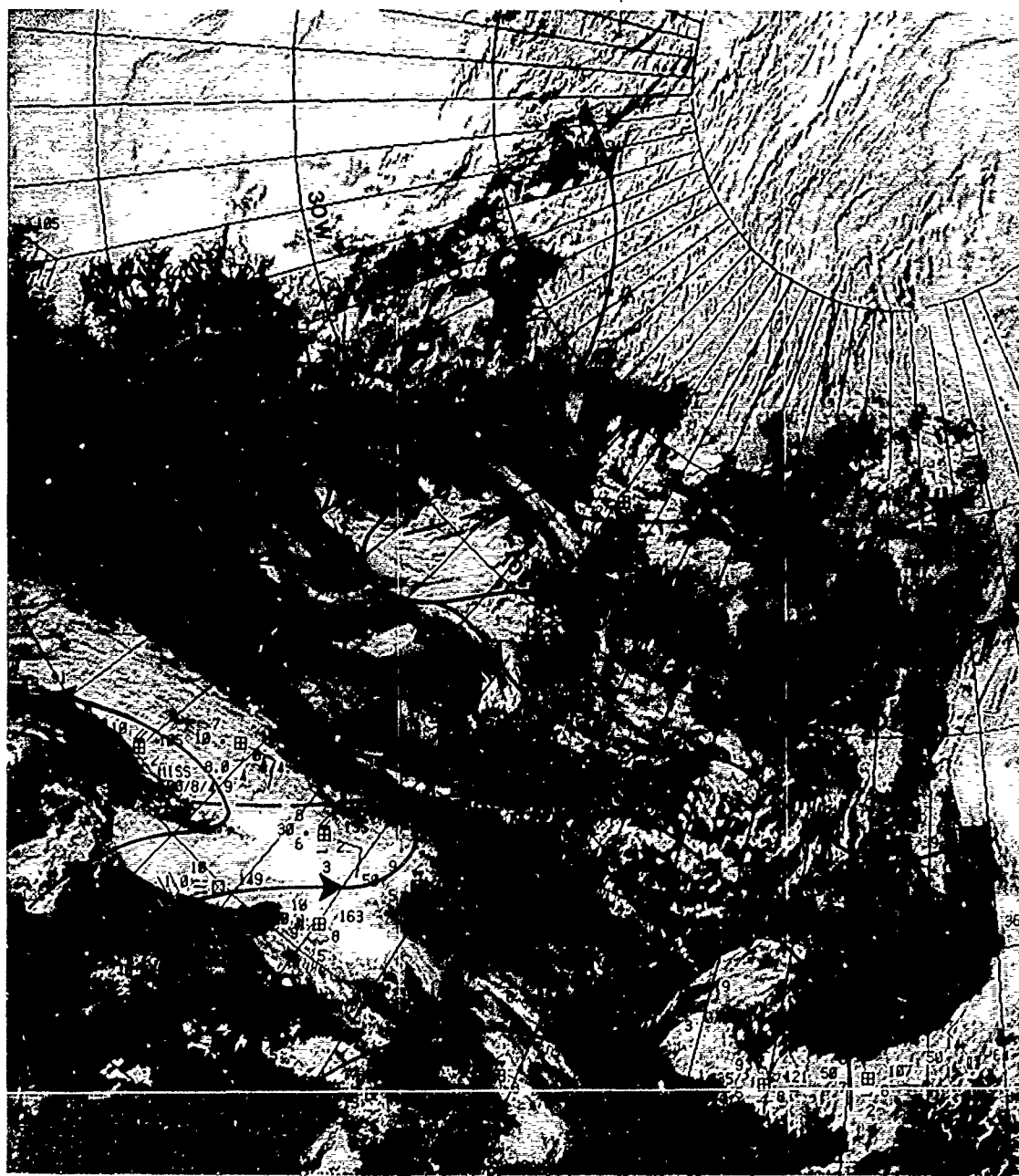
9 July 1984

On this date at 0822 GMT, DMSP visible (LS) data (Fig. 1A-7a) reveal an area from Greenland to Norway. Circled is an area in the right center of the image where small open-celled stratocumulus change to large open-celled stratocumulus very abruptly. A long axis of dilatation characterizes the leading edge of the cloud formation. Arrows have been drawn suggesting the type of flow pattern that might exist in this situation. The pattern suggests a col.



1A-7a. DMSP Visible (LS) Data. 0822 GMT 9 July 1984.

A streamline analysis has been superimposed over DMSP data received a couple of hours earlier at 0641 GMT (Fig. 1A-8a). Surface observations have also been superimposed on the image. The analysis shows that the idea of a col in the region is substantiated. Note especially that the leading edge of the stratocumulus cloud formation seems enhanced, particularly on the east side, and that this edge is logically analyzed as an asymptote of convergence.



1A-8a. DMSP Visible (LS) Data and Streamline Analysis/Surface Observations (0600 GMT). 0641 GMT 9 July 1984.

10 July 1984

DMSP visible (LS) data at 0600 GMT (Fig. 1A-10a) show a scene stretching from Greenland eastward to Novaya Zemlya (lower right). Fog covers a portion of the MIZ on the east coast of Greenland and extends seaward toward Jan Mayen Island. Ice floes can be seen through the transparent layer of fog. The northeastern MIZ of Greenland appears clear by contrast.

A clear slot extends eastward from Jan Mayen toward northern Norway. We should immediately expect the presence of a high pressure center near Jan Mayen and a ridge line over the clear slot.

Figure 1A-11a shows superimposed surface observations and a streamline analysis on the DMSP image. Although this analysis could be drawn in a number of ways, surface observations are adequate to verify that the clear slot overlies a ridge line.

Note that cyclonic flow is shown north of the col area where the overcast stratus suddenly transitions to cumulus cloud lines.

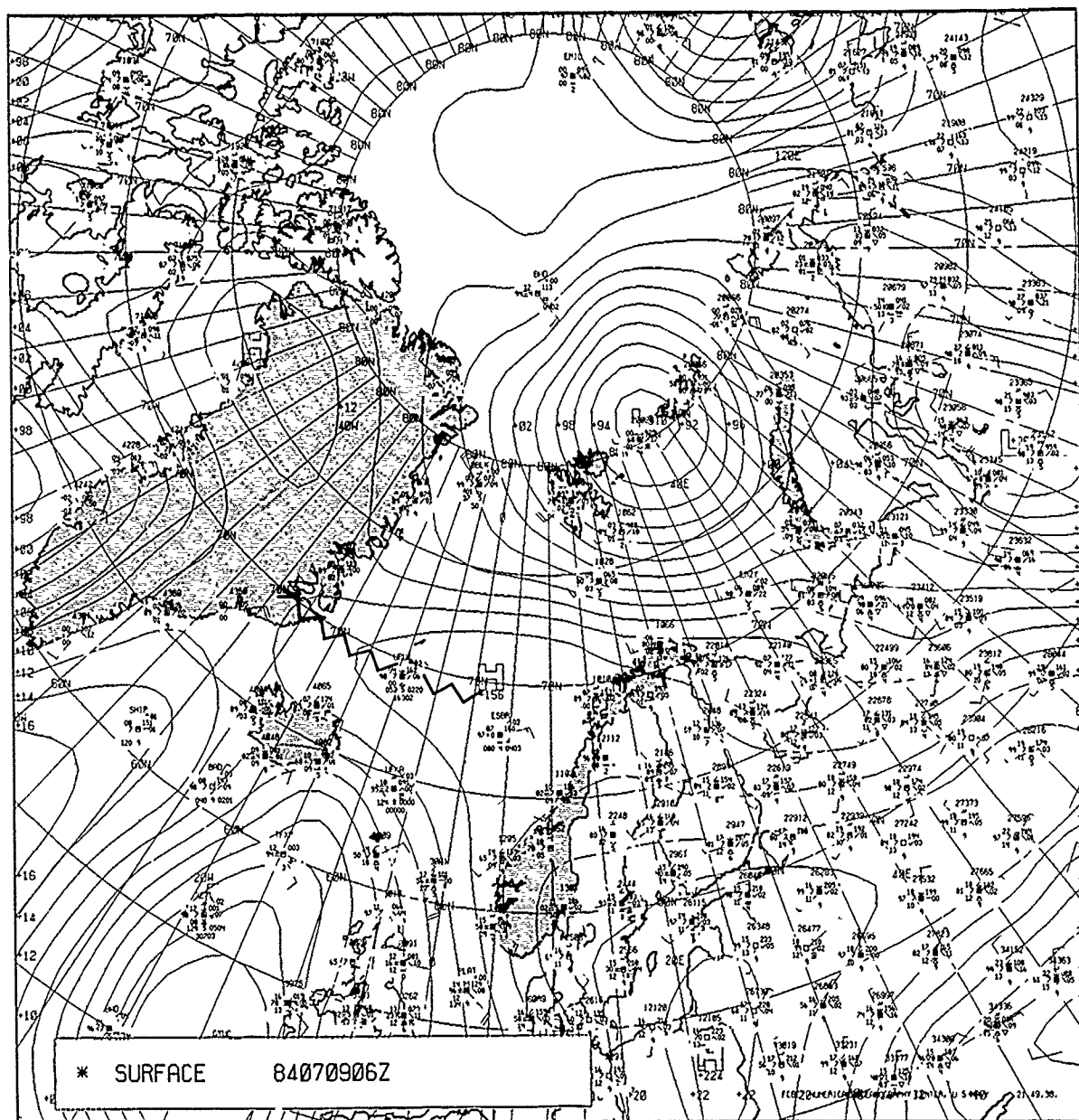
The simultaneous infrared view (Fig. 1A-12a) offers verification that the cloud formation in the Jan Mayen area is very low stratus or fog with a cloud-top temperature almost indistinguishable from that of the sea. The circled area in Fig. 1A-12a is interesting in that a warm gray shade is shown over coastal Greenland, obscuring features apparent in the visible data (Fig. 1A-11a). The gray shade suggests that a thin overcast exists under the inversion. It is difficult, if not impossible, to discern this cloud formation in the visible data.

A number of vortices in this example are also much more evident in the infrared data than in the visible (Figs. 1A-7a and 1A-11a). It is always useful to compare carefully the infrared with the visible data in developing a streamline analysis.

The FNOC surface analysis for 0600 GMT (Fig. 1A-13a) completes this study and shows the ridge extending eastward from near the southern tip of Greenland to the coast of Norway. Fog reports are especially numerous on the south side of the ridge where southerly winds have advected warm, moist air over cooler waters. There is no doubt, however, based on the satellite data that fog is also prevalent along the MIZ and near Jan Mayen Island.

#### Important Conclusions

1. Clear slots in a region of low stratus often coincide with surface ridge lines.
2. Cyclonic flow should be anticipated in regions of cumulus cloud lines.
3. Col areas are sometimes very apparent on satellite data due to abrupt changes in the appearance and type of low stratocumulus cloud formations.
4. Use of infrared data along with visible data is important to assure detection of all details. Some cloud formations such as thin cirrus or thin, transparent stratus are difficult to detect in visible imagery, especially over ice and snow. The same formations are often readily apparent in corresponding infrared data.



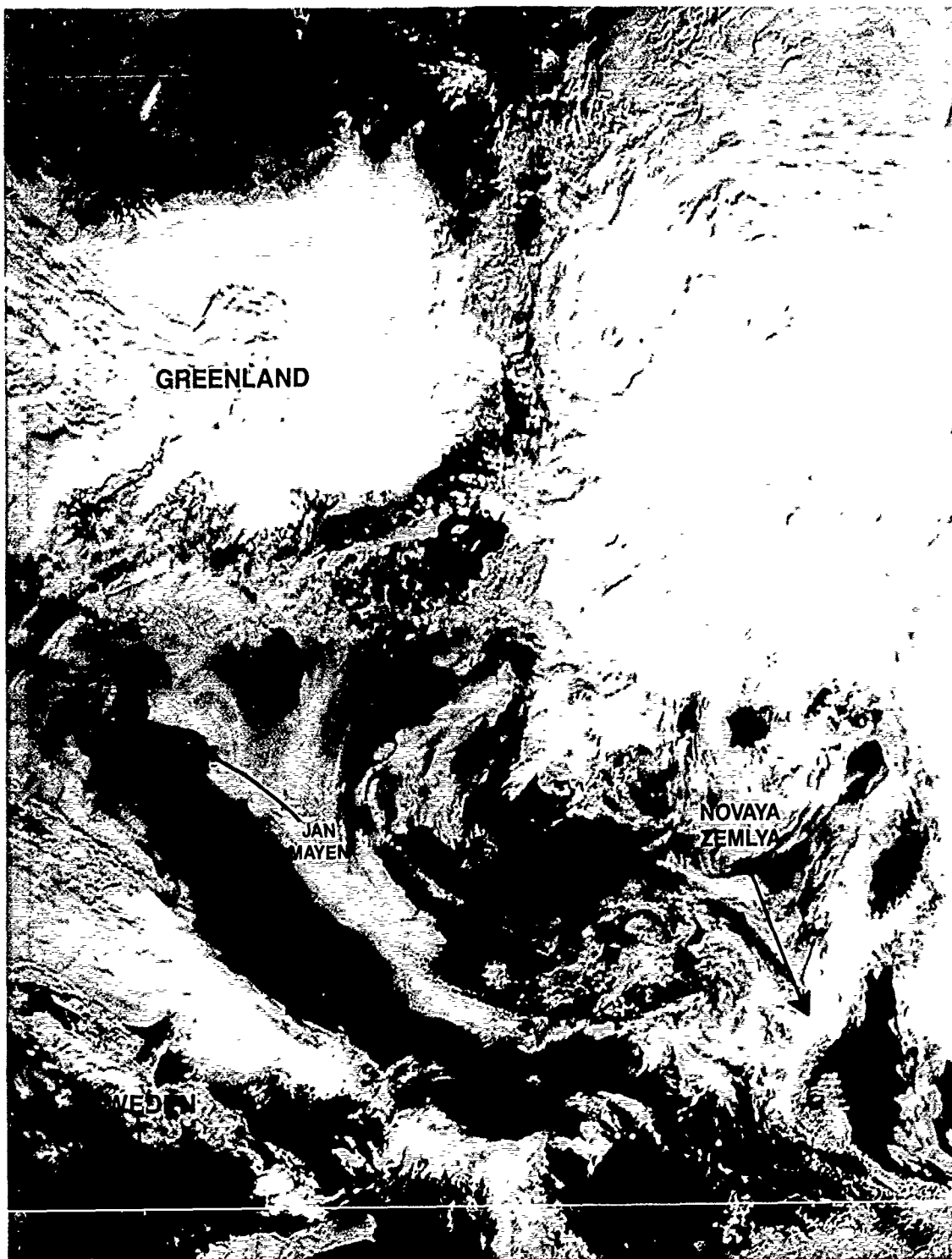
1A-9a. FNOC Surface Analysis. 0600 GMT 9 July 1984.

The FNOC 0600 GMT surface analysis is shown in Fig. 1A-9a. The analysis shows that a ridge line extended across the Norwegian and Greenland Seas toward Scoresby Sund.

The col is just off the Norwegian coast near 70°N and 10°E. A col, by necessity, lies between a high and a low as shown in this analysis.

Note that the Haltenbank (65°N 10°E), a shallow bank off the coast of Norway, is covered with fog (see Fig. 1A-7a). This bank is much colder than adjacent waters. Anticyclonically-turning southerly flow of nearly saturated air over the bank has resulted in the fog formation.



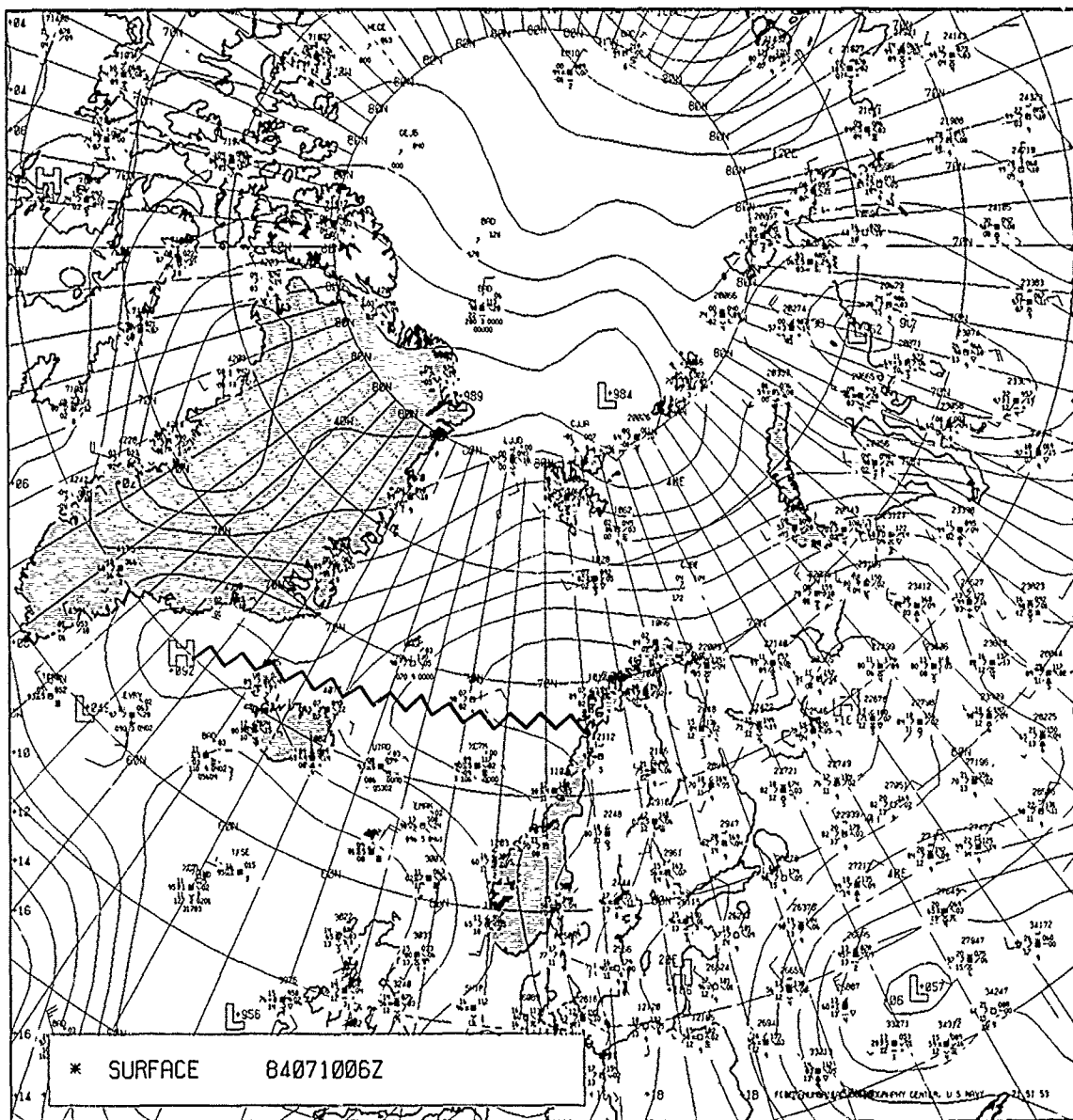


1A-10a. DMSP Visible (LS) Data. 0600 GMT 10 July 1984.





1A-12a. DMSP Infrared (TS) Data. 0600 GMT 10 July 1984.



1A-13a. FNOG Surface Analysis. 0600 GMT 10 July 1984.

## *1B Fog and Stratus Formation*

### *Fog and Stratus Formation Over the Greenland/Norwegian/Barents Seas and Marginal Ice Zone*

Prediction of fog and stratus formation in the Arctic is closely linked to the prediction of movement and location of high pressure centers and ridge lines, and to an understanding of special effects that occur along the marginal ice zone during periods of on-ice flow.

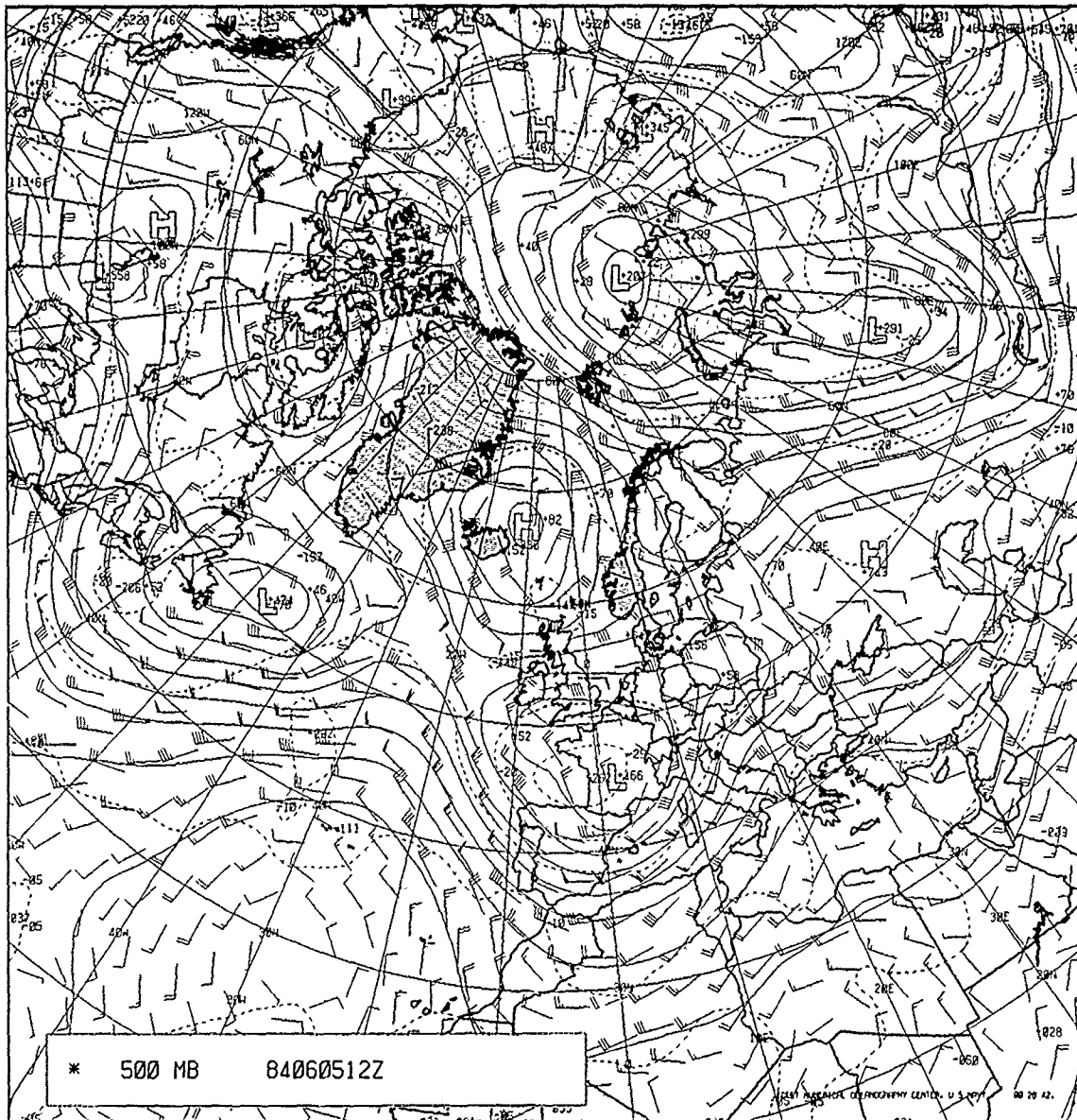
*Case 1 Fog Formation Over the Greenland/Norwegian Seas During a Period of Blocking (5-9 June 1984)*

*Fog Forecasts During a Blocking Event*

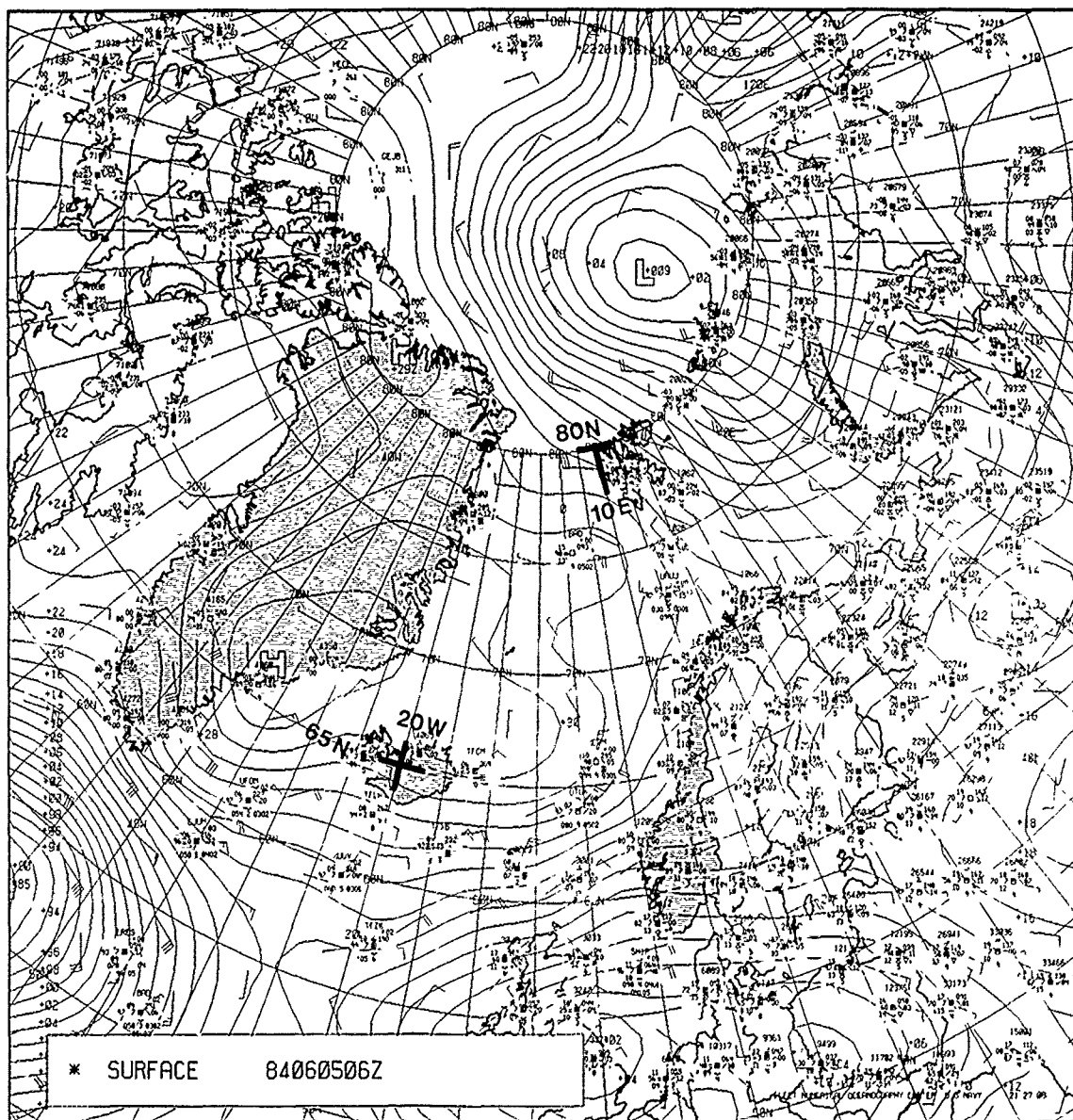
Blocks develop over the North Atlantic with the maximum frequency between December and May, and with the typical block lasting 5 to 15 days (Fett et al., 1981). The block is usually located west of the Greenwich meridian. Operationally, blocks are significant, not only in the manner in which they affect the movement of weather systems around their periphery, but also because of the foggy weather with low ceilings and poor visibility located in the region of the high. Satellite data suggest that a reasonably good forecast for fog can be made by predicting no fog and clear skies near the center of the blocking high on the 24-hr 500-mb prognosis and fog along the edges of the high and under ridge lines emanating from the high.

*5 June 1984*

The 500-mb analysis for 1200 GMT (Fig. 1B-3a) shows a blocking high just northeast of Iceland. The blocking pattern shows the typical split flow where part of the jet east of Newfoundland diverts northward around Iceland and part southward through the Strait of Gibraltar. The low pressure over Spain south of the blocking high is typical of the blocking pattern.



1B-3a. FNOC 500-mb Analysis. 1200 GMT 5 June 1984.



1B-4a. FNOC Surface Analysis. 0600 GMT 5 June 1984.



The surface analysis for 0600 GMT (Fig. 1B-4a) shows the high centered over the southeast coast of Greenland. Numerous reports of fog are shown by surface observations north and southeast of the high center.

DMSP visible data acquired at 0800 GMT (Fig. 1B-5a) shows the region, with the land masses of Greenland, Spitsbergen, Norway, and Scotland clearly visible. Fog and/or low stratus is evident circling the clear area near the image center. The inner edge of the fog pattern is very sharply delineated.

A surface streamline analysis (Fig. 1B-6a) superimposed over the DMSP image shows the likely flow pattern existing over the area. Obviously this pattern could be reconstructed in a number of ways since surface reports are so sparse. The pattern, however, relates reasonably well to what is shown on the surface analysis (Fig. 1B-4a). Note that the clear area centered near  $67^{\circ}\text{N } 3^{\circ}\text{W}$  largely overlies the center of high pressure shown on the 500-mb analysis (Fig. 1B-3a). Fog encircles the outer perimeter of the high.

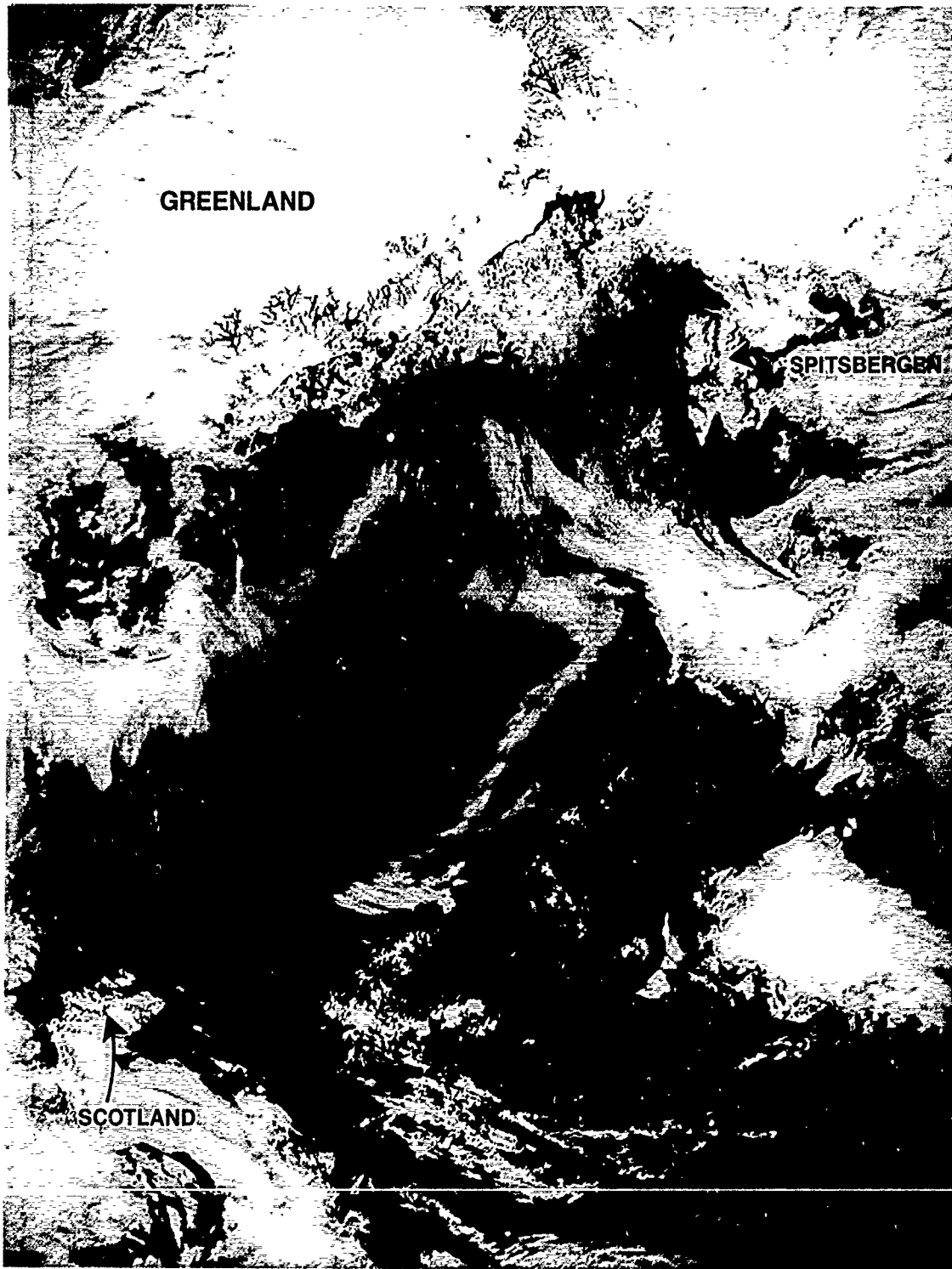
The 24-hr 500-mb prognosis (Fig. 1B-7a) valid for 1200 GMT on 6 June (the following day) shows the block persisting. From this pattern clear skies are anticipated over Iceland and southeast toward the Faroe Islands, with fog north of Iceland toward Greenland and extending eastward to Norway, and fog south of the high under the ridge line.

#### *6 June 1984*

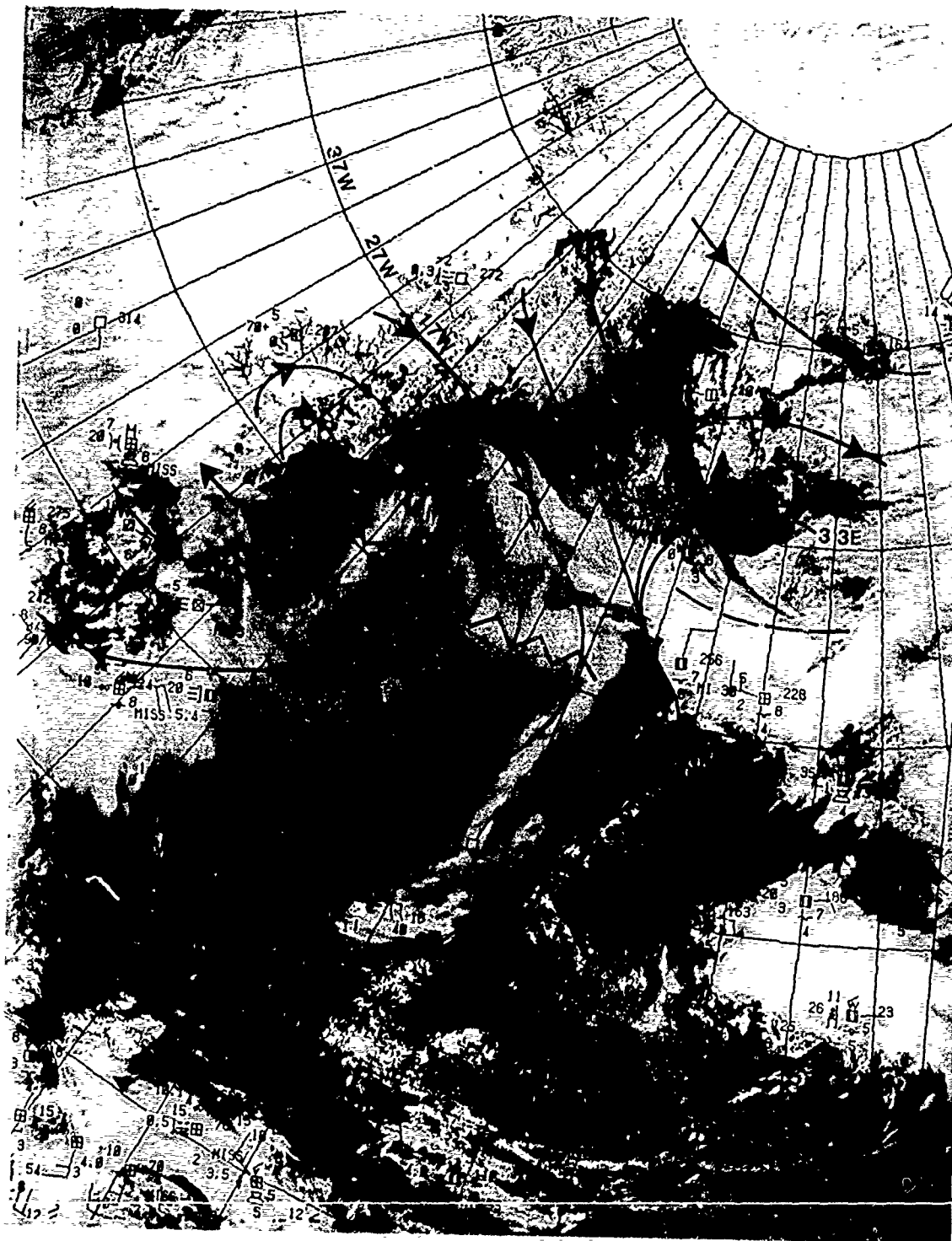
The DMSP data at 0921 GMT (Fig. 1B-8a) reveal very clear conditions over Iceland and generally to the south and northeast. Fog or low stratus is evident mainly well to the east, near Norway, and northwest of Iceland toward Greenland, and to the south of Iceland as forecast. A streamline analysis superimposed over the DMSP data (Fig. 1B-9a) shows the general flow pattern and reports of fog in the region. A small eddy associated with an arctic front is evident to the north moving eastward over the high.

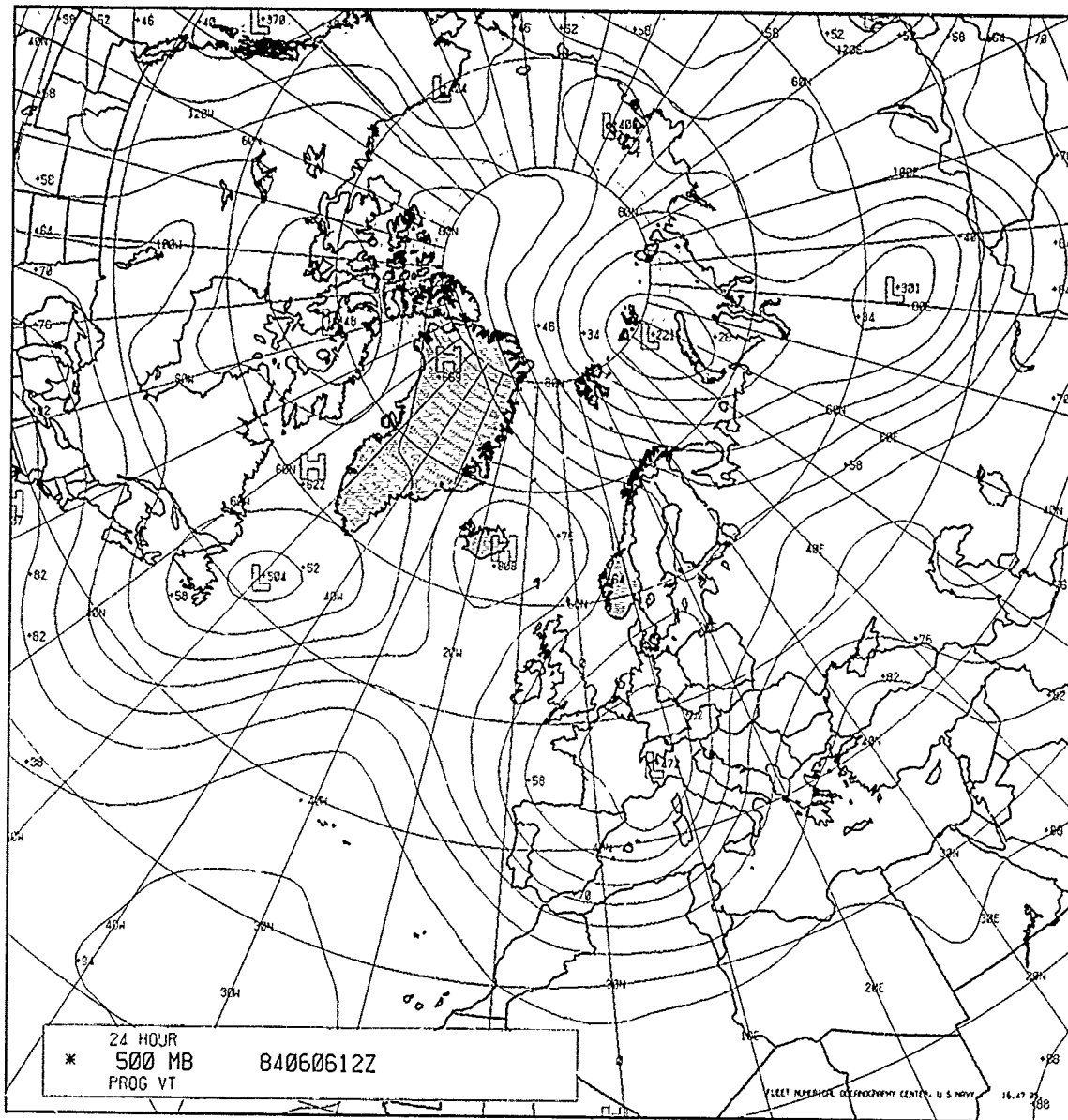
The surface analysis for 1200 GMT (Fig. 1B-10a) does not reveal this feature. Numerous reports of fog, low visibilities, and obscured skies verify fog around the periphery of the high and in the ridge line extending south of Iceland. The 500-mb analysis (Fig. 1B-11a) verifies the continued existence of the block and the split flow separating near  $57.5^{\circ}\text{N } 23^{\circ}\text{W}$ .

The 24-hr 500-mb prognosis valid for 1200 GMT (Fig. 1B-12a) on 7 June shows the block persisting and the center now southeast of Iceland. From this pattern clear skies should be expected in the region between Iceland and the Faroe Islands, with fog extending northeast toward Greenland, eastward toward Norway, and south of the high along the ridge line.



1B-5a. DMSP Visible (LS) Data. 0800 GMT 5 June 1984.



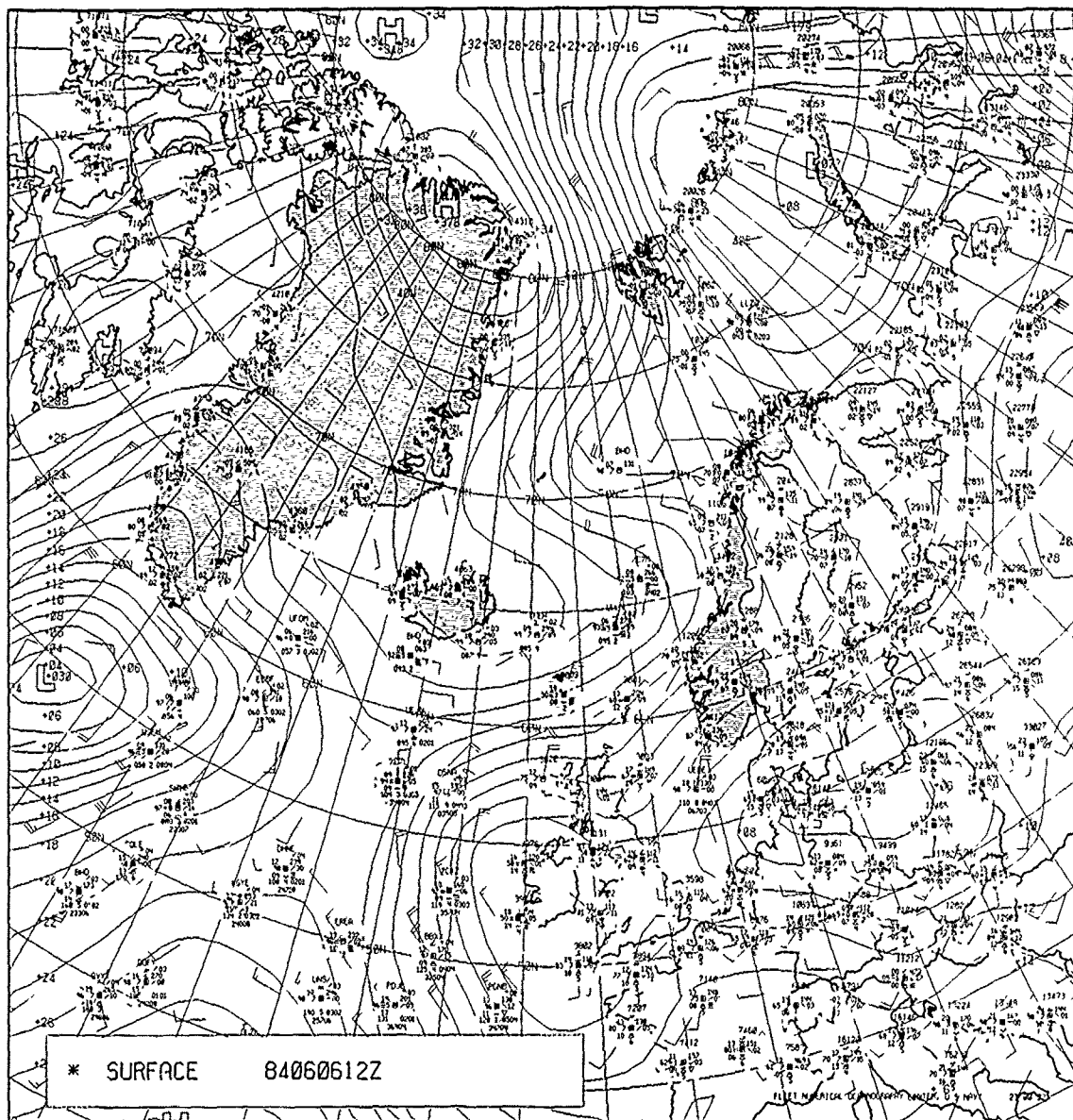


1B-7a. FNOC 24-hr 500-mb Prognosis Valid. 1200 GMT 6 June 1984.

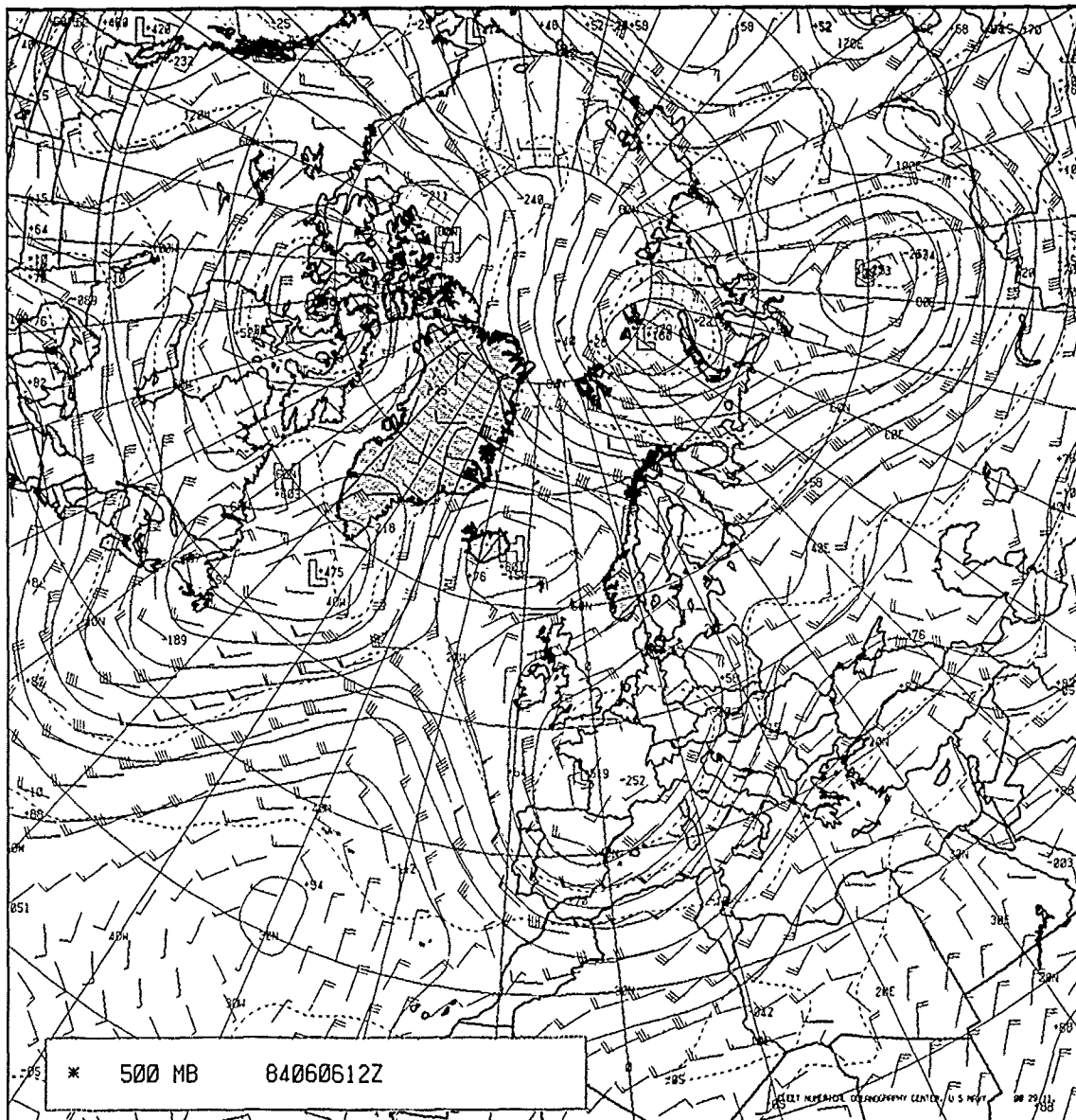


1B-8a. DMSP Visible (LS) Data, 0921 GMT 6 June 1984.





1B-10a. FNOC Surface Analysis. 1200 GMT 6 June 1984.



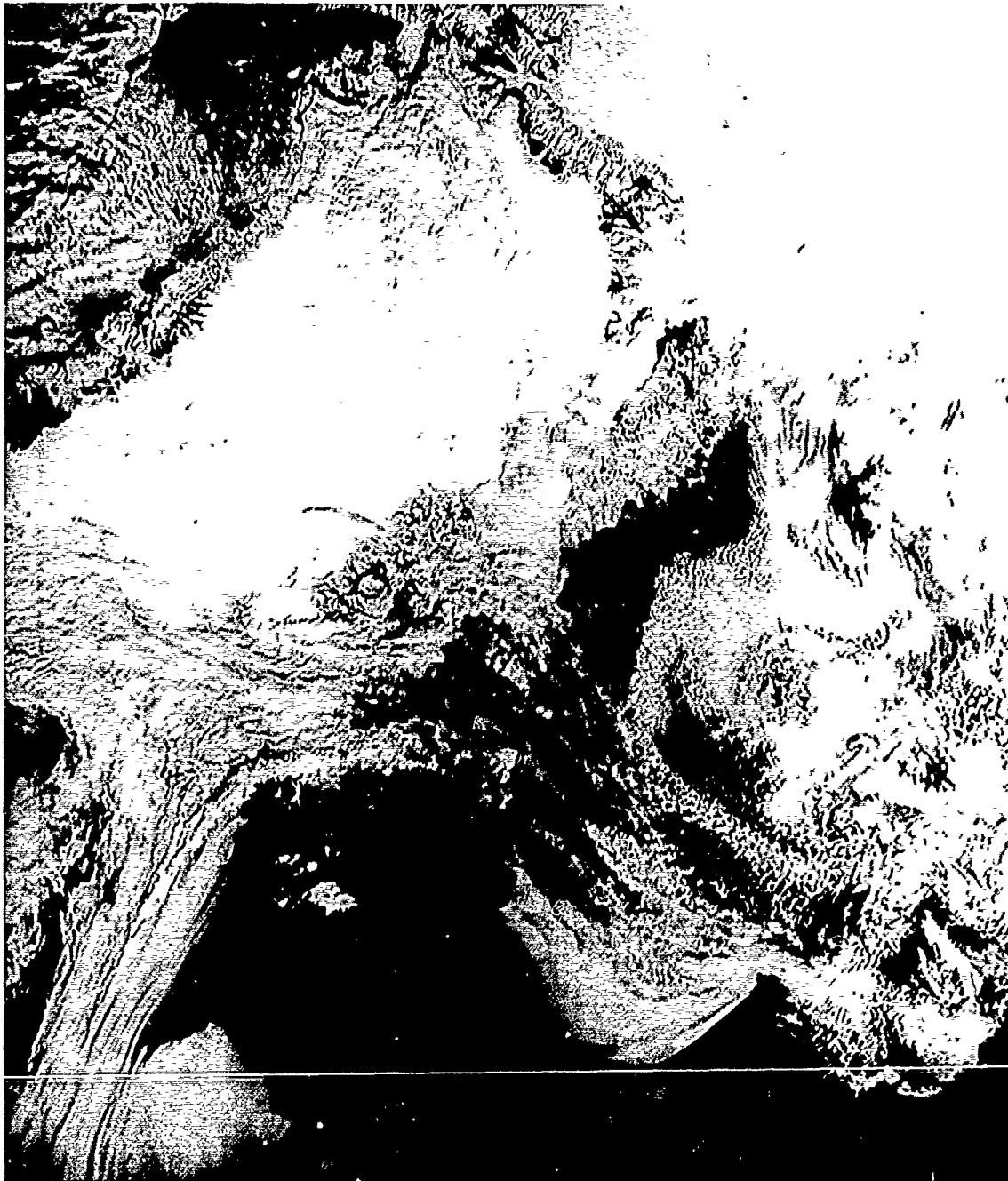
1B-11a. FNOC 500-mb Analysis. 1200 GMT 6 June 1984.





7 June 1984

A DMSP image on this date acquired at 0901 GMT (Fig. 1B-13a) shows that the only clear area in the region is just south and southeast of Iceland. Fog is evident extending from Iceland to Norway; it exists north of Iceland and well to the south and southeast surrounding the Faroe and Shetland Islands, which are creating clear wakes in their lee (to the southwest). Wave clouds,



1B-13a. DMSP Visible (LS) Data. 0901 GMT 7 June 1984.



1B-14a. DMSP Infrared (TS) Data. 0901 GMT 7 June 1984.

similar to ship wakes (Fett and Bohan, 1977) can be seen in the Shetland Islands area. Such wakes imply the existence of a very strong low-level inversion over the area. Simultaneous infrared data are shown in Fig. 1B-14a. These data reveal the warm outline of the Faroe and Shetland Islands and prove that the cloud temperatures in the region are almost indistinguishable from the ocean temperatures, implying very low cloud tops and probable surface fog.

A surface streamline analysis with surface reports superimposed over the DMSP data is shown in Fig. 1B-15a. Note the very low visibilities in the Shetland Island region.

The FNOC surface analysis for 1200 GMT (Fig. 1B-16a) shows the numerous fog reports over the area. Very few reports of fog except in ridge lines can be seen elsewhere on this analysis.

The FNOC 500-mb analysis (Fig. 1B-17a) shows the persistence of the block as an almost perfect example. The 24-hr forecast, however, (Fig. 1B-18a) suggests that the block is weakening. Fog, according to this analysis, would be expected northwestward toward Iceland, southward toward the Canary Islands, and southeast of Iceland toward France. Clear skies would be expected over most of Iceland and Great Britain.

#### *8 June 1984*

DMSP data acquired at 0840 GMT (Fig. 1B-19a) verify the movement of the fog consistent with the change in the forecast 500-mb pattern. Streamlines and surface reports superimposed (Fig. 1B-20a) show the nature of the flow, which is changing in response to the southward movement of a low to the northwest and the high pressure center toward Great Britain.

The surface analysis for 1200 GMT (Fig. 1B-21a) shows additional reports of fog in the region. Note, again, that such reports are concentrated in the region of the blocking high and very few in any other region of the entire analysis covering an immense area. This points to the reliability of using the blocking high and ridge lines in this region for fog forecasts.

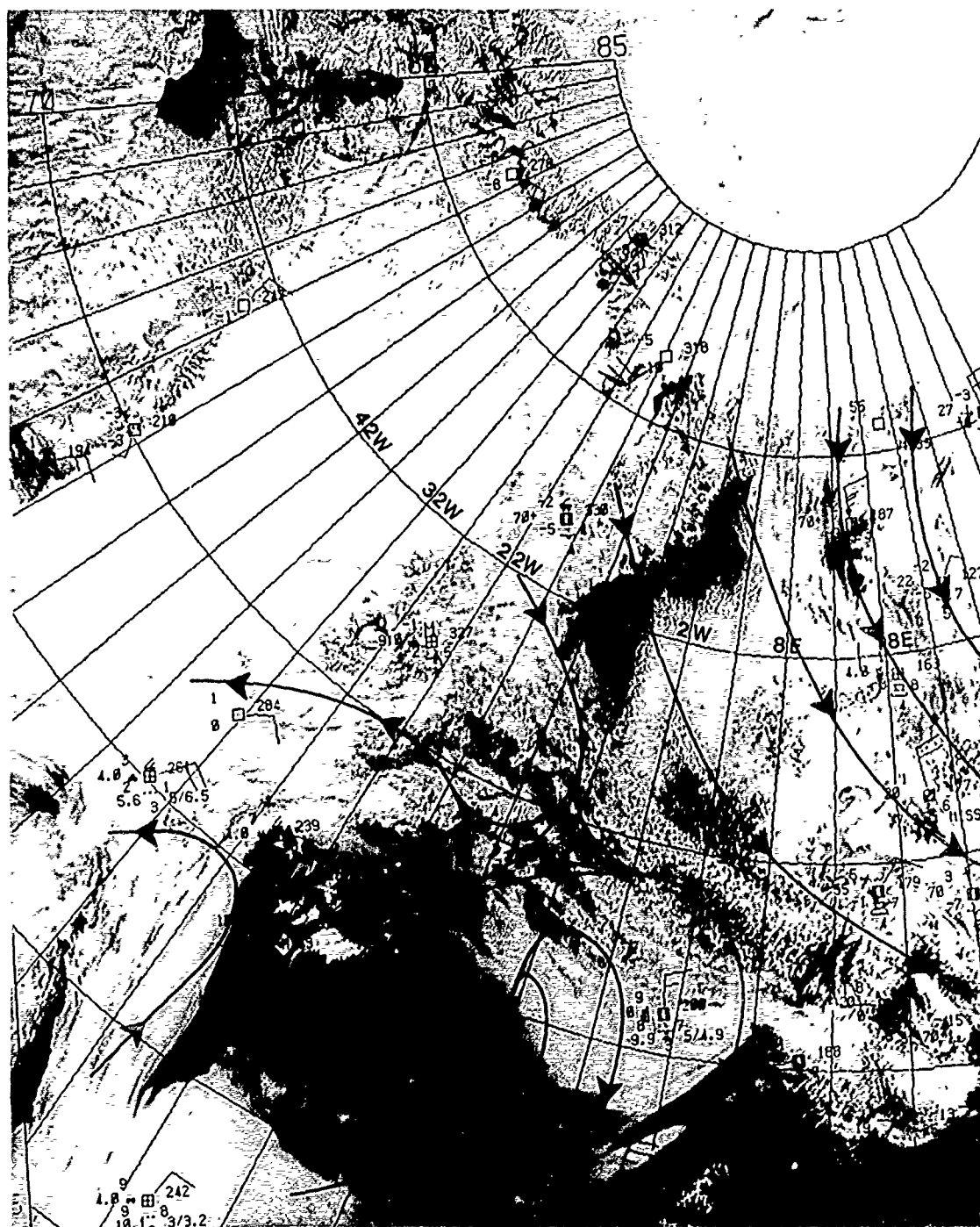
The 500-mb analysis for 1200 GMT (Fig. 1B-22a) continues to show a weakening block while the 24-hr prognosis for 9 June at 1200 GMT (Fig. 1B-23a) shows only a blocking ridge extending southward from Iceland toward the Canary Islands. Fog would be anticipated in patches along this ridge line and over France and southern Great Britain.

#### *9 June 1984*

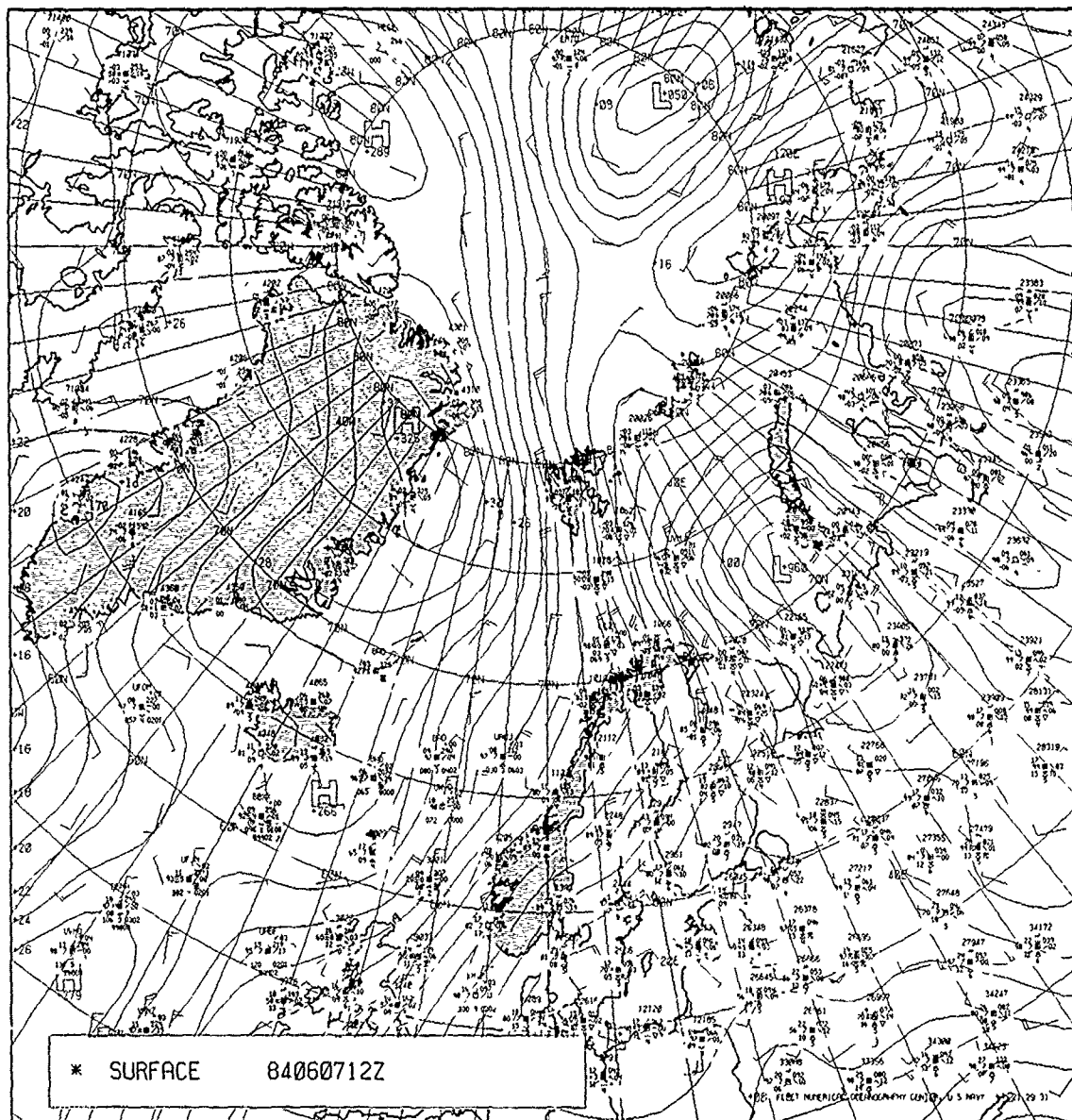
The final DMSP view for 0820 GMT (Fig. 1B-24a) shows only a portion of the region with fog and low stratus apparent west of Great Britain near the ridge line and over France and southern Great Britain.

### **Important Conclusions**

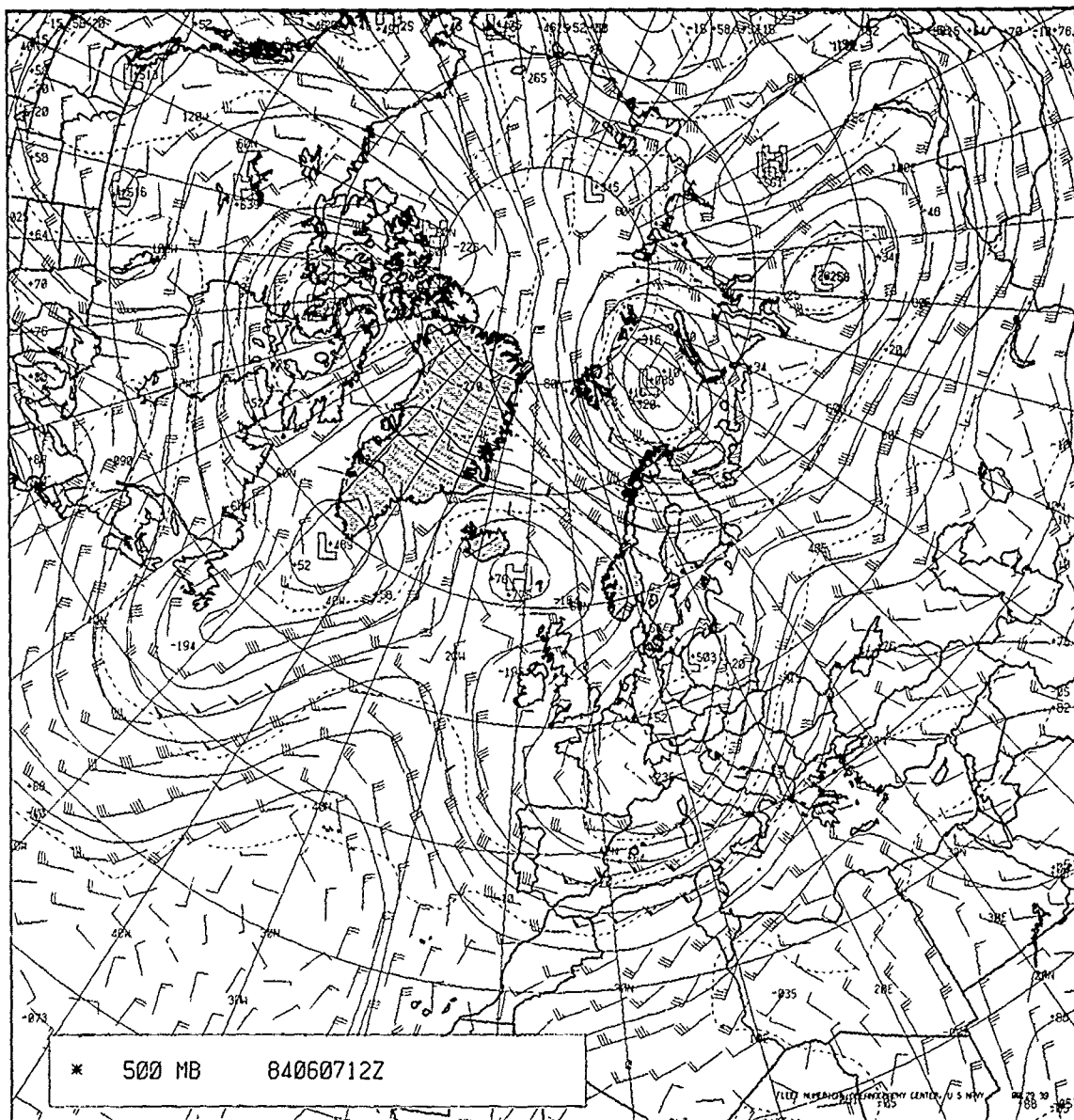
1. Blocking highs radically affect the movement of systems in the Arctic as well as in temperate latitudes.
2. Clear skies are common directly under the blocking 500-mb high position and in trough lines impinging on the high.
3. Fog is intimately associated with blocking highs and can be reliably forecast, using the 24-hr 500-mb prognosis, to lie under ridge lines emanating from the 500-mb blocking high.

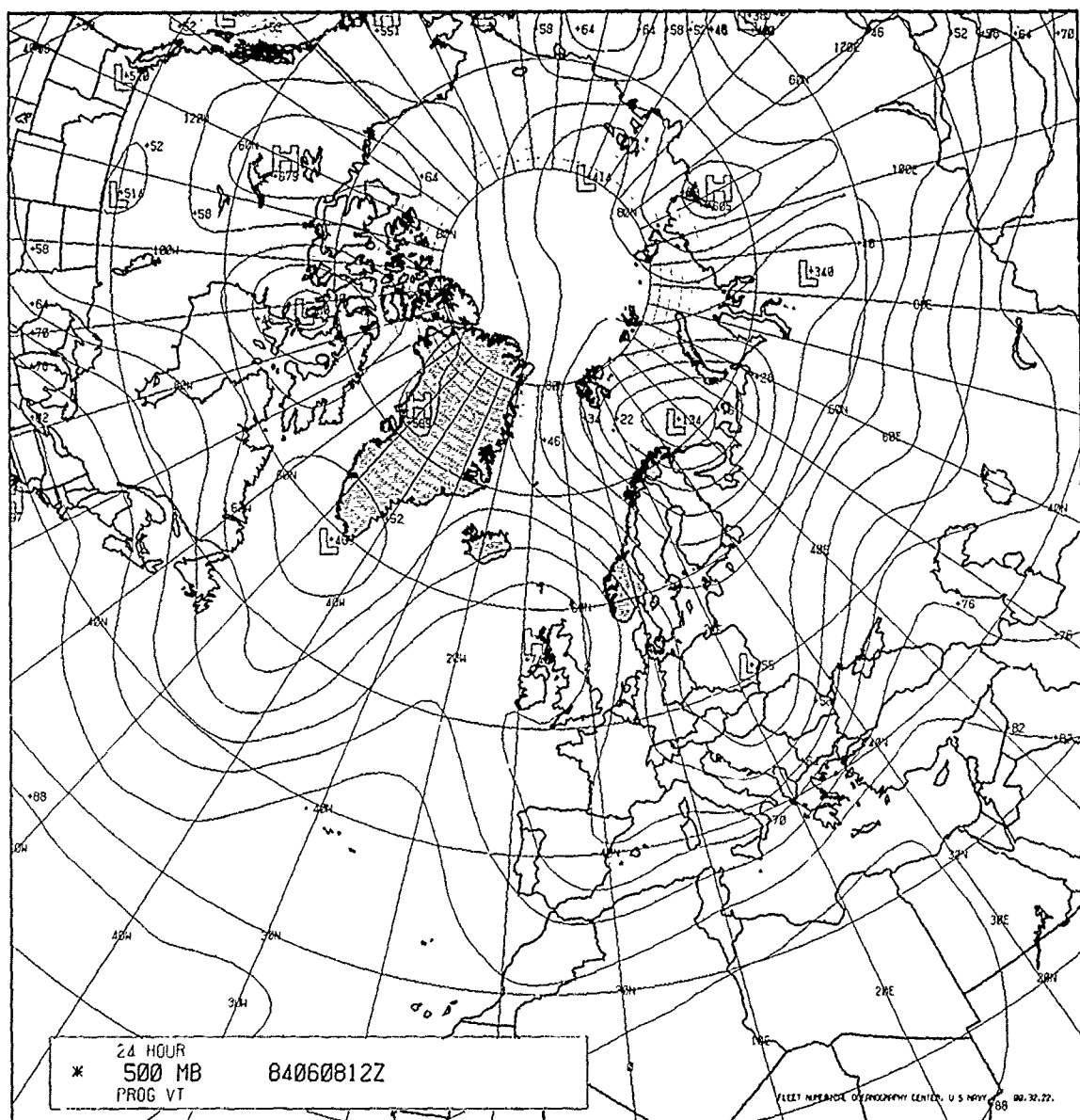


IB-15a. DMSP Infrared (TSS) Data and Streamline Analysis/Surface Observations (1200 GMT). 0901 GMT 7 June 1984.



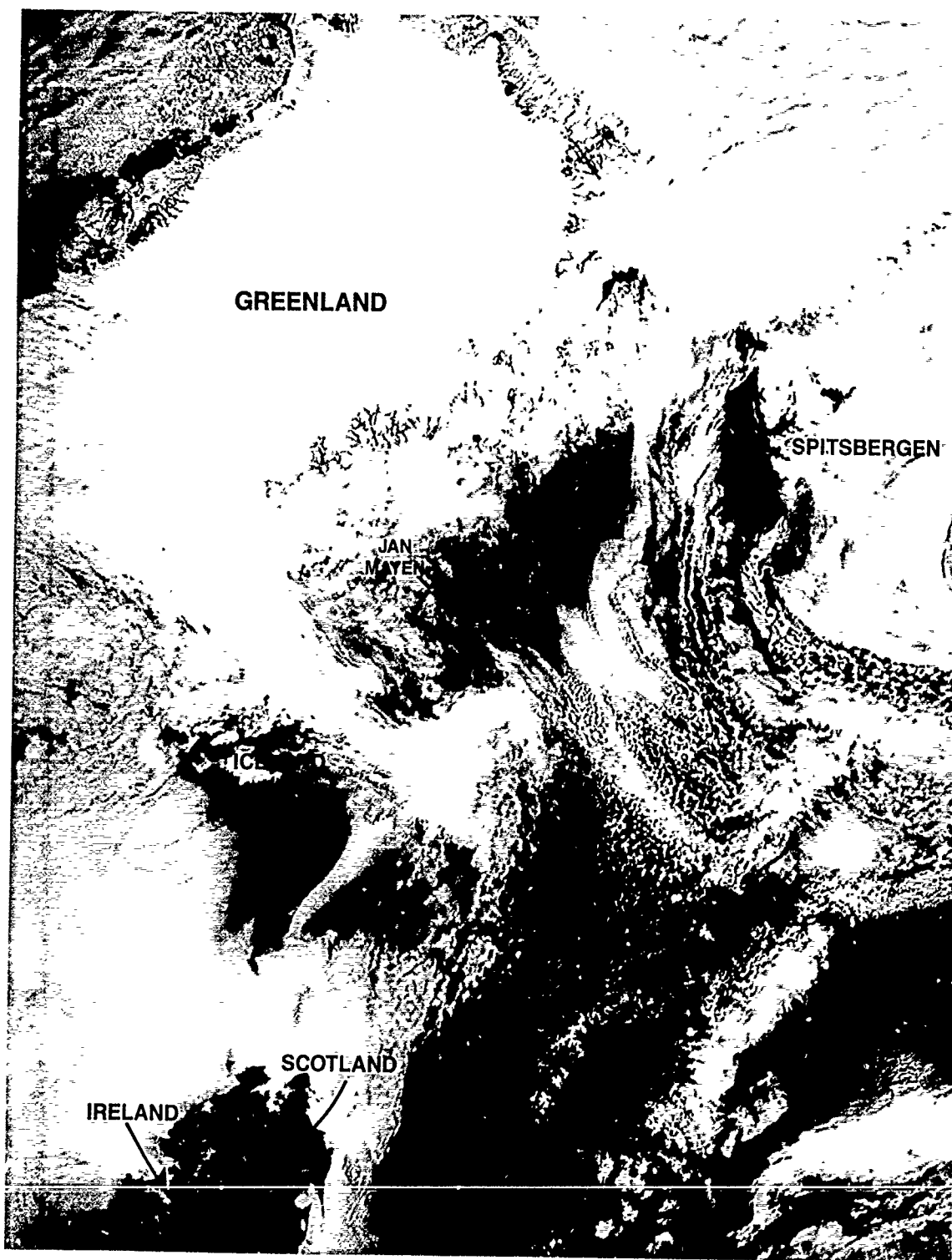
IB-16a. FNOC Surface Analysis. 1200 GMT 7 June 1984.



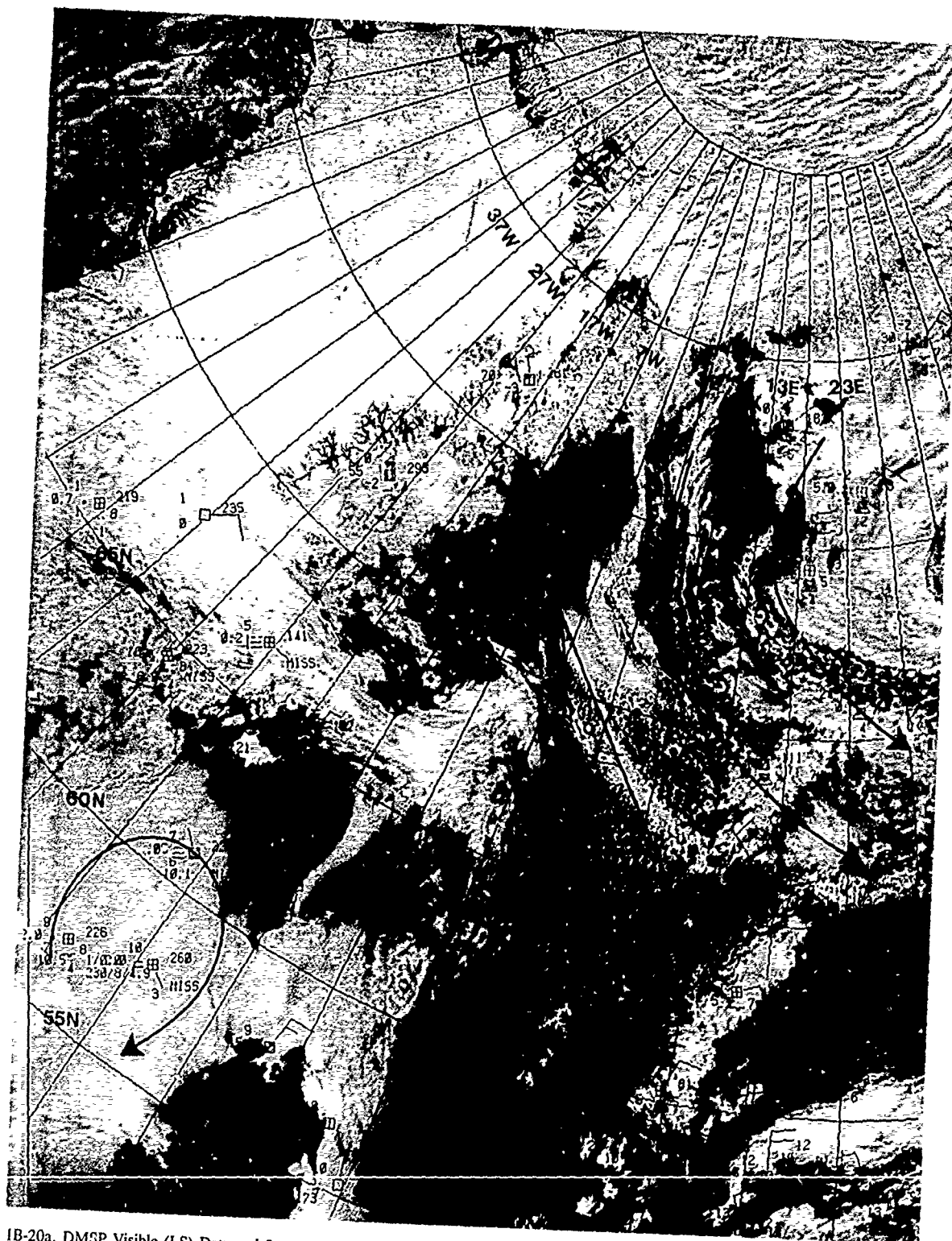


1B-18a. FNOC 24-hr 500-mb Prognosis Valid. 1200 GMT 8 June 1984.

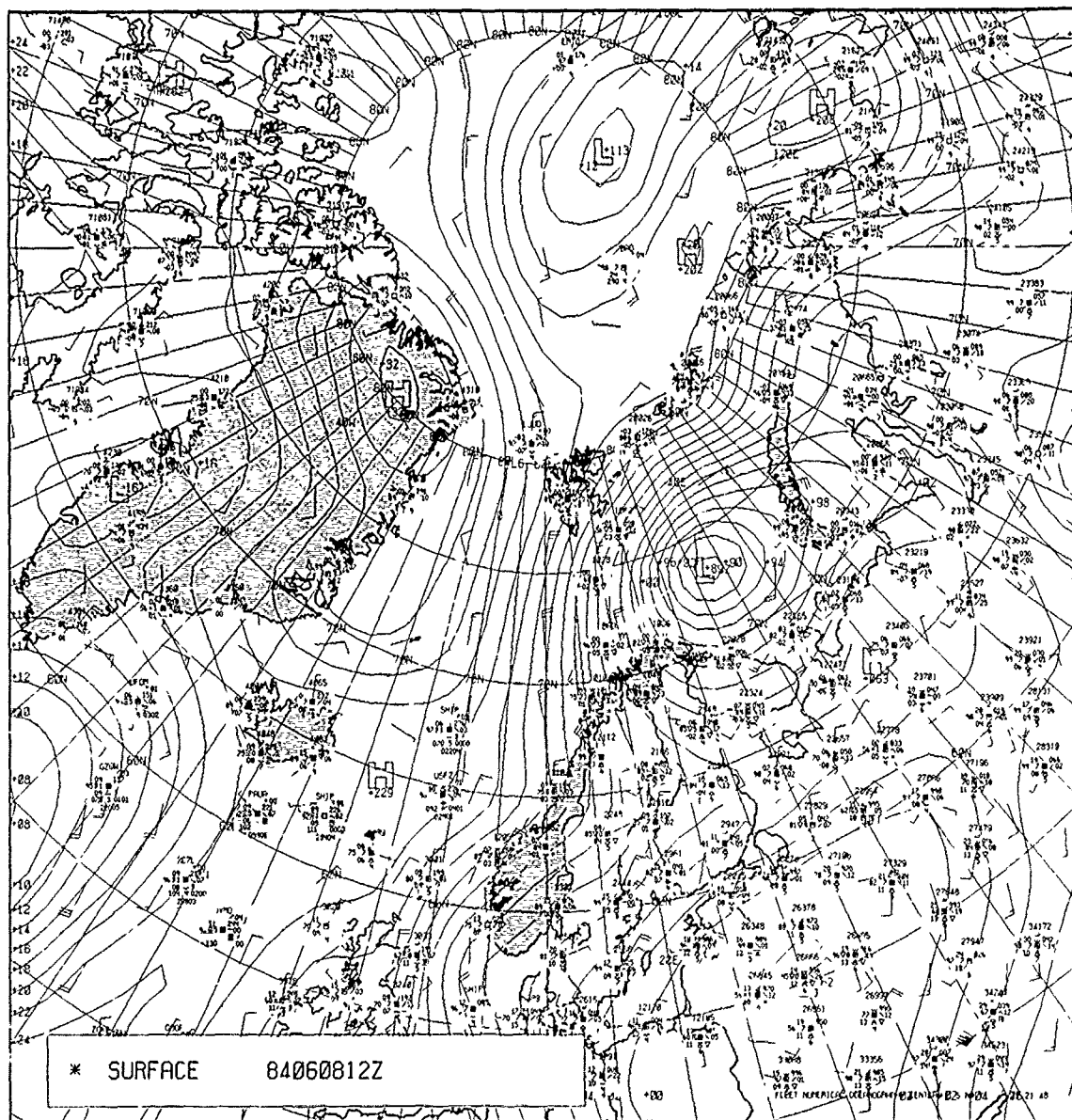




1B-19a. DMSP Visible (LS) Data. 0840 GMT 8 June 1984.

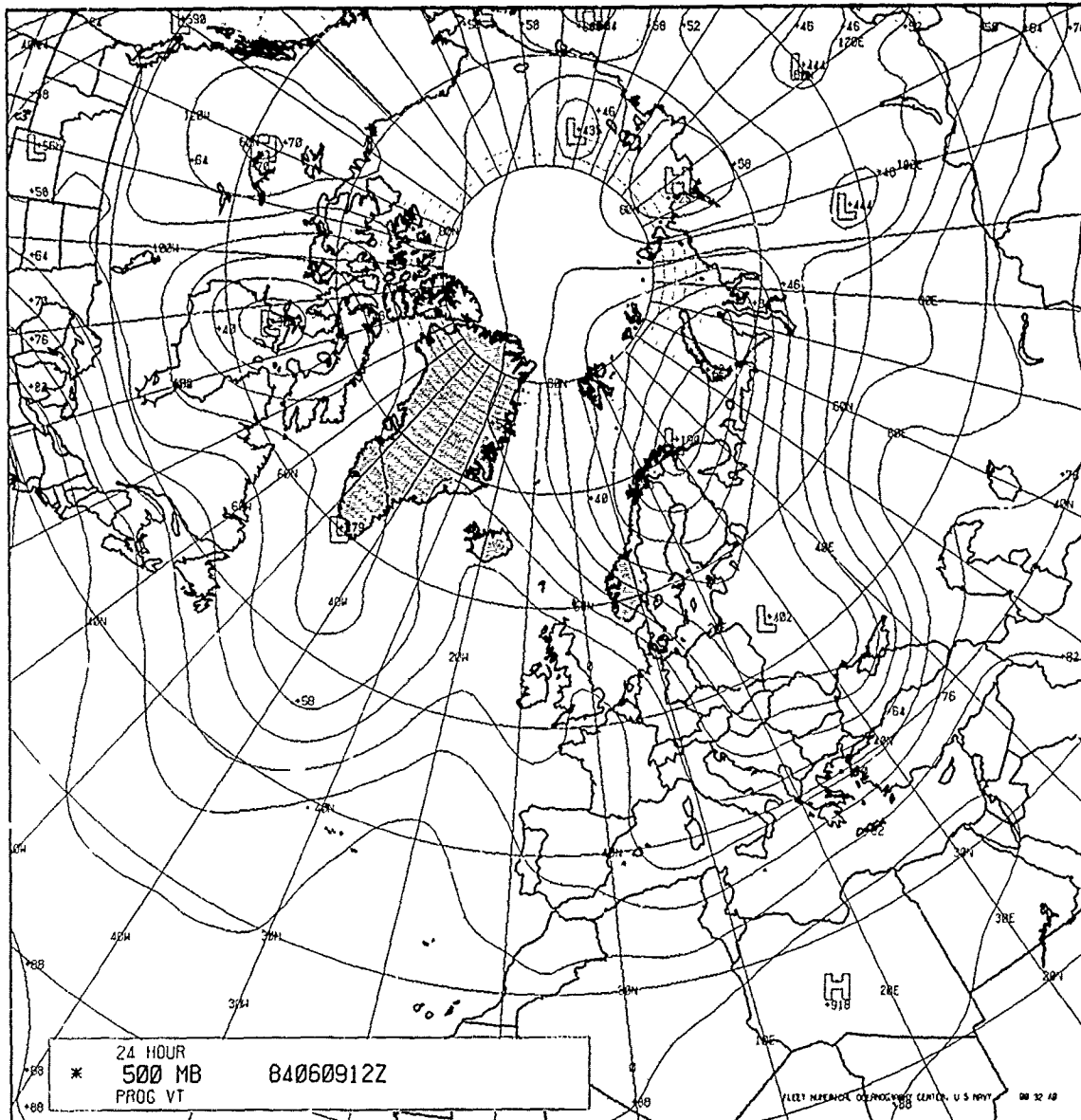


1B-20a. DMSP Visible (LS) Data and Streamline Analysis/Surface Observations (0600 GMT). 0840 GMT 8 June 1984.

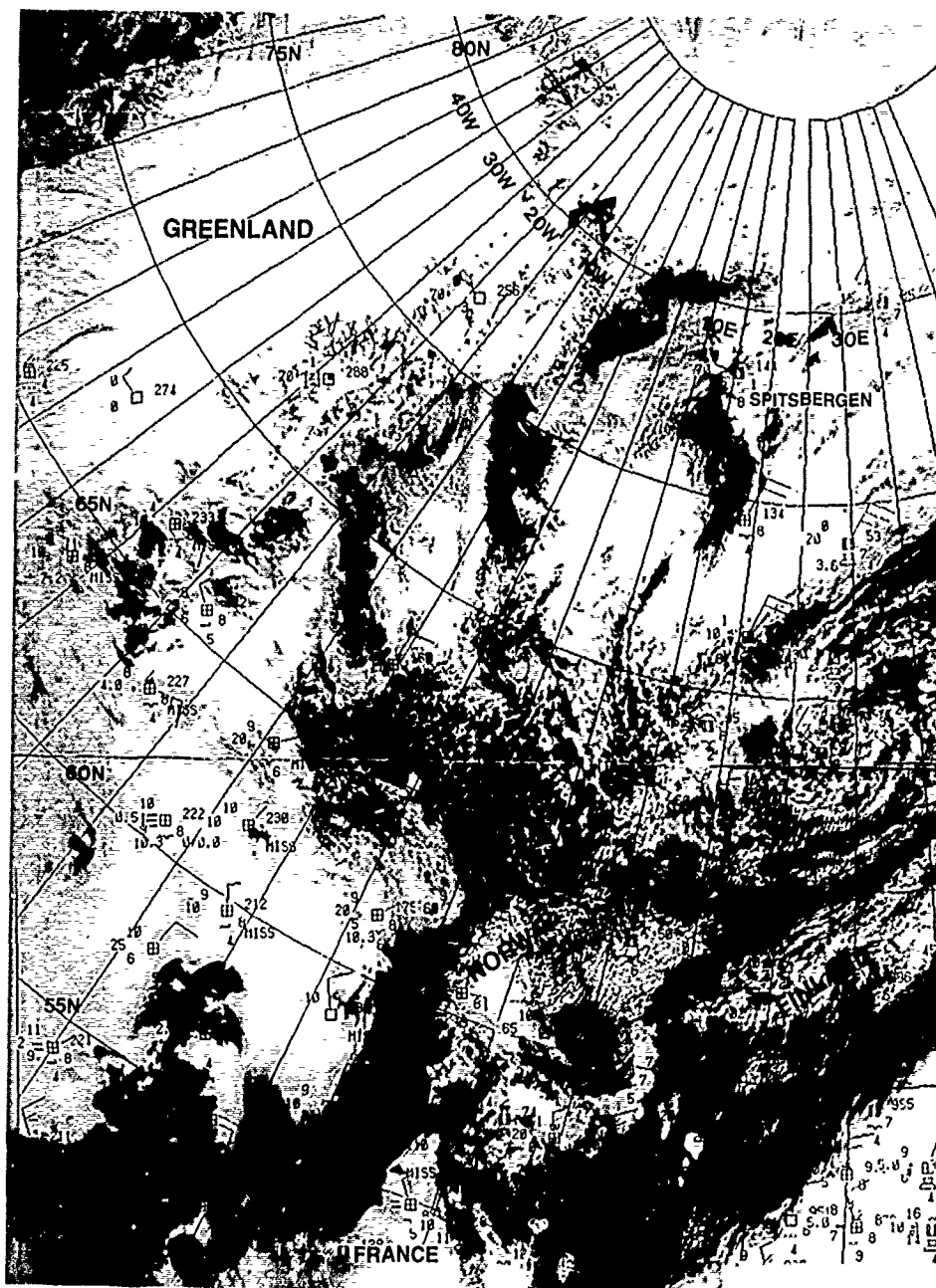


1B-21a. FNOC Surface Analysis. 1200 GMT 8 June 1984.





1B-23a. FNOC 24-hr Surface Prognosis Valid. 1200 GMT 9 June 1984.



IB-24a. DMSP Visible (LS) Data 0820 GMT 9 June 1984.

#### References

- Fett, R.W., and W.A. Bohan 1977. Navy Tactical Applications Guide, Vol. 1, *Techniques and Applications of Image Analysis*. NEPRF Technical Report 77-03, Naval Environmental Prediction Research Facility, Monterey, CA, 93943-5006, 176 pp.
- Fett, R.W., W.A. Bohan, G.A. Stevenson, J. Rosenthal, J.J. Bates, and R.J. Englebreton, 1981: Navy Tactical Applications Guide, Vol. 3, *North Atlantic and Mediterranean Weather Analysis and Forecast Applications*. NEPRF Technical Report 80-07, Naval Environmental Prediction Research Facility, Monterey, CA, 93943-5006, 200 pp.

*Case 2 Fog Formation Over the Greenland Marginal Ice Zone  
(3 April 1987 and 7, 14, and 19 June 1984)*

*Fog and Stratus Formation Over the MIZ*

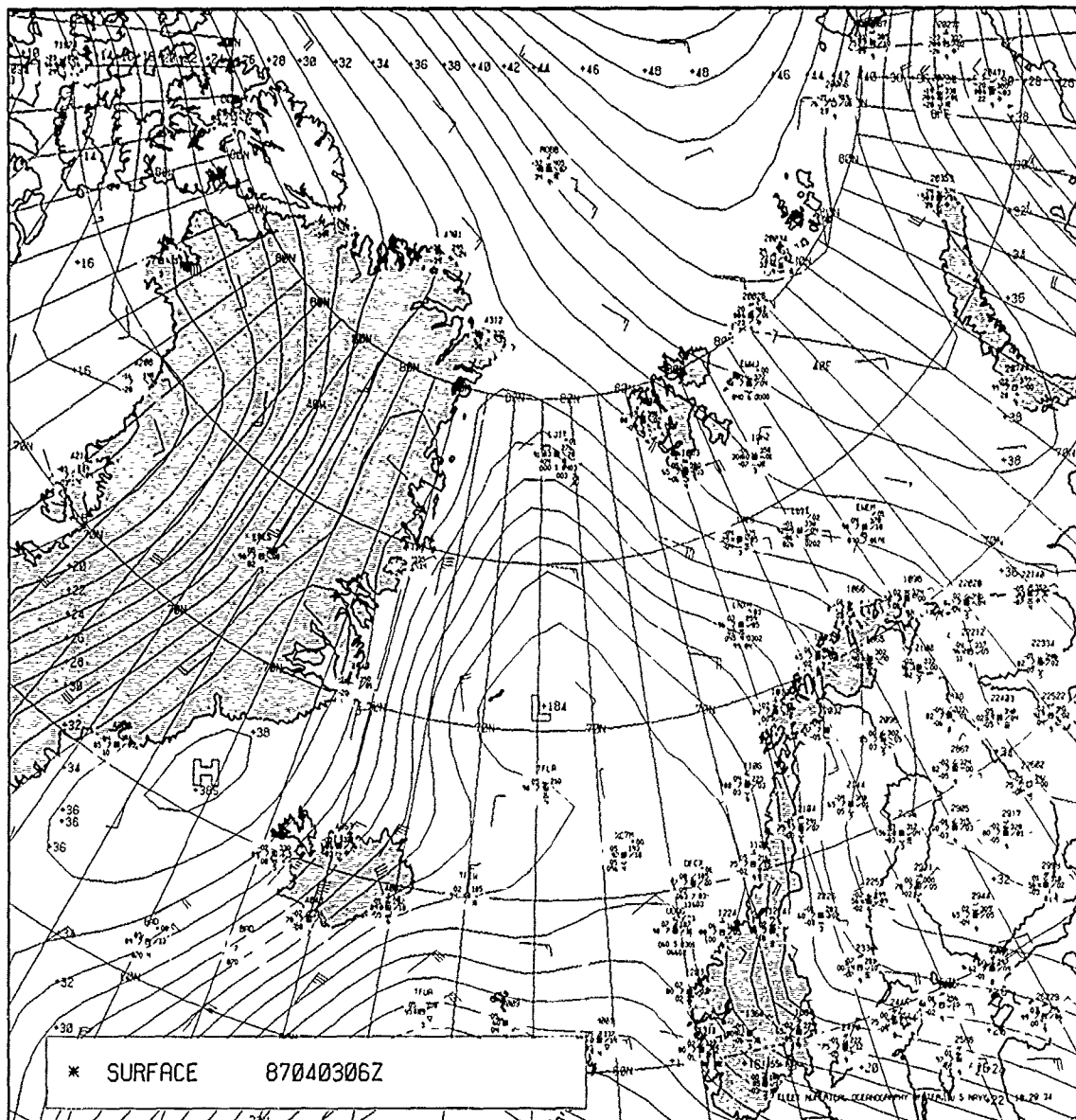
The MIZ, adjacent to the coast of Greenland is characterized by a large horizontal temperature gradient, the isotherms of which run parallel generally to the ice edge and with colder temperatures over the ice. The MIZ is a region of great variability in ice floe size and concentrations with many leads and polynyi that are continually changing in response to the effects of water current and especially wind flow. When the wind blows "on-ice" the MIZ tends to contract; "off-ice" wind conditions cause the MIZ to expand seaward. In the latter case leads enlarge and polynyi expand in size. The ice edge can be driven seaward a few hundred kilometers in just a few days. Open water within the MIZ during a June period (Guest, 1985) was measured at a consistent  $-1.7^{\circ}\text{C}$  while a wet ice surface was measured at a similarly consistent temperature of  $0.0^{\circ}\text{C}$ . Under such conditions when the wind flow is on-ice, or from the sea to the ice, fog formation is commonly observed. In the referenced paper the occurrence of fog was not only correlated with wind direction but also with wind speed. When the winds were blowing on-ice at speeds of  $>5\text{ ms}^{-1}$ , fog occurred 80% of the time. For slower on-ice wind speeds ( $<5\text{ ms}^{-1}$ ) fog was still noted, but the correlation was not as high. It was concluded that lower wind speeds were associated with lower surface humidity fluxes, and that advective cooling effects on the relatively warm, moist marine air were minimized due to the "slow movement of air parcels over the temperature gradient."

Stratus cloud formations were also noted to be less common at lower wind speeds, but quite common at higher wind speeds that cause a higher surface moisture flux, increase the depth of the mixed layer, and tend to concentrate the moisture below the turbulence-induced inversion.

The onset of the fog formation process described in the above comments occurred in what was referred to as either a "frontal" or a "stratus-lowering" fashion and is of primary interest for the purpose of this study. Other less common modes of fog production include fog that has formed as rain or drizzle, which falls from a warm layer into a cool surface layer (usually found in advance of a warm front), and fog that forms over leads or polynyi. In the latter case cold air over the leads and polynyi results in a rapid moisture flux that evaporates into the overlying air, forming a thin patch of fog.

The frontal type of fog formation described by Guest occurs when winds are blowing more or less parallel to the ice edge. The fog front evolves as the wind shifts slightly on-ice. This activity causes immediate cooling of nearly saturated air, capped by an inversion, and the rapid formation of fog. Onboard ship in the MIZ or from an on-ice location, the fog is evident as a shallow bank of clouds touching the surface and approaching the ship. Temperatures were noted to drop by as much as  $4^{\circ}\text{C}$  as the fog bank moved over the ship.

Occurring only half as frequently, given the same wind flow conditions (parallel to the ice), but with higher speeds, fog occurred as the base of a band of stratus gradually lowered until it touched the ice surface. Fog developed in this fashion often lifted to a stratus deck and then quickly lowered again, sometimes repeating the process several times. Inversions were relatively high when stratus-type fog occurrences were noted and relatively low or surface-based when frontal fog occurred.



1B-26a. FNOC Surface Analysis. 0600 GMT 3 April 1987.



This background detail is included in a satellite presentation because the frontal type of fog formation and the stratus-lowering type of fog formation, during periods of a long ice flow, are detectable in satellite visible and infrared imagery. Recognition of the nature of these features enables the satellite meteorologist to understand what is happening on a mesoscale basis and to be able to use this information for an improved synoptic analysis covering a much larger area.

### *3 April 1987*

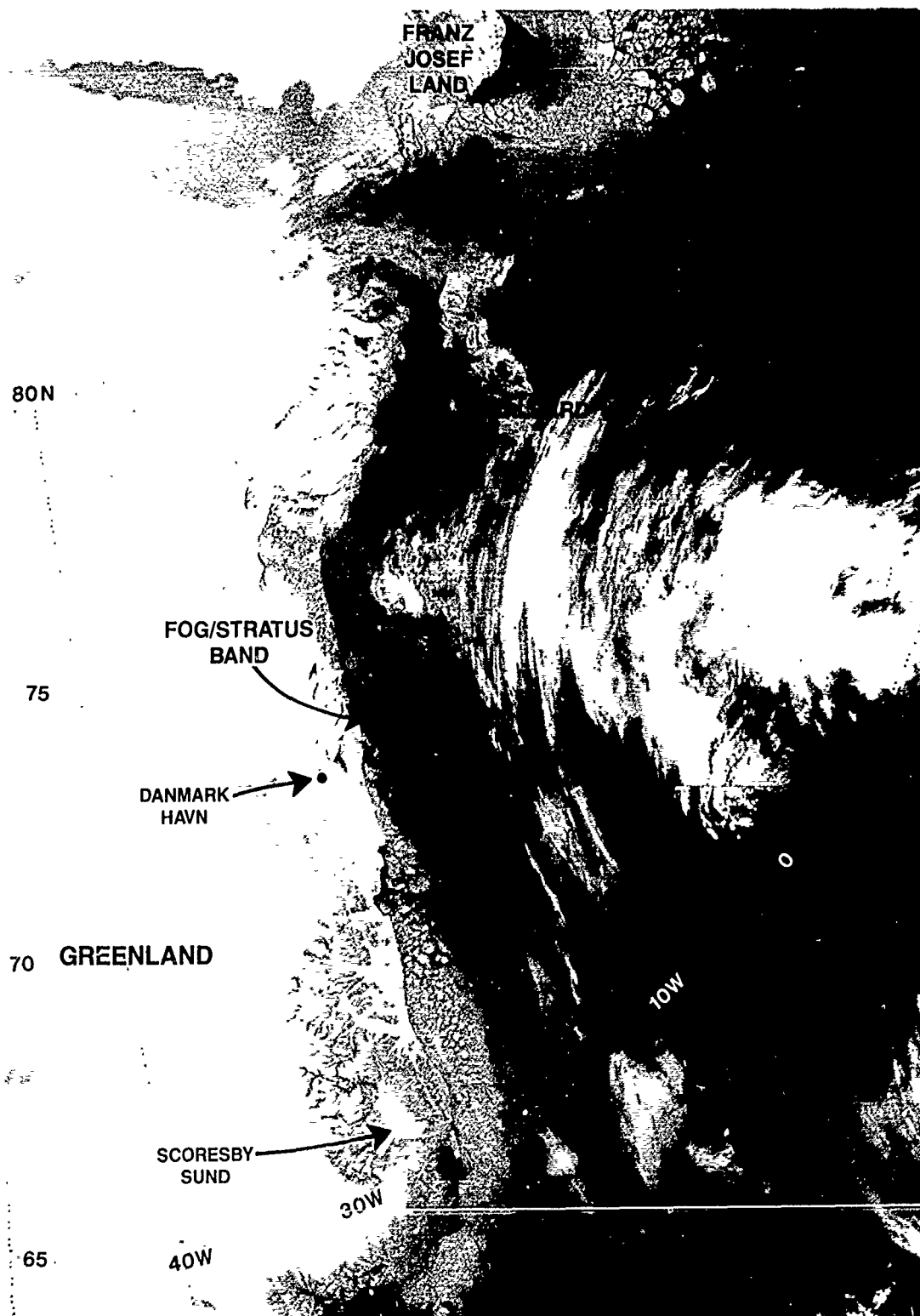
According to the introductory discussion, the potential for frontal-like fog formation along the MIZ of Greenland is high when fairly strong winds ( $> 5 \text{ ms}^{-1}$ ) flow on-ice or roughly parallel to the ice edge bringing relatively warm, moist marine air over the strong temperature gradient that exists along the ice edge. Under such conditions the air will be cooled to saturation and fog or stratus development will occur under the inversion that normally exists, so that the fog is in the cold air under warmer air aloft. Under such circumstances the top of the fog will be at a warmer temperature than the surrounding ice and the fog will appear in satellite infrared data as a warm (dark gray shade) cloud over a cooler (whiter) region.

The FNOC surface analysis at 0600 GMT on 3 April 1987 (Fig. 1B-26a) reveals a flow pattern along the east coast of Greenland conducive to bringing relatively warm, moist marine air into a position over and along the coast of Greenland. The pressure gradient over the MIZ is rather strong in this example, consequently the air parcels would be cooled rapidly in optimum fashion to produce fog.

Figure 1B-27a is a NOAA-9 infrared (Channel [Ch] 4) image that reveals a long band of fog or stratus over the Greenland MIZ stretching from  $80^\circ\text{N}$ , just west of Svalbard, southward to  $70^\circ\text{N}$ , just north of Iceland. The band appears as a dark gray shade, indicating that it is radiating at temperatures warmer than the surface over which it lies.

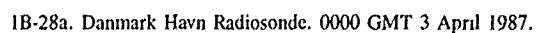
The 0000 GMT radiosonde observation (RAOB) for Danmark Havn ( $76.8^\circ\text{N}$   $18.8^\circ\text{W}$ ) (Fig. 1B-28a) shows the tremendously strong surface-based inversion that existed on this date near the cloud band. Danmark Havn is on the coast of Greenland, west of the fog or stratus band. Inasmuch as the station elevation is only 11 m this sounding should be representative of that near the band, not reflecting, of course, the moisture of the "band" itself. (Note that the image is poorly gridded; however, Danmark Havn is shown in the correct location.) The top of a fog or stratus bank only a few hundred meters thick would radiate at a much warmer temperature than that of the surface under such conditions.

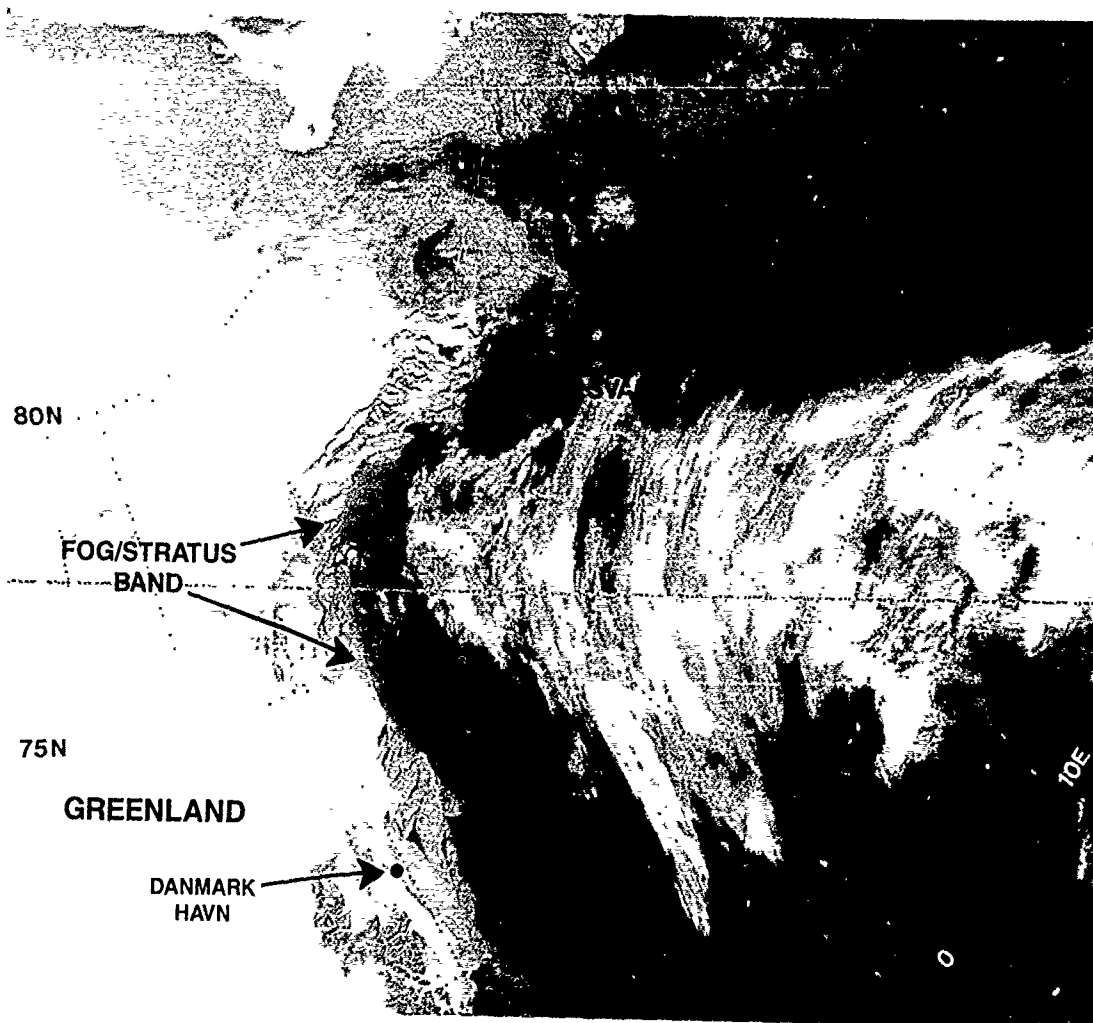
The fog or stratus band was again observed at 1044 GMT by NOAA-10 (Fig. 1B-29a) in another infrared (Ch 4) view. By 1114 GMT just enough daylight was present to observe the band in NOAA-9 visible (Ch 2) imagery (Fig. 1B-30a). An overlay to this image (Fig. 1B-31a) shows the outline of the band. Note that leads in the ice can be seen through the cloud band, indicative of its thin and transparent nature.



1B-27a. NOAA-9 Infrared (Ch 4) Image. 0616 GMT 3 April 1987.

## 4320

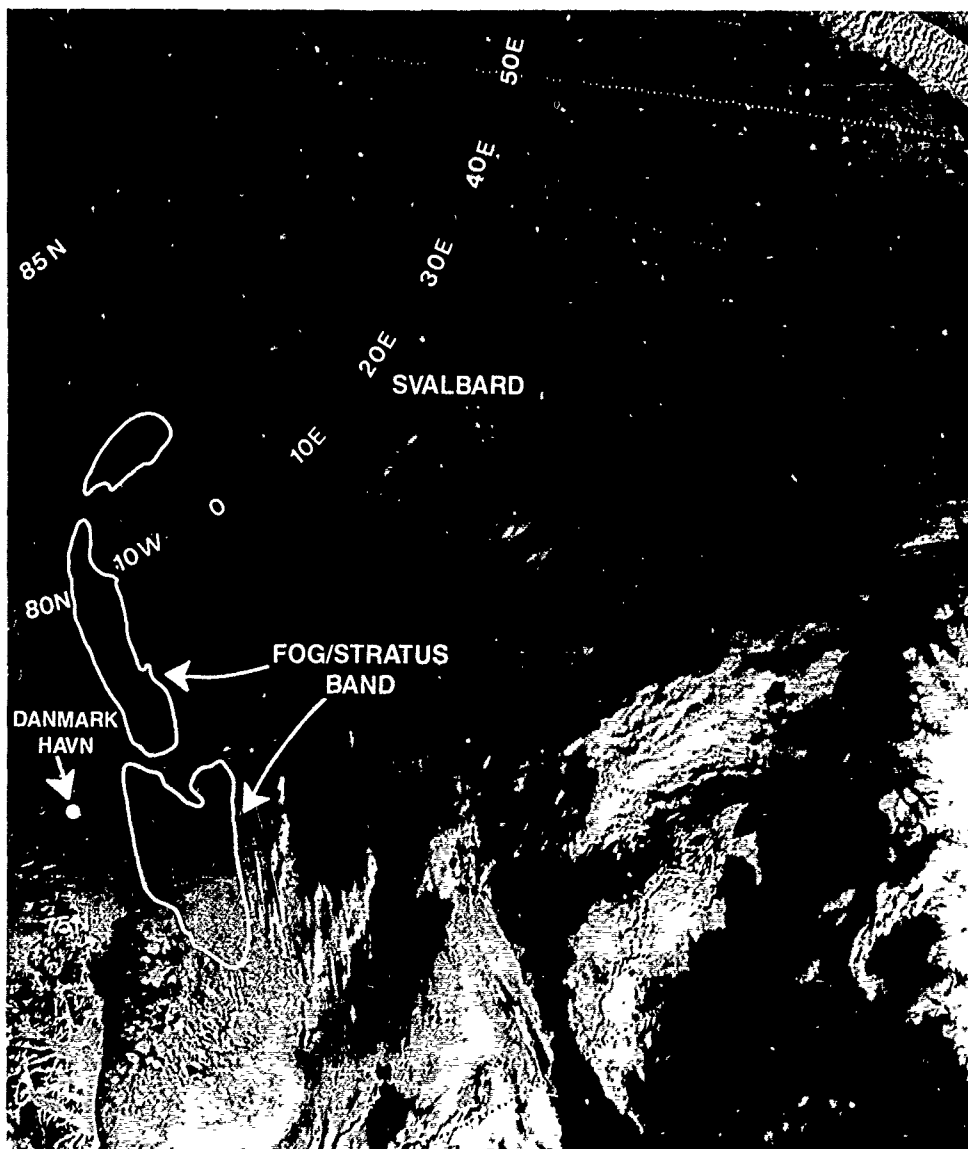




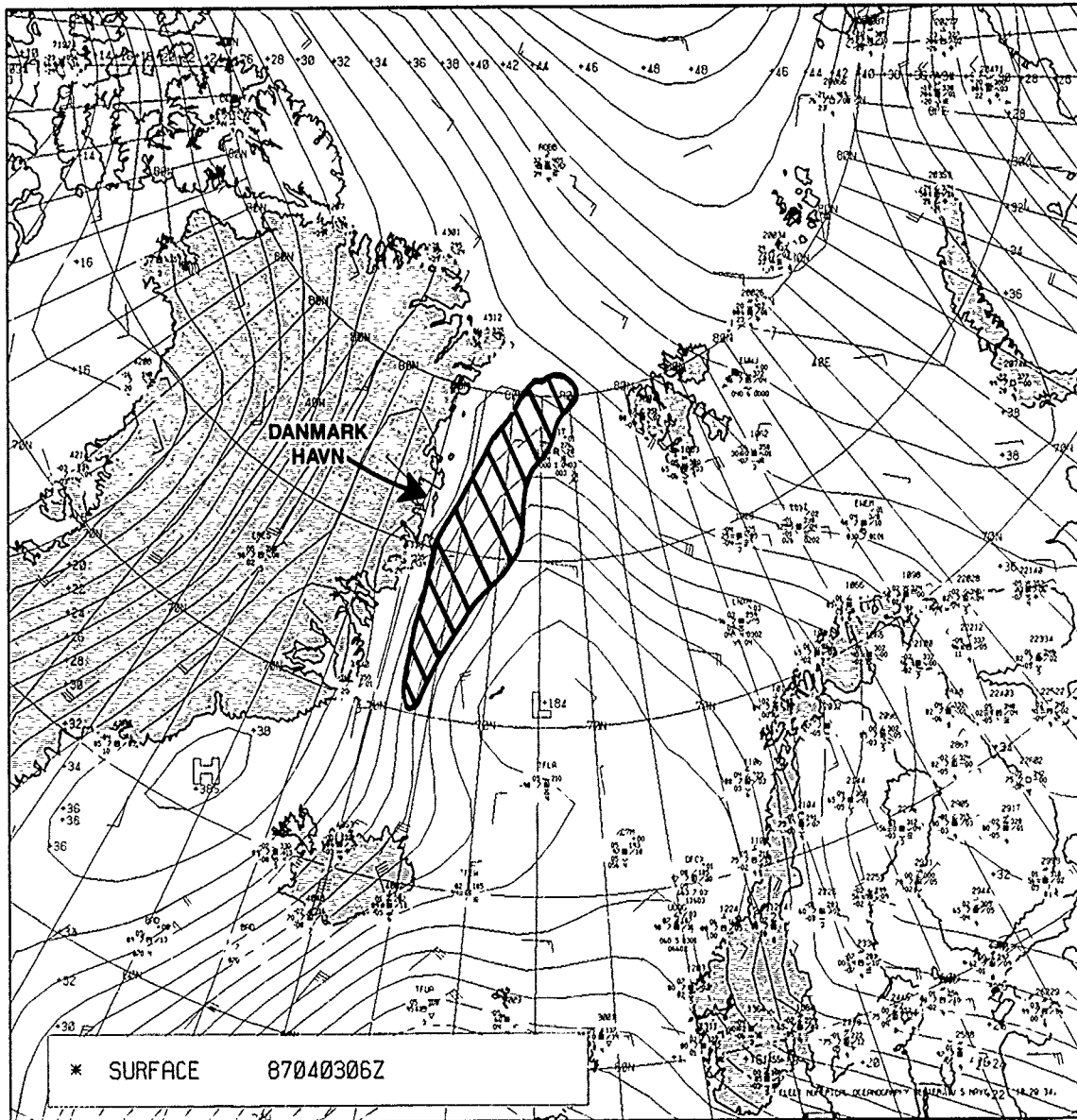
1B-29a NOAA-10 Infrared (Ch 4) Image. 1044 GMT 3 April 1987.



1B-30a. NOAA-9 Visible (Ch 2) Image. 1114 GMT 3 April 1987



1B-31a. NOAA-9 Visible (Ch 2) Image With Cloud Outline. 1114 GMT 3 April 1987.



IB-32a. FNOC Surface Analysis With Cloud Outline. 0600 GMT 3 April 1987.

The location of the band is superimposed on the surface analysis (Fig. 1B-32a) to facilitate comparisons. Unfortunately surface weather observations are not available under the band itself. Note that this fog or stratus band is restricted to the MIZ and does not extend further westward toward or over the coast of Greenland. Examples, which follow, show colder bands paralleling Greenland's coast that overlie part of the coastal terrain. Such bands are not surface based but overlie warmer, drier air in which the surface visibility is excellent.

*7 June 1984*

DMSP infrared data acquired at 1042 GMT (Fig. 1B-33a) show a midlevel cloud formation apparently "banked-up" along the coastal area of northeast Greenland, overlying Danmark Havn (76.8°N 18.8°W). A gridded version of Fig. 1B-33a with surface observations superimposed is shown in Fig. 1B-34a. It can be seen from this latter figure that Danmark Havn is reporting some low stratus and a deck of mixed altocumulus/altostratus; however, low-level visibility is excellent—better than 70 miles.

Simultaneous DMSP visible data (Fig. 1B-35a) reveal the cloud formation with the western edge pressing up against higher terrain. Note that the area north of the cloud over the MIZ is clear and that individual ice floes within the MIZ are resolved. This area shows as a warmer area in Fig. 1B-33a, the infrared view. Note that in this case the cloud tops are colder than the surrounding surface temperature of the MIZ and coastal Greenland.

Figure 1B-36a is the FNOC surface analysis for 1200 GMT with the outline of the cloud formation superimposed. Flow is onshore at this level and also at the 850-mb level (Fig. 1B-37a). This flow pattern permits the introduction of moist marine air over the MIZ and coastal Greenland. Resulting fog or stratus formation may occur initially, as in the first example, where the cloud top is warmer than the underlying surface. Radiation loss from the top of the fog or stratus, however, may eventually cause the cloud to become cooler than the underlying surface so that instability develops. In this case overturning would result in an increase in depth of the mixed layer and a lifting of the fog or stratus as it moved toward the Greenland coast.

The Danmark Havn 1200 GMT RAOB (Fig. 1B-38a) shows a moist region of air between 850- and 700-mb, where the cloud would most likely be located. The layer is essentially isothermal with a mean temperature of about  $-9^{\circ}\text{C}$ , whereas the surface temperature is a warmer  $-2^{\circ}\text{C}$ . The lapse rate is adiabatic below 980 mb indicating a well-mixed layer, consistent with the excellent reported visibility of  $> 70$  miles. The stratus is capped by a subsidence inversion near 650 mb.

The conclusion to be drawn from this example is that similar-appearing cloud formations indicate altostratus/altocumulus cloud formation due to on-ice flow from the surface to 850 mb. Lower levels are unstable due to colder air overlying warmer air, and low-level visibility is excellent. The fog or stratus, once formed, tends to maintain itself (assuming no higher overlying clouds are present) due to the effects of long-wave radiative cooling and reflection of short-wave radiation. The effects of radiation maintain the overturning process, resulting in the collection of moisture under the inversion.

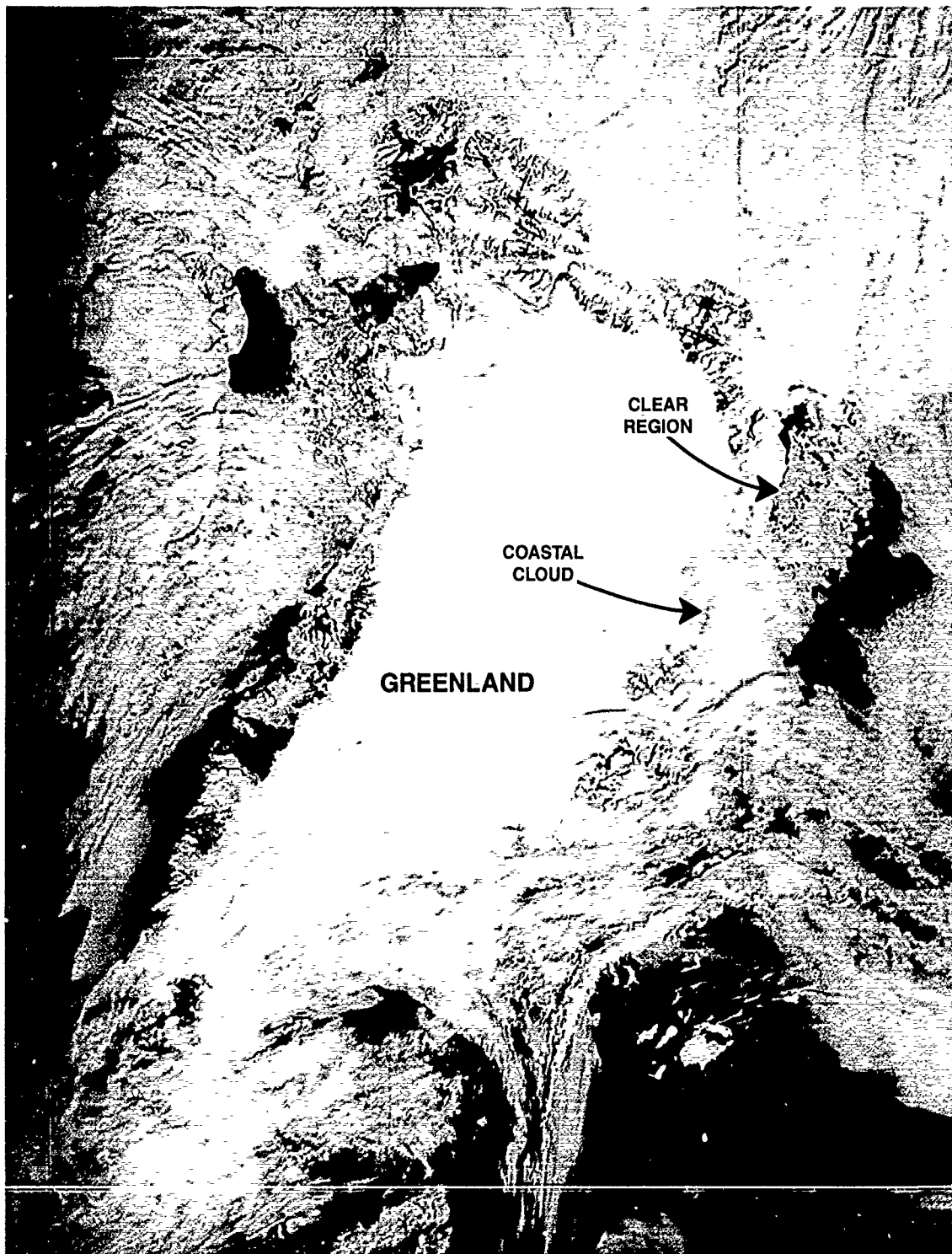




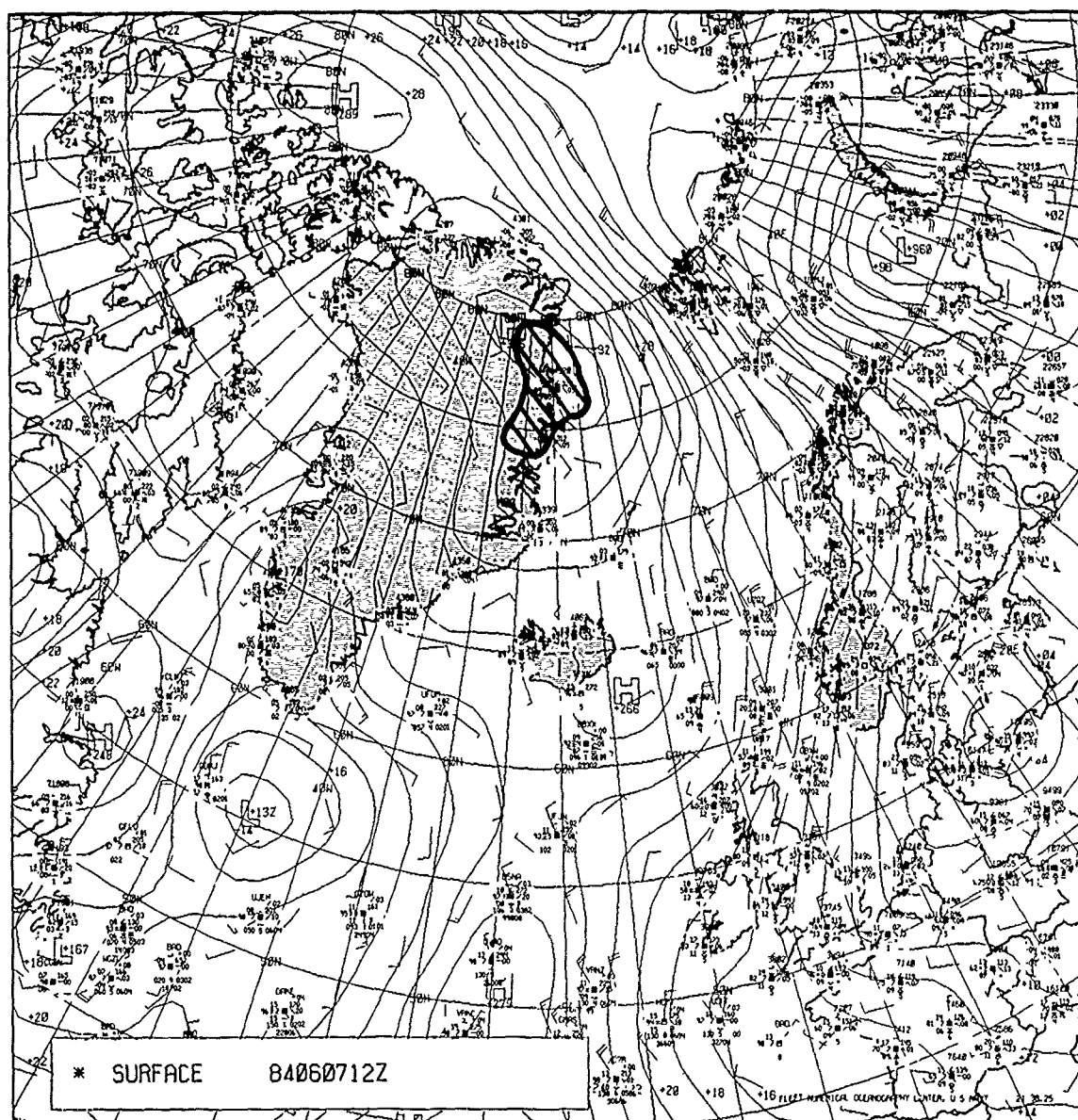
1B-33a. DMSP Infrared (TS) Data. 1042 GMT 7 June 1984.



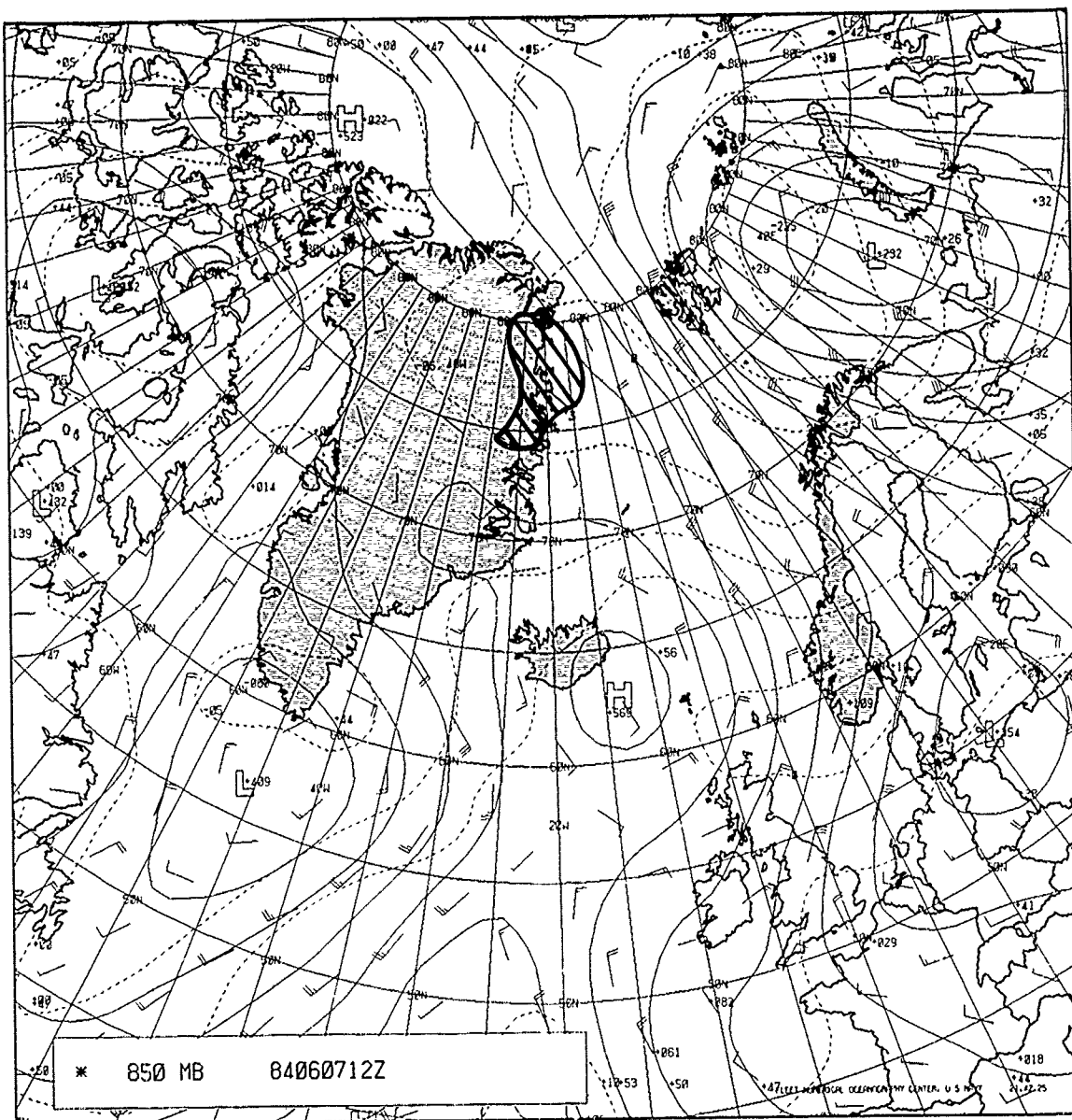
IB-34a. DMSP Infrared (TS) Data and Surface Observations (1200 GMT). 1042 GMT 7 June 1984.



1B-35a. DMSP Visible (LS) Data. 1042 GMT 7 June 1984.



1B-36a. FNOG Surface Analysis With Cloud Outline. 1200 GMT 7 June 1984.



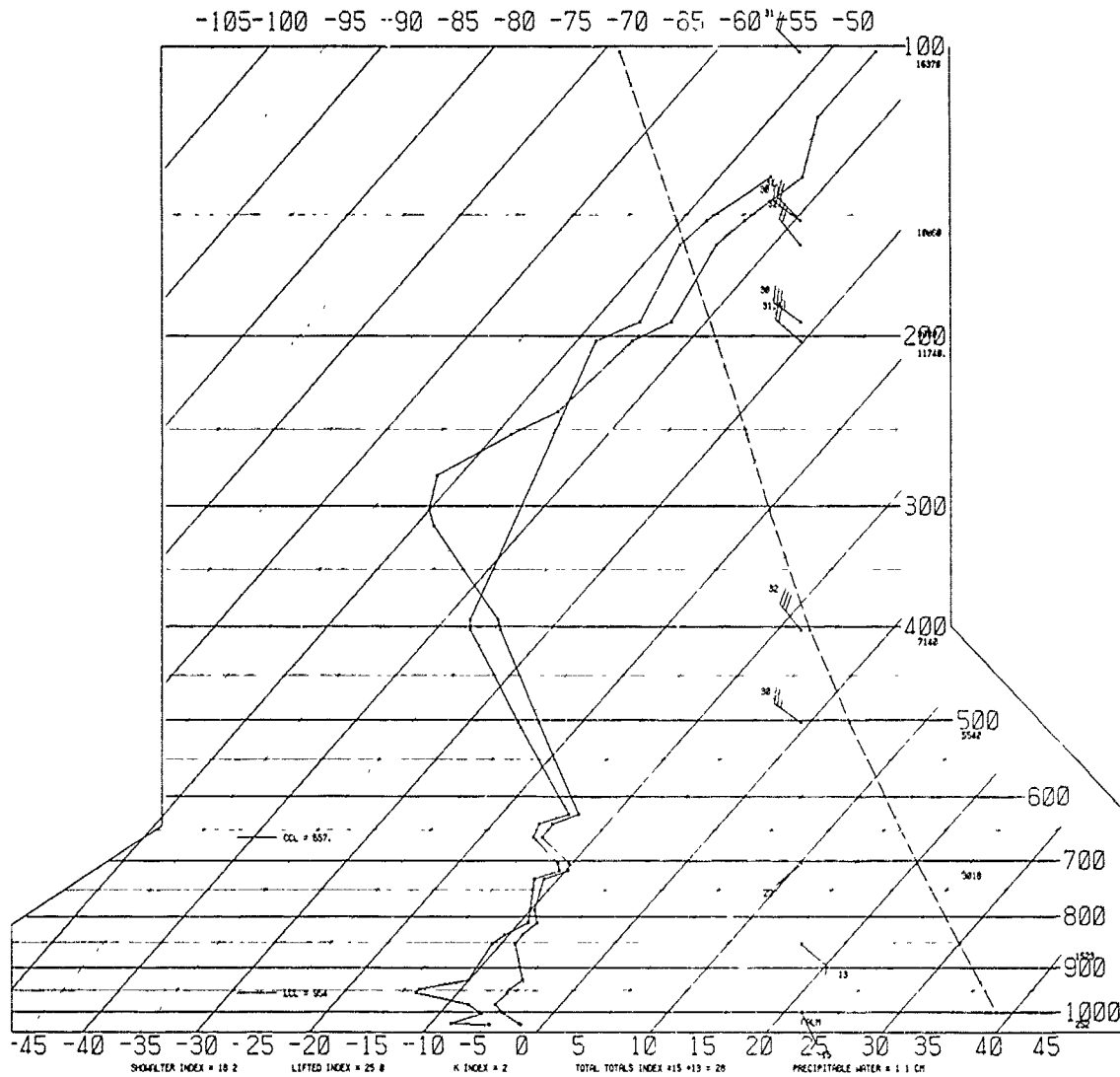
1B-37a. FNOG 850-mb Analysis. 1200 GMT 7 June 1984

# SKEW T, LOG P DIAGRAM

840607

1200Z

4320



IB-38a. Danmark Havn Radiosonde 1200 GMT 7 June 1984.

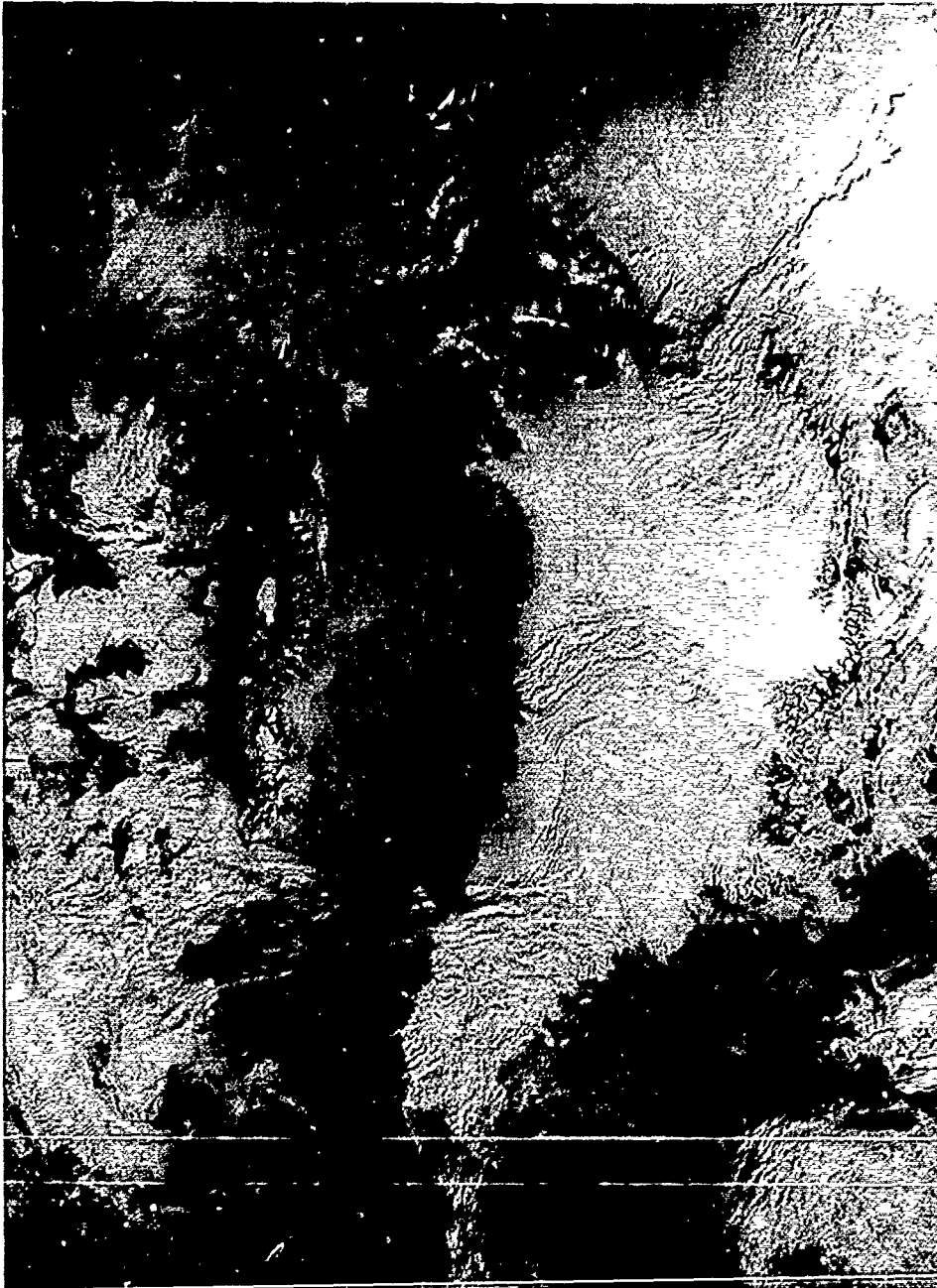
14 June 1984

DMSP infrared data on this date at 1002 GMT (Fig. 1B-39a) reveal another Greenland coastal cloud band oriented parallel to the terrain and apparently "banked-up" against the higher elevations. The cloud band is colder than the underlying land features, and according to the preceding example, and as foreseen, the underlying stations should report altostratus/altocumulus aloft, excellent low-level visibility, and adiabatic or well-mixed sounding with no strong low-level inversion.



1B-39a. DMSP Infrared (TS) Data. 1002 GMT 14 June 1984.

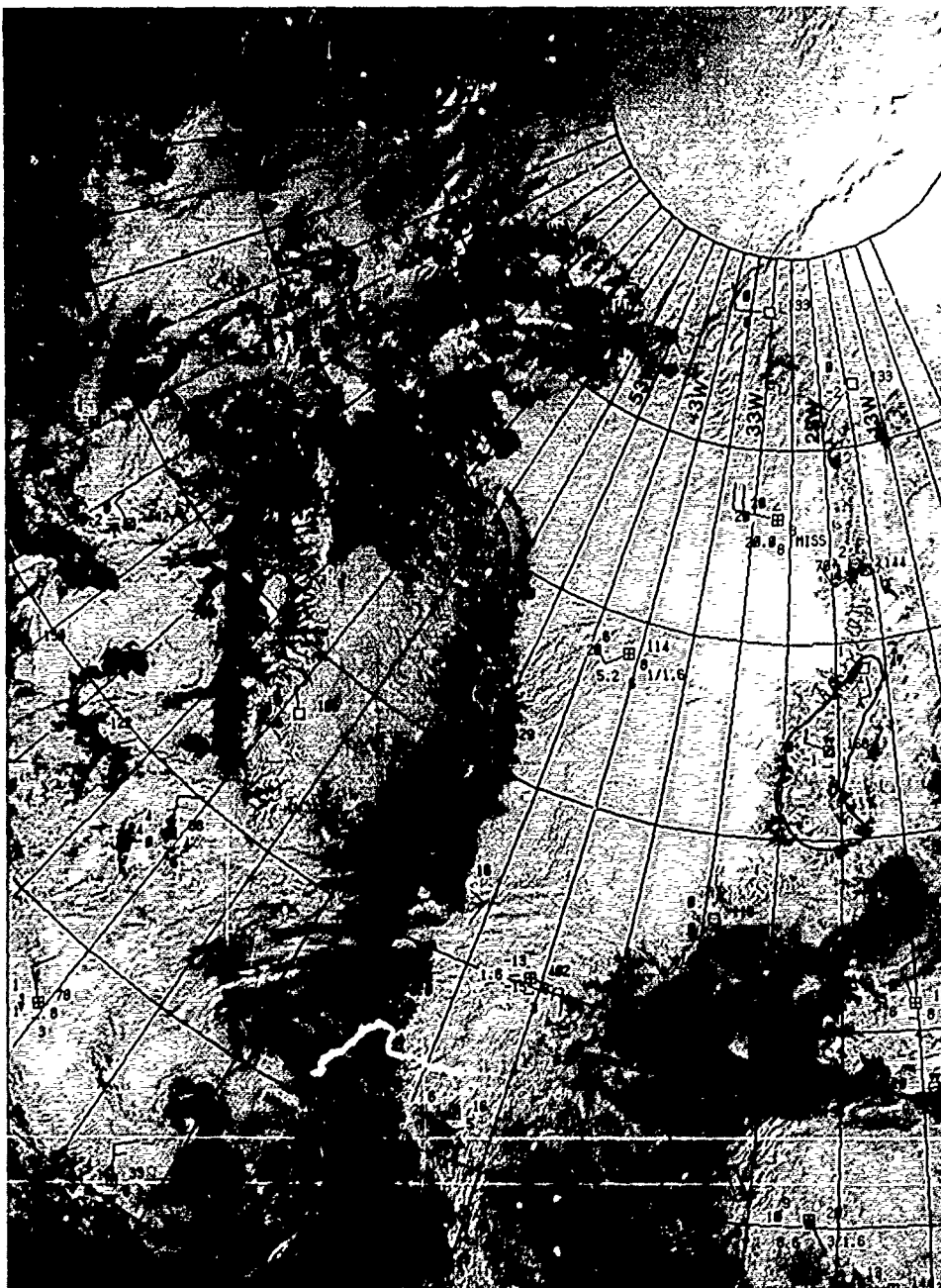
Visible DMSP data a few hours later (1412 GMT) (Fig. 1B-40a) reveal a transparent cloud formation over the region of the band, with terrain features visible through the cloud.

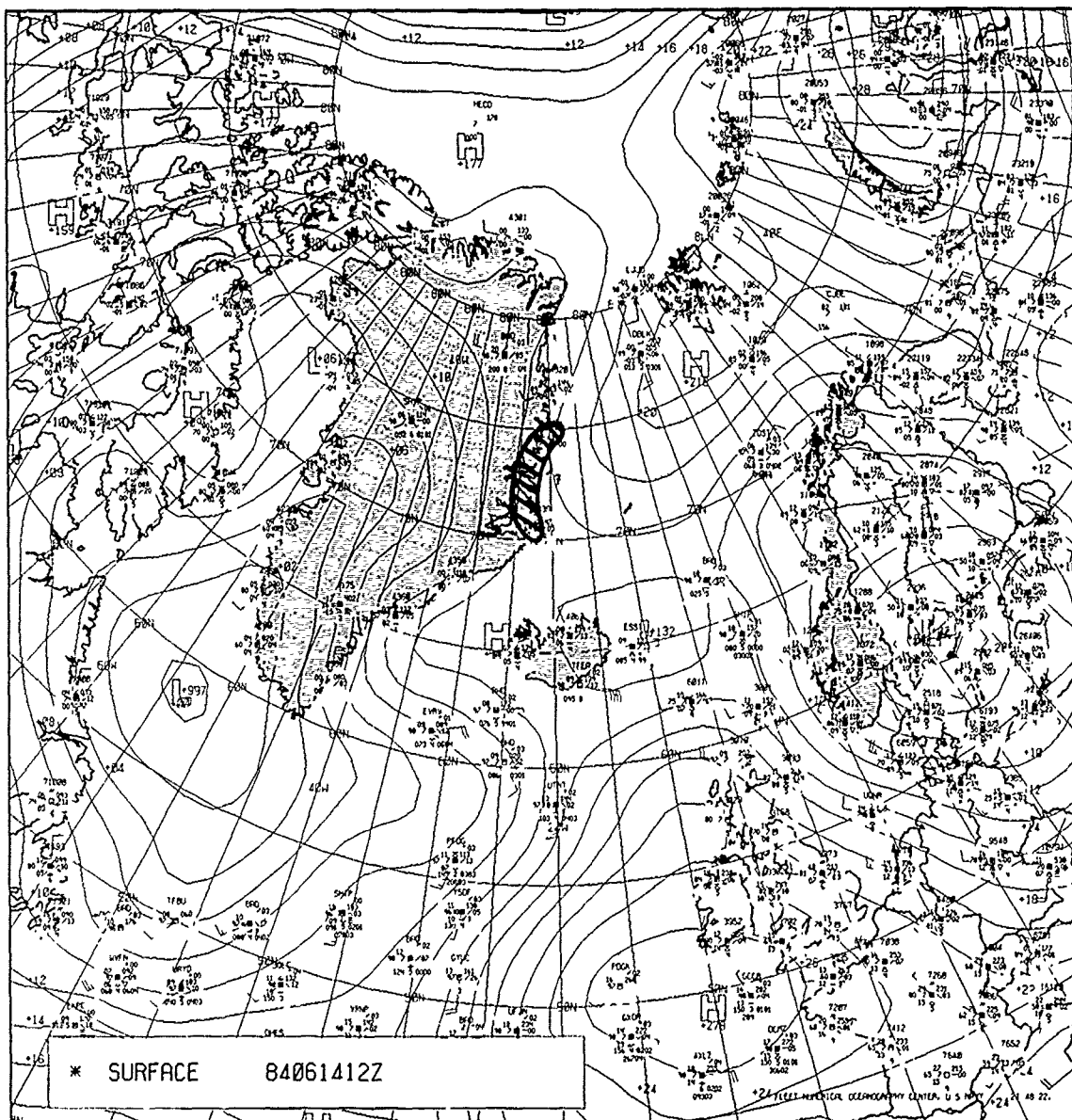


1B-40a. DMSP Visible (LS) Data. 1412 GMT 14 June 1984.



100





1B-42a. FNOG Surface Analysis With Cloud Outline. 1200 GMT 14 June 1984.

The FNOC surface analysis for 1200 GMT with the cloud band outline superimposed (Fig. 1B-42a) reveals that the band is over the coastline of Greenland in a region of onshore surface flow.

Flow at the 850-mb level (Fig. 1B-43a) is somewhat ambiguous over the area but could be onshore.

Unfortunately there are no soundings available in the region of this band to examine the lapse rate structure.

*19 June 1984*

A final case of a Greenland coastal cloud band is shown in Fig. 1B-44a, a DMSP infrared image acquired at 1144 GMT. This band also appears banked-up against the terrain of northeast Greenland, and lies parallel to the coastline.

A grid of the image with surface observations superimposed (Fig. 1B-45a) shows that Danmark Havn is under the band and is reporting broken conditions of altocumulus aloft and surface visibility of >50 miles.

Visible data are not available for this example. Both the surface analysis (Fig. 1B-46a) and the 850-mb analysis (Fig. 1B-47a) reveal the expected conditions of onshore flow.

The Danmark Havn RAOB for this example (Fig. 1B-48a) is classic in revealing the cloud layer between 800- and 850-mb, capped by an inversion, and with a temperature much colder than the surface temperature.

#### Important Conclusions

1. Two types of coastal cloud bands detectable in satellite imagery tend to parallel the coast. The first is a cloud band (type 1) consisting of thin fog or stratus that tends to form over the MIZ under a surface-based inversion during periods of on-ice flow. Leads and polynya can normally be seen through this band in satellite visible imagery because of its thin, transparent nature. The cloud appears as a warm band over the colder MIZ in satellite infrared data. Low-level visibilities in or under such a band are often restricted. A second coastal cloud band (type 2) is quite different in quality. It develops as a result of on-ice flow in the surface through 850-mb level. The cloud band consists of higher level altocumulus or altostratus and in satellite infrared data appears colder than the underlying MIZ. The cloud extends further inland than the type 1 cloud band, frequently banking up against higher coastal terrain. Visibilities under this band are excellent because of an unstable, dry, low-level condition resulting in a deep, well-mixed layer below the cloud base.
2. The rationale to explain the occurrence of type 1 as opposed to type 2 of the Greenland coastal cloud band appears to be linked to a more pervasive intrusion of moist marine air in type 2 occurrences. In fact, type 2 may occur initially as type 1 and then undergo modification as further onshore movement over time takes place, permitting an evolution in nature due to the effects of radiational cooling and resulting instabilities.

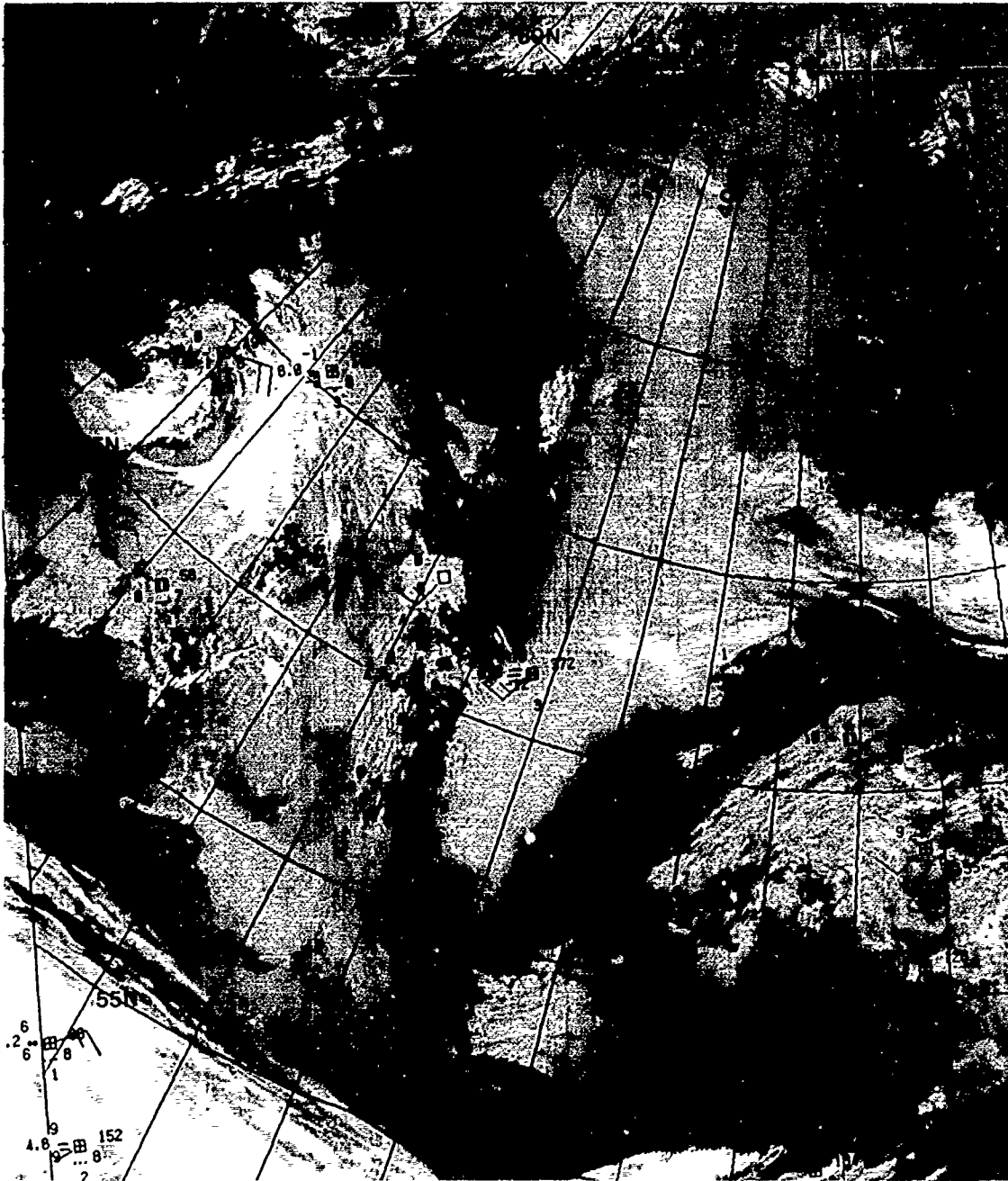
#### Reference

Guest, P., 1985. Forecasting Fog in Marginal Ice Zones (unpublished manuscript). Naval Postgraduate School, Monterey, CA.

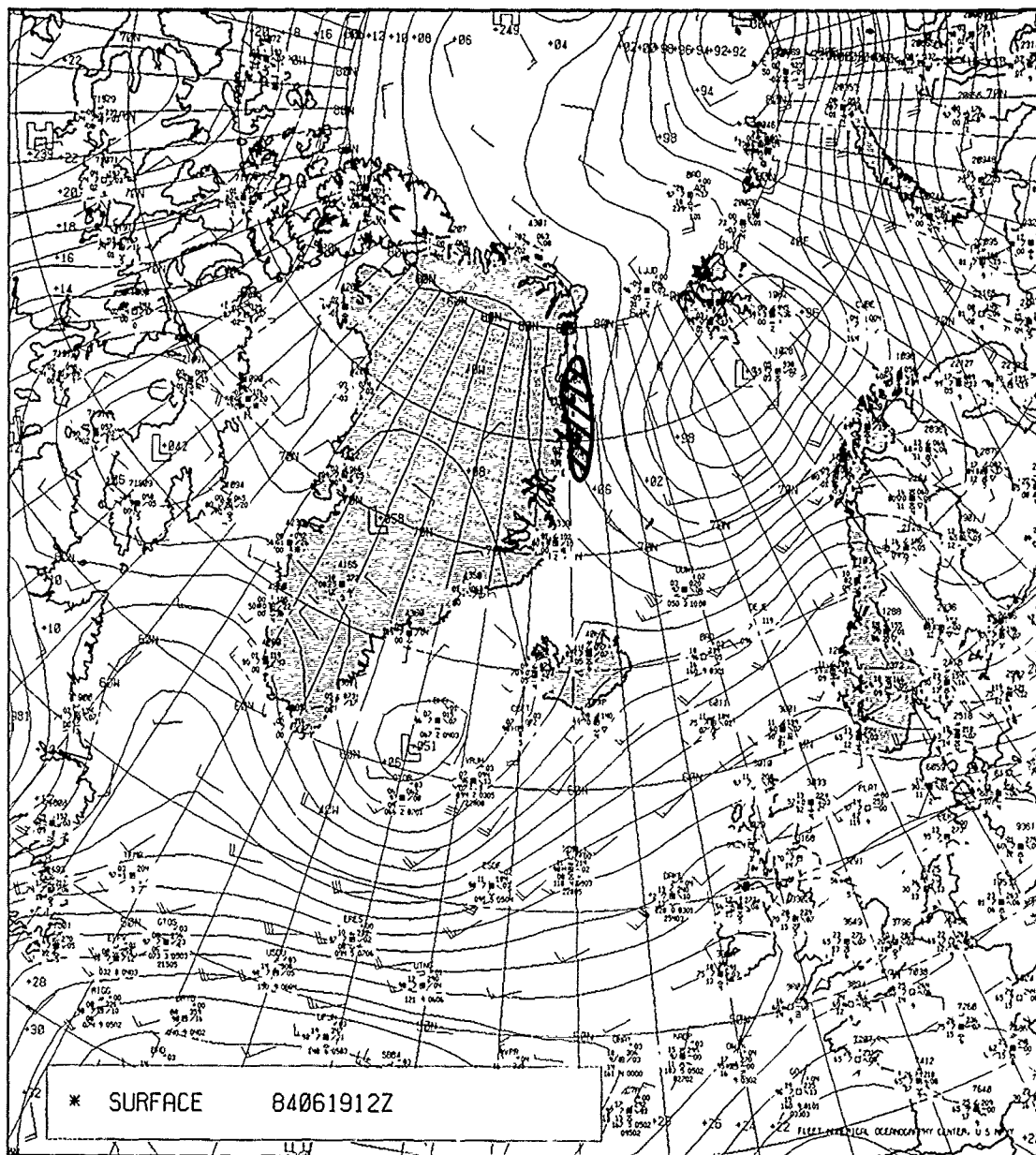




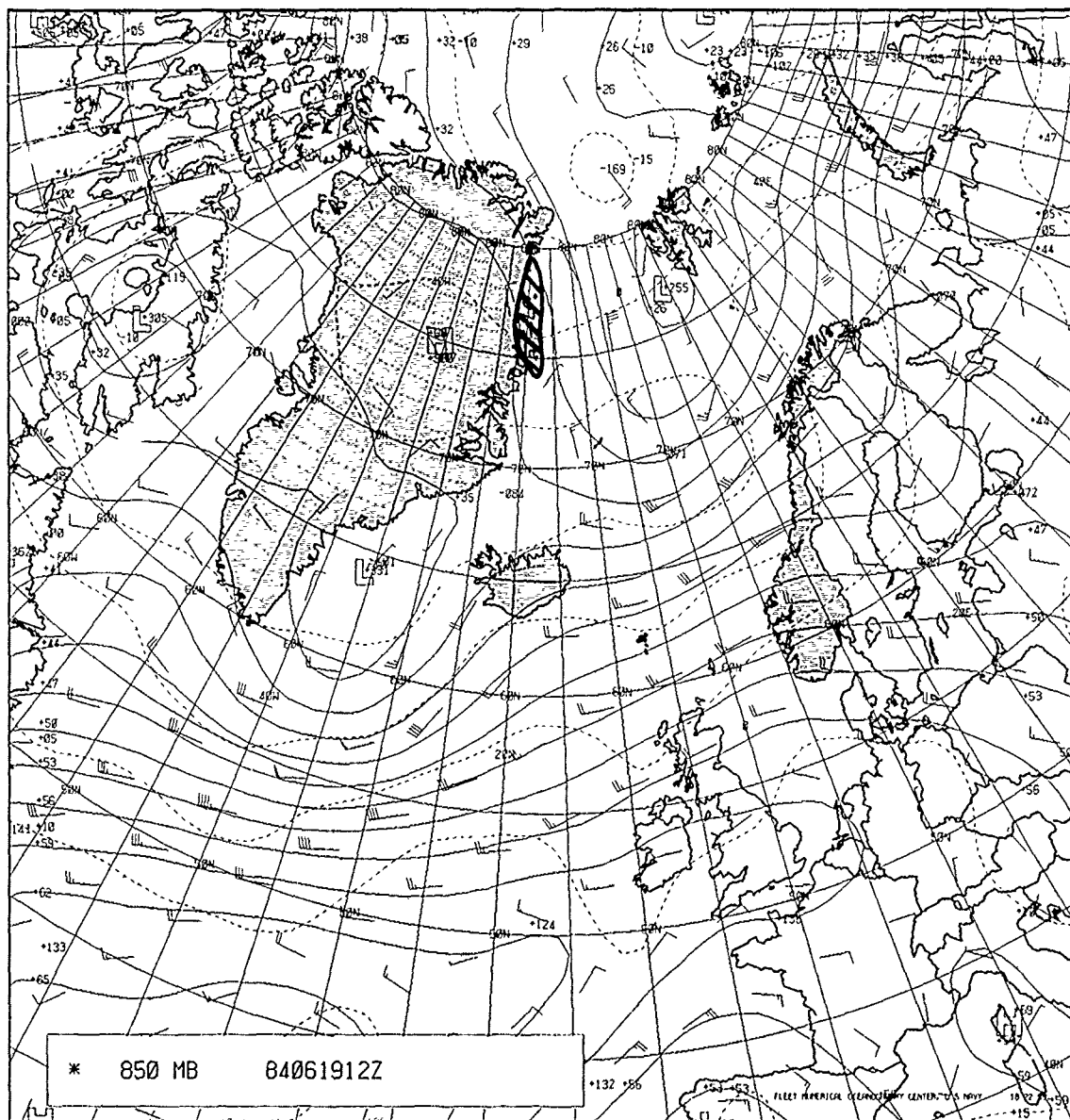
1B-44a. DMSP Infrared (TS) Data. 1144 GMT 19 June 1984.



1B-45a. DMSP Infrared (TS) Data and Surface Observations (1200 GMT). 1144 GMT 19 June 1984.



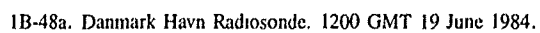
1B-46a. FNOC Surface Analysis. 1200 GMT 19 June 1984.



IB-47a. FNOC 850-mb Analysis. 1200 GMT 19 June 1984.



## 4320



## *1C Sunlint*

### *Sunlint Analysis in the Arctic*

During the summer months sunlint effects, as sensed by polar-orbiting satellites, extend into arctic latitudes. All of the techniques used in sunlint analysis for locating calm sea regions, indicative of high pressure centers or ridge lines, and island barrier effects, useful in determining low-level wind direction, apply, and are useful in arctic satellite analysis.



IC-2a. DMSP Visible (LS) Data. 0625 GMT 7 July 1984.

## *Case 1 Detection of Ridge Lines in the Greenland/North Seas*

### *Sunglint Analysis in the Arctic*

Ridge line detection through use of sunglint patterns over ocean areas in satellite visible imagery has been well documented (see Fett and Bohan, 1977). It is always reassuring, however, to see this capability demonstrated in more unfamiliar areas such as the waters of the Arctic.

*7 July 1984*

Figure 1C-2a is a 0625 GMT DMSP visible (LS) view of Greenland to the north and the United Kingdom to the southeast.

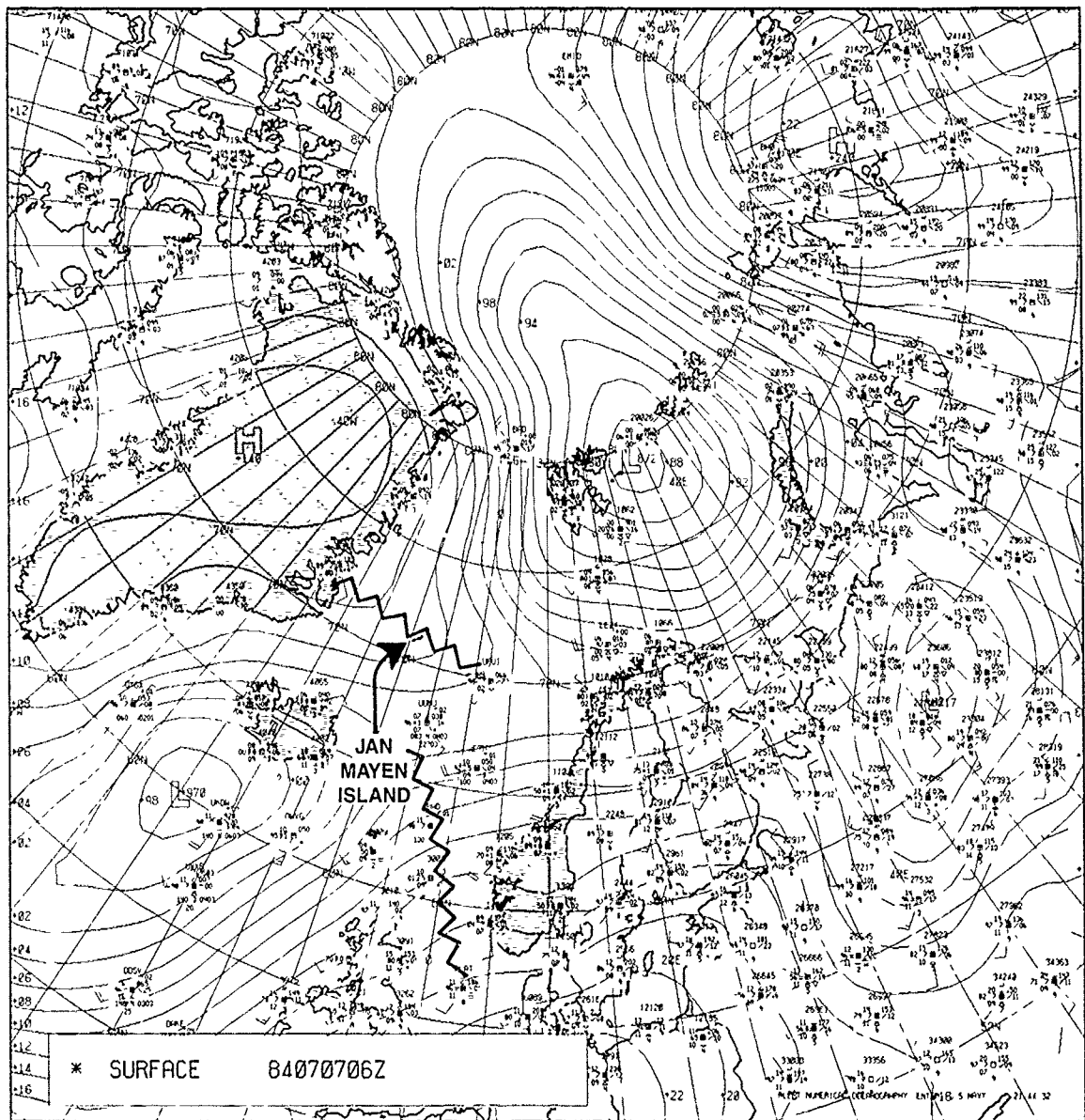
Sunglint affects the eastern portion of this image and has brilliantly illuminated the North Sea and a clear area south of a cloud band east of Scoresby Sund. A dark notch extends into the Scoresby Sund sunglint region. Accordingly, a ridge line should be anticipated through both areas.

Figure 1C-3a is an FNOG surface analysis for 0600 GMT on this date, which in general verifies the ridge line locations. However, a more accurate positioning of the ridge line in the Greenland Sea can be gleaned from a gridded version of the satellite data (Fig. 1C-3b), which shows the ridge line south of 70°N rather than 3° further north, as shown on the surface analysis (Fig. 1C-3a).

The cloud band north of the ridge line can be analyzed as an arctic front separating air that has flowed from off the ice cap and down the MIZ of Greenland from an air mass south of 70°N, which is under the influence of southern flow over the North Atlantic Current waters.

### **Reference**

Fett, R W , and W.A. Bohan, 1977: Navy Tactical Applications Guide, Vol. 1, *Techniques and Applications of Image Analysis*. NEPRF Technical Report 77-03, Naval Environmental Prediction Research Facility, Monterey, CA, 93943-5006, 176 pp



IC-3a. FNOC Surface Analysis. 0600 GMT 7 July 1984.

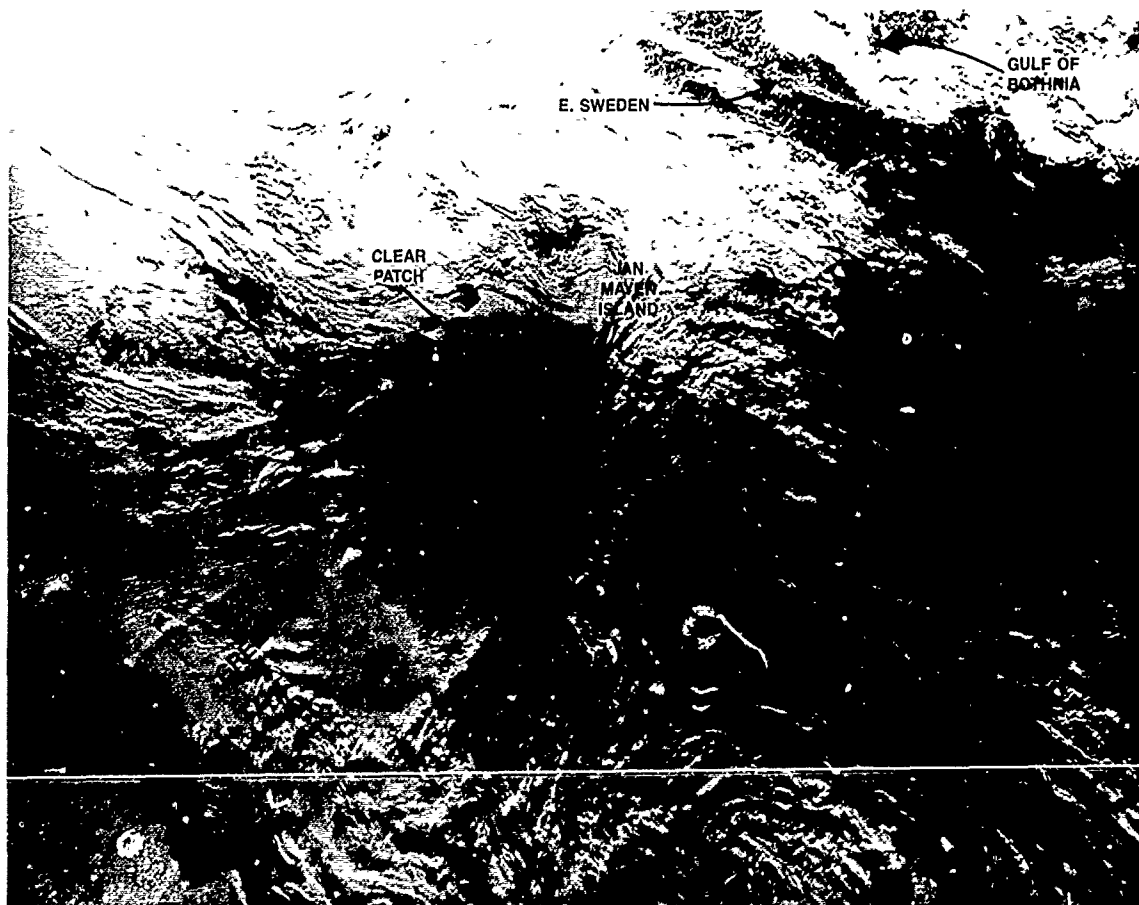
## Case 2 *Detection of High Pressure Centers and Ridge Lines in the Arctic*

### *Use of Clear "Slots" to Define Ridge Line Location*

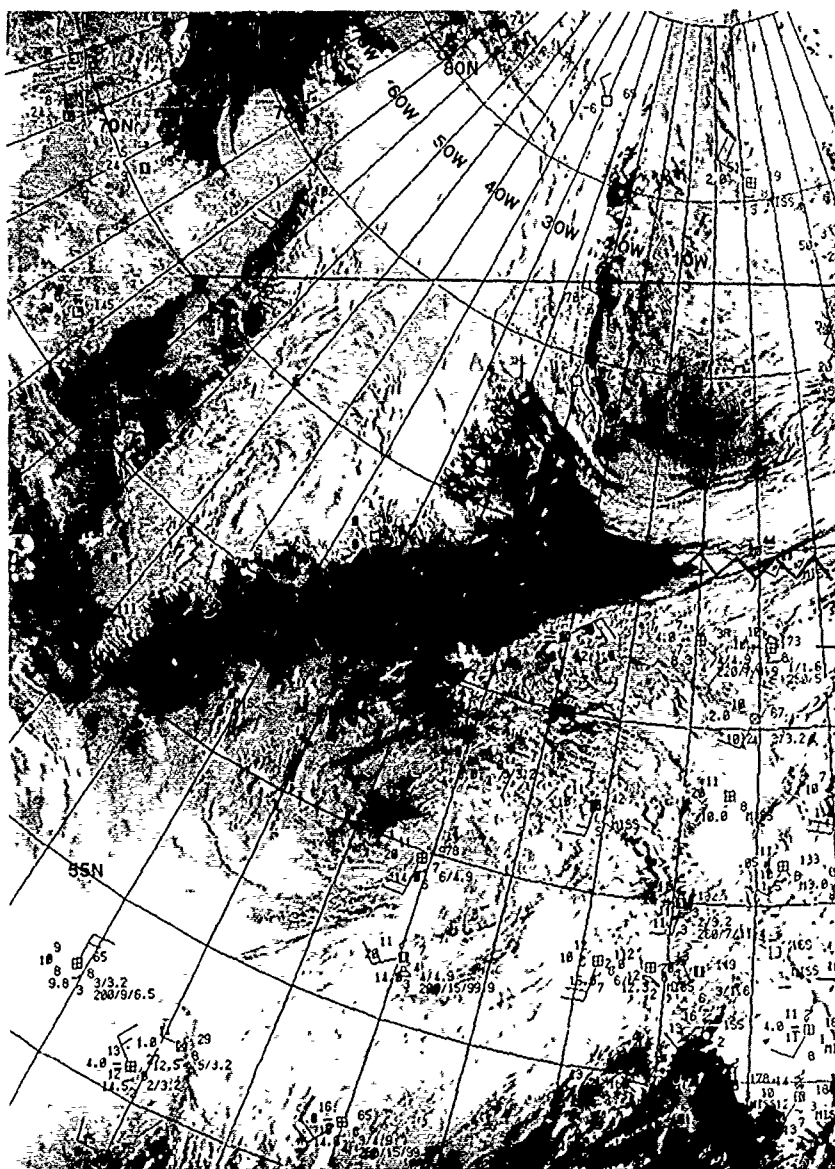
High pressure centers tend to be clear, with low stratus and fog in the outer regions of the circulation. Ridge lines emanating from a high pressure center are often defined by clear "slots" that extend from the center. However, not all clear slots in stratus cloudiness are caused by ridge line influence.

6 July 1984

DMSP visual (LS) data acquired at 0143 GMT (Fig. 1C-4a) show a view extending from Greenland to Scandinavia. The east coast of Greenland in the region from Scoresby Sund and northward for several hundred kilometers is clear, as is the MIZ and near-ice water adjacent to this region. Overcast low fog or stratus is found further east past Jan Mayen Island. These conditions suggest high pressure over the area. Jan Mayen reported obscured skies and fog on the 0000 GMT National Meteorological Center (NMC) surface analysis (not shown). Mt. Beerenberg, (2277 m or 7470 ft) on Jan Mayen can be seen as a white dot in the DMSP data extending upward through the fog. The FNOC 0000 GMT surface analysis (Fig. 1C-5a) verifies a high pressure center near Scoresby Sund with a ridge line extending eastward just north of Jan Mayen Island. Some of the stratus clouds apparent in the satellite imagery (Fig. 1C-4a) are dissipated in a patch over that region.

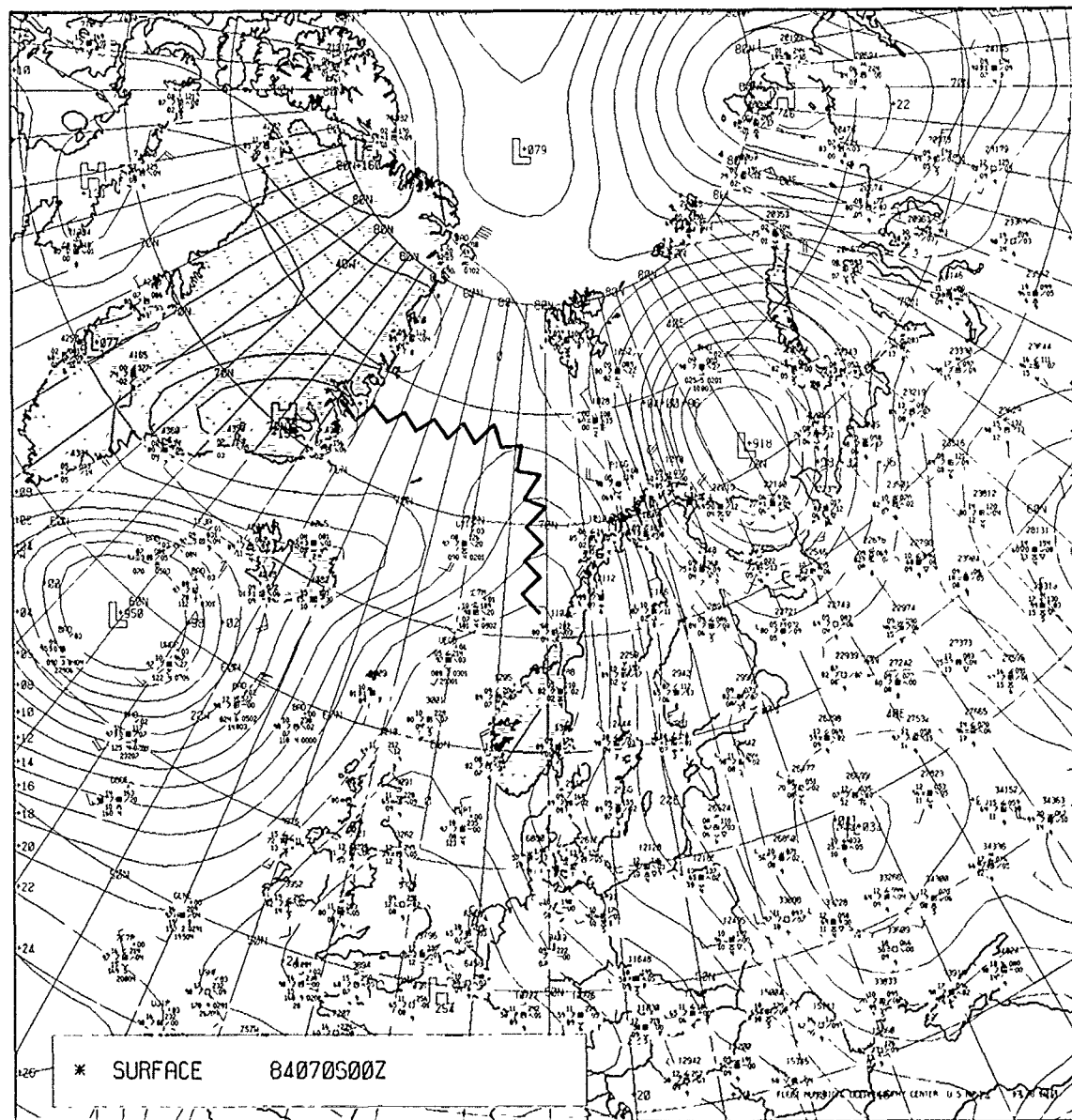


1C-4a. DMSP Visible (LS) Data. 0143 GMT 6 July 1984.



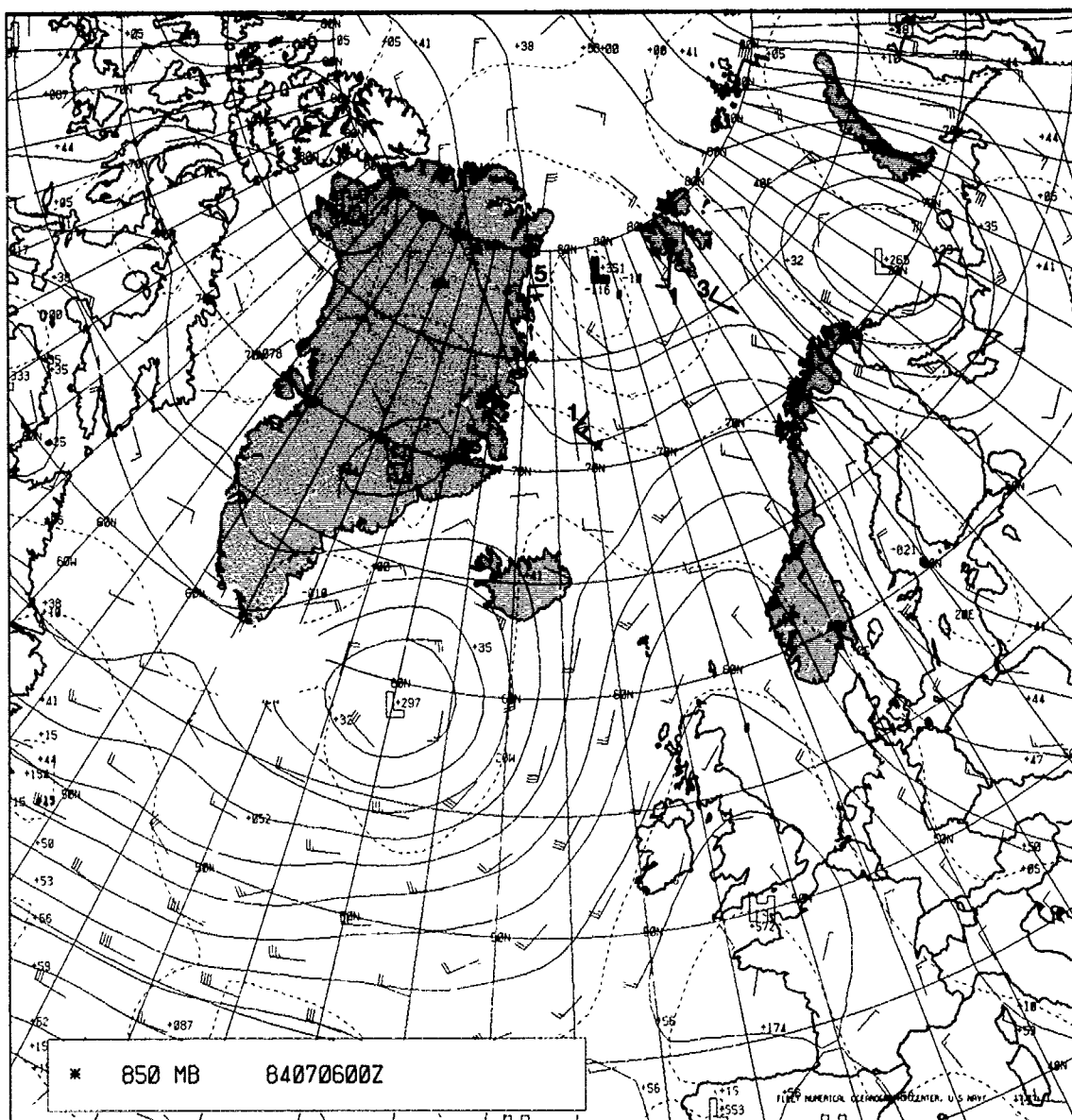
IC-3b. DMSP Visible (LS) Data and Surface Observations (0600 GMT). 0625 GMT 7 July 1984

There is an especially clear slot extending in a north/south direction over Sweden in the region adjacent to the Gulf of Bothnia (Fig. 1C-4a). On first glance the temptation might be to attribute the slot to ridge line influence, but the surface analysis (Fig. 1C-5a) shows that this is not true. The ridge line is off the coast of Norway, and Sweden is in a strong pressure gradient region of northwesterly



1C-5a. FNOG Surface Analysis. 0000 GMT 6 July 1984

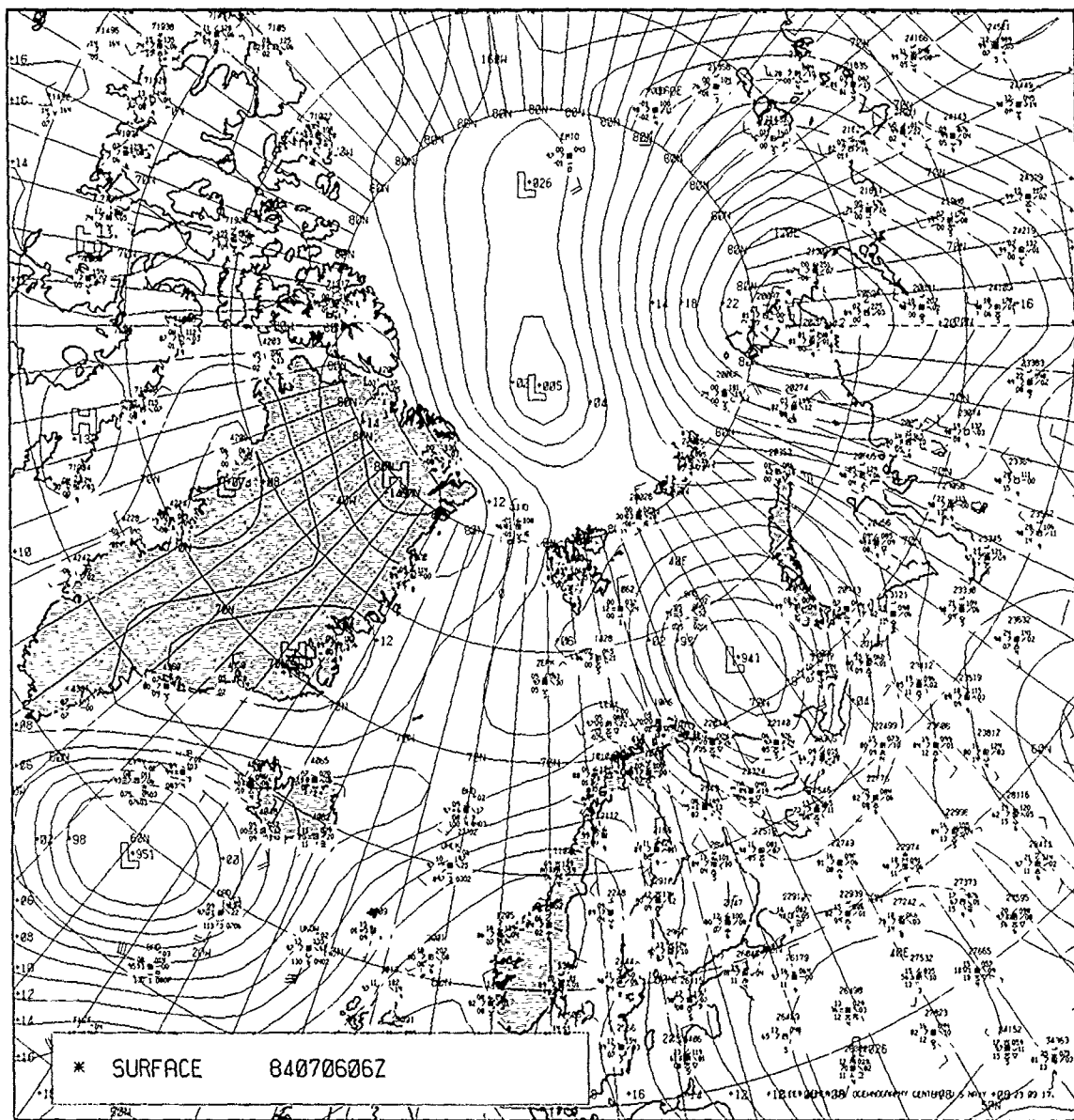




1C-6a. FNOC 850-mb Analysis. 0000 GMT 6 July 1984.

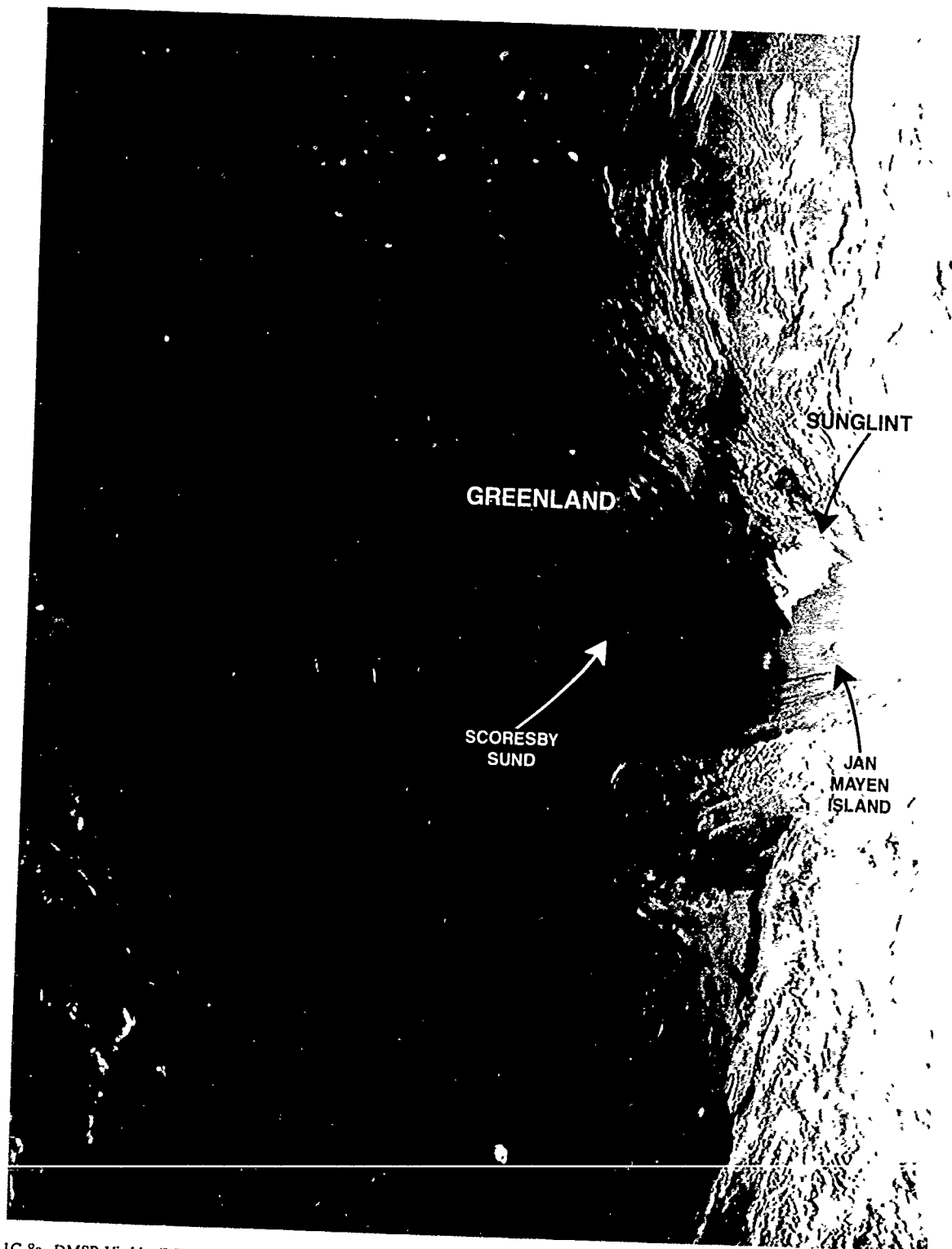
flow. The 850-mb analysis (Fig. 1C-6a) shows that northerly to northwesterly flow also existed at this level. The apparent reason then, for this clear slot, is not ridge line influence but downslope motion of air that has been lifted over the rugged terrain of Norway and western Sweden (losing some of its moisture in the process) and has descended onto the lower, flatter terrain of eastern Sweden. Note that temperatures are higher over Sweden than in Norway (Fig. 1C-5a), and temperature/dew point spreads are larger, indicating dryer air.

The configuration of the ridge line and the satellite-observed cloudiness pattern suggests that a useful analysis and forecasting tool can be derived from this example (i.e., whenever a north/south-oriented ridge line is positioned off the coast of Norway, overcast cloudiness with some convective buildups should be expected over the mountains of Norway and western Sweden, while in general eastern Sweden enjoys unusually clear, dry conditions and an increase in temperature).



1C-7a. FNOC Surface Analysis 0600 GMT 6 July 1984.

The fact that the ridge line off the coast of Norway is not clear may be attributed to a couple of influences. First, warm moist air is being advected around the high over a warm branch of the Gulf Stream that flows northward some distance from the coastline of Norway. Cooler sea surface temperatures are found 50-100 mi off the coast of Norway. These conditions would cause cooling of the warmer moist air and possible condensation to stratus or fog. Secondly, the ridge is very close to the coast of Norway and by 0600 GMT (Fig. 1C-7a) is over the coast. Frictional convergence and lifting of the air over the mountains negates the subsiding influence of the ridge line.



IC-8a DMSP Visible (LS) Data. 0505 GMT 6 July 1984.

An additional view of the area at 0505 GMT is shown in Fig. 1C-8a, a DMSP visible image. In this example sunglint off calm waters illuminates a clear region northeast of Scoresby Sund. Sunglint can also be seen through a break in the overcast cloudiness south of Jan Mayen. Note that the island and cloud south of the island casts shadows on the lower overcast. The two small areas of sunglint, however, do not exhibit a shadow effect.

The 0000 GMT sounding for Jan Mayen (Fig. 1C-9a) reveals calm surface winds and saturated low-level conditions, capped by an inversion at 998 mb (200 m or about 600 ft). Since Jan Mayen has the highest terrain at 2277 m (7470 ft) it is evident that this terrain projects thousands of feet above the lower overcast cloud deck to produce the shadow effect in Fig. 1C-6a.

#### **Important Conclusions**

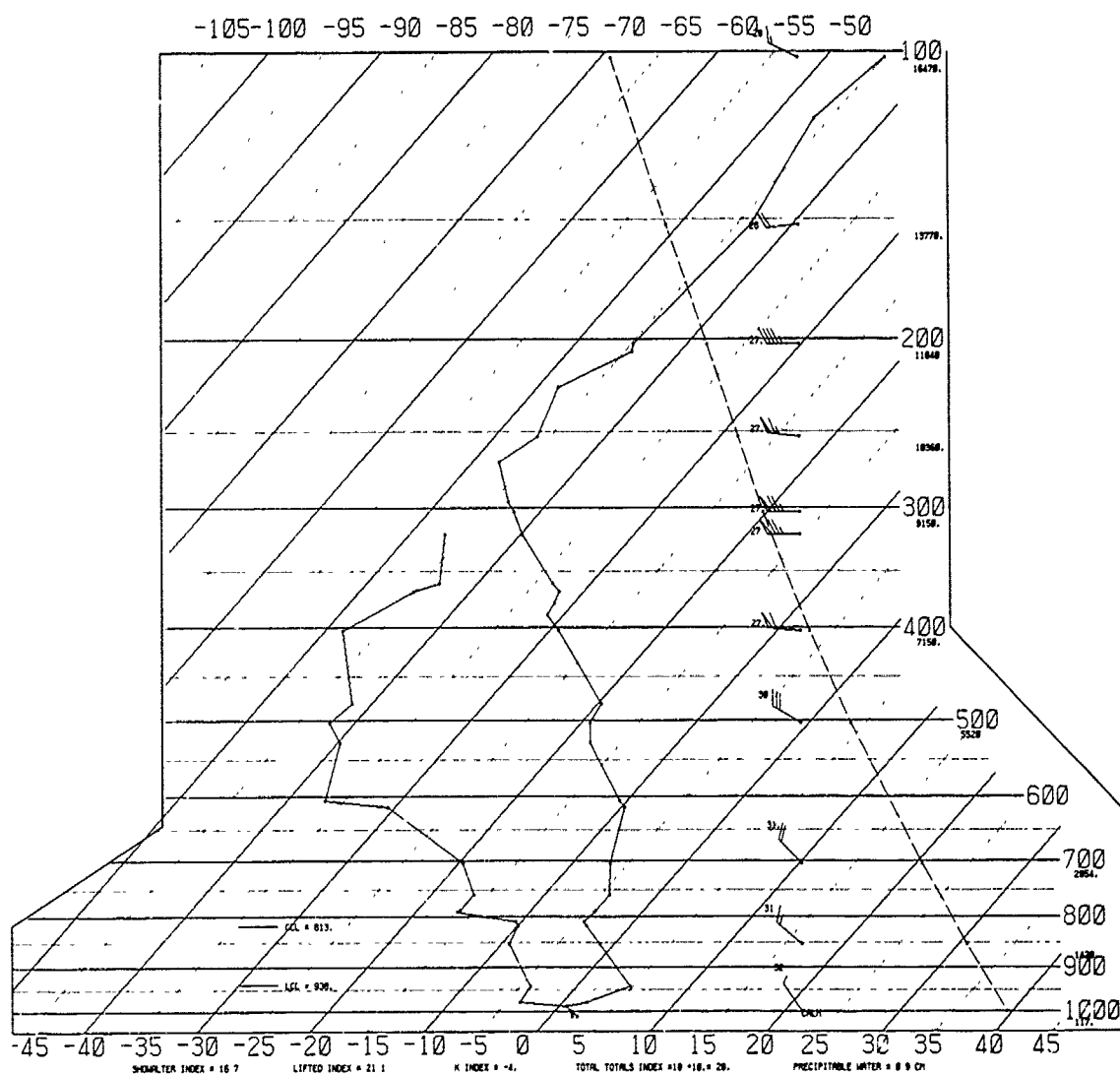
1. High pressure areas and ridge line locations can be detected reliably using satellite imagery.
2. Superposition of surface reports in satellite data assists greatly in the analysis and interpretation of the satellite imagery.
3. Clear slots in stratus often denote ridge lines, but over land areas in the region of mountains may be an effect of downslope winds.

# SKEW T, LOG P DIAGRAM

840706

0000Z

1001



1C-9a. Jan Mayen Radiosonde Data. 0000 GMT 6 July 1984.

*Case 1 Satellite Detection of a Southward-Moving Front  
Barents Sea (7-8 April 1987)*

*7 April 1987*

NOAA-9 infrared (Ch 4) HRPT data on this date at 0533 GMT (Fig. 1D-2a) reveal an area centered near Svalbard. A portion of northern Norway can be seen near the southern extremity of the image.

Orographic cloud effects can be seen with plumes evident extending southward from the terrain of Svalbard. These plumes are aligned with cyclonically curved cloud streaks extending north-northwest of Svalbard and to the southeast of the region over the ice pack south of Franz Josef Land. North-northeastern flow is implied by cloud streets in the Fram Strait.

The plumes are even more evident a few hours later in NOAA-10 Channel 4 data received at 0737 GMT (Fig. 1D-3a). The cyclonically-curved cloud streaks lead to another area of orographically-induced cloud plumes stretching eastward from the elevated terrain of central Novaya Zemlya. Faint cloud plumes are evident extending westward from the polynya southwest of the Franz Josef Land island group. Using these and other cloud alignment indications as tracers a suggestion of a low or trough can be seen, with the possible center between the edge of the Barents Sea ice pack and Franz Josef Land.

The 0600 GMT surface analysis (Fig. 1D-4a), prepared by the Northern Norway Forecast Center at Tromsø, Norway, shows a low center just west of central Novaya Zemlya. The satellite evidence and surface observations on the analysis suggest that this low center is misplaced and should have been positioned further north.

By using the polynya cloud plume indications in Fig. 1D-3a, which indicate northeasterly flow in agreement with the 20 kt north-northeasterly wind plotted on the surface analysis (Fig. 1D-4a) over Franz Josef Land, a trough would be indicated coincident with the arctic front near Nordauslandet. A buoy located near 80.7°N 20°E confirmed trough passage as pressure fell from 1018.2 mb on 7 April at 0000 GMT to 1013.8 mb by 0600 GMT and then rose continuously to 1017.6 mb by 0000 GMT on 8 April. The temperature fell from -14°C at 0000 GMT on 7 April to -22.4°C 12 hr later, behind the arctic front.

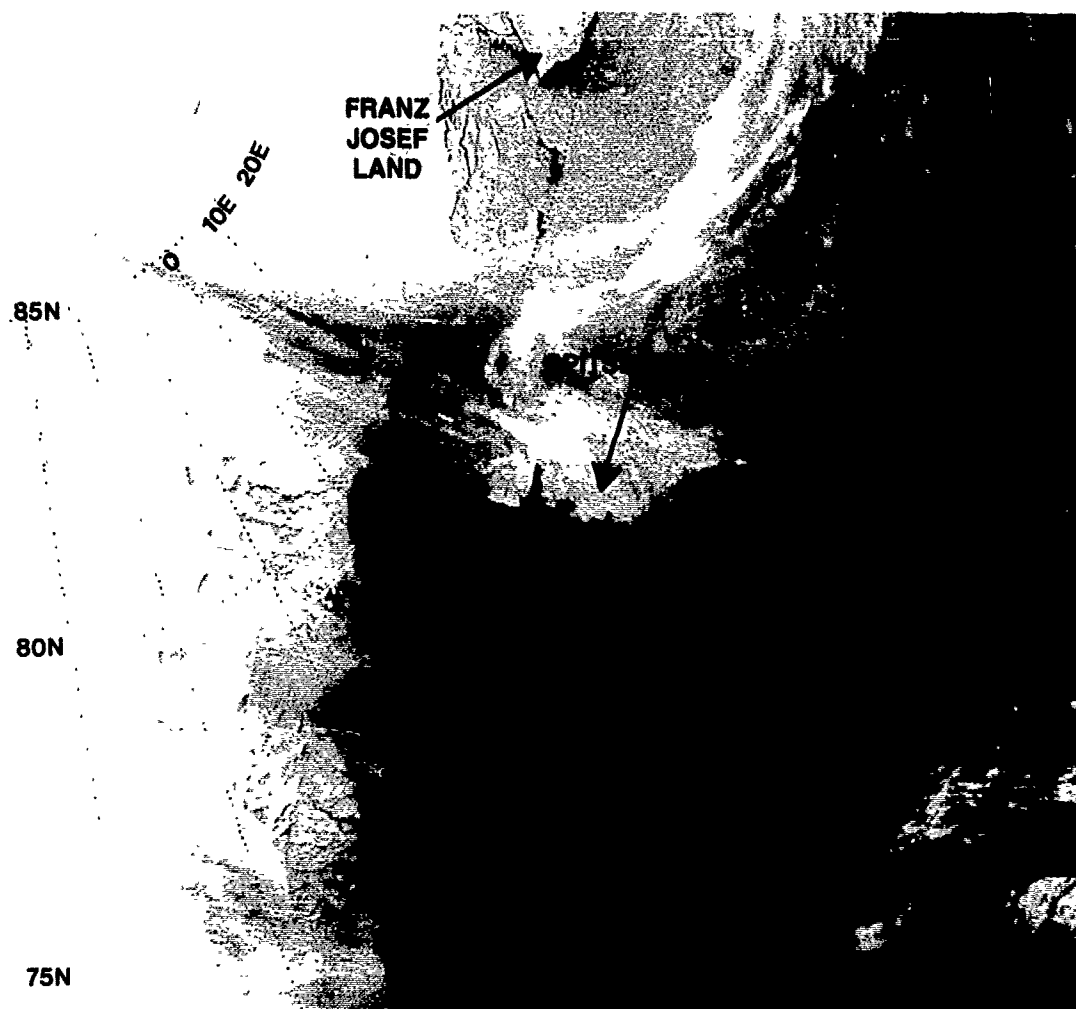
The FNOC 700-mb analyses for 7 April at 0000 and 1200 GMT (Figs. 1D-5a and 1D-6a) and for 8 April at 0000 GMT (Fig. 1D-7a) show westward movement of the low center associated with the arctic front from a position east of Novaya Zemlya to a position west of the island. The -25°C isotherm has been enhanced to show the progression of colder air toward Svalbard and over the Barents Sea. This progression was accompanied by a similar movement of stronger winds associated with the arctic front at the periphery of the low.

Fortunately satellite data are available at frequent enough intervals to show the evolution and movement of the arctic front as it moved over the Barents Sea during the ensuing 24 hr. Figures 1D-8a and 1D-9a are NOAA-10 Channel 4 views at 0917 and 1057 GMT, respectively. These show the extension with time of the orographic plume over Nordauslandet, which remains apparently "anchored" over the higher terrain where new cloud particles are continuously being formed. The westward movement of the low, however, causes a similar westward drift of the source region of cloud formation; by 1213 GMT, in a NOAA-9 visible (Ch 2) image (Fig. 1D-10a), the source of cloud formation has moved from Nordauslandet near 80°N 22°E to Spitsbergen near 80°N 12°E.

## *1D Arctic Fronts*

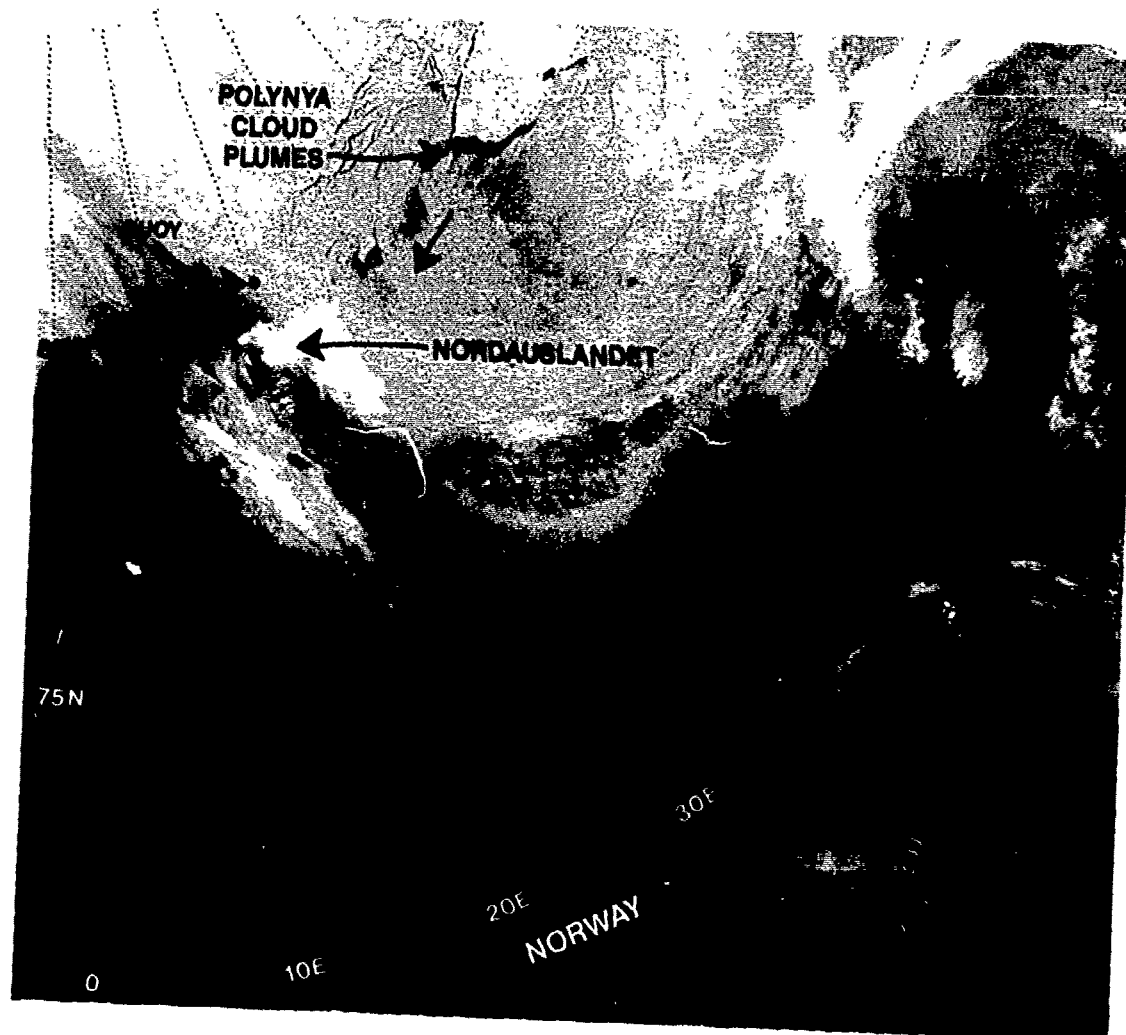
### *Characteristics of Arctic Fronts*

In classical meteorology frontal zones are characterized by a band of convergence in which moisture is maximized. The front is also a structure having a strong horizontal temperature gradient with a thermal wind component that produces a wind maximum along the front with a jet stream at higher elevations. Over the Arctic ice cap, where moisture is not as abundant as in lower latitudes, the front may appear somewhat ill-defined as a fragmented band of higher and lower level cloudiness. Due to moisture content and high wind speeds, however, the associated flow will produce orographic cloud effects wherever elevated terrain is encountered as near-saturated air is lifted to condensation. The plume from the orographic barrier is an indication of strong winds aloft and at the level of the terrain. When this plume is aligned with other banded cloudiness and when the plume and band are noted to translate, spreading generally southward with time, assumptions can be made that an arctic front has formed, that high wind speeds may be encountered at the surface and at low and upper levels near the front, and that cold surge effects may appear as cold arctic air moves southward behind the front and over the open sea to the south of the ice edge.

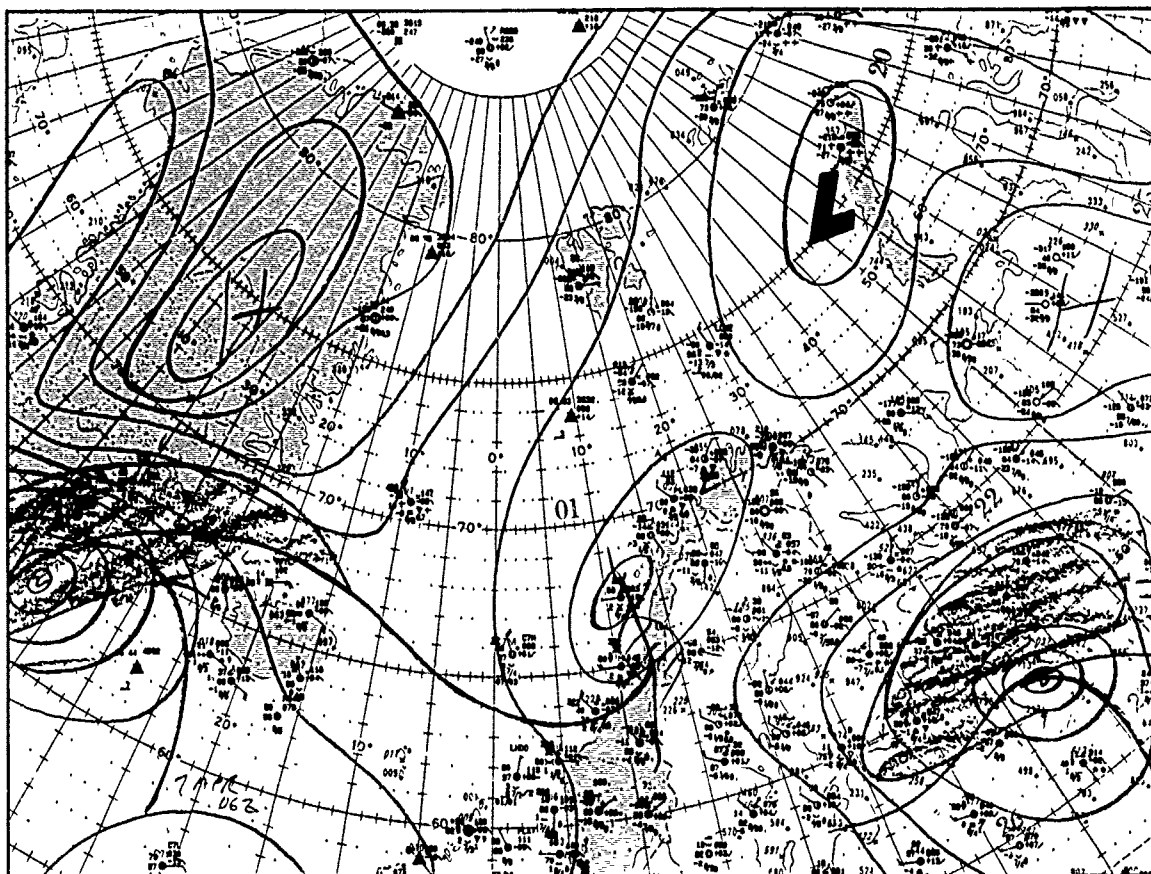


1D-2a. NOAA-9 Infrared (Ch 4) HRPT Data. 0533 GMT 7 April 1987.

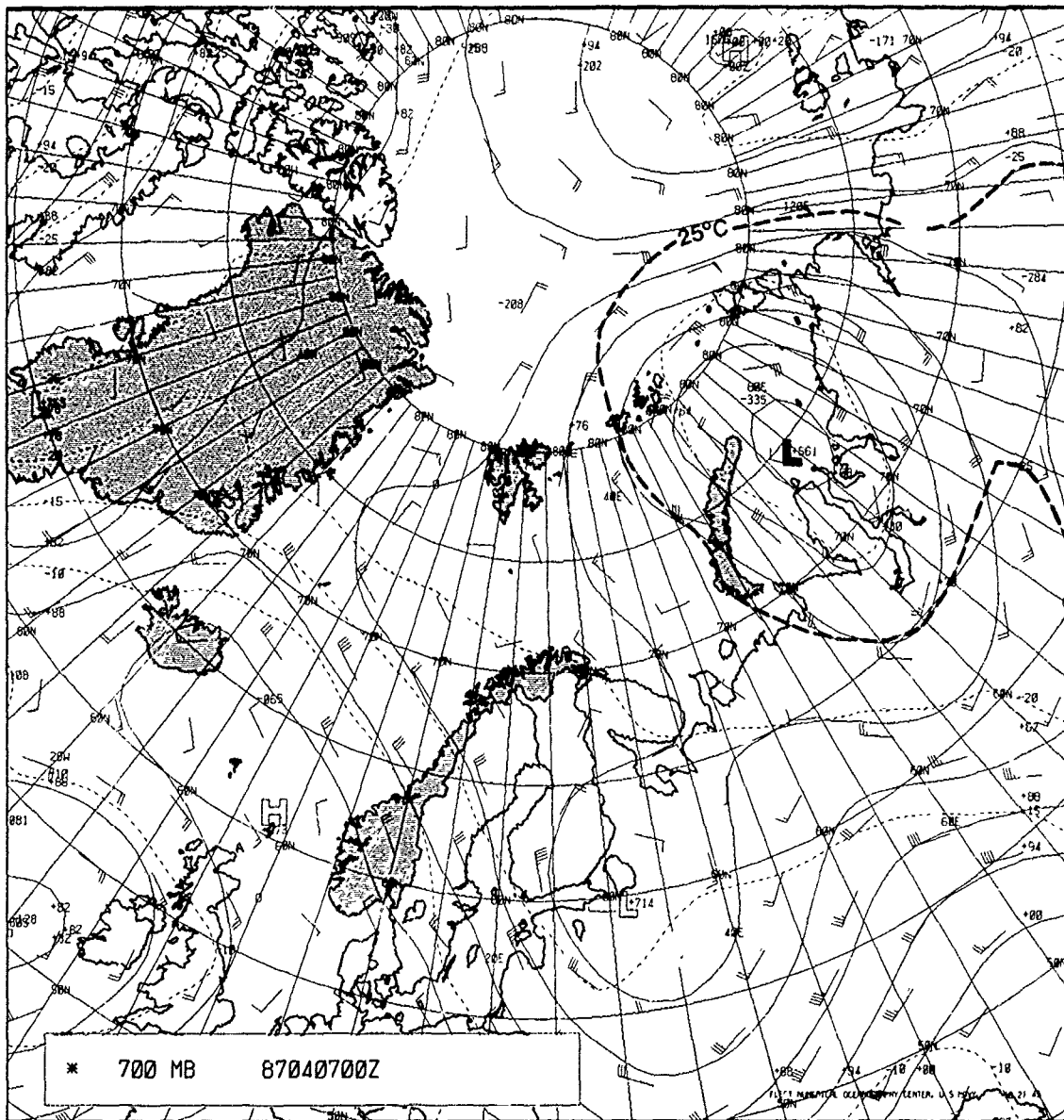




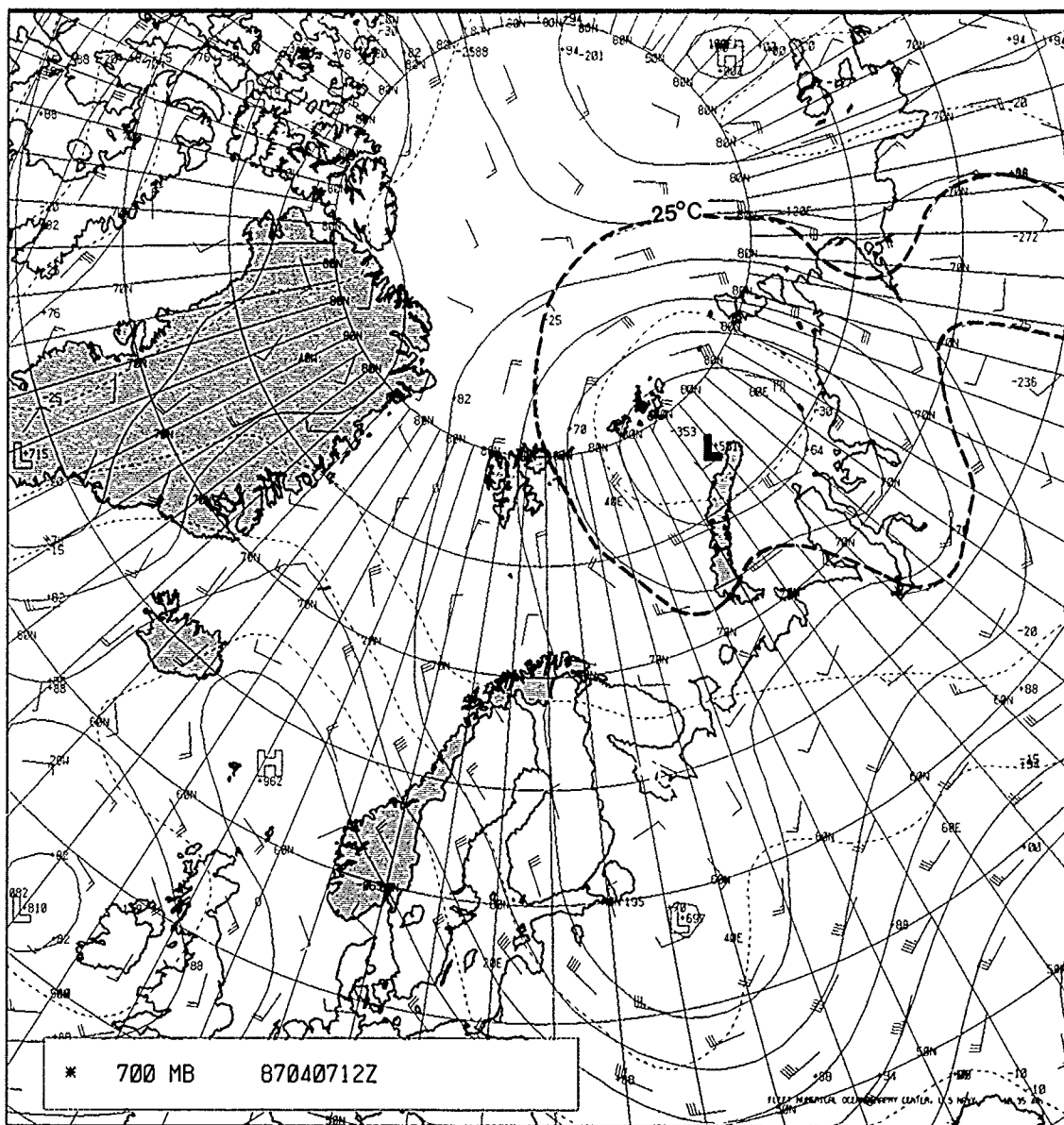
1D-3a. NOAA-10 Infrared (Ch 4) HRPT Data. 0737 GMT 7 April 1987.



1D-4a. Northern Norway Forecast Center (Tromsø) Surface Analysis 0600 GMT 7 April 1987.

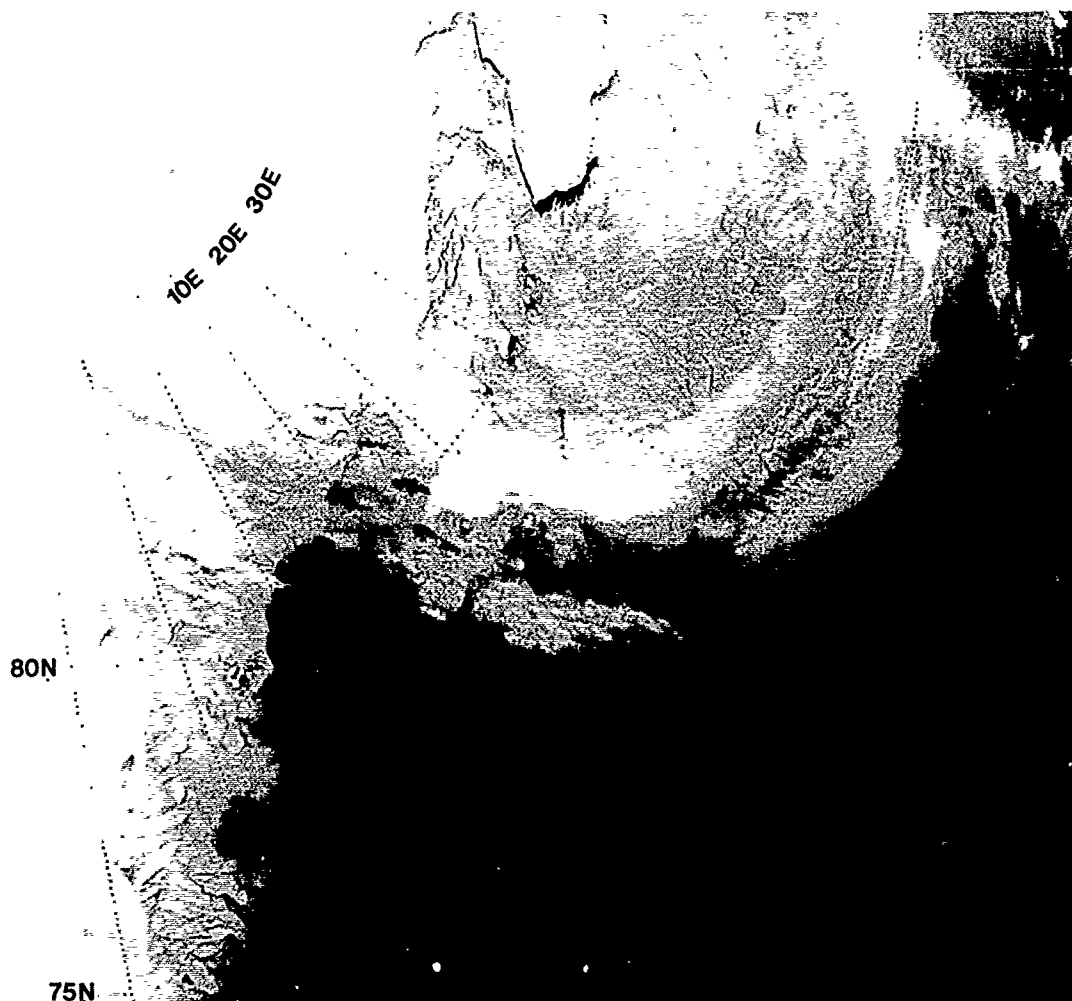


1D-5a. FNOC 700-mb Analysis 0000 GMT 7 April 1987.

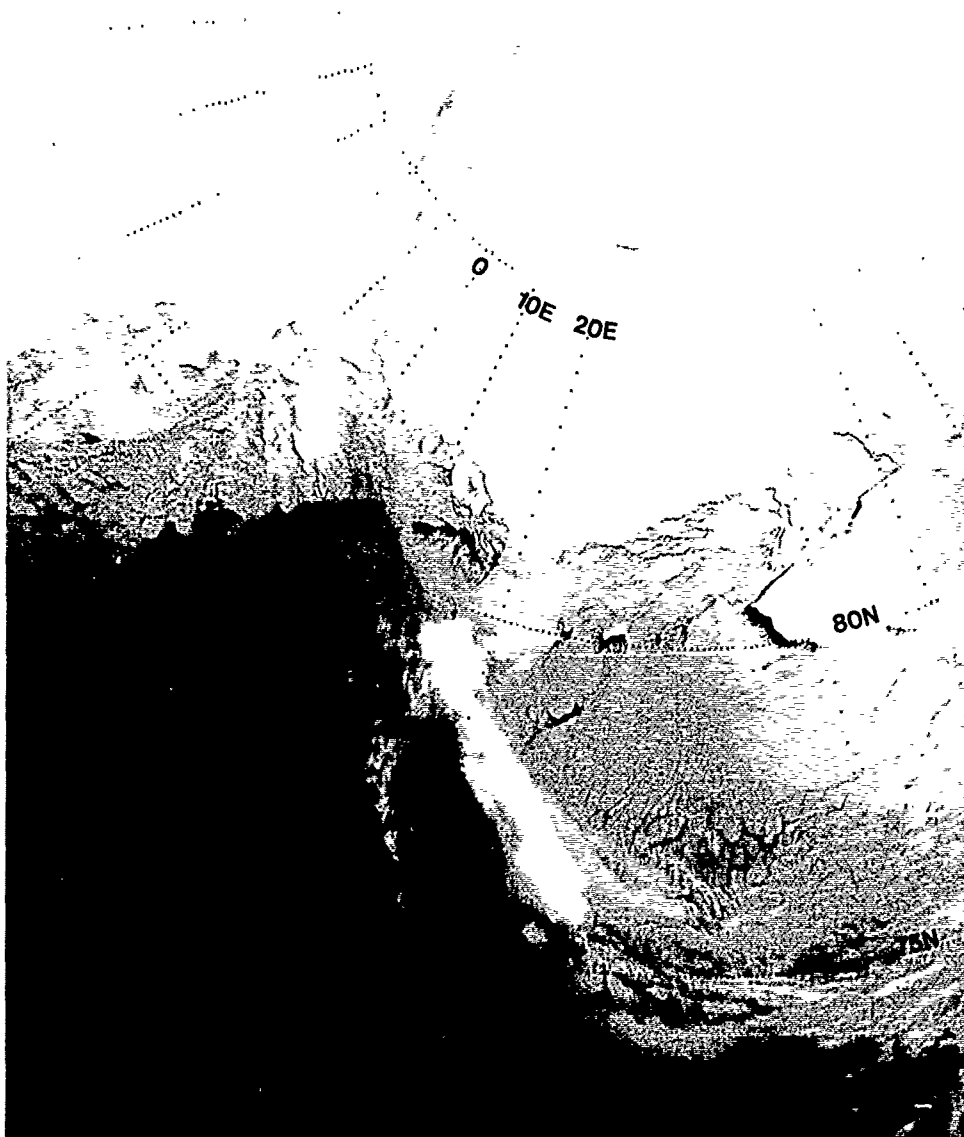


ID-6a FNOC 700-mb Analysis. 1200 GMT 7 April 1987.

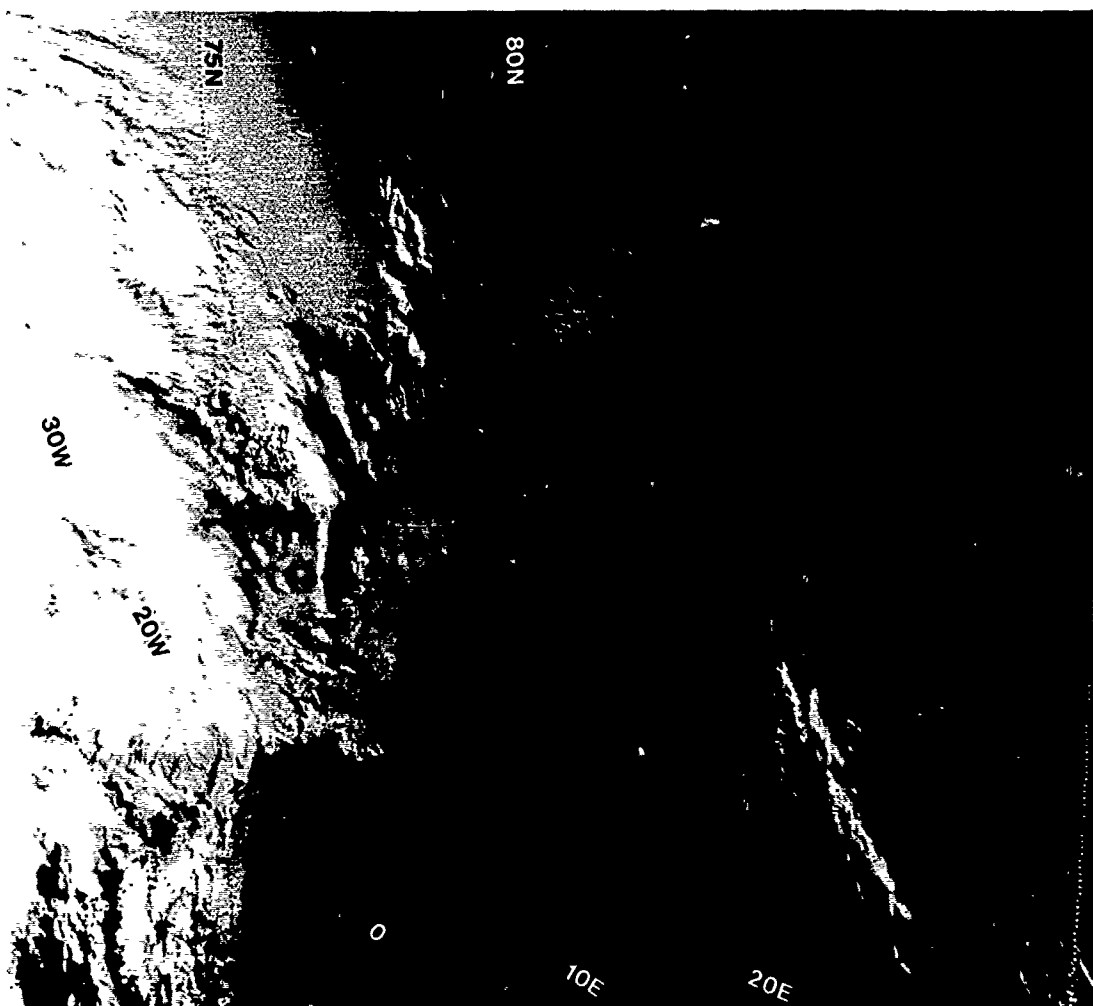




1D-8a. NOAA-10 Infrared (Ch 4) HRPT Data. 0917 GMT 7 April 1987.



1D-9a. NOAA-10 Infrared (Ch 4) HRPT Data. 1057 GMT 7 April 1987.



1D-10a. NOAA-9 Visible (Ch 2) HRPT Data. 1213 GMT 7 April 1987.



Figure 1D-12a is the RAOB for 8 April at 0000 GMT. The sounding reveals the expected strong winds at lower levels with probable cloud formation just under the inversion near 900 mb. The highest terrain in Novaya Zemlya, under the cloud, is 1965 ft (599 m). The base of the inversion is at the 900-mb level at about 3200 ft (1000 m), so it appears that the cloud is being formed in this region with winds of 240 degrees at 30 kt. This direction coincides perfectly with cloud striations over that area shown in Fig. 1D-11a.

The Northern Norway Forecast Center's 0000 GMT surface analysis for 8 April (Fig. 1D-13a) shows the low center west of Novaya Zemlya. In this analysis there is no indication of an arctic front in the region. However, the isobaric analysis suggests that one could easily be drawn, essentially as the satellite data (Fig. 1D-11a) indicate, through the inverted trough west of Spitsbergen to the region of Bear Island and then eastward past the south side of the low and over the southern tip of Novaya Zemlya.

The ship report from Lance (LBHC) just west of northern Spitsbergen is especially interesting in that the ship is reporting a 30-kt northerly off-ice wind in fog, with a visibility of 2.5 mi (4 km). This ship is a Norwegian oceanographic research vessel, consequently the report can be considered very reliable. (It also continues to report fog and high winds for the next several 3-hr reports.) Of interest is the fog reported under conditions of high wind speed off-ice flow over the ocean. However, cold arctic air moving from the strong surface-based inversion over the ice onto the relatively warm water of the Fram Strait will initially erode the inversion only slightly. The strong heat and moisture flux into the air will initially condense into fog or stratus trapped under the low inversion. Only after the air has traveled 100 km or so over the water does the mixed layer deepen and roll cloud convection, with better visibilities, occurs. At 0300 GMT Lance (LBHC) reported winds of 40° at 30 kt in snow showers with a visibility of only 0.3 mi (0.5 km). The temperature was  $-13.7^{\circ}\text{C}$  with a dewpoint of  $-14.0^{\circ}\text{C}$ . The position of Lance (LBHC) at that time is shown in Fig. 1D-11a, an image taken approximately 45 min after the surface observation. This figure shows the ship very near the ice edge, in a position where fog formation under such conditions would be likely.

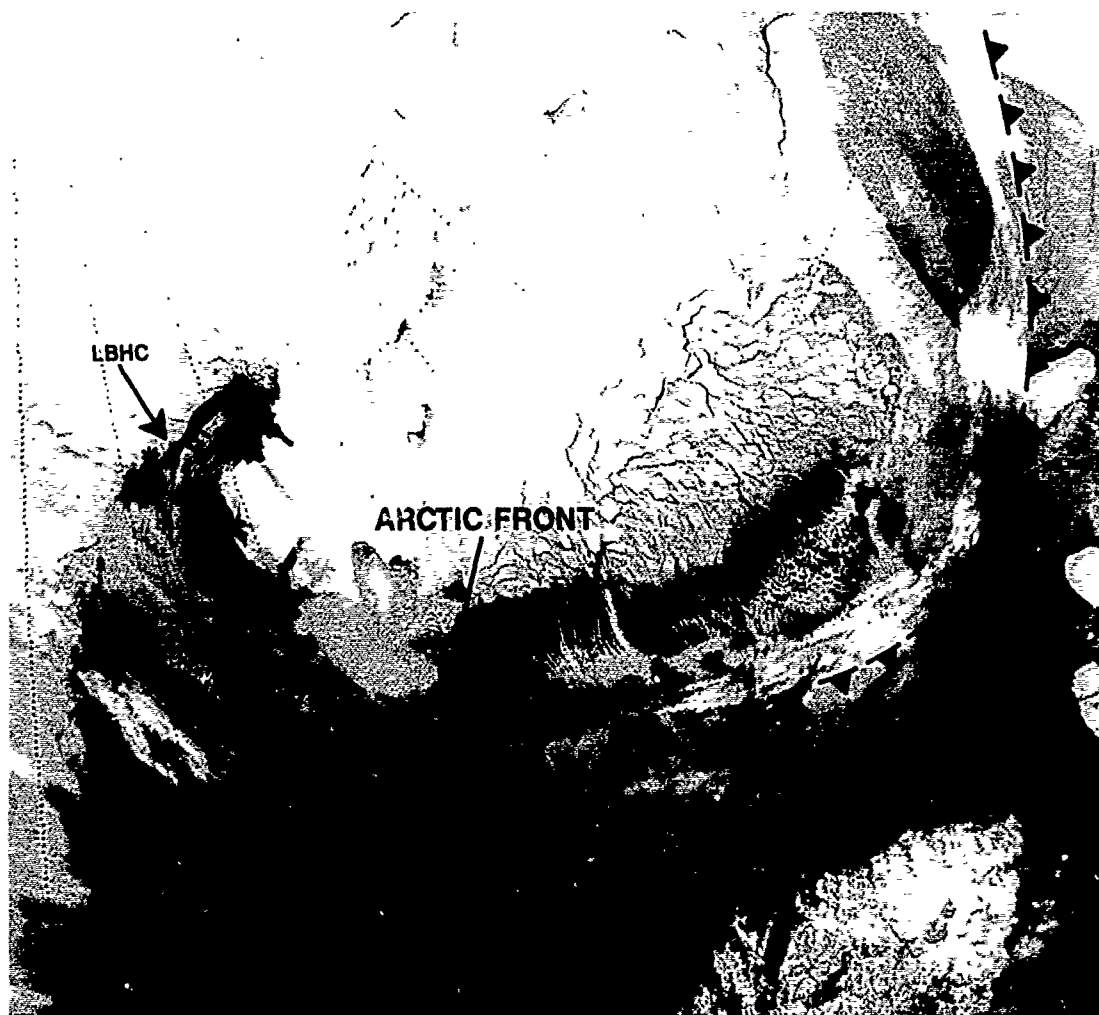
The final two NOAA-10 infrared (Ch 4) images for this example are shown in Figs. 1D-14a and 1D-15a taken on 8 April at 0715 and 1034 GMT, respectively. These figures show the further progression of the front and in particular the outbreak of cloud plumes from open leads in the pack ice north of the Barents Sea.

In the region where the cloud plumes are occurring stronger winds from aloft have broken through the inversion to reach the surface. Cloud plumes will not develop in light wind situations. The high winds produce a greater stress upon the ice pack and tend to open new water areas within the leads. A careful comparison of Figs. 1D-14a and 1D-15a with Figs. 1D-2a and 1D-3a reveals that the ice edge has moved southward by almost a degree, especially in the area approaching Novaya Zemlya.

Expansion of the ice in this region is also an effect of the low pressure system over the region. Since ice tends to move at an angle of about  $30^{\circ}$  to  $40^{\circ}$  to the right of surface wind flow, it follows that the lows tend to cause an expansion of ice floe regions radially outward while high pressure systems cause compaction.

8 April 1987

By early 8 April, at 0341 GMT, the front has moved past Spitsbergen and off into the Barents Sea as revealed in NOAA-9 infrared (Ch 4) data (Fig. 1D-11a). These data show the arctic front in the Fram Strait, the Barents Sea, and passing over the southern end of Novaya Zemlya where another orographic plume is generated, indicative of high wind speeds at lower levels. Coincidentally the front passes over a radiosonde station on Novaya Zemlya (Marlyye Karamakuly, Station 207440, 72.6°N 52.7°E).



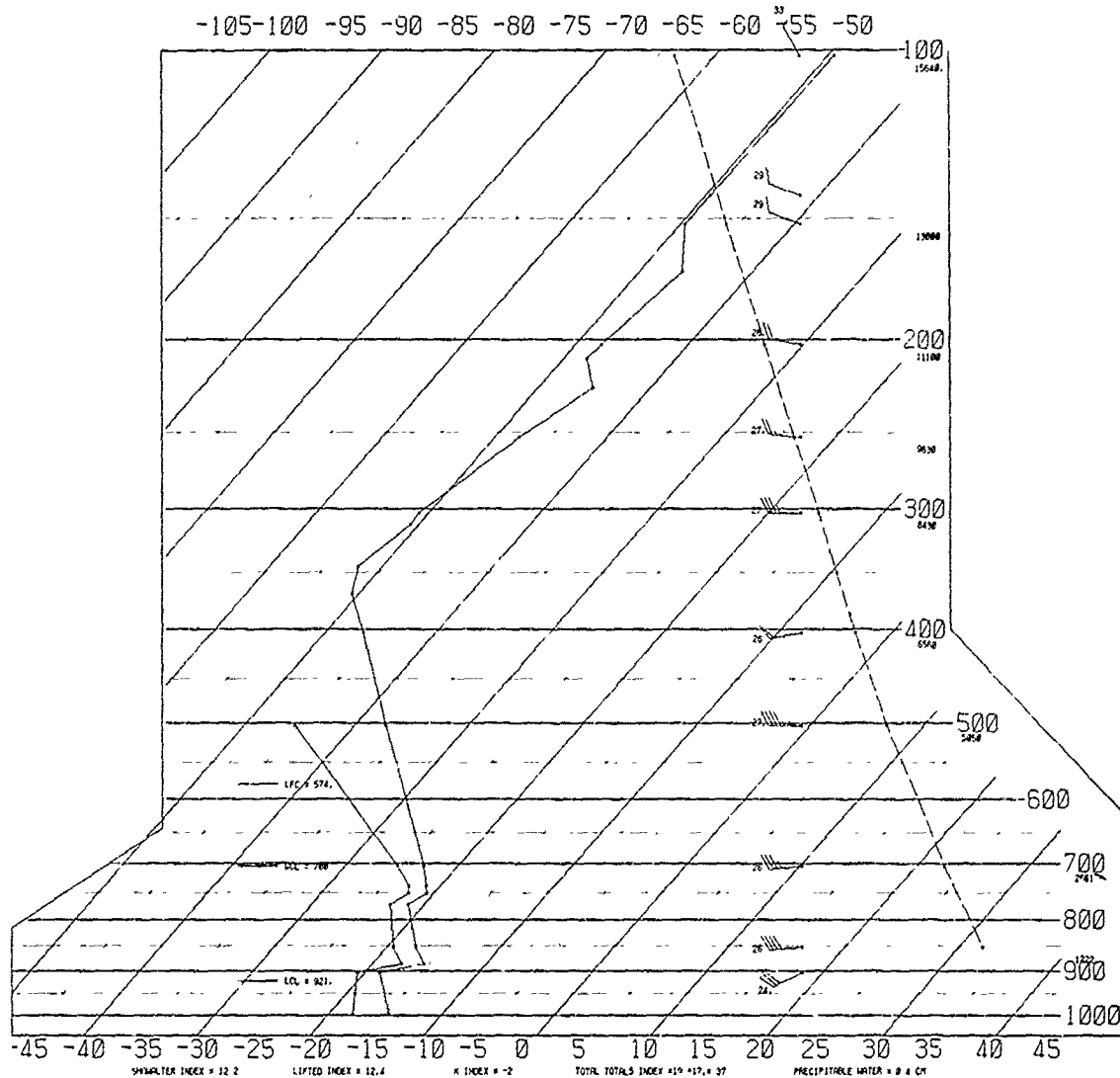
1D-11a. NOAA-9 Infrared (Ch 4) HRPT Data. 0341 GMT 8 April 1987.

# SKREW T, LOG P DIAGRAM

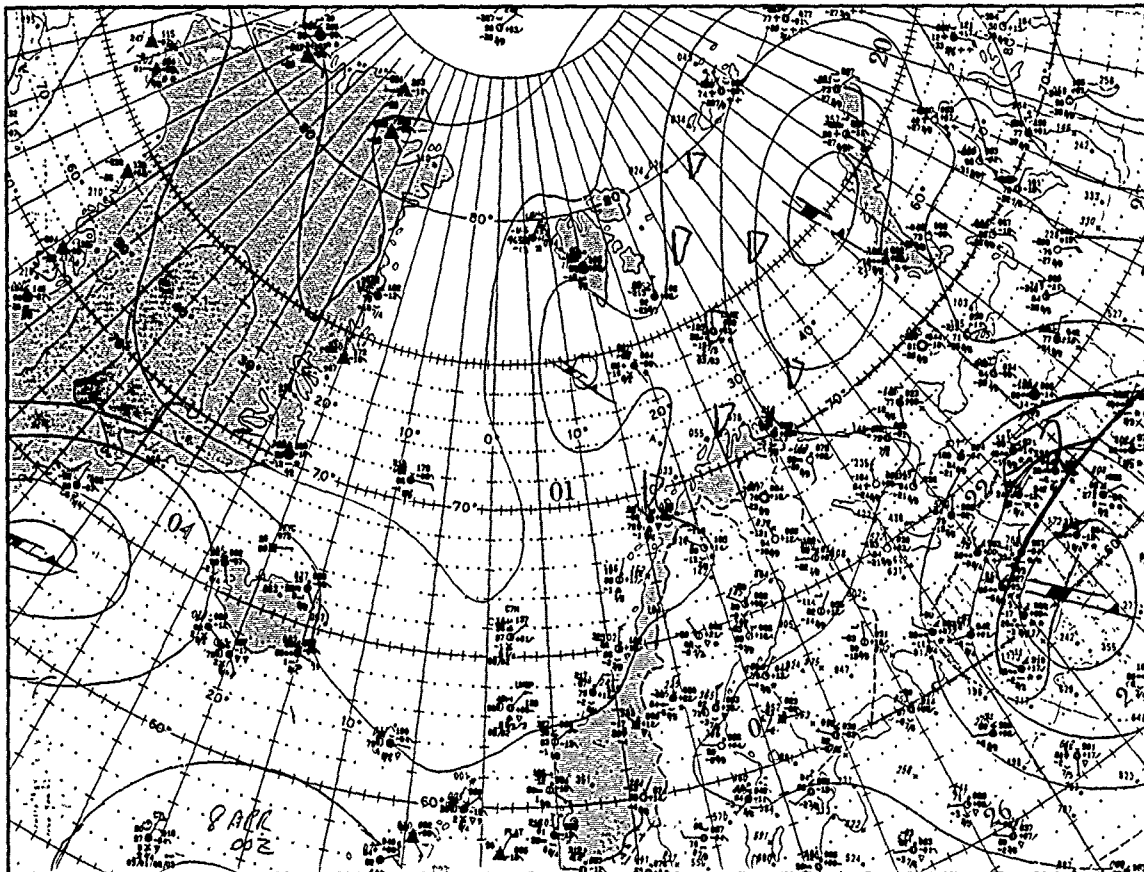
870408

0000Z

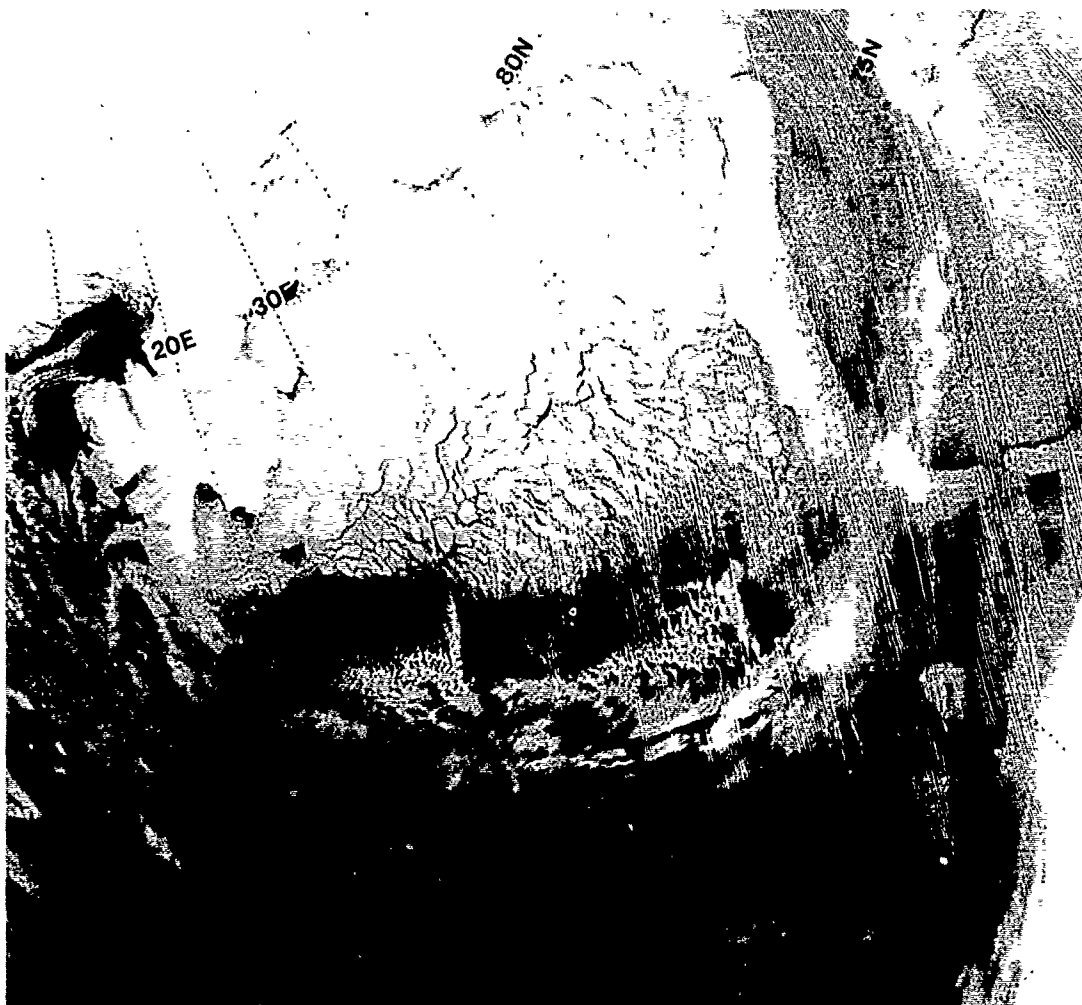
20744



1D-12a Mariyye Karamakuly Radiosonde Data. 0000 GMT 8 April 1987.



ID-13a. Northern Norway Forecast Center (Tromsø) Surface Analysis. 0000 GMT 8 April 1987.



ID-14a NOAA-10 Infrared (Ch 4) HRPT Data. 0715 GMT 8 April 1987.



1D-15a, NOAA-10 Infrared (Ch 4) HRPT Data, 1034 GMT 8 April 1987.

#### Important Conclusions

1. Cloud plumes over elevated terrain in the Arctic are indicative of strong winds at low levels and, if other streaks or banded cloudiness are observed aligned with the plumes, may indicate the position of an arctic front.
2. Movement of a cloud plume from its initially observed anchored position may indicate similar movement of the arctic front.
3. Fog formation over open water near the ice edge can occur under conditions of strong off-ice flow.
4. Low pressure systems over ice floe regions cause an expansion of the ice area and result in increased leads and open water areas. High pressure systems result in ice floe compaction.
5. Cloud plumes extending from leads in the ice pack are indicative of strong surface winds and a disruption of the normal surface-based inversion over the ice.
6. High quality satellite data at frequent intervals are required to optimize arctic front detection and to monitor movement and development. Surface and upper air observations are, however, important complementary data that aid in analysis and interpretation of effects.

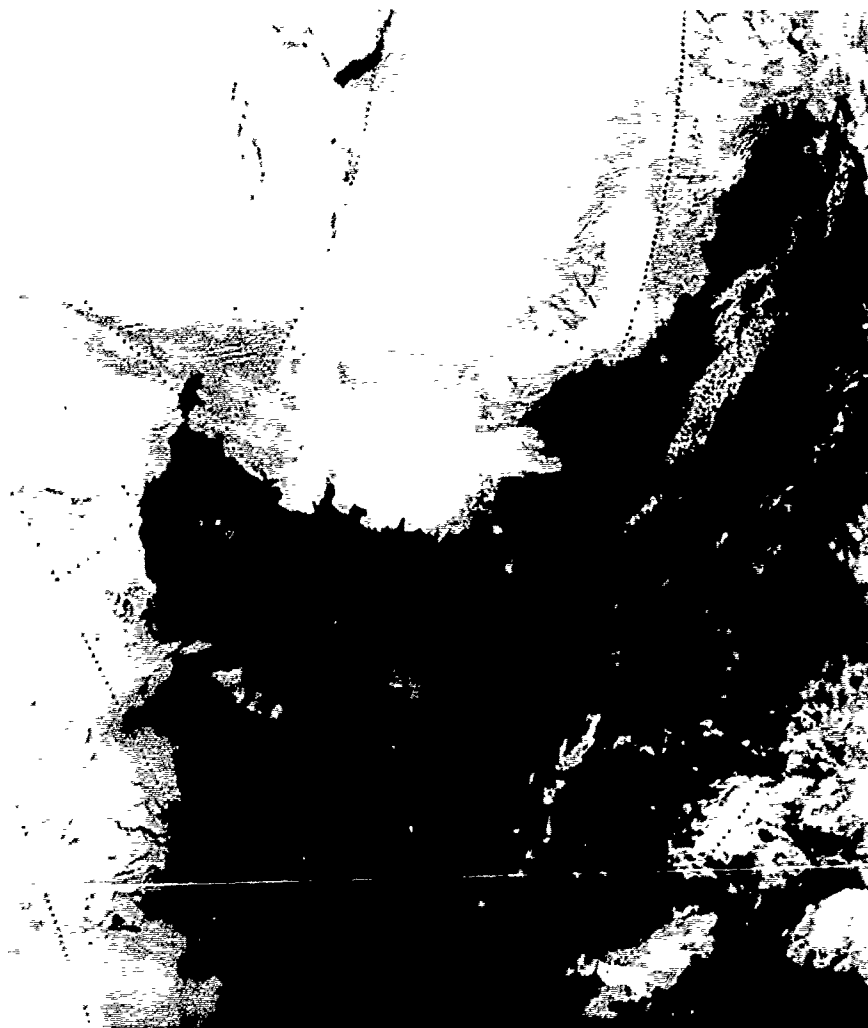
*Case 2 Southward Movement of the Barents Sea Ice Edge Following Arctic Frontal Passage (7-12 April 1987)*

*Ice Movement Following Arctic Frontal Passage*

Factors governing the movement of ice are manifold and complex but include the effects of wind, ocean current, and internal stress. In the Barents Sea, away from land, internal stress factors may be minimal. During a strong wind event it is the force of the wind, causing surface stress, which becomes overpowering. Significant ice movement can be observed by satellite in 24 hr or less. Strong winds are observed over the ice during and following arctic frontal passage as it moves from the ice cap southward into the open water of the Barents Sea.

*Barents Sea—7-12 April 1987*

Passage of an arctic front southward into the Barents Sea was documented during the period 7-8 April 1987 (see Case 1). Figure 1D-16a shows the area on 7 April 1987 at 0533 GMT as viewed in NOAA-9 infrared (Ch 4) data.



1D-16a. NOAA-9 Infrared (Ch 4) HRPT Data. 0533 GMT 7 April 1987.

When the same overlay is applied to the following day's Channel 4 data, which was acquired by NOAA-10 at 0715 GMT (Fig. 1D-18a), there is evidence of a small but perceptible movement of the ice edge southward of its former limit. This movement has occurred as the arctic front, north of the ice edge (Fig. 1D-16a), has moved to the south of the ice in the central Barents Sea (Fig. 1D-18a). Note that the winds on the north side of Spitsbergen have shifted from northerly (Fig. 1D-17a) to easterly (Fig. 1D-18a), as the front moved past.

Effects of arctic front passage are readily evident in the cloud plumes extending from open leads in the ice pack and in the cloud lines, which imply strong northerly flow in the area south of the ice edge.

Continued southward movement of the ice edge away from its original position on 7 April, in response to northerly flow, is evident on 9 April 1987 as revealed in NOAA-10 Channel 4 data acquired at 0653 GMT (Fig. 1D-19a). Cloud plumes along the southern portion of the ice edge show continued evidence of northwesterly flow tending to stress the ice in a southward direction.

NOAA-9 visible (Ch 2) data (Fig. 1D-20a), acquired at 1140 GMT, show cloud plumes near the southern portion of the ice that indicate continued westerly to northwesterly flow. Due to the Coriolis effect the ice tends to move about  $20^\circ$  to the right of the wind, consequently southerly ice motion continues in that area. The large cloud plume from Kvitoya and cloud streaks to the northwest suggest the presence of a new arctic front at that location, as indicated on the overlay.

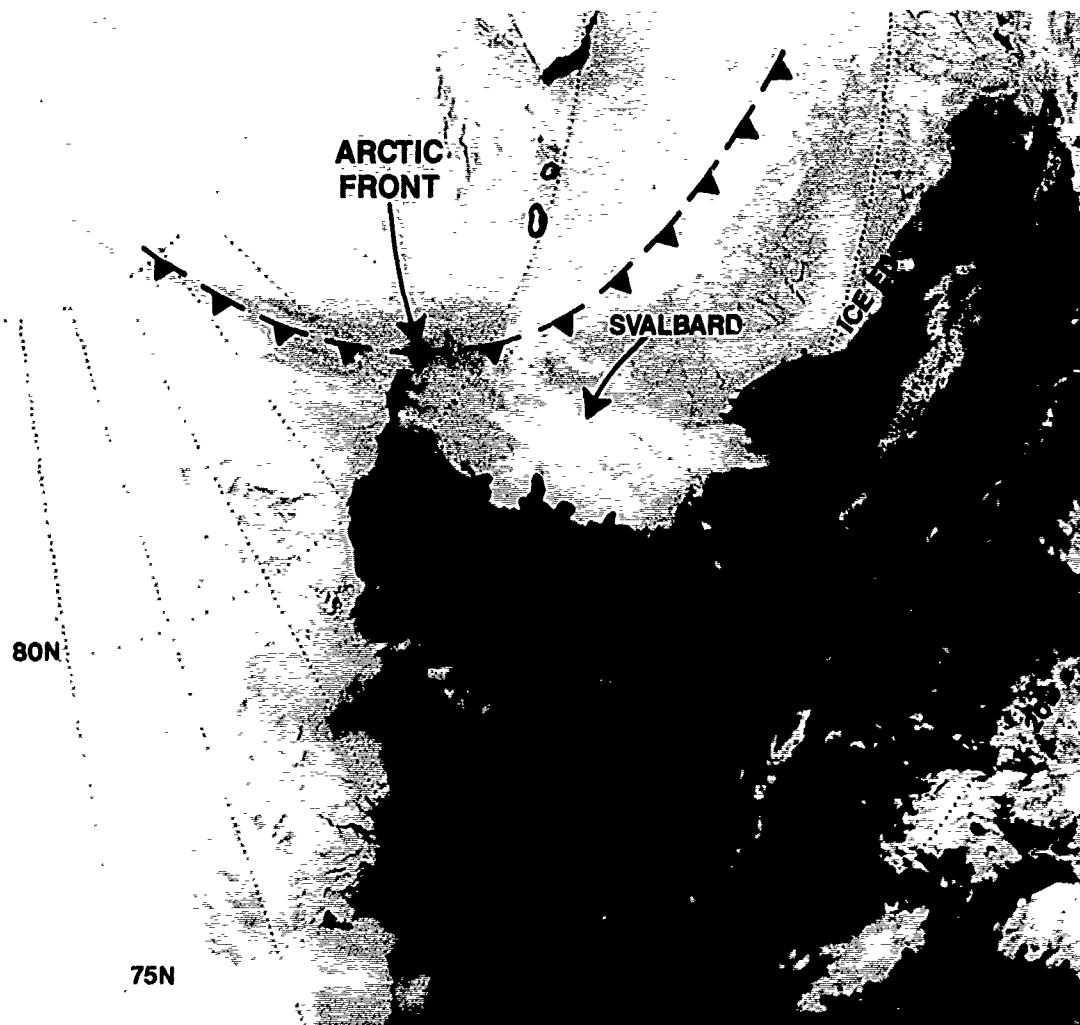
The FNOC surface analysis for 10 April 1987 at 1200 GMT (Fig. 1D-21a) shows the very strong gradient existing over the western Barents Sea at this time. The analysis implies sustained winds of 25 kt at the surface over the region from a northerly direction. The computer-drawn isotherm analysis (dashed lines) does not emphasize the strong thermal gradient that should exist near the arctic front. Isotherms should bulge northward over the warm water of the Fram Strait and dip more sharply southward over the cold ice east of Svalbard to reflect the reality of the situation. The force of the northerly flow over the ice is emphasized by an observation from the ship LUXE ( $75^\circ\text{N } 30^\circ\text{E}$ ) on the FNOC surface analysis 6 hr later (1800 GMT) (Fig. 1D-22a). At this time the ship reports sustained winds of 35 kt from the northwest.

The new arctic front to the north did not move significantly as indicated by its position in NOAA infrared (Ch 4) data acquired the following day (11 April 1987) at 0930 GMT (Fig. 1D-23a). Its location is revealed by cloud streaks passing over Svalbard and then southeastward to the southern portion of Novaya Zemlya, where cloud plumes are formed along the ridge line. Note that large polynya are being formed on the south side of the islands between Svalbard and Franz Josef Land. The presence of a cloud plume from the polynya south of Kvitoya verifies open water in that region.

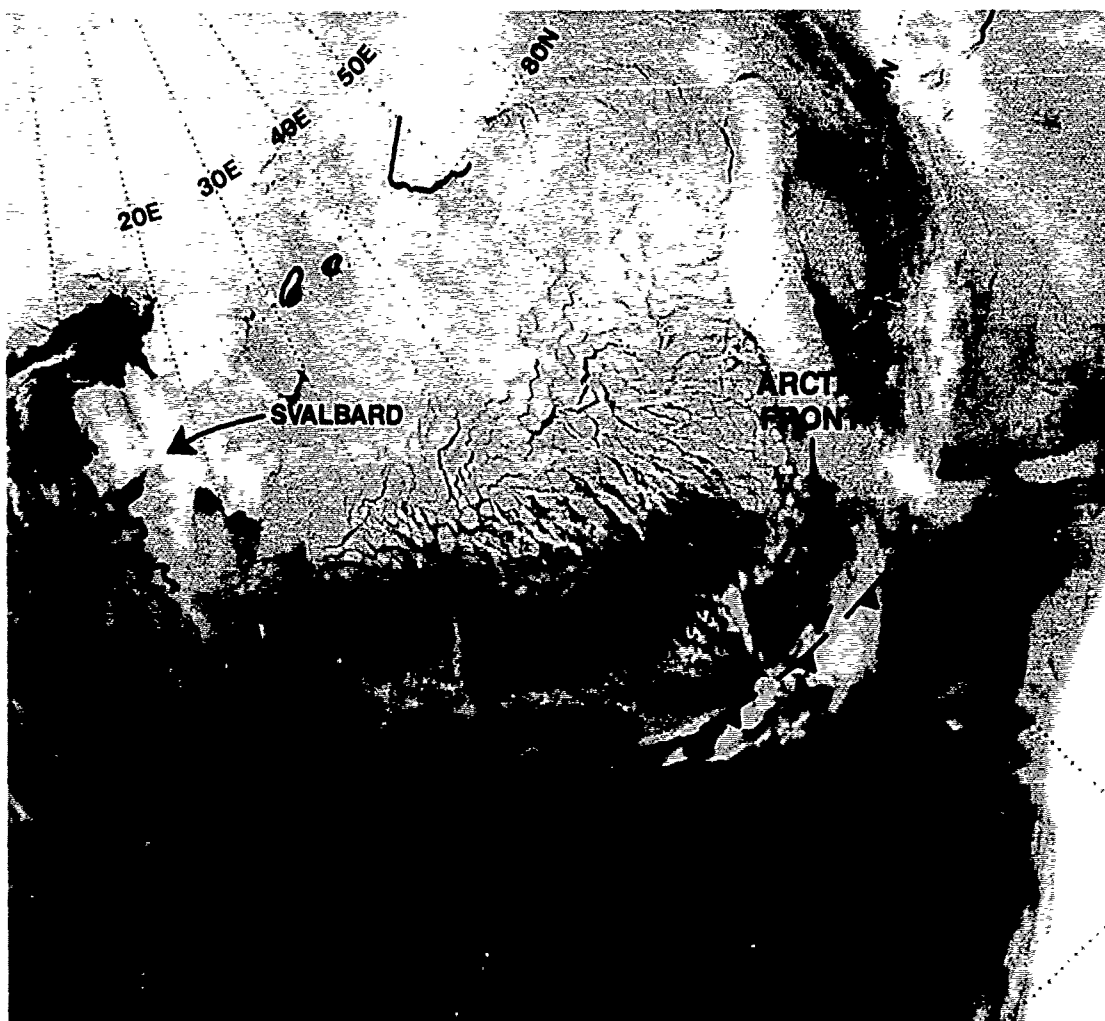
A final view of the region on 12 April 1987, in infrared (Ch 4) data acquired by NOAA-9 at 0258 GMT, is shown in Fig. 1D-24a. This figure shows the dramatic southward extension of the ice edge that occurred in comparison to the initial ice edge position on 7 April—5 days earlier. A comparison of Fig. 1D-24a with Fig. 1D-18a on 8 April, when changes were first noted in the ice edge position, helps give an appreciation for the dramatic increase in polynya development and lead extension. The coincident movement of arctic fronts associated with this change is also of great interest. The new arctic front has apparently passed Svalbard as winds north of Spitsbergen again change from northerly to easterly and a renewed outbreak of northerly flow is apparent over the ice and into the Barents Sea. Figure 1D-25a shows the FNOC 12 April 1987 0000 GMT surface analysis on which the position of the arctic front has been superimposed. From this figure the arctic front can be seen as it defines the southward limit of northerly flow. The point could be made that if such movement could be accurately analyzed and forecasted, periods of dramatic southward ice extension could also be predicted. Obviously the accurate analysis of satellite data can greatly assist this effort.



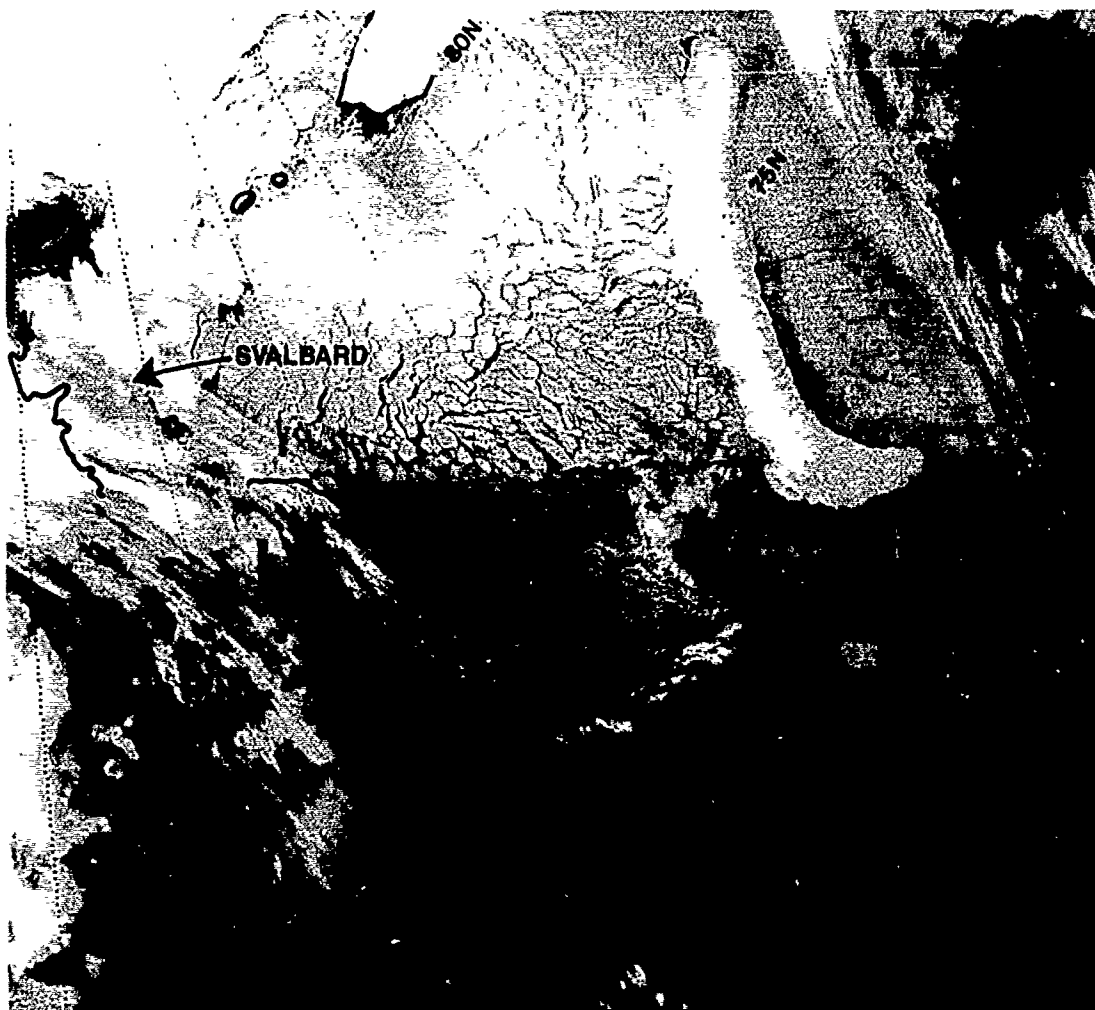
Although the ice edge is not clearly delineated in this image because of cloud obscurations its limit is closely defined by the overlay superimposed on Fig. 1D-17a. The position of the arctic front is also indicated on the overlay.



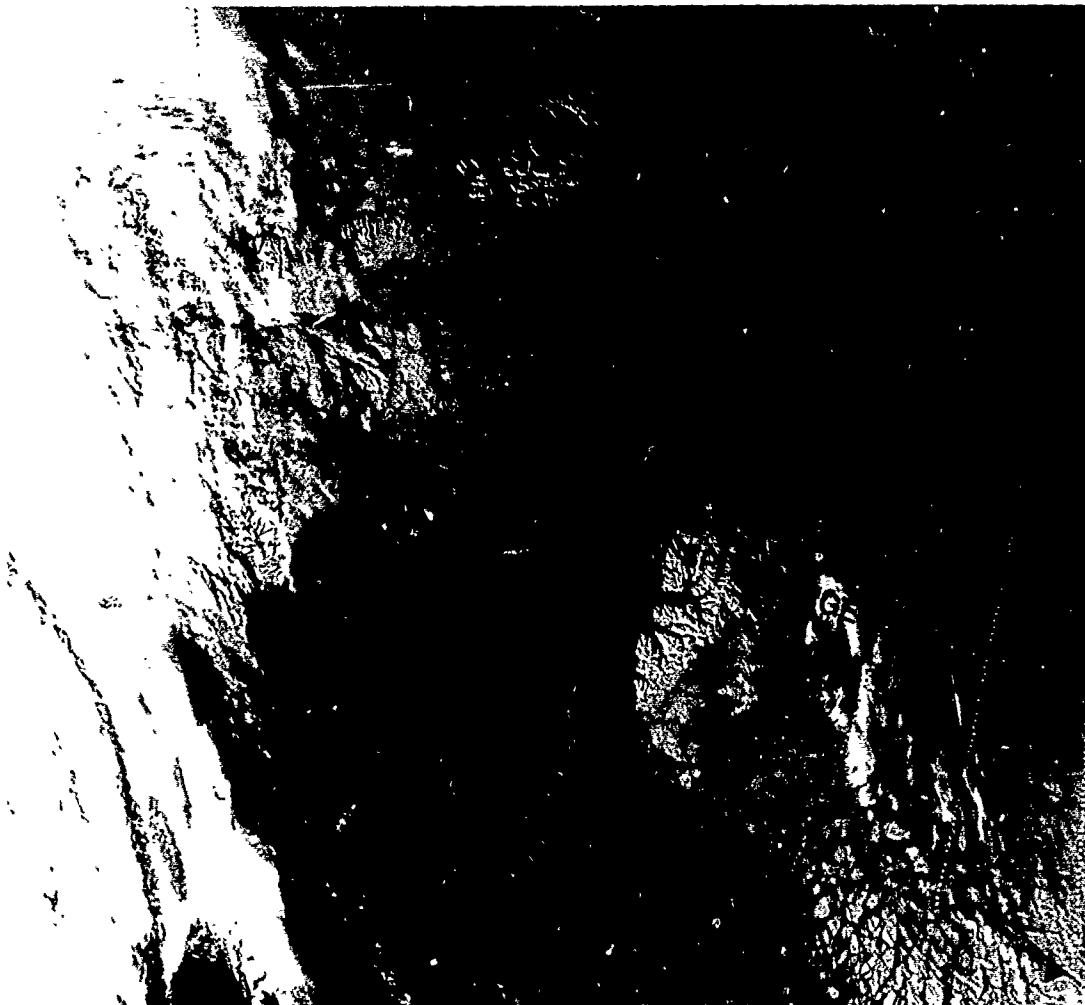
1D-17a. NOAA-9 Infrared (Ch 4) HRPT Data and Overlay. 0533 GMT 7 April 1987.



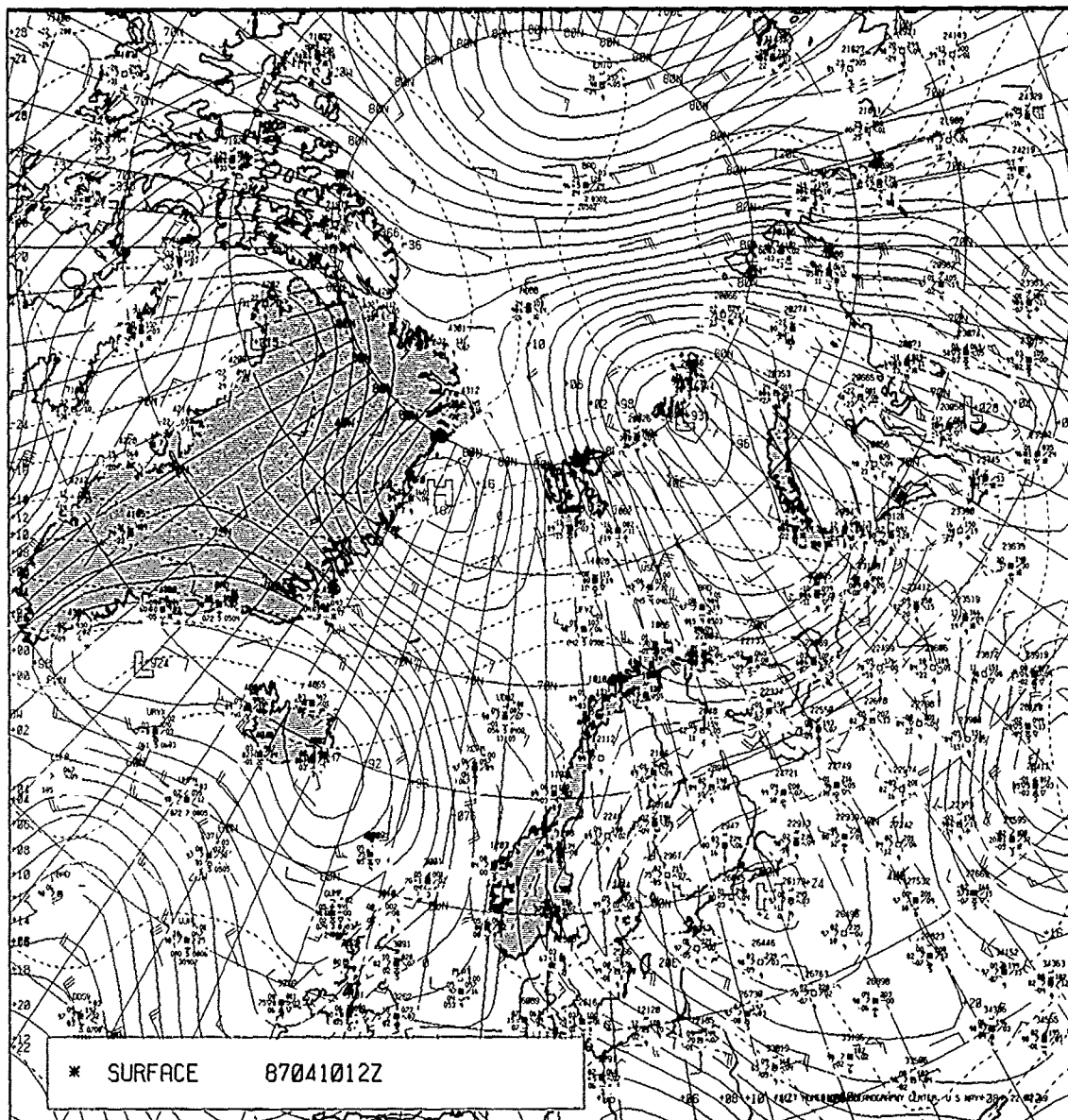
1D-18a. NOAA-10 Infrared (Ch 4) HRPT Data and Overlay. 0715 GMT 8 April 1987.



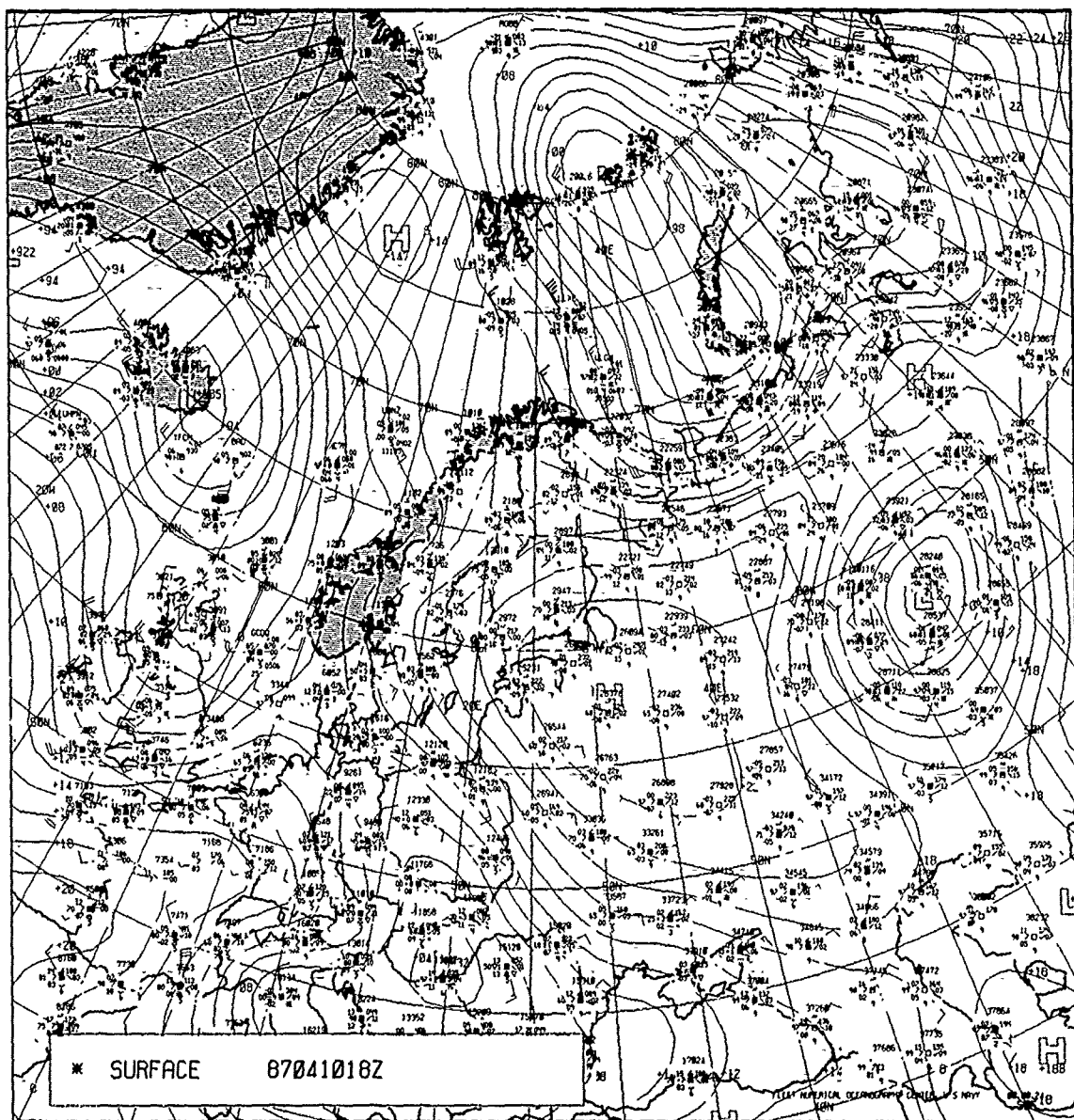
ID-19a NOAA-10 Infrared (Ch 4) HRPT Data. 0653 GMT 9 April 1987.



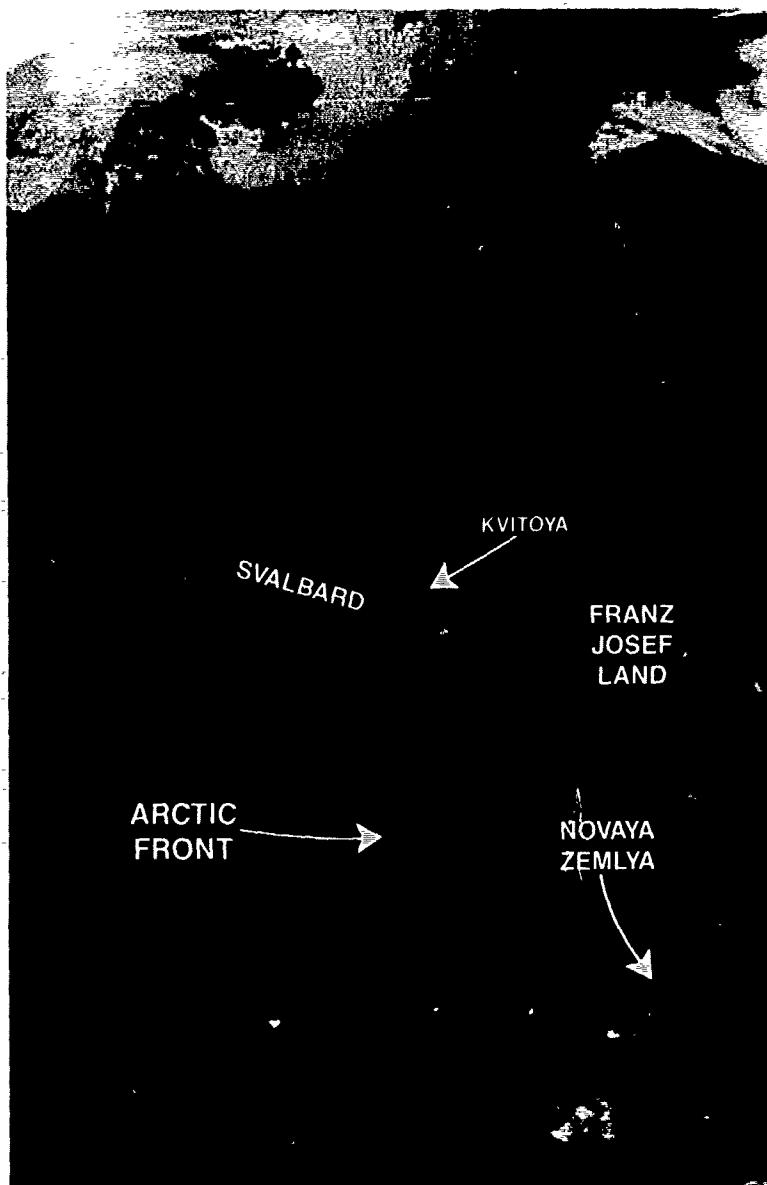
1D-20a NOAA-9 Visible (Ch 2) HRPT Data. 1140 GMT 9 April 1987



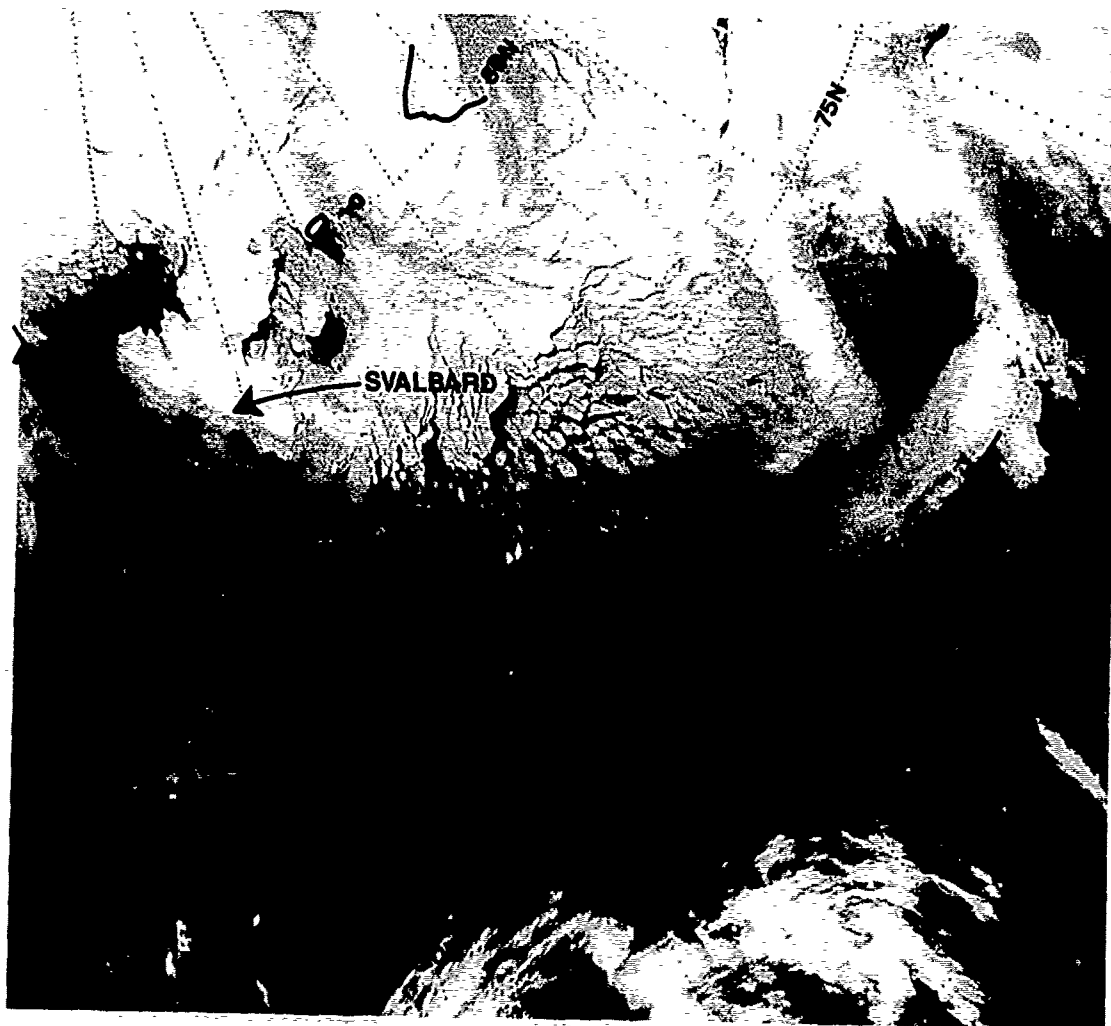
ID-21a. FNOC Surface Analysis. 1200 GMT 10 April 1987.



1D-22a. FNOG Surface Analysis. 1800 GMT 10 April 1987.



1D-23a. NOAA-10 Infrared (Ch 4) Data. 0930 GMT 11 April 1987.



1D-24a. NOAA-9 Infrared (Ch 4) Data. 0258 GMT 12 April 1987.



### *Case 3 Off-Ice Flow From the Greenland Marginal Ice Zone*

#### *Off-Ice Flow With Cold Air Aloft*

In the typical cold surge example cumulus cloud lines are generated as the cold air over the ice pack flows out over much warmer water. The flux of heat and moisture from the ocean into the cold air drives a vertical circulation of air into the base of the clouds with sinking motion between adjacent cloud lines. Typically, the height of the base of the mixed layer increases downstream over the water and individual cloud element sizes become larger in the same downstream sense.

Under conditions of cold temperatures aloft enhanced convection occurs almost immediately at the beginning of the cloud line and the usual growth of cloud element size downstream is not observed.

*7 July 1984*

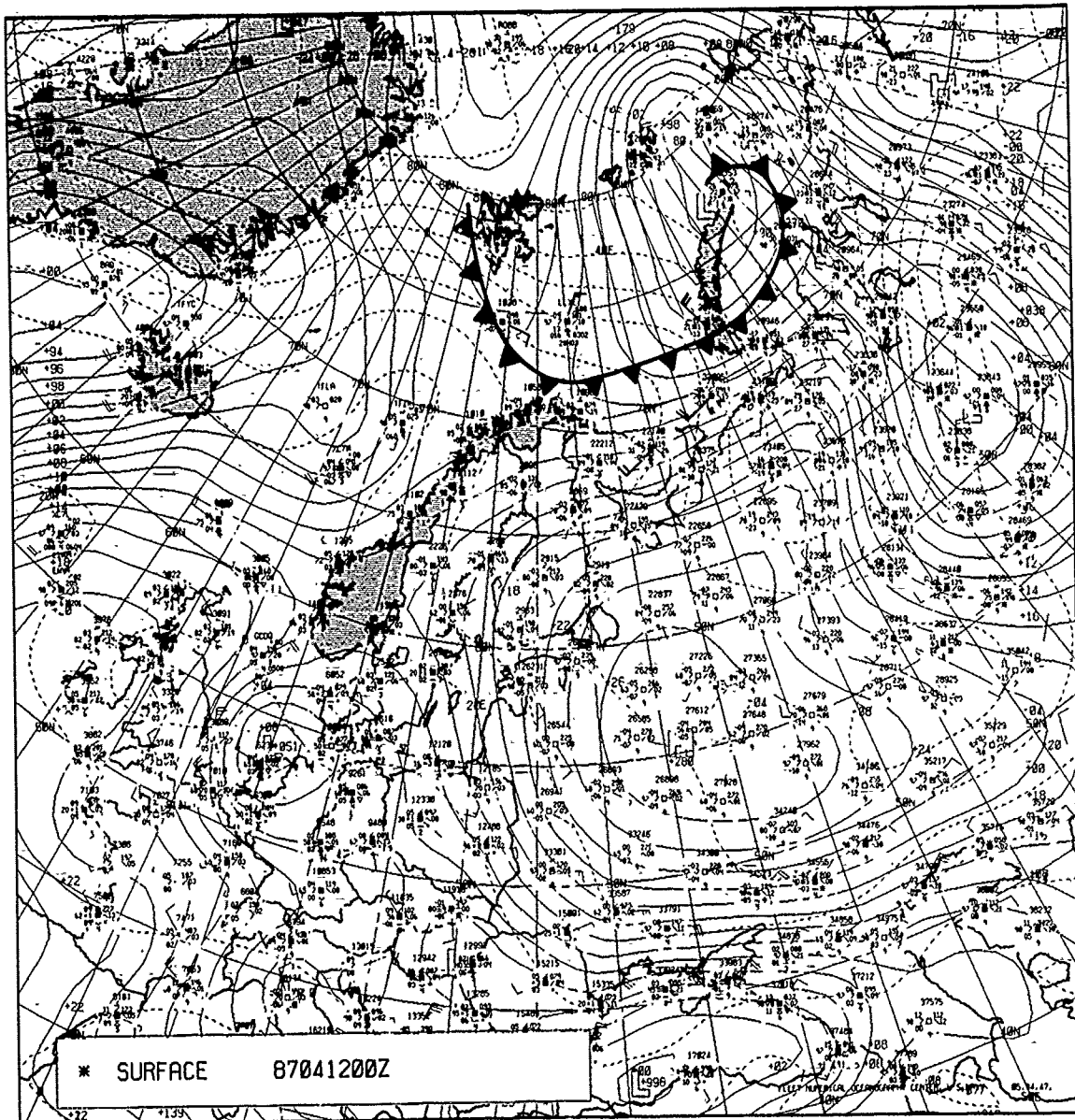
DMSP visual (LS) data taken at 0647 GMT (Fig. 1D-26a) show the area between Greenland and Scandinavia.

A large cloud plume curves cyclonically over Waltershausen Glacier and extends out over the Greenland Sea. This plume apparently formed as northwesterly flow was lifted up over the 6000-8000-ft mountains that surround the glacial area (Fig. 1D-27a). Curvature of the plume implies a trough in the region deep enough to extend through the 700-mb level and the probable existence of an arctic front at that location. Trough presence is confirmed by the 0000 GMT 850-mb analysis (Fig. 1D-28a) and 500-mb analysis (Fig. 1D-29a). A DMSP infrared depiction of the region at 0625 GMT (Fig. 1D-30a) shows that the plume was very cold, indicating an extension to high altitudes.

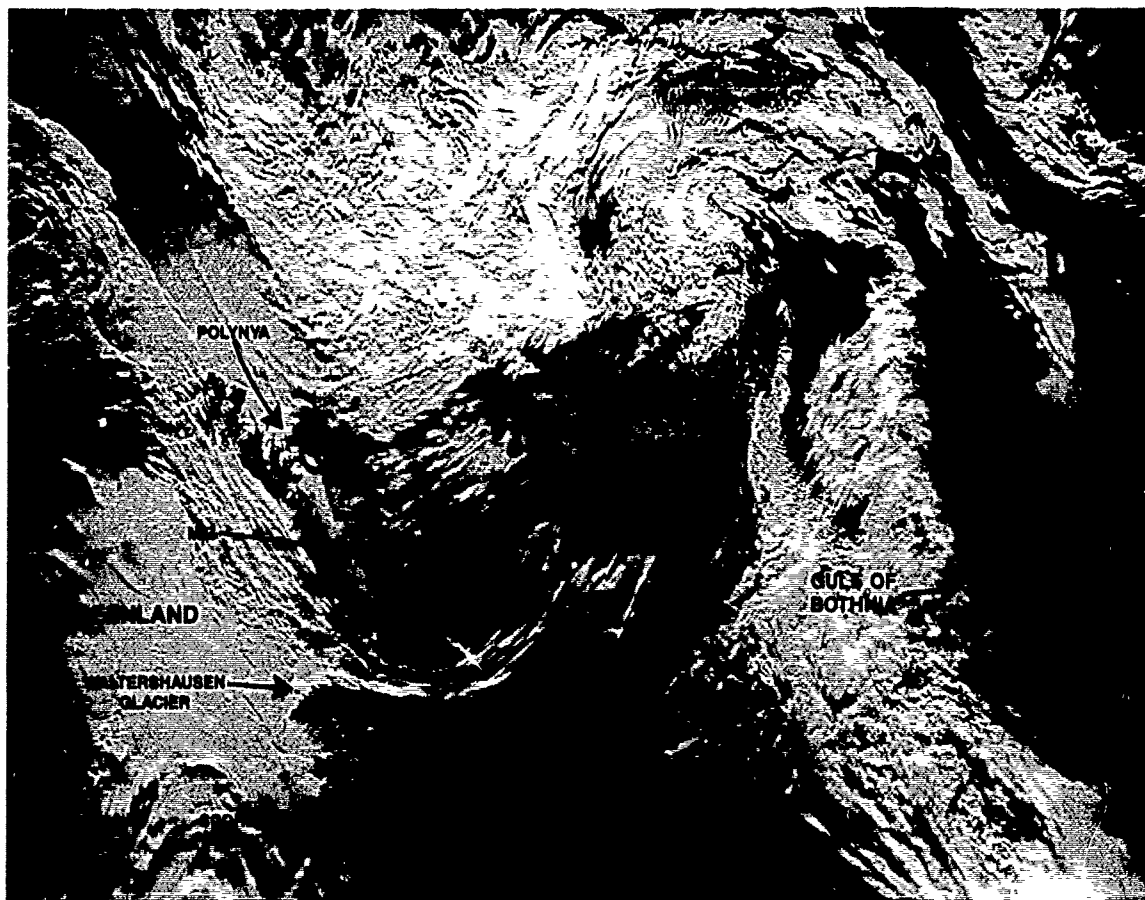
A pool of cold air (temperatures  $< -25^{\circ}\text{C}$ ) is shown over the Fram Strait (between Svalbard and Greenland) on the 500-mb analysis (Fig. 1D-29a). This air happens to overlie a region of off-ice flow, shown clearly in the DMSP depiction of Fig. 1D-26a. Off-ice flow is indicated by convective cloud streaks that begin over the MIZ and extend out over the open water. The edge of the MIZ can be discerned through portions of the sometimes semi-transparent cloud pattern. Cloud production apparently begins where cold air encounters breaks, leads, and polynyi in the MIZ, which is constantly changing in response to wind and current.

The fact that these clouds do not look like the typical cloud formations noted under subsiding cold surge conditions can be attributed to the cold conditions aloft. Air parcels, warmed and moistened by exposure to open water, upon rising, would tend to accelerate upward by being warmer and less dense than the surrounding air. Upon condensation latent heat release would contribute to further upward movement or convective buildup. Note in Fig. 1D-30a that the cloud line region exhibits cold temperature characteristics of midlevel to upper levels. This logic can be applied in reverse, deducing, through the appearance of cloud lines in satellite data, the presence of such cold upper level conditions (which also tend to be associated with upper level troughs).

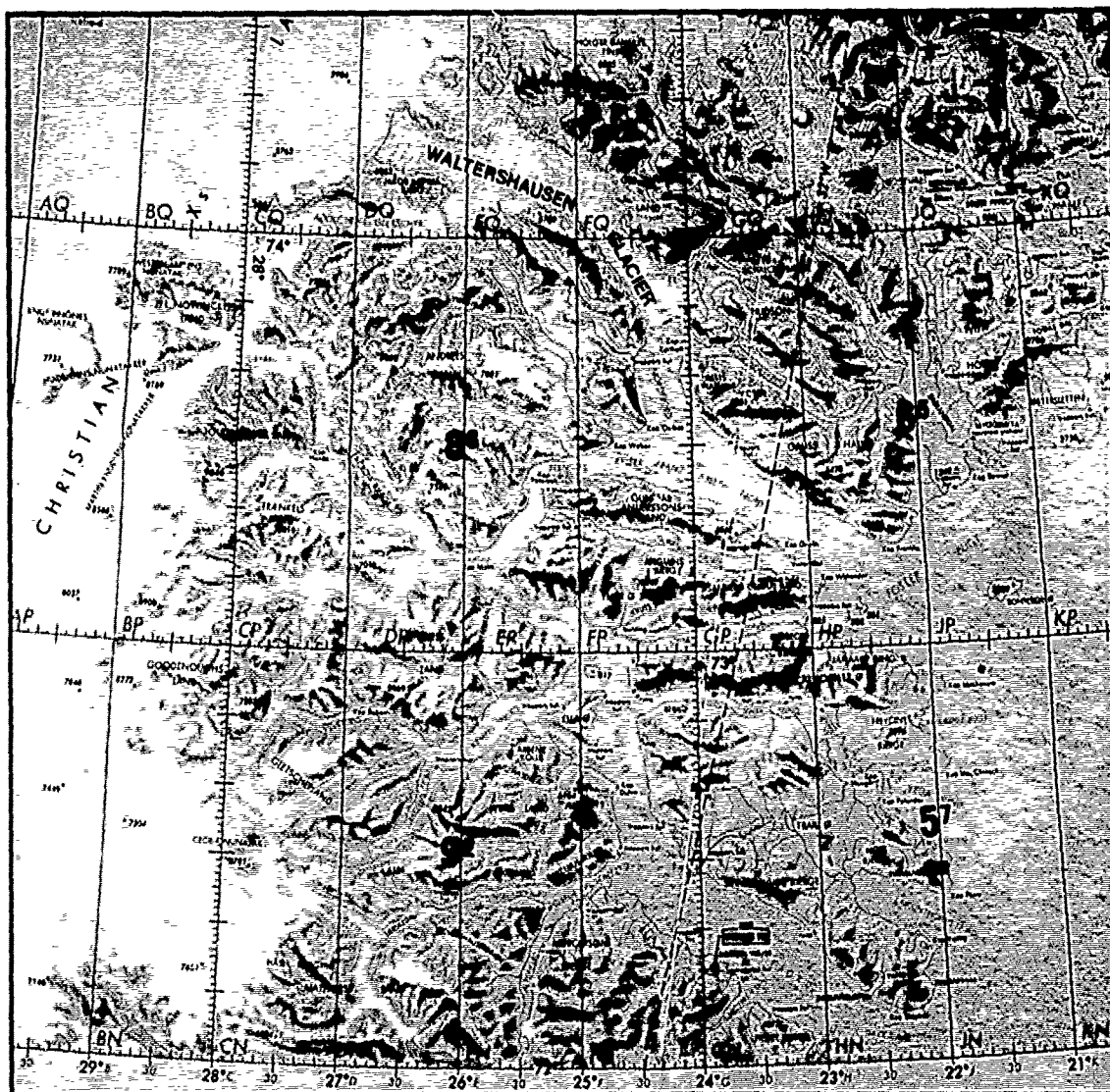
The surface analysis for 0600 GMT (Fig. 1D-31a) is interesting in that it shows a strong north/south-oriented packing of isobars through the Fram Strait. The isobars are oriented nearly normal to the cloud line orientation and to the direction of actual low-level flow, judging by wind reports on the surface analysis and implications of the cloud line orientation in the satellite data.



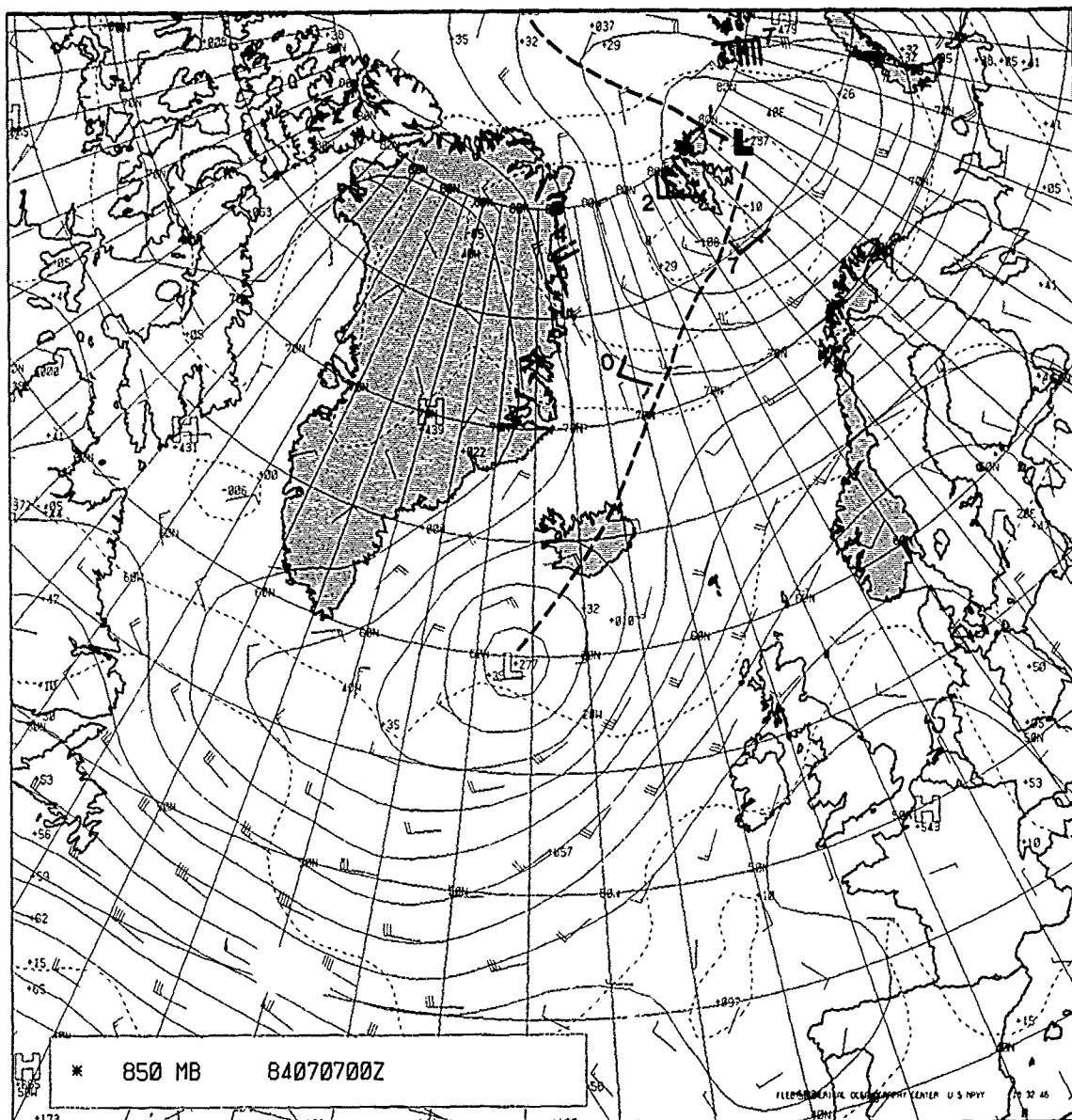
1D-25a. FNOC Surface Analysis. 0000 GMT 12 April 1987.



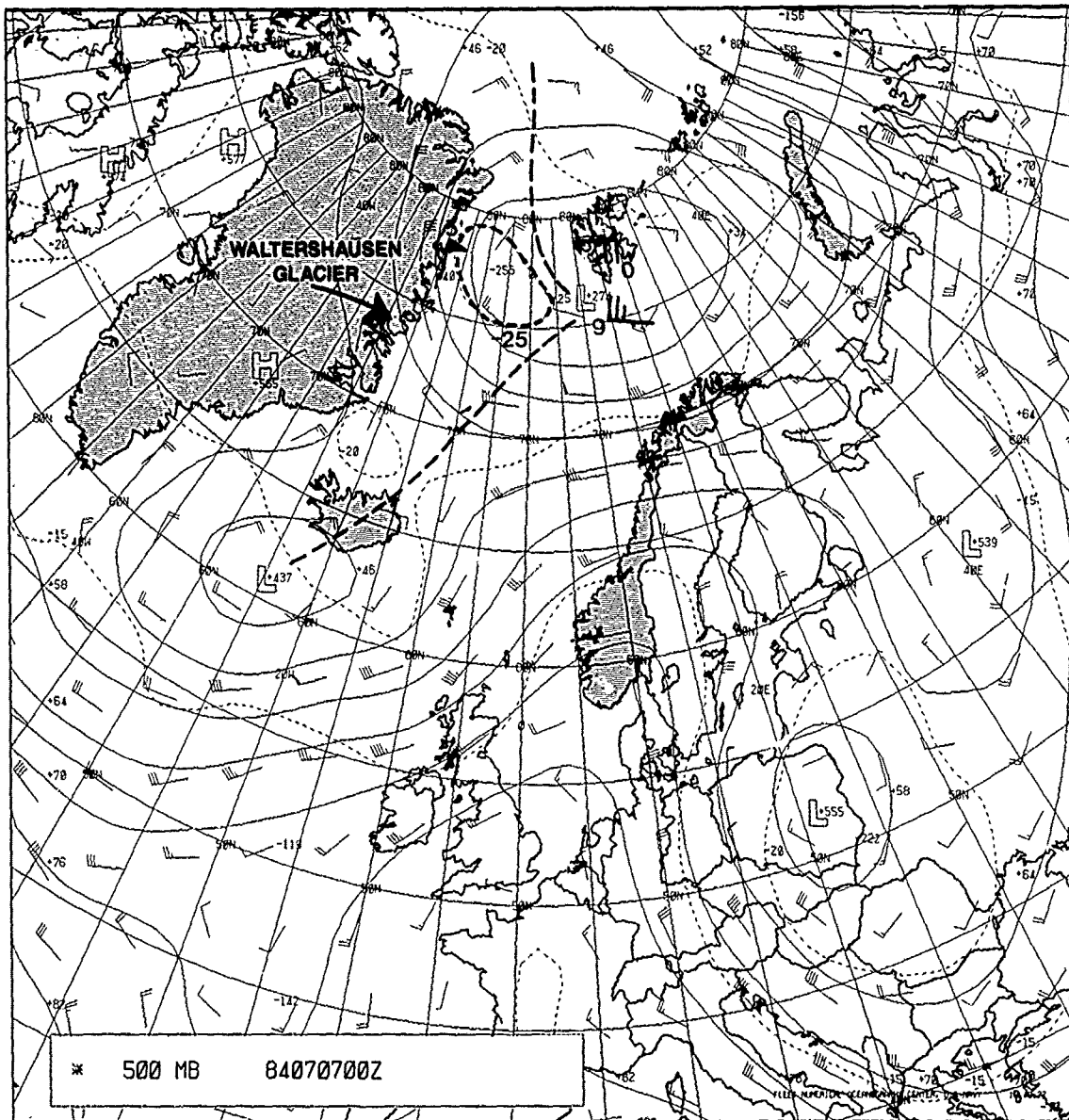
1D-26a. DMSP Visible (LS) Data, 0647 GMT 7 July 1984.



ID-27a. Greenland Eastern Coastal Features.



ID-28a. FNOC 850-mb Analysis. 0000 GMT 7 July 1984.

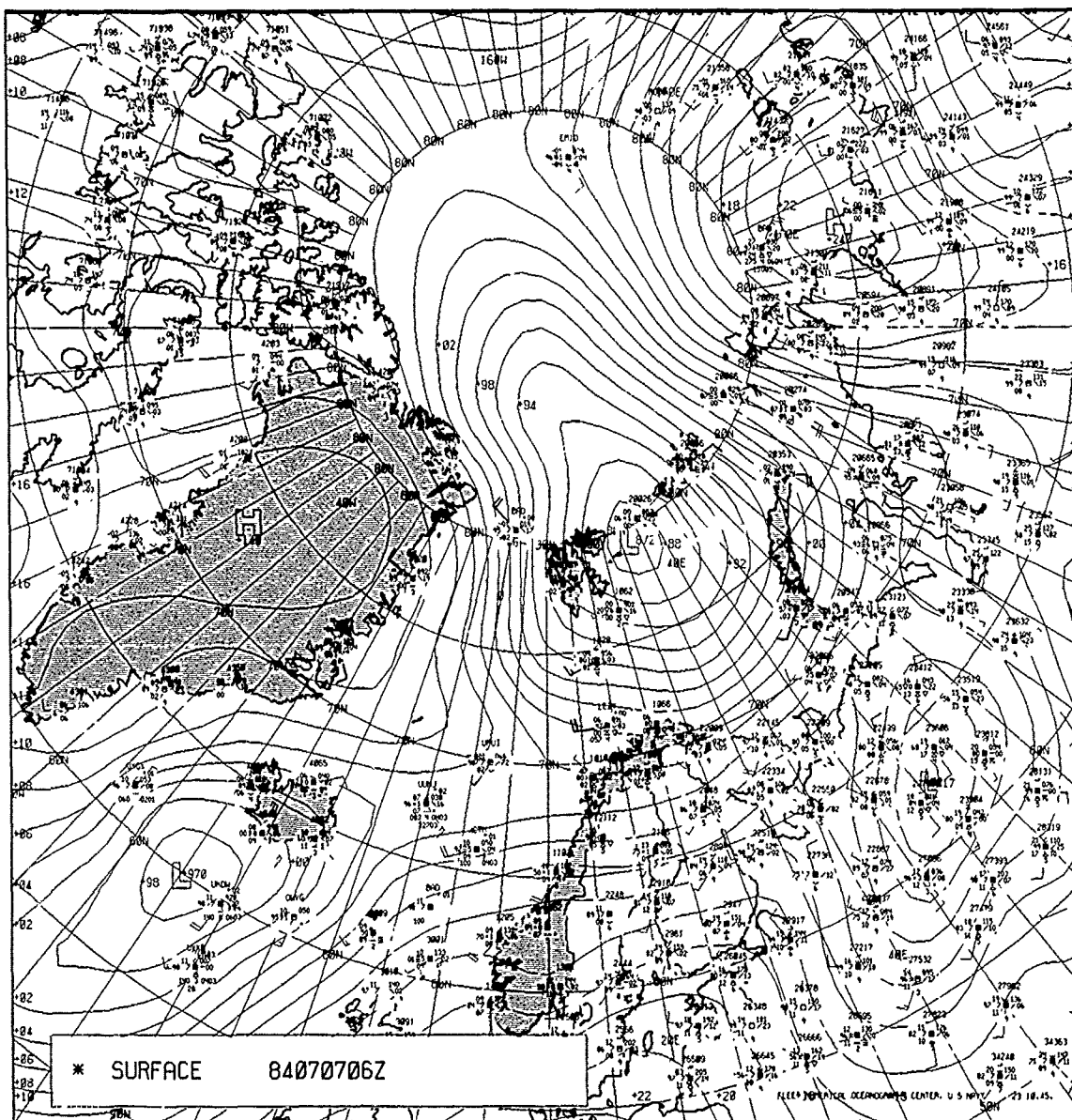


ID-29a. FNOC 500-mb Analysis. 0000 GMT 7 July 1984.



1D-30a DMSP Infrared (TS) Data, 0625 GMT 7 July 1984.





1D-31a. FNOC Surface Analysis. 0600 GMT 7 July 1984.



The most logical cause for such strong cross-isobaric flow is a downward flux of momentum from aloft (from the 850-mb level or higher). Such vertical mixing is implied by the convective nature of the cloud lines in this example. Referring to the 850-mb (Fig. 1D-28a) and 500-mb (Fig. 1D-29a) analyses it can be seen that the flow pattern at those levels becomes much more westerly and more aligned with the cloud lines shown in the satellite imagery.

It may be concluded that whenever cloud lines or wind barbs in the Arctic show strong cross-isobaric flow, unstable conditions exist and there is a strong probability that the area is under the influence of an upper cold trough or low. Conversely, the more typical cold surge effects are stable events; in these examples cross-isobaric flow at the surface should not be extreme (i.e., the cross-isobaric angle of flow should be  $< 30^\circ$ ) and the winds should veer with height on passing through the inversion.

One final interesting feature in Fig. 1D-26a is the clear slot over the pack ice that extends in a northerly direction from the northeastern tip of Greenland.

The precise cause of this feature is not known—almost no observations except the satellite evidence exists in that region. The 500-mb (Fig. 1D-29a) upper level trough overlies this feature and may be a source of subsidence into the slot. At the surface (Fig. 1D-31a) the clear slot is located in the tight pressure gradient region, which is causing an advection of cold ice cap air down to the coastline of northeastern Greenland. Note that the first cyclonic turning of cloud streaks occurs where the cold arctic air crosses a polynya off the northeast corner of Greenland. Additional cloud lines develop as the cold air moves southward over the MIZ. As discussed earlier, the downward transfer of momentum from winds at upper levels appears to be the cause of the turning of northerly winds coming down the clear slot to west-northwesterly winds in the cold air outbreak over the MIZ and the northern Greenland Sea.

#### Important Conclusions

1. Cross-isobaric low-level flow in the Arctic commonly implies strong vertical mixing and the presence of a cold upper level trough or low over the region.
2. Cloud lines and cloud plumes are often excellent indicators of flow direction at a particular level.
3. The source region for westerly off-ice flow noted over the MIZ of northeastern Greenland can be the Arctic ice pack near the North Pole rather than Greenland itself. Northerly flow, in this case, is deflected to westerly flow by a downward transfer of westerly wind momentum components from aloft.

Figure 1E-2a shows an almost perfectly developed example from the Southern Hemisphere acquired over the Indian Ocean on 7 June 1984 at 0538 GMT (north is to the top of the figure). A suggested streamline analysis, based only on the satellite data, is shown in Fig. 1E-3a. The pattern in the Southern Hemisphere is formed by a core of southerly flow that splits into a low on the right side and a high on the left side in a perfectly balanced composition. The top of the formation is capped by a deformation zone or col. Relative positions of the high and low are reversed in the Northern Hemisphere.

An example of this type of flow pattern on a much smaller and less developed scale is shown in NTAG, Vol. 1, Sec. 2B (Fett and Bohan, 1977). In that example a plume of smoke from a forest fire near Los Angeles, driven by Santa Ana winds, split over the ocean in a similar fashion.

In the present instance an example of such a formation is found over Scandinavia and the Bering Sea.

### *Case 1 A Summer Fleur-De-Lis Cloud System Pattern Norwegian/Barents Seas*

*14 July 1984*

DMSP visible (LS) data acquired at 0215 GMT (Fig. 1E-4a) shows the area between Greenland and Novaya Zemlya. Much low-level cloudiness covers the Greenland, Norwegian, and Barents Seas suggesting the presence of high pressure over much of the region. The only really clear area of ocean is seen southwest of Novaya Zemlya. The land area of Russia south of the Kara Sea is also remarkably clear with sunglint illuminating the Usa River in the region from west Usa to west Vorkuta. The river has its source in the western foothills of the Ural Mountains. The clearness of the area suggests that the major high pressure center or ridge should be in that region.

A well-defined cyclonic cloud system centered near the Gulf of Bothnia appears southwest of the suspected high center near Novaya Zemlya.

The FNOC surface analysis for 0000 GMT (Fig. 1E-5a) shows major synoptic features. A high is found near the southern tip of Novaya Zemlya. A ridge line extends from the high westward across Svalbard and into central Greenland. A ridge also extends southward from Novaya Zemlya into Russia.

The low center is shown near the Gulf of Bothnia. The adjacent positioning of the high and low in this fashion suggests the fleur-de-lis pattern. In this example the low is fully developed and apparent as a vortex. The high is not as obvious as in Fig. 1E-2a, the Southern Hemisphere case, but is manifested by clear skies and a surrounding suppressed region of stratus-type clouds. The southerly flow can then be visualized coming in from south of the Usa River, turning cyclonically into the low and anticyclonically around the high. The long streaks of clouds apparent to the west of Novaya Zemlya represent the cap of the fleur-de-lis pattern where an asymptote of convergence should be found.

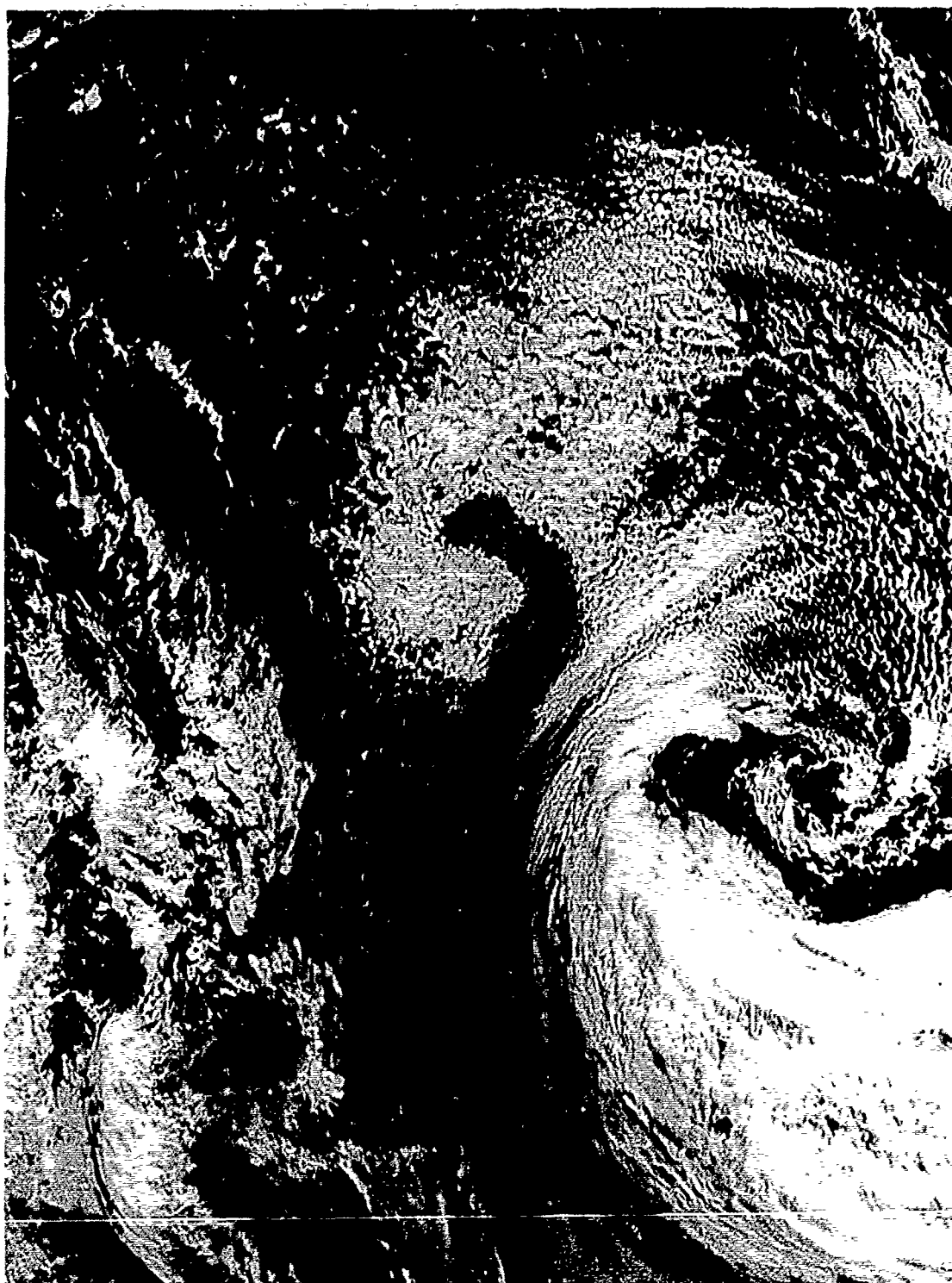
Wind observations from the surface analysis (Fig. 1E-5a) indicate that a col region exists between Svalbard and Novaya Zemlya and that an asymptote of convergence could be drawn somewhere in that region.

The pattern on the 850-mb analysis for 1200 GMT (Fig. 1E-5b) is especially evident as shown by the streamlines superimposed over that figure. The position of the asymptote of convergence on this example corresponds closely to the position of the cloud streaks shown in Fig. 1E-2a.

## *1E The Fleur-De-Lis Cloud System Pattern*

### *Deformation Zone Analysis*

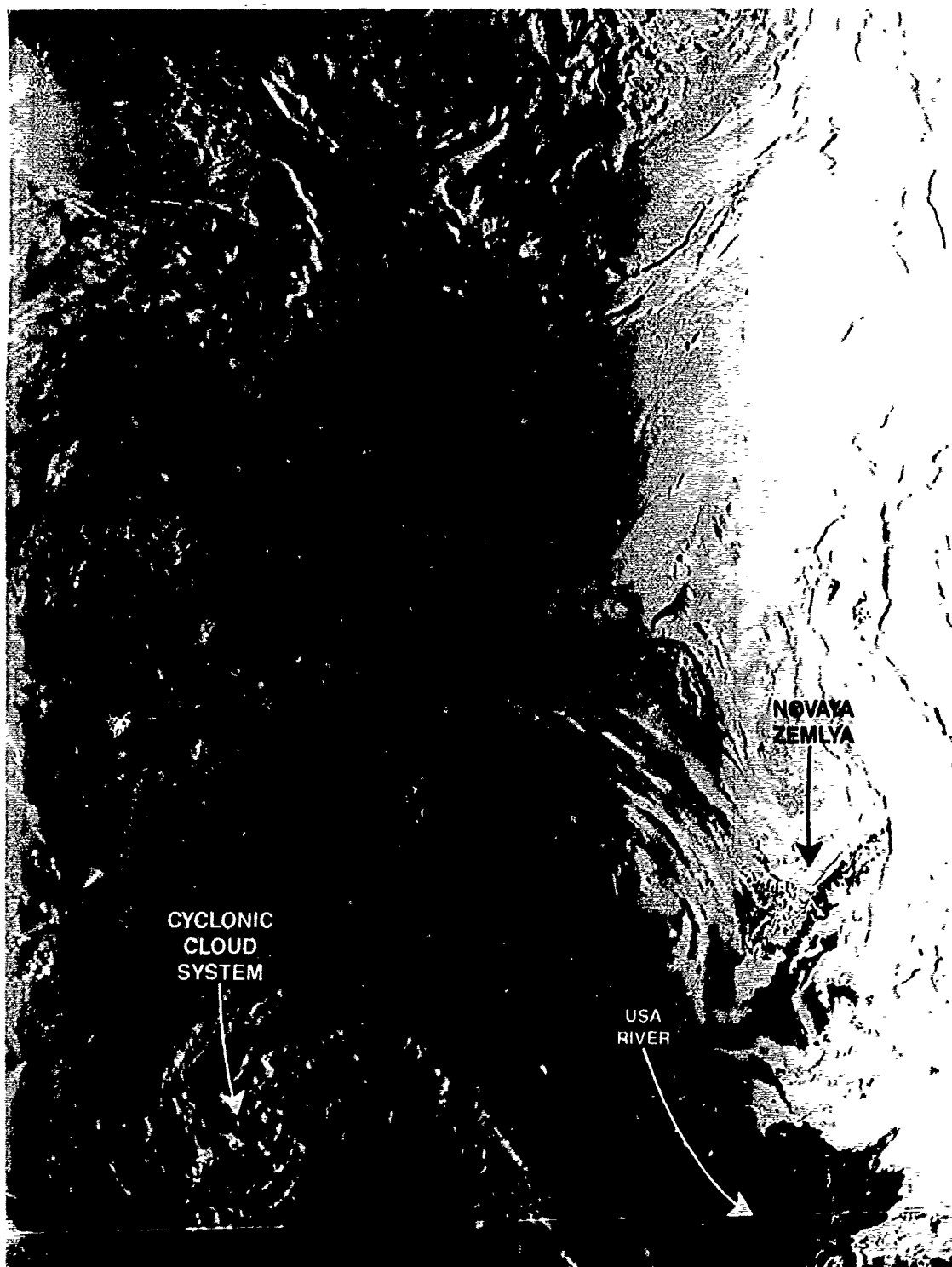
There is a pattern of cloud system formation that is seen quite frequently in satellite data in several scales of magnitude. The pattern is associated with deformation zones in both the atmosphere and the ocean. The pattern was referred to as a "fountain-like pattern" by Weldon (1979) and in its fully developed form resembles the fleur-de-lis—the coat of arms insignia of the former royal family of France. This symbol has a central plume with curved petals on either side, the left-hand petal turning counterclockwise and the right-hand petal turning clockwise (cyclonic and anticyclonic).



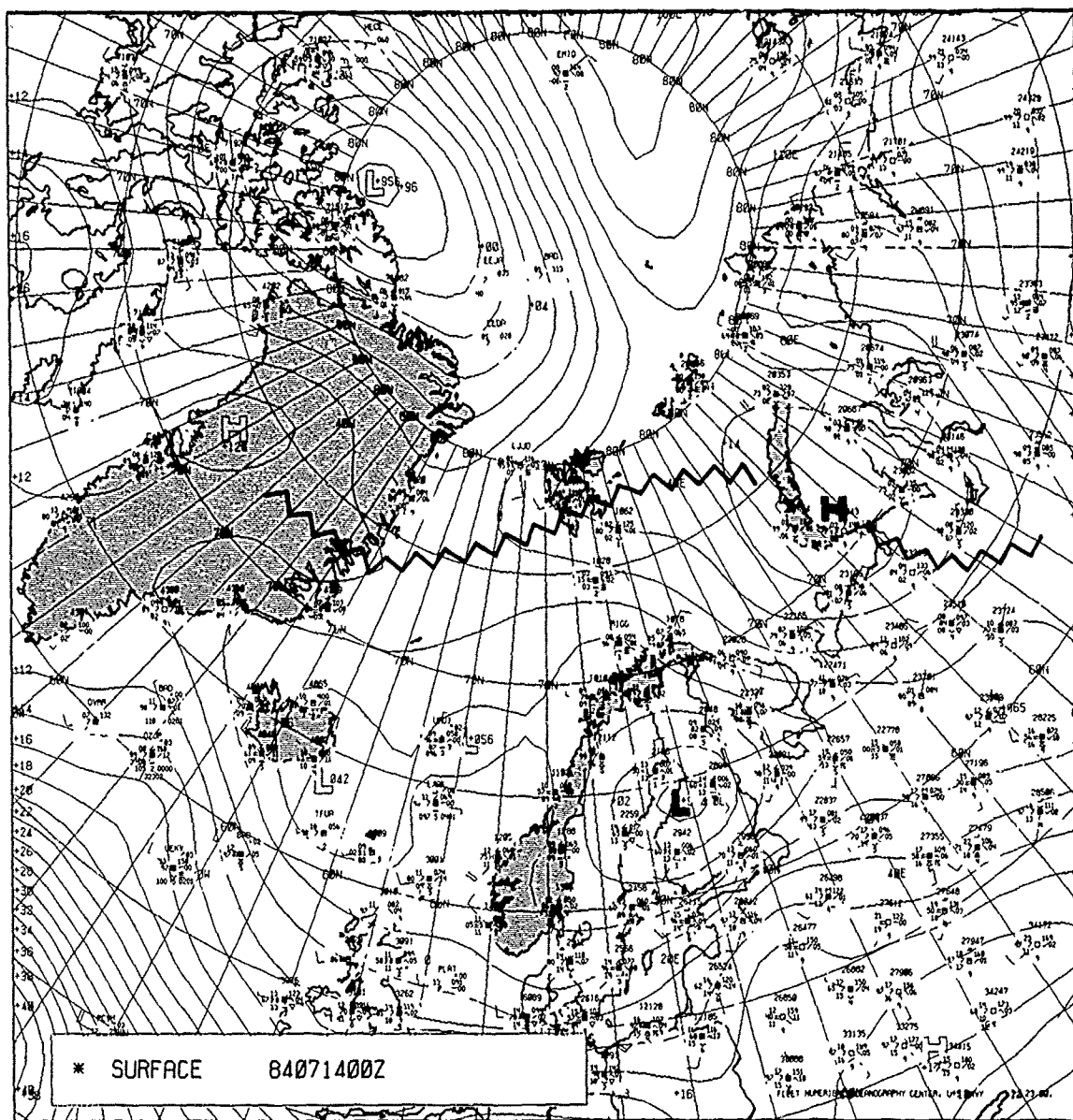
1E-2a. DMSP Visible (LS) Data. 0538 GMT 7 June 1984.



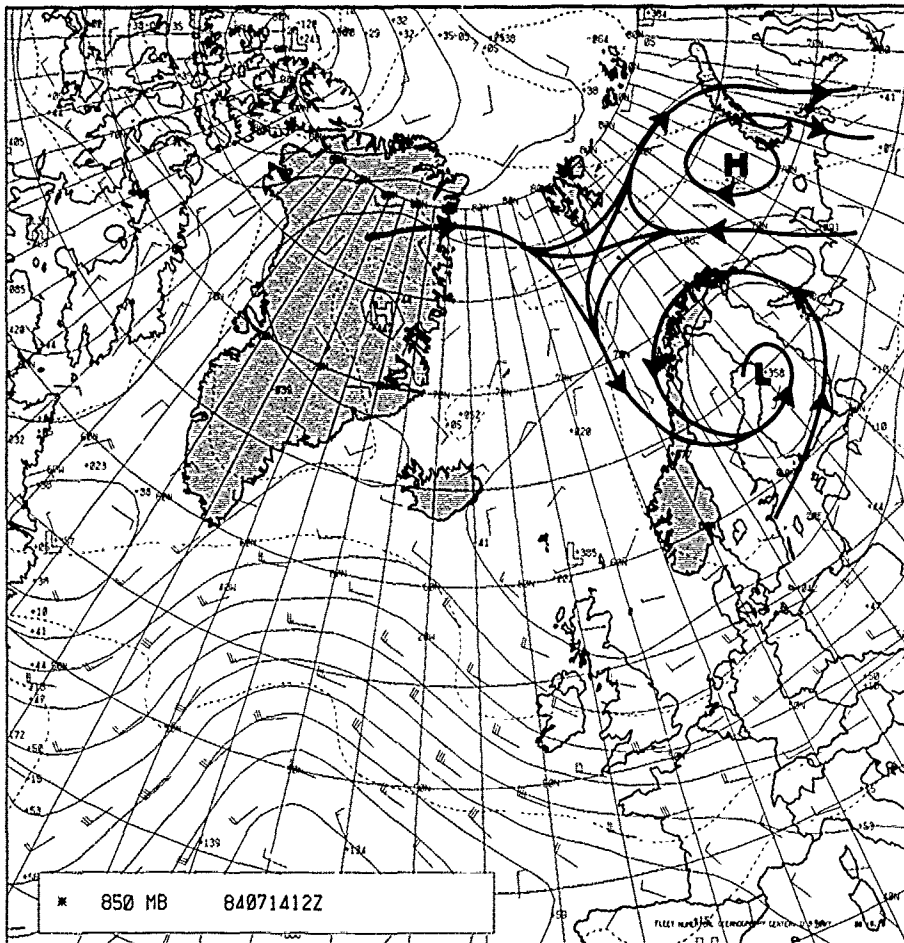
1E-3a. DMSP Visible (LS) Data and Streamline Analysis. 0538 GMT 7 June 1984.



1E-4a. DMSP Visible (LS) Data. 0215 GMT 14 July 1984.



1E-5a. FNOC Surface Analysis. 0000 GMT 14 July 1984.



1E-5b. FNOC 850-mb Analysis. 1200 GMT 14 July 1984

#### Important Conclusions

1. The fleur-de-lis cloud system pattern is a recurring pattern apparent in satellite imagery in a variety of scales.
2. Knowledge of the attributes of this pattern enables the satellite meteorologist to understand flow patterns with a high degree of accuracy over areas of little or no conventional information.

#### References

- Fett, R.W. and W.A. Bohan, 1977: Navy Tactical Appl. Guide, Vol. 1, *Techniques and Applications of Image Analysis*, NEPRF Technical Report 77-03, Naval Environmental Prediction Research Facility, Monterey, CA 93943-5006, 176 pp.
- Weldon, R., 1979: Satellite Training Course Notes, Part IV, *Cloud Patterns and the Upper Air Wind Field*. Applications Division, National Environmental Satellite Service, NOAA, Washington, DC., 79.



Fig. 2A-2a shows an example of a reversed shear configuration on 1 November 1985. The figure shows an analysis of the 1000-mb height contours (solid lines) indicating a low over the Norwegian Sea. The 1000- to 850-mb thickness analysis (dashed lines) reveals that the thermal wind west of the low center is southerly (parallel to the thickness lines, with cold air to the left). The thermal wind, then, opposes northerly low-level flow about the low center.

The importance of a pre-existent low-level condition maximizing vorticity in polar low development was discussed by Rasmussen (1985) and because of its importance is quoted below:

"As already mentioned, polar lows develop in different synoptic situations. A common feature for all these developments, however, seems to be that low-level relative vorticity is present in the area prior to the development. We may think therefore of a basic mechanism for *all* polar low development working in the following way. First low-level vorticity is formed in one way or another, depending on the actual place and situation. If then it is possible for deep convection to proceed, then CISK can take over and through a rapid development concentrate the already available vorticity into a polar low."

The term "CISK," an acronym for "conditional instability of the second kind," is described very clearly in the following quote and illustration from Rasmussen:

"CISK in its most simple way works in that way that convection associated with an initial small perturbation, i.e., a small low at the surface, will heat the surrounding atmosphere, which is assumed conditionally unstable. The heating will cause a local high pressure at upper levels from which the air will diverge (Fig. 2A-2b). Provided this upper level divergence is stronger than the low-level convergence, further pressure fall will result at the surface, i.e., the initial small low will deepen. This again results in increased convergence at low levels, especially in the boundary layer towards the center of the low so that the convection will increase, i.e., a positive feedback process is possible."

When surface observations are available in the region of polar low development an analysis of the 3-hr pressure change reveals falling isallobaric patterns ahead of the low and strong rises to the rear. Fig. 2A-3a shows such a pattern in the area where a polar low developed near 70°N, 0° at 1200 GMT on 1 November 1985. Six hours later (Fig. 2A-3b) the pattern is even more pronounced as the pattern and storm are displaced southward. Note, as is typical in a polar low development, that the polar low is on the periphery or west of the analyzed low center. Very seldom are conventional observations adequate to define the polar low in its initial development.

In the Norwegian report referenced previously the criteria for selecting areas where polar low development is likely are also given. These are:

1. There must be cold air advection at the sea surface.
2. The thickness of the layer 850 to 500 mb must be below 3960 m. This limit should vary with the sea surface temperature: when the sea surface temperature is low, the limit should be lowered.
3. The curvature of the contour lines in the 500- to 700-mb levels must be cyclonic or zero.

It is probable that polar lows develop differently in different regions through either baroclinic instability or CISK and at times through a combination of these processes and others. In the "others" category is a third potential, described by Shapiro *et al.* (1987), in which essentially unmodified cold arctic air moving southward over the ice, turned cyclonically over the water, wrapping itself "about a warm(er) inner air mass, thereby isolating it from its warm air source..."

# Section 2

## *Polar Lows*

### *2A Polar Lows*

Characteristics of Polar Lows ..... 2A-1

Polar Low Development in Association With Boundary  
Layer Fronts ..... 2A-6

### *Case Studies*

1 *Polar Low Development in the Denmark Strait* ..... 2A-10

2 *Polar Low Development in the Greenland/  
Norwegian Seas (13-14 February 1984)* ..... 2A-20

3 *Polar Low Development as a Seclusion Process  
(25-27 February 1984)* ..... 2A-42

4 *Polar Low Development in Association With Boundary  
Layer Fronts (11-13 December 1982)* ..... 2A-74

5 *Polar Low Development on a Track From the North Pole  
to Northern Norway (5-9 June 1984)* ..... 2A-118

6 *Polar Low Development From a Cold Surge in the  
Fram Strait (19-23 December 1983)* ..... 2A-138

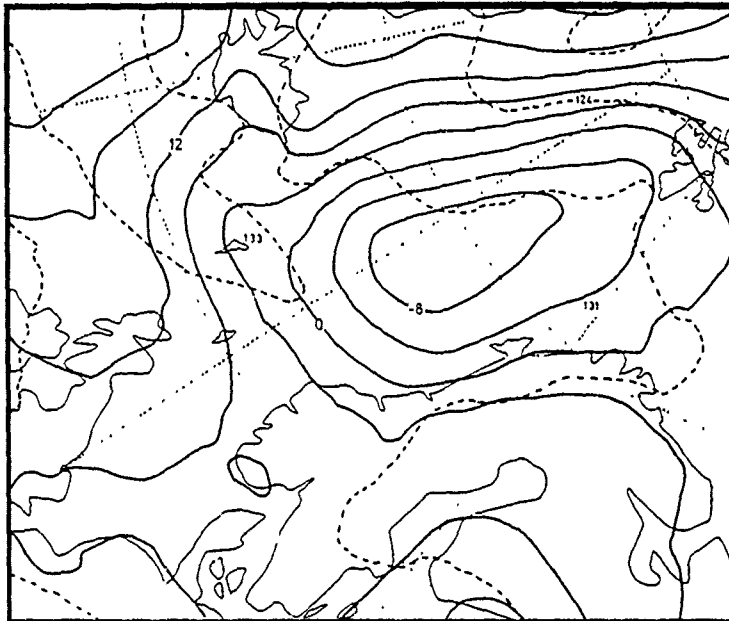
## 2A Polar Lows

### *Characteristics of Polar Lows*

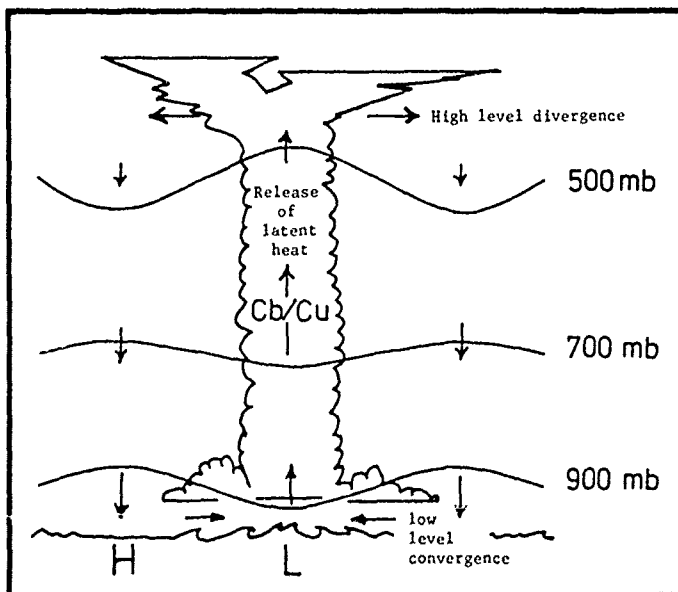
Polar lows are intense, subsynoptic-scale lows that occur generally north of and/or west of the arctic front, on the cold air side of the 500-mb polar jet, and quite often in areas of pronounced low-level cyclonic shear. Polar lows are typified by an atmosphere exhibiting conditionally unstable conditions through the lower troposphere and midtroposphere. Vertical shear in the vicinity of polar lows is generally weak. The geostrophic wind accompanying polar vortices displays this characteristic and tends to back with height. Polar lows differ from midlatitude lows not only in size but often in the mechanism for development, the speed of development and often dissipation, and in their internal structure. The attribute last mentioned is still a subject of some speculation. For example, on the one hand Carleton (1985) concludes that "... a cold core and little vertical tilt distinguish the polar low in the mean." On the other hand Shapiro *et al.* (1987), in their analysis "of the first research aircraft observations of the three-dimensional structure of a polar low," found that "... the polar low possessed a warm inner core, whose layer-averaged thickness temperature exceeded the exterior environmental temperature at 200 km from the low center by 4 K." Temperature analyses at 300 m, 850 mb, and the 580- to 1013-mb thickness all indicated a warm core structure.

Rasmussen (1983) also noted that the polar low circulation is strongest near the surface and weakens upward implying a warm core structure at lower levels. This type of structure agrees very well with the observation that polar lows quite frequently develop in reversed shear atmospheric conditions. In reversed shear the thermal wind in the lower troposphere opposes the surface flow. Opposition can be established in a number of ways. Quite commonly it occurs when a cold pool of air moves to the south of a surface low.

In that type of configuration westerly low-level flow around the vortex is opposed by an easterly thermal wind component. The Norwegians (Midtbo *et al.*, 1986) note that "Investigations on the growth of baroclinic waves are generally dealing with occasions when the thermal wind and the progression of the disturbance are in the same direction. In case of a reversed shear flow the baroclinic instability takes place in a different way. The wind at the steering level is northerly and directed nearly opposite to the thermal wind." They also note that the surface wind speeds are generally stronger than expected when compared with ordinary unreversed situations.



2A-2a. Norwegian 1000-mb Numerical Analysis From LAM 50, 0000 GMT 1 November 1985. Solid Lines Indicate Height Contours of 1000-mb Level (Each 4 Decameter), Dashed Lines Indicate 1000-850-mb Thickness (Each 4 Decameter).



2A-2b Schematic Illustrating the CISK Mechanism (Rasmussen, 1985).

This process was first described by Bergeron (1928), who termed the process a "seclusion." The importance of the Shapiro study is that the classic definition of a polar low, being one that necessarily develops in a homogeneous cold polar air stream behind the arctic front, is shown to be incorrect, at least in some instances.

Another important mode of development, believed to be of primary importance in the Bear Island region, was advection of an upper level low across the ice edge in the region of pronounced sea surface temperature gradient (Rasmussen, 1985). It is hypothesized that the upper cold core low caused the formation of a polar low of the same horizontal scale through the initiation of convection, which transformed the initial cold core system to a low-level warm core system by the release of latent heat and further development through the CISK mechanism.

Regional differences in polar low appearance from a satellite perspective also suggest variations in the dynamics of polar low evolution. The comma cloud or PVA is the most frequent mode of development in the North Pacific, while variations of a spiral vortex predominate in the North Atlantic. Forbes and Lottes (1985) made a distinction between polar lows and polar vortices based on a deficit pressure consideration. In a study of 133 polar vortices in the North Atlantic, they were able to distinguish nine categories of cloud configurations accounting for differences in cloud patterns, depth, and type (stratiform or convective). Of the nine categories, only categories 1 (comma, deep spiral) and 2 (merry-go-round or ring of vortices) had sufficient deficit pressure (6-mb or greater) to merit the title of "polar low." It was noted, however, that most of the more intense polar lows evolved from less intense categories to the higher category numbers. This condition does not guarantee that all of the low category vortices would evolve to higher categories since many of them originated and existed only briefly before dissipation.

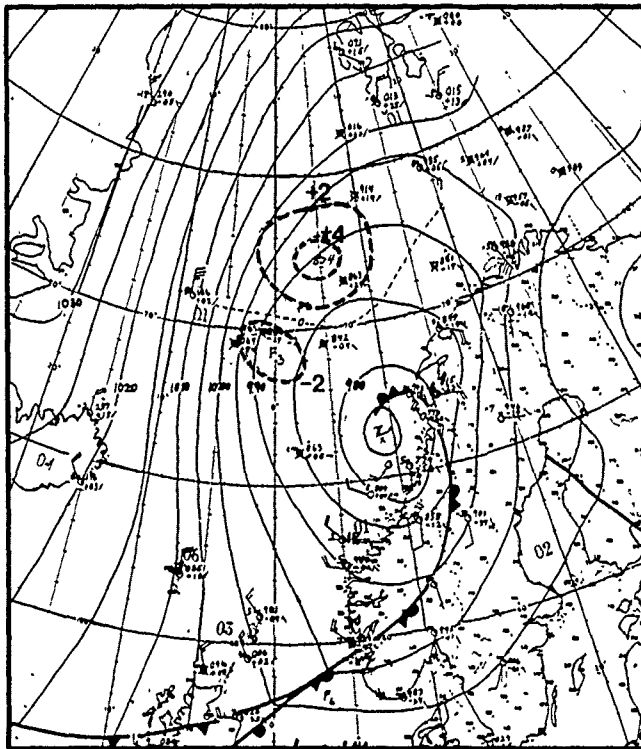
From a climatological point of view, Businger (1985) composited 500-mb data and 1000- to 500-mb thickness fields during outbreaks of well-developed polar lows over the Norwegian and Barents Seas. Results of his studies indicated the tendency for significant negative 500-mb temperature and height anomalies over this region when mature polar lows were present. Ridging simultaneously was dominant over the west coast of Greenland. This produced northerly upper and lower level flow over the Norwegian Sea as much as 3 days prior to polar low development. The northerly flow over warmer waters produced a condition of low static stability and the development of low-level baroclinicity.

Forcing by migratory short waves aloft with strong positive vorticity advection, just prior to polar low development, appeared to be involved in the more intense polar low developments. Businger also suggests that topographic forcing by the high Greenland Plateau may be involved in the development of the negative height anomaly over the Norwegian Sea.

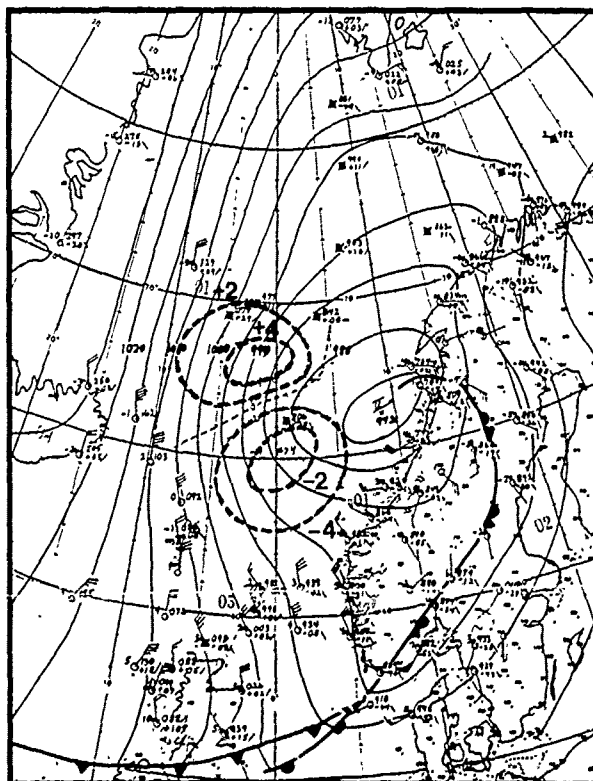
The role of boundary layer fronts (BLF) in polar low development (Fett, 1989) was apparent in a number of examples noted in the Greenland, Norwegian, and Barents Seas. Such fronts developed as cold arctic air moved from over the ice pack onto the relatively warmer water of the open seas. The frontal boundary, often appearing much like a "rope cloud," showed a tendency to develop small mesoscale vortices along its length (and particularly at the southern extremity of a north-south oriented line). Such vortices often failed to develop due to lack of upper level support. However, when an upper cold low or cold trough moved into the regions of BLFs, polar low development often occurred.

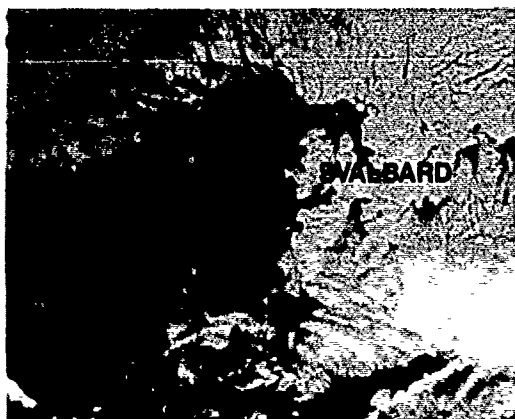
Figure 2A-4a is an example of a BLF moving southward, marking the limit of a cold surge through the Fram Strait on 19 December 1983. A vortex developed along the front on 20 December, and by 21 December (Fig. 2A-4b) polar low development had occurred (see Section 2A, Case 6).

2A-3a. Norwegian Surface Pressure Analysis.  
1200 GMT 1 November 1985.

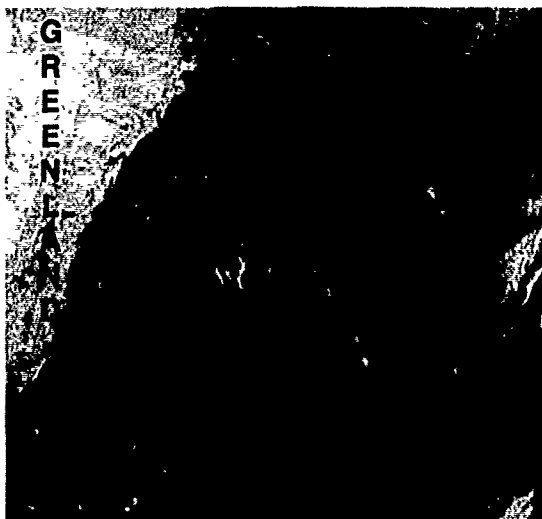


2A-3b. Norwegian Surface Pressure Analysis.  
1800 GMT 1 November 1985.



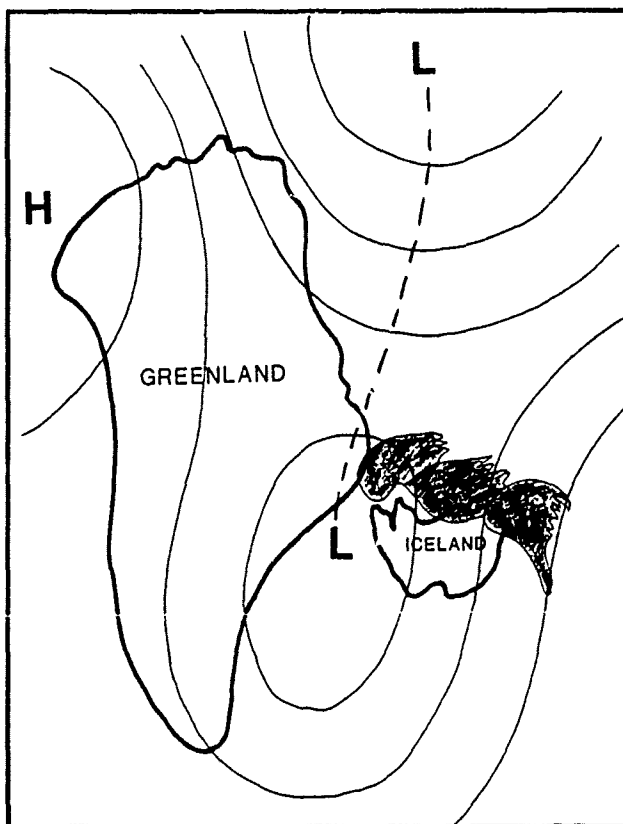


2A-4a. A DMSP Nighttime Visual Image Acquired on 19 December 1983 at 2318 GMT. Svalbard Is in Upper Right Corner of Image.



2A-4b. A DMSP Nighttime Visual Image Acquired on 21 December 1983 at 1913 GMT. Spitsbergen Is in Upper Right Corner of Image.

2A-4c. Precursor Surface Conditions Leading to Polar Low Development.



### *Polar Low Development in Association With Boundary Layer Fronts*

During the Marginal Ice Zone Experiment (MIZEX) of March and April 1987 documentation was obtained concerning the nature and movement of a westward propagating boundary layer front that crossed the Fram Strait (see Section 3C, Case 1). The frontal boundary, apparent as an enhanced north/south-oriented cloud line, was a baroclinic zone separating colder air that had surged off the ice pack and frozen land area of Svalbard in southeasterly flow, from air that had been resident for some time over the Fram Strait. Wind speeds were higher, up to about 25 kt in the southeasterly flow east of the front and lighter in the general northerly flow west of the front. Therefore, vorticity was also maximized at the frontal boundary, which also was positioned in a pressure minimum region that could be analyzed as a col area between two mesoscale high pressure centers or as a sharp inverted trough in isobaric analysis. The boundary layer height was higher, about 2000 m on the east side of the front and lower, about 1000 m west of the front. The area was generally clear of clouds above the boundary layer.

The German research vessel, Valdivia (call sign DESI), measured a 5°C temperature drop crossing the frontal boundary shortly after it had formed just west of Spitsbergen. During the 4-day period of noted frontal movement, mesoscale vortices were observed to form near the southern end or base of the inverted trough. Smaller vortex-like perturbations were also noted forming along the enhanced cloud line that represented the frontal boundary.

Figure 2A-6a shows the frontal zone on 25 March 1987. Note that the area east of the front to the coast of Spitsbergen is covered by a thin low overcast. In this region the cold arctic air was rapidly being warmed and moistened by a warm branch of the Gulf Stream, which extends into the Fram Strait. Light to moderate snow and snow showers were reported in that overcast region.

Figure 2A-7a shows the region again on 26 March 1987 at 1100 GMT. Cloud lines clearly delineate the off-ice flow and southeasterly wind flow direction leading to the frontal boundary. Note at this time that two mesoscale vortices are apparent at the southern end of the frontal boundary. These vortices dissipated fairly rapidly, probably due to unfavorable high pressure conditions aloft.



Based on a number of polar low developments a satellite-observed pattern was identified that enabled a high reliability 24-hr prediction of polar low development (Fett, 1987). A precursor indication was the development of an elongated band of convective cloudiness, normally coinciding with an asymptote of convergence at the surface, leading into a low pressure area. Figure 2A-4c shows an example of such a band based on an actual polar low development. South of the band deep open-celled convections are an indication of an upper cold low or cold trough over the region (Fig. 2A-5a). A streamline analysis at the 500-mb level in this figure shows a tendency for the flow to turn anticyclonically over the convective band. Vorticity advection is also maximized in the region of the band by this type of upper level flow. The cold pool of air south of the band results in a reversed shear situation (described earlier) where the thermal wind opposes any low-level cyclonic circulation. When this configuration is detected polar low development within the band can be anticipated in 24 hr or less.

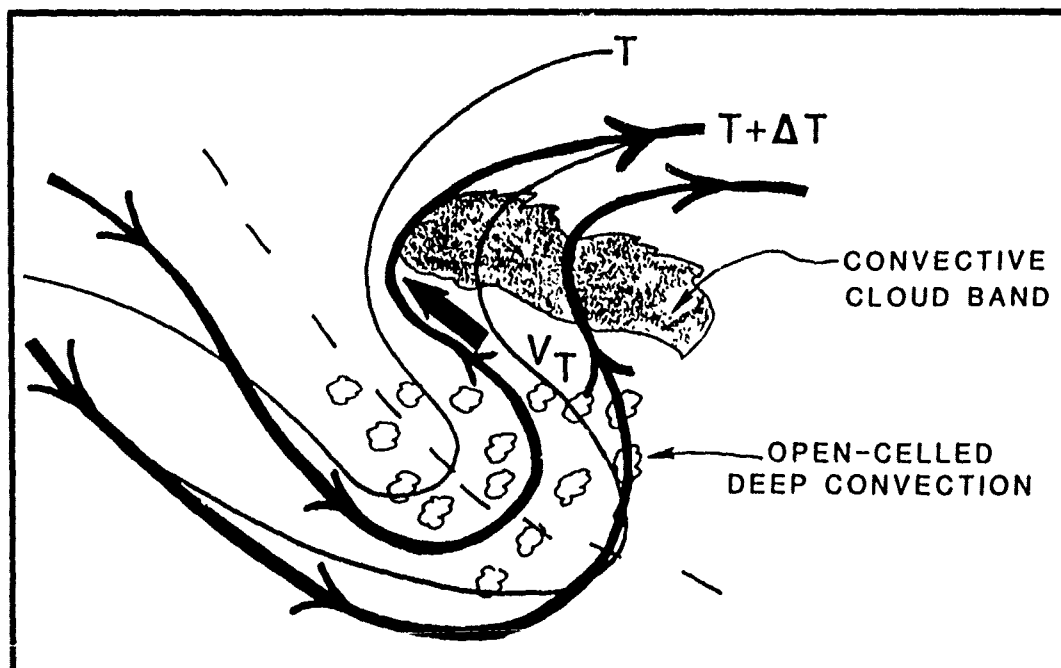
The major differences between developing polar lows and nondevelopers are that the developing storm has more favorable vorticity advection, is positioned in a more baroclinic region, is located in a more northerly latitude, and is typified by a steeper lapse rate, particularly in the 700- to 500-mb layer.

In the seas surrounding Norway polar lows occur most frequently in December and January, with a distinct minimum in February (Wilhelmsen, 1986). Their speed of movement averages  $8$  to  $13 \text{ ms}^{-1}$  over sea and  $15$  to  $20 \text{ ms}^{-1}$  over land. Dissipation proceeds rapidly after landfall, however.

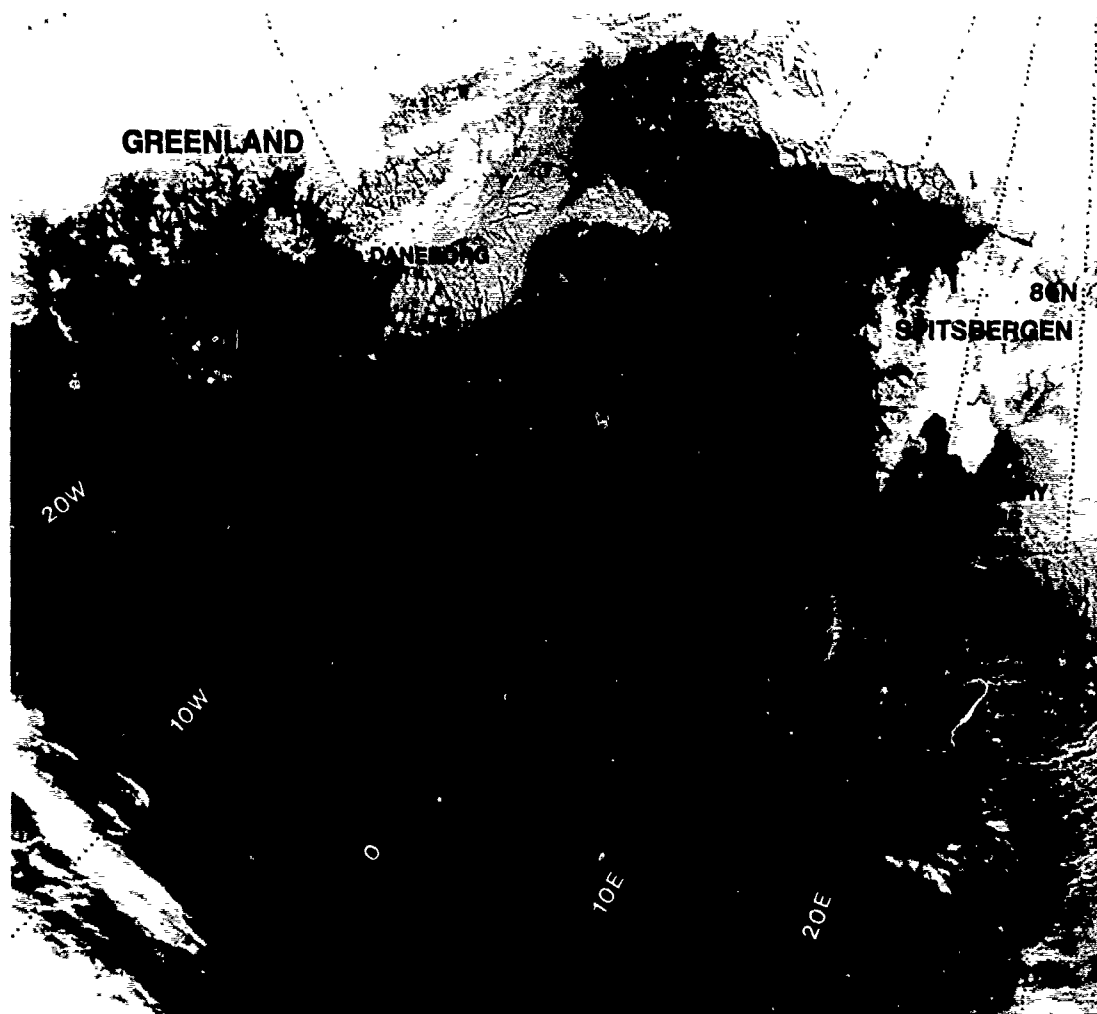
Tracks of polar lows are associated with temperatures of about  $-20^\circ\text{C}$  near points of origin near ice and up to  $0^\circ\text{C}$  over open water. Small pressure drops are noted in advance of polar lows (see Figs. 2A-3a and 2A-3b), with sharp rises occurring in a narrow zone behind the low.

Polar lows are a difficult phenomena to forecast and seldom are forecast by numerical methods. Their life cycle can be completed in as little as 6 to 12 hr, or as long as 2 to 3 days; wind speeds can gust to  $60 \text{ ms}^{-1}$  and seas can build to 15 m or higher; structural icing is common and very hazardous for ships because of below freezing ambient air temperature in high winds and resulting spray. Sudden unexpected encounters with polar lows have cost the Norwegians an average loss of three ships a year over a time span of many years because of these effects.

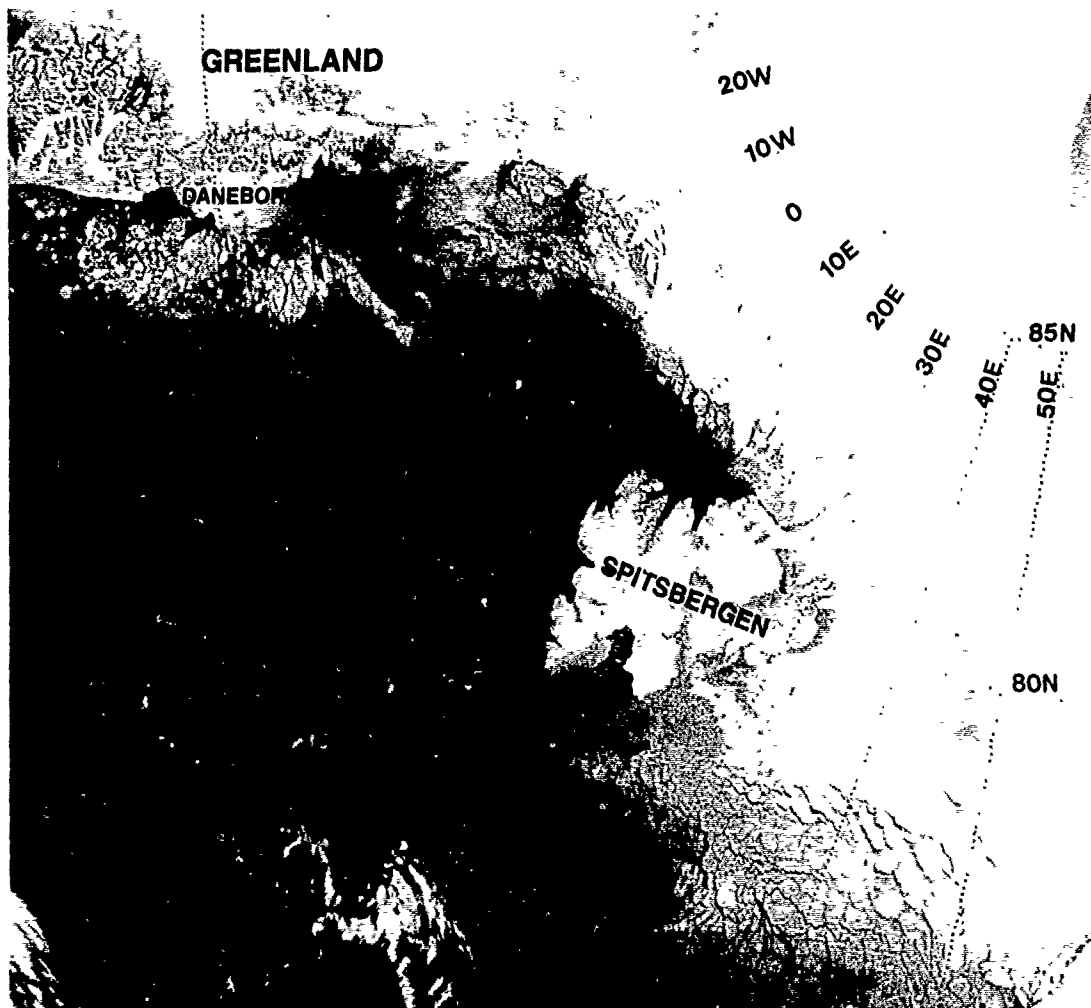
Satellite images every few hours are an essential requirement in detecting polar lows and monitoring their evolution.



2A-5a. Precursor 500-mb Conditions Leading to Polar Low Development.



2A-6a. NOAA-9 Infrared HRPT (Ch 4) Data. 1251 GMT 25 March 1987.

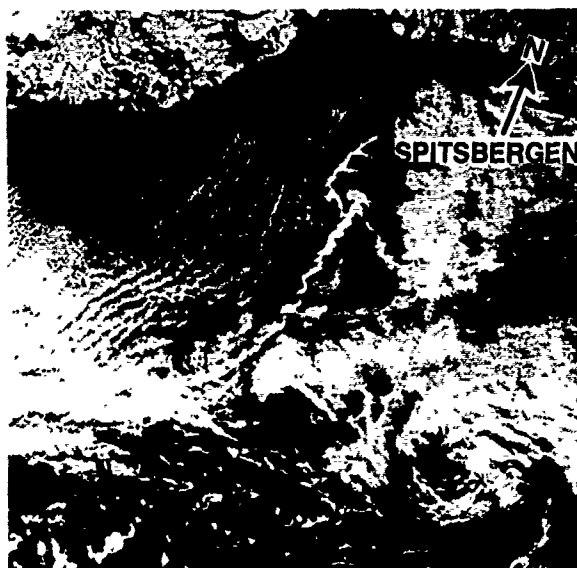


2A-7a. NOAA-9 Infrared HRPT (Ch 4) Data. 1100 GMT 26 March 1987.

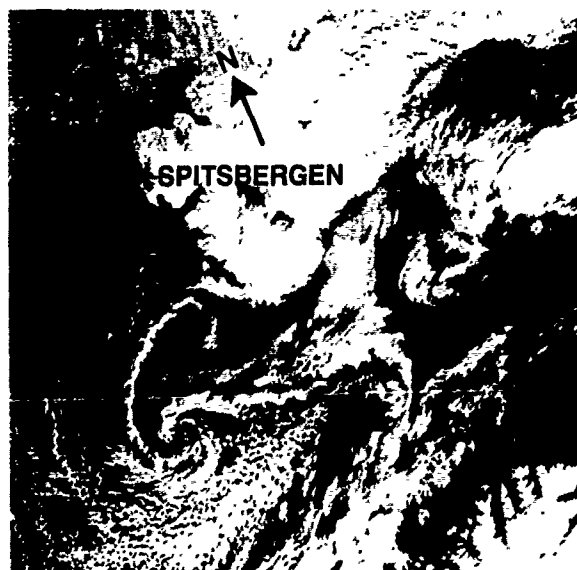
Similar appearing boundary layer fronts have been observed in this region on other occasions. Figure 2A-8a shows an example on 18 April 1983 at 1220 GMT. Vortex development is again apparent at the southern end of the frontal boundary. Its further development is documented a day later in Fig. 2A-8b at 0741 GMT. This vortex also failed to develop further.

The example presented in Case 4 of this section is of an intense polar low development that in its initial state appeared to develop similarly to the vortices noted above, at the base of a north/south-oriented boundary layer front in the Fram Strait. A case study of this development has been published (Rasmussen, 1985); however, the relationship of the development to a pre-existent boundary layer front was not described.

2A-8a. DMSP Infrared (TS) Data.  
1220 GMT 18 April 1983.



2A-8b. DMSP Infrared (TS) Data.  
0741 GMT 19 April 1983.



## *Case 1 Polar Low Development in the Denmark Strait*

*13 December 1986*

The region off the southeast tip of Greenland is a notable area favorable for cyclogenesis. Under conditions of westerly flow the high plateau of the ice cap, with elevations approaching 10,000 ft, acts as a mountain barrier similar to the Rockies in promoting the development of a lee trough. Additionally, low-level thermal baroclinicity is enhanced because of the juxtaposition of the marginal ice zone in that region and a branch of the warm Gulf Stream, which turns counterclockwise to meet the cold southward-flowing East Greenland Current (Fig. 2A-10a). This baroclinicity extends through the Denmark Strait where the Irminger Current flows northward past Iceland.

On 13 December, at 0600 GMT, the FNOC computer-produced surface analysis (Fig. 2A-11a) showed a deep low of about 950 mb just off the southwest coast of Iceland. Near simultaneous NOAA-9 APT data (Fig. 2A-12a), somewhat surprisingly, do not show a classic cloud vortex center at or near that location. A frontal band is evident sweeping west to east across the lower portion of the data and then curling back north of Iceland and into the central portion of Greenland. A broad overcast element of this band extends from the coast of Greenland to Iceland and seems to coincide with the surface trough in the same area (Fig. 2A-11a). The cyclonic curvature of convective cloud lines south of this band seems to indicate the existence of a mesoscale trough not revealed in the synoptic-scale analysis. Note the huge convective clusters of cumulonimbus immediately east of this mesoscale trough axis.

By 1051 GMT, NOAA 10 APT infrared data (Fig. 2A-13a) suggest that this mesoscale trough had deepened and an overcast comma-shaped feature appears near the trough axis. Heightened cumulonimbus activity is evident, as before, east of the trough.

The 1200 GMT FNOC surface analysis (Fig. 2A-14a) indicates that the major low center (949.3 mb) has moved westward toward Greenland. Pressures at Keflavik and Reykjavik both increased 18-19 mb compared to their 0600 GMT readings in support of such a movement.

The 500-mb analysis (Fig. 2A-15a) suggests a cause for the enhanced cumulonimbus activity over the region. Temperatures of  $-35^{\circ}\text{C}$  exist south of Iceland at this level and this isotherm essentially defines the region of maximum convective activity.

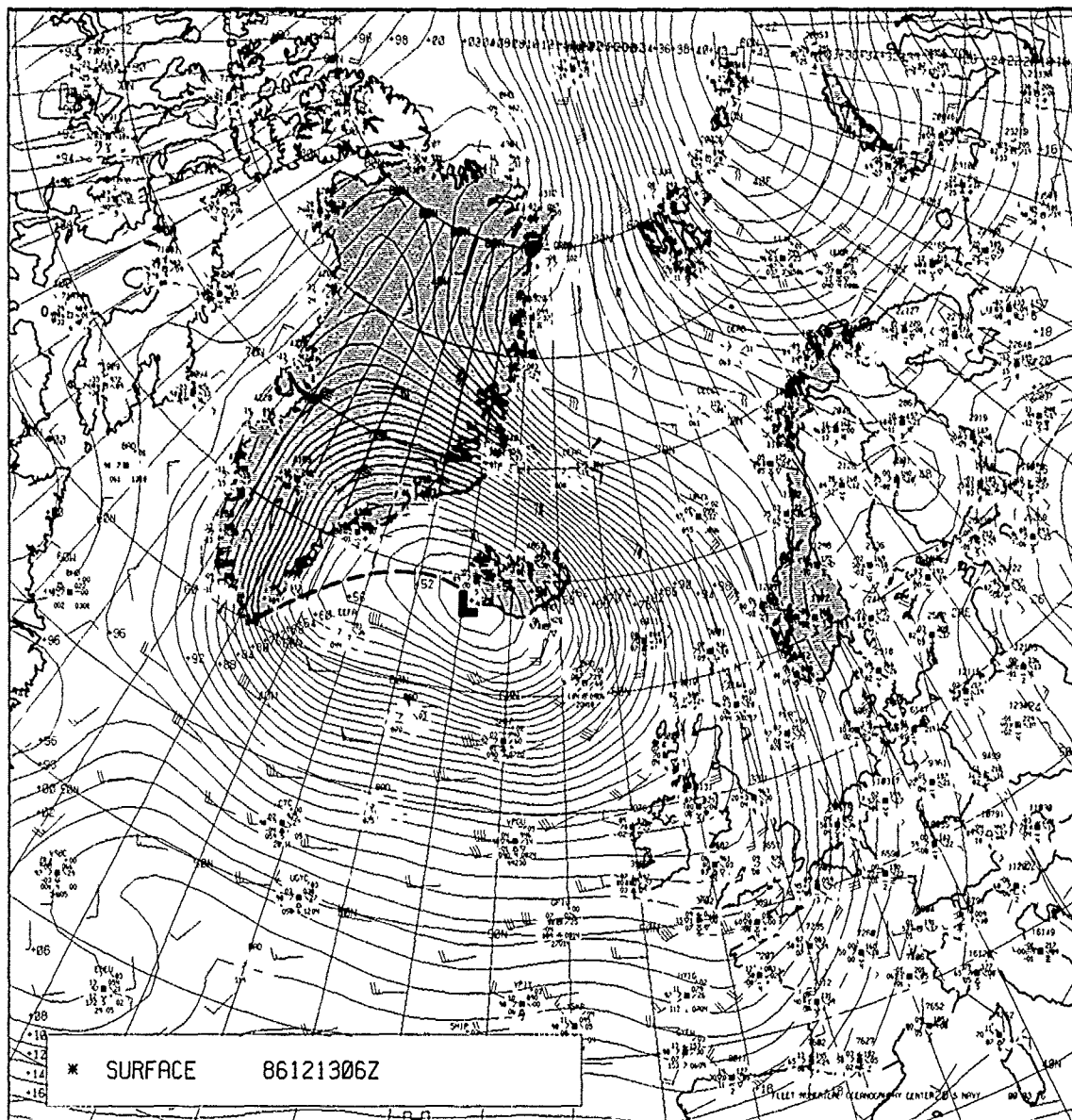
Succeeding NOAA APT passes on this date at 1420 GMT (Fig. 2A-16a), 1601 GMT (Fig. 2A-17a), 1904 GMT (Fig. 2A-18a), and 2045 GMT (Fig. 2A-19a), show movement of the cloud cluster associated with the mesoscale trough up northward through the Denmark Strait (apparently steered by the major low pressure circulation) and reveal that the feature develops into a hook-shaped vortex (Fig. 2A-18a) with a nearly cloud-free eye by the time of Fig. 2A-19a. Such vortices are a class of polar lows of moderate severity. Inasmuch as this particular system was an embedded feature in a larger scale circulation that had a strong pressure gradient extending out for hundreds of miles, its individual intensity is difficult to assess. Similar appearing vortices, however, are typically so embedded and have produced sustained winds at Keflavik of over 50 kt.

# References

- Bergeron, T., 1928: Über Die Dreidimensional Verknüpfende Wetteranalyse I. *Geophys. Publ.* (6), 111 pp.
- Businger, S., 1985: The synoptic climatology of polar low outbreaks. *Tellus*, 37A, 419-432.
- Carleton, A.M., 1985: Satellite climatological aspects of the polar low and instant occlusion. *Tellus*, 37A, 433-450.
- Fett, R.W., 1989: Polar Low Development Associated with Boundary Layer Fronts in the Greenland, Norwegian, and Barents Seas. In *Polar and Arctic Lows*, P.F. Twitchell, E.A. Rasmussen, and K.L. Davidson (Eds.), A. Deepak Publishing, Hampton, Virginia, 313-322.
- Fett, R.W., 1987: Satellite Detection of Precursor Conditions Leading to Polar Low Development. AES Canadian Meteorology and Oceanography Society, Preprint volume of the Second Workshop on Operational Meteorology, 14-16 October 1987, Halifax, Nova Scotia.
- Forbes, G.S., and W.D. Lottes, 1985: Classification of mesoscale vortices in polar airstreams and the influence of the large-scale environment on their evolutions. *Tellus*, 37A, 132-155.
- Midtbo, K.H., M. Naustvik, V. Hoem, and J.C. Smits, 1986: *Polar low forecasting, Part 1, Methods and evaluation*. Polar Low Project, Technical Report No. 19, Norwegian Meteorological Institute, 122 pp.
- Rasmussen, E., 1983: A review of mesoscale disturbances in cold air masses. In *Mesoscale Meteorology—Theories, Observations, and Models*, D.K. Lilly and T. Gal-Chen (Eds.), D. Reidel Publishing Co., Dordrecht, Holland, 247-283.
- Rasmussen, E., 1985: A Polar Low Development Over the Barents Sea. Polar Low Project, Technical Report No. 7, Norwegian Meteorological Institute, Oslo, Norway, 42 pp.
- Shapiro, M., L.S. Fedor, and T. Hampel, 1987: Research aircraft measurements of a polar low over the Norwegian Sea. *Tellus*, Vol. 39A (4), 272-306.
- Wilhelmsen, K., 1986: Climatological Study of Gale Producing Polar Lows Near Norway. *Tellus*, Vol. 37A (5), 451-459.

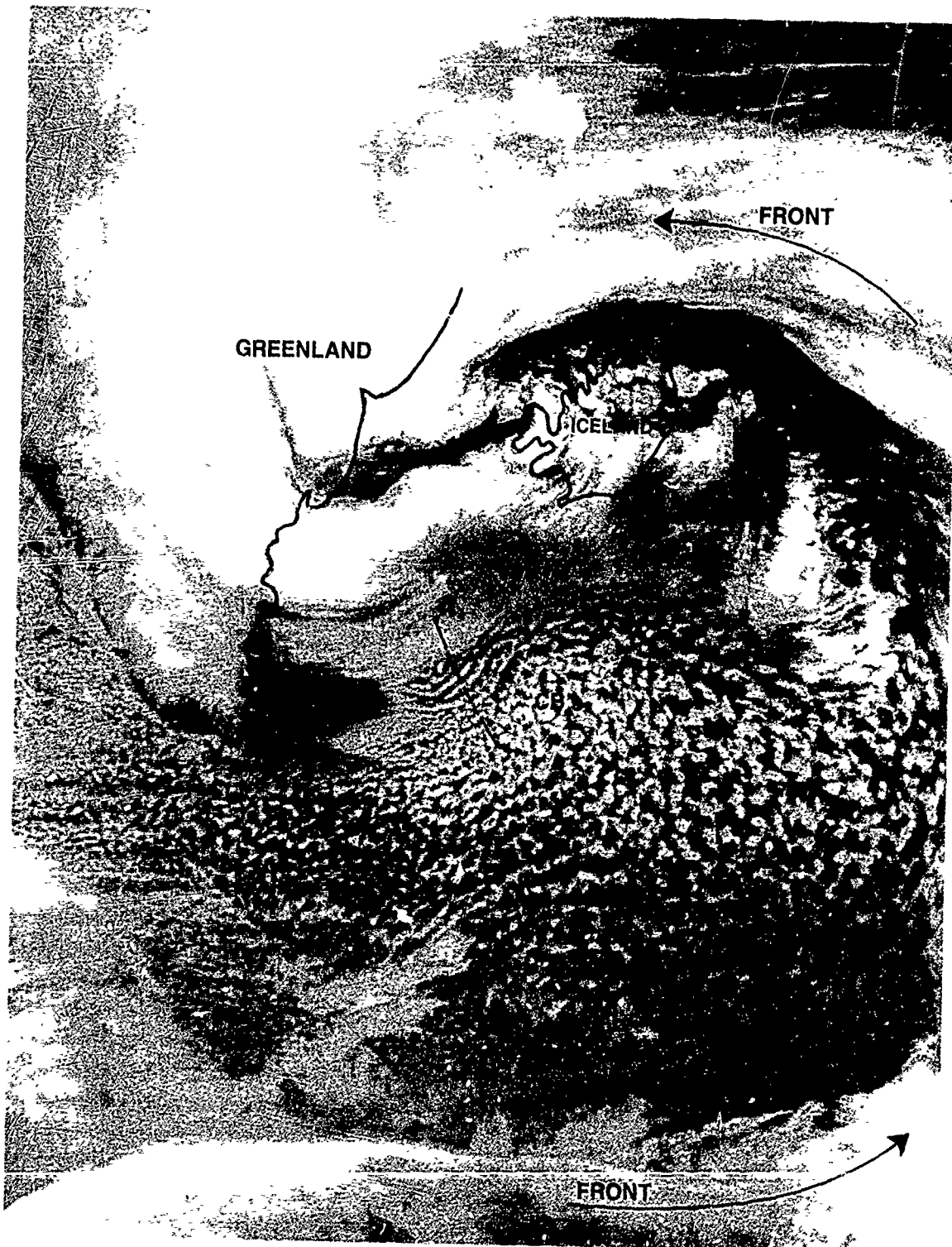


2A-10a. Oceanographic Features of the Greenland/Norwegian Seas.



2A-11a. FNOC Surface Analysis. 0600 GMT 13 December 1986.

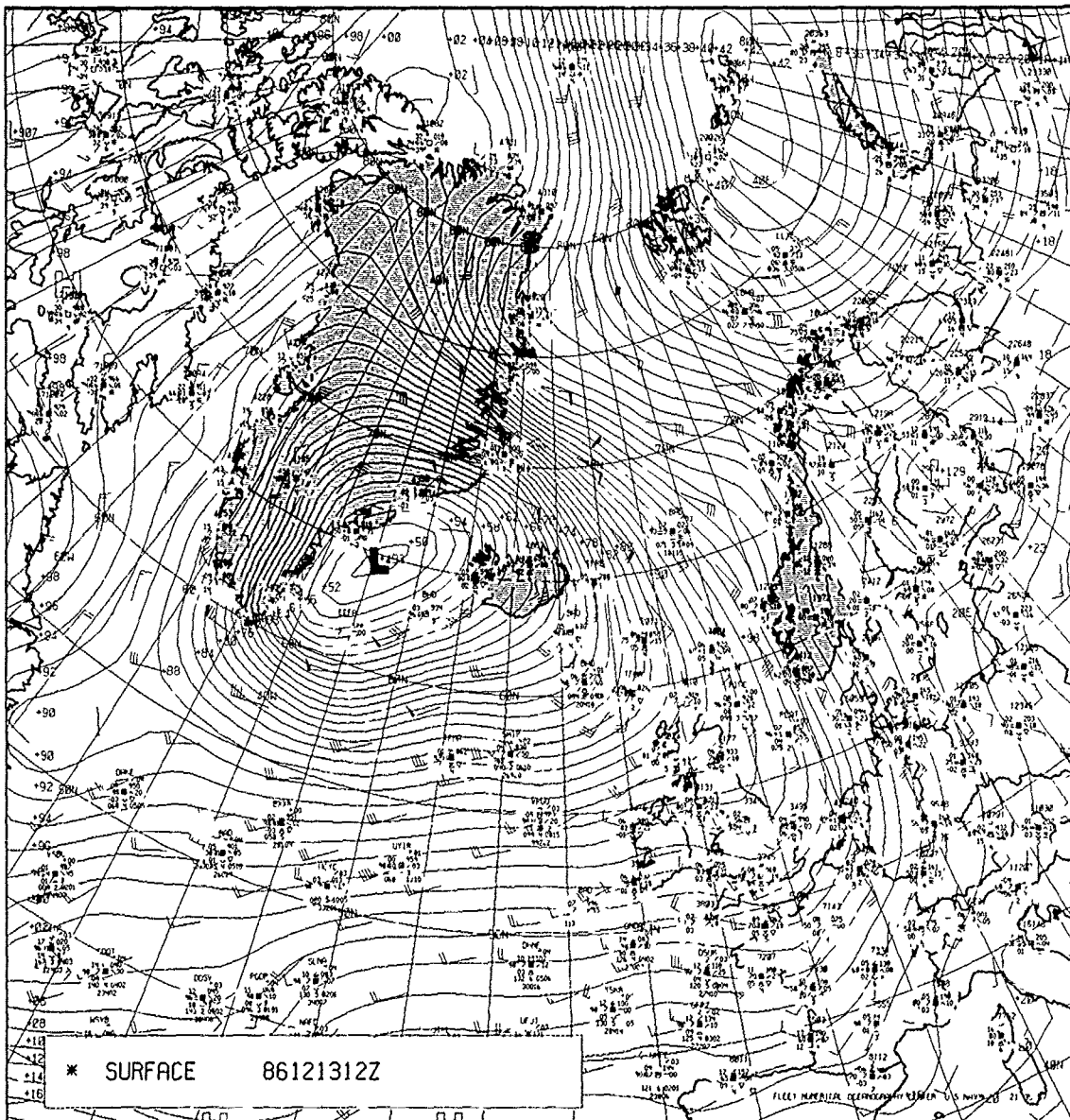




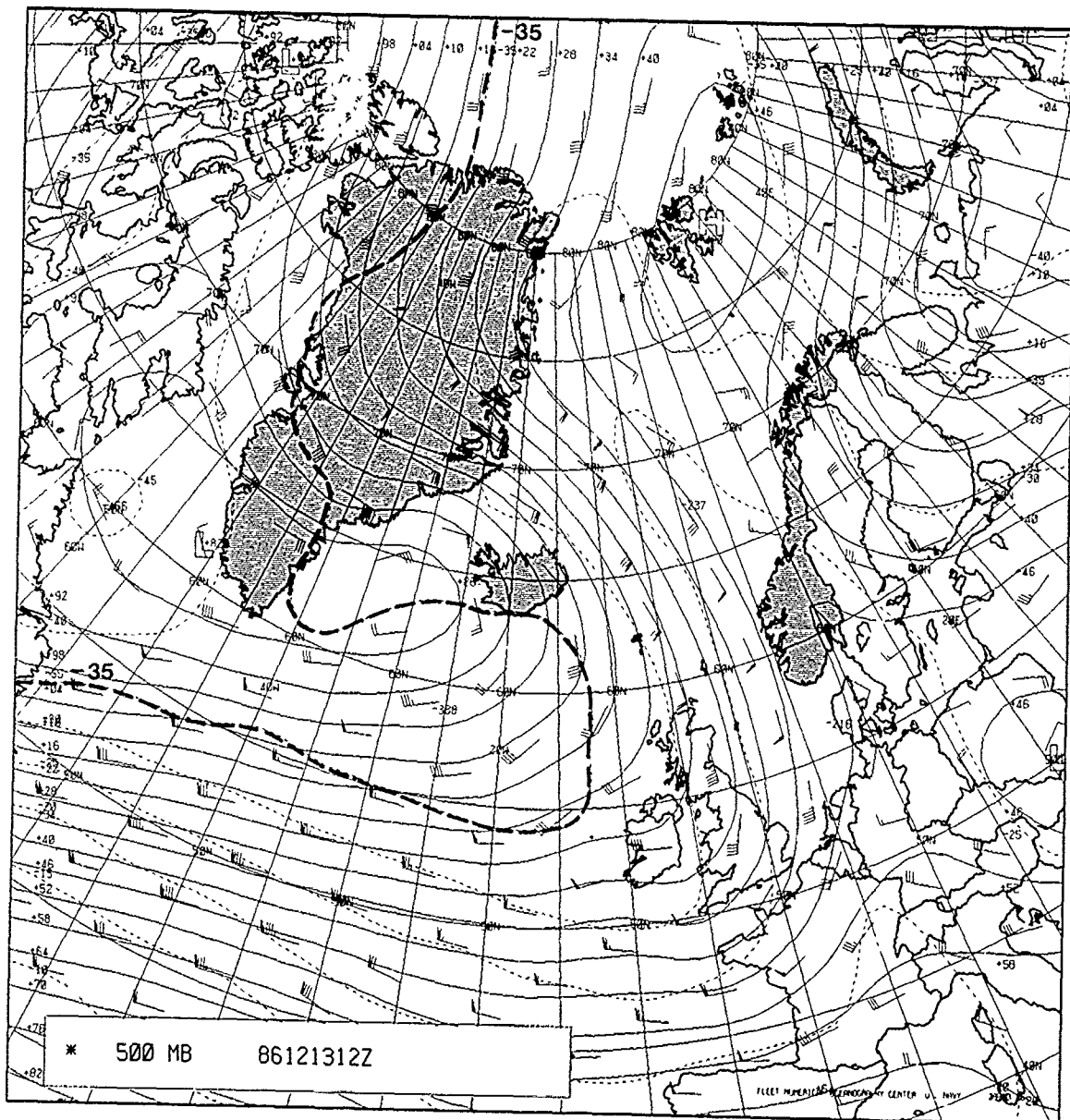
2A-12a NOAA-9 APT Infrared Data 0600 GMT 13 December 1986



2A-13a. NOAA-10 APT Infrared Data. 1051 GMT 13 December 1986



2A-14a. FNOC Surface Analysis. 1200 GMT 13 December 1986.



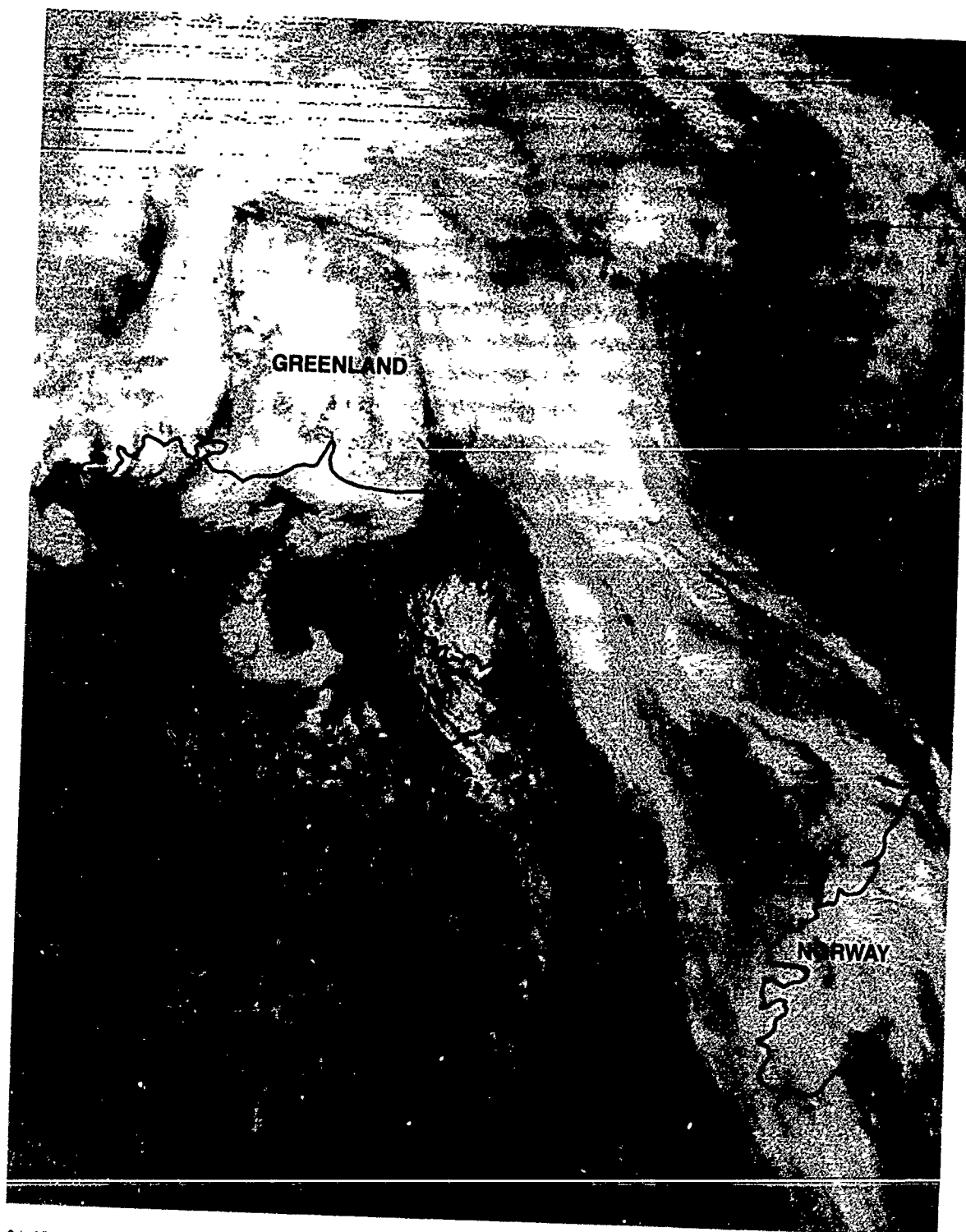
2A-15a. FNOC 500-mb Analysis. 1200 GMT 13 December 1986.



2A-16a NOAA-9 APT Infrared Data, 1420 GMT 13 December 1986.



2A-17a NOAA-9 APT Infrared Data 1601 GMT 13 December 1986



2A-18a NOAA-10 APT Infrared Data 1904 GMT 13 December 1986



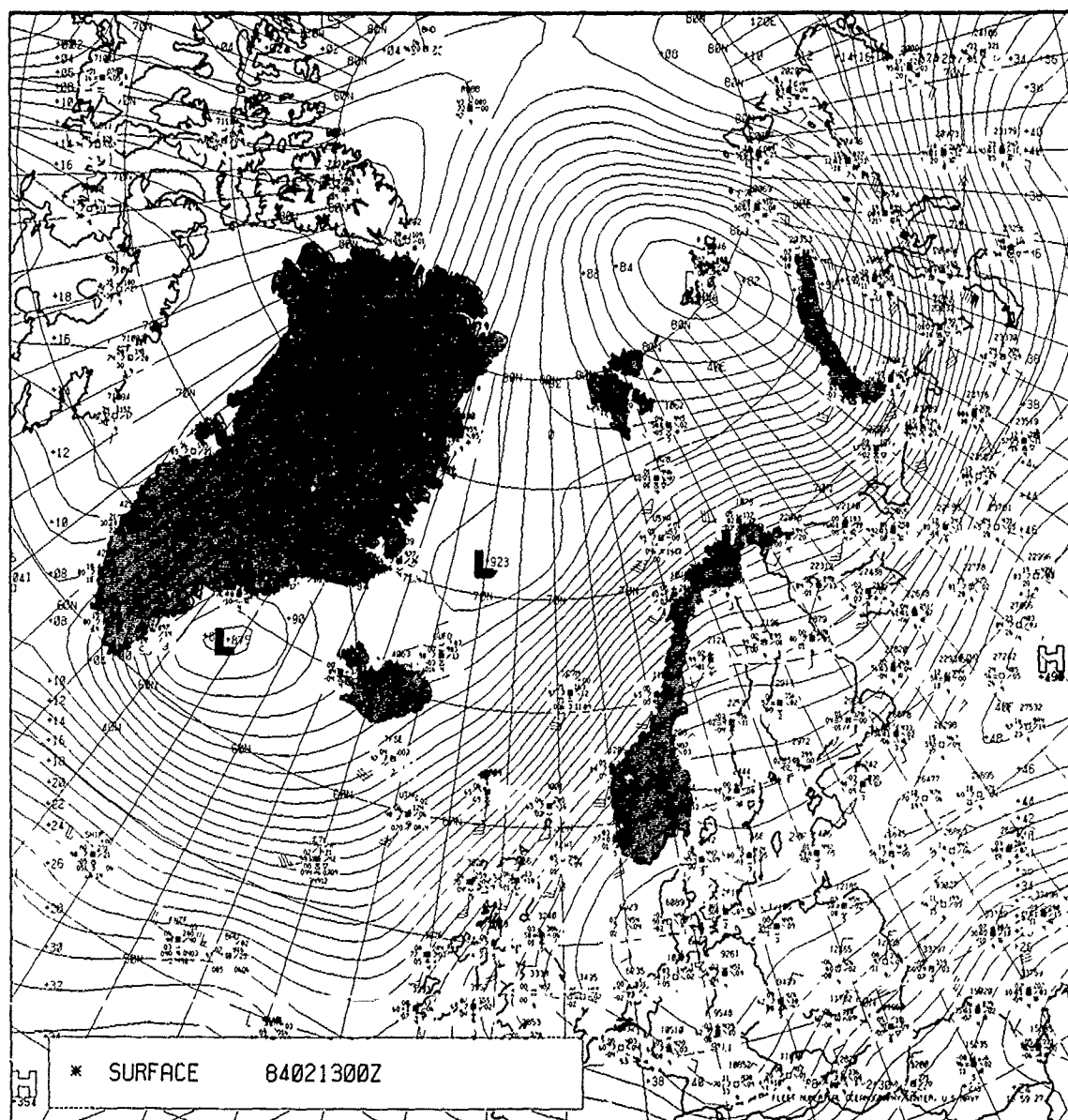
2A-19a. NOAA-10 APT Infrared Data. 2045 GMT 13 December 1986



## Case 2 Polar Low Development in the Greenland/Norwegian Seas (13-14 February 1984)

13 February 1984

The FNOC surface analysis for 0000 GMT (Fig. 2A-20a) reveals multiple lows in a northeast/southwest elongated trough extending from Franz Josef Land in the north to a low off the east coast of Greenland, near its southern tip. A very strong gradient exists on the east side of the trough promoting a vigorous 30- to 45-kt southwesterly flow. Reduction to sea level problems lead to a fictitious representation of the isobaric pattern illustrated over Greenland, which implies strong northerly flow. In fact the flow at the surface over Greenland is largely southerly. Some indication of this can be seen from the lone wind report at station 4165 (Dye 2, 66.5°N 46.3°W) where a wind of 160/10 kt



The important point of this study is that the polar low is developed within, but offset from a general low pressure region adjacent to an unusually enhanced field of open-celled cumulonimbus. Five-hundred-millibar data revealed very cold temperatures in association with an upper trough in the area of the disturbance. From a satellite perspective the enhanced convection is the clue that an upper cold trough is in the area. This information serves to pinpoint the location where polar low development can occur.

#### **Important Conclusions**

1. The Denmark Strait region is a favored region for cyclogenesis.
2. Polar lows can develop in this region in 14 hr or less.
3. Polar low development is a mesoscale development that may and often does occur within a larger scale circulation, as an offset or short-wave development some distance from the main low pressure center.
4. Polar lows often develop within or adjacent to a field of especially enhanced open-celled cumulonimbus. Such development signals the favorable upper level cold trough support noted in many polar low developments.
5. By combining the satellite evidence with other known factors favorable for polar low production (see introduction) the forecaster can be alerted to the exact area where this potential exists.

DMSP infrared data acquired at about 0600 GMT on 13 February combining several orbits in mosaic format are shown in Fig. 2A-22a. For perspective in comparing these data with later images, attention should be focused on systems labeled 1 through 3. System 1 contains a low center just off the coast of Labrador with a frontal zone apparent as an overcast stratus band that dips southward and extends eastward ultimately looping up to connect with system 2, a low center and cloud complex off the southeast tip of Greenland.

System 3 is a low center near Spitsbergen that represents a northward extension of a meridional frontal system extending deep into the midlatitudes. Bulging cloudiness west of the frontal zone between systems 2 and 3 is south of a low center indicated in Fig. 2A-20a.

The cloud complex of system 2, consisting of an east-west oriented band of convective cloud clusters and a field of open-celled cumulonimbus containing a vorticity center near  $63^{\circ}\text{N } 29^{\circ}\text{W}$ , is the system of special interest for the purpose of this study. The heavy convective buildups south of the banded cloudiness develops only under conditions of cyclonically curved low-level flow (also implied by the vorticity center on the northwest side of the convective buildups), with an upper cold low or trough aloft.

The FNOC 500-mb analysis (Fig. 2A-23a) verifies this condition with a cold thermal trough indicated in alignment with the pressure trough extending south of Iceland.

The NMC depiction of all three systems in their surface analysis is shown in Fig. 2A-24a. This analysis shows frontal connections to each of the three systems. Broadly speaking, the DMSP data relate reasonably well to the FNOC (Fig. 2A-20a) and NMC (Fig. 2A-24a) analyses. In particular the elongated cloud band extending from just west of the United Kingdom northeastward past Spitsbergen (near  $15^{\circ}\text{E } 78^{\circ}\text{N}$ ) relates well to the strong southwesterly flow and probable frontal band existing in that area, and system 1 exhibits the classical frontal cloud pattern structure seen in the midlatitudes.

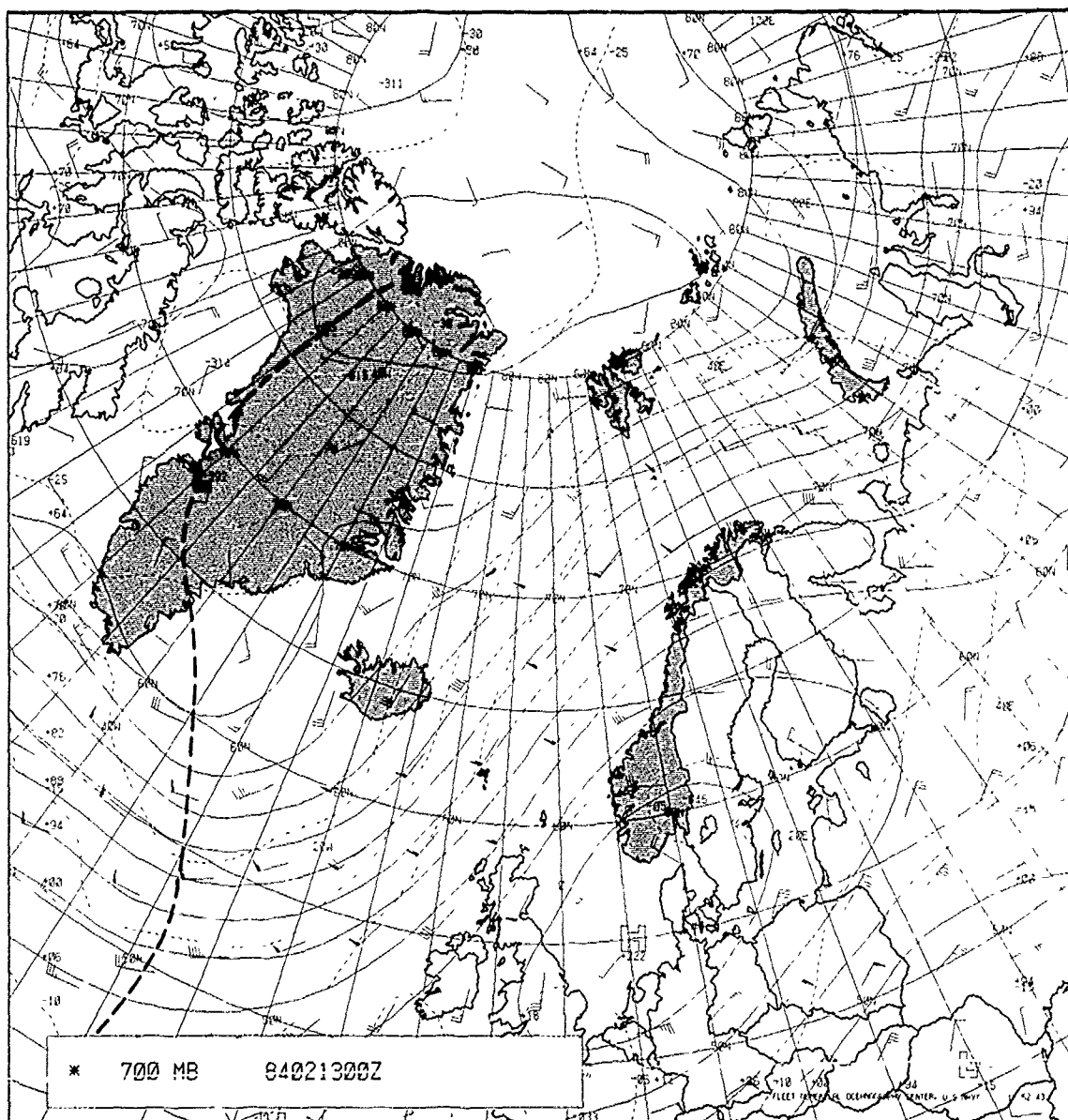
System 2, showing the enhanced open-celled cumulonimbus and a broad east-west-oriented convective band of cloud clusters, is not classical in terms of appearance as an occluded front and low center indicated in the NMC surface analysis (Fig. 2A-24a).

If the convective cloud band pattern of system 2 is transposed on the surface analysis, and a streamline analysis of flow characteristics is also superimposed (shown in Fig. 2A-25a), it can be seen that the band lies along a convergence asymptote leading into the storm center. Flow turns cyclonically to the south of this band through the field of open-celled cumulus and cumulonimbus. The vorticity center suggested by the satellite data near  $63^{\circ}\text{N } 29^{\circ}\text{W}$  is about 180 nm east of the analyzed low pressure center.

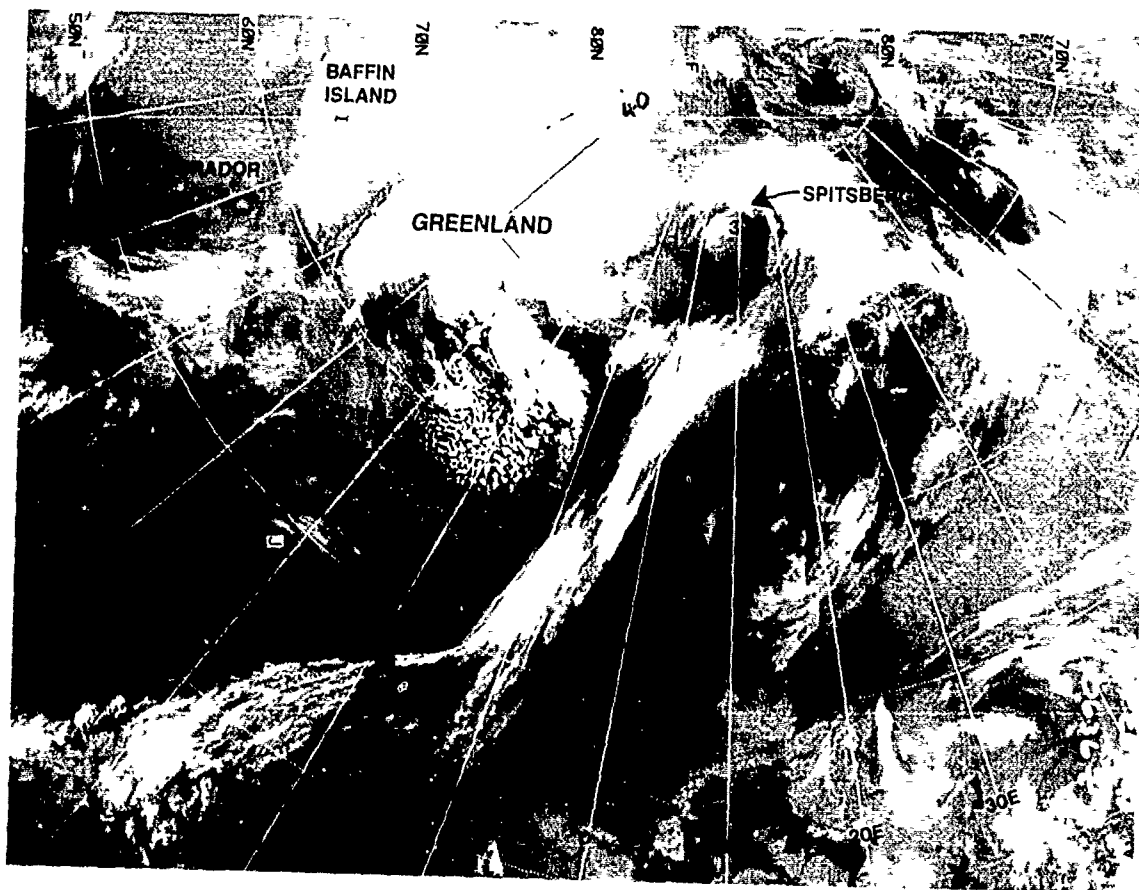
A similar transposition of the pattern onto the 500-mb analysis (as shown in Fig. 2A-26a) reveals the enhanced convective developments under a cold trough with temperatures below  $-35^{\circ}\text{C}$ . Cold temperatures aloft and positive vorticity advection have apparently destabilized the atmosphere and triggered such development.

The satellite data (Fig. 2A-22a) reveal that open-celled cumulus, quite suppressed in the western portion of the area, enlarge downstream toward the east, implying strong heating and moistening from below and an increase in the height of the boundary layer to the point where the inversion is destroyed in the region of heaviest convection. In this region it can be inferred that an almost neutral layer replaces the stable inversion-dominated layer further west. The east-west-oriented convective band to the north of the open cells does not lie within the position of the upper level trough but is in a region to the northeast characterized by anticyclonically-turning flow where positive vorticity advection is maximized. That the flow is anticyclonic at the cloud top region is implied by the cirrus streaks on the north edge of the convective band that turn anticyclonically.

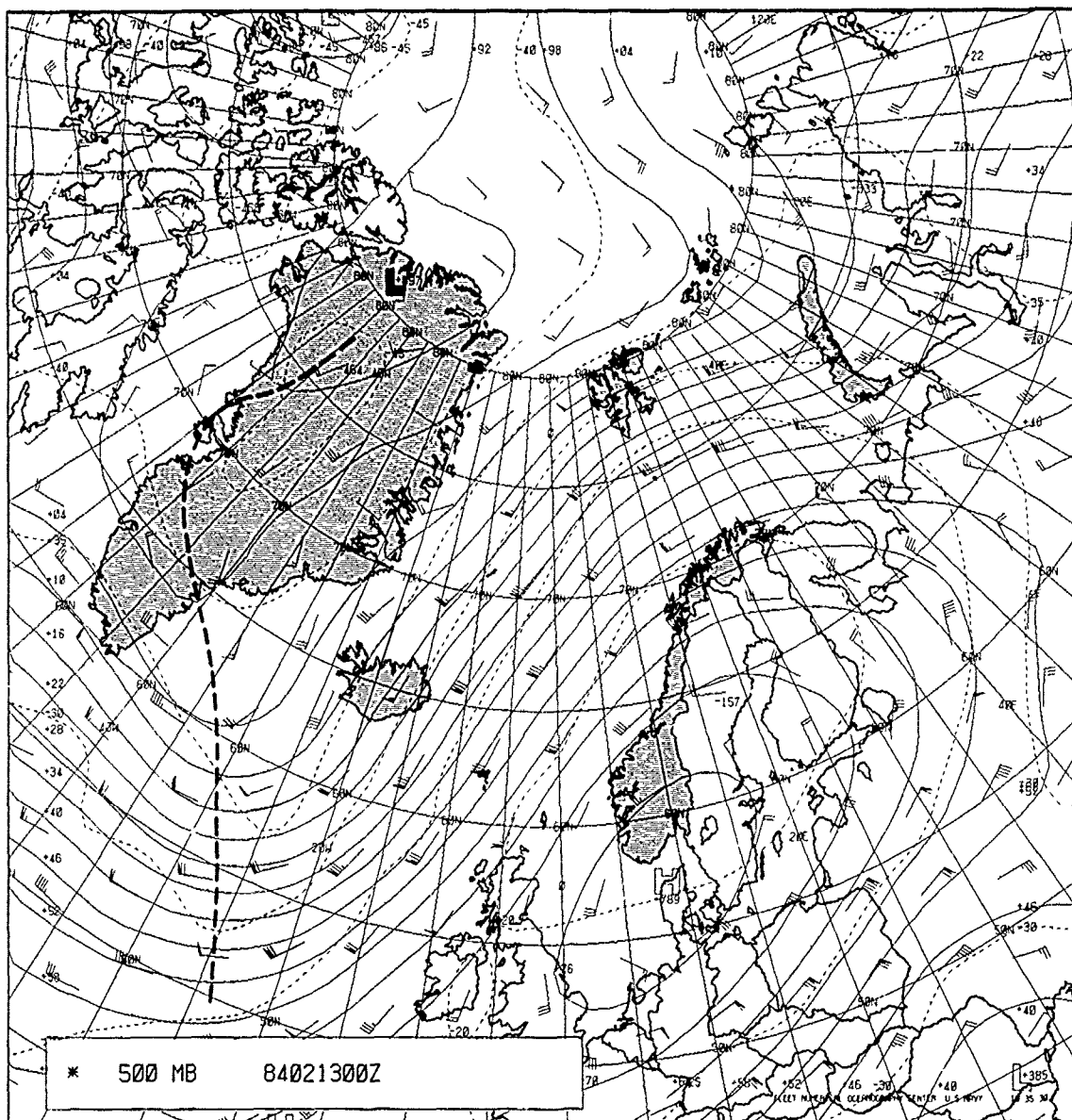
is reported. Figure 2A-21a is the 700-mb analysis, which reflects more accurately surface conditions at the 10,000 ft elevation, typical of the ice cap over Greenland. The analysis shows largely southerly flow over the ice cap and that the trough at this level is displaced well to the west rather than over the open sea as shown at the surface (Fig. 2A-20a).



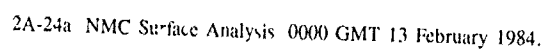
2A-21a. FNOC 700-mb Analysis. 0000 GMT 13 February 1984.

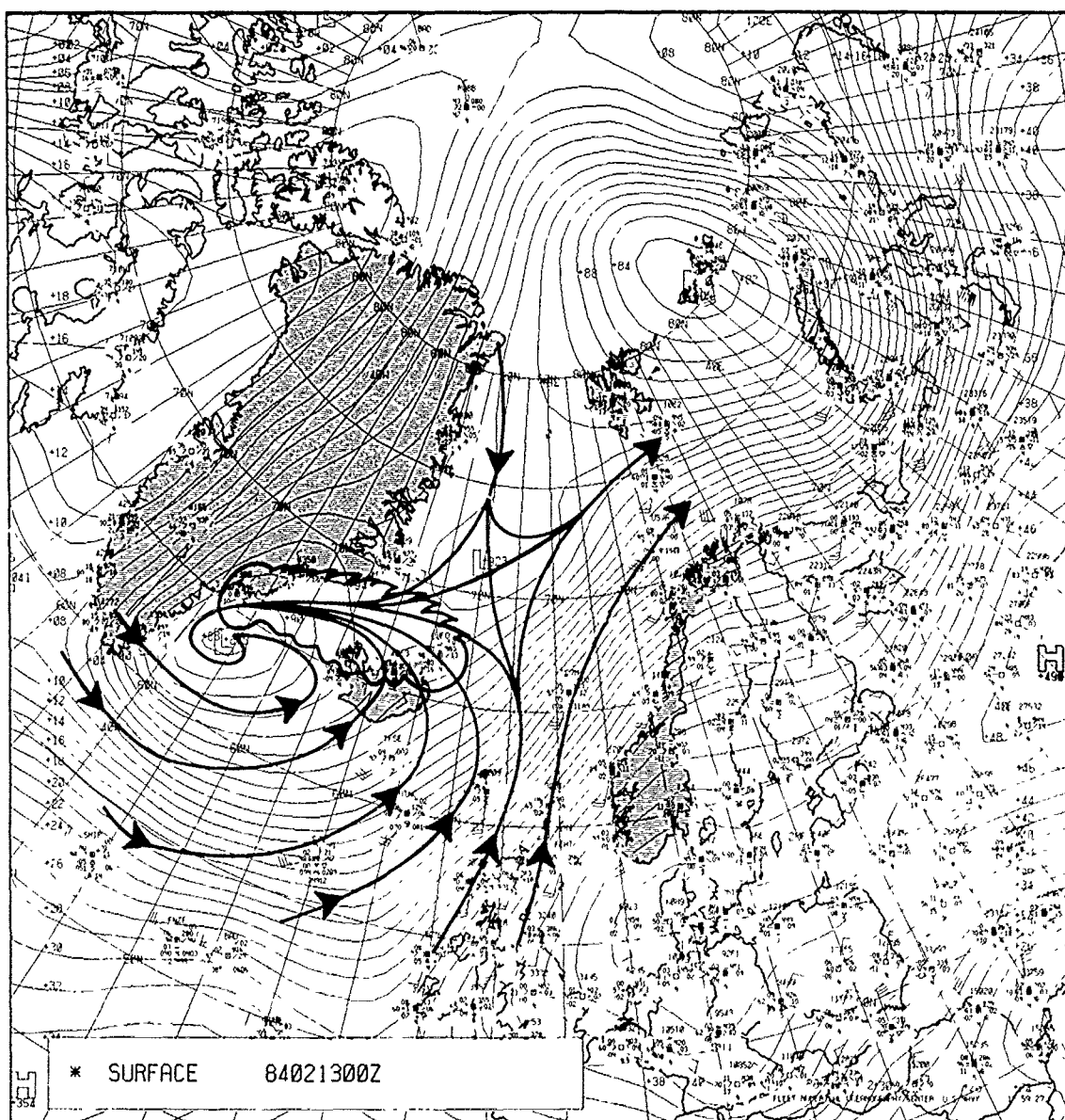


2A-22a DMSP Infrared (LS) Data 0600 GMT 13 February 1984.

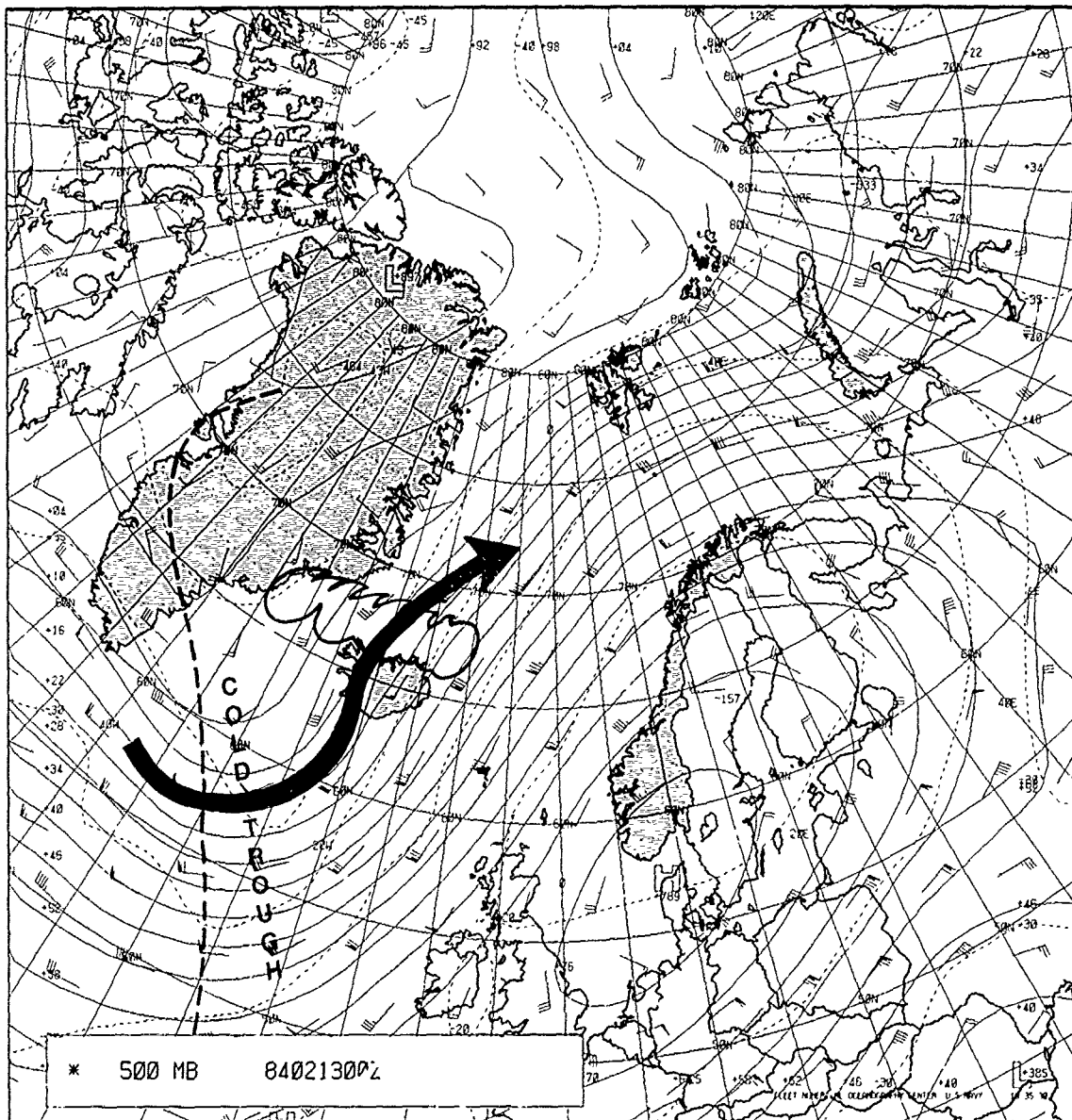


2A-23a. FNOC 500-mb Analysis. 0000 GMT 13 February 1984





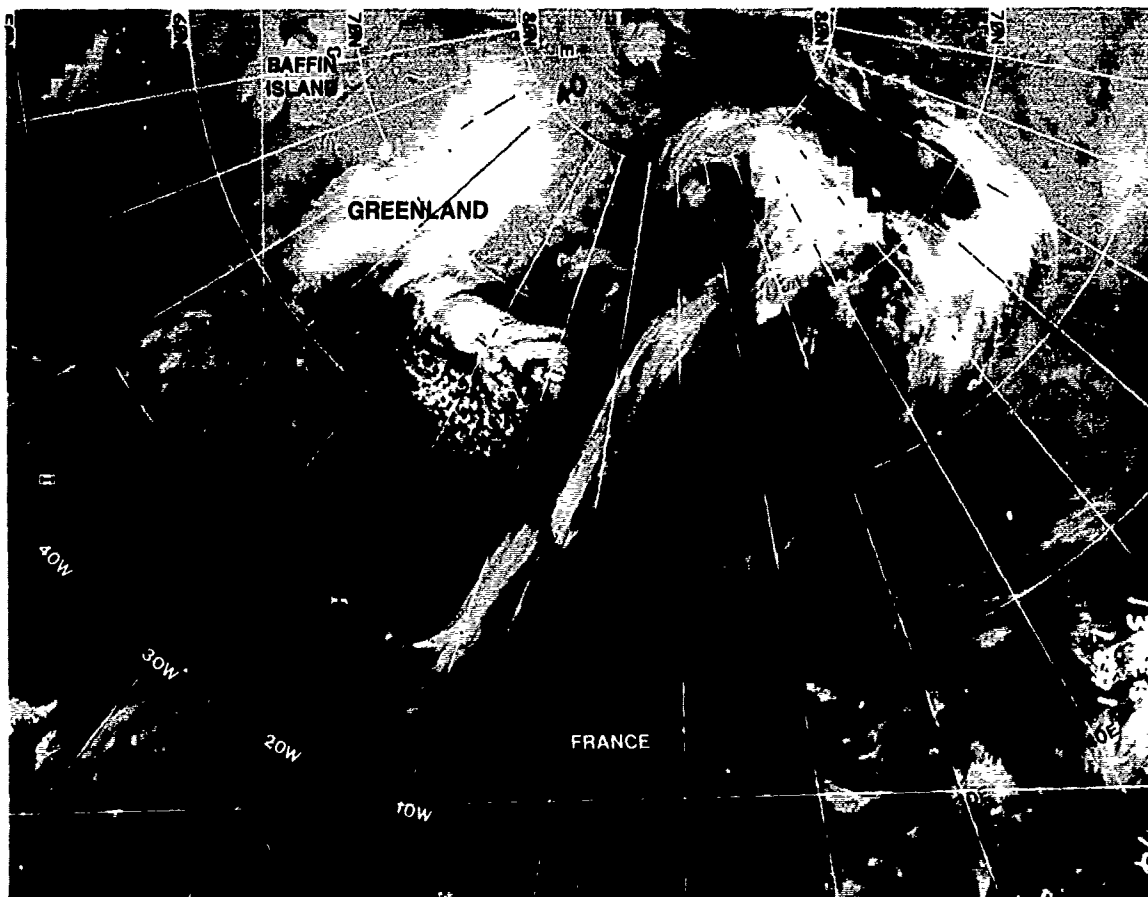




2A-26a. FNOC 500-mb Analysis With Cloud Outline 0000 GMT 13 February 1984

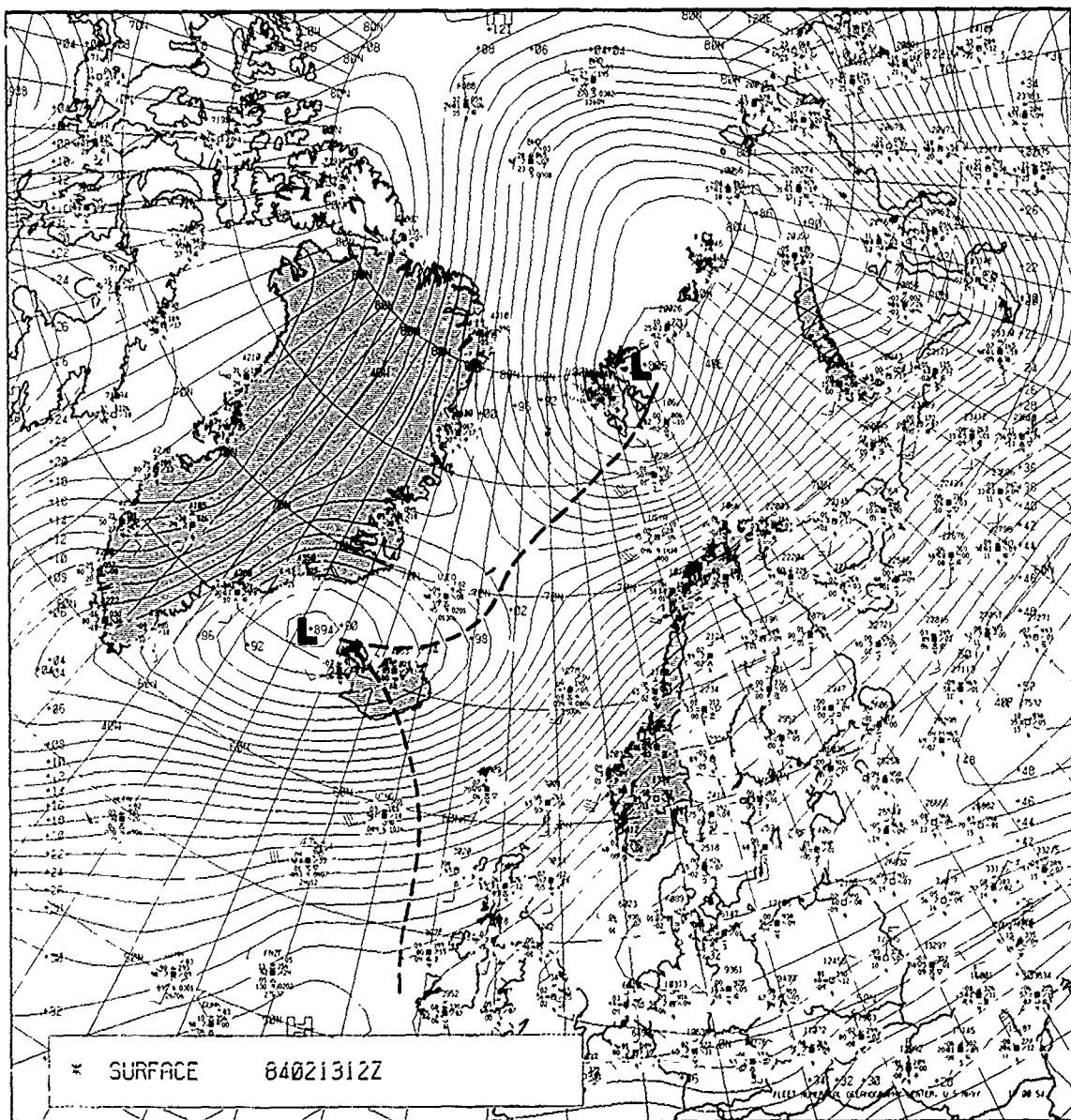
It is of great interest that the positive vorticity advection and anticyclonic flow occur directly over the convective band, which at the surface lies within the trough of low pressure. The coincidence of such a flow pattern favoring upper level divergence with the surface pattern and satellite data indicating low-level convergence implies strong upward vertical motion within the band. Such motion within a moist environment tends to reinforce the upper ridge through release of the latent heat of condensation and to favor continued advection of the colocated features (the band and the opened-cellular convection) as recognizable entities until an important change in intensity occurs. This could come about as a sudden explosive development of a cluster within the band as a polar low, for example, or a decay of the system due to unfavorable conditions such as advection over terrain or advection of the features from areas of warmer to areas of colder water.

The distinctive pattern is easy to track as it appears a few hours later (0839 GMT) in another DMSP mosaic (Fig. 2A-27a) and in a NOAA-7 mosaic (Fig. 2A-27b) at 1353 GMT. Note the northeastward movement and cyclonic rotation of the system when compared with the position and alignment shown in Fig. 2A-22a.

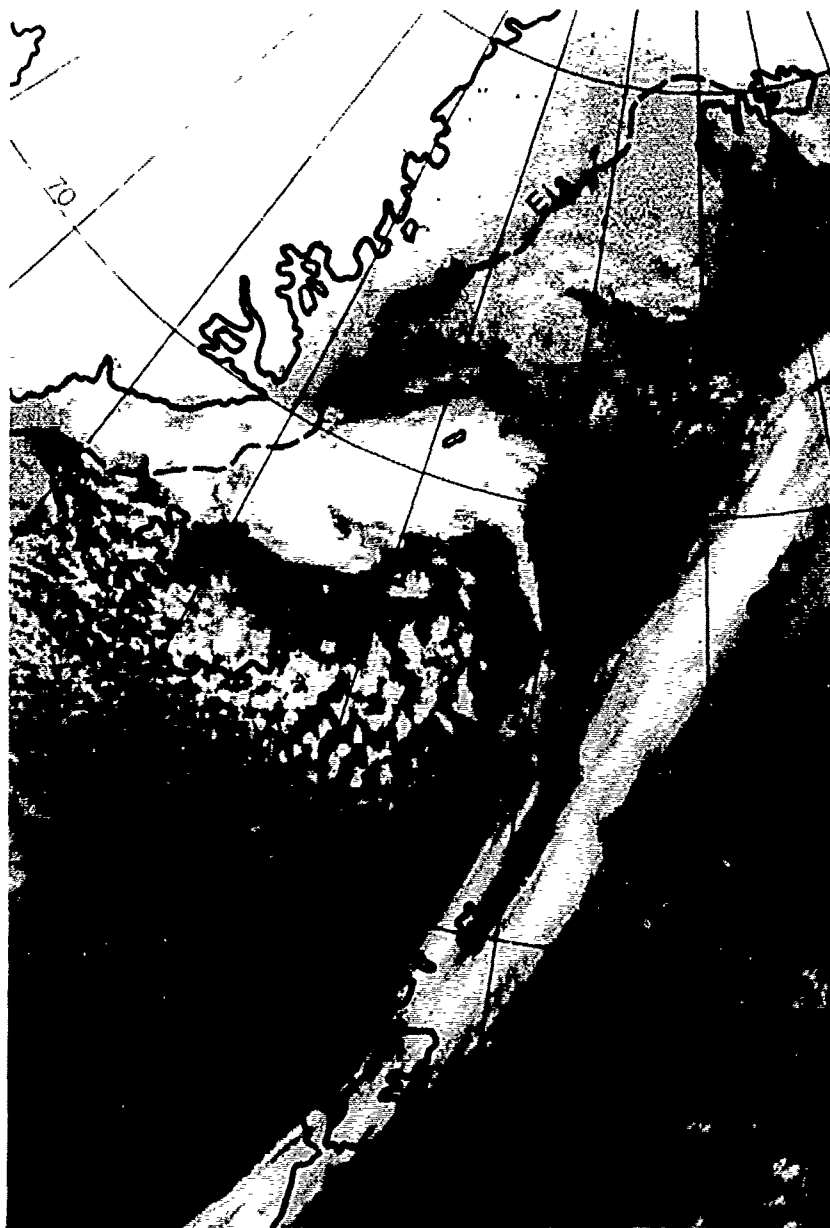


2A-27a. DMSP Infrared Mosaic Data. 0839 GMT 13 February 1984.

The FNOC surface analysis for 1200 GMT (Fig. 2A-28a) shows the low pressure center still retained within the Denmark Strait with no signs of vortex development to the northeast in the region of the convective band. The 500-mb analysis for 1200 GMT (Fig. 2A-29a) is of special interest in that it shows the cold trough moving over and along with the region of heavy convection south of the overcast band.



2A-28a. FNOC Surface Analysis. 1200 GMT 13 February 1984



2A-27b. NOAA-7 Infrared Mosaic Data. 1353 GMT 13 February 1984.

14 February 1984

Good views of this system were not obtained again until about 11 hr later at 0053 GMT on 14 February (Fig. 2A-30a). Nevertheless, the distinctive patterns of systems 1, 2, and 3 are easy to identify and they have appeared to move logically from the earlier positions.

System 1 has intensified and moved past the southern tip of Greenland; system 2 centered about 5° due south of Spitsbergen has retained the enhanced cumulus convection, symptomatic of cold unstable conditions aloft, and the clustered cloudiness with middle and upper level cloud shields; while system 3 is revealed by the jet stream cirrus streaks that progressed eastward. A cloud vortex associated with system 3 appears well to the east near 77°N.

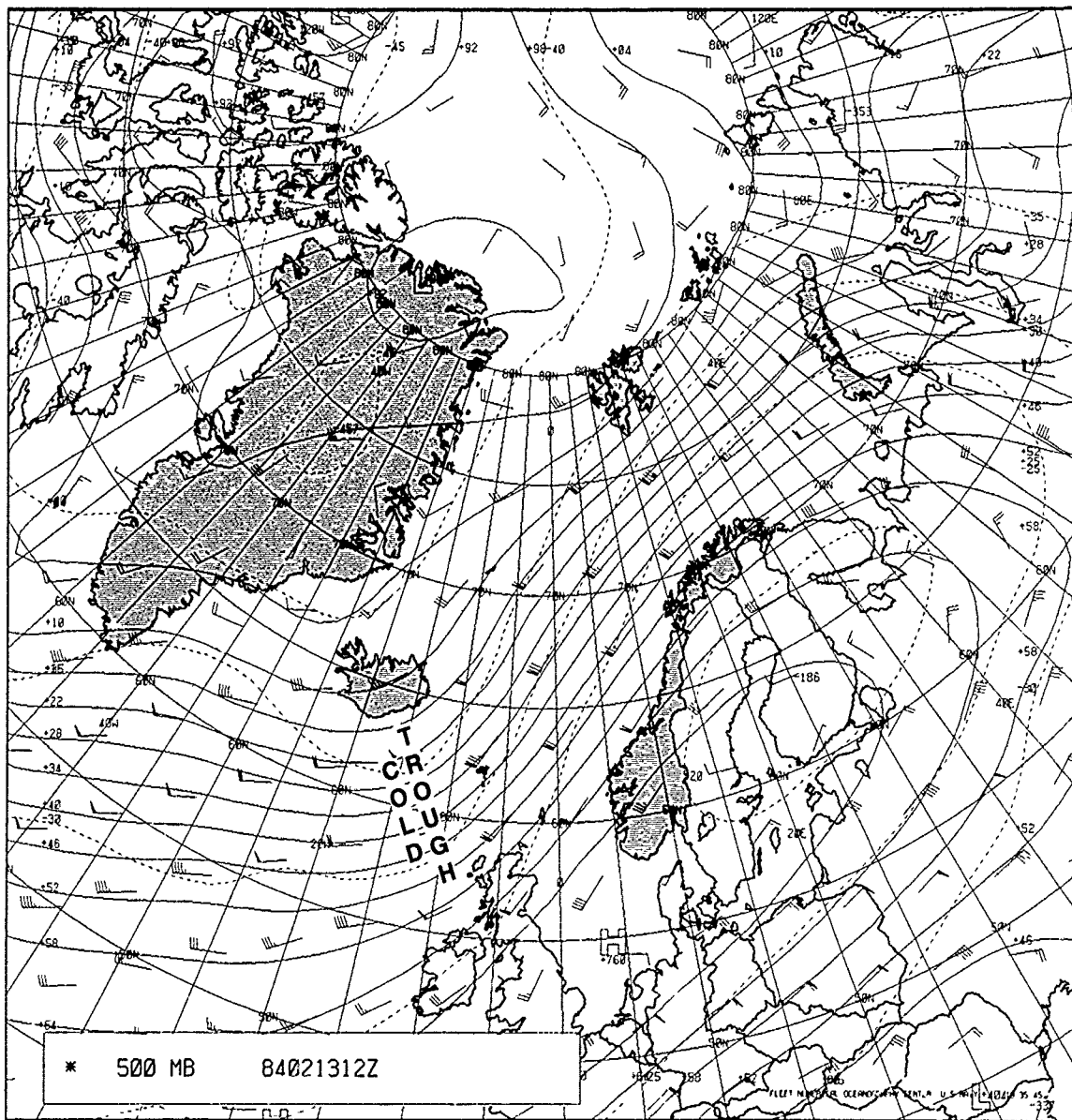
System 2 was penetrated by a NOAA P-3 aircraft on this date, which flew from Bodø, Norway to Spitsbergen and returned, releasing dropsondes enroute to document the structure of the system between Bodø and Spitsbergen and of a northerly low-level coastal jet found along the west coast of Spitsbergen (Shapiro and Fedor, 1986).

There is a suggestion (curved cloud bands) in the DMSP mosaic (Fig. 2A-30a) that system 2 contains two separate vorticity centers and possible centers of circulation. One is indicated in the vicinity of 68°–69°N and about 1°W, and the other near 73°N, and about 12°E. The circulation centers become even more apparent about 7 hr later (0817 GMT) in another DMSP infrared mosaic (Fig. 2A-31a). It can be seen from this latter mosaic that convective cloudiness of the southern-most center is already impacting on the Bodø, Norway region.

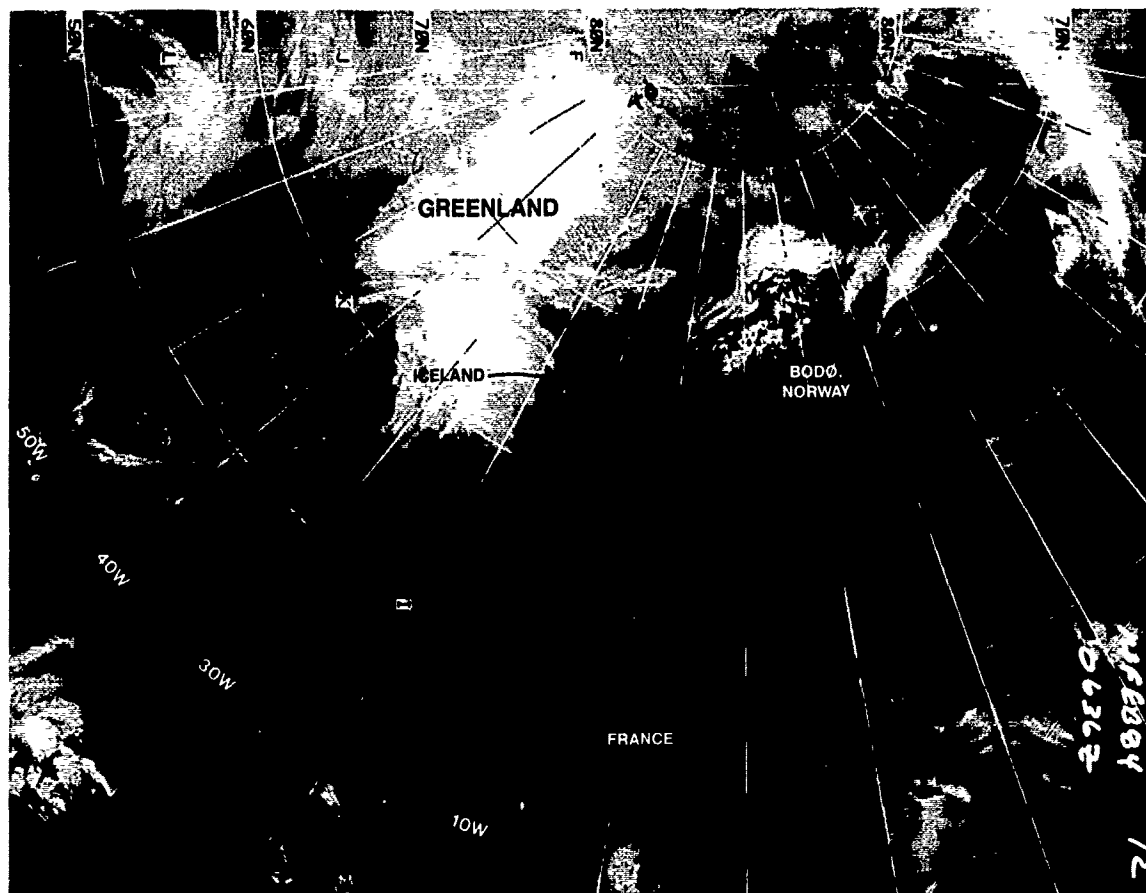
The FNOC surface analysis for 0000 GMT (Fig. 2A-32a), with cloud outlines shown by the DMSP data (Fig. 2A-30a) superimposed, shows neither of these vorticity or circulation centers specifically. Both are located on the east side of what is shown as a trough. The convective activity appears just in advance of the cold trough at the 500-mb level (Fig. 2A-33a), which has moved from south of Iceland (Fig. 2A-21a) northeastward toward the coast of Norway. Flow over the cloud cluster south of Spitsbergen suggests a tendency to curve anticyclonically over this feature.

The 1200 GMT FNOC surface analysis with the outline of the cloud cluster shown in Fig. 2A-30a superimposed (Fig. 2A-34a) reveals that this cluster is now within a strong cyclonic circulation. A low center could easily have been analyzed in the surface analysis over this area. In fact more detailed surface analyses derived from the report by Shapiro and Fedor (1986) shows the development of two polar lows in that area on 14 February (Fig. 2A-35a). The development in that analysis is shown to be associated with the leading edge of cold air or the arctic front moving south from the Fram Strait region. The analysis shows the characteristic large pressure rises of greater than 10 mb in 3 hr often noted following passage of polar lows.

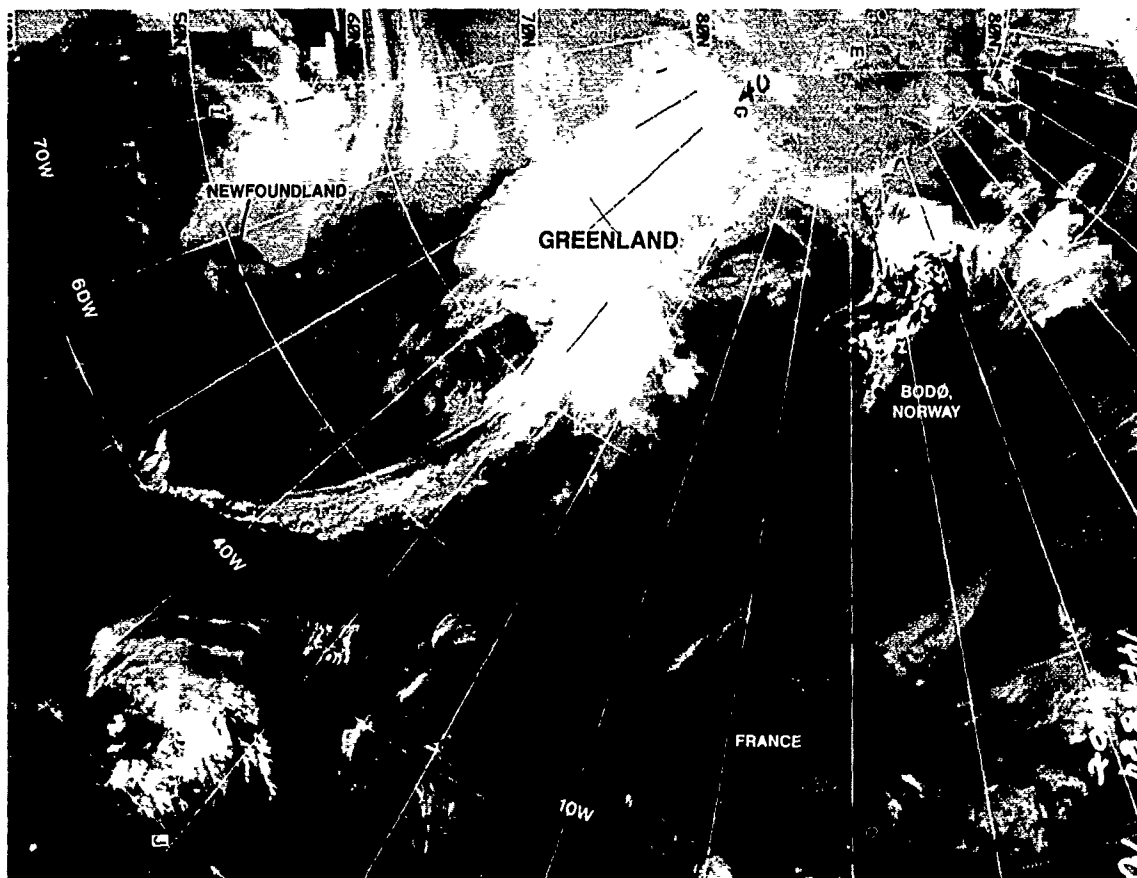
Shapiro's streamline analysis, based on flight data plus conventional observations (Fig. 2A-36a), is particularly interesting in that maximum winds of 70 kt were found south of the storm center. Some computer-enhanced images, (Fig. 2A-37a), prepared by Shapiro and Fedor, show NOAA HRPT infrared data of the storm area that more clearly reveal the spiral structure of clouds defining the storm centers and verify the extreme vertical development of cumulonimbus clouds in the area south of the center. The HRPT data were obtained in direct-readout mode from the Tromsø, Norway telemetry station. The Fig. 2A-37a view was acquired at 0440 GMT on 14 February at Tromsø and shows various enlargements and a temperature slice (revealing only the coldest temperatures) (Fig. 2A-37a[D]) of the storm area. The spiral vortex is clearly implied by cloud curvature and is labeled L in Fig. 2A-37a(A) with an enlargement of the area shown in Fig. 2A-37a(C). The temperature slice showing only the coldest temperature-radiating cloudiness (210 K) suggests cloud tops near 400 mb, based on comparison with the 0000 GMT 14 February 1984, Bear Island rawinsonde. Note that the tops of cumulonimbus convection to the south are also shown in this temperature slice, confirming deep convection in that region.



2A-29a. FNOC 500-mb Analysis. 1200 GMT 13 February 1984.

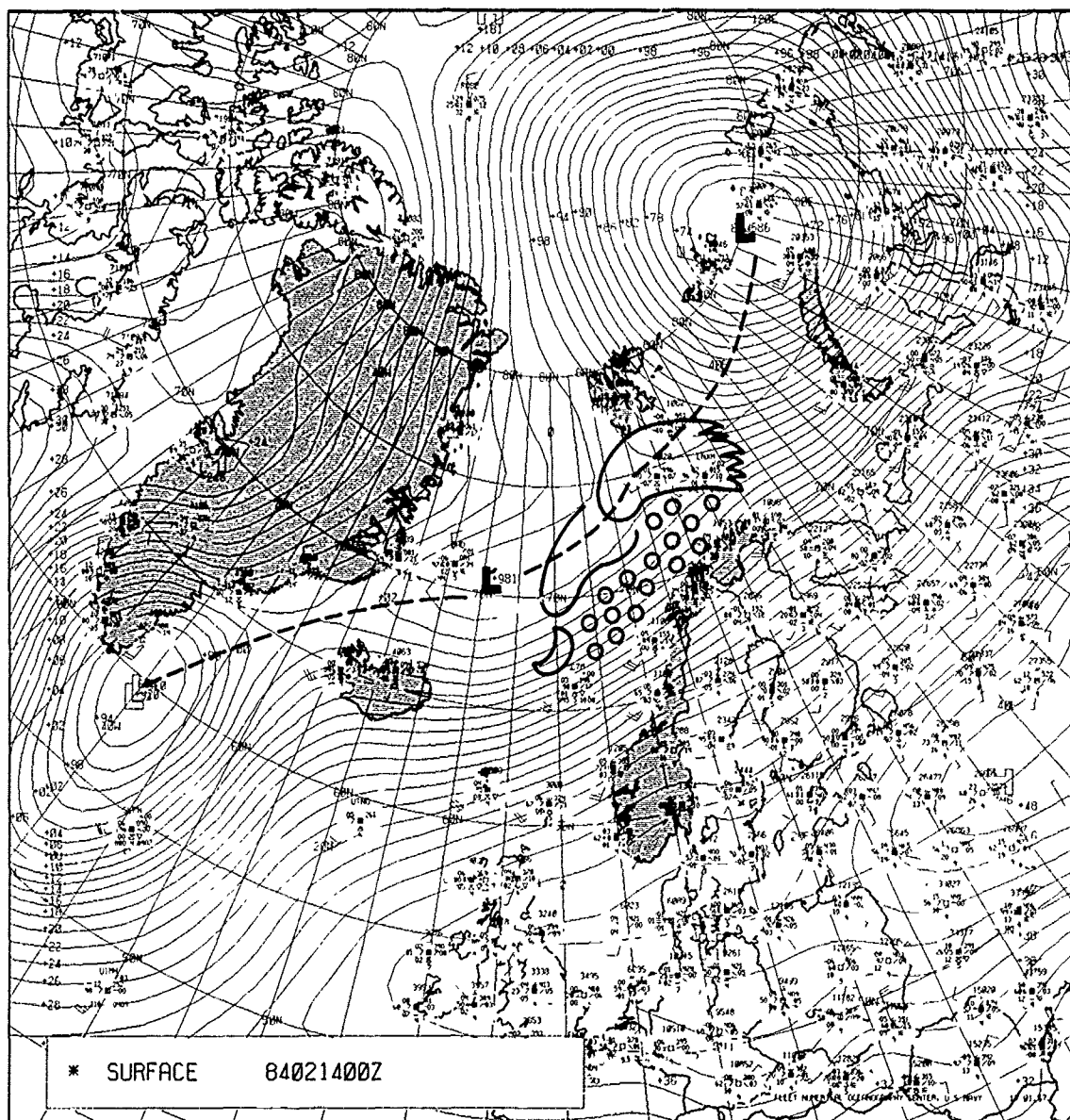


2A-30a. DMSP Infrared Mosaic Data. 0053 GMT 14 February 1984.

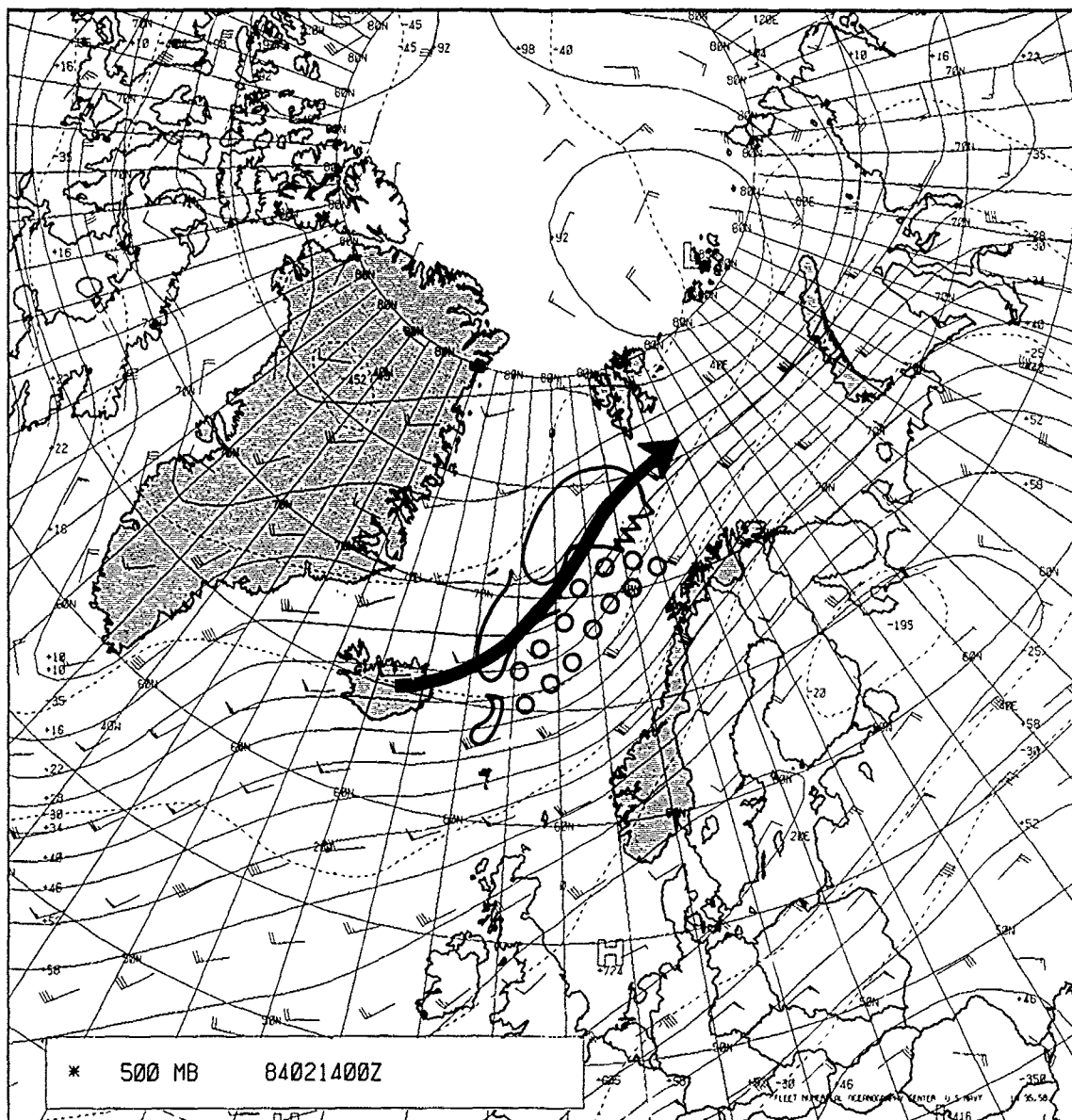


2A-31a. DMSP Infrared Mosaic Data. 0817 GMT 14 February 1984.

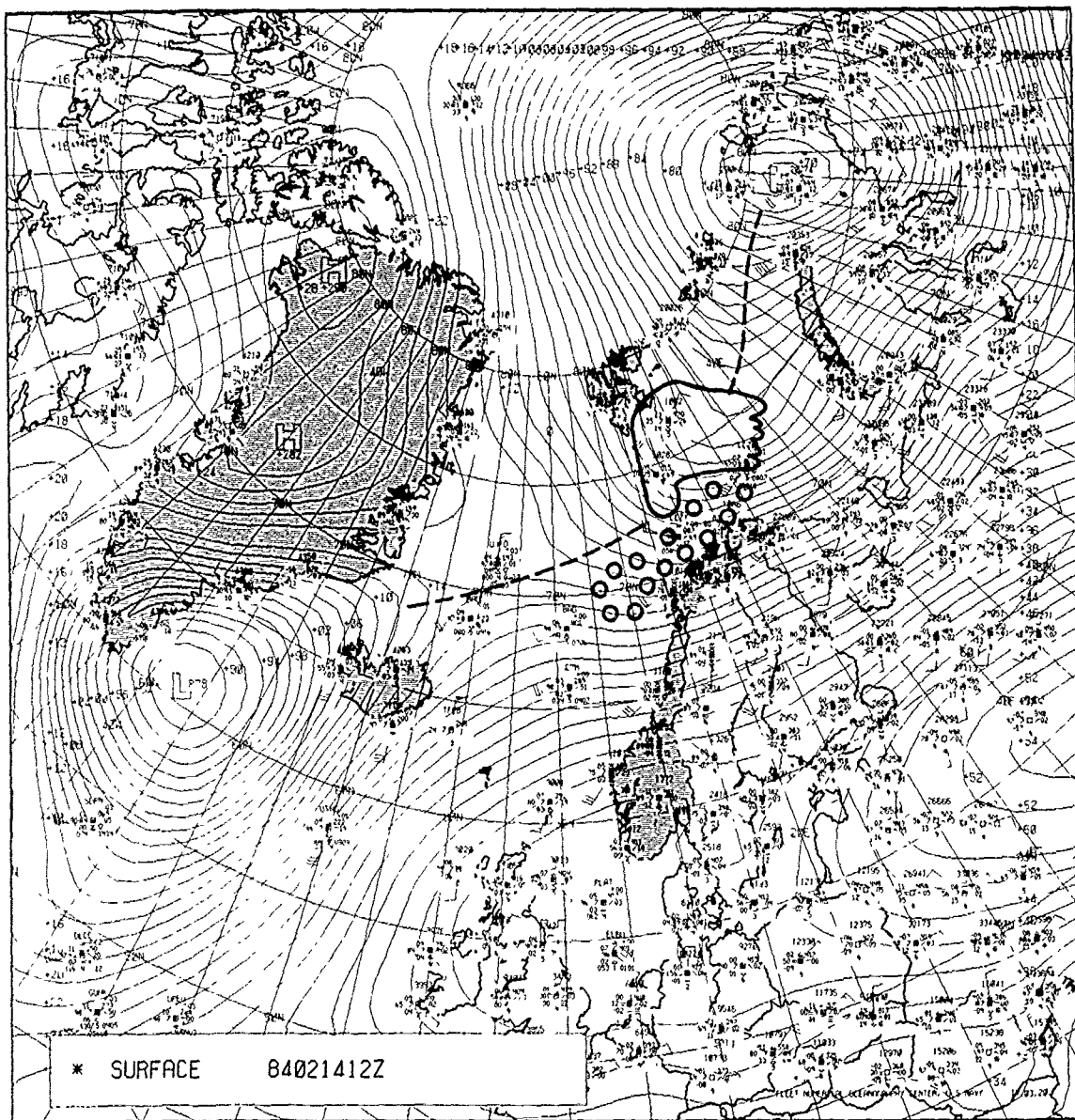




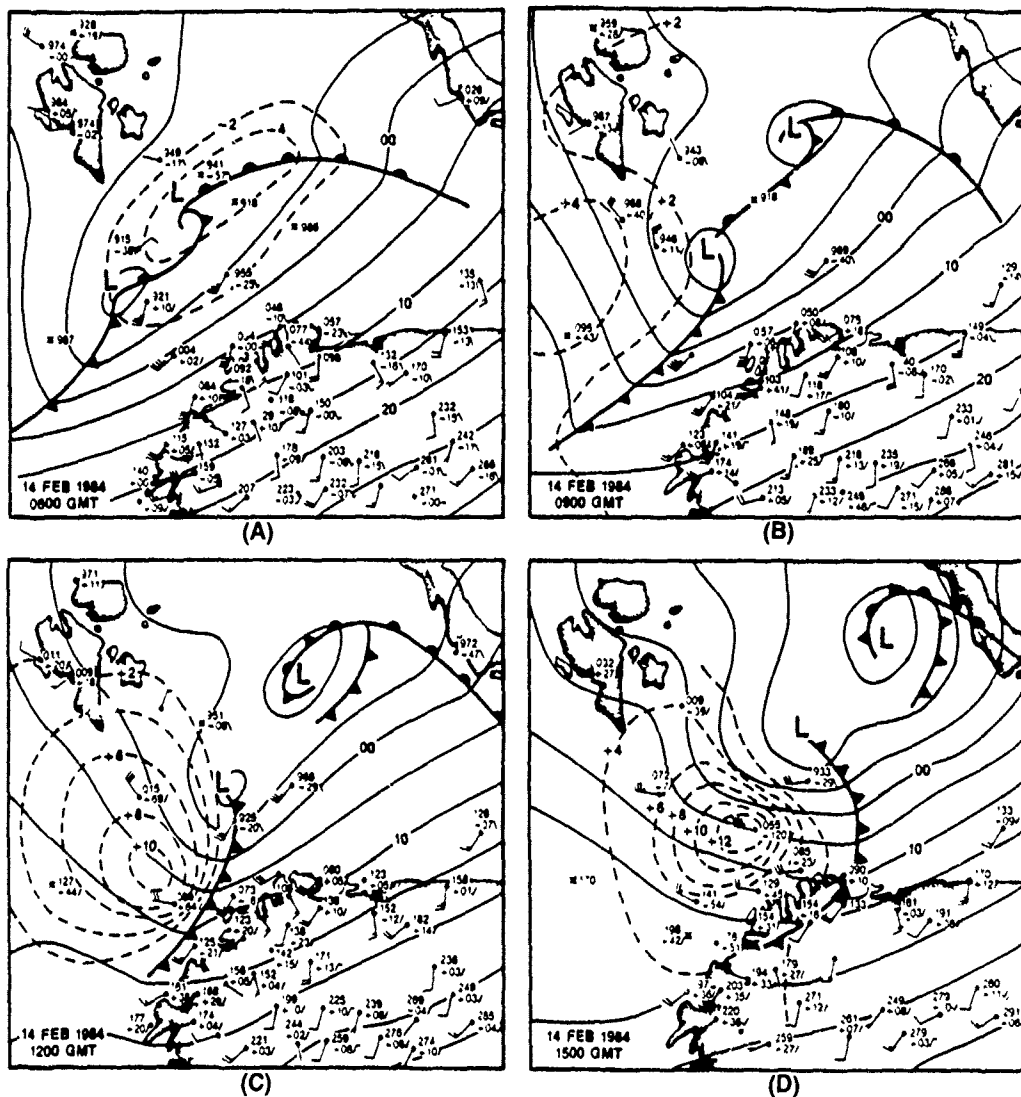
2A-32a. FNOG Surface Analysis With Cloud Outline. 0000 GMT 14 February 1984.



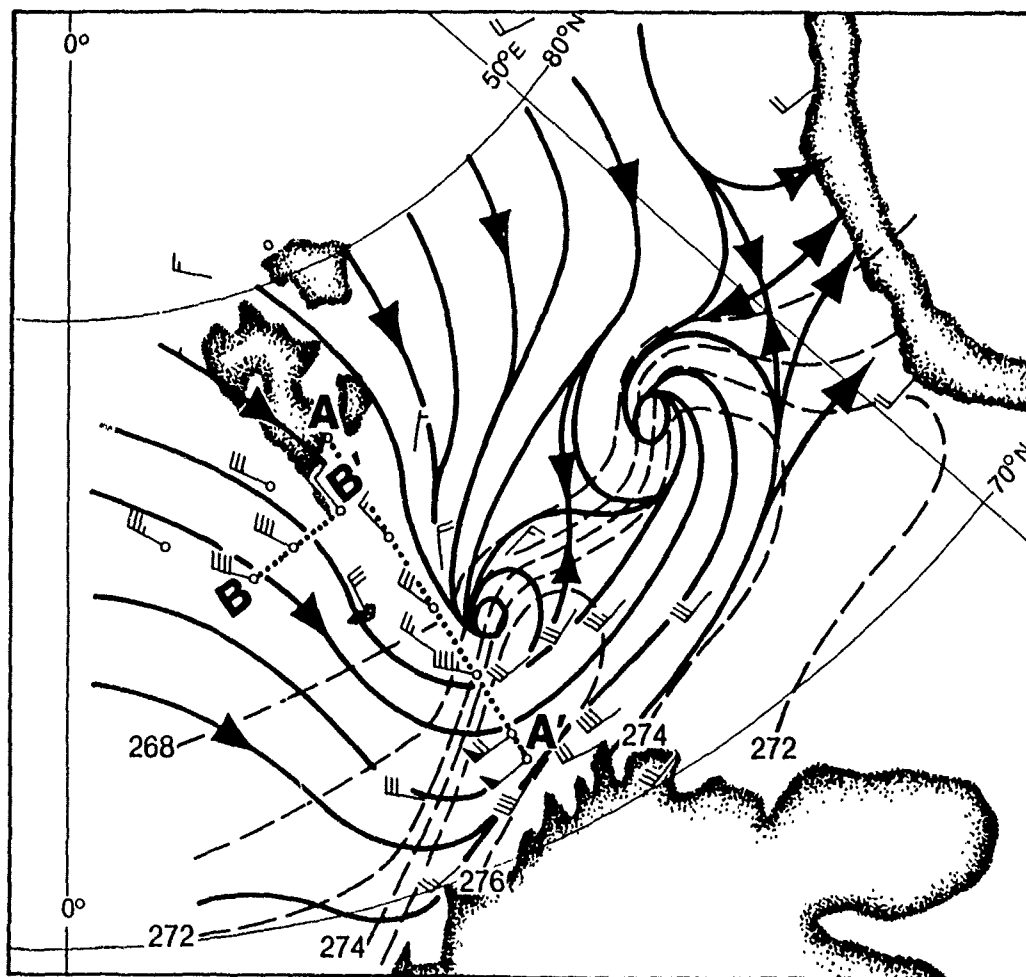
2A-33a. FNOC 500-mb Analysis With Cloud Outline. 0000 GMT 14 February 1984.



2A-34a. FNOG Surface Analysis With Cloud Outline 1200 GMT 14 February 1984.



2A-35a. Detailed Surface Analysis. 0600, 0900, 1200 and 1500 GMT 14 February 1984 (Shapiro and Fedor, 1986).



2A-36a. Surface Streamline Analysis. 1200 GMT 14 February 1984 (Shapiro and Fedor, 1986).

A later NOAA HRPT infrared view of the area (0945 GMT) is shown in Fig. 2A-38a. This depiction more clearly shows the further development of  $L_1$  as a spiral vortex (Figs. 2A-38a[A,B,C]) and a second polar low development  $L_2$  (Figs. 2A-38a[A,D]) further to the east. Note the characteristic cumulonimbus cloud clusters south of each of the systems indicating cold temperatures aloft.

A final view of the storms at 1622 GMT (Fig. 2A-39a) shows the dissipation of  $L_1$  and intensification of  $L_2$ .

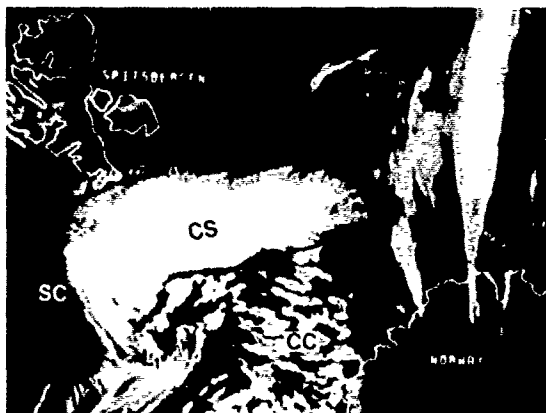
The FNOC 500-mb charts for 14 February at 1200 GMT and 15 February at 0000 GMT (Figs. 2A-40a and 41a), with the cloud cluster outline superimposed over Fig. 2A-40a, reveal movement of the cold trough rapidly eastward following the surface manifestations of the polar low systems. A slight tendency toward anticyclonic flow based on Bear Island's wind of  $280^\circ$  at 65 kt is revealed in the 1200 GMT analysis (Fig. 2A-40a).

#### Important Conclusions

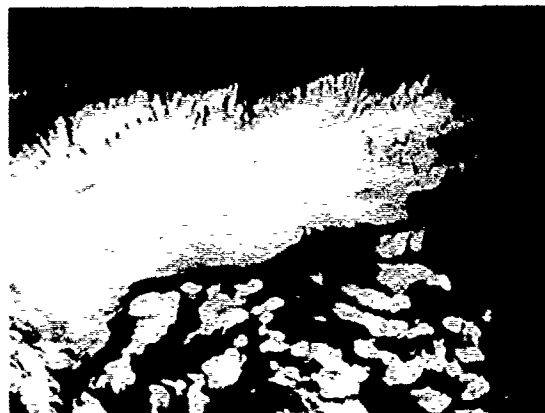
1. Elongated bands of cloud clusters associated with asymptotes of convergence leading into low centers in the Greenland/Norwegian Seas region with heavy convective activity to the south are precursor signs of possible polar low development.
2. Deep open-celled convection over marine areas is associated with cyclonically turning low-level flow with an upper cold low or cold trough at the 500-mb level
3. Multiple polar low developments may occur within the elongated band forming or a convergence asymptote leading into a low pressure center.
4. Despite the weaker appearance of polar lows in comparison to hurricanes, winds of 70 kt or more are common

#### Reference

Shapiro, M.A., and L.S. Fedor. 1986: *The Arctic Cyclone Expedition, 1984 Research Aircraft Observations of Fronts and Polar Lows Over the Norwegian and Barents Seas, Part I. Polar Lows Project*, Technical Report No. 20, NOAA/ERL/Wave Propagation Laboratory, Boulder, CO 80303, 56 pp



(A)



(B)



(C)

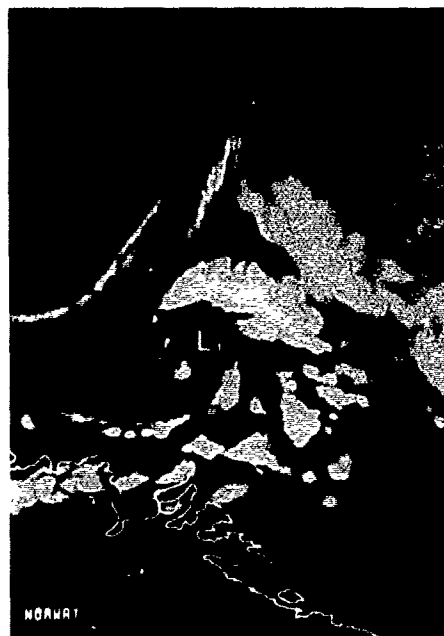


(D)

2A-37a Computer-Enhanced NOAA HRPT Infrared Images. 0440 GMT 14 February 1984 (Shapiro and Fedor, 1986).



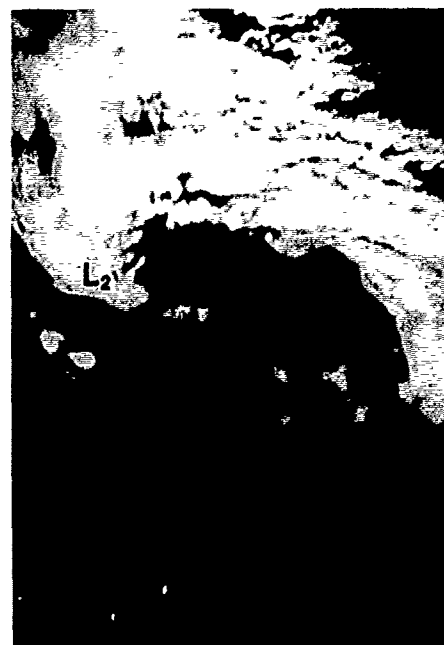
(A)



(B)



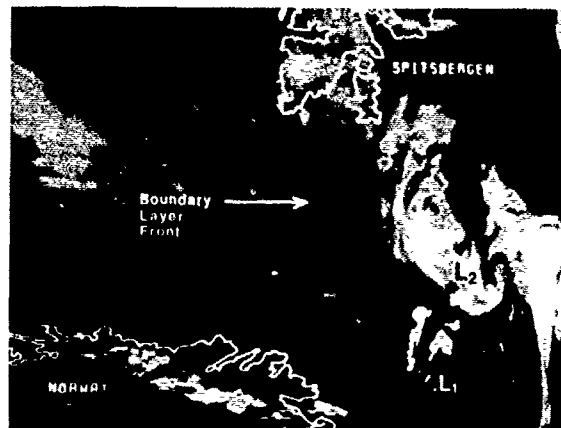
(C)



(D)

2A-38a. Computer-Enhanced NOAA HRPT Infrared Images 0945 GMT 14 February 1984 (Shapiro and Fedor, 1984).





(A)

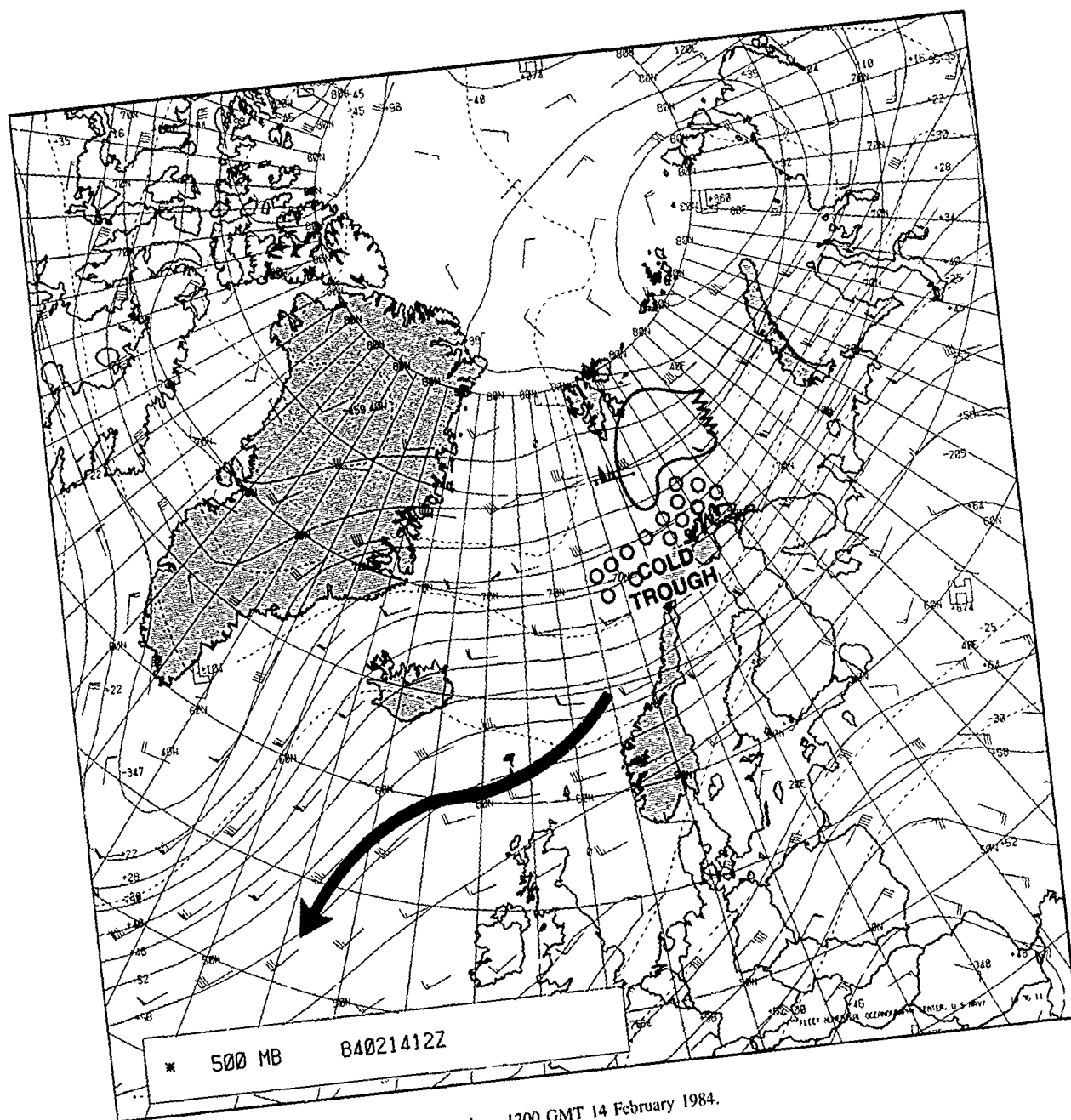


(B)

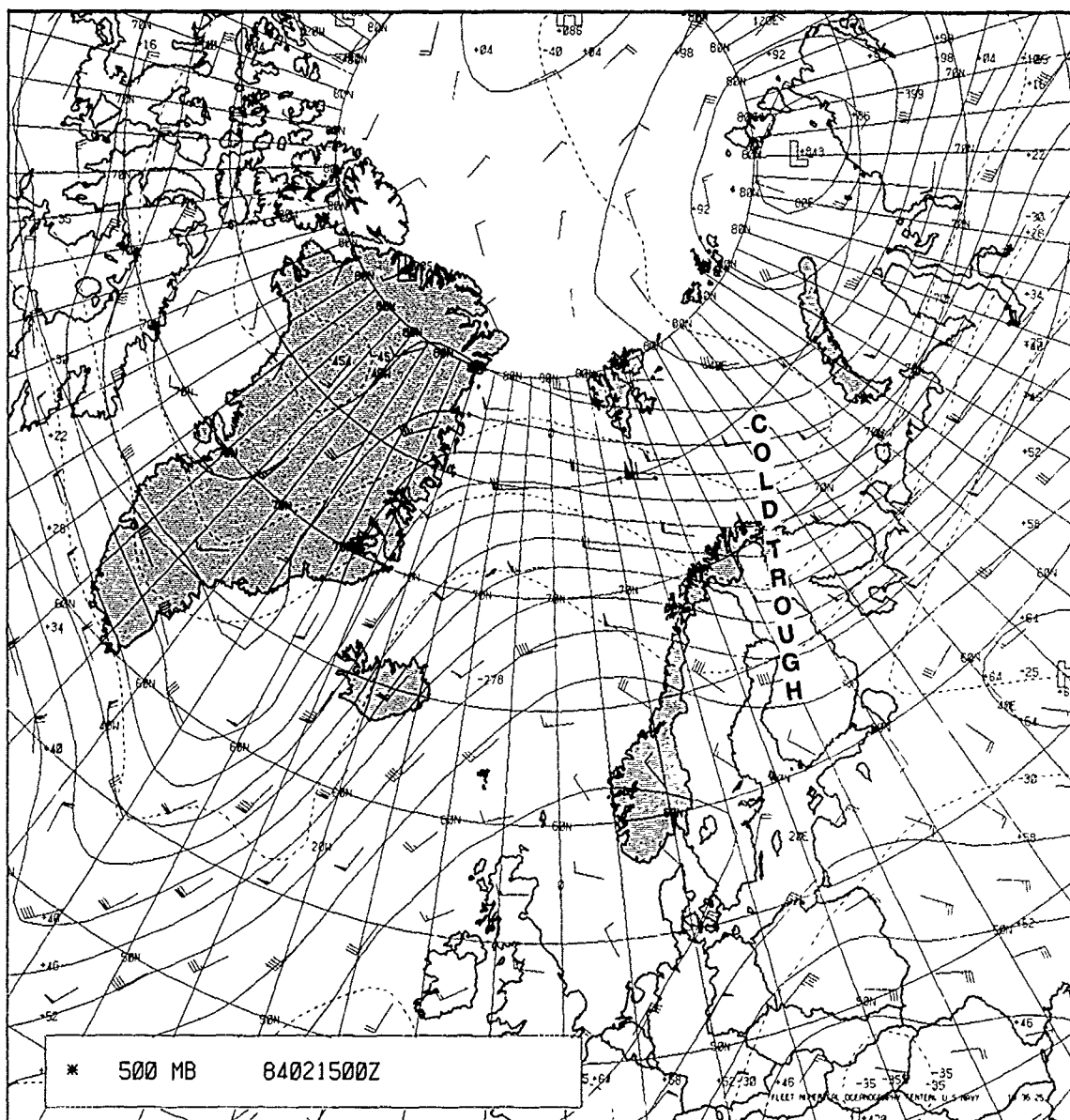


(C)

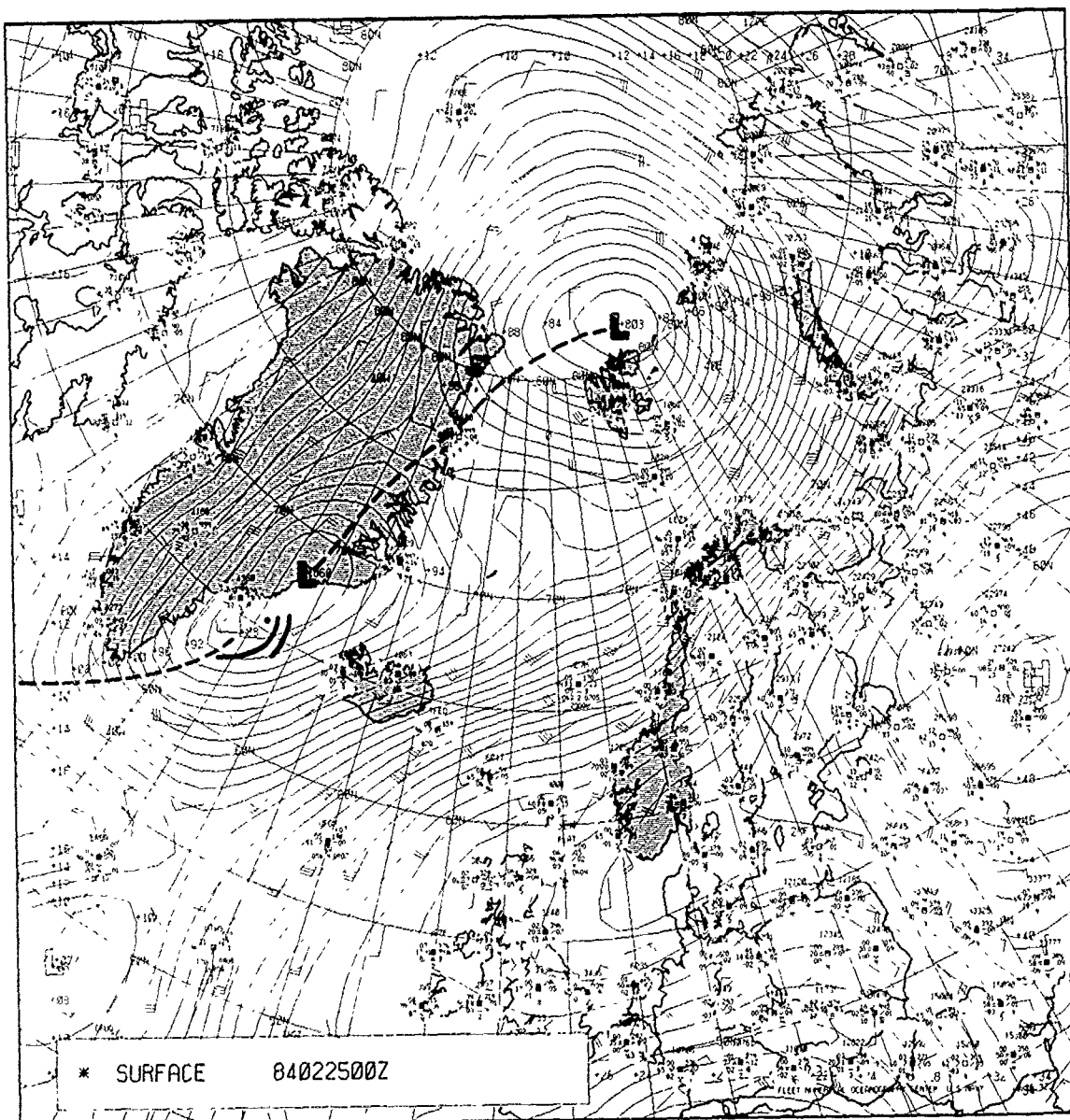
2A-39a. Computer-Enhanced NOAA HRPT Infrared Images.  
1622 GMT 14 February 1984 (Shapiro and Fedor, 1986).



2A-40a. FNOC 500-mb Analysis With Cloud Outline. 1200 GMT 14 February 1984.



2A-41a. FNOC 500-mb Analysis. 0000 GMT 15 February 1984.



2A-42a. FNOC Surface Analysis 0000 GMT 25 February 1984.

### Case 3 Polar Low Development as a Seclusion Process (25-27 February 1984)

#### *Problems Related to the Definition of Polar Lows*

As noted earlier the proper definition of a polar low is still a subject of some debate. From a satellite perspective, cloud vortices in the Arctic take on many different appearances. Forbes and Lottes (1985) distinguished between nine categories of polar vortices based on the appearance of various cloud configurations.

From a satellite perspective, warm-core systems should have an appearance different from cold core systems. The former are typified by the presence of anticyclonic flow over the storm area at upper elevations while cold core systems remain cyclonic with height. Cirrus striations should therefore display a different alignment above the respective systems.

Research studies show examples of apparently both types of development. It also appears possible for a cold core system to evolve into a warm core system so that both structures could be observed in a single storm evolution. The question of intensity is of special interest. When does a polar vortex become strong enough to be classified as a polar low? Forbes and Lottes (1985) decided to use the concept of deficit pressure. Once a central pressure of a polar vortex was measured or estimated, this value was subtracted from a smoothed value obtained at the same position. The smoothed value was obtained from an analysis that was drawn by ignoring all observations in the area of the vortex. Forbes and Lottes estimated that previously documented polar lows had deficit pressures ranging from 4 to 24 mb and decided, for their purposes, to adopt a threshold deficit pressure of 6 mb.

Essential to an early definition of polar lows was that they were small-scale synoptic or subsynoptic disturbances that developed in the cold air masses poleward of major fronts or jet streams. In the first research aircraft flight into a polar low, however, Shapiro *et al.* (1987) documented that this development occurred in a "seclusion" process in which cold arctic air encircled and essentially entrapped a warmer air mass by wrapping around it and separating this air mass from the source air mass to the north. This process was originally described by Bergeron (1928) as a seclusion. The case study that follows describes the polar low evolution investigated by Shapiro. It establishes the fact that not all polar lows develop within a cold polar air stream behind the arctic front.

#### *25 February 1984*

The FNOC surface analysis for 0000 GMT (Fig. 2A-42a) shows two low pressure systems of interest: one near the north coast of Spitsbergen and the other on the southeast coast of Greenland. Strong southwesterly flow bringing relatively warm, moist air into arctic regions is evident flowing past the United Kingdom, the west coast of Norway, and northeastward past Novaya Zemlya into Franz Josef Land. Offshore or off-ice westerly flow is indicated in the region between northern Greenland and Spitsbergen.

The strong pressure gradient and derived computer-produced wind field shown over Greenland is fictitious because of the ice fields that produce "ground-level" elevations of over 10,000 ft (3,270 m). The ice, in some areas, is as thick as 11,188 ft (3,410 m) and elevations of 6,500 to 10,000 ft prevail over most of the island. Due to this problem the 700-mb wind field (Fig. 2A-43a) is more representative of actual conditions at the surface than the surface analysis. This analysis shows two low centers over northern Greenland displaced well to the west of the surface (Spitsbergen) low position at that latitude, with a trough extending southward to southern Greenland. Note that this chart does not suggest strong northerly surface flow as indicated by the surface analysis (Fig. 2A-42a), but southwesterly flow over most of Greenland east of the trough axis.

Conditions at the 500-mb level (Fig. 2A-44a) indicate double cold low centers over northern Greenland with short-wave troughs extending southward and east-southeastward from the centers. A cold pool of air ( $-40^{\circ}\text{C}$ ) overlies the region of the low center. The strong southwest current past Iceland is evident on all of the upper level charts. This flow produces strong cyclonic shear and vorticity in the region along a line between Iceland and Spitsbergen.

A mosaic of DMSP imagery early on 25 February (Fig. 2A-45a) reveals, very clearly, the vortex ( $L_1$ ) northeast of Spitsbergen. Less distinctive, but quite evident is the vortex off the coast of Greenland ( $L_2$ ). The low center is implied by spiral bands of stratocumulus suggesting a center just off the southeast coast. A cold surge of arctic air is shown by west-northwest- and east-southeast-oriented cloud lines in the Davis Strait flowing past the southern tip of Greenland, and further north off the east coast of Greenland, by east-west-oriented cloud lines in the Fram Strait. A third low ( $L_3$ ) well to the south seems part of the scenario that basically shows a series of vortices or waves developing along the band of cloudiness defining a frontal system tending to connect or coming close to connecting  $L_1$ ,  $L_2$ , and  $L_3$ .

The NMC surface analysis (Fig. 2A-46a) shows cold and warm front positions associated with the low centers and the cloud banded structure displayed in Fig. 2A-45a. Note the disagreement of this analysis with the FNOC surface analysis (Fig. 2A-42a) in its depiction of a low center ( $L_4$ ) northeast of Iceland where the FNOC chart shows a ridge.

An individual DMSP infrared image at 0425 GMT (Fig. 2A-47a) shows the vortex north of Spitsbergen and the cloud lines flowing off the marginal ice zone south of the Fram Strait driven by strong westerly winds.

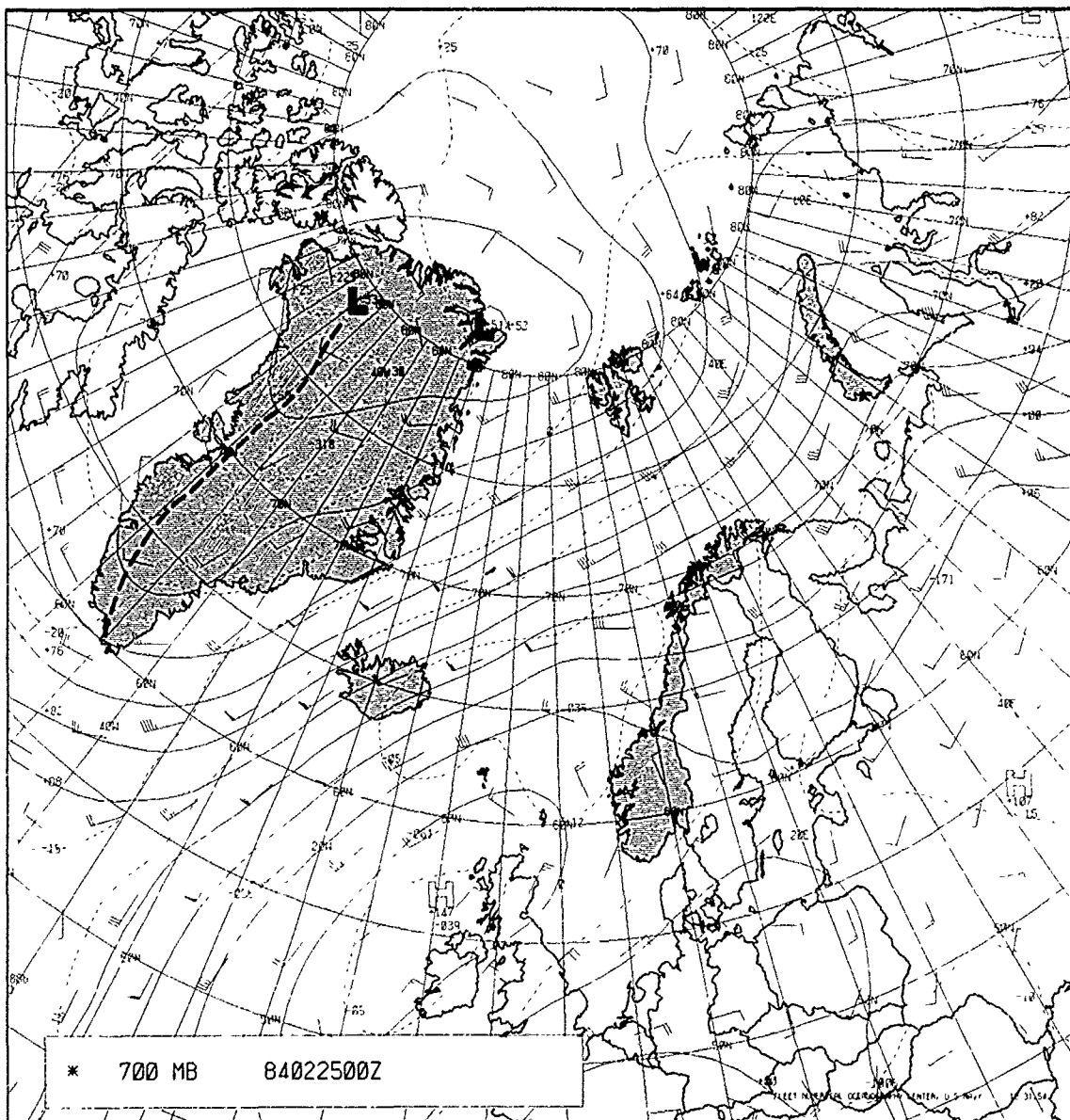
Figure 2A-48a shows another DMSP infrared image with surface reports superimposed much later in the day, at 2027 GMT. The image reveals stratocumulus cloud lines and surface reports defining the vortex west of Iceland essentially on the marginal ice zone along the southeast coast of Greenland. The vortex is obviously weak, containing no middle or upper level cloud structure, despite the apparent strength suggested by the surface analyses. The break in the north-northeast-flowing cirrus cloud band is terrain-induced due to the topography of Iceland. Note that the westerly flow from off the ice edge near  $75^{\circ}\text{N}$  appears to have ceased.

#### 26 February 1984

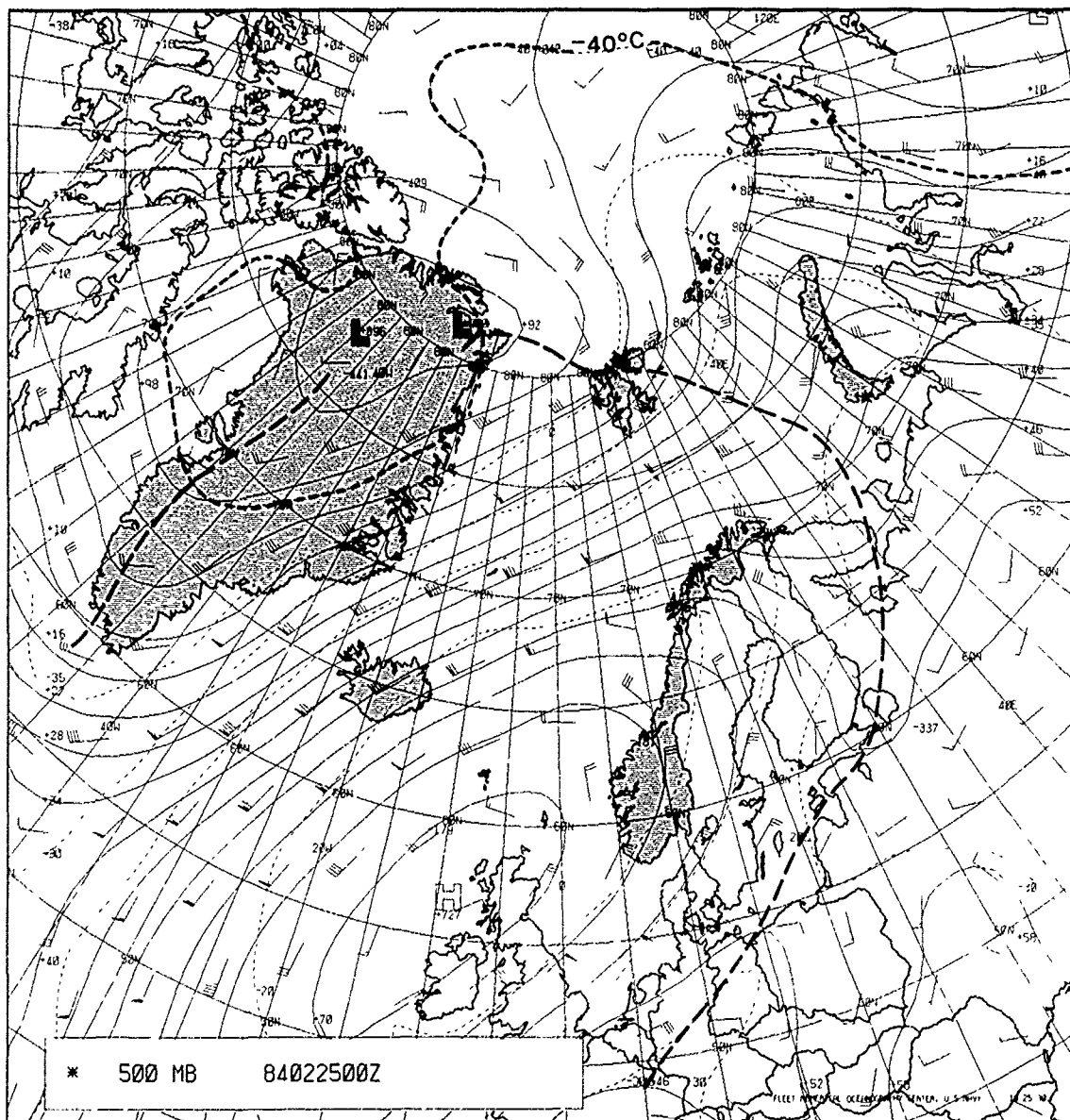
The FNOC surface analysis for 0000 GMT (Fig. 2A-49a) shows little change in the position of the low centers noted 24 hr earlier (Fig. 2A-42a). The trough connecting the centers, however, has moved significantly eastward over the Greenland and Norwegian Seas. Winds along the northeastern coast of Greenland have turned to a more northerly direction permitting very cold air to be advected southward without much temperature change. The low off Greenland is indicated to have filled about 5.5 mb. High pressure is beginning to build in the north-western Greenland region.

The 500-mb analysis (Fig. 2A-50a) reveals a movement of the trough to a more easterly position and movement of the low center to a position just north of Spitsbergen. Jet force winds are evident streaming northeastward past Iceland into the Norwegian Sea.

The jet streak passing into the Norwegian Sea is clearly indicated in a DMSP mosaic early on 26 February (Fig. 2A-51a). The jet axis is located on the northern edge of the elongated cloud band extending over the Norwegian Sea. A break in this band continues to occur over Iceland. Low  $L_1$  is vaguely apparent north of Spitsbergen near  $80^{\circ}\text{N}$ .

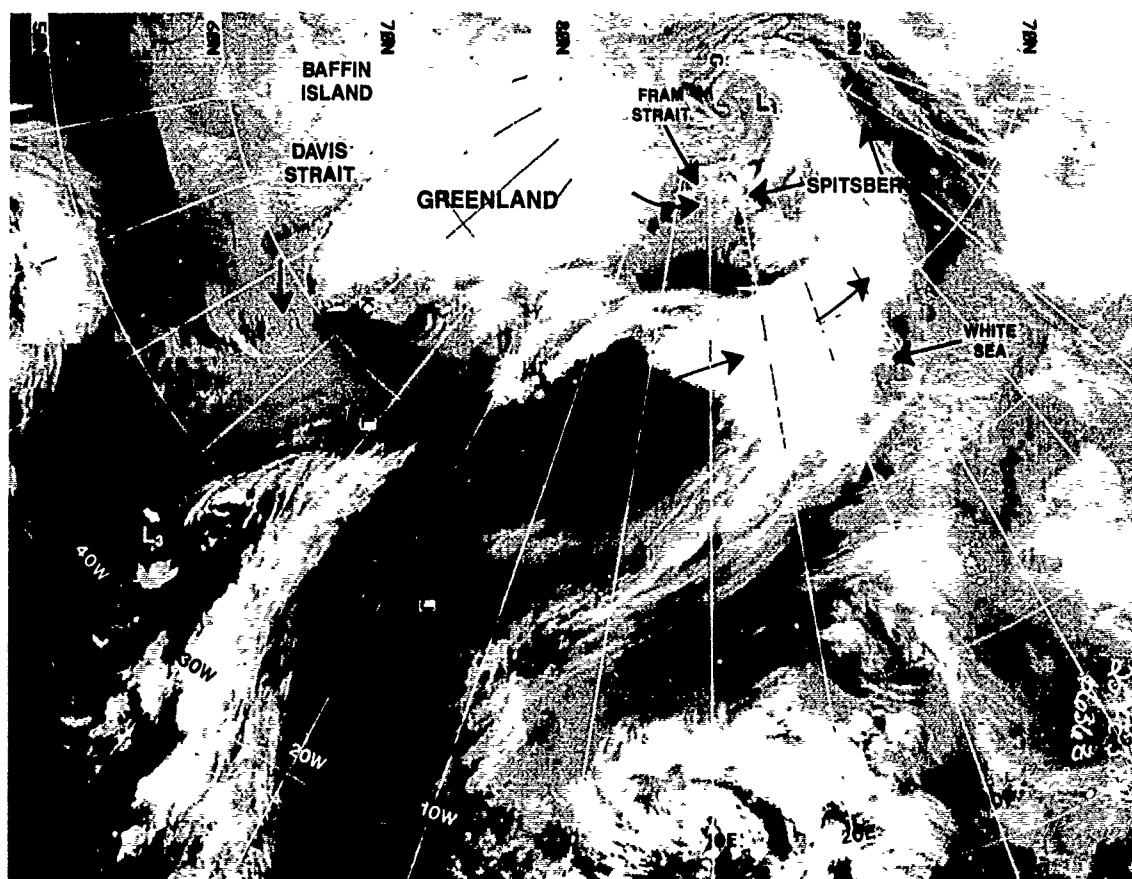


2A-43a. FNOC 700-mb Analysis. 0000 GMT 25 February 1984.

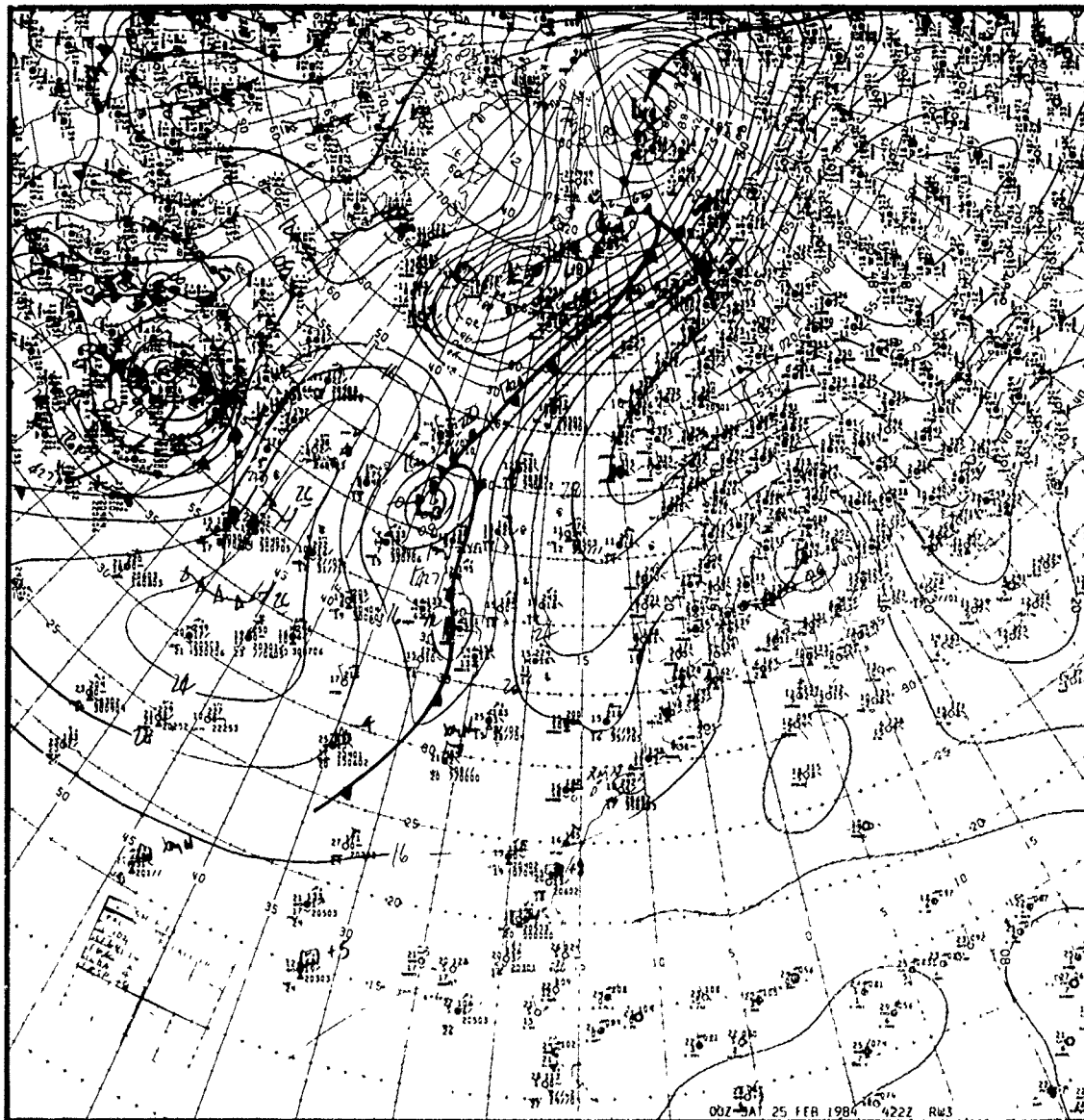


2A-44a. FNOC 500-mb Analysis 0000 GMT 25 February 1984.

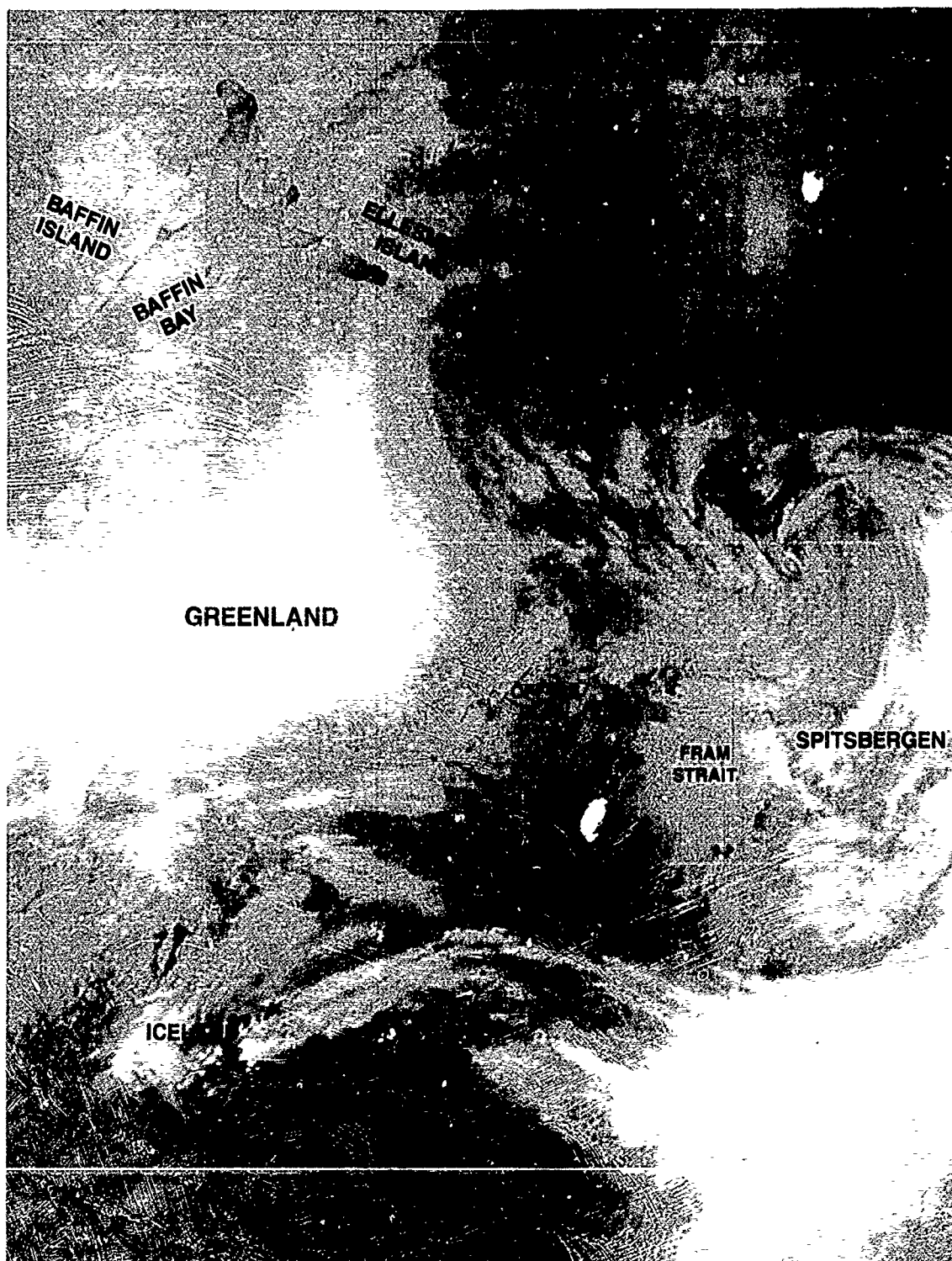




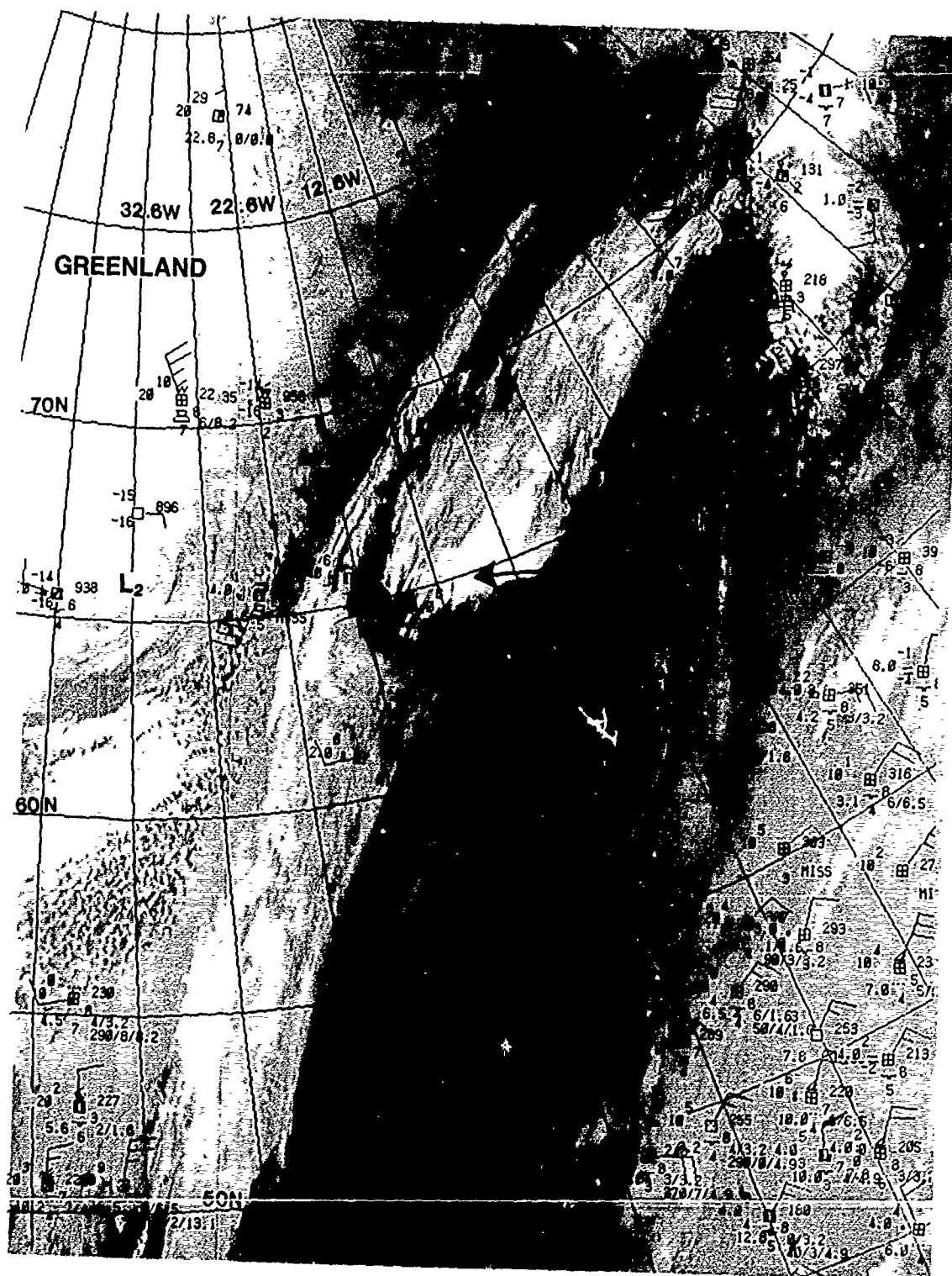
2A-45a. DMSP Infrared Mosaic Data. 0636 GMT 25 February 1984.



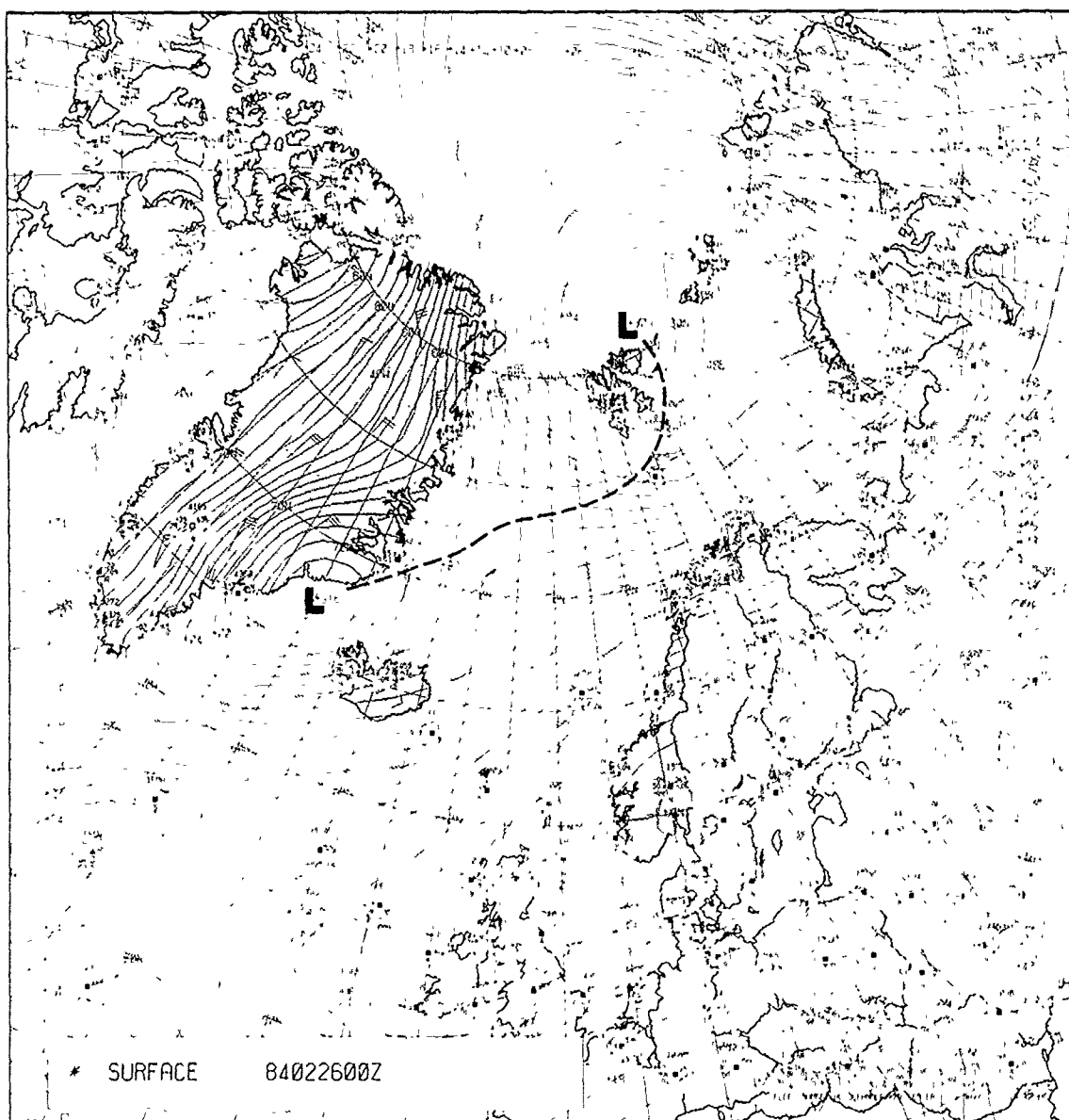
2A-46a NMC Surface Analysis 0000 GMT 25 February 1984



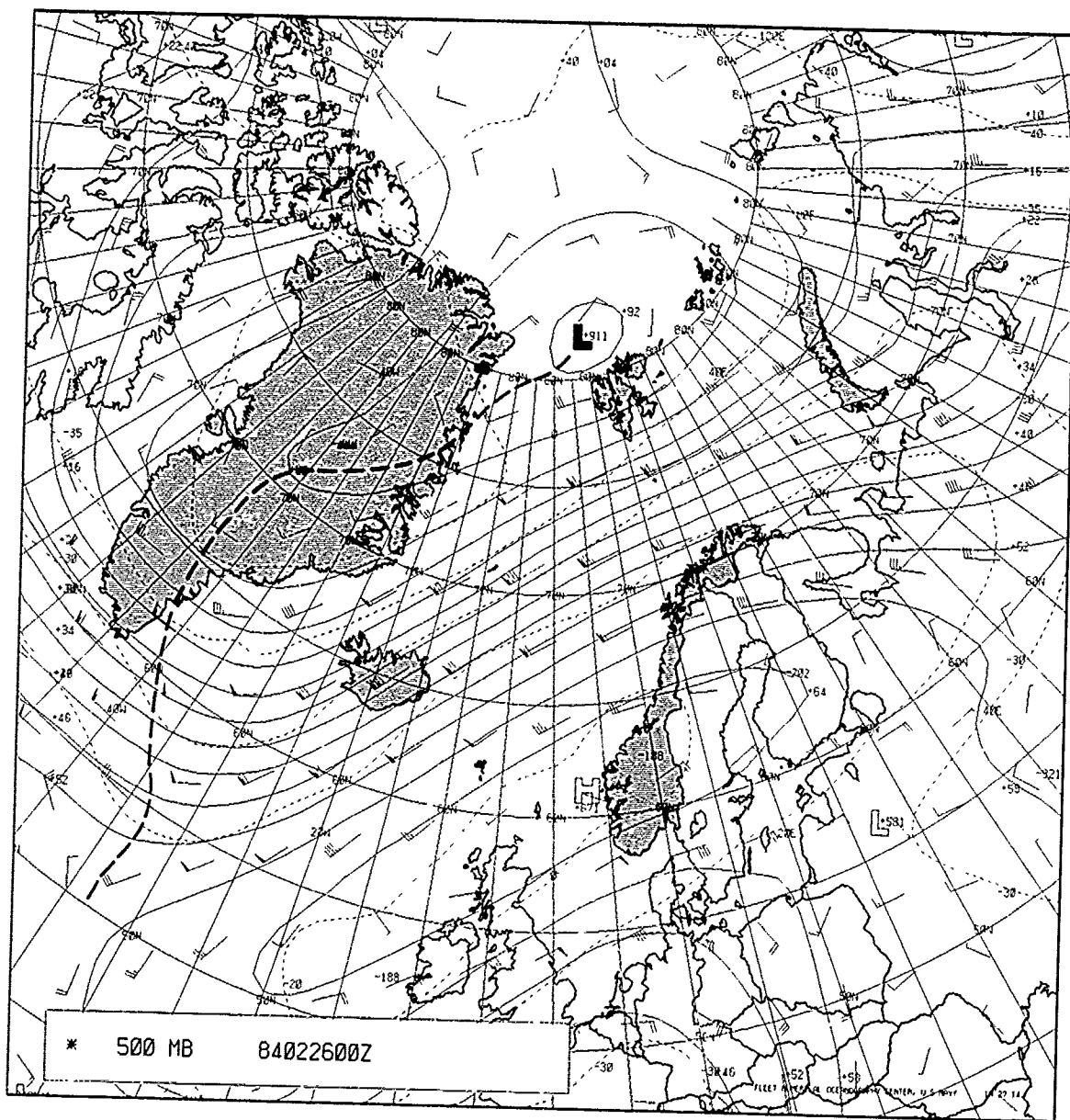
2A-47a. DMSP Infrared (I S) Data, 0425 GMT 25 February 1984.



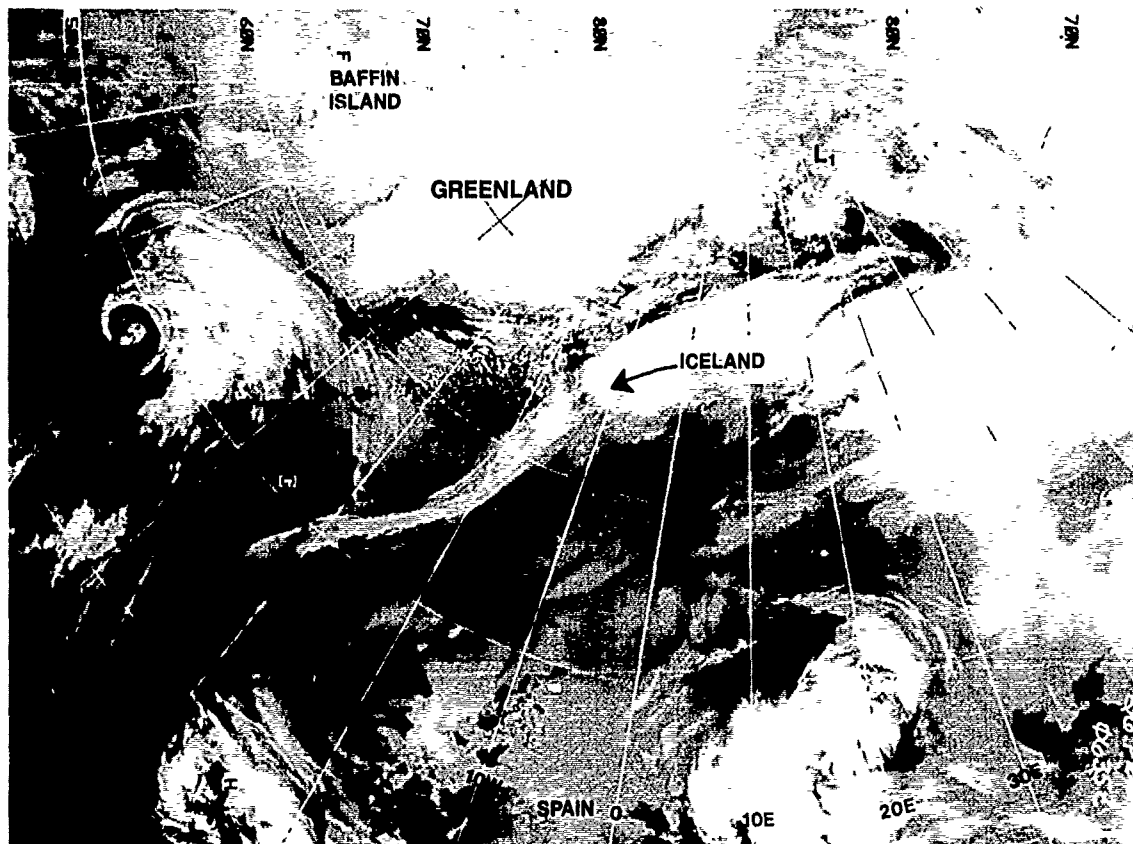
2A-48a. DMSP Infrared (LS) Data. 2027 GMT 25 February 1984.



2A-49a FNOC Surface Analysis 0000 GMT 26 February 1984



2A-50a. FNOC 500-mb Analysis. 0000 GMT 26 February 1984.



2A-51a. DMSP Infrared Mosaic Data. 0635 GMT 26 February 1984



2A-52a. DMSP Infrared (LS) Data. 2006 GMT 26 February 1984.



The low off the coast of Greenland is not well defined on this mosaic, but appears clearly in a DMSP infrared image at 2006 GMT (Fig. 2A-52a) just west of Iceland, which is partially obscured by the banded cloud structure west of the storm center. A streamline analysis, based on surface reports superimposed on this image, is shown in Fig. 2A-53a. The analysis clearly reveals the low center west of Iceland, and a trough extending northeastward past Jan Mayen Island. Note, near the top of the image at about 72°N, the elongated band of overcast cloudiness that extends westward from an anticyclonically curved band of jet stream cirrus cloudiness. Such a development is suspiciously similar to Weldon's description of Meridional Trough (type I) Cyclogenesis (see NTAG, Vol. 4, Sec. 2A, p. 2A-7). The anticyclonically curved cirrus streak is indicative of a short-wave ridge in advance of a short-wave trough moving up the frontal cloud band. Weldon describes how comma-shaped vorticity areas (cloud masses) emerge and move outward from under the cirrus shield and undergo cyclogenesis. His further description seems especially applicable to this example: "Although the tops of the clouds in the comma-head region are normally middle level, they often reach cirrus level, but are lower than the cirrus deck to the right of the jet axis." The elongated cloud band in Fig. 2A-53a seems to conform to this description.

A DMSP infrared mosaic (Fig. 2A-54a) at 2148 GMT shows this cloud band at about 72°N with another, not too dissimilar band, appearing just south of 70°N. The latter band, with  $L_2$  immediately to the south, was the band destined for significant cyclogenesis, while the band to the north seemed to persist as a significant baroclinic zone.

The outline of these cloud bands has been superimposed on the FNOC 1800 GMT surface analysis (Fig. 2A-55a). The cloud bands are shown to lie along the trough line connecting  $L_1$  to  $L_2$ . The band north of 70°N is in the col region separating  $L_1$  from  $L_2$ . Such an area is an ideal region for frontogenesis. Fig. 2A-56a is a schematic showing how such col regions act to concentrate the isotherms between air, which is cold to the northwest and warm to the southeast, creating a frontogenetic zone.

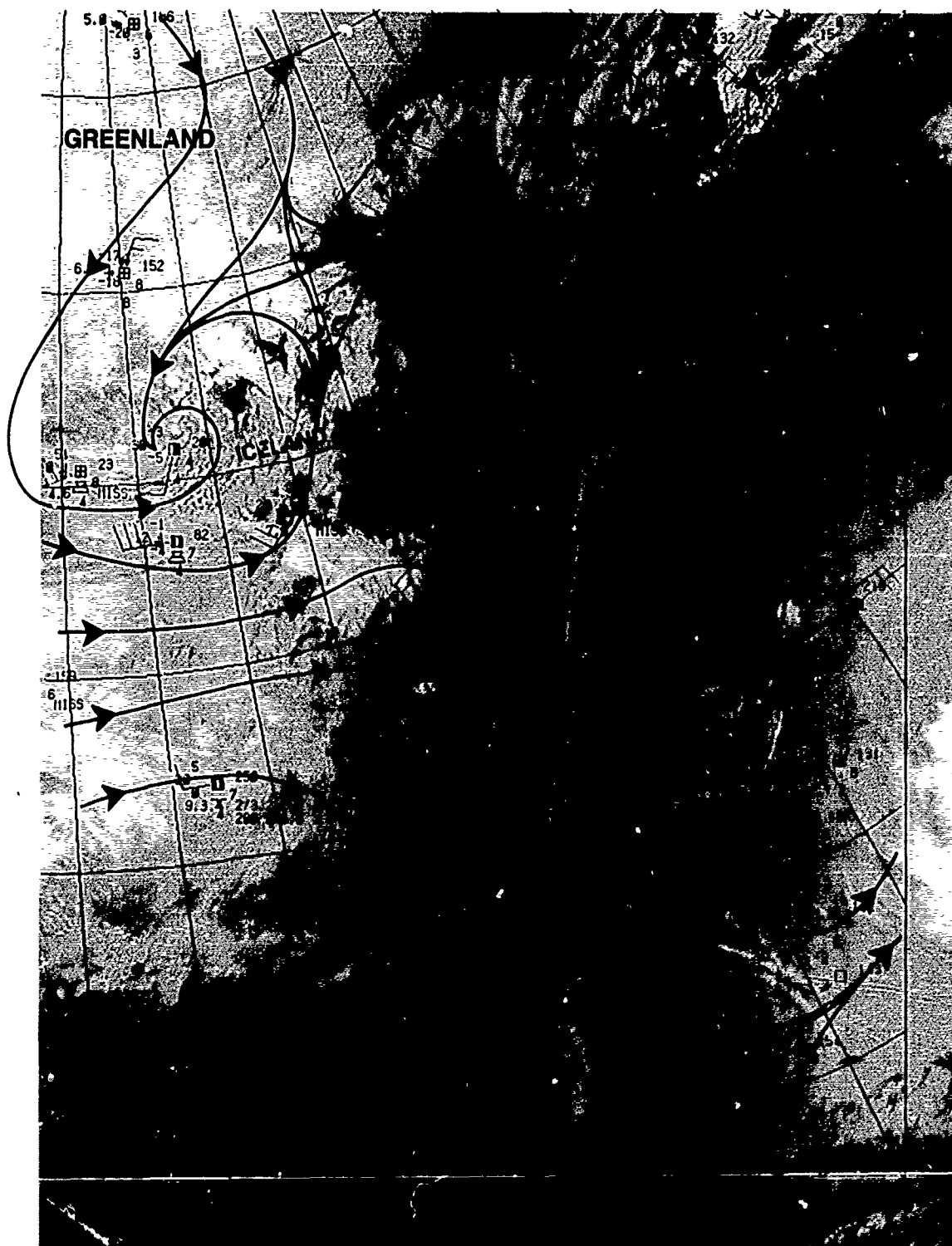
A comparison of Fig. 2A-55a with Fig. 2A-42a shows that the westerly flow through the Fram Strait has changed to northerly, permitting cold arctic air to flow southward along the ice-covered east coast of Greenland, past Scoresby Sund and Iceland, and creating an arctic frontal boundary south of Iceland and a frontogenetic (cyclogenetic) zone in the col region to the northeast near Jan Mayen.

#### 27 February 1984

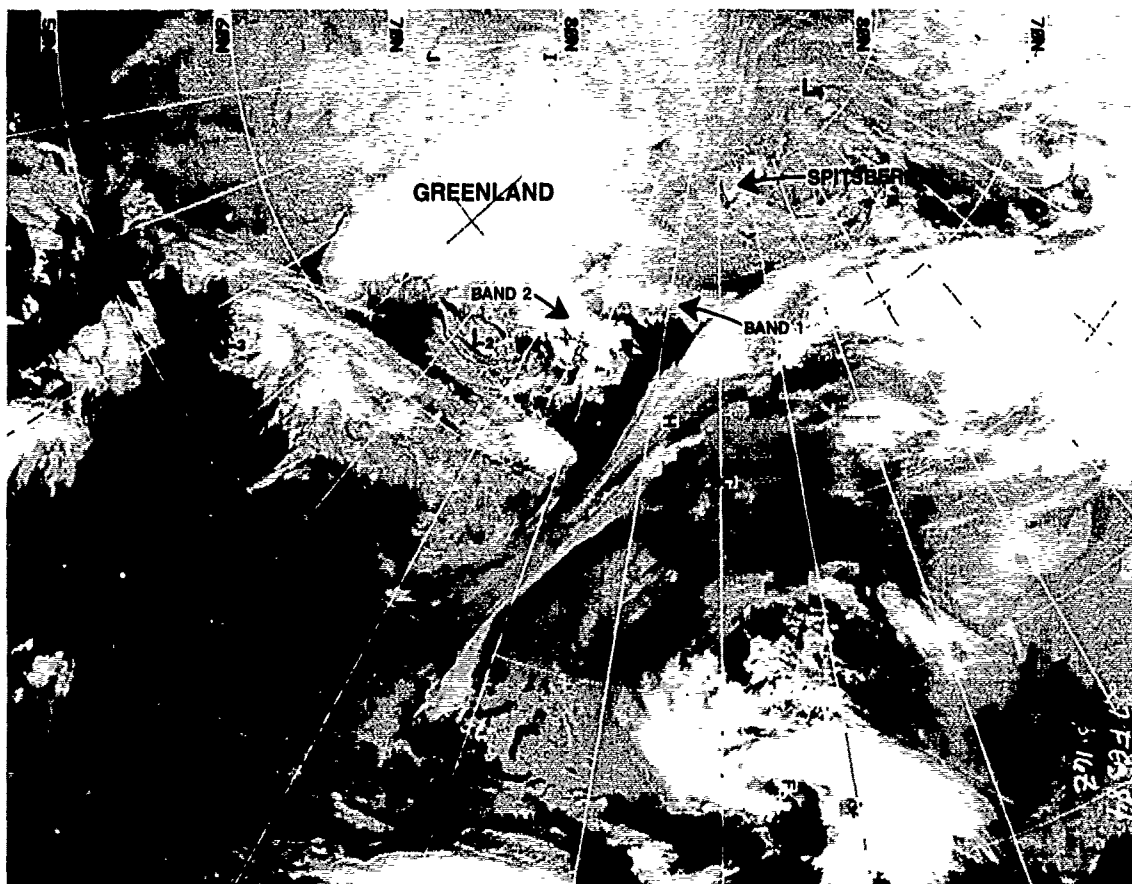
On 27 February the FNOC 0000 GMT surface analysis (Fig. 2A-56b) shows a significant eastward movement of both  $L_1$  and  $L_2$  and of the trough connecting them. Both lows are indicated to have filled slightly during the preceding 24-hr period. A high pressure cell has continued to build over northwestern Greenland.

Succeeding surface analyses on the 27th at 0600, 1200, and 1800 GMT (Figs. 2A-57a, 2A-57b, and 2A-58a, respectively) show  $L_2$  moving rapidly and deepening as it approaches the north coast of Norway. A speed of movement of 60 kt is implied by the change of position between 0600 and 1200 GMT. Based on satellite imagery and research aircraft results, observations show that these analyses are erroneous and grossly over-simplify the developments that actually occurred. Chief among these was the development and dissipation of a polar low of near-hurricane intensity and the development and dissipation of at least three other vortices in the region of what has been analyzed as a single low.

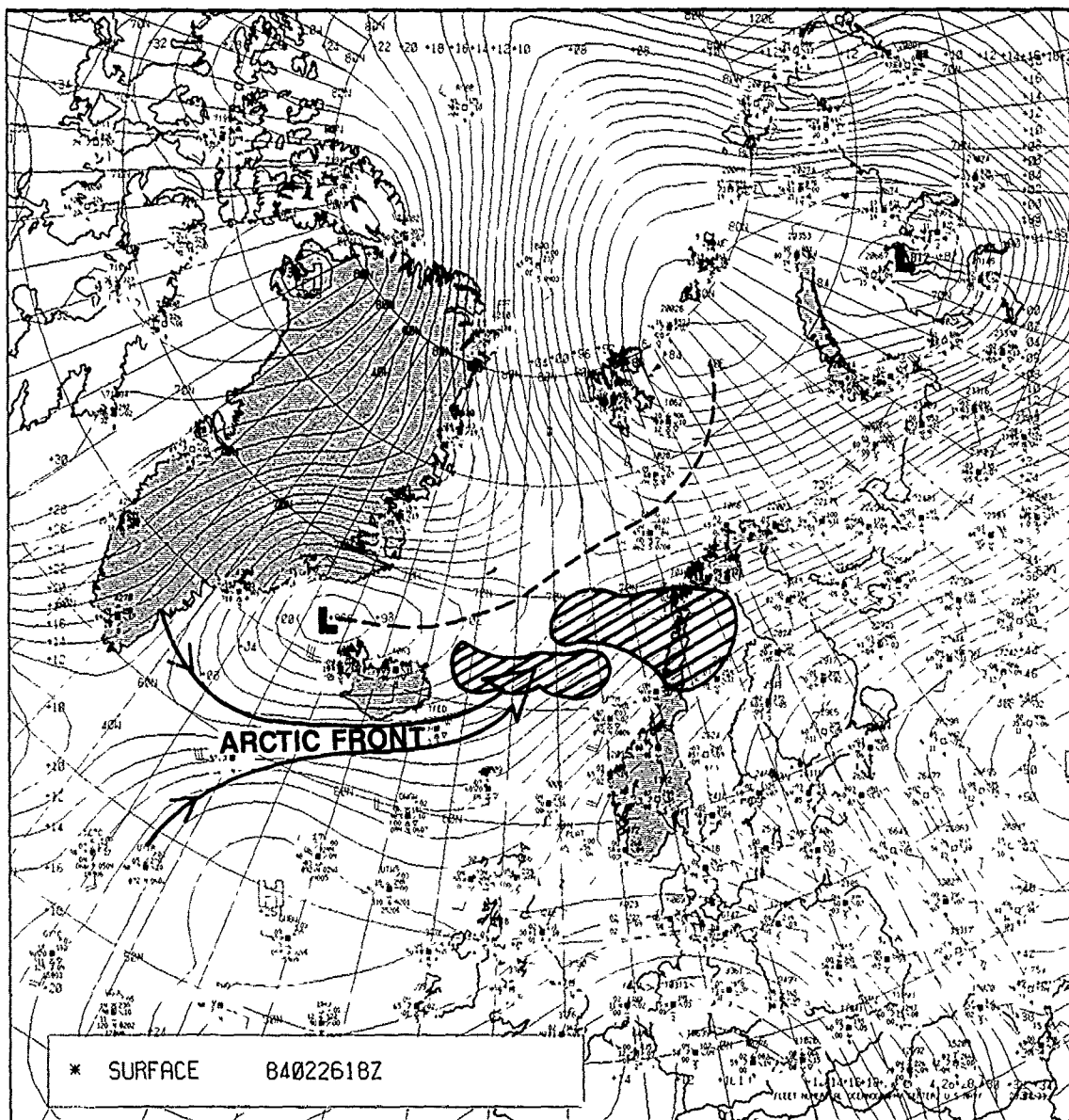
A DMSP infrared mosaic over the region at 0524 GMT (Fig. 2A-59a) reveals an apparent strengthening of individual cloud clusters within the cloud band nearest  $L_2$ . At least three separate comma-shaped cloud masses are evident, while the band to the north also appears to have intensified, creating cloudiness that reaches higher (colder) elevations.



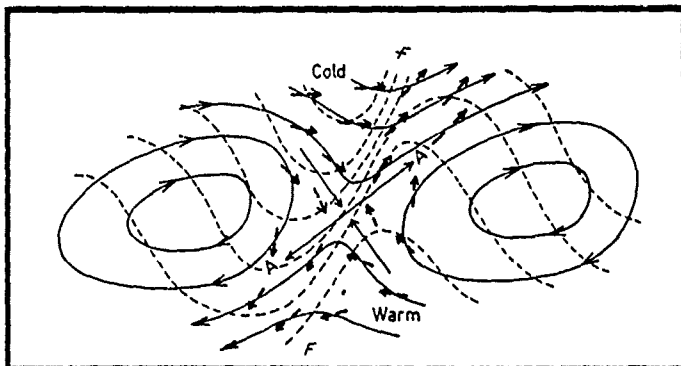
2A-53a. DMSP Infrared (LS) Data With Surface Observations (1800 GMT) and Streamline Analysis.  
2006 GMT 26 February 1984.



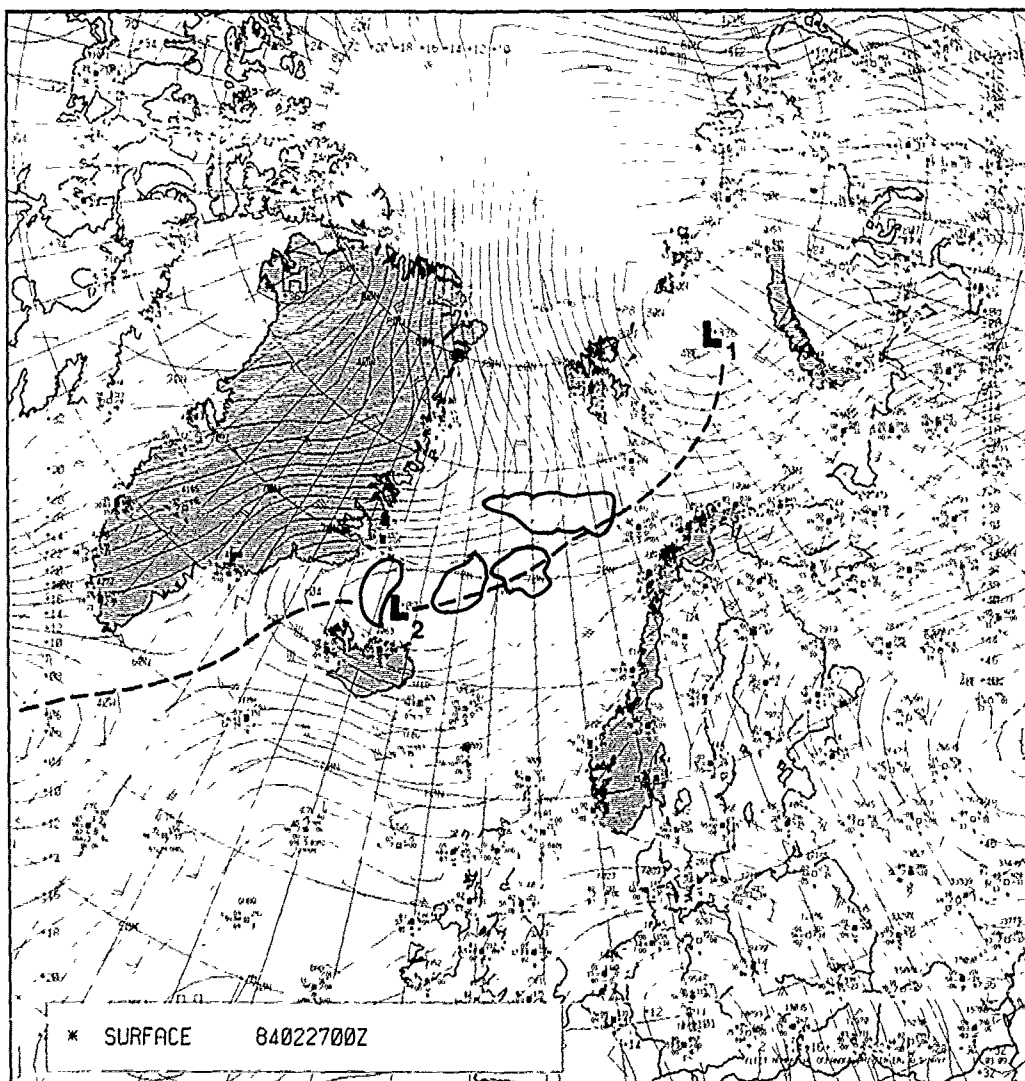
2A-54a. DMSP Infrared Mosaic Data. 2148 GMT 26 February 1984.



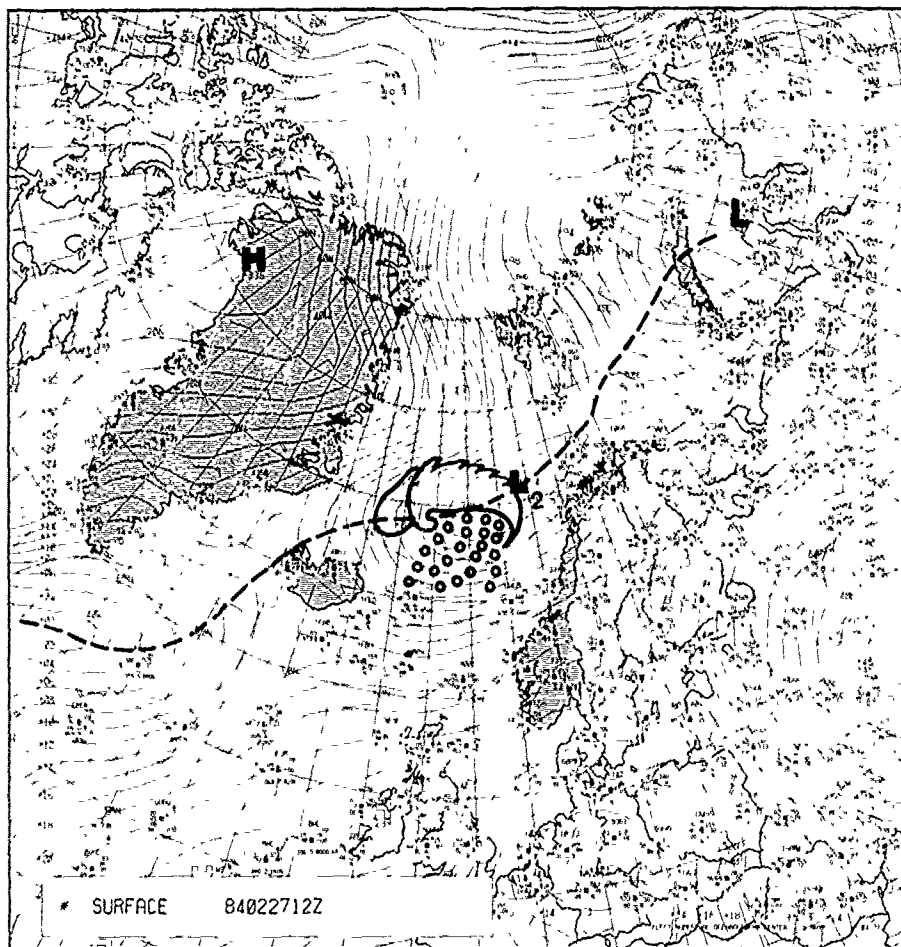
2A-55a. FNOC Surface Analysis and Cloud Outline. 1800 GMT 26 February 1984.



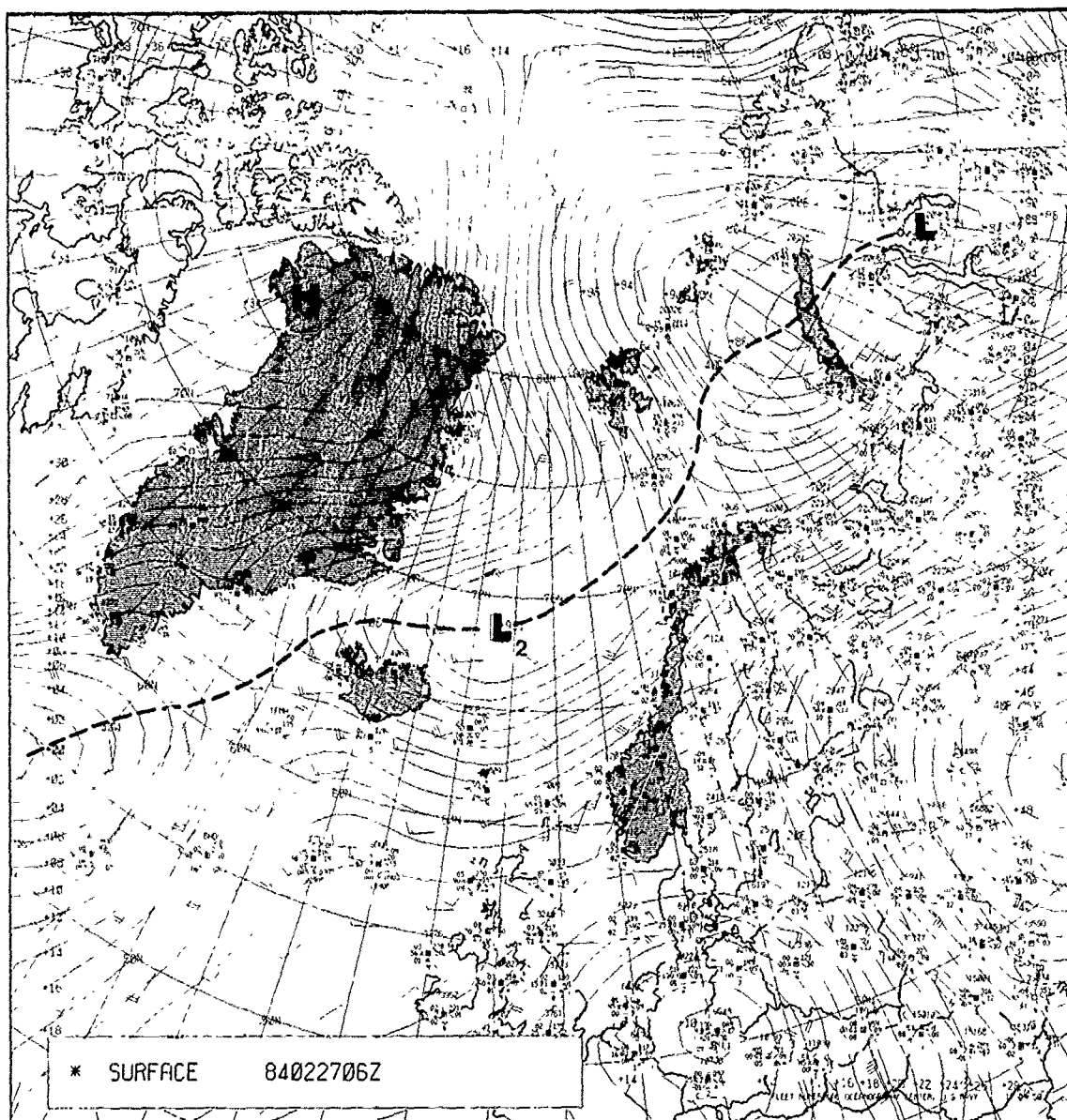
2A-56a. A Schematic Illustrating Frontogenesis in a Col.



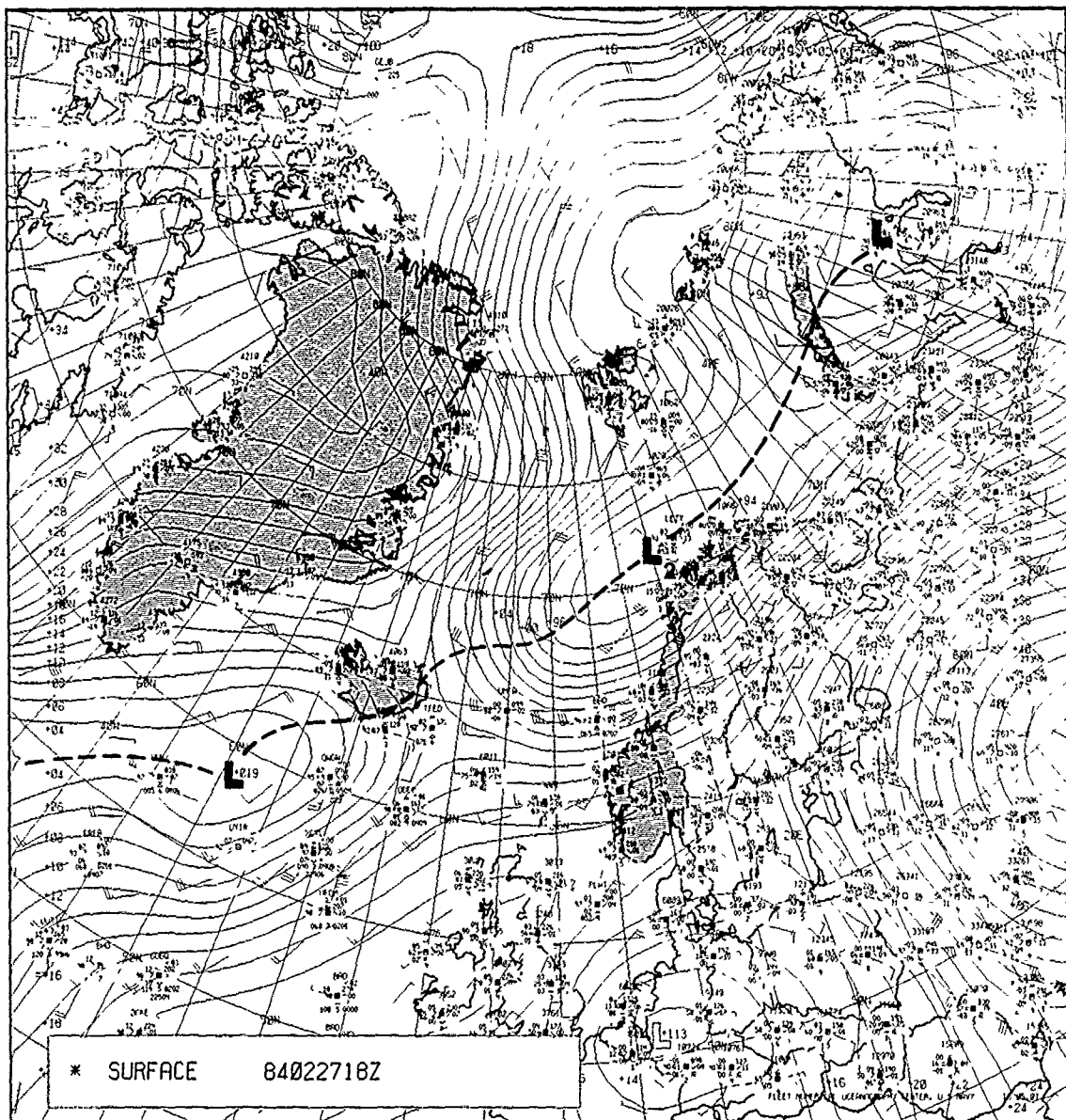
2A-56b. FNOC Surface Analysis. 0000 GMT 27 February 1984.



2A-57b. FNOC Surface Analysis. 1200 GMT 27 February 1984.

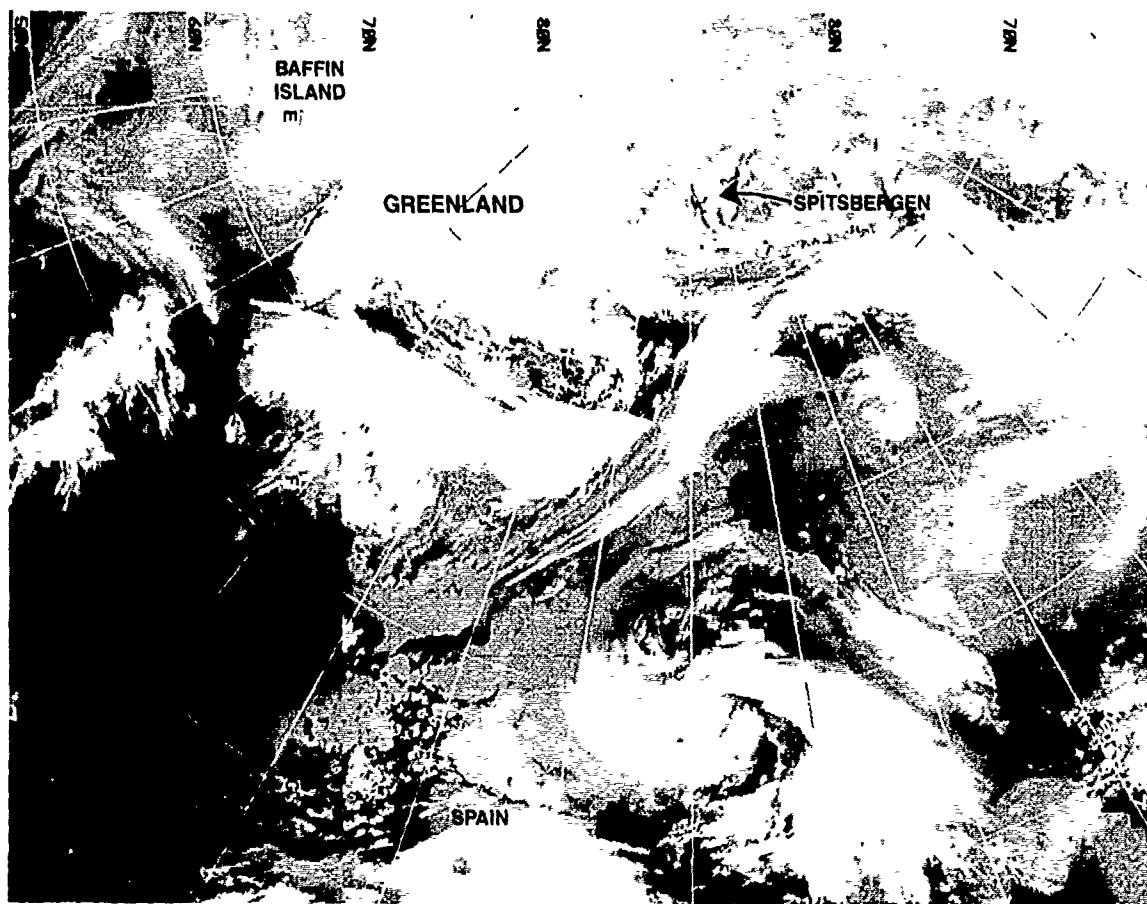


2A-57a FNOC Surface Analysis. 0600 GMT 27 February 1984



2A-58a. FNOC Surface Analysis. 1800 GMT 27 February 1984.





2A-59a. DMSP Infrared Mosaic Data. 0524 GMT 27 February 1984.



2A-60a. DMSP Infrared (LS) Data. 0524 GMT 27 February 1984.

The individual DMSP infrared data used in the mosaic are shown in Fig. 2A-60a. Strong westerly jet force winds were blowing aloft past Iceland in a jet streak with core winds of over 100 kt just south of the island, as shown on the 300-mb analysis for 0000 GMT (Fig. 2A-61a). Orographic lifting has produced a bright cloud on the southeast side of the island over terrain that rises to 2119 m. A series of gravity waves extends eastward from the high terrain reflecting the effect of these strong winds. A streamline analysis, based on surface observations superimposed on Fig. 2A-60a (Fig. 2A-62a), shows that the cloud clusters are embedded in a broad trough region. Lack of surface observations over much of the region prevents a more detailed analysis. The jet streak's location places the easternmost cloud cluster in the front left quadrant of the jet core. This is the most favorable position to influence cyclogenesis.

The 500-mb analysis for 0000 GMT (Fig. 2A-63a) is also of interest. This analysis shows a cold trough extending south of the cloud band with flow turning anticyclonically over the eastern portion of the cloud band. Such a flow pattern promotes positive vorticity advection and upper level divergence favorable for intensification. Therefore, it comes as no surprise that the easternmost cluster is the one destined for explosive development during the next few hours.

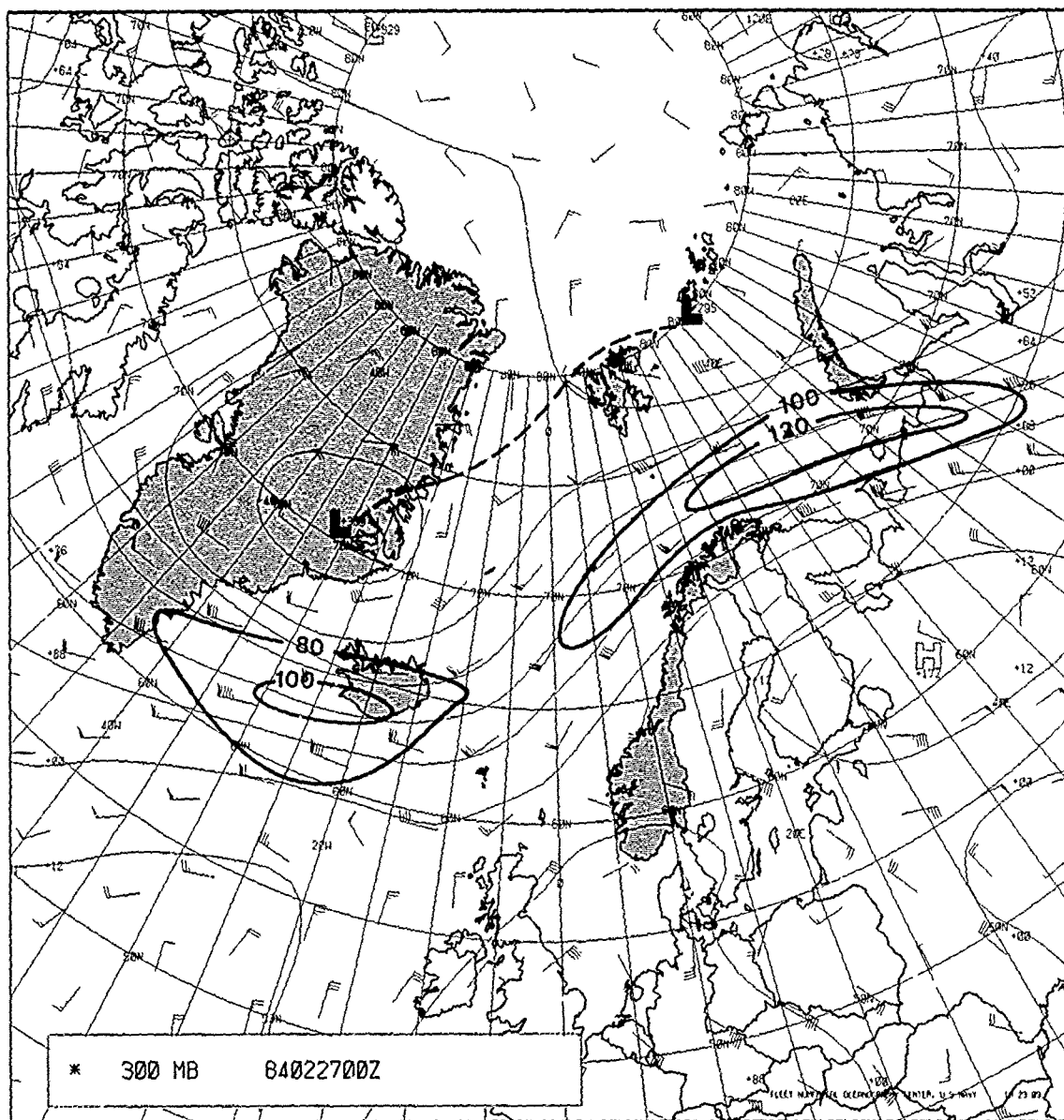
A NOAA P-3 flew into this storm approximately 7 hr after the DMSP data shown in Figs. 2A-59a and 2A-60a. Letdown from 580-mb to the 300-m level was in the vicinity of 69°N 3°W. A dropwindsonde was released just prior to descent. Telemetered wind reports from the instrument indicated an increase of winds at the 2-km (6562 ft) level to  $25 \text{ ms}^{-1}$ . At 150 m (492 ft) they exceeded  $30 \text{ ms}^{-1}$  wind speeds indicative of an intense polar low. The aircraft continued descent to 300 m where clear views of the ocean revealed wind-driven sea swell with a height of 12 m (39.4 ft). Such conditions certainly could not have been anticipated based on the contemporary surface analyses previously shown.

The evolution in appearance of the polar low complex from 0725 GMT to 1340 GMT is shown in Figs. 2A-64a(A), 2A-64a(B), 2A-64a(C), and 2A-64a(D). Jan Mayen Island appears just north of the center of Fig. 2A-64a as a short white dash. Note movement of the polar low cloud complex eastward toward the west coast of Norway, south of Jan Mayen and the progressive strengthening and establishment of a circulation center in the easternmost vortex. Referring back to Fig. 2A-56b, where cloud outlines have been superimposed, it can be seen that the cloud cluster complex east of  $L_2$  has developed in the shear region and baroclinic zone between cold arctic air coming down from the Fram Strait and warmer, moist, southwesterly flow coming up past the east coast of Iceland.

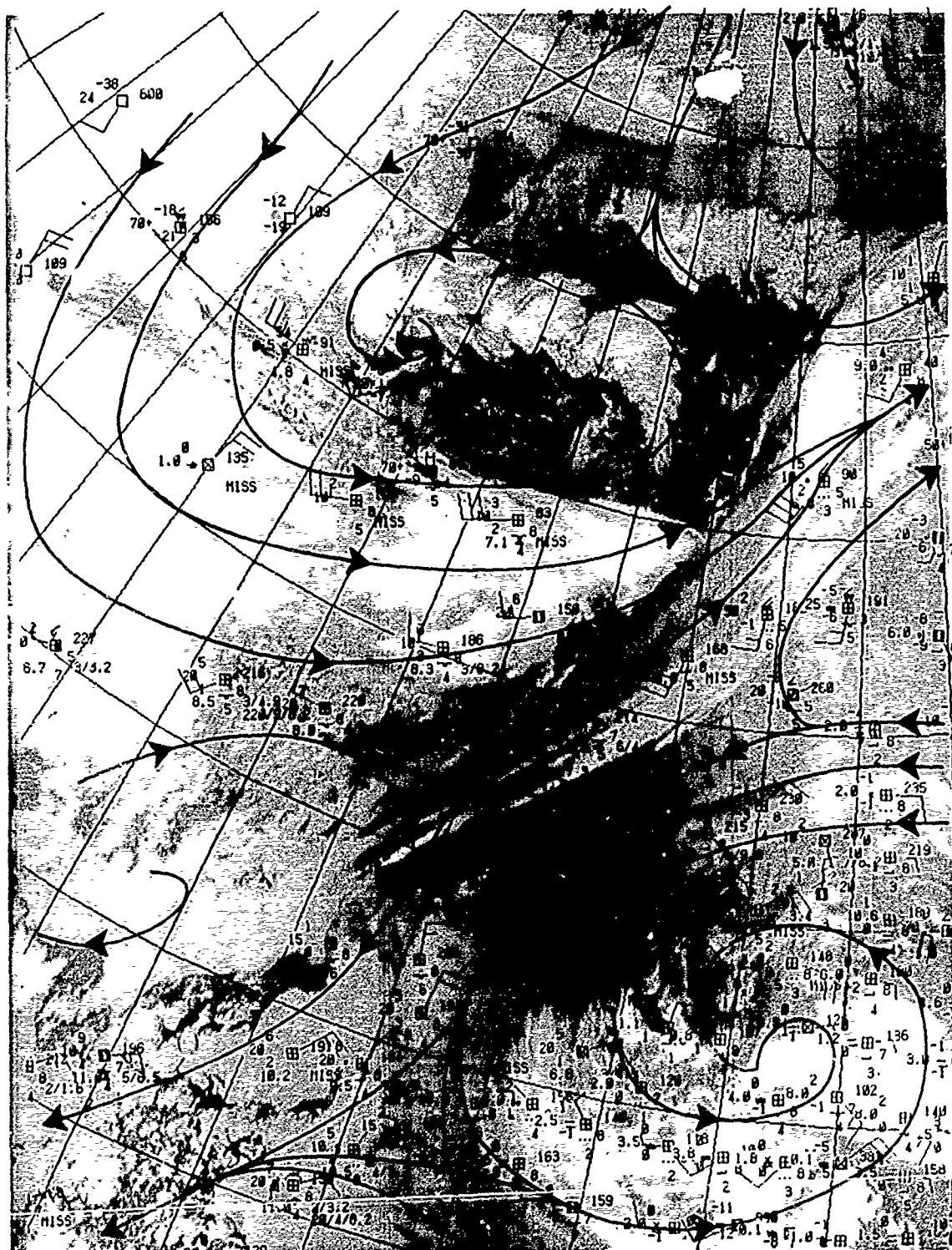
The NOAA P-3 aircraft passed near the cloud free "eye" of the storm at 1336 GMT and during the following 3 hr gathered wind data as shown in Fig. 2A-64b and pressure data shown in Fig. 2A-65a. The compact nature and intensity of this storm is well revealed in these figures.

Figure 2A-65b is a DMSP mosaic showing the storm near its peak intensity. The location is near 69°N 3°W. NOAA-7 also passed over the storm at 1340 GMT, close to the time of the DMSP pass, and its view is shown in Fig. 2A-66a for comparison. The pronounced cold air advection revealed by cloud streets in the Fram Strait and along the marginal ice zone is evident in this figure.

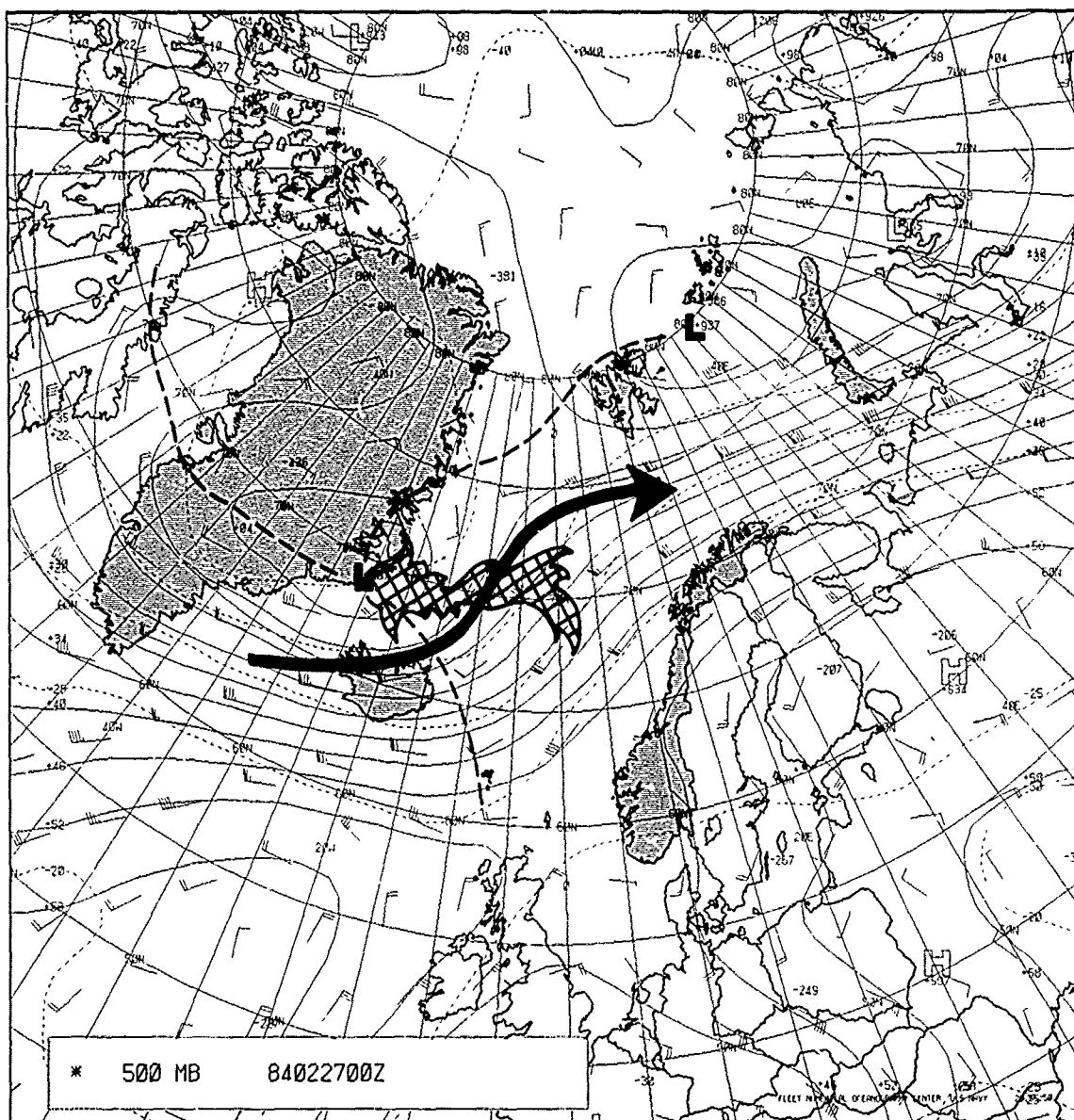
The 500-mb analysis for 1200 GMT (Fig. 2A-67a) with cloud outlines superimposed shows persistence of the cold trough south of the storm center. The cold temperatures aloft apparently destabilized the atmosphere promoting the deep convection in the southern quadrants of the storm. The tendency toward anticyclonic flow over the overcast band leading into the storm center is also suggested by this analysis. (Winds shown on this analysis are computer-derived and obviously could vary from actual conditions that could emphasize or de-emphasize this feature.)



2A-61a. FNOC 300-mb Analysis. 0000 GMT 27 February 1984.



2A-62a. DMSP Infrared (LS) Data With Surface Observations (0600 GMT) and Streamline Analysis  
0624 GMT 27 February 1984.



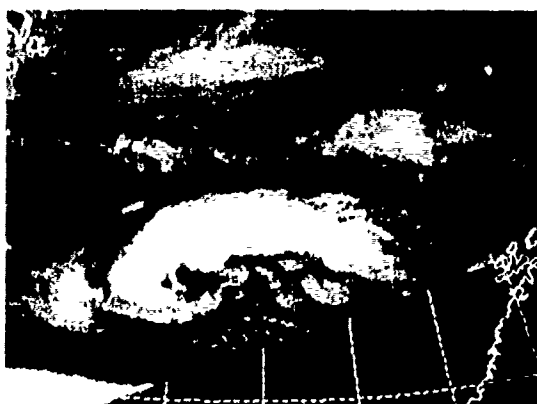
2A-63a. FNOC 500-mb Analysis. 0000 GMT 27 February 1984.



(A)



(B)



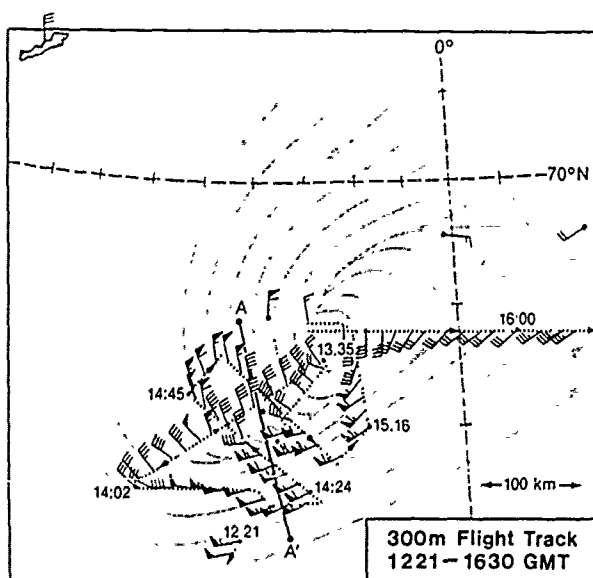
(C)

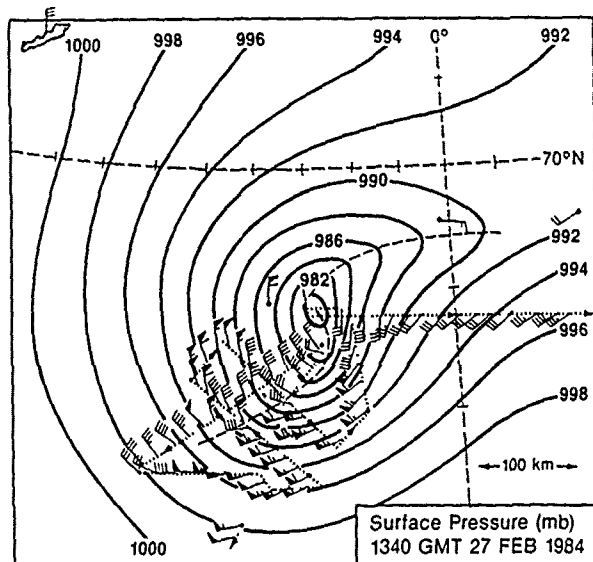


(D)

2A-64a. Successive NOAA 4-km-Resolution Infrared Images at (a) 0725 GMT, (b) 1005 GMT, (c) 1230 GMT, and (d) 1340 GMT (Shapiro, et al., 1987).

2A-64b. Three-Hundred-Meter Flight Track Data During Period 1221-1630 GMT 27 February 1984 (Shapiro et al., 1987).

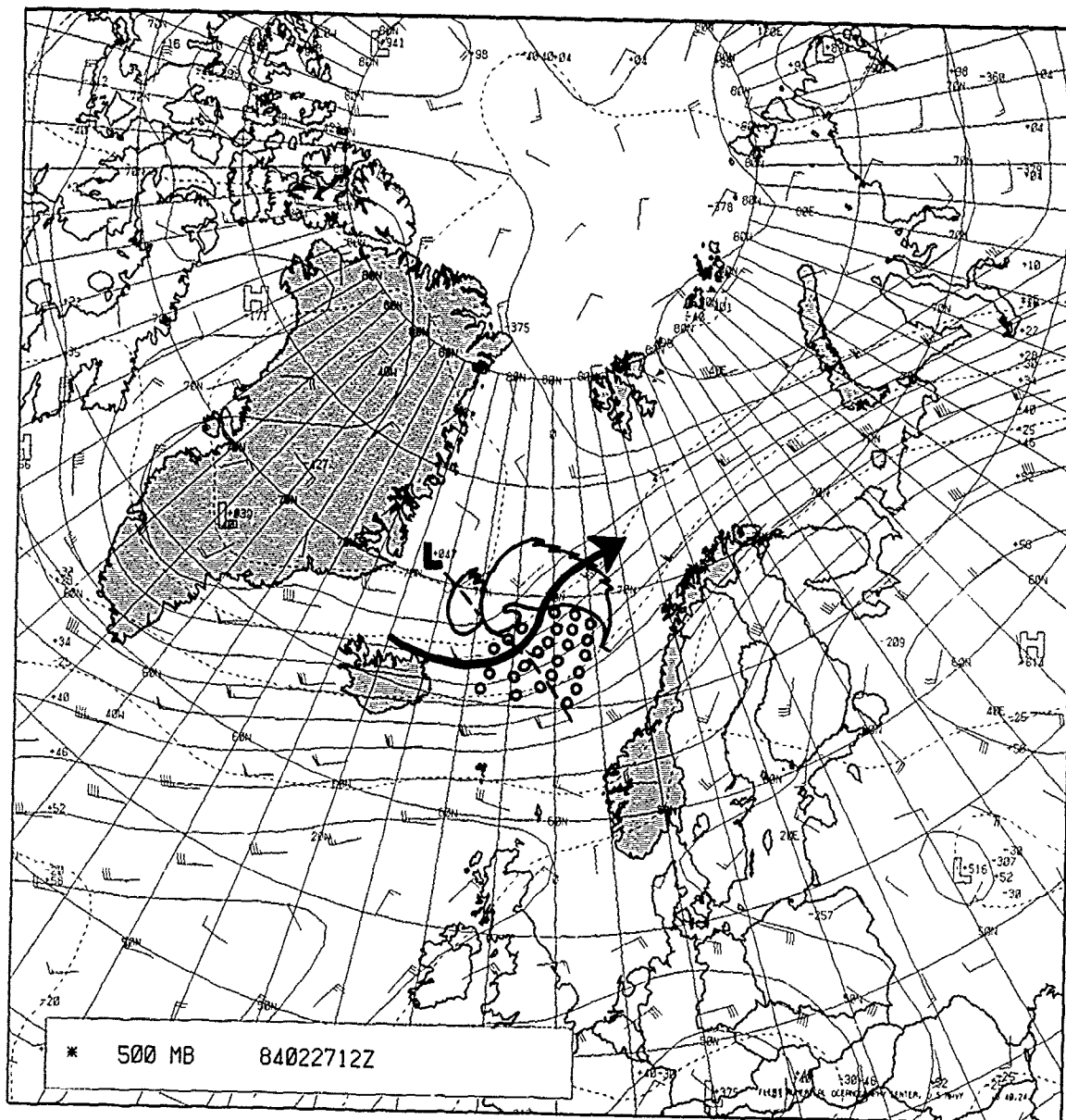






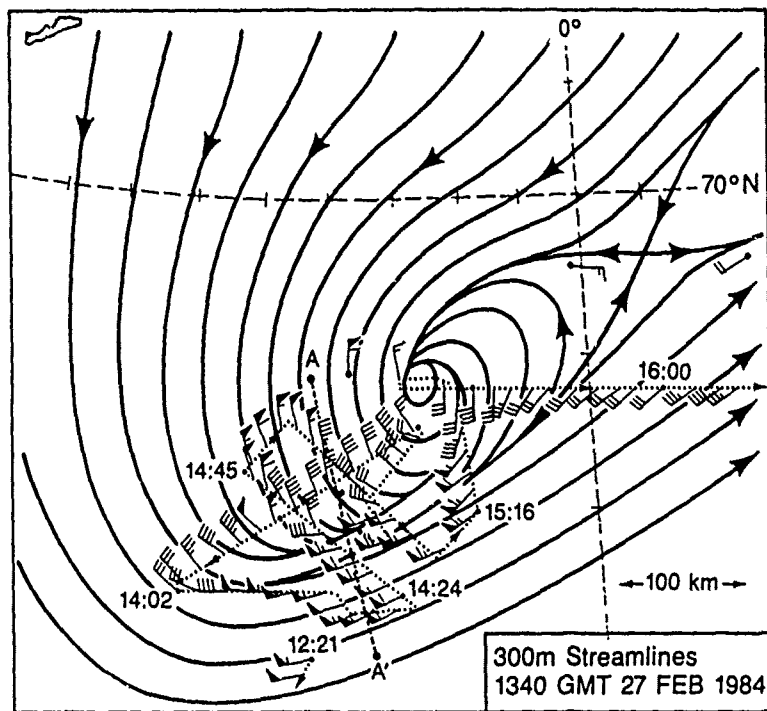


2A-66a. NOAA-7 Infrared Data. 1340 GMT 27 February 1984.



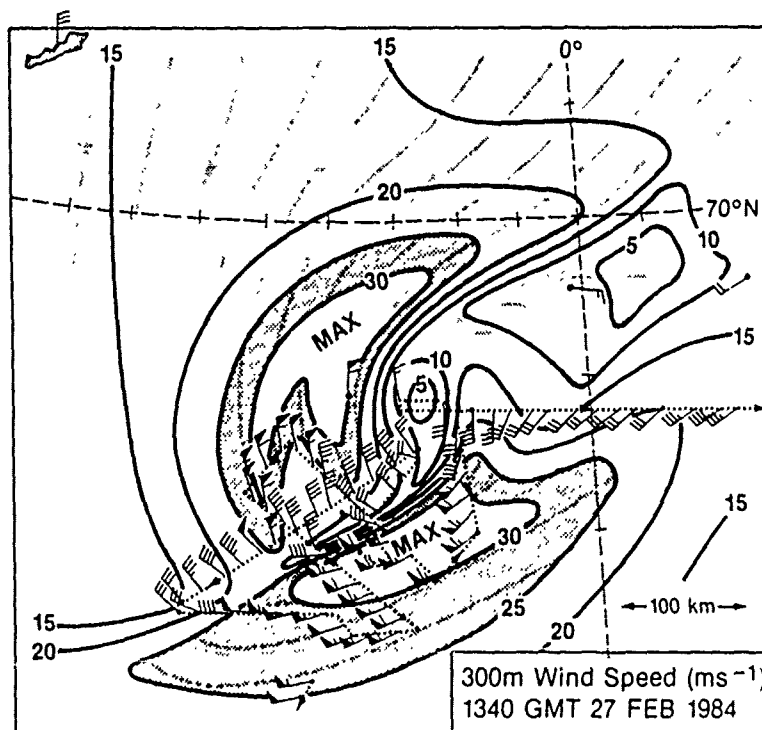
2A-67a. FNOG 500-mb Analysis and Cloud Outline. 1200 GMT 27 February 1984.

2A-68b.  
 (A). Three-Hundred-Meter Streamlines.  
 1340 GMT 27 February 1986  
 (Shapiro, et al., 1987).



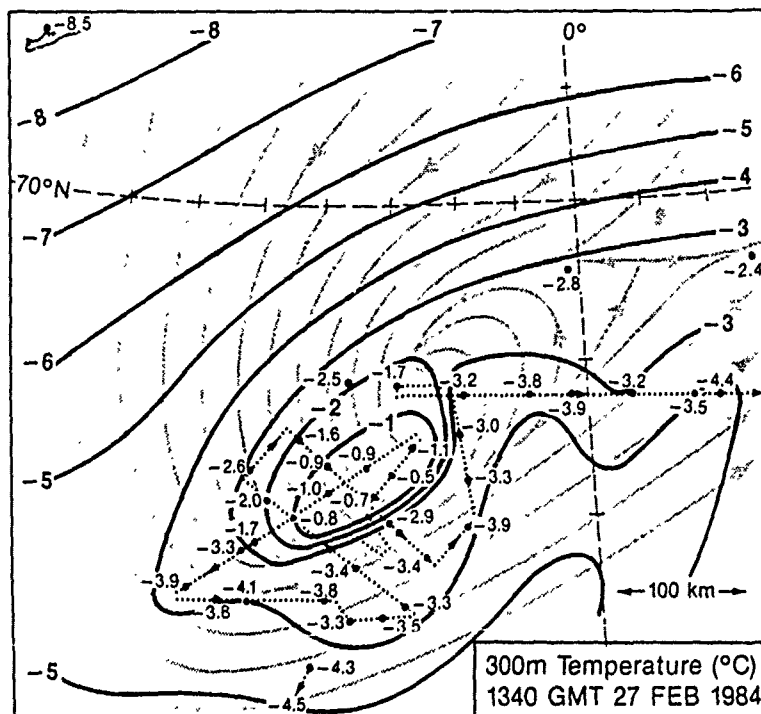
(A)

(B). Three-Hundred-Meter Wind Speed ( $\text{ms}^{-1}$ ).  
 1340 GMT 27 February 1986  
 (Shapiro et al., 1987).



(B)

Flight data indicated that this asymptote was strongly convergent and contained the heaviest precipitation encountered in the storm area. Note from the isotach analysis (Fig. 2A-68b[B]) that this asymptote was associated with a minimum wind speed area separating strong northerly to northwesterly flow from strong westerly to southwesterly flow. Latent heat release from this band may certainly have been a contributing factor to the warm core structure. Shapiro *et al.* (1987), however, examined the 850-mb thermal structure and the 1013- to 580-mb thickness pattern and found that all three analyses (300-m, 850-mb and 1013- to 580-mb thickness) indicated a warm core structure.

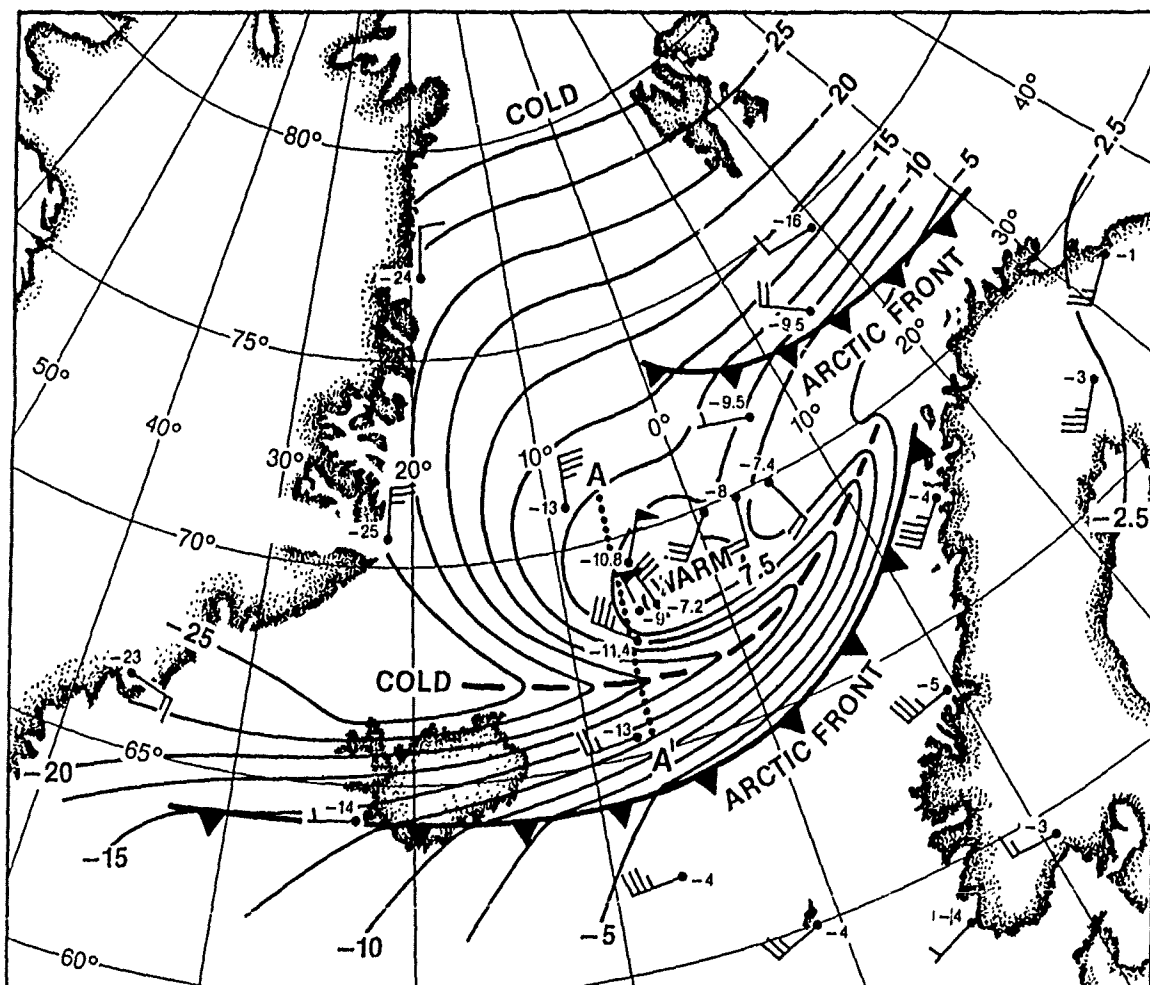


2A-68a. Three-Hundred-Meter Temperature (°C).  
1340 GMT 27 February 1984 (Shapiro et al., 1987).

The 850-mb analysis (Fig. 2A-69a) is especially interesting. This analysis shows that air flowing southward along the ice-covered east coast of Greenland experienced little temperature increase until it left the coastal ice region. As this cold surge turned cyclonically past Iceland, forming an arctic front, the air flow essentially entrapped a warmer air mass by wrapping around it, separating this air mass from the source air mass to the south. This process was originally described by Bergeron (1928) as a seclusion.

The temperature analysis is important in showing this entrainment process. Without the analysis, Shapiro summarizes, "...one might *incorrectly* conclude that the polar low developed within a cold polar air stream behind the arctic front."

Unfortunately the seclusion process obscures the issue as to what extent latent heat release caused the warm core or to what extent it was formed by the seclusion itself.



2A-69a. Eight-Hundred and Fifty-Millibar Temperature ( $^{\circ}\text{C}$ ). 1200 GMT 27 February 1986 (Shapiro et al., 1987).

2A-70a. NOAA-7 Infrared  
HRPT Data. 1524 GMT  
27 February 1986.



2A-70b. NOAA-8 Infrared  
HRPT Data. 1823 GMT  
27 February 1986.



The polar low began to weaken shortly after the view of the storm at 1340 GMT (Fig. 2A-66a), and a new development became more active to the northeast. Figs. 2A-70a and 2A-70b are NOAA-7 and NOAA-8 views of the polar low as it weakened at 1524 GMT and at 1823 GMT. Cold air seems to have more progressively engulfed the storm circulation and perhaps weakened or destroyed its warm core nature.

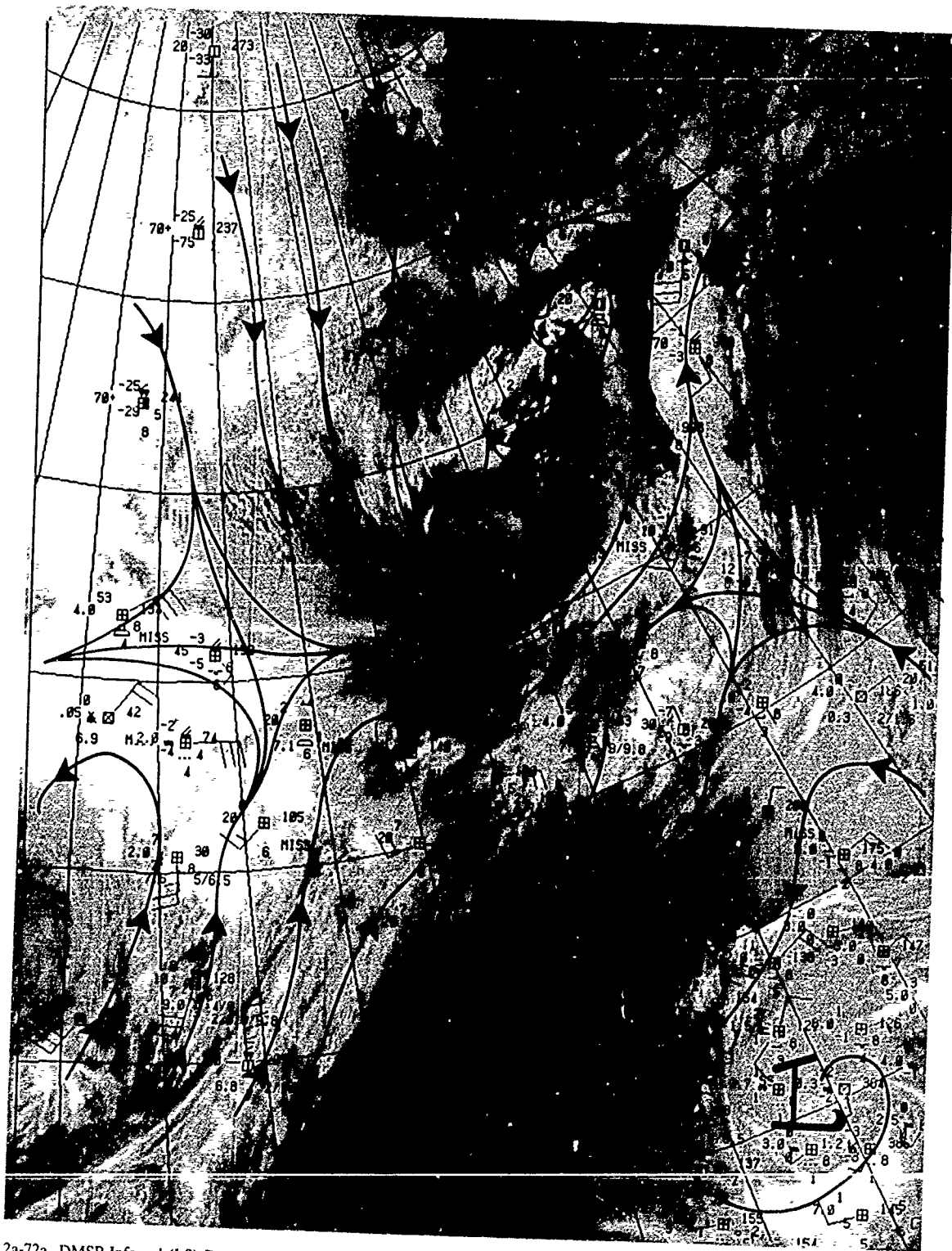
A DMSP infrared orbit at 1945 GMT (Fig. 2A-71a) shows the vastly decreased storm circulation and associated convection (compare with Fig. 2A-69a). Also apparent is the development of a second center to the north. A streamline analysis, which is superimposed on the DMSP image based on the indicated surface reports (Fig. 2A-72a), clearly shows a second circulation center near 72°N and 13°E. This is very close to the low position shown on the 1800 GMT FNOC surface analysis (Fig. 2A-58a). Note, however, that the original polar low to the southeast is not even shown in this analysis. The alternate development and dissipation of the separate mesoscale centers within the synoptic-scale analysis has created the false impression that  $L_2$ , first shown off the southeast coast of Greenland west of Iceland in Fig. 2A-45a on 25 February, is the same low appearing off the northern coast of Norway on 27 February (Fig. 2A-58a), when in fact three (and maybe even four or five) separate low developments were involved. Figure 2A-73a (from Shapiro *et al.*) illustrates the evolution of the complete system on 27 February.

The example illustrates the need for high quality satellite imagery every 1 to 2 hr since some of the cyclonic systems had *life cycles* as short as 6 hr.



2A-71a. DMSP Infrared (LS) Data. 1945 GMT 27 February 1986.





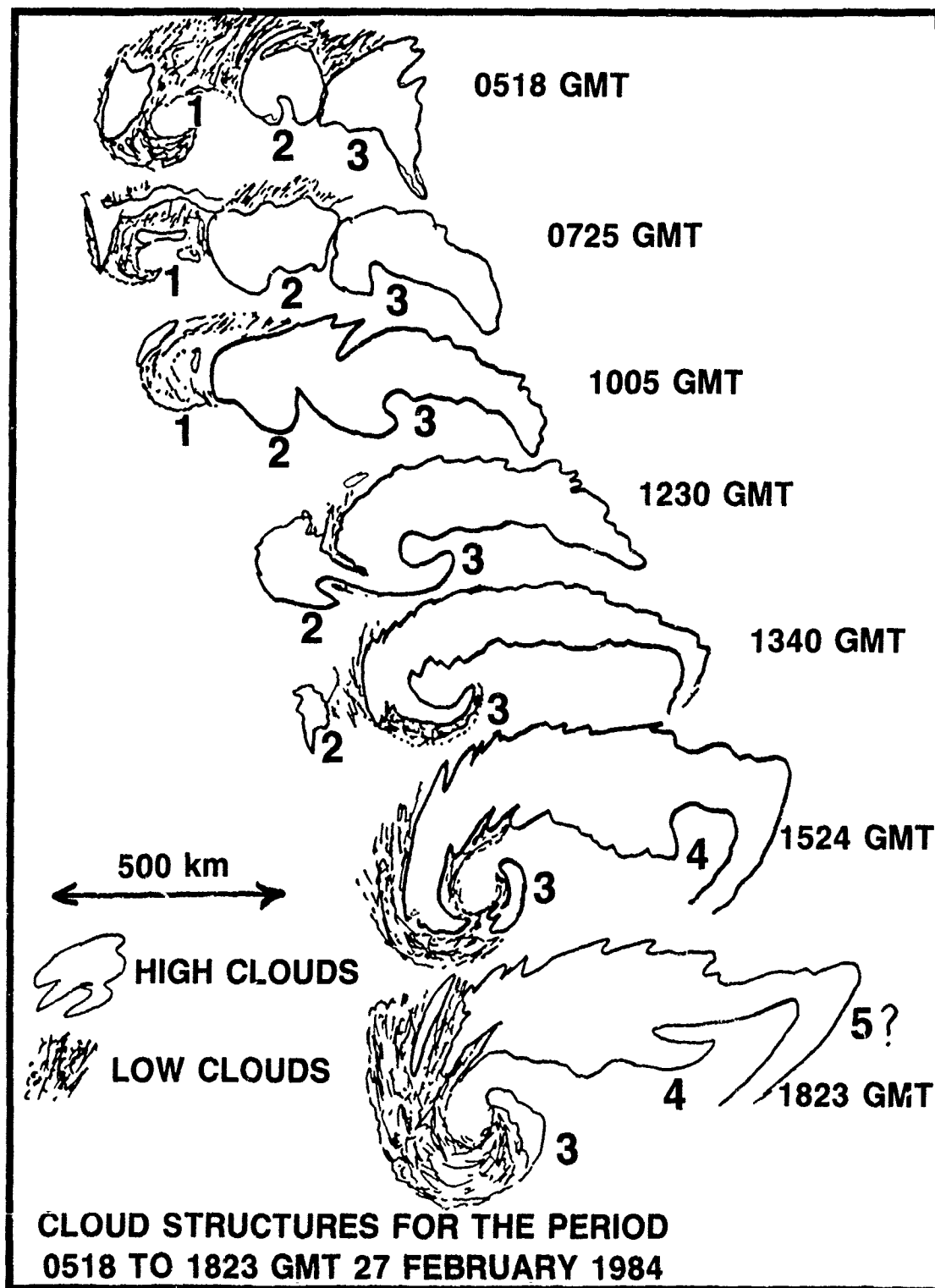
2a-72a. DMSP Infrared (LS) Data, Surface Observations and Streamline Analysis 1945 GMT 27 February 1986.

### Important Conclusions

1. Satellite data every 1 to 2 hr are required to detect polar low development since the complete life cycle of the storm may be completed in as short a time span as 6 hr.
2. Despite their small size, polar lows can generate hurricane-force winds. Therefore, they are extremely dangerous. Normal surface analyses without benefit of satellite input cannot be relied on for polar low detection, movement, and intensity estimates.
3. Seasonal polar low development can be anticipated when ridge or high pressure conditions are detected building over northern Greenland, and deep trough conditions, connecting low centers near 80°N and 60°N, are noted with the trough moving eastward across the Greenland and Norwegian Seas. Development may occur along the trough axis near the col region between low centers, where shearing is greatest, separating northerly from southerly flow.
4. Upper level flow patterns and jet streaks seem to play an important role in polar low development. In particular, superposition of the left exit region of a jet stream maximum (jet streak) over an area favorable for development and a cold 500-mb trough promoting anticyclonic flow over the disturbed area favor such development.
5. The surface analysis in terms of pressure gradient and winds is inaccurate over the island of Greenland. The 700-mb level is more representative of surface conditions over Greenland.
6. Lows appearing quite intense off the southeast coast of Greenland on surface analyses are apt to be much weaker than indicated. Comparison with satellite data is necessary to deduce true intensity.

### References

- Bergeron, T., 1928: Über Dreidimensional verknüpfende wetteranalyse I. *Geofys. Publ.* 5, No. 6, 111 pp.
- Forbes, G.S., and W.D. Lottes, 1985: Classification of mesoscale vortices in polar airstreams and the influence of the large-scale environment on their evolutions. *Tellus*, 37A, 132-155.
- Shapiro, M., L.S. Fedor, and T. Hampel, 1987: Research aircraft measurements of a polar low over the Norwegian Sea. *Tellus*, 39A (4), 272-306.



2A-73a. A Schematic Showing Evolutionary Changes in Polar Low Development on 27 February 1984 (Shapiro et al., 1987).

11 December 1982

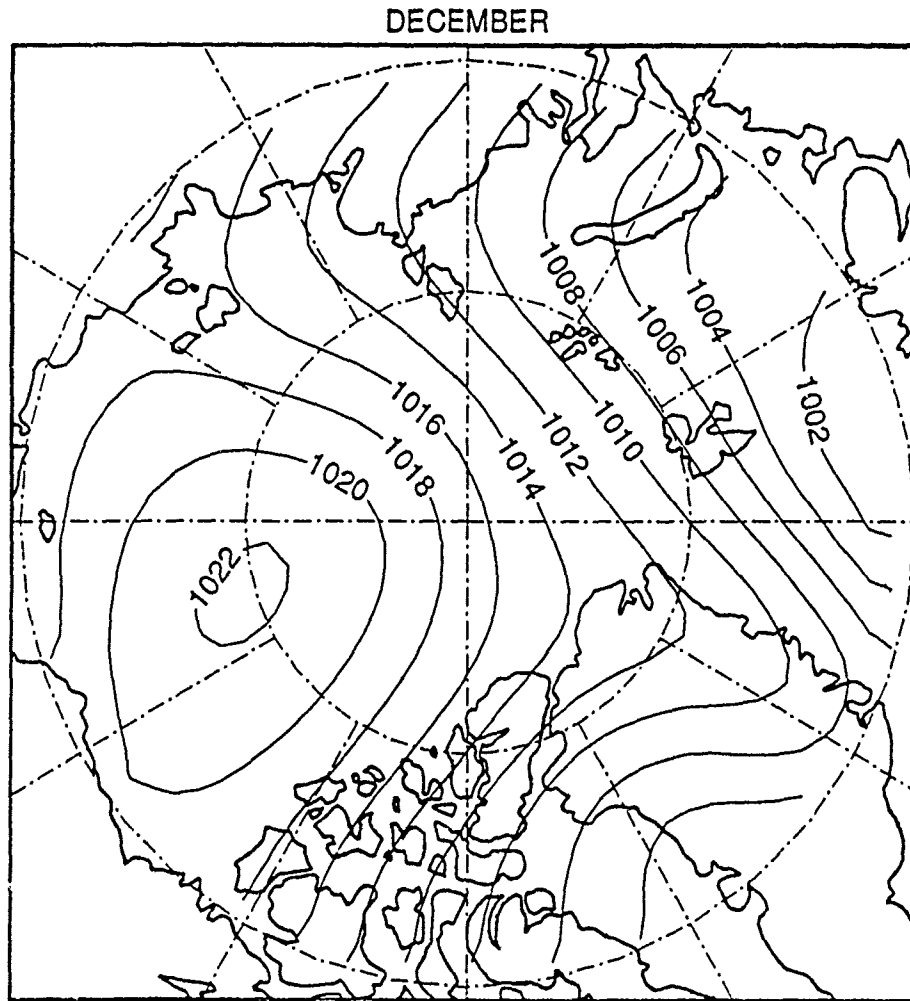
ANALYSIS 00Z 11 DEC 82 PS 6721 REPORTS CUT= 3

FLEET NUMERICAL OCEANOGRAPHY CENTER, U.S. NAVY 15 54, 05

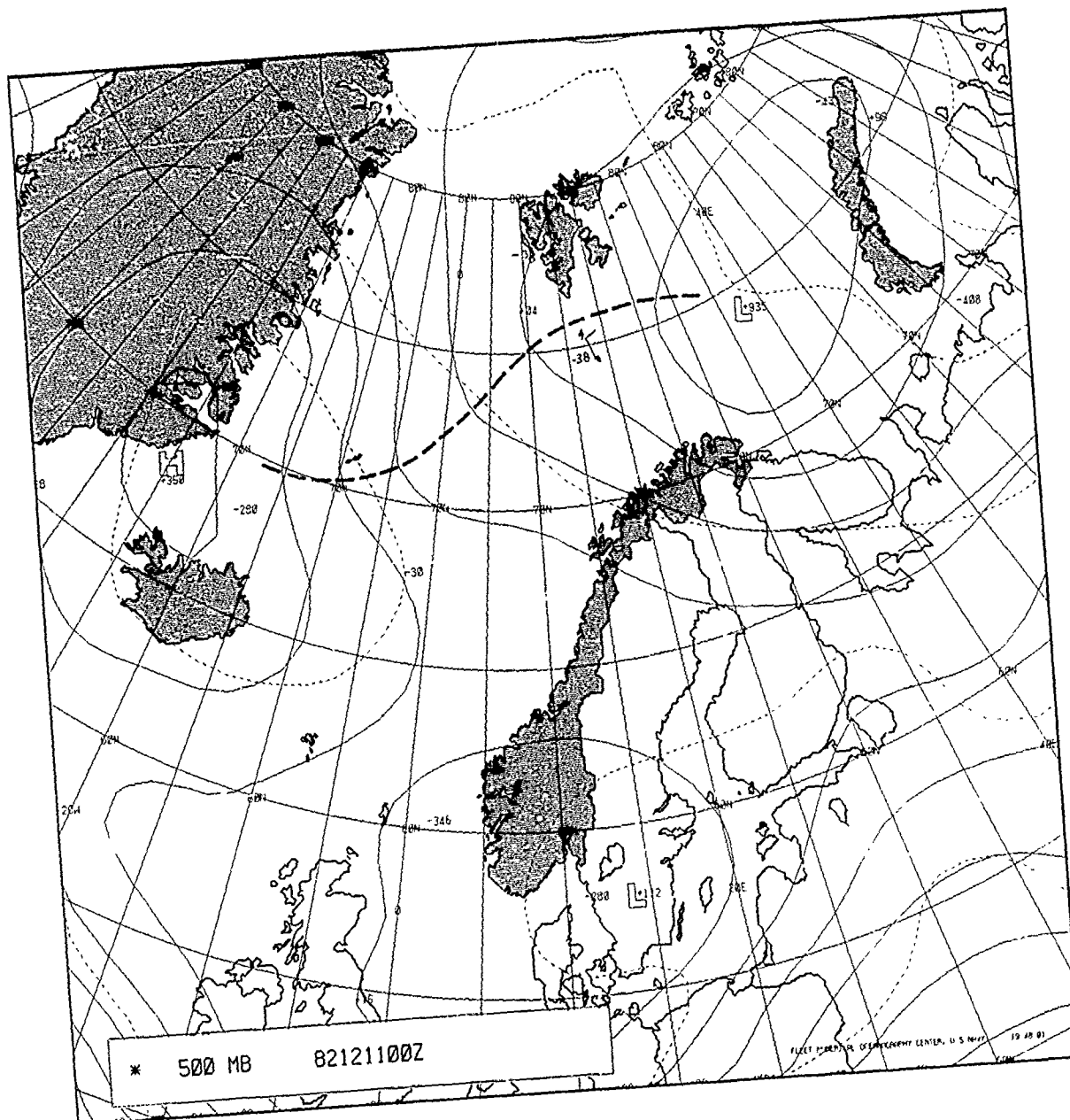
2A-74a. FNOc Surface Analysis. 0000 GMT 11 December 1982.

Northeasterly flow is suggested north of these systems extending from Franz Josef Land, past Svalbard, and down to the area of Iceland where the flow is more northerly. This pattern is not too dissimilar from the mean monthly surface pressure pattern for December (Fig. 2A-75a), which also implies north-easterly flow in the same areas.

Actual wind observations at Barentsburg, Spitsbergen (Fig. 2A-74a), however, are at odds with the analysis indicating southerly flow at Barentsburg with a speed of 4 kt, which persisted from the south at 2 to 4 kt under generally clear skies, until reports at 1800 and 2100 GMT. At this time the winds turned calm, and pressure, which had been rising, started to fall.



2A-75a. Mean Monthly Surface Pressure Pattern for December.



2A-76a FNO 500-mb Analysis. 0000 GMT 11 December 1982.

Winds at Hopen (76.5°N 25.1°E) also suggest that the 0000 GMT analysis may be inaccurate in that they are reported to be blowing from 320° at 21 kt—an angle almost perpendicular to the isobars. These discrepancies are pointed out not to achieve “the” correct analysis, but rather in appreciation of the fact that polar lows generally do not evolve near the center of low pressure, such as is shown in the middle of the Barents Sea. Instead as a short-wave feature, polar lows move around the periphery of the major low. Wind reports that vary drastically from the isobaric analysis are often a clue that the analysis is incorrect and that something may be developing.

Axes of short-wave troughs extending from 500-mb lows are areas frequently associated with polar low evolution.

The 500-mb analysis for 0000 GMT (Fig. 2A-76a) shows such a short-wave trough extending westward from the Barents Sea low between Svalbard and Bear Island.

### *12 December 1982*

A significant change occurred in the weather at Barentsburg by the time of the 0000 GMT surface analysis (Fig. 2A-77a). At this time, skies changed from clear to overcast and continuous snow began falling as the winds picked up to 8 kt and shifted to the northeast. Pressure continued falling. The temperature warmed up to -14°C in comparison to -23°C 24 hr earlier. The warmer temperatures may be a reflection of adiabatic warming due to downslope flow over Barentsburg from the nearby mountains.

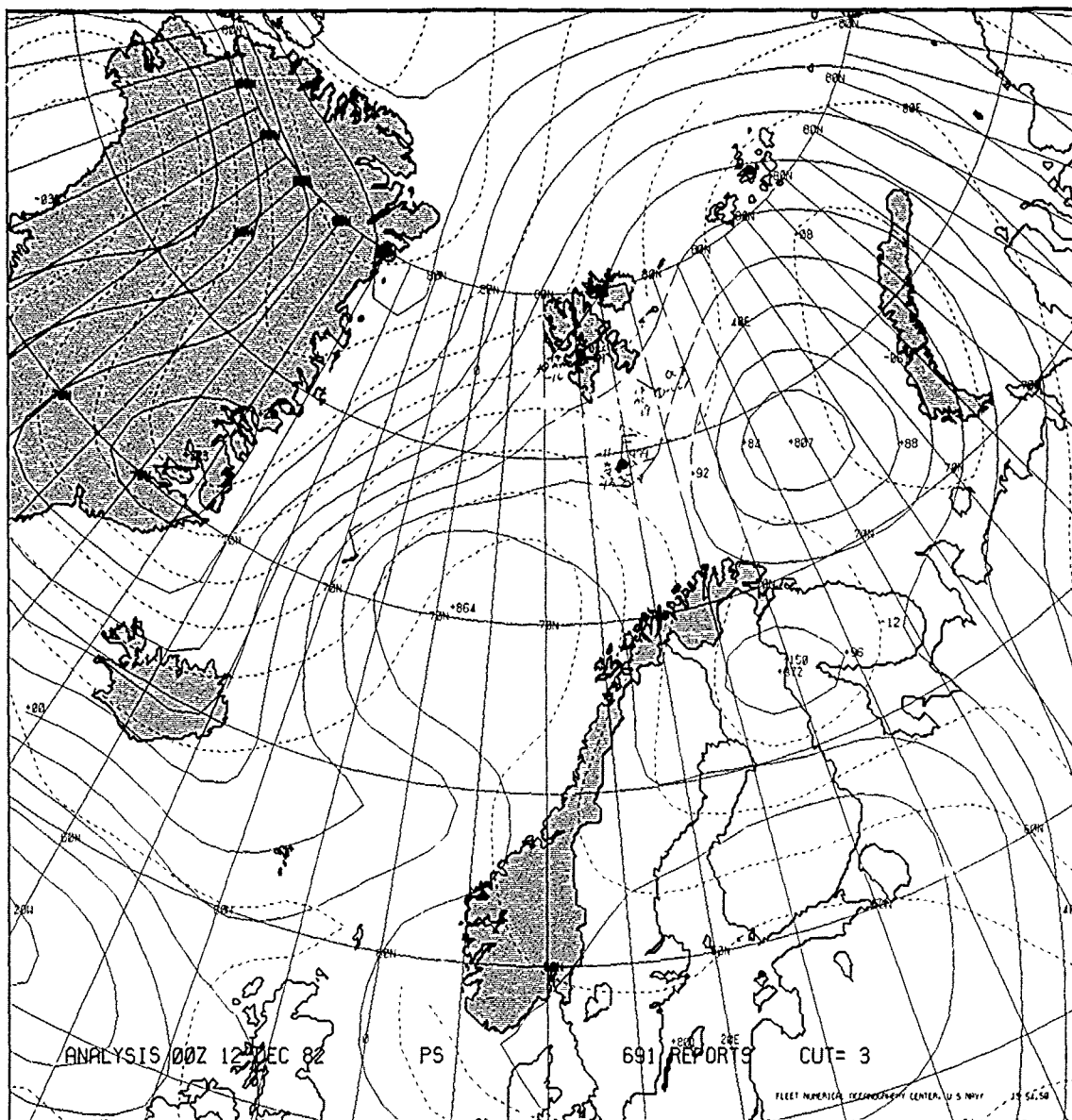
The 500-mb analysis (Fig. 2A-78a) showed the main Barents Sea low moving northwest toward Svalbard. The 500-mb temperatures in Barentsburg and Bear Island dropped from -38°C to -42°C and -43°C, respectively. A minor short-wave trough could be analyzed at 500 mb between Bear Island and Barentsburg, although it is not indicated in the computer-drawn analysis.

NOAA-7 data acquired at about 0355 GMT (Fig. 2A-79a) reveal a small vortex with a well-defined center in the area between Bear Island and Barentsburg.

A much better view of this system is shown in Fig. 2A-79b, a NOAA-7 image acquired 9 hr later at 1257 GMT. The point of immediate interest is that this vortex, similar to the vortices shown in Figs. 2A-80a, 2A-80b, and 2A-80c, is linked to a boundary layer front, which extends northward into the Fram Strait. The difference between this vortex and the others is that this vortex was destined within 12 hr to develop into an intense polar low.

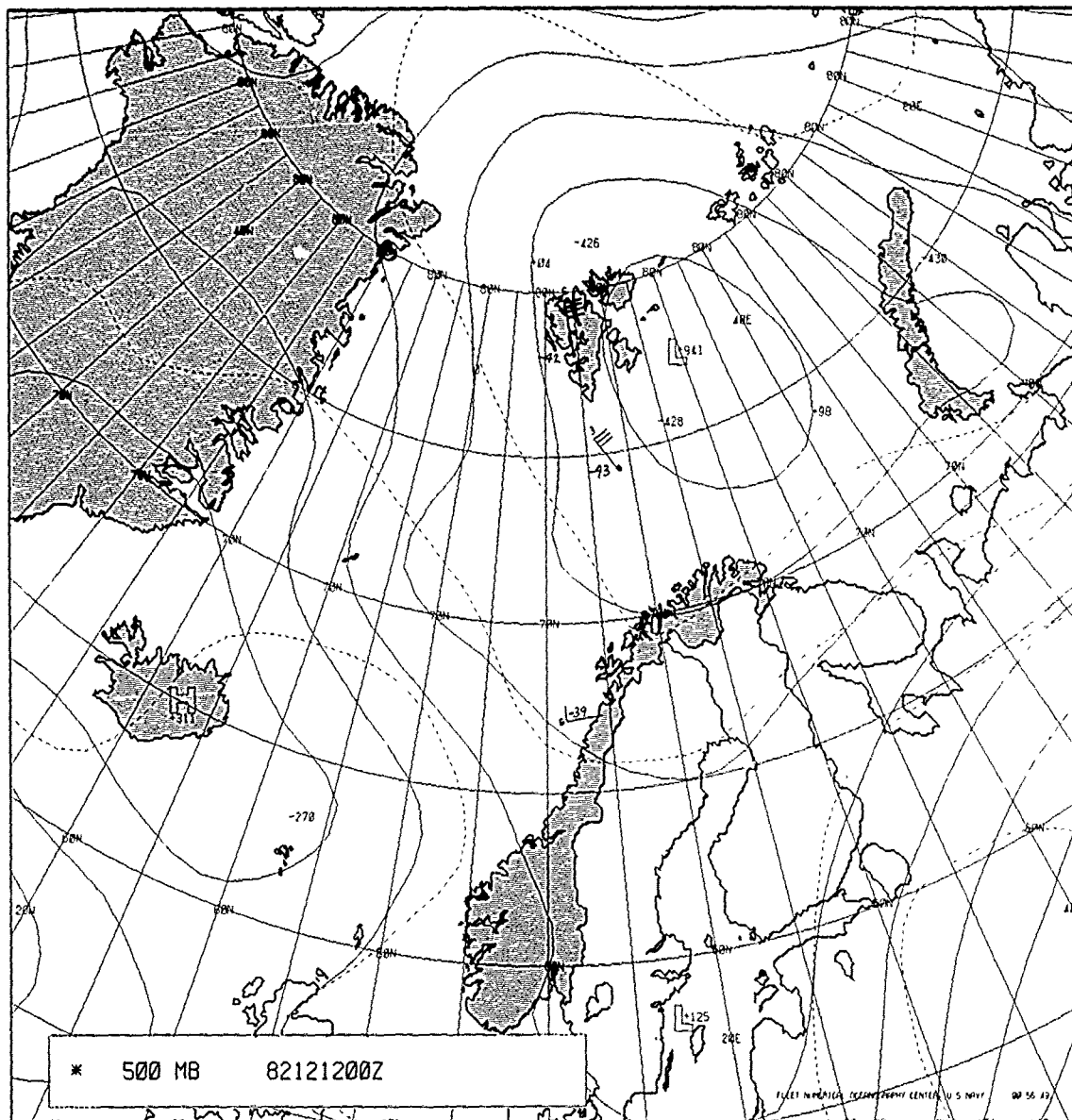
Fig. 2A-81a shows the surface analysis at 1200 GMT, within a few minutes of the time of the NOAA-7 data. The outline of the storm and a streamline analysis have been superimposed over the surface analysis to illustrate flow relationships to cloud vortex structure. The analysis suggests that the vortex has formed on the south end of a boundary layer front, formed as cold anticyclonically turning air flows off the ice onto the north Norwegian Sea. Southeasterly winds lead up to the boundary layer front.

The 500-mb analysis (Fig. 2A-82a) is very suspect showing a low center east of Bear Island, which is reporting a southeast wind at 32 kt. RAOB data from Bear Island (Fig. 2A-83a) taken at 0000 GMT show northerly flow, which had persisted for some time (see Figs. 2A-76a and 2A-78a). This flow changed to southerly at all levels on the 1200 GMT sounding (Fig. 2A-83b), indicating that an upper cold-core low had passed from east to west of that station by 1200 GMT.



2A-77a. FNOC Surface Analysis 0000 GMT 12 December 1982.





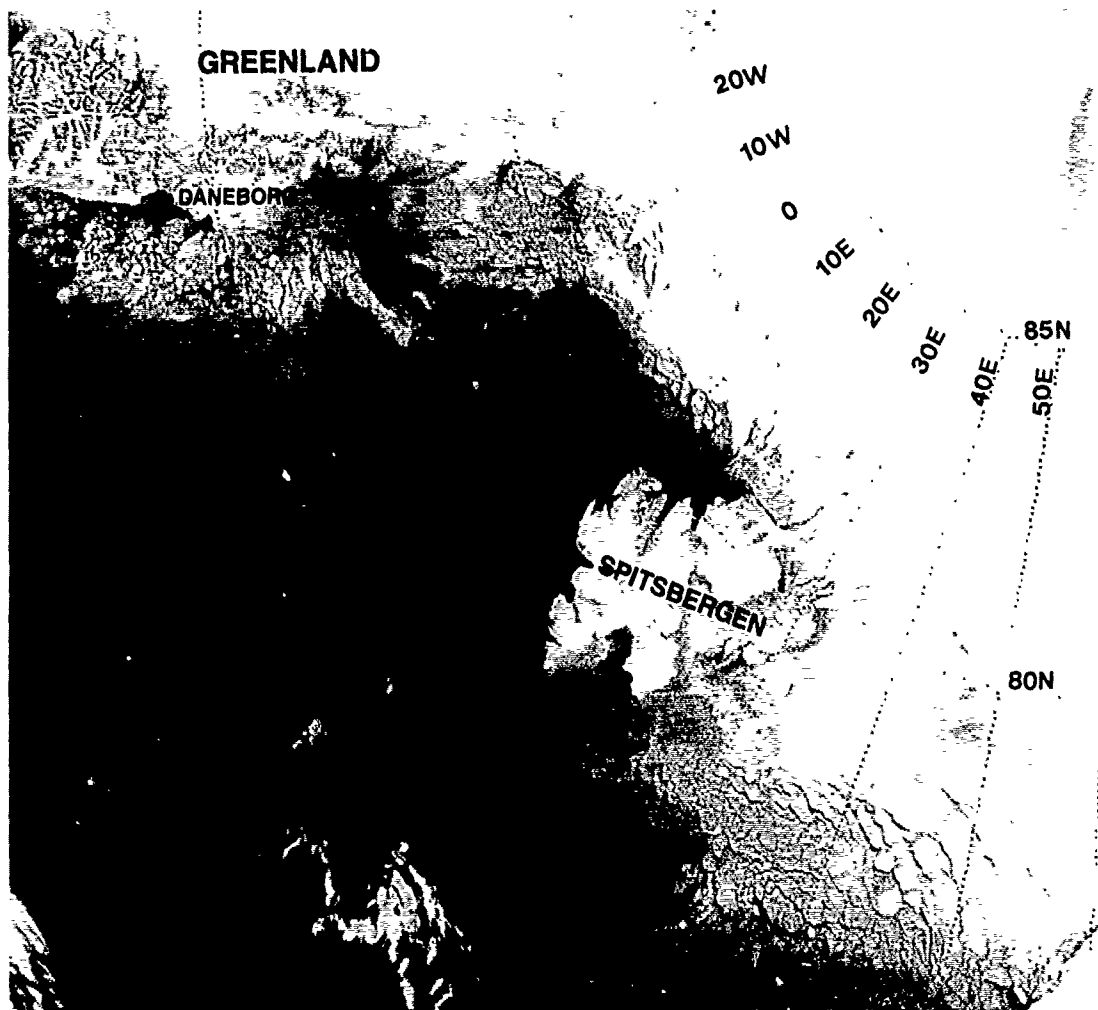
2A-78a. FNOC 500-mb Analysis. 0000 GMT 12 December 1982.



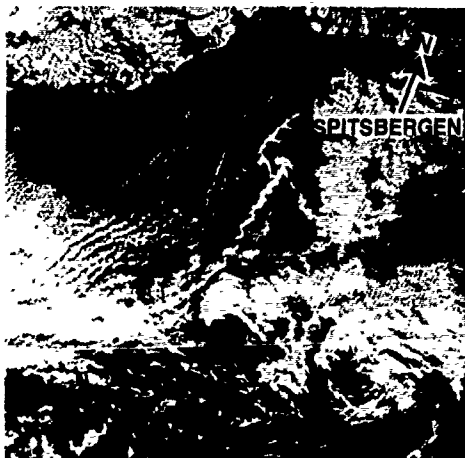
2A-79a. NOAA-7 Infrared Data.  
0355 GMT 12 December 1982.



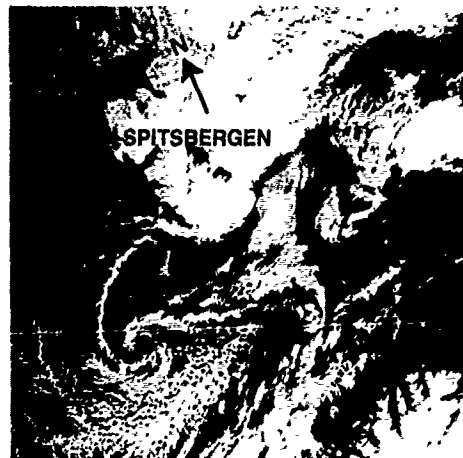
2A-79b. NOAA-7 Infrared Data. 1257 GMT 12 December 1982.



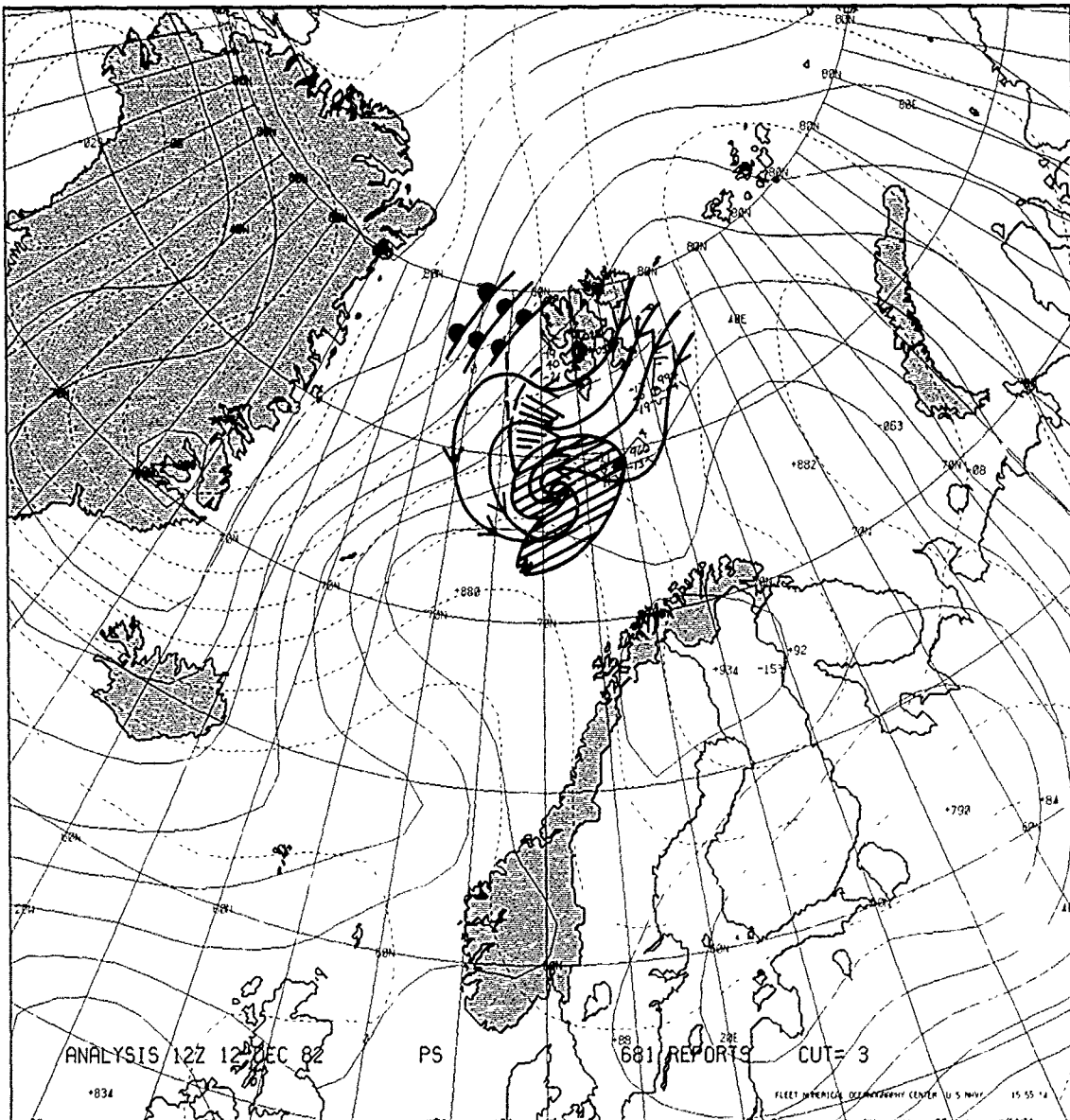
2A-80a. NOAA-9 Infrared HRPT (Ch 4) Data. 1100 GMT 26 March 1987.



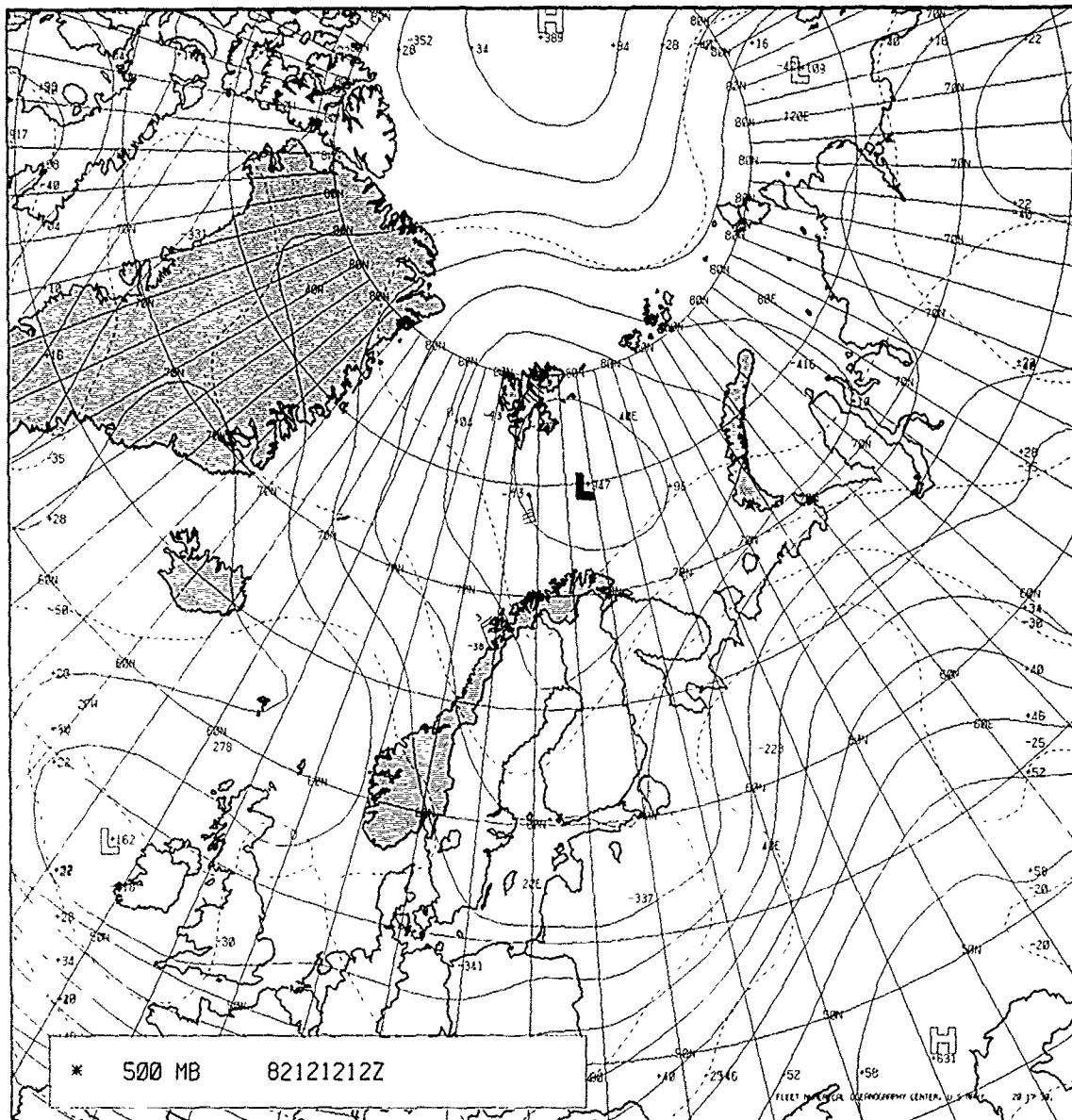
2A-80b. DMSP Infrared (TS) Data.  
1220 GMT 18 April 1983.



2A-80c. DMSP Infrared (TS) Data.  
0741 GMT 19 April 1983.



2A-81a. FNOC Surface Analysis. 1200 GMT 12 December 1982.



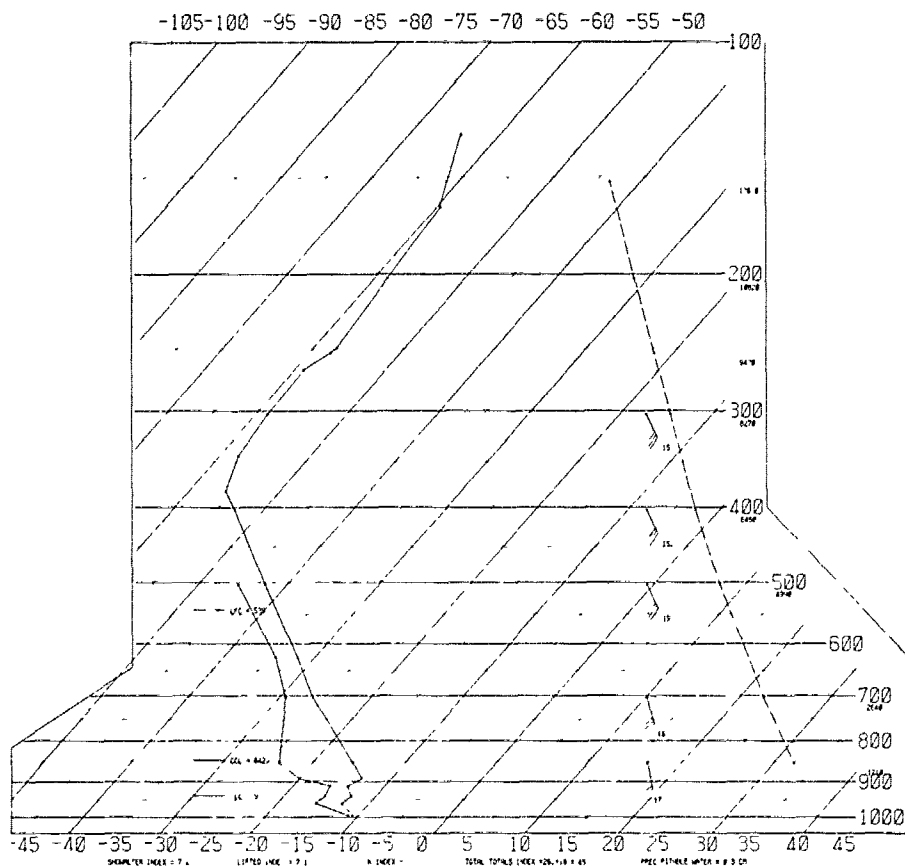
2A-82a FNOC 500-mb Analysis. 1200 GMT 12 December 1982.

# SKREW T. LOG P DIAGRAM

821212

1200Z

1028



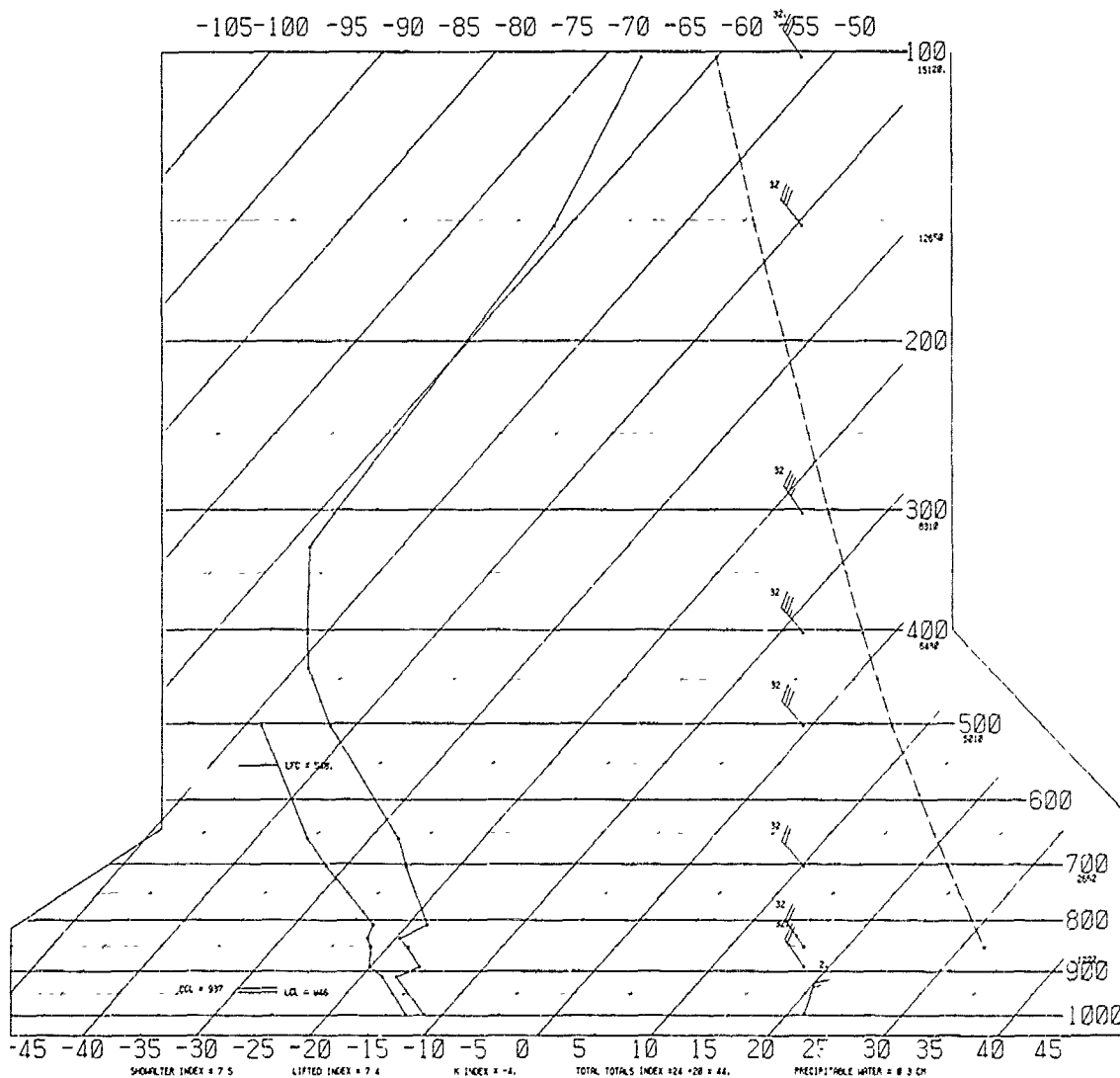
2A-83b. Radiosonde Analysis for Bear Island. 1200 GMT 12 December 1982.

# SKEW T, LOG P DIAGRAM

821212

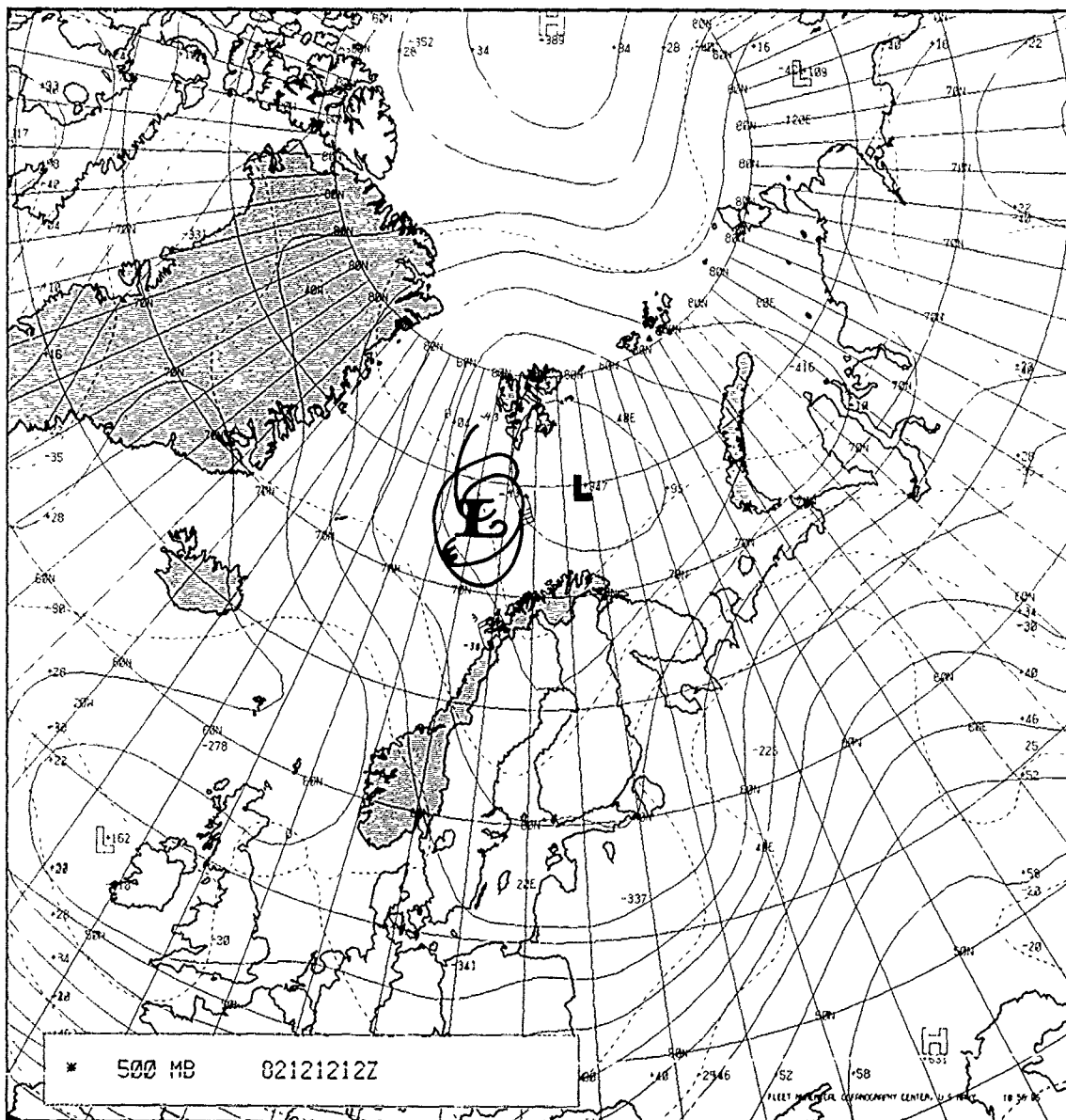
0000Z

1028



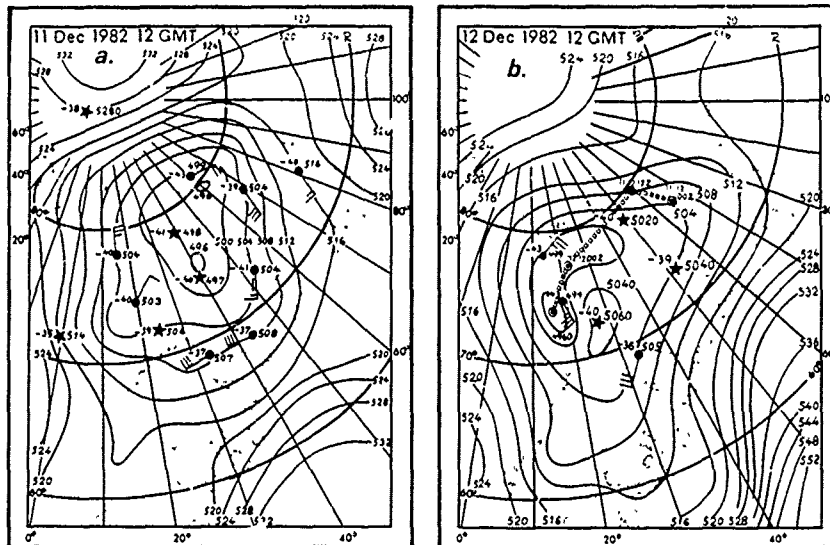
2A-83a Radiosonde Analysis for Bear Island, 0000 GMT 12 December 1982.

Figure 2A-84a, a modified analysis of Fig. 2A-82a, shows where a low cell might be located—in this case directly over the developing vortex. This FNOG analysis did not incorporate satellite sounding data. Rasmussen (1985) shows 500-mb charts (Fig. 2A-85a) for 11 and 12 December at 1200 GMT, which incorporate such data. The 12 December 1200 GMT chart is especially interesting in that it shows a small high pressure cell flanking the cold core low. This configuration provides an efficient outflow channel, similar to that of a hurricane and may explain the rapid intensification that had occurred or was occurring at the time of the image. It is also suggestive of the CISK mechanism illustrated in Fig. 2A-85b, which tends to build high pressure at upper levels and force the explosive deepening process typical of polar lows.

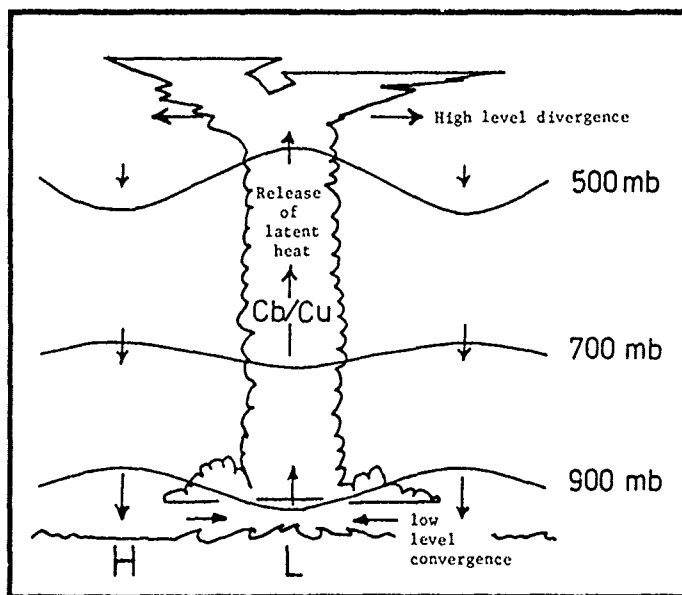


2A-84a FNOG 500-mb Analysis (Modified). 1200 GMT 12 December 1982.





2A-85a Five-Hundred-Millibar Analysis. 1200 GMT 11 and 12 December 1982  
(Rasmussen, 1985).



2A-85b Schematic Illustrating the CISK Mechanism  
(Rasmussen, 1985).



2A-86a. NOAA-6 Infrared Data.  
1804 GMT 12 December 1982



2A-86b. NOAA-6 Infrared Data With  
Boundary Layer Front Position Indicator  
1804 GMT 12 December 1982.

Another view of the storm area as seen by NOAA-6 (Fig. 2A-86a) was acquired at 1804 GMT. The position of the boundary layer front can still be discerned on this image. Its position is marked in Fig. 2A-86b for clarification.

Figure 2A-87a, the 1800 GMT surface analysis with the outline of the storm superimposed, shows that Bear Island, with wind of  $50^\circ$  at 20 kt, is not reflecting the cyclonic circulation about the storm. This is not surprising since polar lows are typified by intense hurricane-force winds restricted to small areas around the storm center. As is usual in polar low development, the vortex does not appear near a surface low pressure center but is offset on the periphery.

### *13 December 1982*

Detailed surface analyses developed for this date by Rasmussen (1985) are shown in Fig. 2A-88a. These analyses further emphasize the mesoscale nature of the polar low development: note the continuous easterly off-ice flow reported by Barentsburg (the station in the upper left of the analysis). This activity relates well to the continued westward propagation of the boundary layer front across Fram Strait, north of the developing storm.

A NOAA-7 infrared image (Fig. 2A-89a) shows the storm at 0250 GMT. The storm at this time gives all appearances of being a fairly intense vortex, showing a hurricane-like eye and tight spiral banding around the center of circulation. The boundary layer front is not well defined, but may correspond to the enhanced band of convective clouds that leads into the southwest quadrant of the storm from the north.

Another area of interest in the image is the east/west elongated band of convective cloudiness, extending east of the storm into the Barents Sea. Multiple polar low development occurs frequently along such bands as illustrated previously by Shapiro (1987) who referred to the process as a "downstream amplification, i.e., the triggering of new cyclones... along the leading edge of the west-east-oriented northerly cold-air Arctic outbreak."

The 500-mb analysis for 0000 GMT (Fig. 2A-90a) with cloud outlines superimposed suggests that the upper low is directly superimposed over the cloud vortex. Lack of additional observations at this level precludes a more detailed analysis.

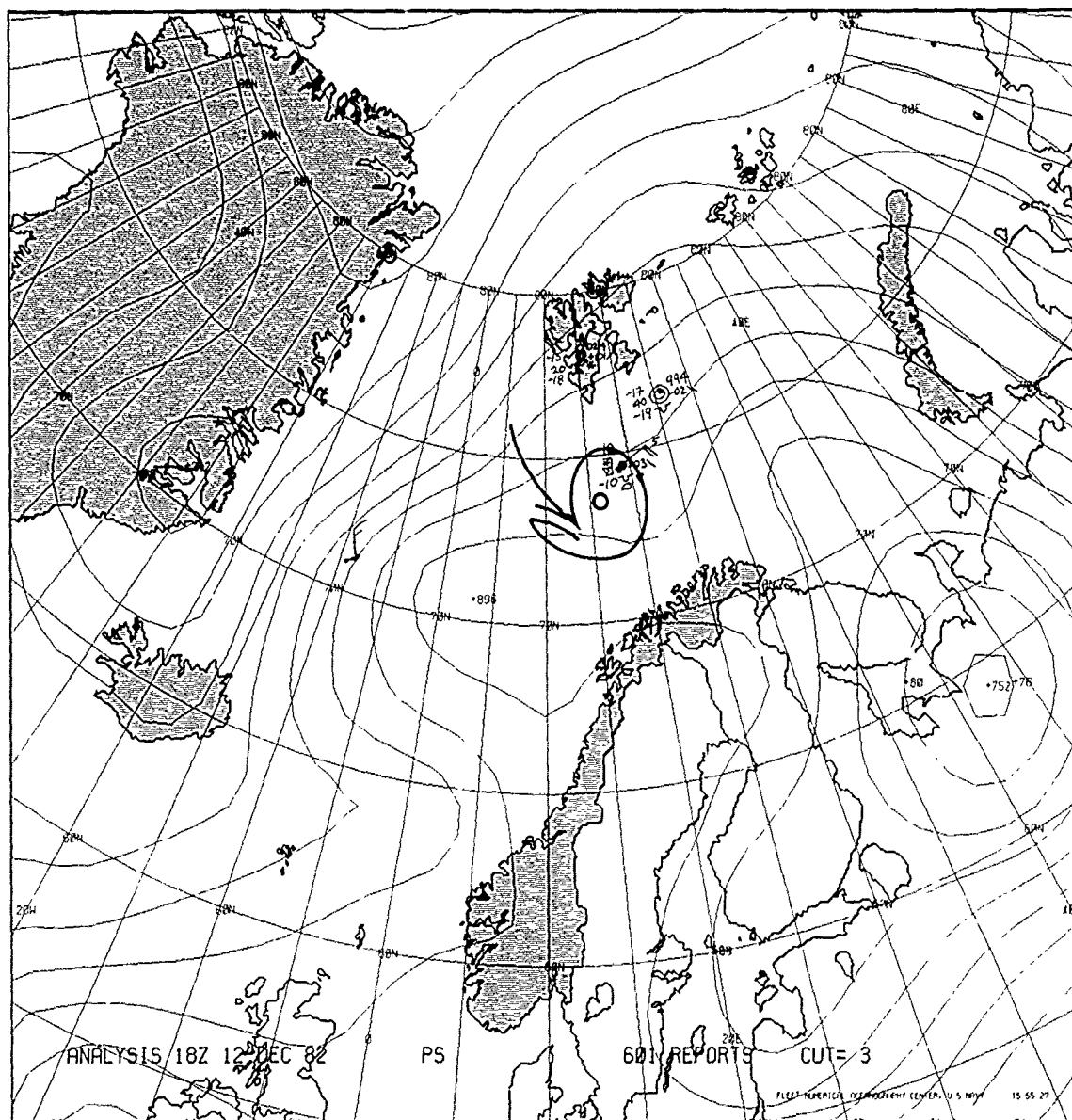
It is evident that very cold temperatures and low pressure aloft are associated with the storm development.

A final detailed view of the storm as revealed in NOAA-7 infrared data at 1245 GMT is shown in Fig. 2A-91a. The original polar low "A" southwest of Bear Island (denoted by an "X") is at its peak intensity and a secondary disturbance "B" appears to be generating. There are also numerous mesoscale vorticity centers noticeable along the remnants of the planetary boundary layer front extending southward from the Fram Strait into the southwest quadrant of polar low "A."

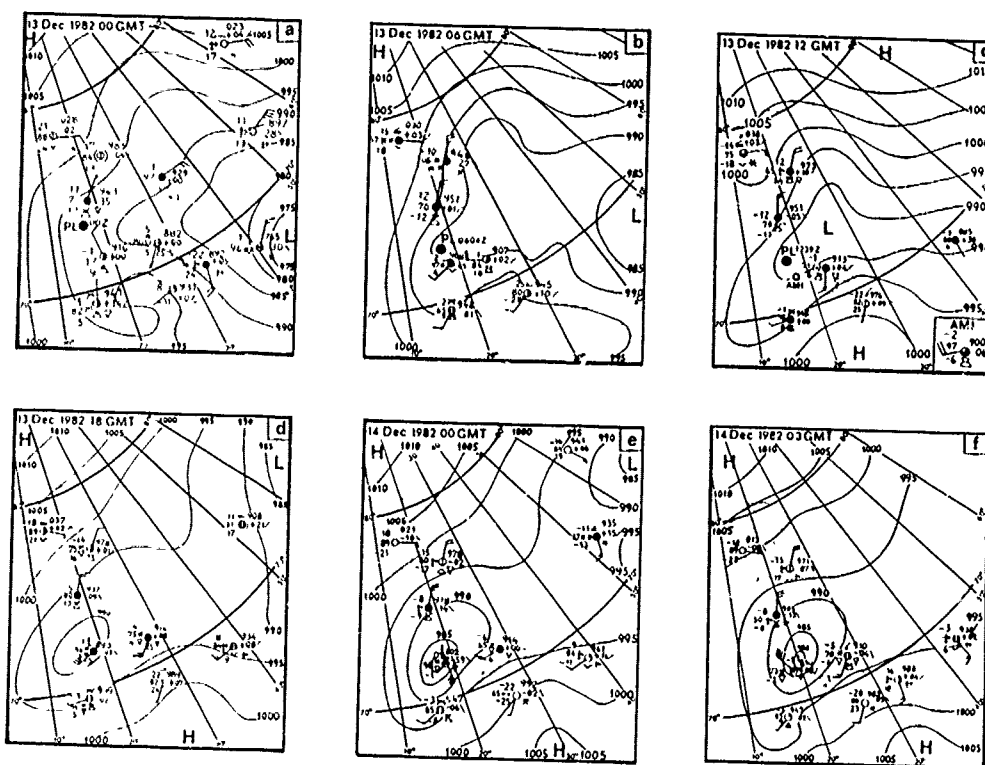
None of these features are apparent in the 1200 GMT FNOC surface analysis (Fig. 2A-92a). It is particularly interesting to note that the storms, in typical fashion, have developed hundreds of miles from analyzed low pressure centers. The col region in which they have developed, between centers of an elongated trough connecting lows, has been previously noted as a favored location for polar low development.

### *Additional Examples*

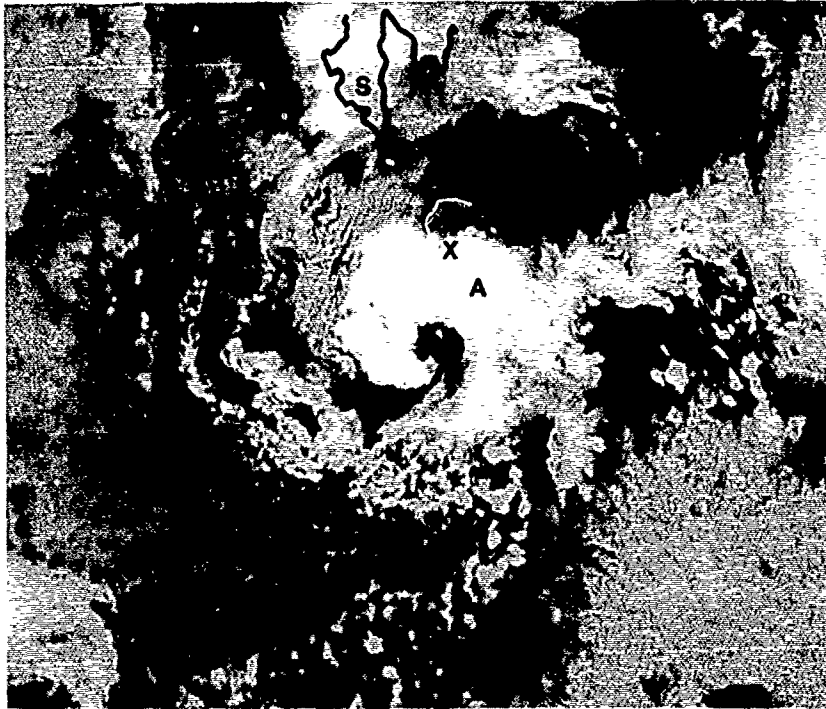
One example of polar low evolution along a boundary layer frontal zone in the Fram Strait has been shown. Based on a survey of satellite data over several years showing polar low development in this region and in the Barents Sea, boundary layer frontal linkage appears to be atypical though probably not the exclusive mode of polar low generation in that region.



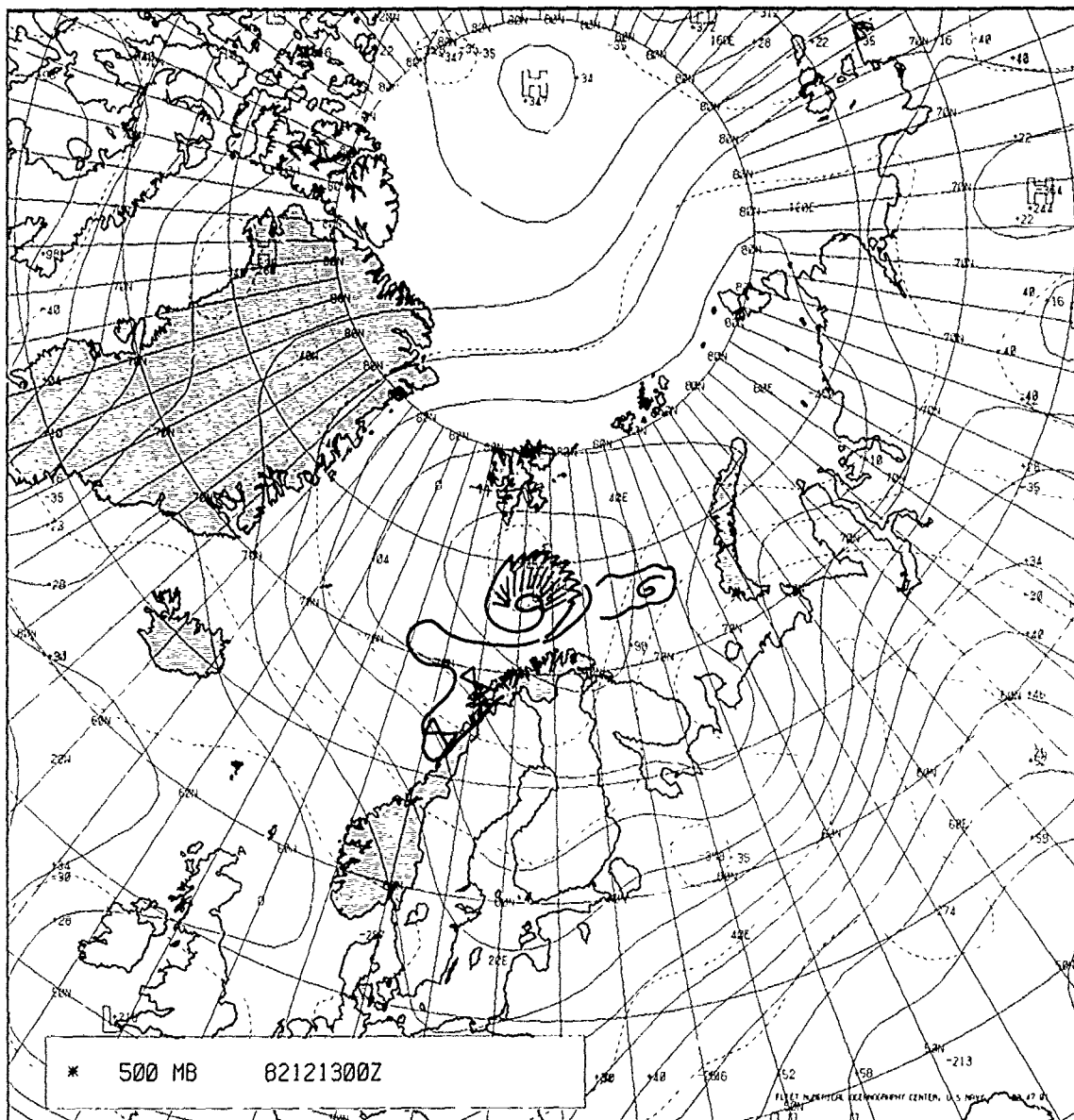
2A-87a. FNOG Surface Analysis With Cloud Outline. 1800 GMT 12 December 1982.



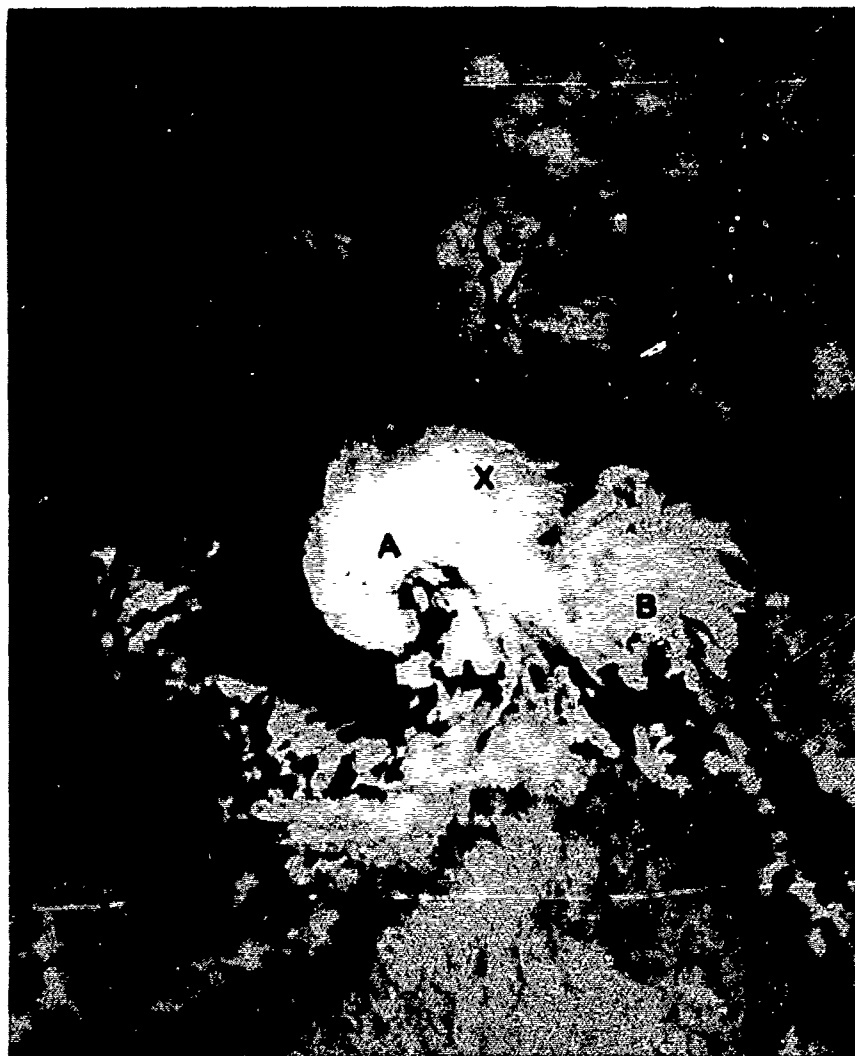
2A-88a. Surface Analysis. 13 December 1982 (Rasmussen, 1985)



2A-89a. NOAA-7 Infrared Image. 0250 GMT 13 December 1982.

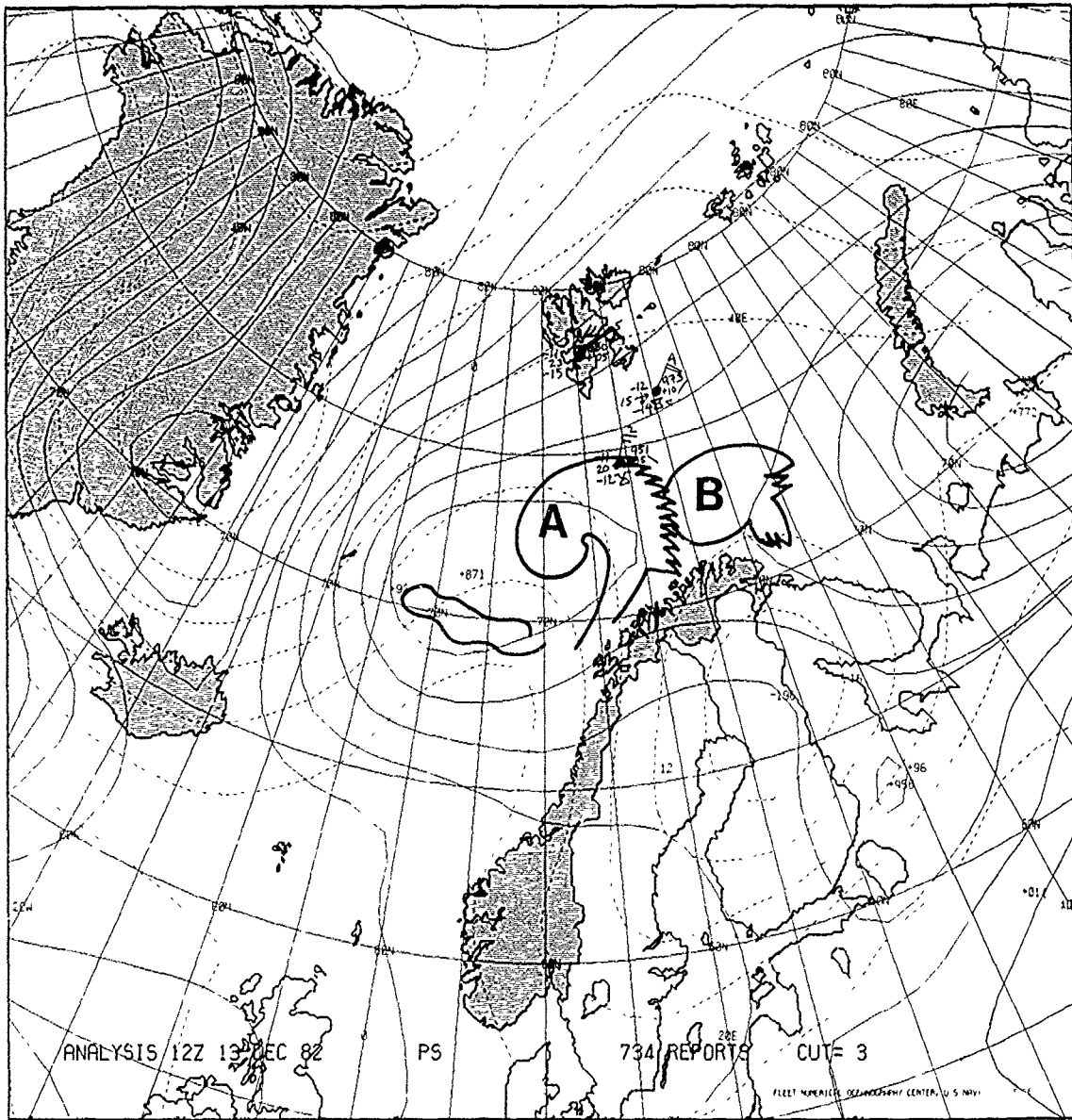


2A-90a FNOC 500-mb Analysis, 0000 GMT 13 December 1982



2A-91a. NOAA-7 Infrared Data. 1245 GMT 13 December 1982.



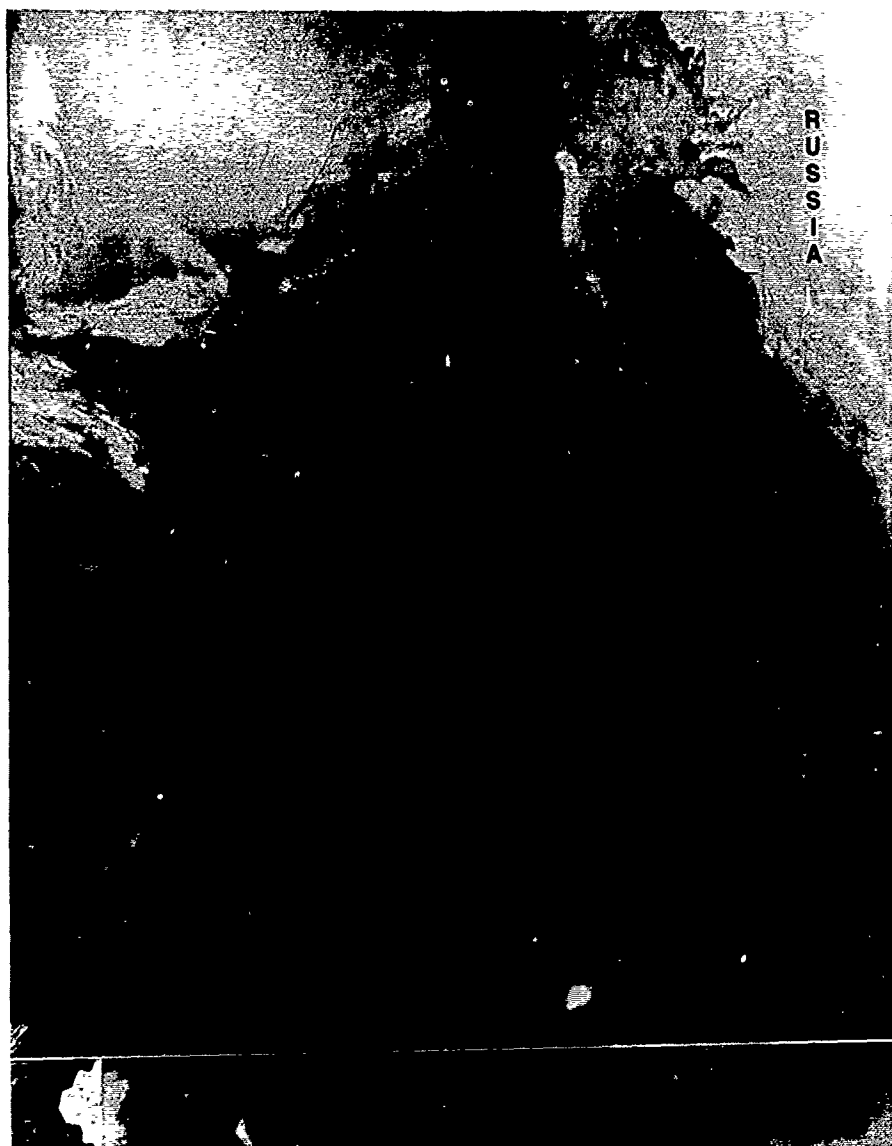


2A-92a. FNOG Surface Analysis. 1200 GMT 13 December 1982.

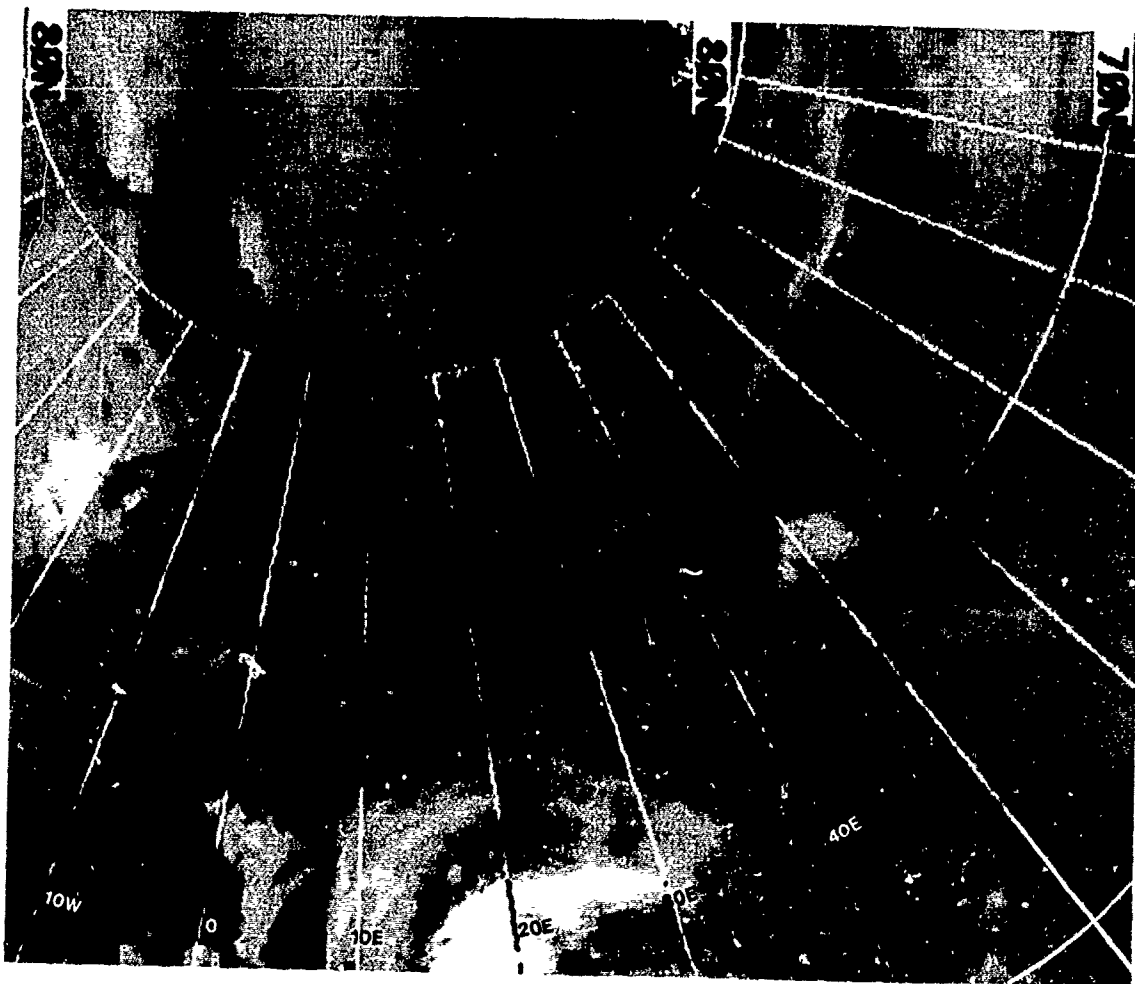
Some additional examples will be shown without going into detailed documentation with charts and analyses to illustrate and provide a "feel" for the variety of effects.

*Example 1. Polar Low Evolution on Boundary Layer Fronts West of Novaya Zemlya (2-3 December 1983)*

Figure 2A-93a is a DMSP infrared view on 2 December 1983 at 1637 GMT showing a boundary layer front apparent as a long enhanced line of clouds oriented generally north/south, just west of Novaya Zemlya. The island of Kolguyev appears near its southern extremity. Numerous small vorticity centers are apparent along the frontal boundary.



2A-93a. DMSP Infrared (TS) Data. 1637 GMT 2 December 1983.



2A-94a. DMSP Infrared Mosaic. 0840 GMT 3 December 1983

A DMSP infrared montage, with data in the region of Novaya Zemlya acquired on 3 December 1983 at about 0840 GMT (Fig. 2A-94a), shows that two larger scale cloud vortices or polar lows have developed along that front boundary. The southernmost vortex appears to be the most intense.

A final DMSP infrared view of the system later in the day, at 1616 GMT, is shown in Fig. 2A-95a. The system did not deepen significantly beyond this stage.

*Example 2. Eastward-Moving Polar Low Development in the Barents Sea (6-7 December 1983)*

Figure 2A-96a, another example, is a DMSP infrared image acquired on 6 December 1983 at 0414 GMT. This image shows a boundary layer front extending south-southwest of Spitsbergen. Numerous small vorticity centers are apparent along the frontal boundary. Additional wave-like disturbances are also revealed further south along the coast of Norway. The southernmost of these shows convective development indicative of a cold low aloft. It has been found that the most severe polar lows are connected in some fashion to such upper cold lows. The attention here, however, is in following developments associated with the northernmost frontal boundary.

On the following day, 7 December 1983, at 0030 GMT, DMSP infrared data (Fig. 2A-97a) reveal vortex development at the base of the frontal boundary. Faintly discernible to the north are higher level clouds swirling about an upper cold low over the ice with the center just east of Spitsbergen. The upper cold low is a large-scale synoptic feature with a circulation dominating the Barents and Kara Seas region as shown in the 500-mb analysis on 7 December at 0000 GMT (Fig. 2A-98a).

Good satellite data are lacking during the next several hours; but it appears that the upper cold low moved southward over the ice to the open water of the Barents Sea and either caused intensification of the vorticity center in Fig. 2A-97a, or absorbed it in an explosive development. Fig. 2A-99a shows the area at about 1250 GMT. A hook-shaped cloud band defines the beginning of an intense polar low development. Figure 2A-100a is an additional DMSP infrared view revealing the intense-appearing system at 1633 GMT. The complete system is even better shown in Fig. 2A-101a, a DMSP infrared view at 1814 GMT. Note the attachment of this polar low to the planetary boundary layer front stretching westward and then northward toward Spitsbergen.

*Example 3. Polar-Low Development From Southward Moving Boundary Layer Fronts in the Fram Strait (19-20 December 1983)*

Boundary layer fronts in the Fram Strait and other locations move in the direction of the low-level flow or surge. Quite often such a surge occurs from north to south between Spitsbergen and Greenland.

Figure 2A-102a shows such a surge through the Fram Strait in a DMSP infrared view on 19 December 1983. An enhanced cloud line looking much like a rope cloud delineates the frontal position. Note that open-celled cumulus clouds in the strait do not exist all the way up to the frontal boundary but change form to overcast stratus 40 to 60 nm behind the front. Winds are believed to turn strongly anticyclonically in this region to a northeasterly direction. This causes a change from open to closed cell or overcast stratus and helps create the cyclonic vorticity maximized at the frontal location. (See Fig. 2A-80a as an example of strong anticyclonic turning of the wind near the frontal boundary).

On 20 December at 2025 GMT (Fig. 2A-103a), a cloud vortex is observed in the DMSP nighttime visual data. In this image the pronounced anticyclonic turning of the winds from northerly to northeasterly, in the flow leading to the vortex, is revealed by the change in alignment of cloud streets in that area.

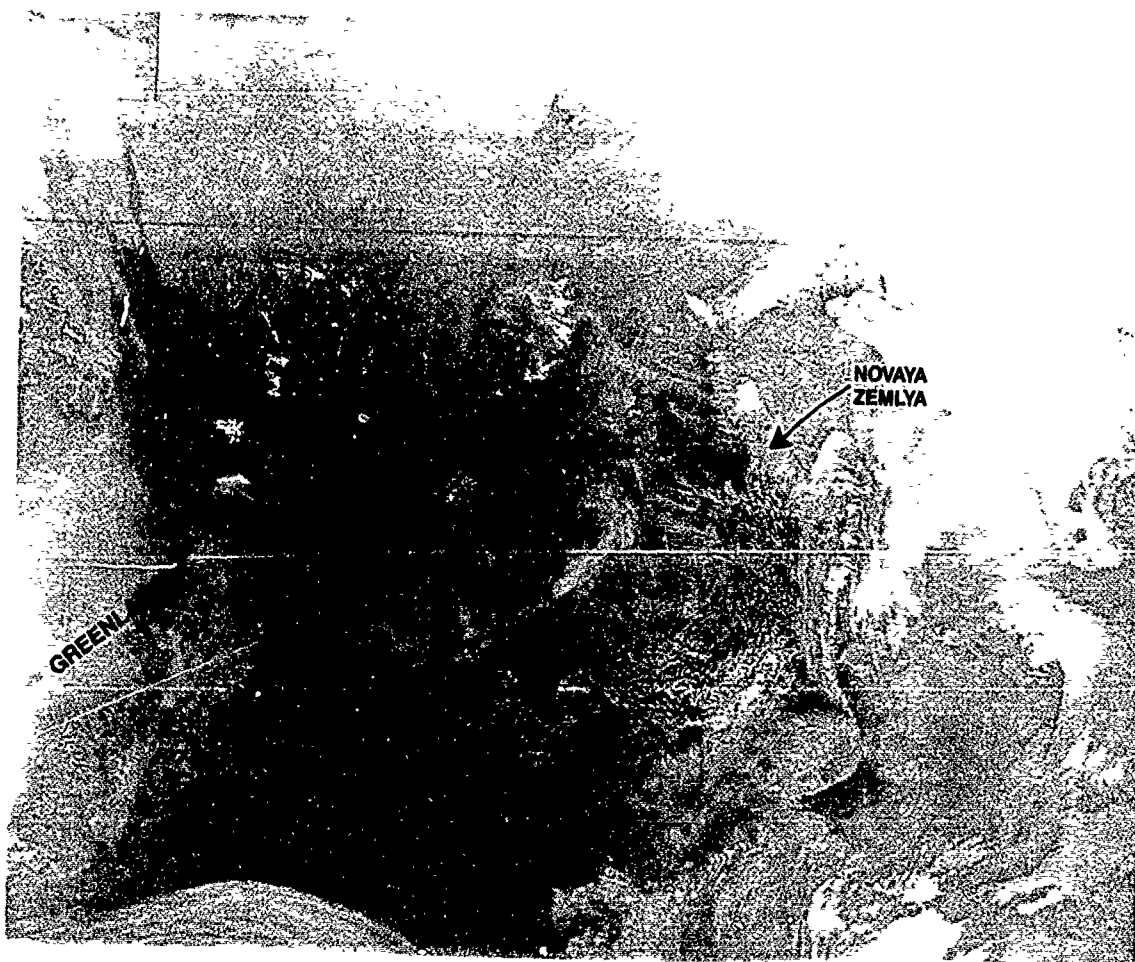
By 1913 GMT, as revealed by another DMSP nighttime visual image (Fig. 2A-104a), a significant polar low had evolved.



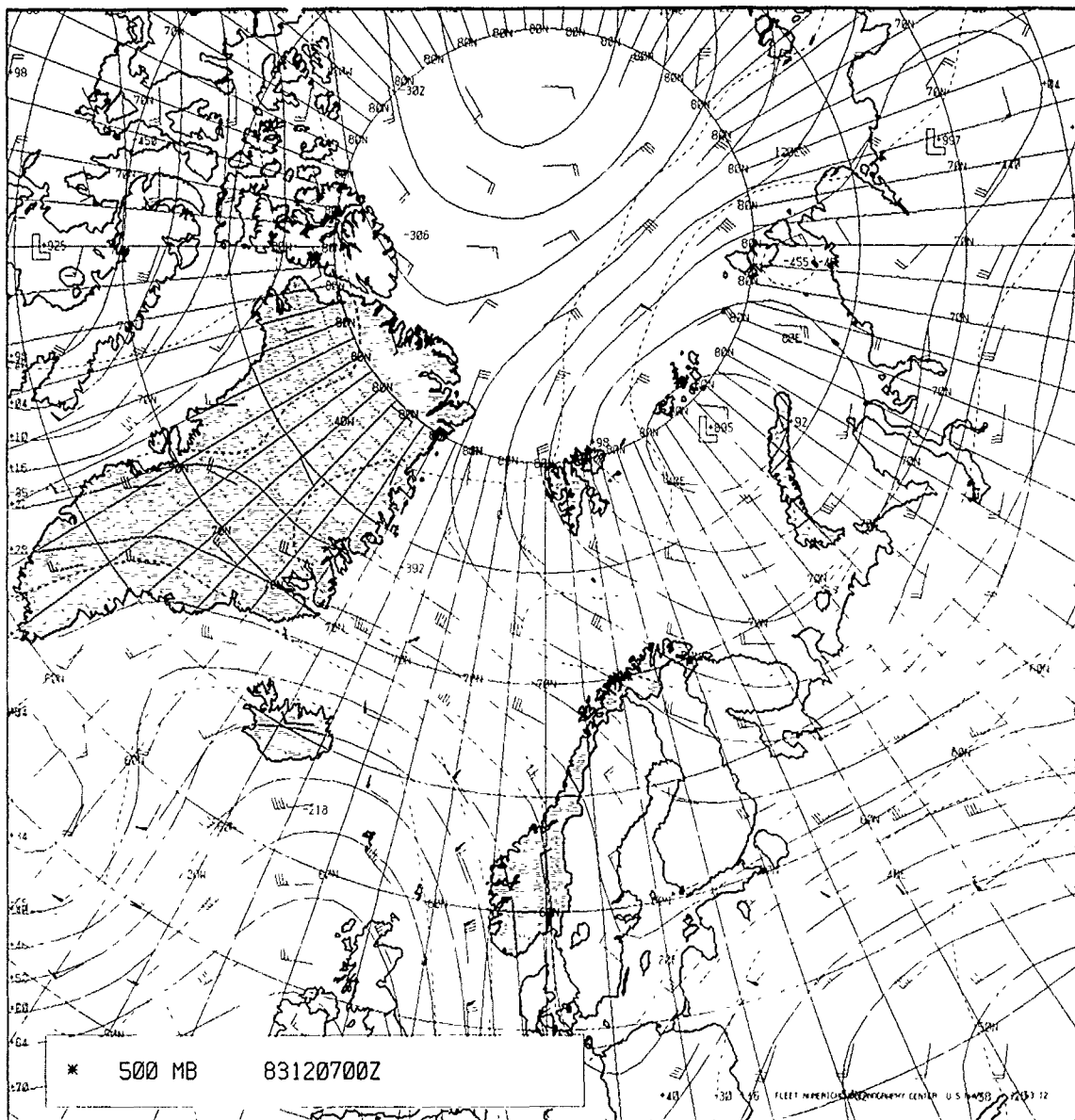
2A-95a DMSP Infrared (TS) Data 1616 GMT 3 December 1983.



2A-96a. DMSP Infrared (TS) Data. 0414 GMT 6 December 1983

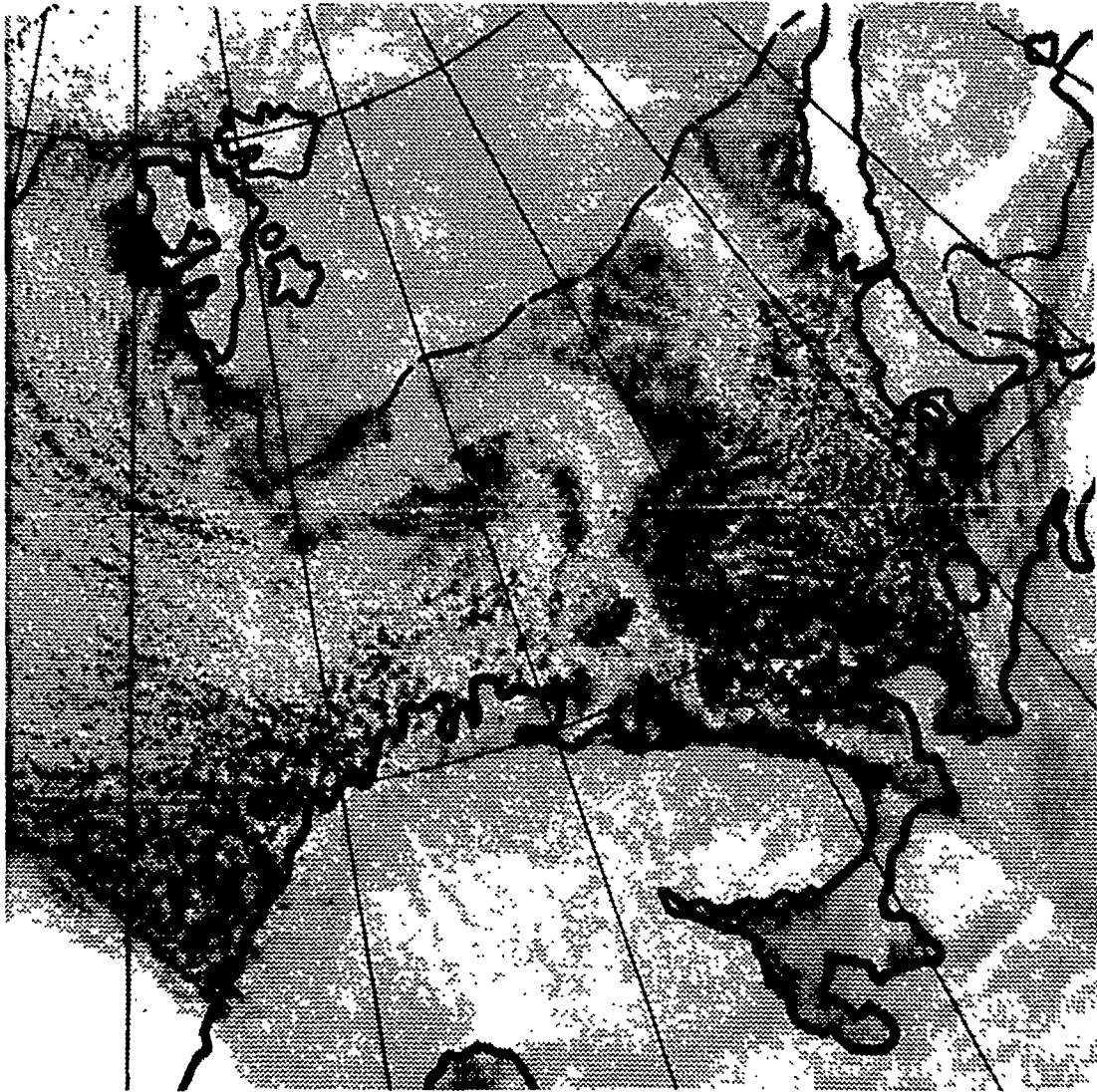


2A-97a DMSP Infrared (TS) Data 0030 GMT 7 December 1983

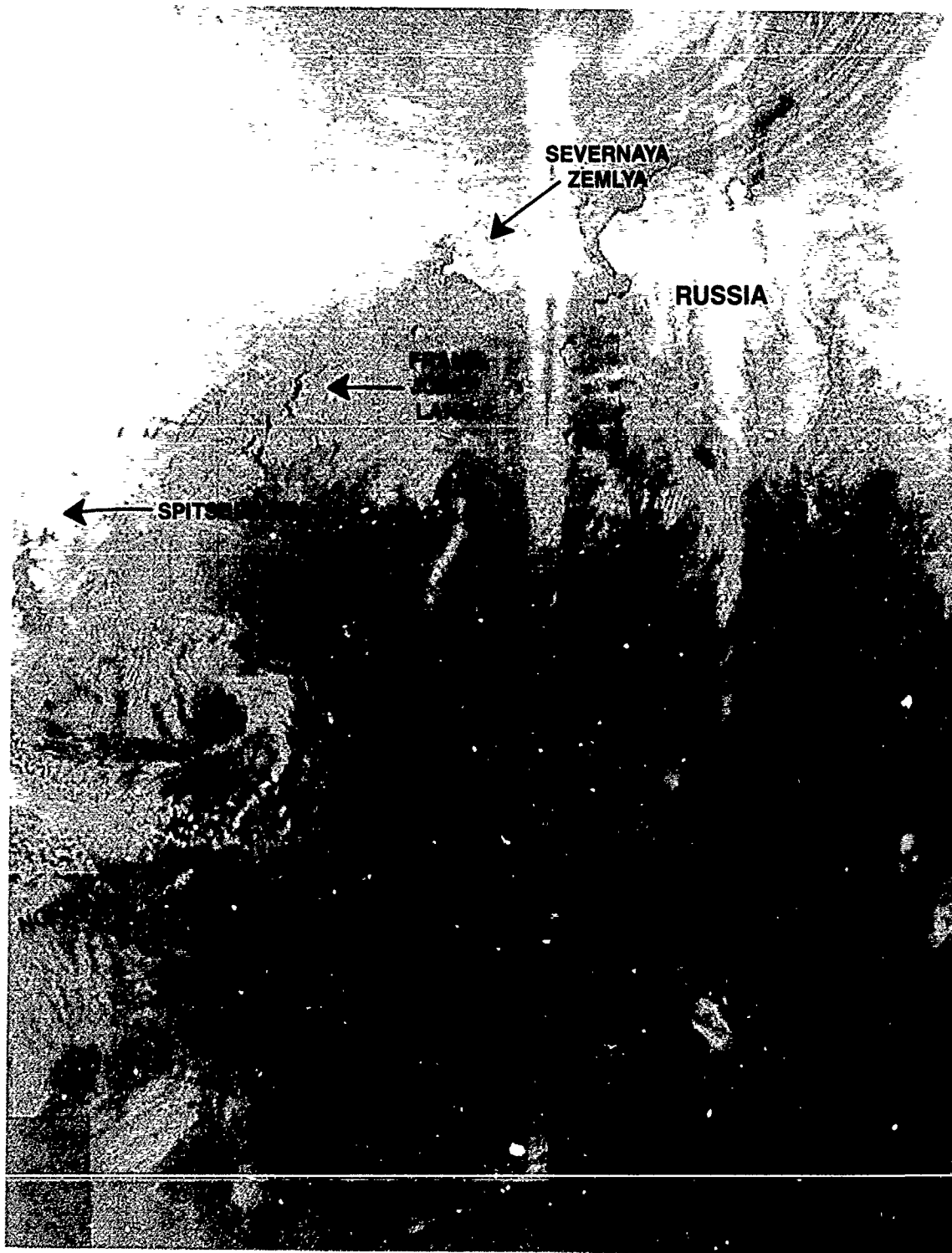


2A-98a. FNOC 500-mb Analysis. 0000 GMT 7 December 1983.





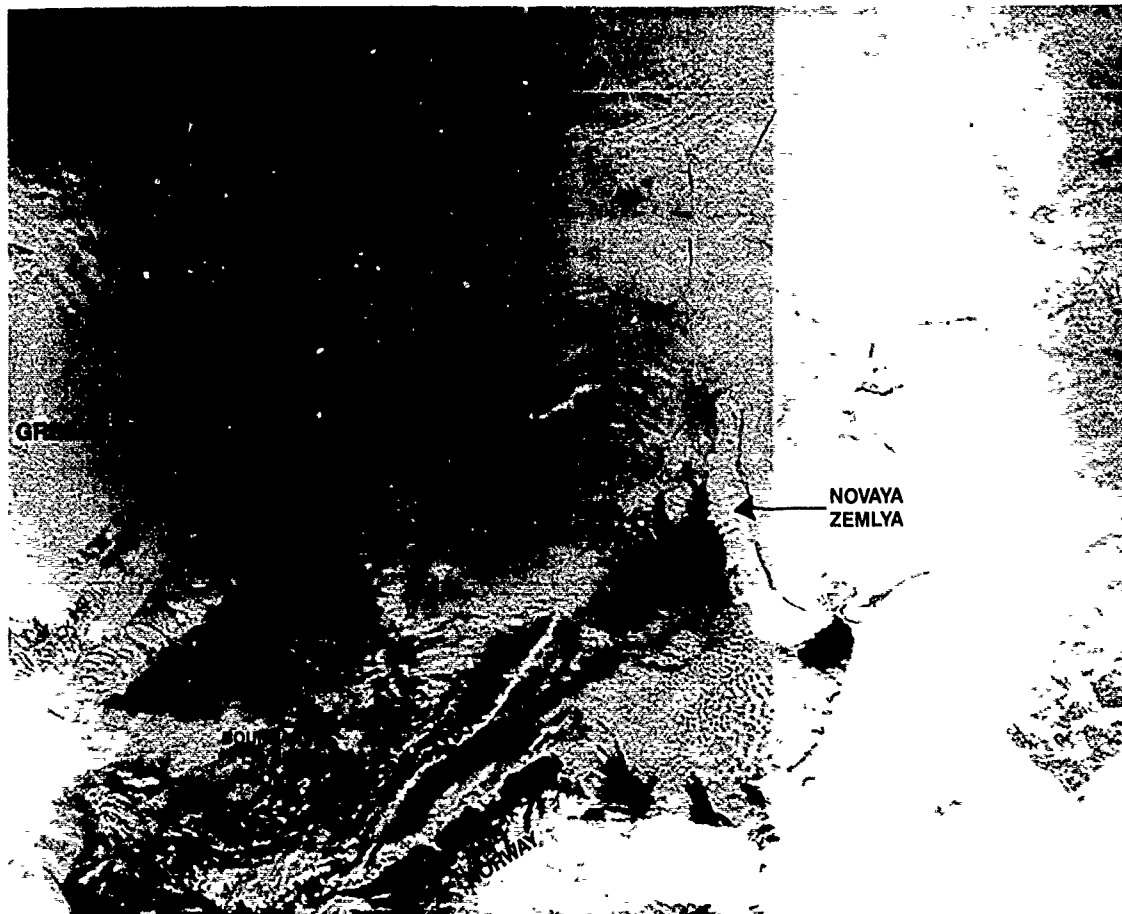
2A-99a DMSP Infrared (TS) Data. 1250 GMT 7 December 1983



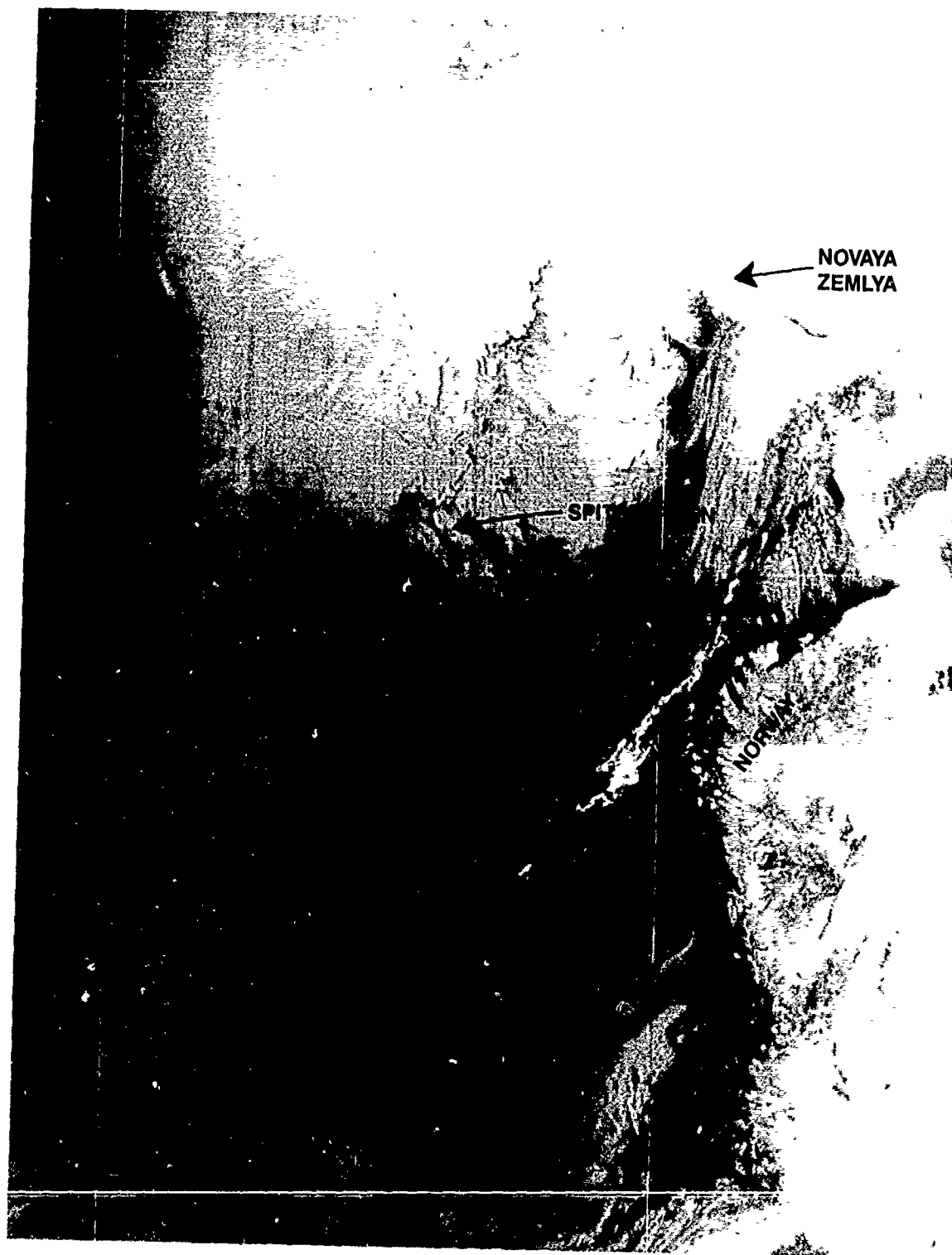
2A-100a DMSP Infrared (TS) Data 1633 GMT 7 December 1983



2A-101a. DMSP Infrared (TS) Data 1814 GMT 7 December 1983.



2A-102a. DMSP Infrared (TS) Data 2318 GMT 19 December 1983.



2A-103a. DMSP Nighttime Visual (LS) Data. 2025 GMT 20 December 1983.

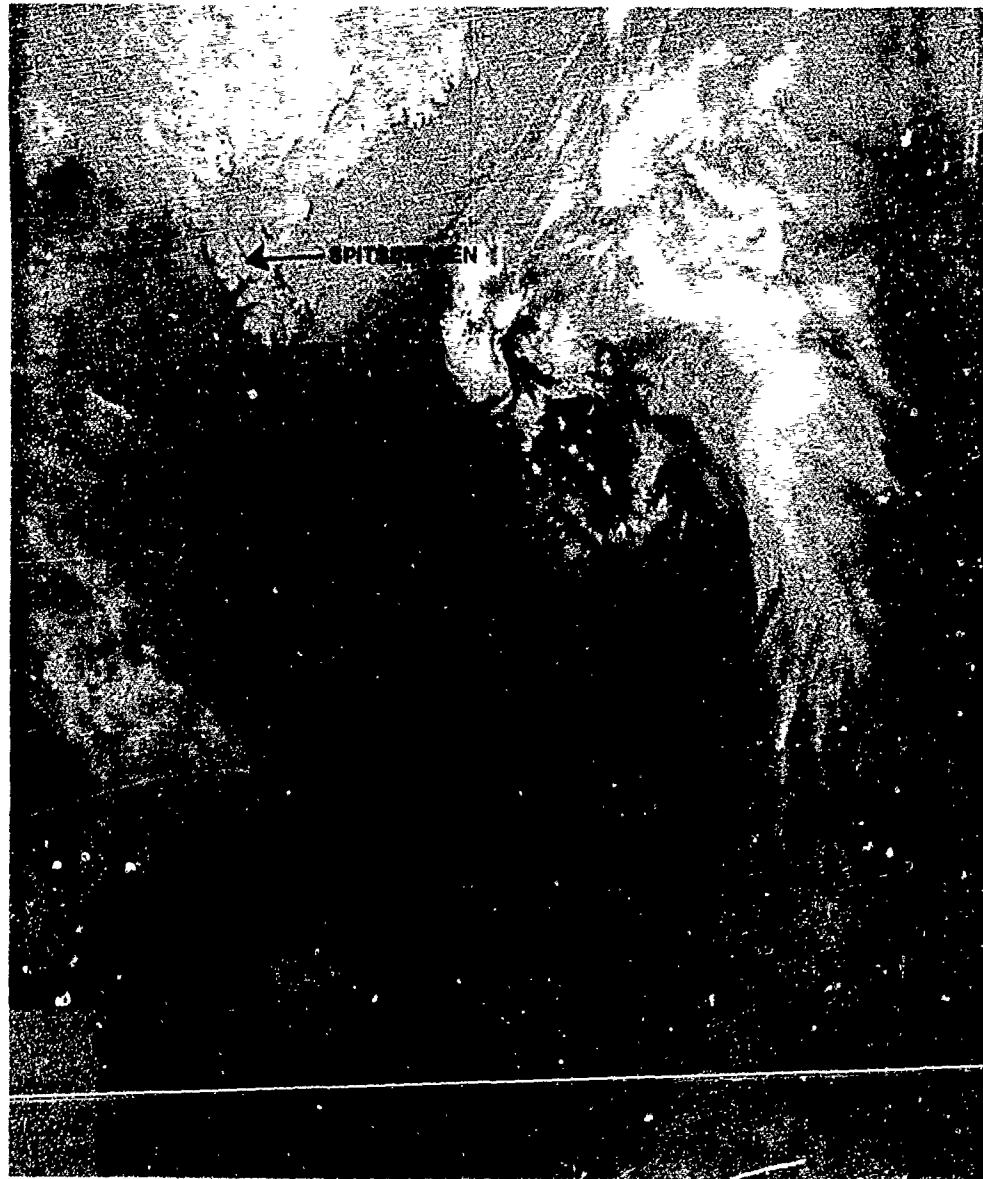


2A-104a DMSP Nighttime Visual (LS) Data. 1913 GMT 20 December 1983.

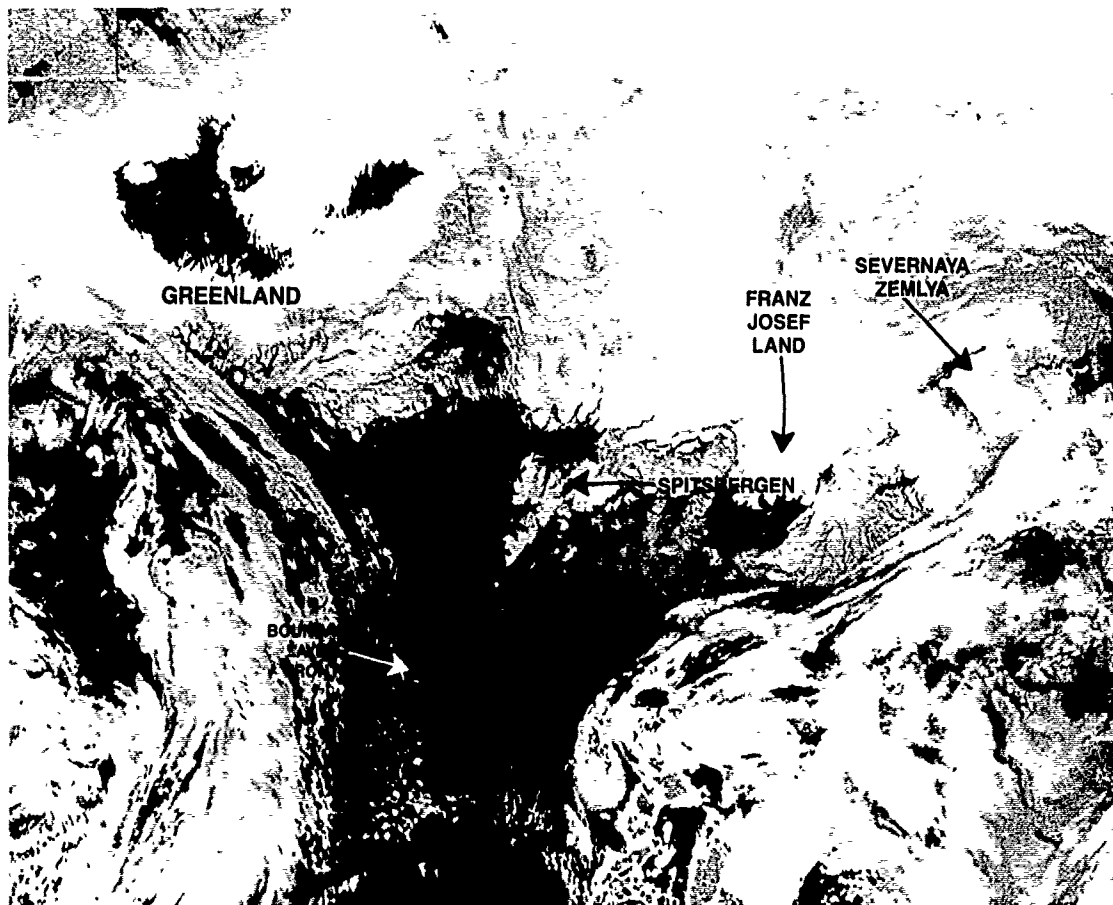
*Example 4. Polar Low Development in Interaction With a Cold Trough Aloft—18-22 November 1983*

Boundary layer fronts in the Arctic without upper level support in the form of a cold low or cold trough are still operationally significant, and are frequently associated with mesoscale vortices that form along the trough axis. Such vortices generally do not deepen in any significant fashion. In contrast intense polar lows require further development of instability through a deep layer of the atmosphere. This condition is provided when cold trough or lows move over the region of the boundary layer front. An example of such development is shown in the next series of images.

Figure 2A-105a is a DMSP infrared image acquired on 18 November 1983 at 1810 GMT. The image shows a boundary layer front extending from the southern tip of Spitsbergen to the north coast of Norway. It is apparent from the pattern of open-celled stratocumulus west of the front that the boundary layer is deeper in this region than on the east side of the front where open cells are much smaller in diameter.



2A-105a DMSP Infrared (TS) Data. 1810 GMT 18 November 1983.



2A-106a. DMSP Infrared (TS) Enhanced Data. 2047 GMT 18 November 1983



The area for several miles east of the front is overcast. Winds in this area have shifted from northerly to southeasterly. This activity can be verified in a DMSP enhancement acquired at 2047 GMT (Fig. 2A-106a). These data clearly reveal the southeasterly orientation of cloud lines leading up to the front from the east (similar to Fig. 2A-80a). The flow changes back to northerly immediately west of the boundary layer front. This produces strong cyclonic vorticity at the frontal boundary, favorable for vortex formation.

On the following day, 19 November at 2112 GMT, DMSP data (Fig. 2A-107a) reveal that vortex development did occur along the frontal boundary and also at a secondary frontal boundary immediately to the west. These vortices appeared very weak in nature and are not apparent on the following day, 20 November at 2323 GMT (Fig. 2A-108a).

The image is very interesting for at least a couple of reasons. First a careful look in the region just east of the frontal boundary shows that cloud lines, especially noticeable in the northern portion of the front, are turning again to align with southeasterly flow. In fact there is some rather marked cyclonic turning indicating strong vorticity in the region near Bear Island ( $74.6^{\circ}\text{N } 19^{\circ}\text{E}$ )

Secondly, cloud plumes over the Fram Strait indicate northwesterly flow aloft, while plumes from Novaya Zemlya indicate southeasterly flow. These plumes imply a closed upper level low over the ice just east of Svalbard. Upper cold lows in the vicinity of boundary layer fronts over the water often lead to intense polar low development. One such image properly interpreted gives advance warning of this potential.

The FNOC 500-mb analysis (Fig. 2A-109a) verifies the presence of the cold core low aloft over the area.

By 1848 GMT on 21 November (Fig. 2A-110a) it is apparent from the DMSP data that something important is happening along the frontal boundary. Convection appears to be quite intense and there is evidence of multiple vorticity centers along the overcast band defining the boundary layer front.

Aloft the FNOC 500-mb analysis (Fig. 2A-111a) for 0000 GMT on 22 November reveals the cold low over the frontal region. A strong polar jet from the northwest coincides with the northern edge of cirrus cloudiness streaming across the Greenland/Norwegian Seas toward southern Norway.

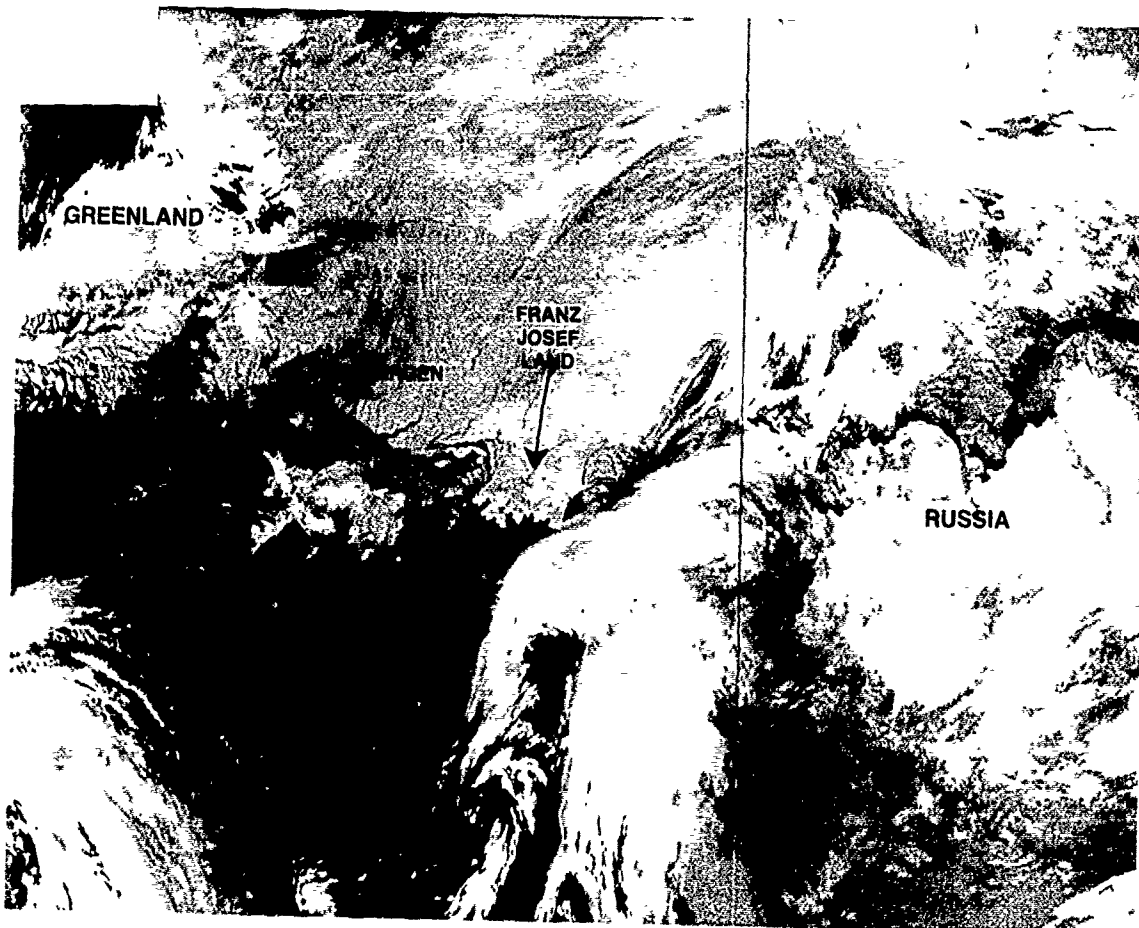
DMSP nighttime visual data at 2302 GMT (Fig. 2A-112a) again suggest several centers of vorticity along the frontal band but the southernmost one appears to be most intense at this time.

Intensification continues as shown by DMSP data at 0043 GMT on 22 November (Fig. 2A-113a), and by 1555 GMT (Fig. 2A-114a) an intense polar low has formed.

A second center is shown forming southwest of the main low in DMSP nighttime visual data acquired at 2150 GMT (Fig. 2A-115a). This image shows a new boundary layer front moving eastward past Spitsbergen across the Fram Strait, again with southeasterly winds behind it in its northern extremity.

Eastward movement of the front is verified by the progression shown in Fig. 2A-116a, DMSP nighttime visual data on 23 November at 0022 GMT.

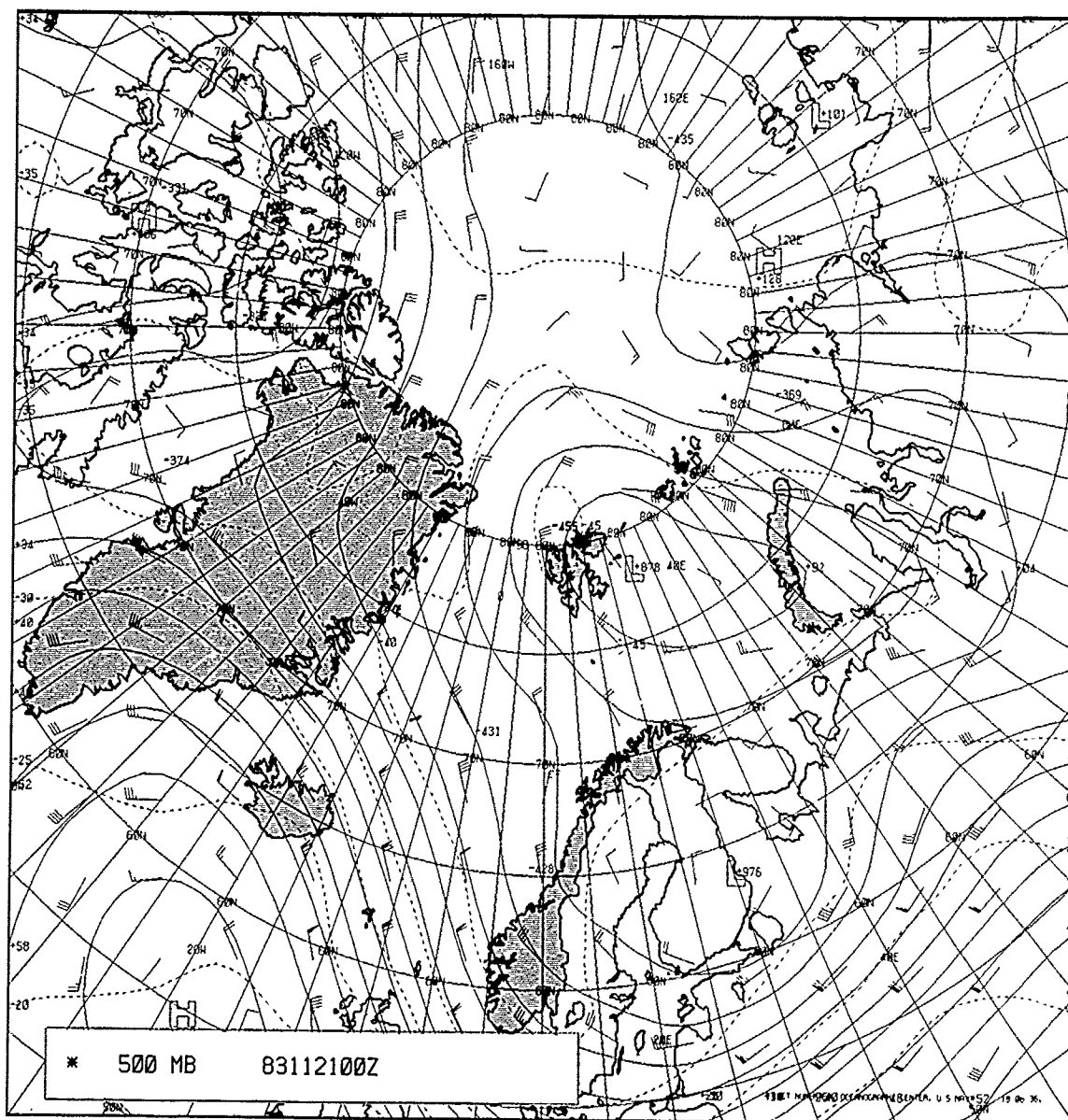
A final nighttime visual view at 0203 GMT (Fig. 2A-117a) shows the well-defined polar low and a series of waves along the frontal boundary east of Spitsbergen.



2A-107a. DMSP Infrared (TS) Data 2112 GMT 19 November 1983



2A-108a DMSP Infrared (TS) Data 2323 GMT 20 November 1983

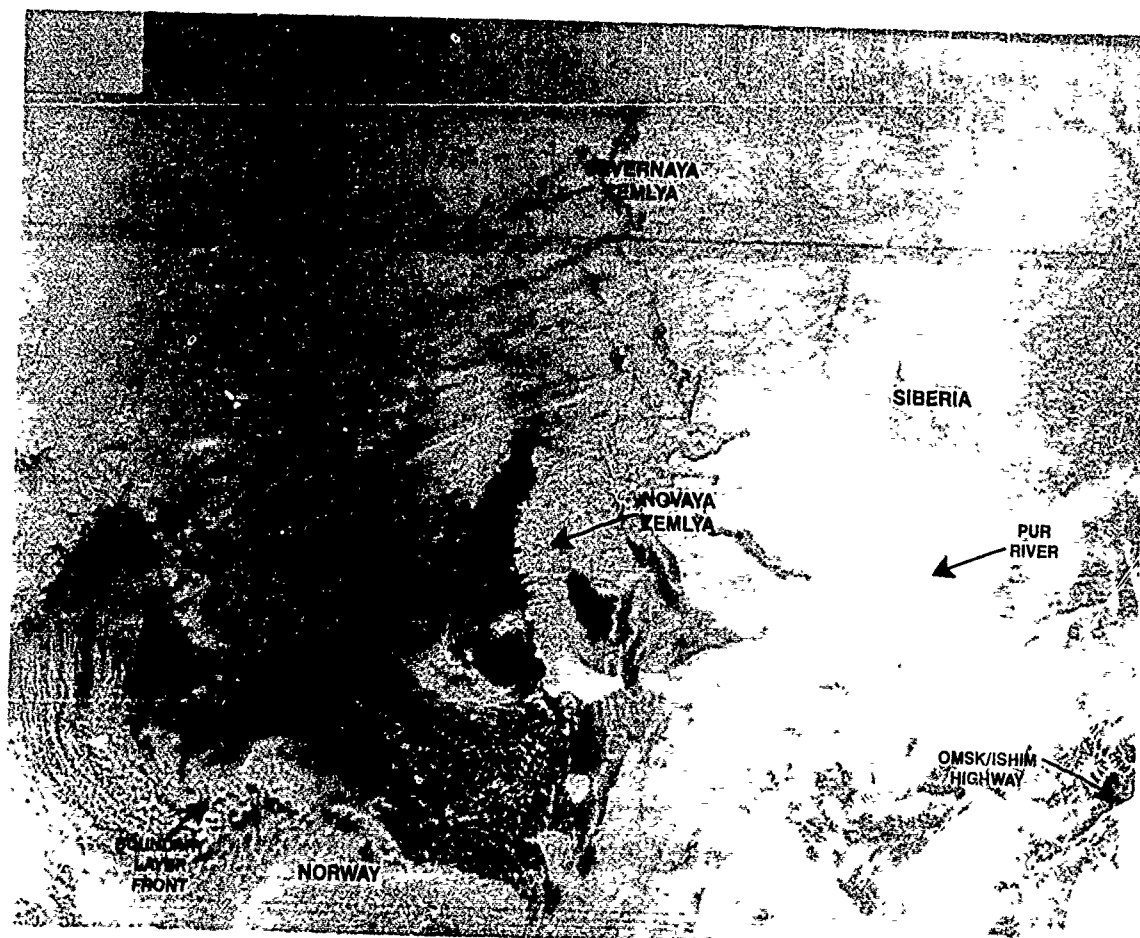


2A-109a. FNOC 500-mb Analysis. 0000 GMT 21 November 1983.



2A-110a. DMSP Infrared (TS) Data 1848 GMT 21 November 1983.





2A-112a DMSP Nighttime Visual (LS) Data 2302 GMT 21 November 1983



2A-113a. DMSP Infrared (TS) Data 0043 GMT 22 November 1983





2A-114a DMSP Infrared (TS) Data. 1555 GMT 22 November 1983



2A-113a DMSP Nighttime Visual (LS) Data 2150 GMT 22 November 1983



2A-116a DMSP Nighttime Visual (LS) Data 0022 GMT 23 November 1983

### Important Conclusions

1. Several examples of boundary layer frontal movement in the Greenland, Norwegian, and Barents Seas region have been shown. The boundary layer front separates air that has moved from over the ice and onto the water from air that has been resident over the water for some time and hence, strongly modified.
2. Vorticity tends to be maximized along the frontal boundary so that vortex formation is common, particularly at the base of the front. Normally such vortices are weak and do not undergo intense development. When an upper cold low or trough moves in the vicinity of a boundary layer front, however, intense and often explosive polar low development can occur.
3. It is unlikely that this is the only mode of polar low development in the described region but it appears to be a frequent and often favored mode of development.
4. Although not convincingly demonstrated in this study, conventional analyses are generally not adequate in terms of detecting boundary layer frontal or polar low formation and movement.
5. Satellite data at frequent intervals (every 2 or 3 hr) are required to definitively monitor such developments.

### References

- Rasmussen, E., 1985. *A Polar Low Development Over the Barents Sea* Polar Low Project, Technical Report No. 7, DNMI, The Norwegian Meteorological Institute, Oslo, Norway, 42 pp.
- Shapiro, M. A., 1987: Research aircraft measurements of a polar low over the Norwegian Sea *Tellus*, 39A, 272-306.



2A-117a DMSP Nighttime Visual (LS) Data. 0203 GMT 23 November 1983

*Case 5 Polar Low Development on a Track From the North Pole to Northern Norway  
(5-9 June 1984)*

*Modes of Polar Low Development*

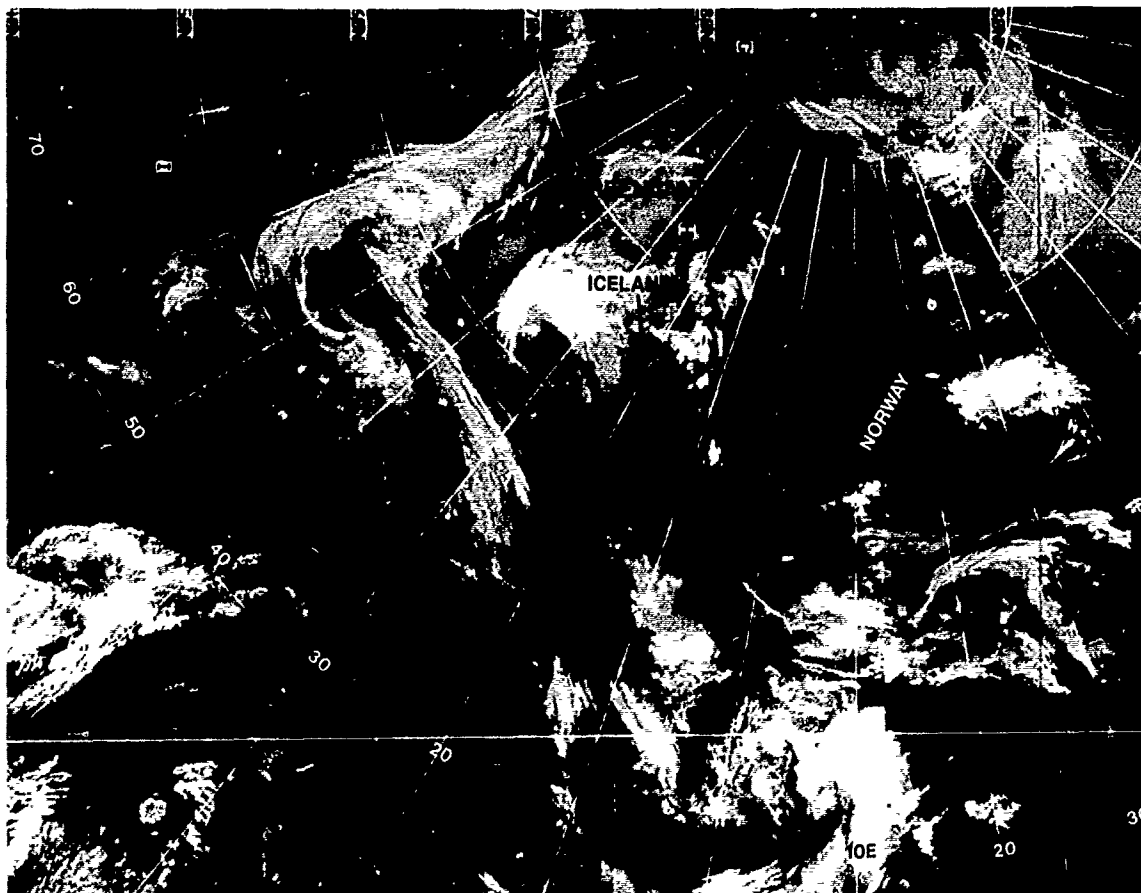
Polar low development has been noted to occur in the Arctic when an upper cold low and a surface low, roughly superimposed, move from over the pack ice or ice cap to an open body of water. (See NTAG, Vol. 8, Part 2, case of polar low development in the Chukchi Sea.)

This method of polar low production differs from the polar lows that develop along a low-level boundary front. In the latter case, development occurs when an upper cold low moves separately into the vicinity of a BLF that is situated over an open body of water.

In the present example the upper cold low and the surface low are evident and quite well defined near the North Pole, three days prior to polar low formation. The evolution of the polar low occurred as a separate event within the circulation of the parent system as the upper cold low and surface low moved southward from the ice cap, to a position over the Barents Sea on a track toward northern Norway.

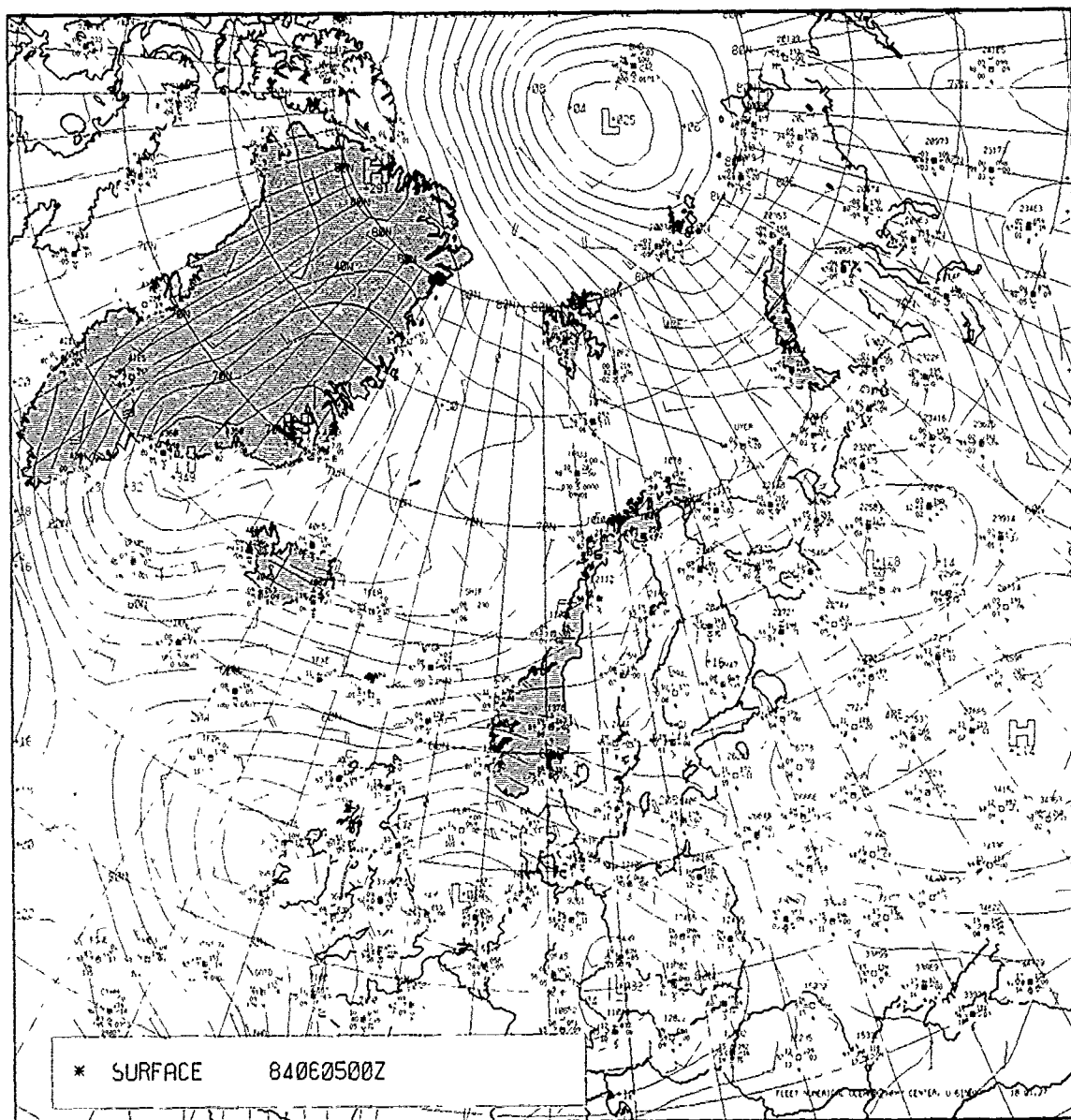
*5 June 1984*

A DMSP mosaic on this date at about 1120 GMT (Fig. 2A-118a) shows evidence of a vortex centered southeast of the North Pole near 85°N 50°E. Cirrus and/or middle cloud striations, evident in this infrared depiction, clearly delineate the vertical structure. Note the outline of Greenland (near "H") and the warm outline of Norway southwest of the vortex on the right-hand side of the image.

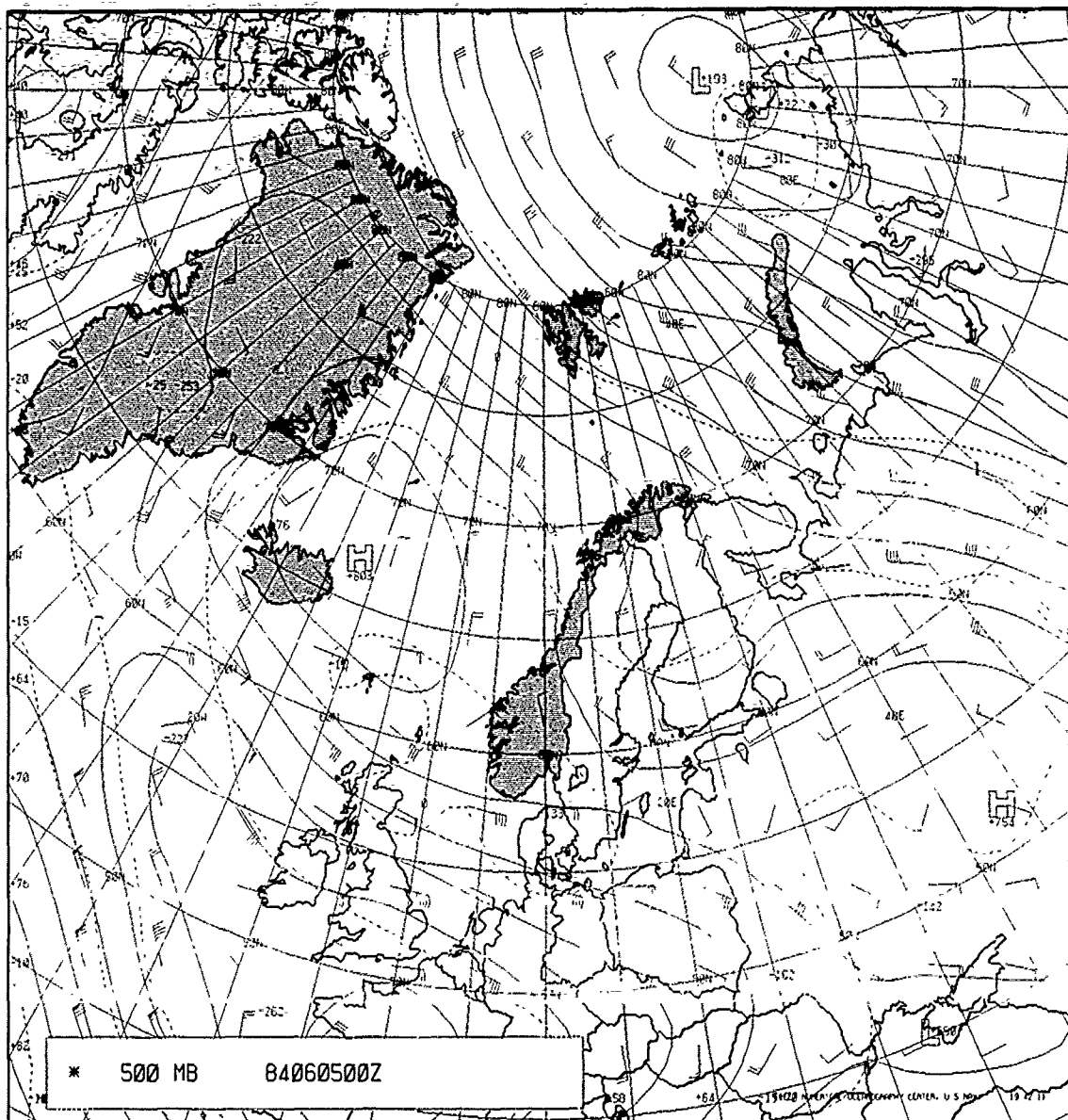


2A-118a. DMSP Infrared (TS) Mosaic Data. 1120 GMT 5 June 1984.

The FNOC surface analysis for 0000 GMT (Fig. 2A-119a) shows a low center of 1002.5 mb in that general area. Temperatures are not too cold, only slightly below freezing.



2A-119a. FNOC Surface Analysis. 0000 GMT 5 June 1984.



2A-120a. FNOC 500-mb Analysis. 0000 GMT 5 June 1984.



At 500 mb (Fig. 2A-120a) an upper cold low is indicated southeast of the surface low, near Severnaya Zemlya (North Land).

The features are equally evident 12 hr later at 1200 GMT with the surface low apparently moving southward and showing a pressure of 1001.8 mb (Figs. 2A-121a and 2A-122a).

#### *6 June 1984*

The DMSP infrared mosaic on this date at about 1010 GMT (Fig. 2A-123a) shows that the low has indeed moved southward to near 80°N 50°E. Note that comma-shaped cloud masses exist south of the center, indicating the extension of a trough southward along about 50°N.

The 0000 GMT surface analysis (Fig. 2A-124a) shows the low center over Franz Josef Land and verifies the extension of a trough southward over Novaya Zemlya. The upper cold low (Fig. 2A-125a) is centered with a cold pool of air ( $-30^{\circ}\text{C}$ ) over the surface disturbance.

The 1200 GMT analyses (Figs. 2A-126a and 2A-127a) show continued southward movement, with the 500-mb low slightly trailing the surface feature. Central pressure of the surface low is around 1007 mb, an increase from earlier days.

#### *7 June 1984*

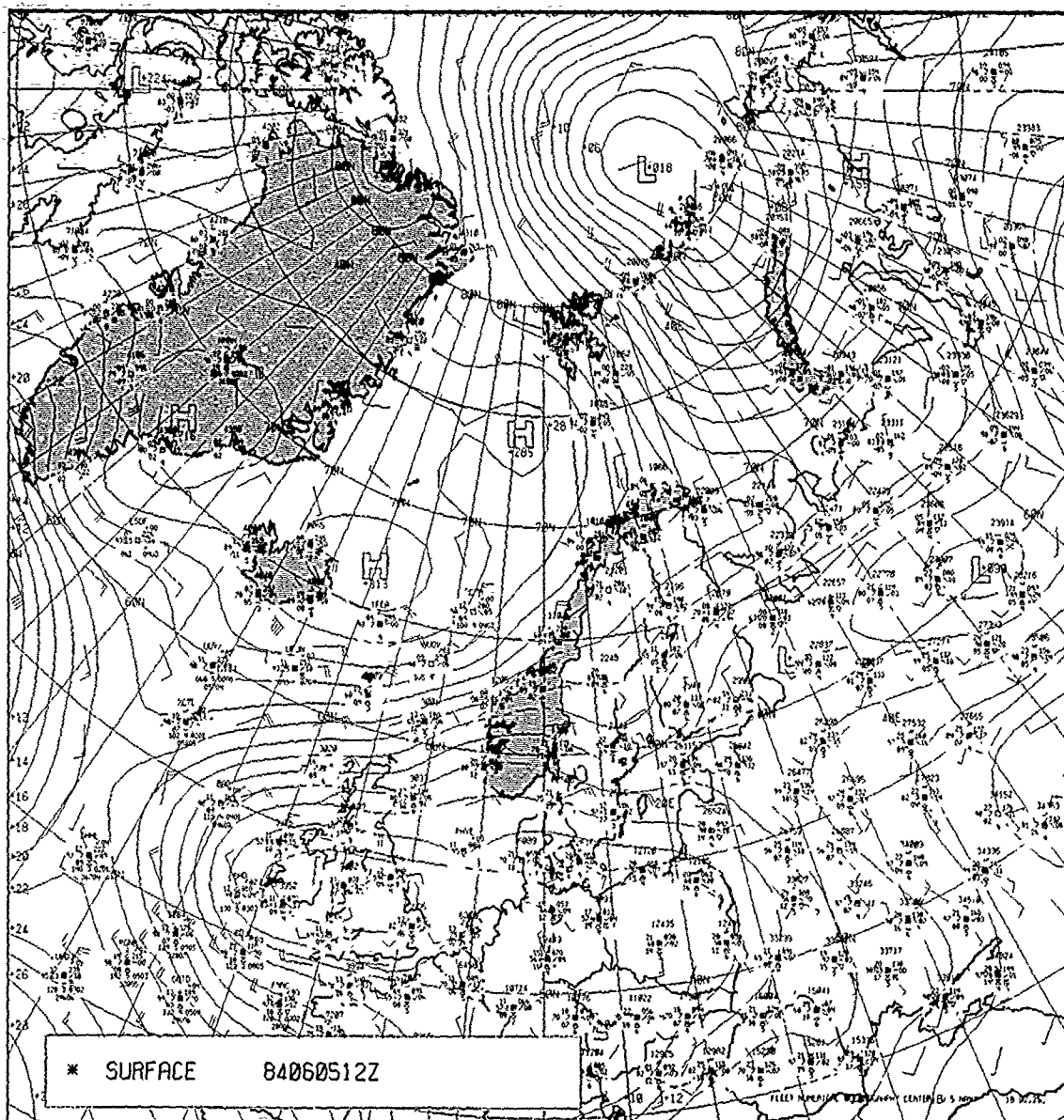
Visible DMSP data (LS) acquired at 0719 GMT (Fig. 2A-128a) now show a major change in the appearance of the system as strong convective activity breaks out over the open water of the Barents Sea. Two comma-shaped convective patterns are apparent in the open-celled convection along 39°E between 70° and 77°N latitude. There is also a hook-shaped pattern suggesting vortex formation near 74° and 50°E. This formation is occurring along a major convective band adjacent to the open-celled convection. The appearance of the system at this time is typical of precursor conditions previously shown to indicate potential for polar low evolution within 24 hr (Fig. 2A-129a). This figure shows the 500-mb pattern associated with polar low evolution with the trough or low and coldest air directly over the enhanced convection.

The actual 500-mb analysis for 0000 GMT (Fig. 2A-129b) shows the upper cold low with its center considerably to the northeast. A cold trough does extend, however, from the low center southward over the convective region toward Novaya Zemlya. A surface low (Fig. 2A-130a) is also indicated about 5° east of the apparent vortex center shown in the DMSP data (Fig. 2A-128a). Central pressure at this time has decreased to 1000.9 mb. The lack of observations in the region undoubtedly contribute to some of these apparent discrepancies in the central position of the low. There is also a time difference—the satellite data being about 7 hr later than the analyses.

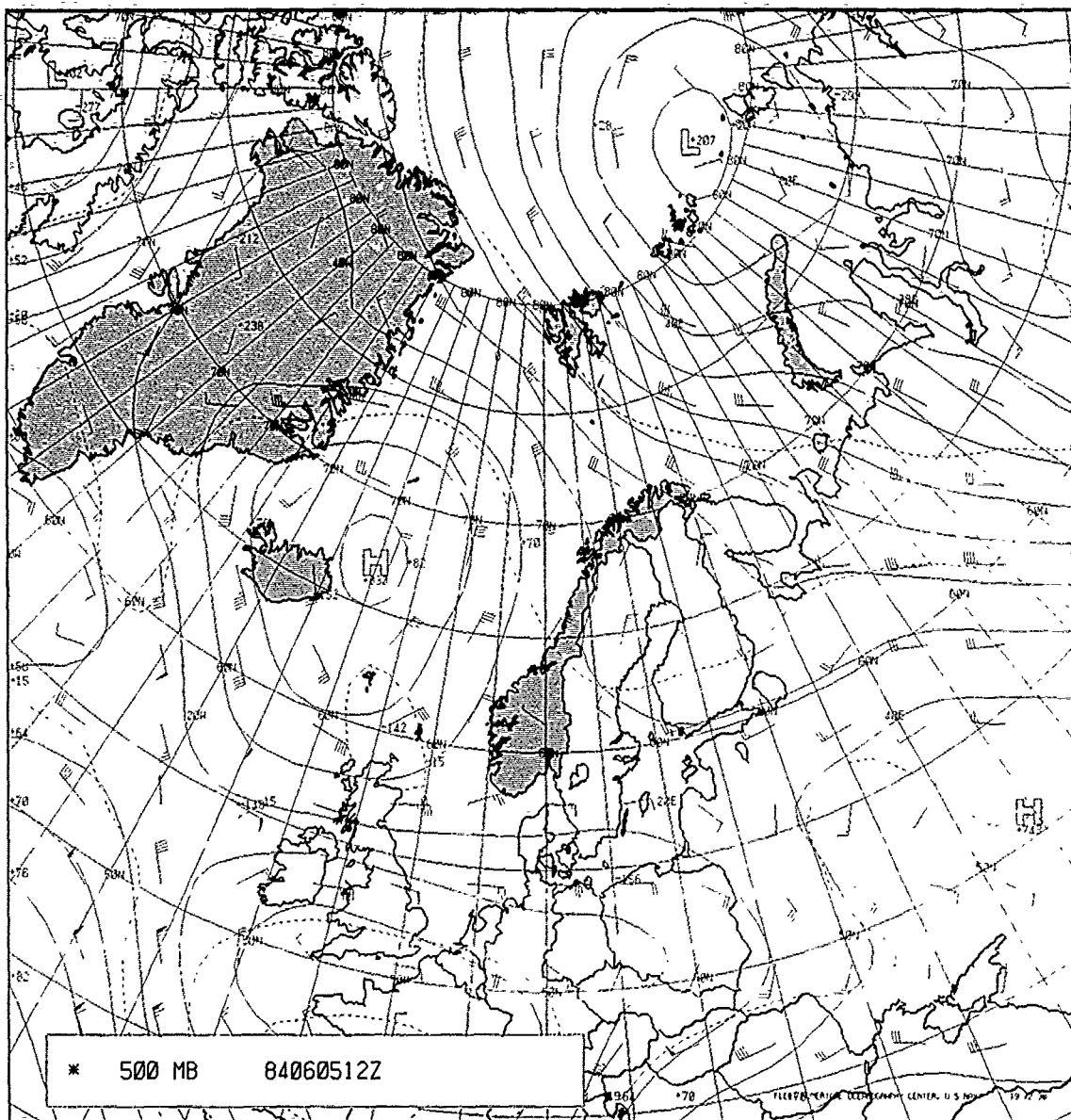
The 1200 GMT surface and 500-mb analyses are shown in Figs. 2A-131a and 2A-131b, respectively. The lower and upper level circulations are well maintained during this time period with surface pressure dropping to 996.0 mb.

#### *8 June 1988*

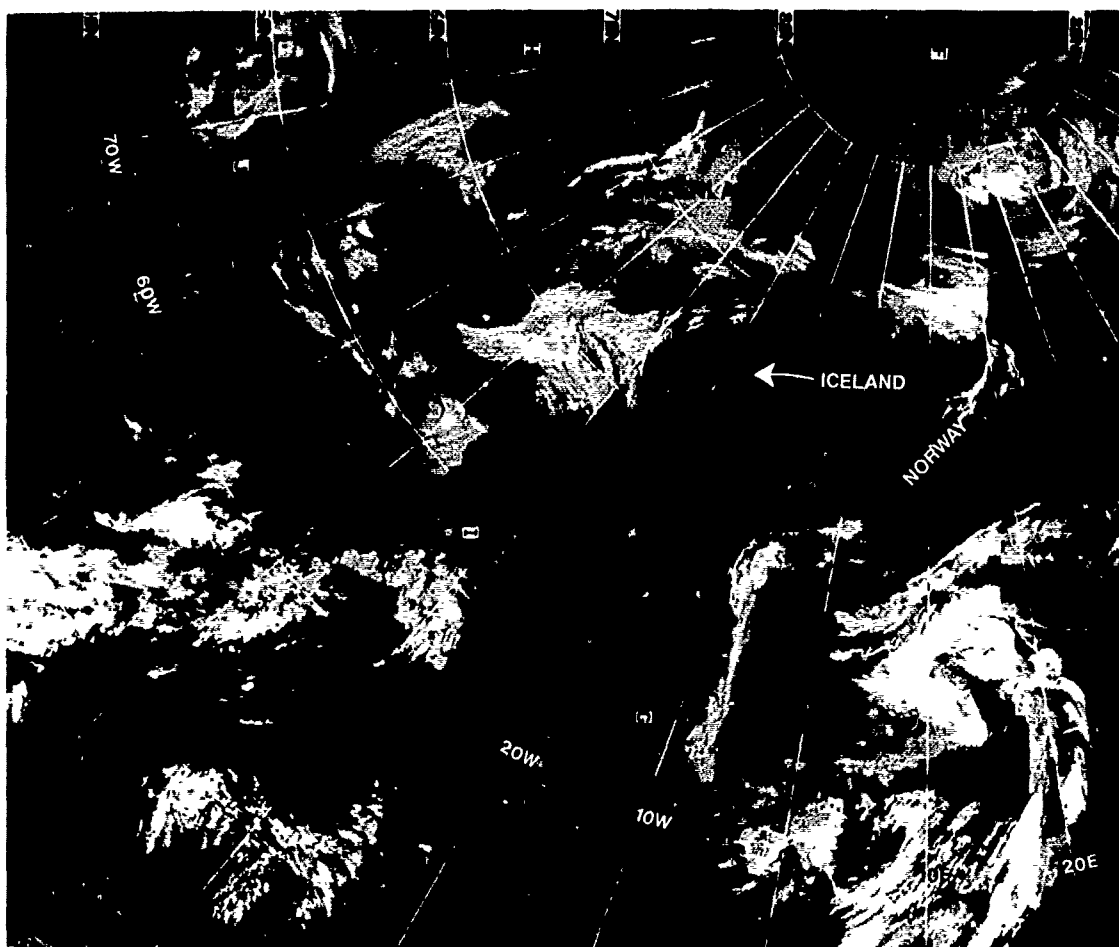
The surface analysis on this date at 0000 GMT (Fig. 2A-132a) shows the low center near the southern tip of Novaya Zemlya with a surface pressure of 994.7 mb. At 500 mb (Fig. 2A-133a) a cold pool of air and an upper low covers the Barents Sea. No indication can be derived from those analyses that an intense polar low has developed in the region.



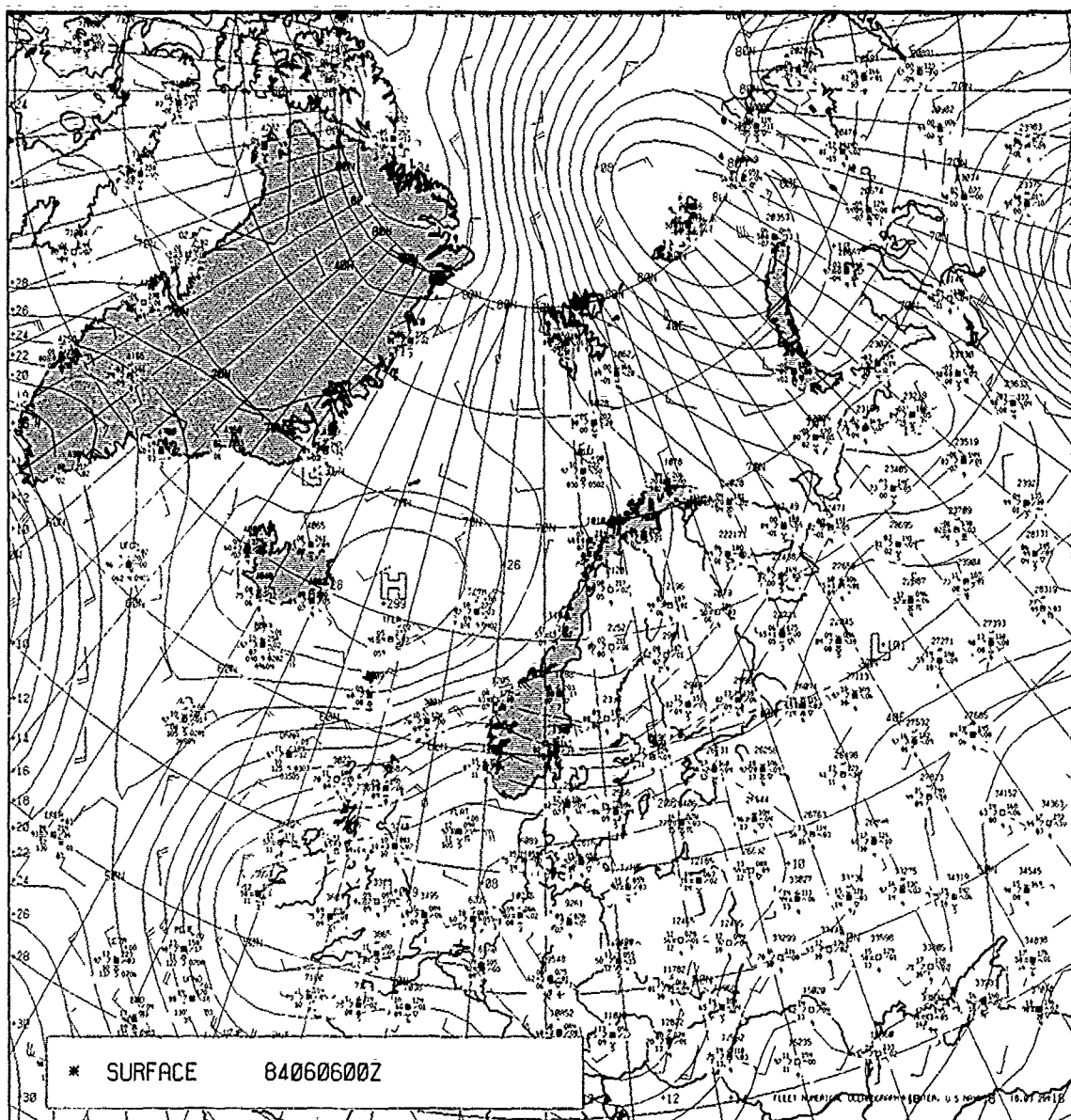
2A-121a. FNOC Surface Analysis. 1200 GMT 5 June 1984.



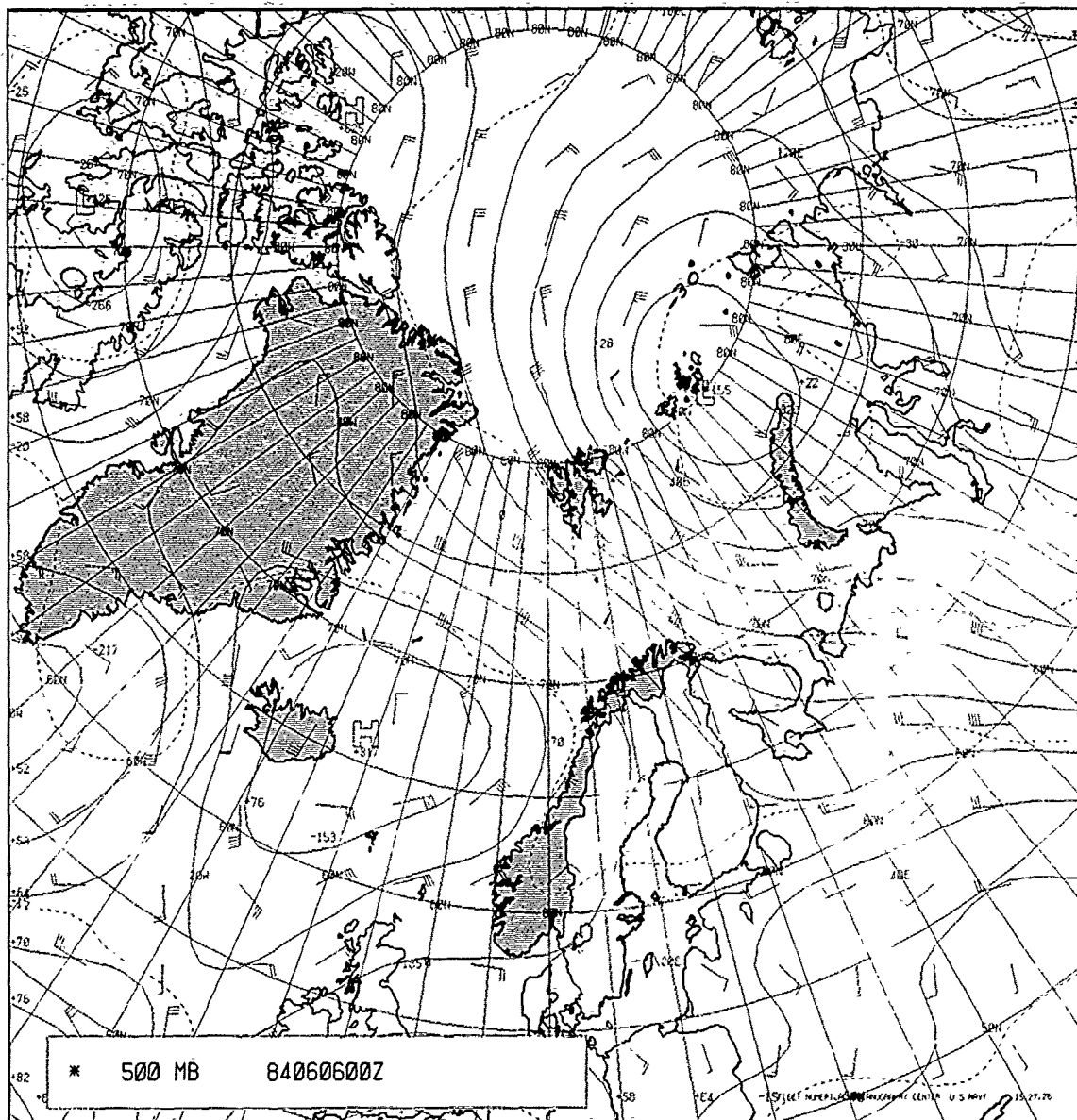
2A-122a. FNOC 500-mb Analysis, 1200 GMT 5 June 1984.



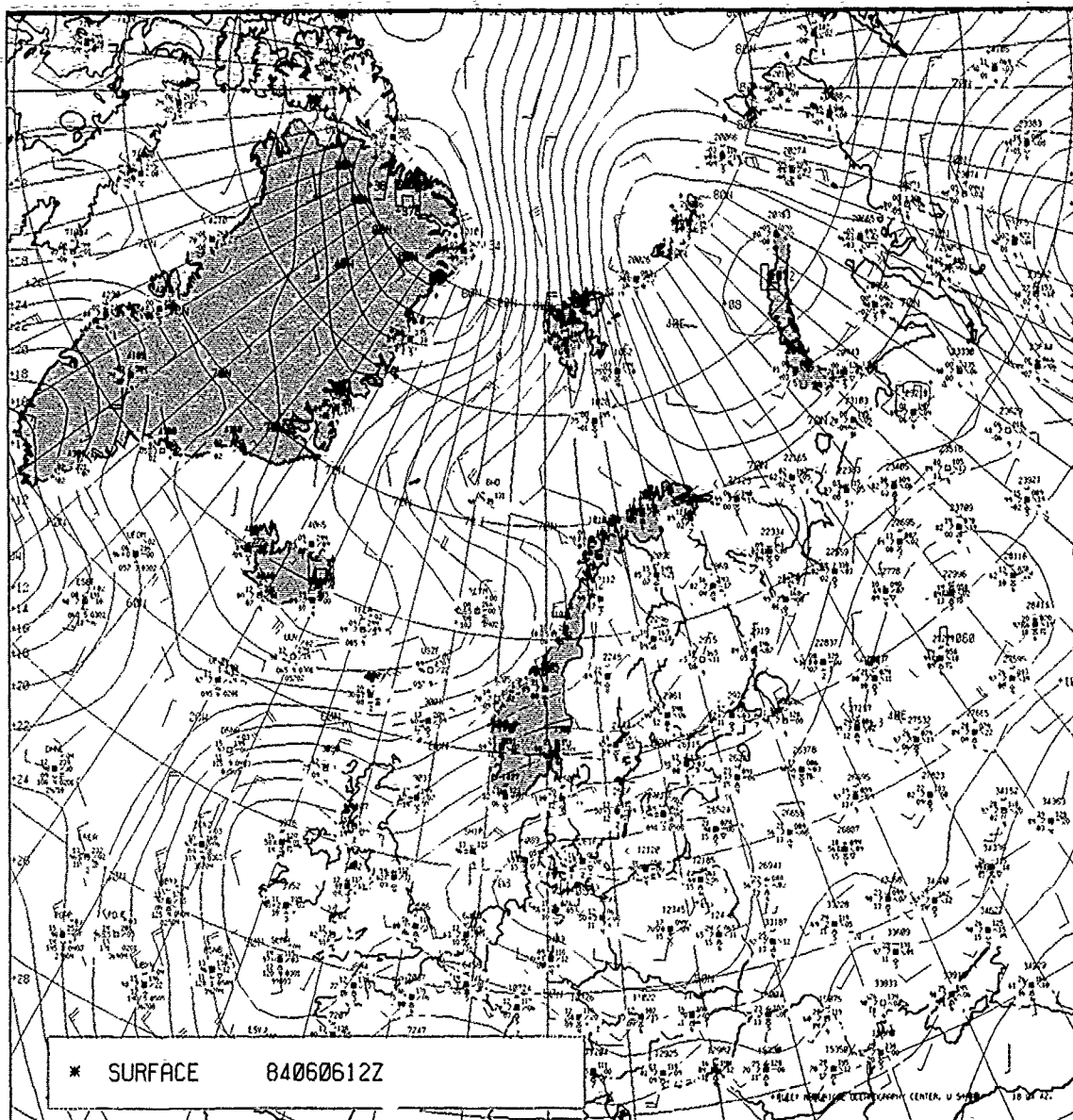
2A-123a DMSP Infrared (TS) Mosaic Data. 1010 GMT 6 June 1984.



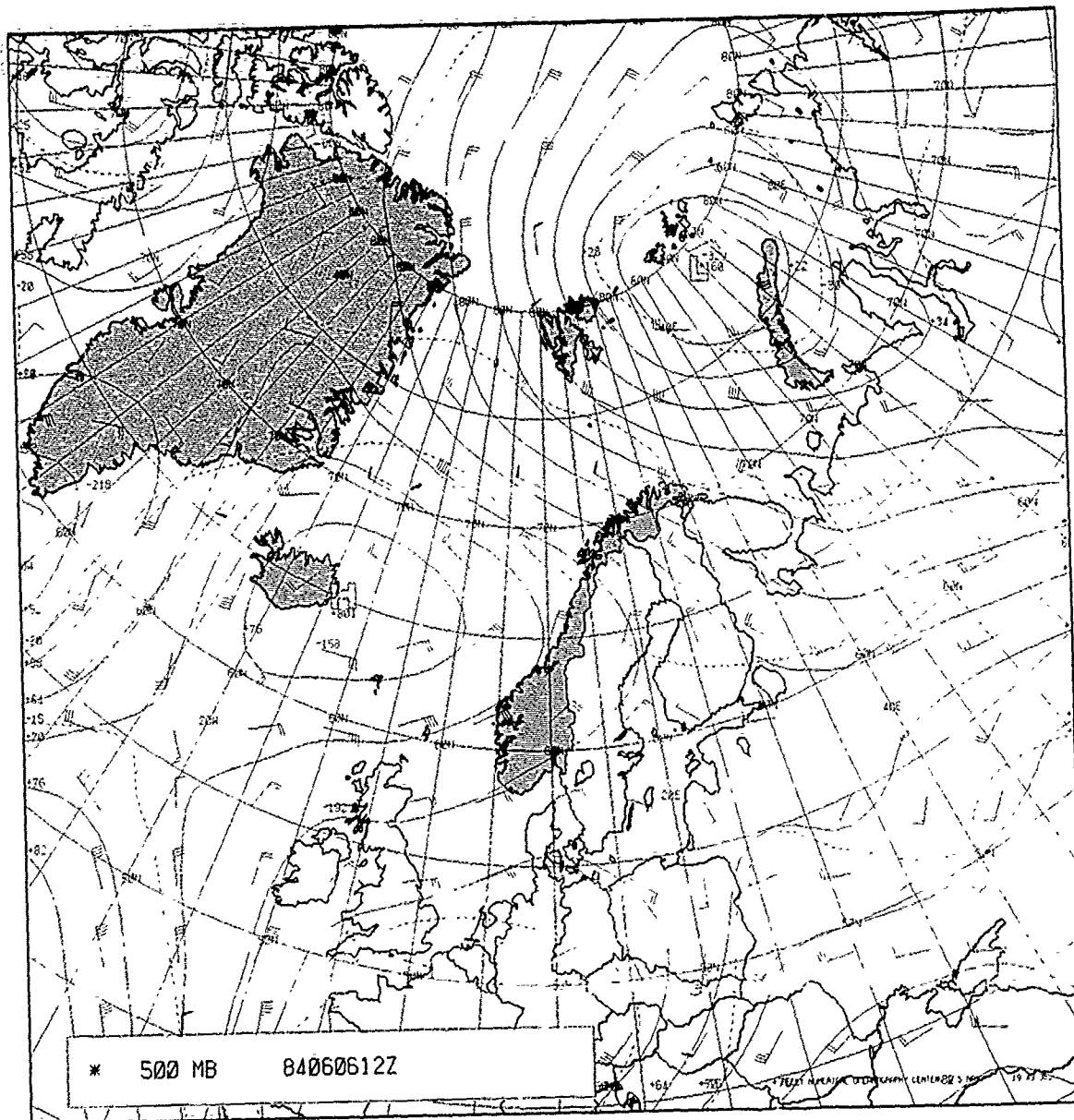
2A-124a. FNOG Surface Analysis. 0000 GMT 6 June 1984.



2A-125a. FNOC 500-mb Analysis. 0000 GMT 6 June 1984.

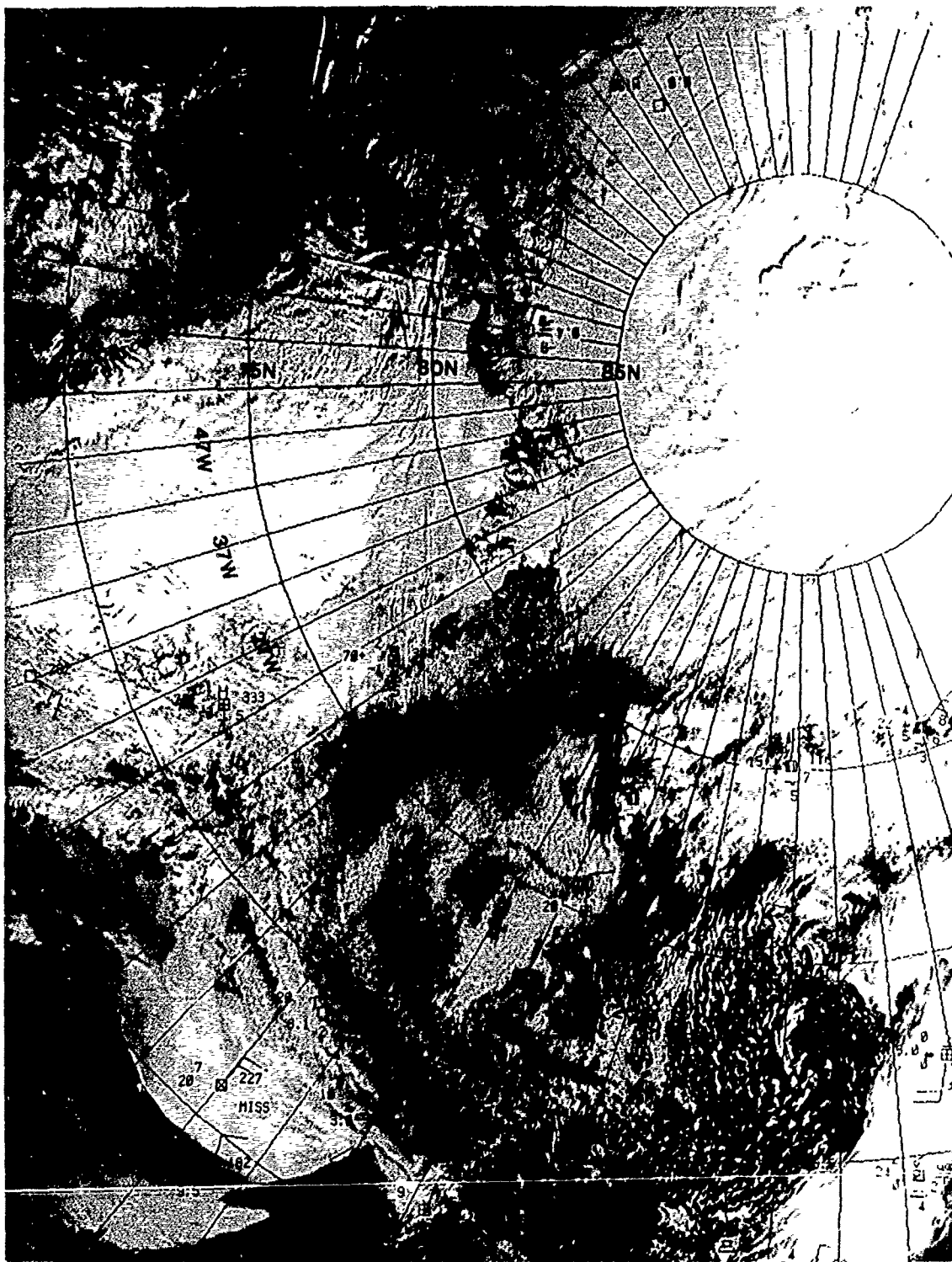


2A-126a. FNOC Surface Analysis. 1200 GMT 6 June 1984.

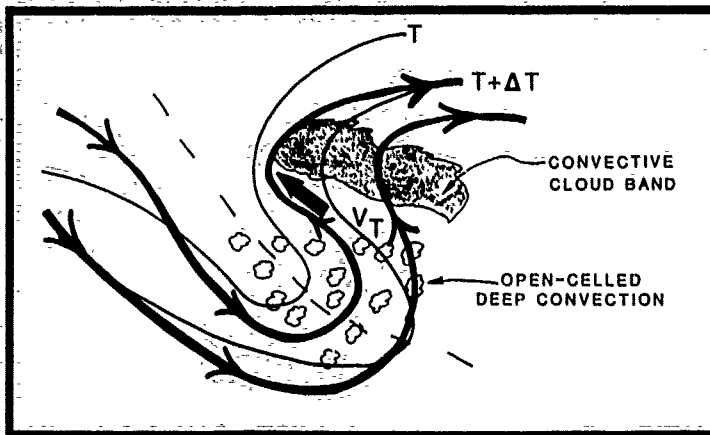


2A-127a. FNOC 500-mb Analysis. 1200 GMT 6 June 1984.

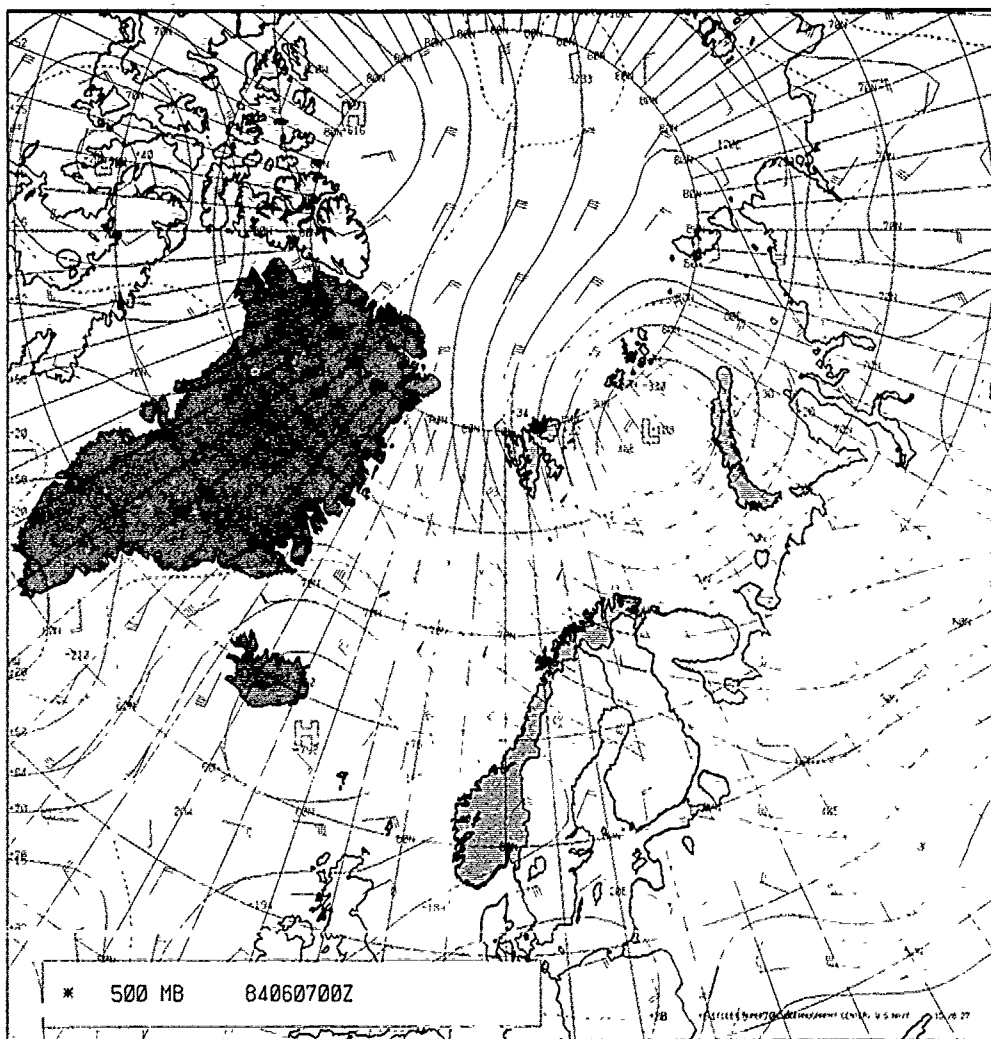




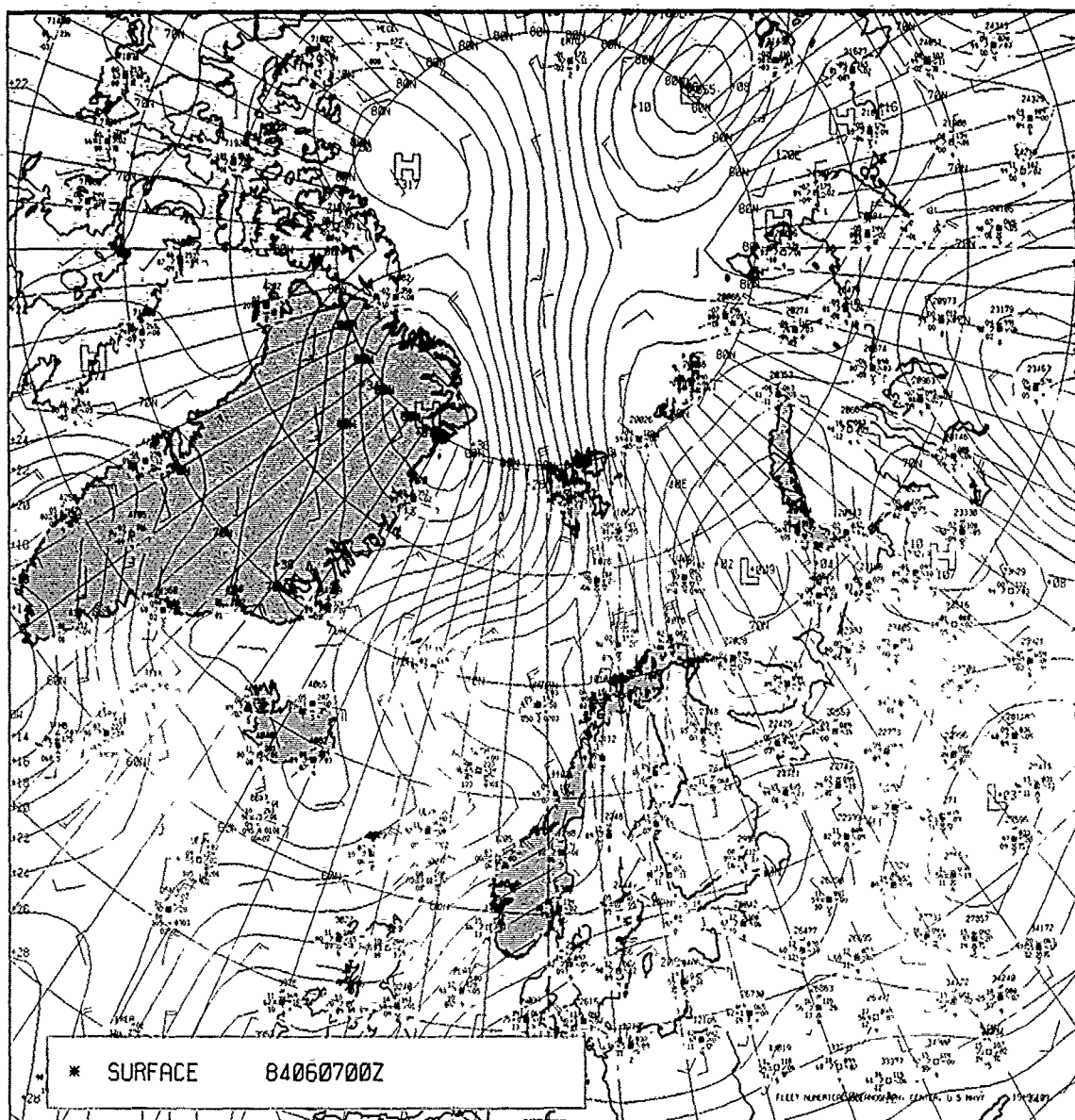
2A-128a DMSP Visible (LS) Data. 0719 GMT 7 June 1984.



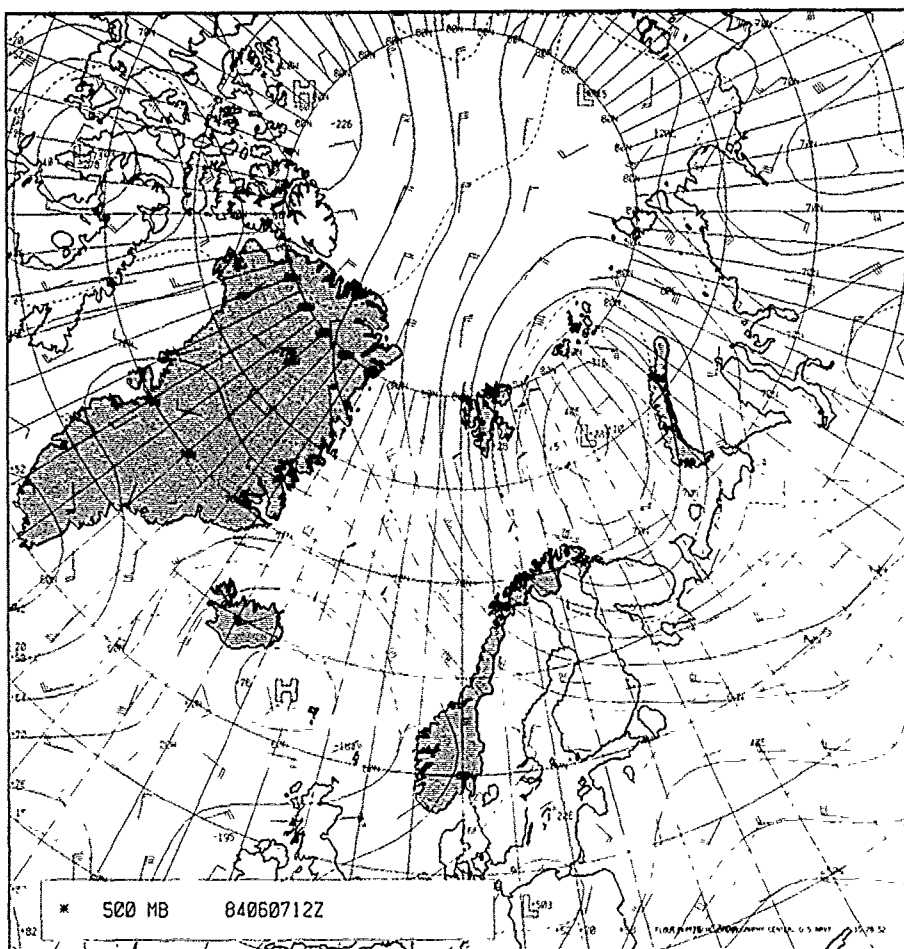
2A-129a. Precursor 500-mb Pattern Favorable for Polar Low Development.



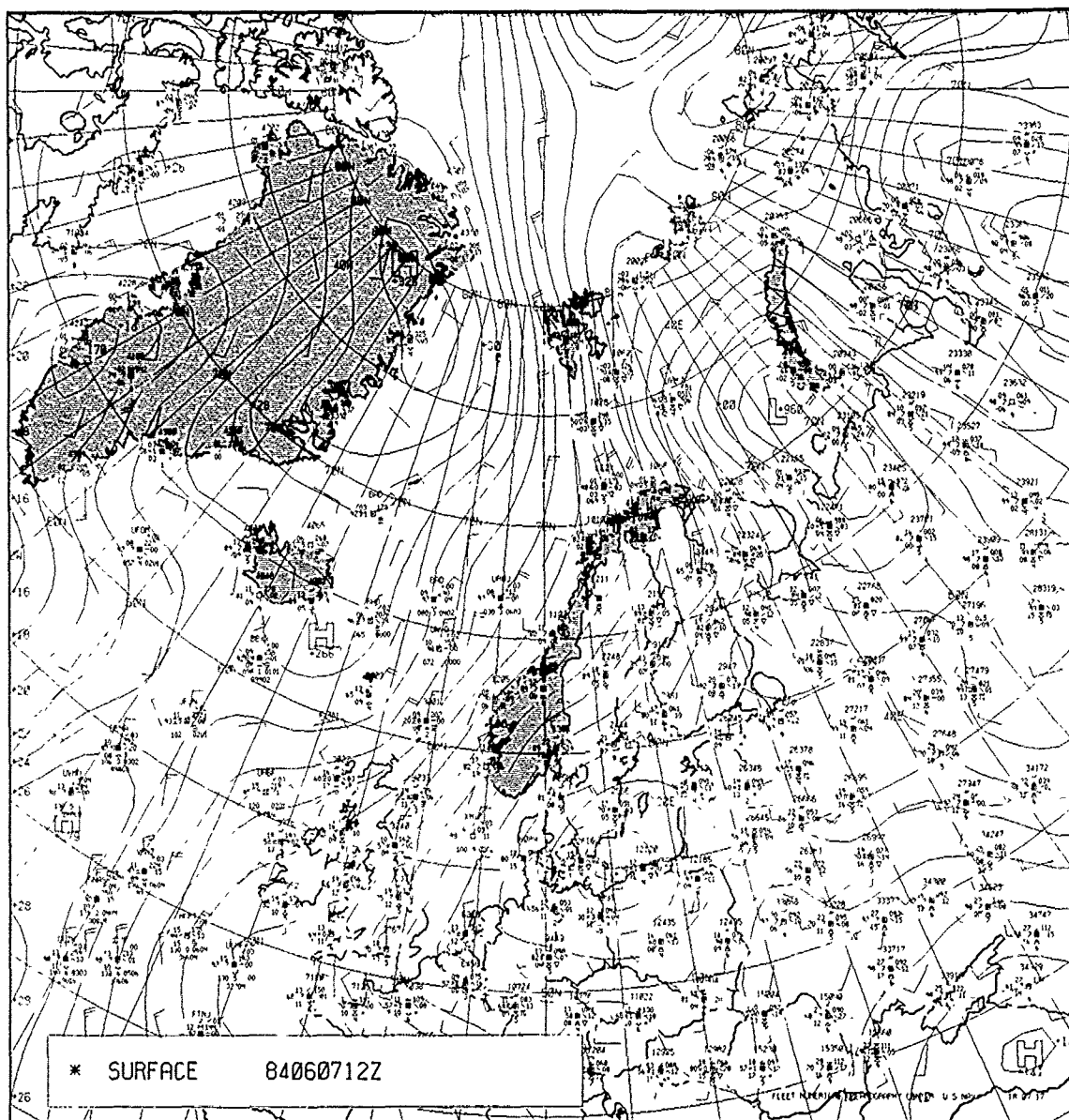
2A-129b. FNOC 500-mb Analysis. 0000 GMT 7 June 1984.



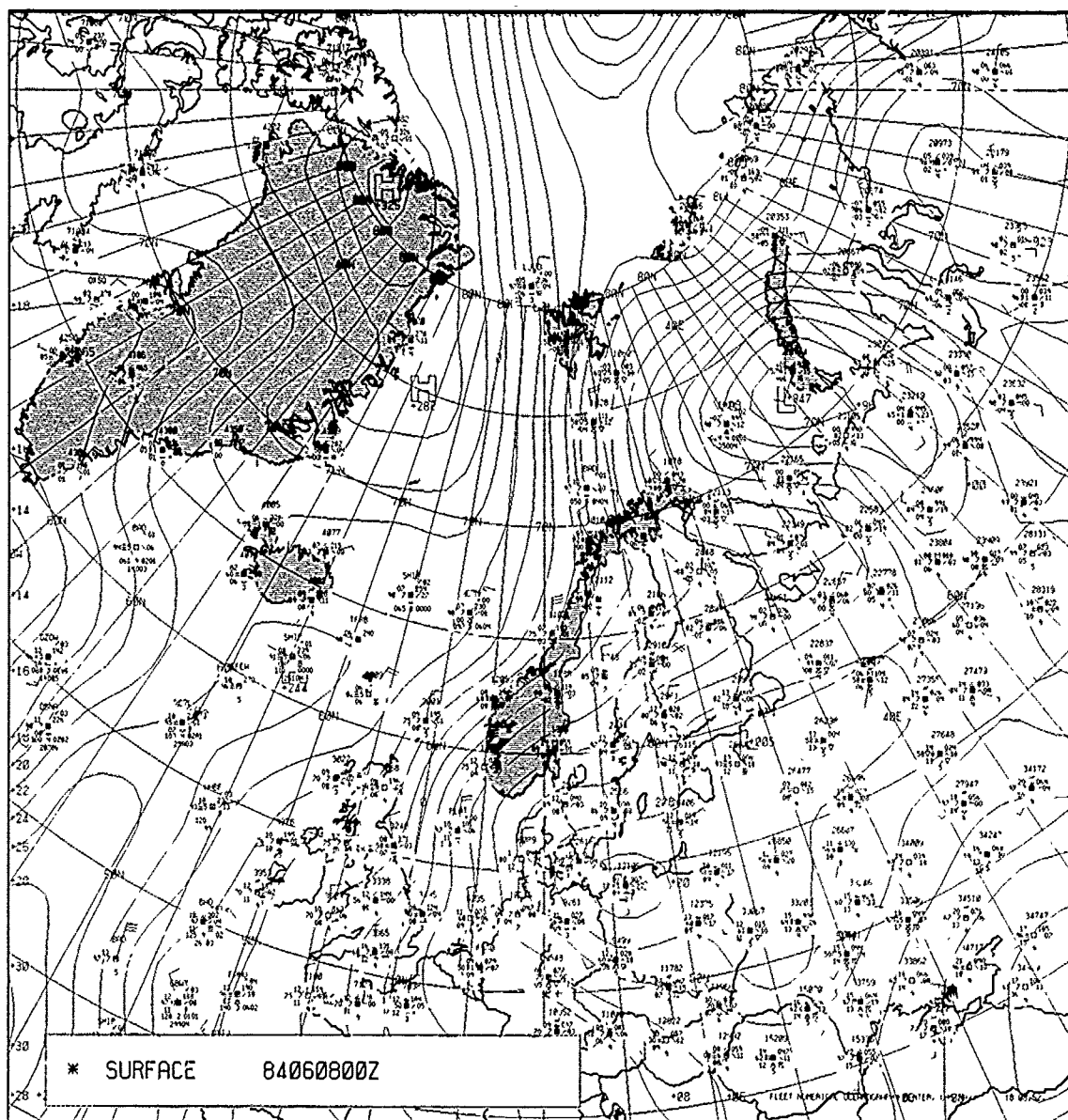
2A-130a. FNOC Surface Analysis. 0000 GMT 7 June 1984.



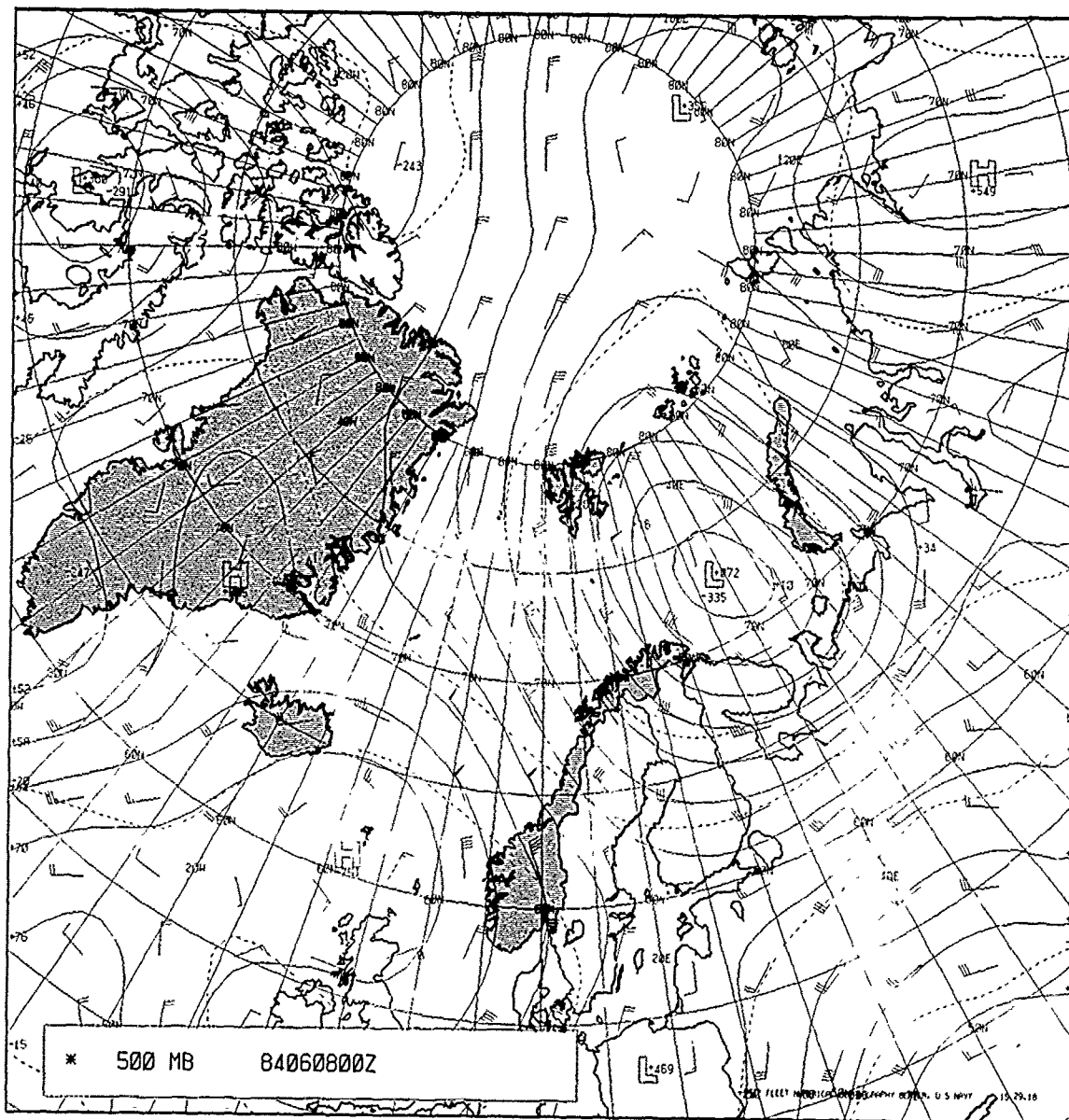
2A-131b. FNOC 500-mb Analysis. 1200 GMT 7 June 1984.



2A-131a. FNOG Surface Analysis. 1200 GMT 7 June 1984.

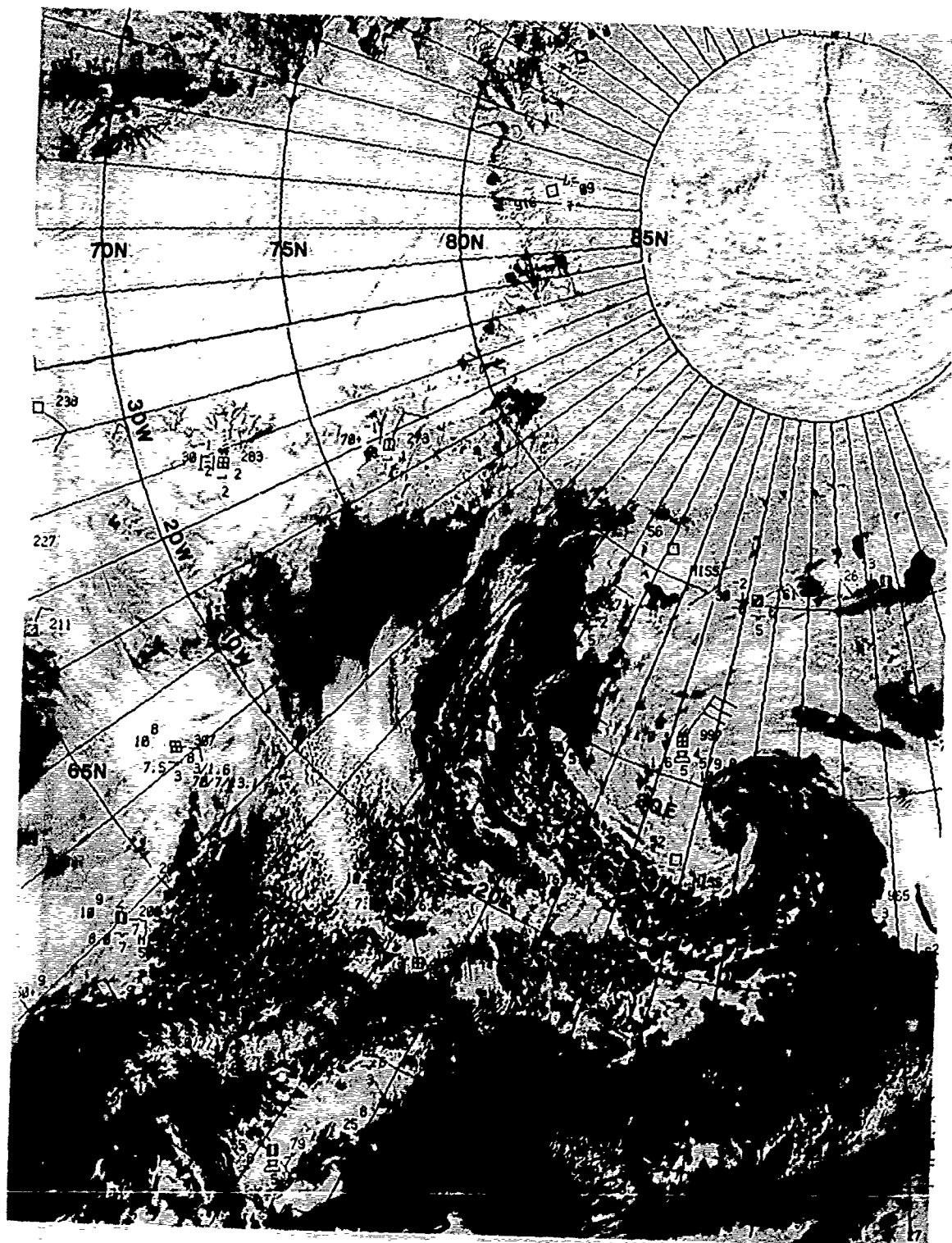


2A-132a. FNOC Surface Analysis. 0000 GMT 8 June 1984.



2A-133a. FNOC 500-mb Analysis. 0000 GMT 8 June 1984.





2A-134a. DMSP Infrared (TS) Data. 0659 GMT 8 June 1984.



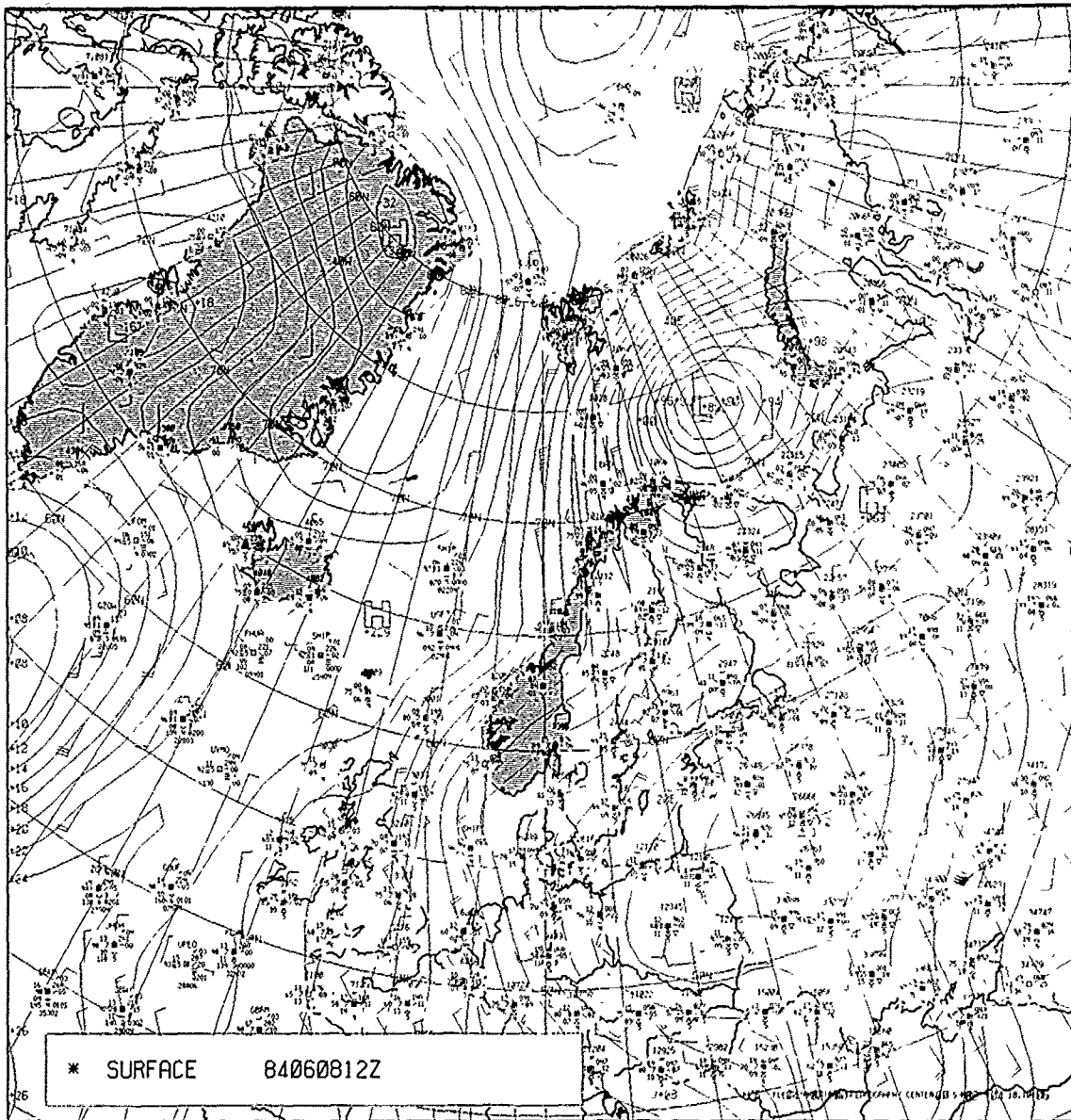
Satellite data at 0659 GMT (Fig. 2A-134a), however, confirm such development. A tight spiral low with its center near 74°N 38°E indicates strong (probably greater than 50 kt) winds exist in a small area within a couple of degrees of the storm center. The 1200 GMT surface analysis (Fig. 2A-135a) now shows a center very near the satellite position and with a central pressure dropping to 989.2 mb. Unfortunately no ships are in the region to confirm the storm's central intensity. At 500 mb (Fig. 2A-136a) the low is shown to be maintained, covering most of the region between Greenland and Russia.

#### *9 June 1984*

A final view of the storm as it moved on-shore over northern Norway is shown in Fig. 2A-137a. The storm at this time is breaking up due to loss of heat flux from the sea and impact with mountainous terrain. Nevertheless 0600 GMT surface reports superimposed on the image still indicate that at least one station within the storm's circulation is reporting sustained winds of 40 kt. The storm is therefore a major event to the north coast of Norway and the adjacent region of Finland and Russia's Kola Peninsula. The storm would have had a serious impact on any naval operation within the area as it approached and moved on through.

#### **Important Conclusions**

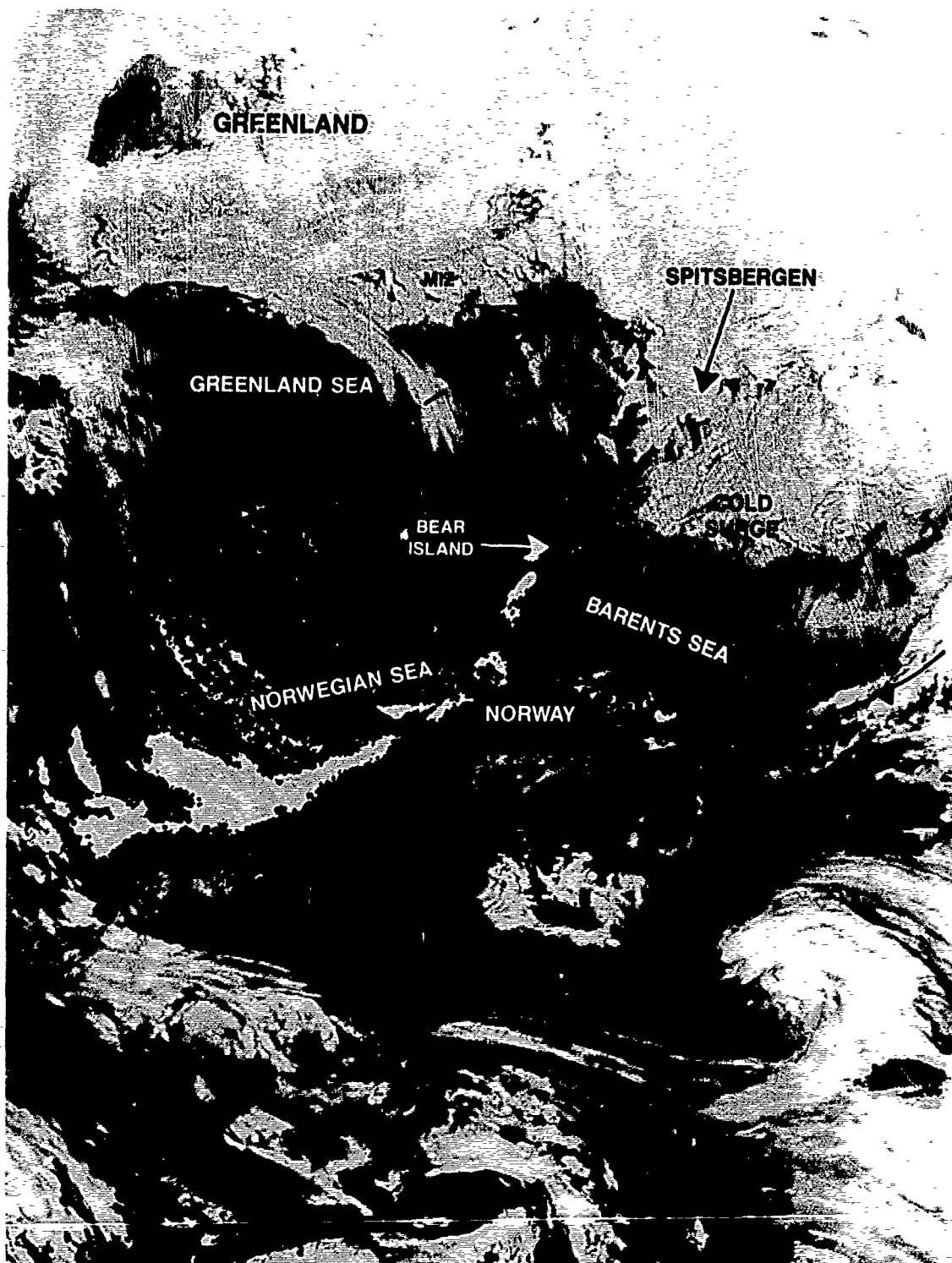
1. The track of this storm was interesting in that it moved southward from near the North Pole to northern Norway. Definition of the system was quite good in the FNOC surface and 500-mb analyses, except at the most important time—when polar low evolution was occurring within the larger scale circulation as the system moved southward from off the ice pack into the relatively warm waters of the Barents Sea.
2. The key to predicting polar low evolution could be found in satellite data 24 hr in advance as heavy convective cells were noted adjacent to a heavy convective band over the Barents Sea on 7 June (Fig. 2A-128a).



2A-135a. FNOC Surface Analysis. 1200 GMT 8 June 1984







2A-138a. DMSP Infrared (TS) Data: 0302 GMT 19 December 1983.

## *Case 6 Polar Low Development From a Cold Surge in the Fram Strait (19-23 December 1983)*

*19 December 1983*

A DMSP infrared (TS) enhanced view of the region of the Greenland, Norwegian, and Barents Seas at 0302 GMT is shown in Fig. 2A-138a. A cold surge in progress is evident over the Barents Sea. This activity would suggest the presence of an arctic front at its leading edge as shown.

A series of vortices in low stratus cloudiness over the Fram Strait indicate the presence of a BLF moving westward toward the marginal ice zone of Greenland. This movement normally implies the anticyclonic flow depicted east of the BLF.

A gridded version of the image is shown in Fig. 2A-139a for comparison. The grid fits quite well in the northern portion. Polynya effects in the lee of some of the islands are of interest.

The FNOC surface analysis at 0600 GMT (Fig. 2A-140a) provides verification of the northerly surge across the Barents Sea. An arctic front could be positioned as shown. Note, however, that the temperatures of the arctic air have been considerably modified as indicated by observations along the north coast of Norway, due to the passage of air over the relatively warm water of the Barents Sea—thus conditions inland ahead of the front are colder than along the coast.

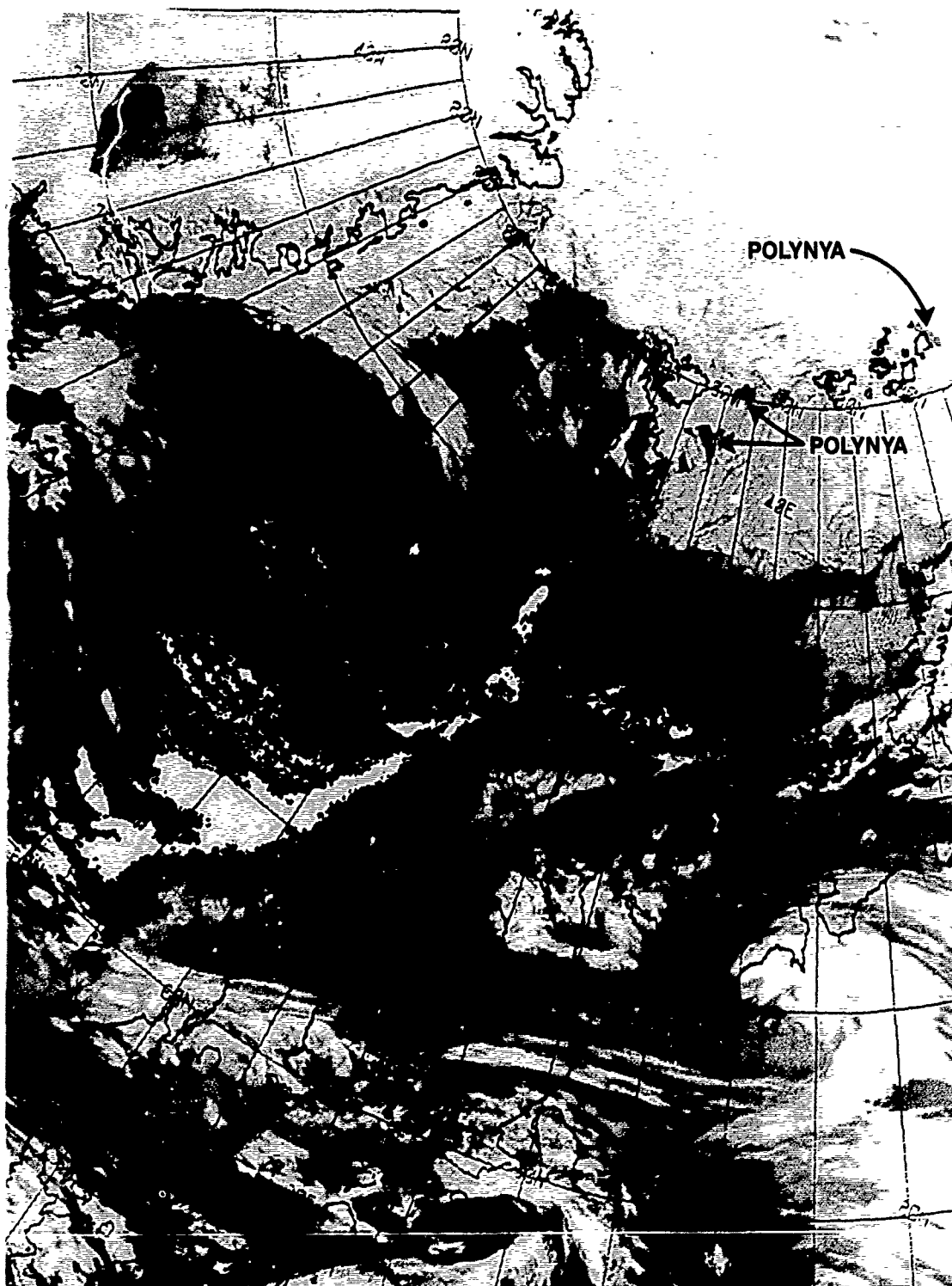
The high pressure shown in the Fram Strait is not inconsistent with the anticyclonic flow over that region indicated in Fig. 2A-138a. Observations are too sparse, however, to indicate the BLF trough. This must be inferred from the satellite data.

By 1700 GMT DMSP data (not shown) indicated that a cold surge had commenced within the Fram Strait. This development is verified by the FNOC surface analysis for 1800 GMT (Fig. 2A-141a) and a DMSP infrared (TS) view at 1905 GMT (Fig. 2A-142a), where north/south-oriented cloud lines can be seen over the Fram Strait between Spitsbergen and the Greenland MIZ. The cold surge apparently commenced as the high pressure cell near the Fram Strait (Fig. 2A-140a) moved westward (Fig. 2A-141a) and the pressure gradient over the Fram Strait intensified.

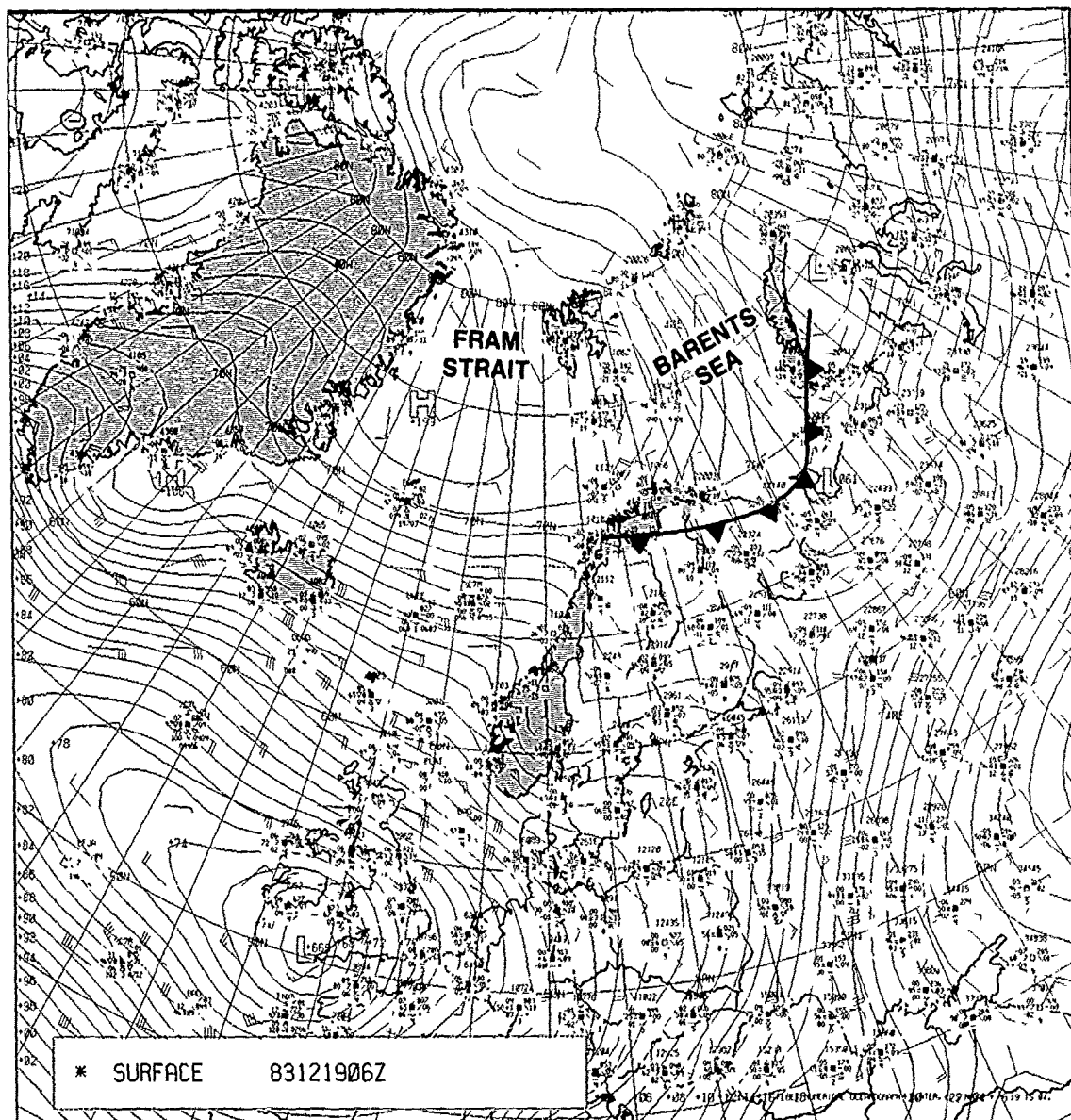
A DMSP infrared (TS) view of the region at 2137 GMT (Fig. 2A-143a) reveals the surge more clearly and shows the typical BLF appearing at the leading edge of the cold surge as an enhanced cumulus cloud line. It is along this cloud line that multiple vortices are noted to develop (one seems to be evident in this image near the southwestern tip of Spitsbergen). Such vortices usually are weak and undergo no significant development of operational importance. When upper level conditions show a cold low or trough moving over the region, however, intense development and polar low genesis are often observed.

*20/21 December 1983*

The FNOC 500-mb chart series starting at 0000 GMT 20 December and ending on 21 December at 1200 GMT (Figs. 2A-144a to 2A-147a) reveal the movement of a cold upper level trough drifting southward over the Fram Strait during this period.

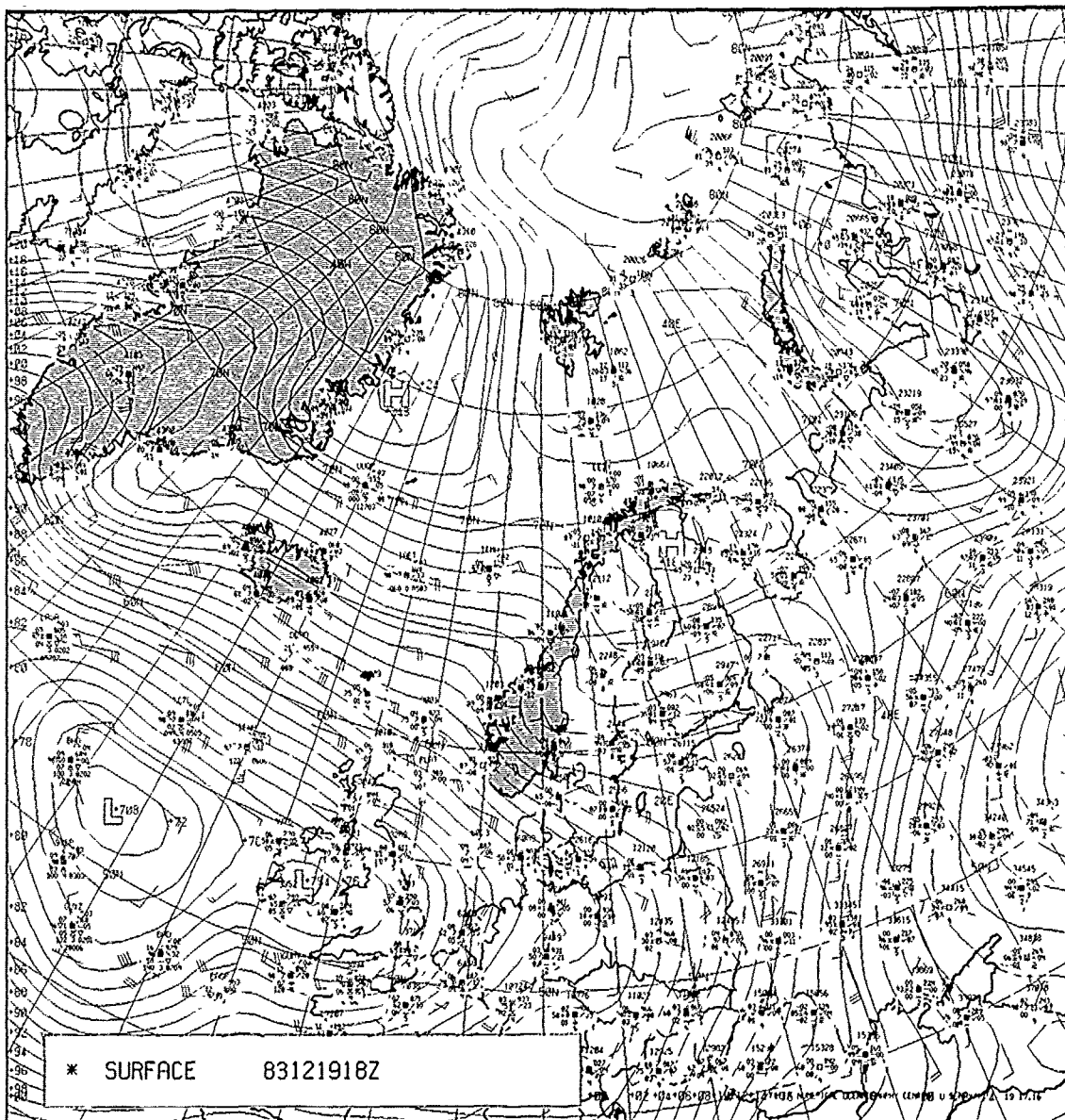


2A-139a. Gridded DMSP Infrared (TS) Data: 0302 GMT 19 December 1983.

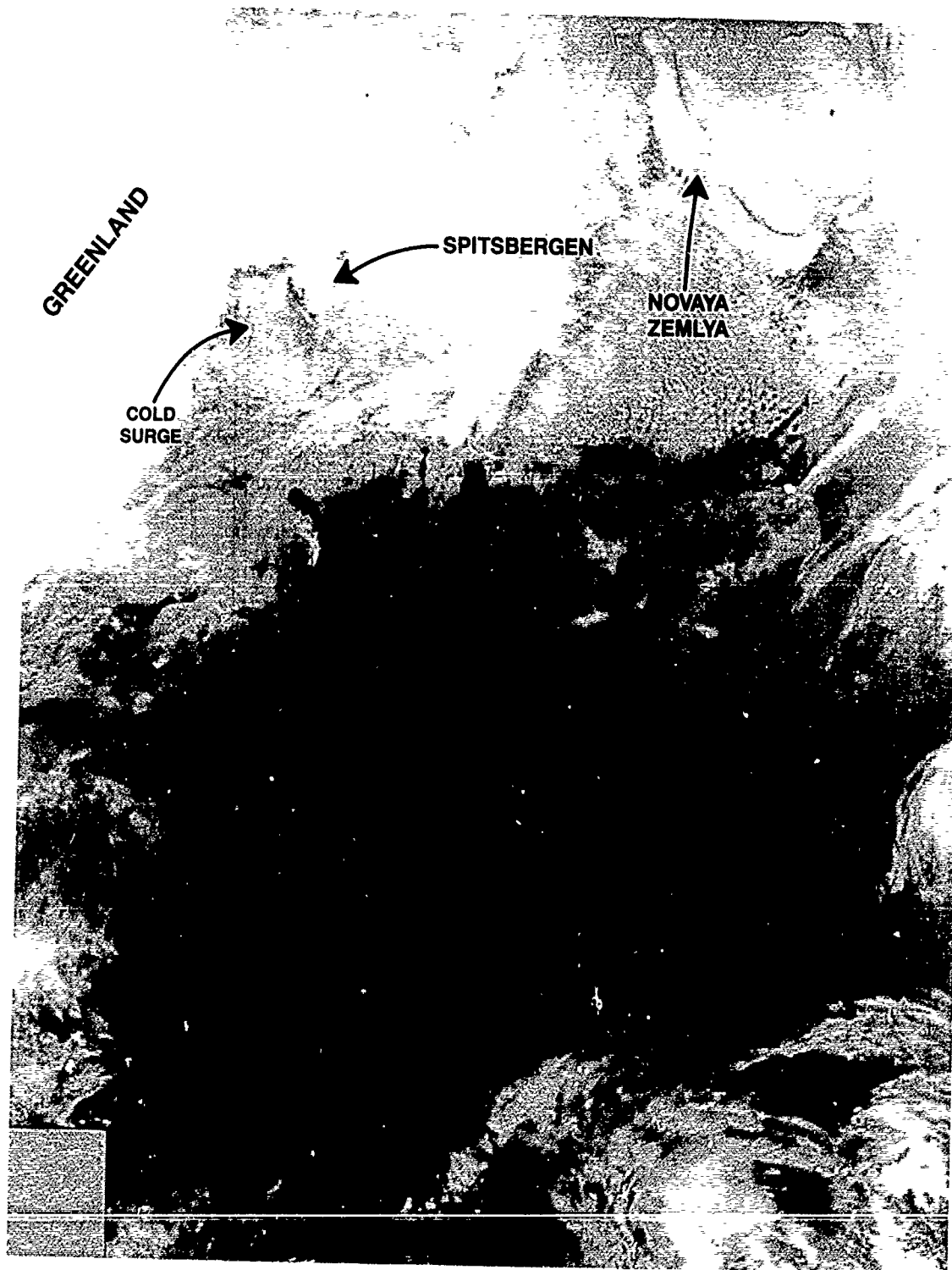


2A-140a. FNOC Surface Analysis. 0600 GMT 19 December 1983.





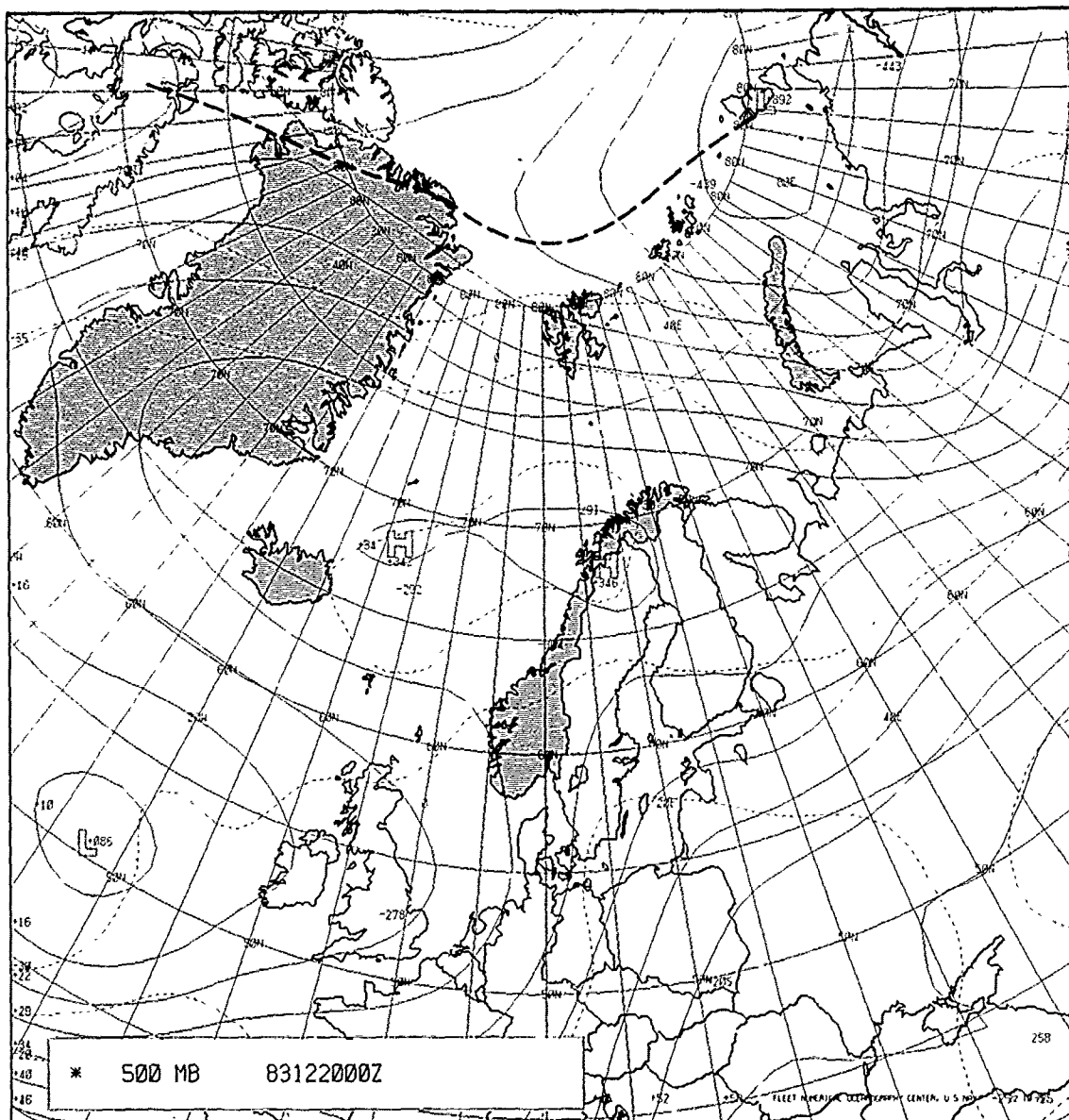
2A-141a. FNOC Surface Analysis, 1800 GMT 19 December 1983.



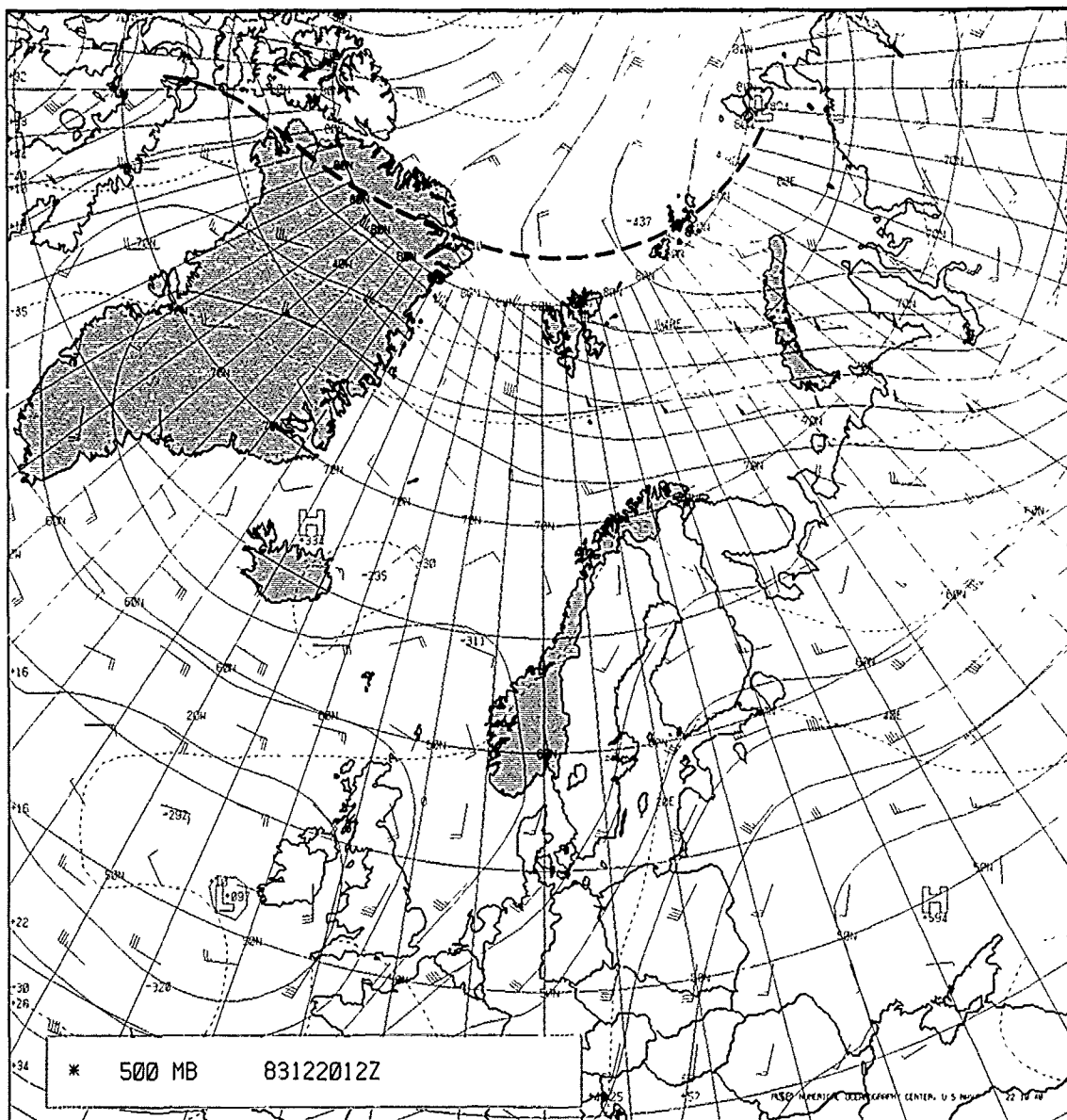
2A-142a. DMSP Infrared (TS) Data. 1905 GMT 19 December 1983.



2A-143a. DMSP Infrared (TS) Data. 2137 GMT 19 December 1983.

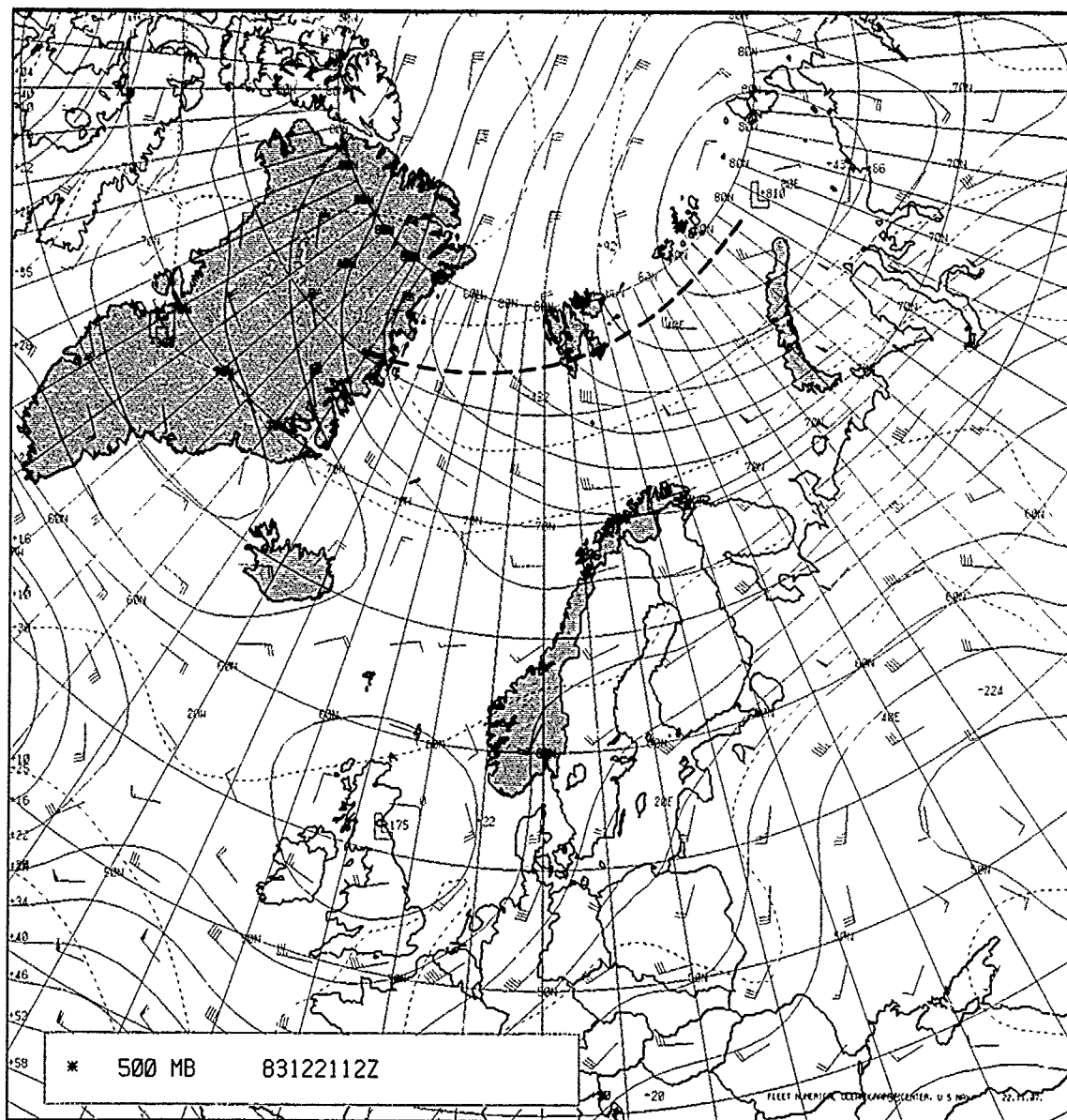


2A-144a. FNOC 500-mb Analysis. 0000 GMT 20 December 1983.



2A-145a. FNOC 500-mb Analysis. 1200 GMT 20 December 1983.





2A-147a. FNOC 500-mb Analysis, 1200 GMT 21 December 1983.





The FNOC surface analyses for the same time series (Figs. 2A-148a to 2A-151a) begin by showing continued northerly flow through the Fram Strait (Fig. 2A-148a). Note, however, that the analysis of Fig. 2A-148a has been made without benefit of a weather observation from Jan Mayen Island (70.09°N 8.7°W). The Jan Mayen observation has been plotted and shows a northwest wind of about 3 kt and a pressure of 1018.2 mb. The 1018.2 mb pressure is about 4 mb less than the analyzed 1022-mb isobar passing over the station. Twelve hours later the 1200 GMT analysis (Fig. 2A-149a) ignores a ship located near 76°N, 0°, which reports a southeast wind of 30 kt and a pressure of 985.2 mb. The report was considered poor. Jan Mayen (not plotted) was reporting a north-northwest wind of 10 kt at the same time. Together the two station reports would suggest low pressure between the two stations. Continued strange discrepancies include a ship report near Jan Mayen on 21 December 0000 GMT analysis (Fig. 2A-150a) showing a north-northwest wind perpendicular to the analyzed gradient. This discrepancy continued to the 1200 GMT analysis (Fig. 2A-151a) where Jan Mayen (not plotted on the original analysis) is reporting a northwest wind at 25 kt while the ship (UUOR) was reporting a north wind at 15 kt, again at a large angle to the isobars. Jan Mayen and the ship indicated falling 3-hr pressure tendencies of  $-1.2$  and  $-2.9$  mb, respectively, indicative of approaching low pressure.

The satellite data provide evidence to resolve what was really happening. DMSP nighttime visual data on 19 December at 2318 GMT (Fig. 2A-152a) reveal the cold surge and BLF in excellent detail. Near the BLF on the north side open celled stratocumulus suddenly change to overcast stratiform, indicating a sudden sharp anticyclonic turning of the wind from northerly to northeasterly. Winds would be expected to turn again northerly at the frontal boundary to provide the maximization of cyclonic vorticity concentrated along this line.

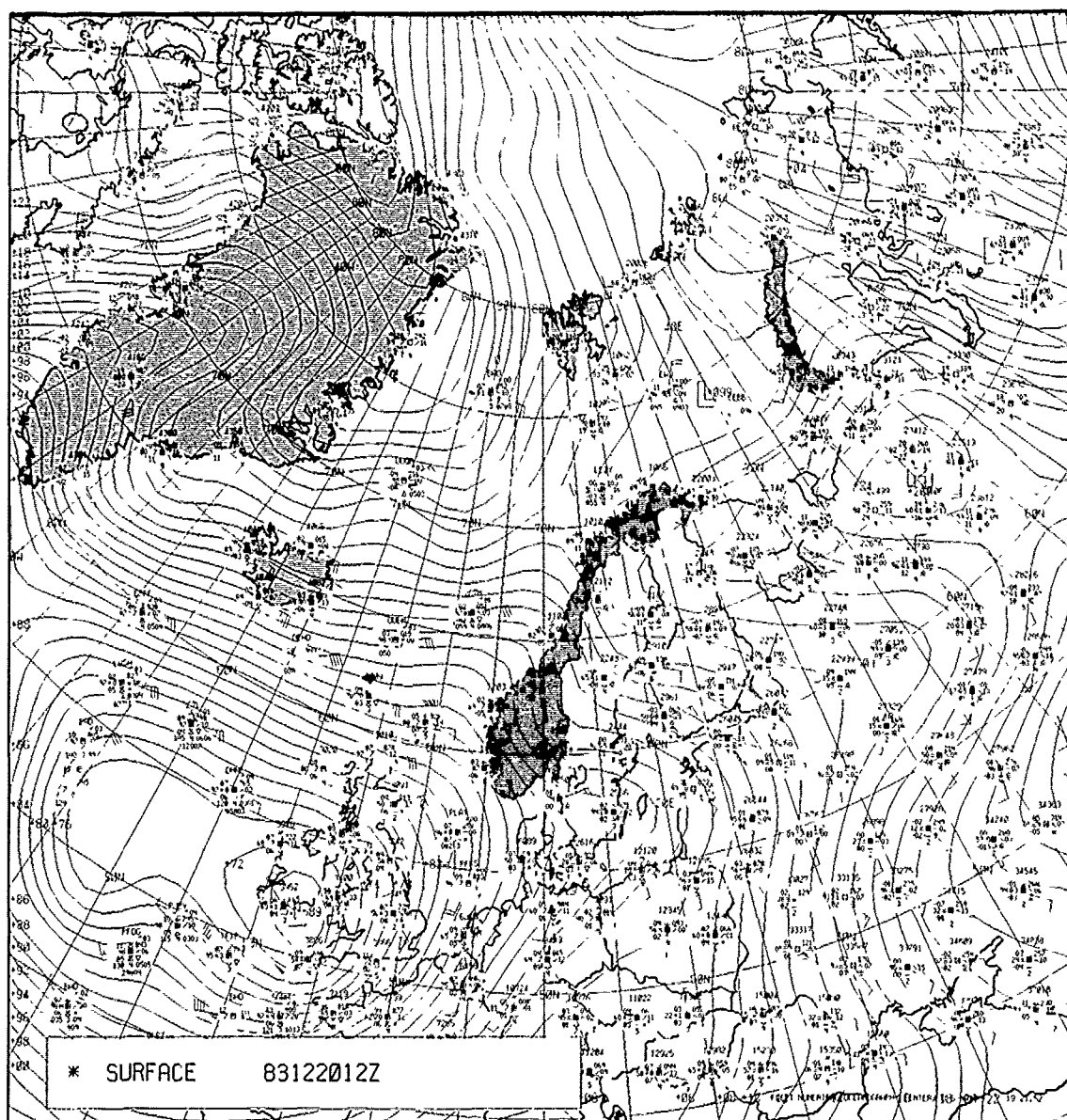
By 20 December at 0100 GMT, in DMSP enhanced infrared (TS) data (Fig. 2A-153a), the overcast cloudy region seems to enlarge and it is difficult to locate the exact position of the BLF itself.

Good quality DMSP infrared data were not available until nearly 19 hr later when a pass at 1844 GMT (Fig. 2A-154a) revealed a large vortex at the position of the BLF. A gridded version of the image (Fig. 2A-155a), with superimposed wind observations from the FNOC analyses for 20 December 1200 GMT (Fig. 2A-149a) and from Jan Mayen for 1800 GMT, suggests an appreciable and probably moderately intense vortex with the center at point X (Fig. 2A-155a) between the two observations.

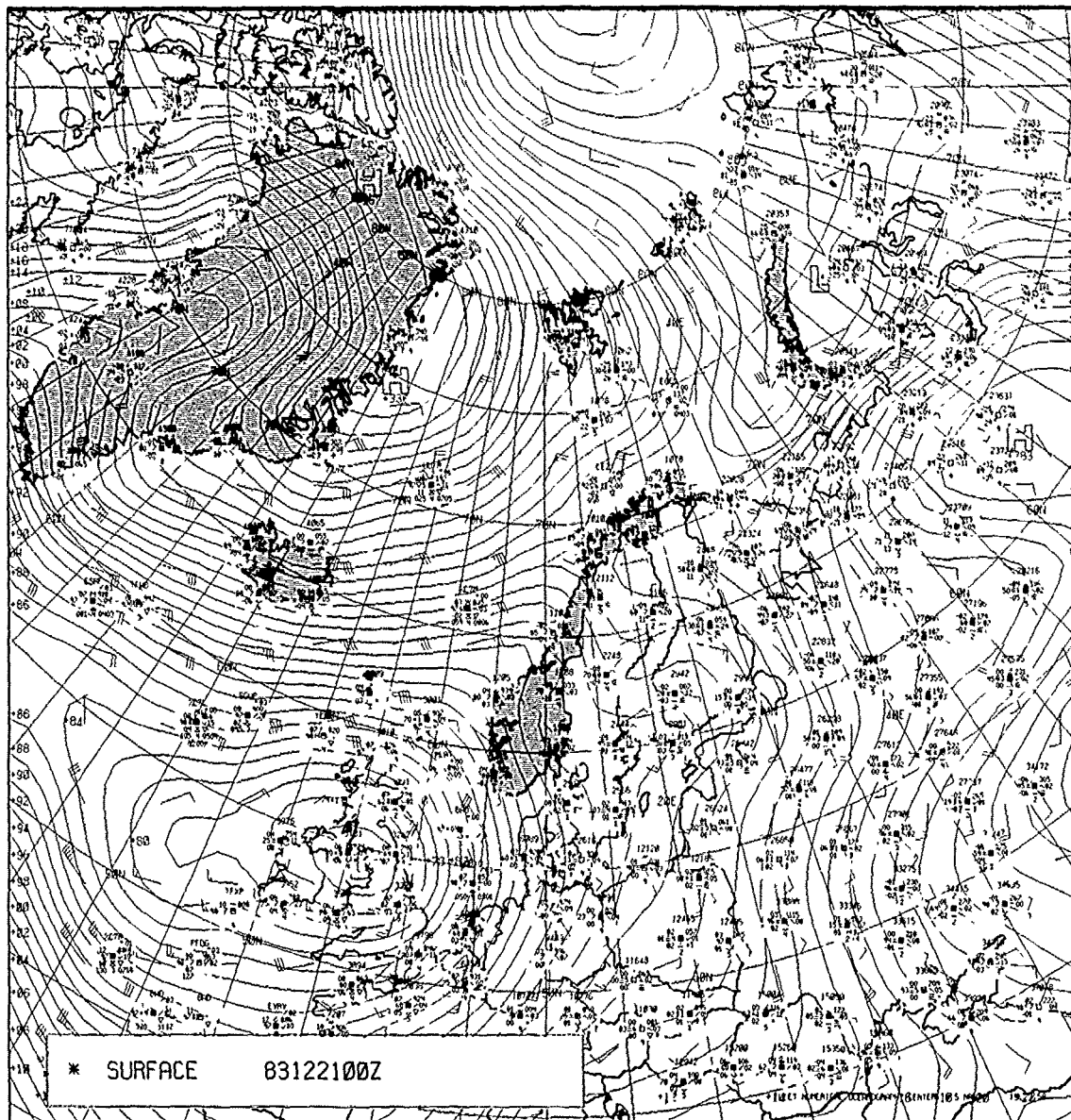
The vortex appears with greater clarity at 2025 GMT in a DMSP nighttime visual depiction (Fig. 2A-156a). In this image the strong anticyclonic-turning of the winds near the outer edge of the vortex is clearly depicted by the curvature of cloud streets in the region. A wake effect in the southward lee of Jan Mayen Island indicates northerly low-level flow at that location in agreement with the nearby ship observation shown in Fig. 2A-150a. The position of the 500-mb trough has also been superimposed on this image. It can be seen that development is occurring in advance of this trough in a region of positive vorticity advection.

There is also a suggestion in this image that the BLF in the region east of the vortex has moved independently southward, and that minor vortex developments are occurring in that region.

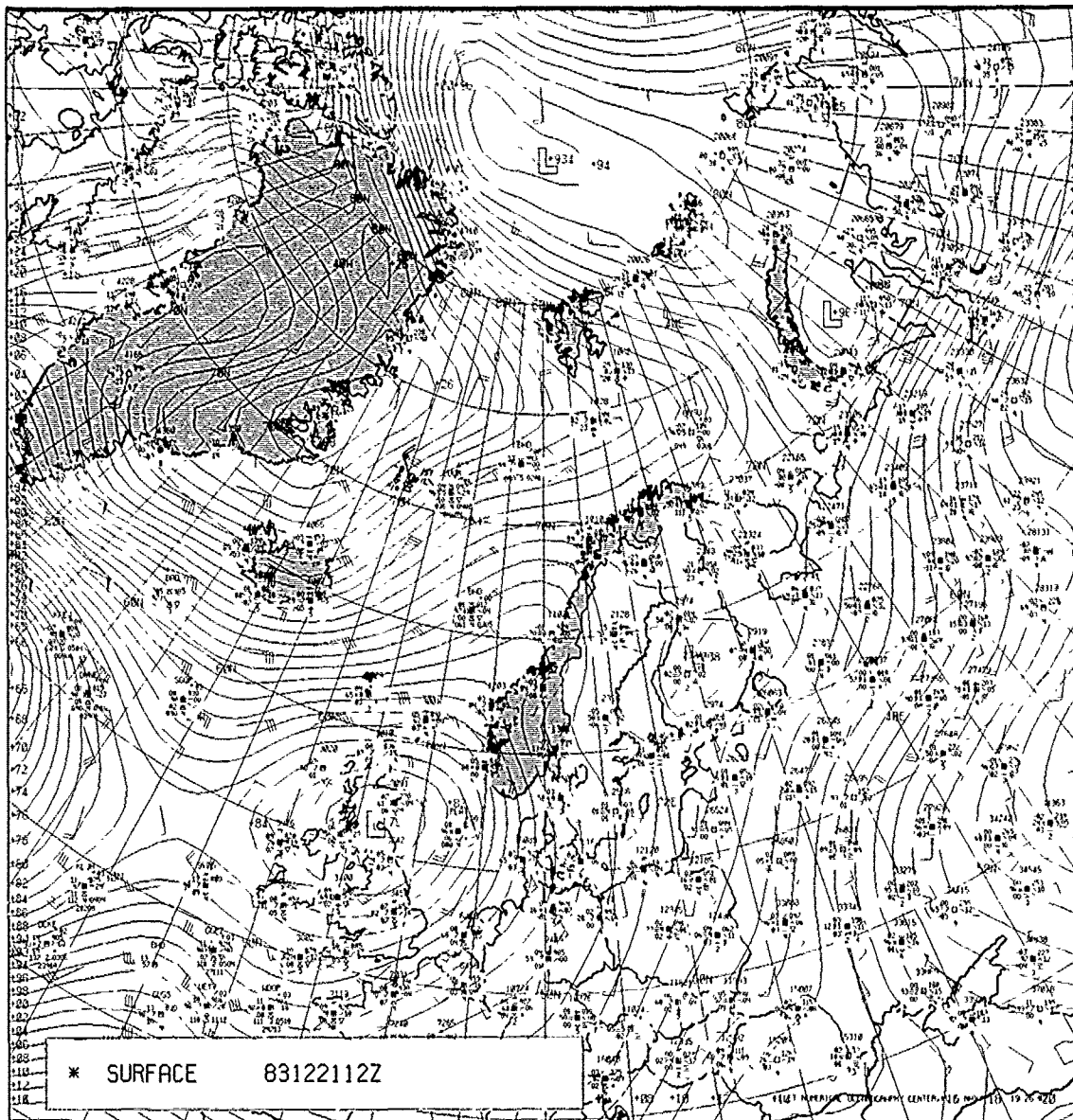
This suggestion is verified by the appearance of a well-defined small-scale vortex in DMSP infrared (TS) acquired at 2116 GMT (Fig. 2A-157a). The major vortex is not well developed through the middle troposphere at this time as can be seen by the relatively warm temperatures of the overlying cloudiness.



2A-149a. FNOC Surface Analysis. 1200 GMT 20 December 1983



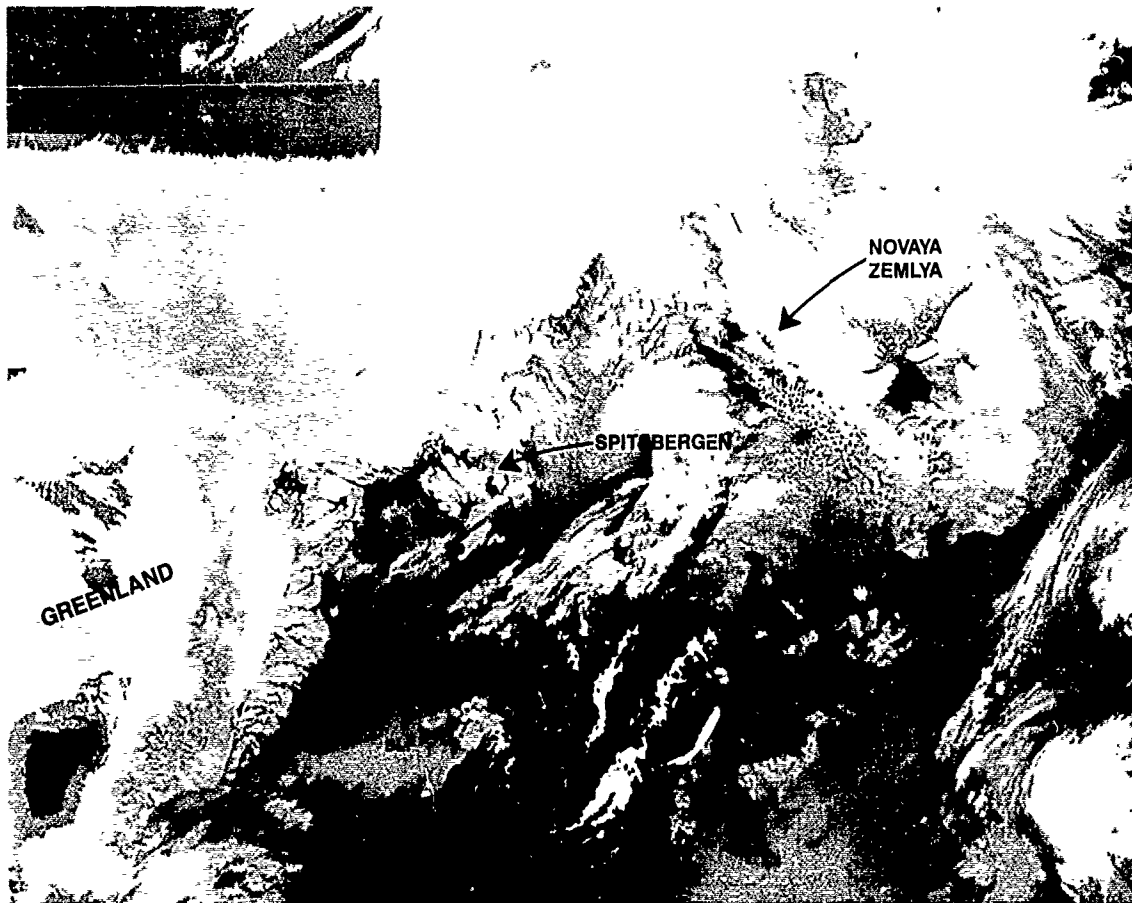
2A-150a. FNOC Surface Analysis. 0000 GMT 21 December 1983.



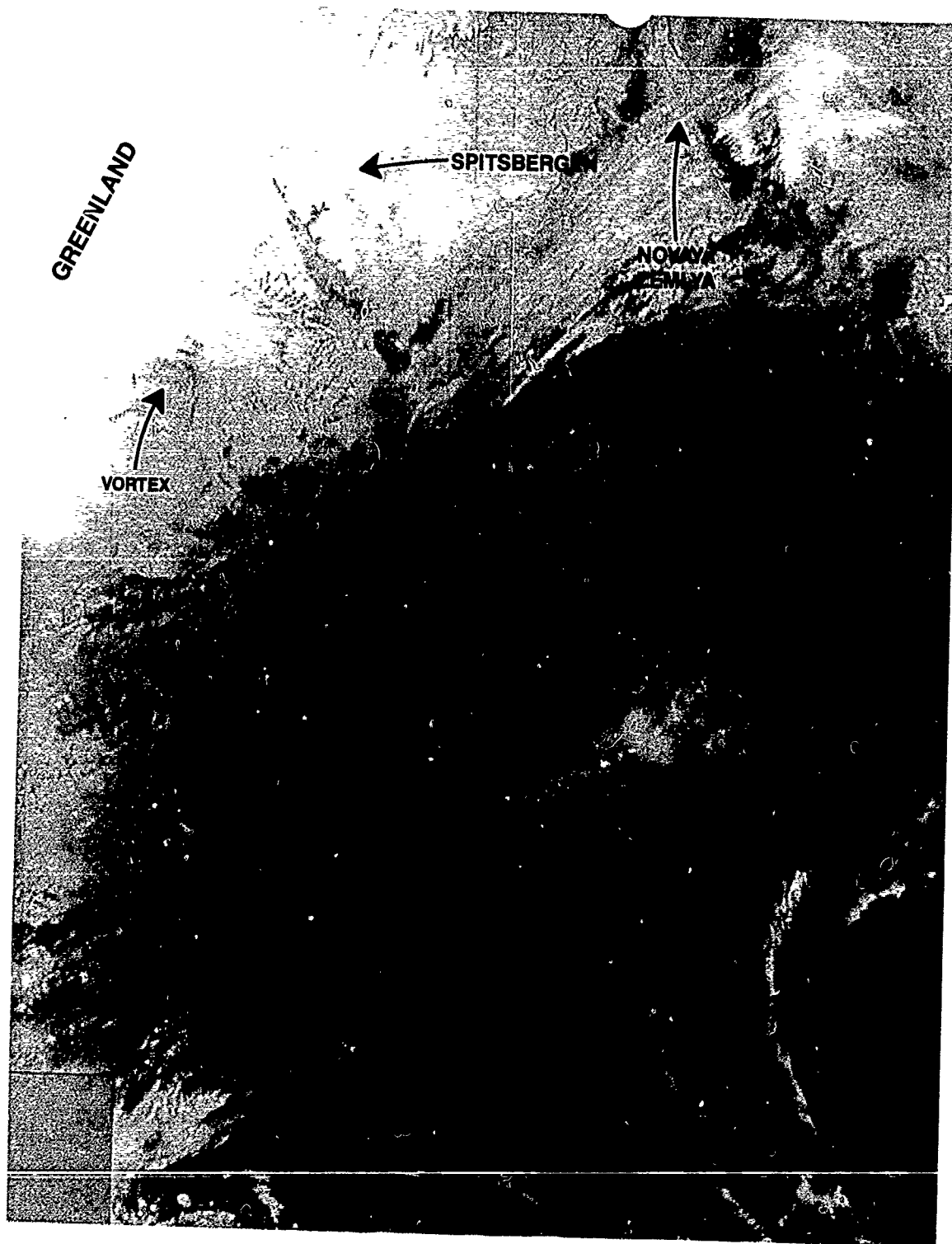
2A-151a. FNOC Surface Analysis. 1200 GMT 21 December 1983.



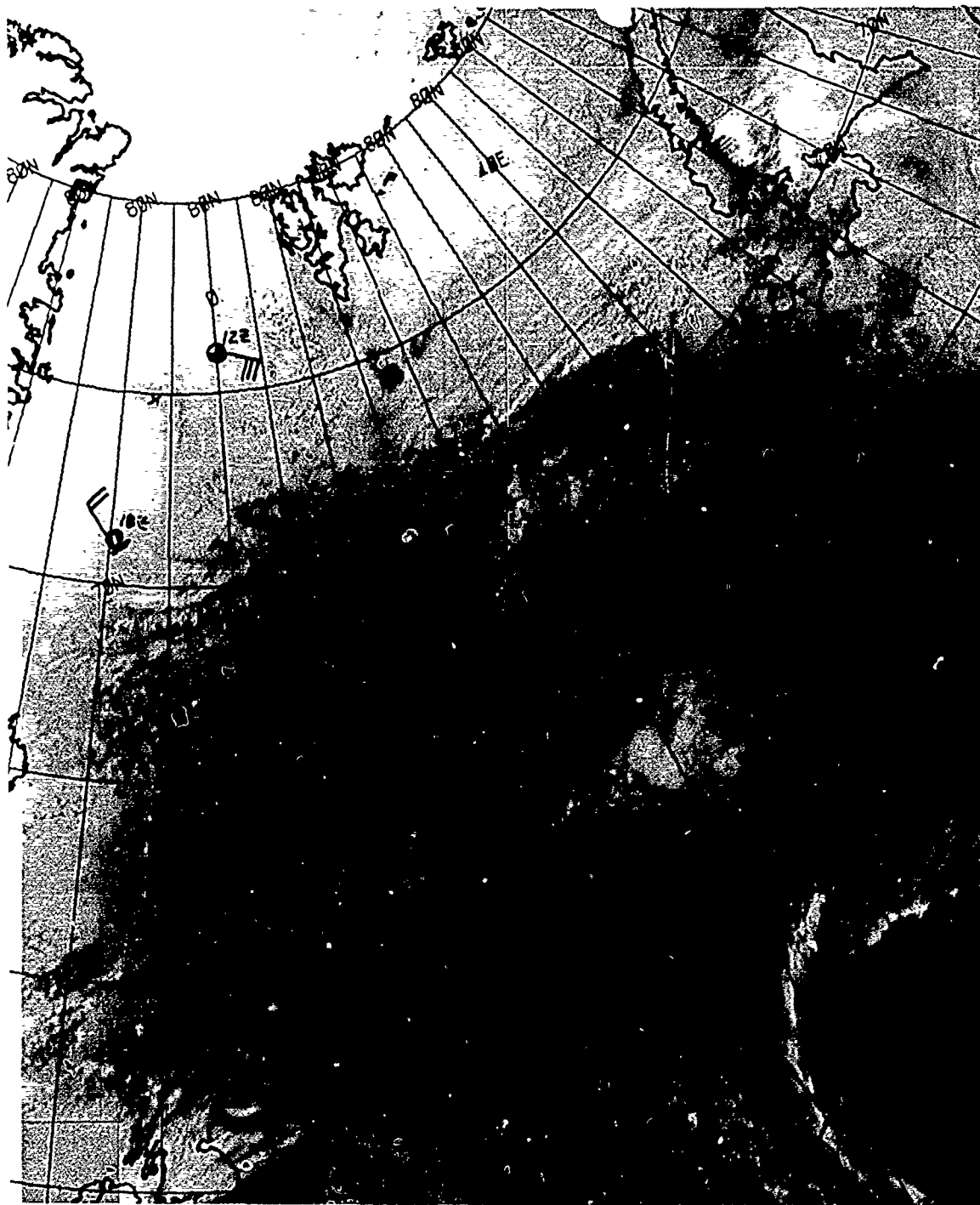
2A-152a. DMSP Nighttime Visual (LS) Data, 2318 GMT 19 December 1983.



2A-153a. DMSP Enhanced Infrared (TS) Data. 0100 GMT 20 December 1983

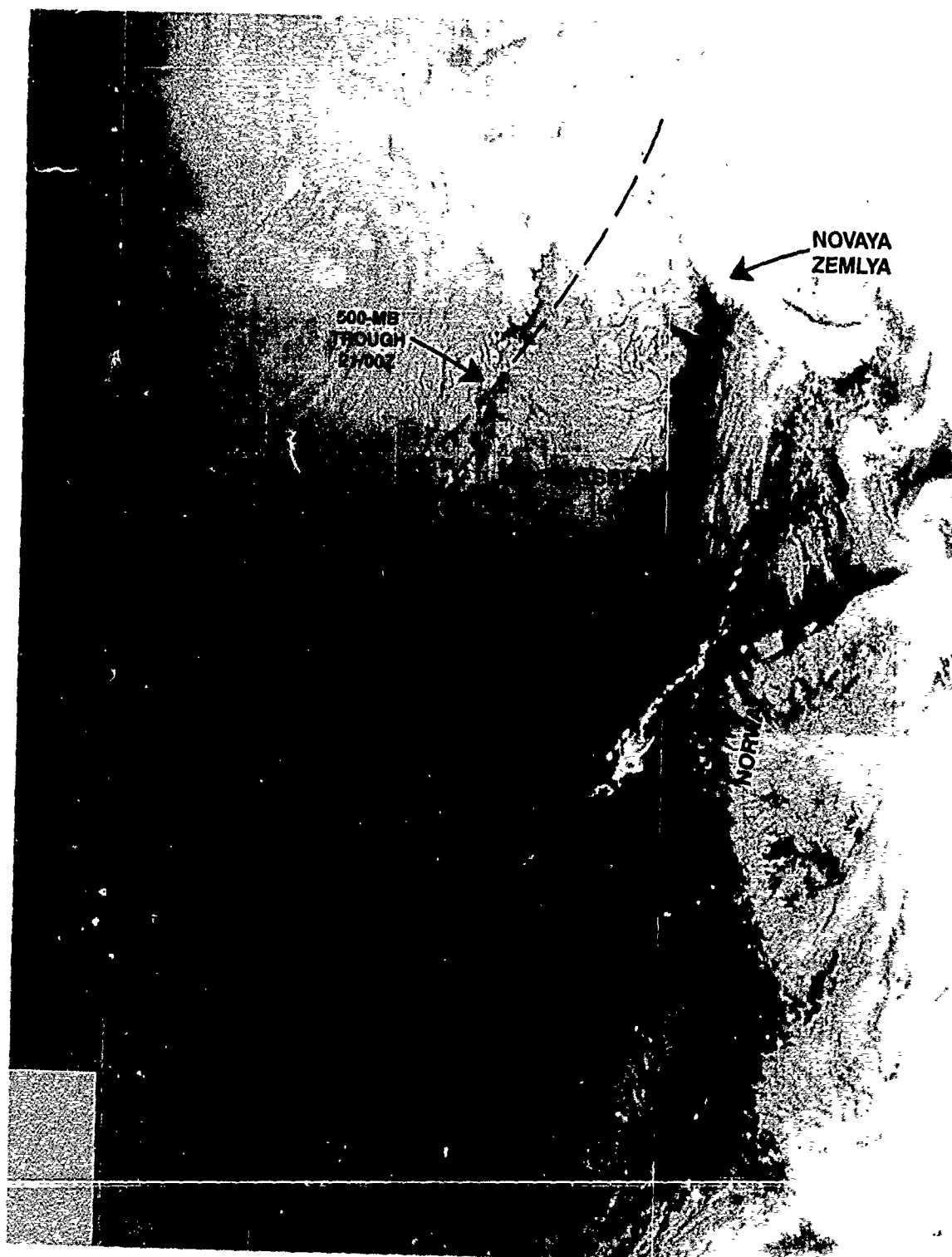


2A-154a DMSP Infrared (TS) Data 1844 GMT 20 December 1983.

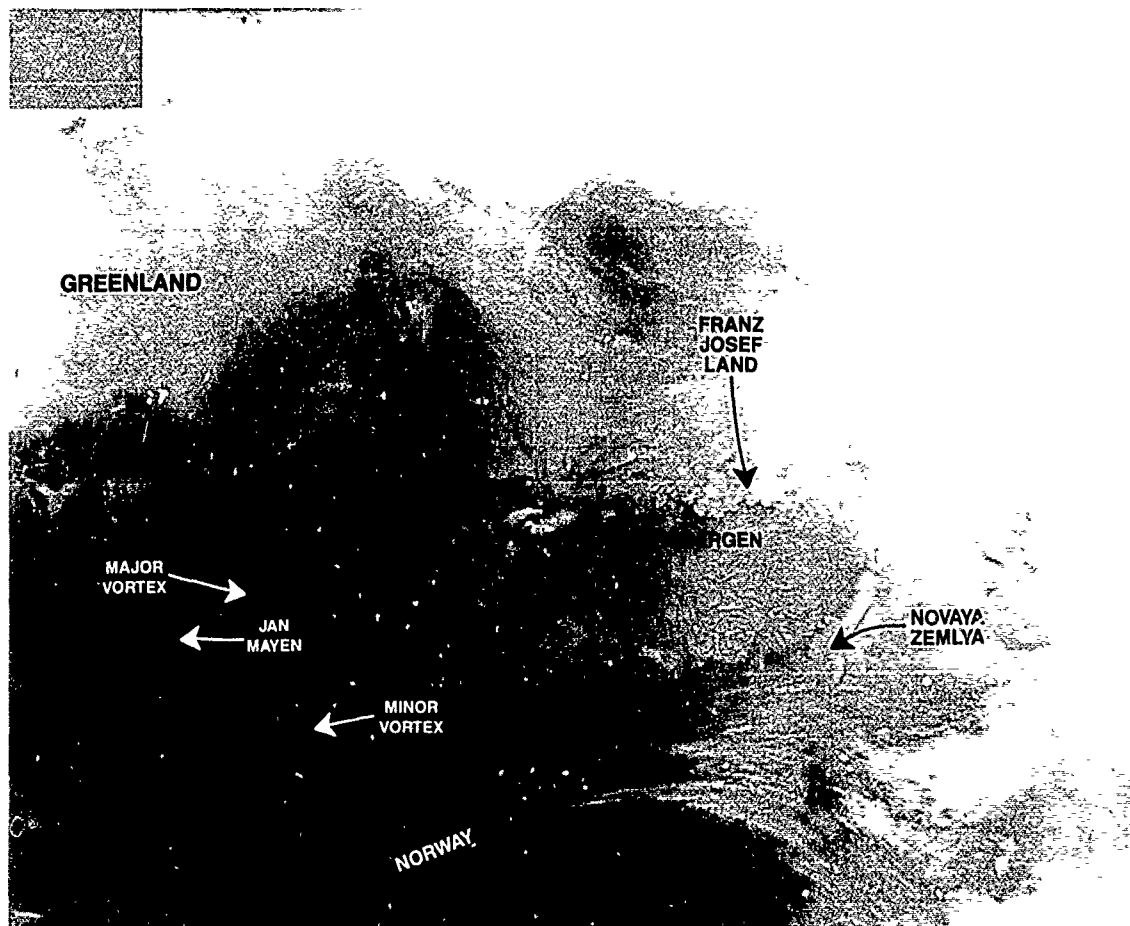


2A-155a. Gridded DMSP Infrared (TS) Data 1844 GMT 20 December 1983.





2A-156a, DMSP Nighttime Visual (LS) Data. 2025 GMT 20 December 1985



2A-157a. DMSP Infrared (TS) Data 2116 GMT 20 December 1983



2A-158a. DMSP Infrared (TS) Data. 0038 GMT 21 December 1983.

The storm seems to undergo further development a few hours later on 21 December, however, as DMSP infrared (TS) enhanced imagery at 0038 GMT (Fig. 2A-158a) reveals a much colder cloud deck associated with the vortex. The circulation about the vortex center cannot be extensive since Jan Mayen, based on DMSP infrared (TS) enhanced data at 0220 GMT (Fig. 2A-159a), continues to show lee effects to the south, indicative of northerly low-level flow. This relates well to the northerly winds shown near Jan Mayen on the 0000 GMT 21 December surface analysis (Fig. 2A-150a) and proves that the FNOC analysis in this region is inaccurate.

At 0401 GMT DMSP visible nighttime (LS) data (Fig. 2A-160a) reveal little apparent intensification of the major vortex as the northerly low-level flow continues to be in evidence past Jan Mayen, where a well-developed field of Von Karmen vortices is evident to the southward lee.

Two secondary vortices have developed on the BLF east of the major vortex, which is north of Jan Mayen Island. This is an interesting and apparently not atypical development (see Cases 2-4 in this section). Often multiple development of polar lows occur within a single BLF complex as one vortex intensifies following the sudden "flare-up" and equally sudden decrease in intensity of another. It is not clear from Fig. 2A-160a which, if any, of the vortices is destined to undergo the intensification normally associated with polar lows (i.e., adequate enough to produce winds around the vortex in excess of 50 kt). The westernmost vortex has been labeled "main vortex" because it appears basically larger than the other two (though obviously still weak).

Another point of interest in this figure is the contrast between the size and density of cellular cloud forms in the Barents Sea as opposed to those in the Fram Strait and in the area west of Bear Island. The latter cloud cells are much larger and imply a thicker mixed layer.

The implied low inversion over the Barents Sea is verified by the Bear Island sounding for 0000 GMT 21 December (Fig. 2A-161a). Bear Island is surrounded by ice, as can be seen in Fig. 2A-160a, and is representative of conditions over the ice extending up to Spitsbergen—and more representative of conditions over the Barents Sea than those of the Fram Strait, where a warm branch of the Gulf Stream accentuates atmospheric heating effects and contributes to a deeper mixed layer.

DMSP enhanced infrared (TS) data at 0542 GMT (Fig. 2A-162a) show that a BLF is beginning to move westward in the region just west of Bear Island. The plausibility of such movement is supported by the due easterly winds reported at Bear Island in the FNOC 0600 GMT surface analysis (Fig. 2A-163a). Note also, in the DMSP data, Fig. 2A-162a, that an enhanced cloud line and some suggestion of cloud curvature/vortex development seem to be taking place in the region southwest of Bear Island.

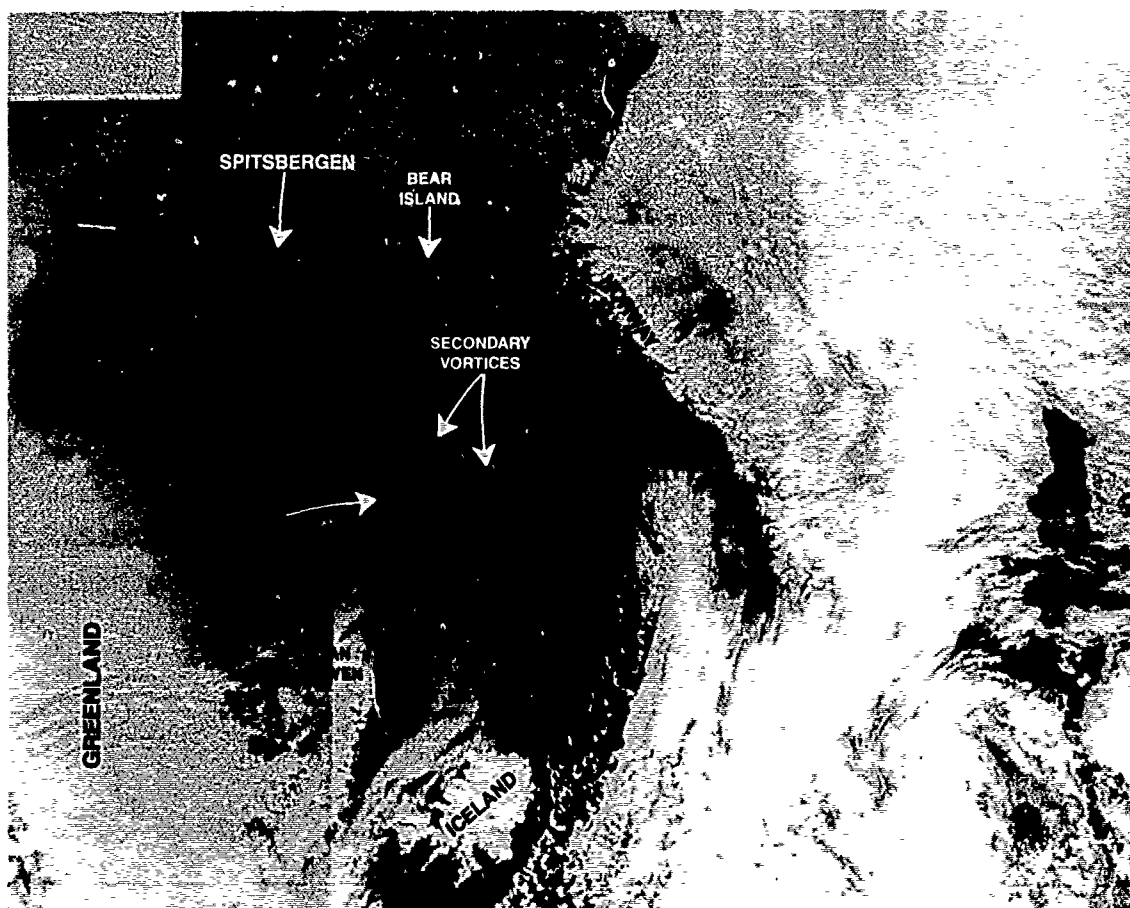
The main cloud system, however, shows little additional development at this time.

About 4.5 hr later a DMSP infrared (TS) mosaic at 1004 GMT 21 December (Fig. 2A-164a) reveals that the major cloud system has apparently intensified and taken on the appearance of a comma cloud often noted during rapid intensification. A comparison of this figure with Fig. 2A-162a shows that the BLF west of Bear Island has moved considerably further to the west following the movement of the comma cloud.

A DMSP nighttime visual (LS) image at 1732 GMT (Fig. 2A-165a) suggests that the system has evolved to polar low status. Winds of 40 to 50 kt would be anticipated under the cloud shield in the northern semicircle of the storm with lesser wind speeds to the south. The existence of a minor vortex in the southeast quadrant of the storm emphasizes the much lighter winds in that region.



2A-159a. DMSP Enhanced Infrared (TS) Data. 0220 GMT 21 December 1983.



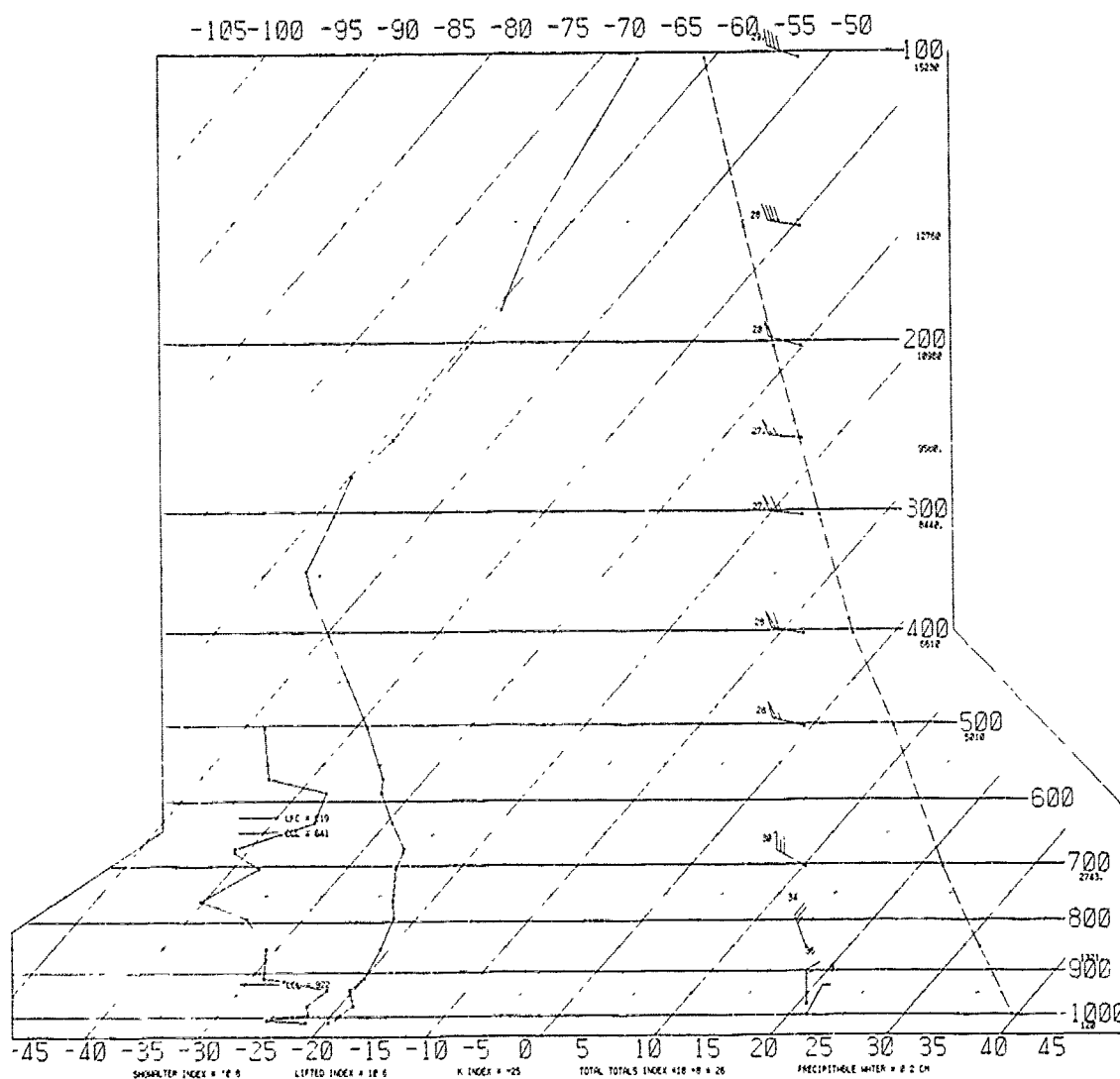
2A-160a. DMSP Nighttime Visual (LS) Data. 0401 GMT 21 December 1983.

# SKREW T. LOG P DIAGRAM

831221

0000Z

1028

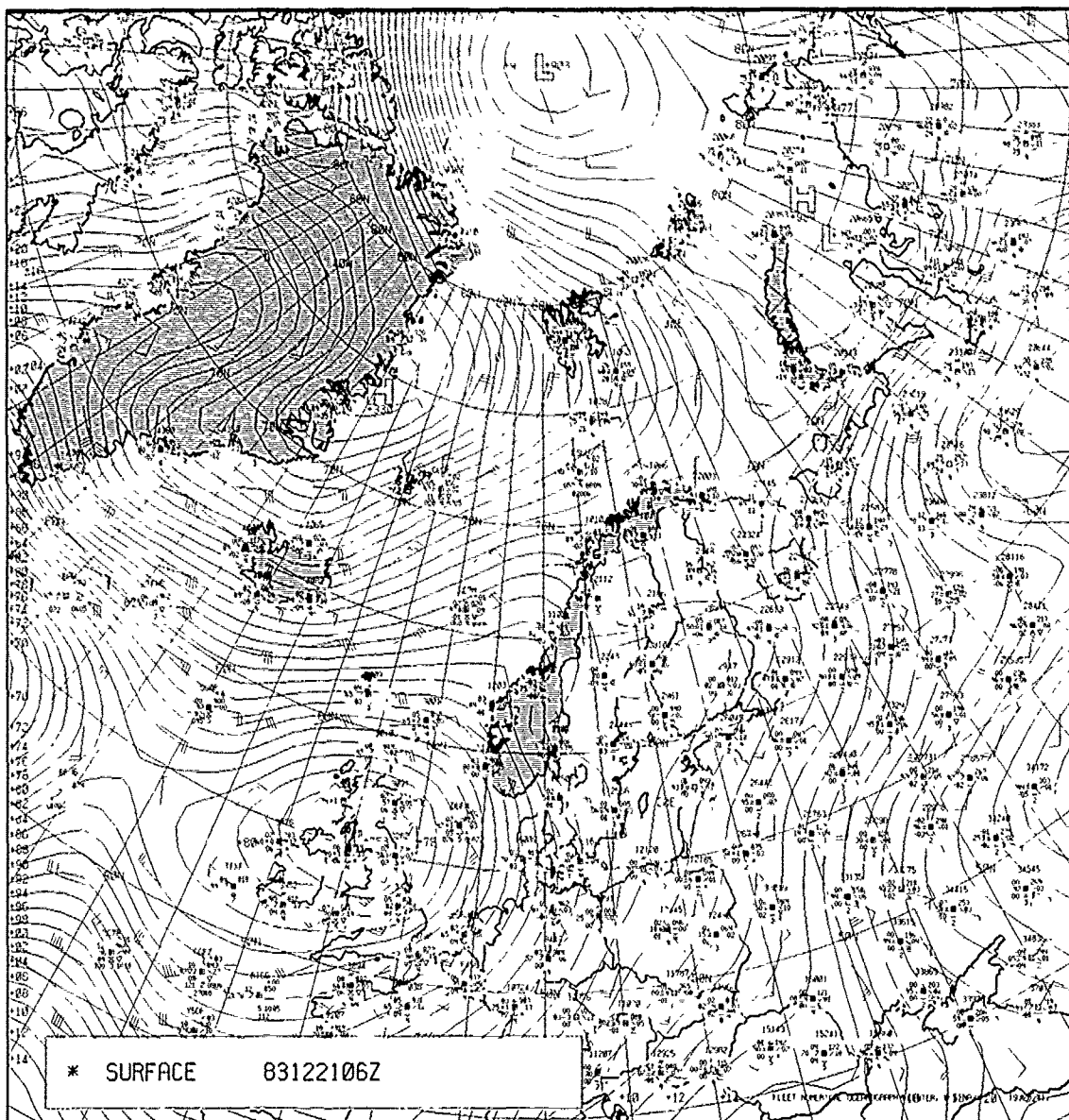


2A-161a. Radiosonde Analysis for Bear Island. 0000 GMT 21 December 1983.

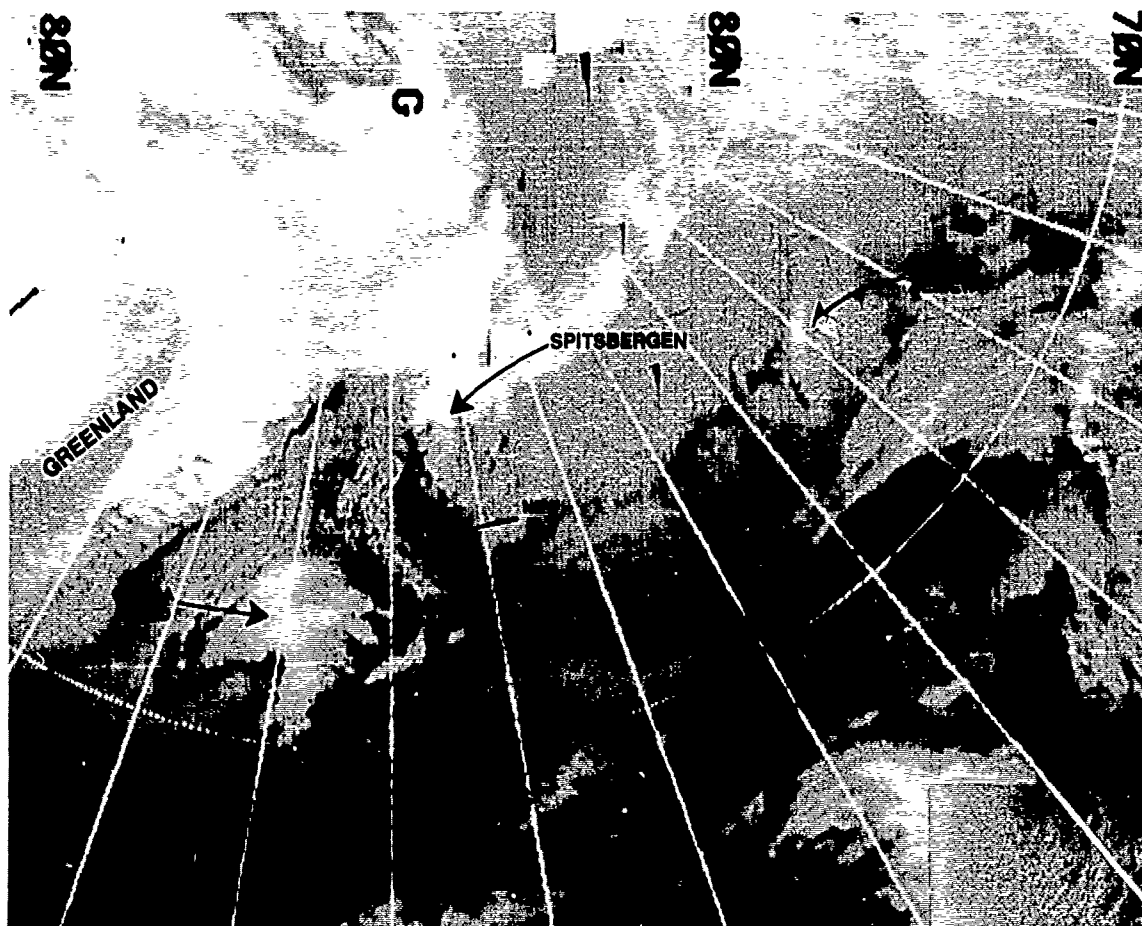


2A-162a. DMSP Enhanced Infrared (TS) Data. 0542 GMT 21 December 1983.

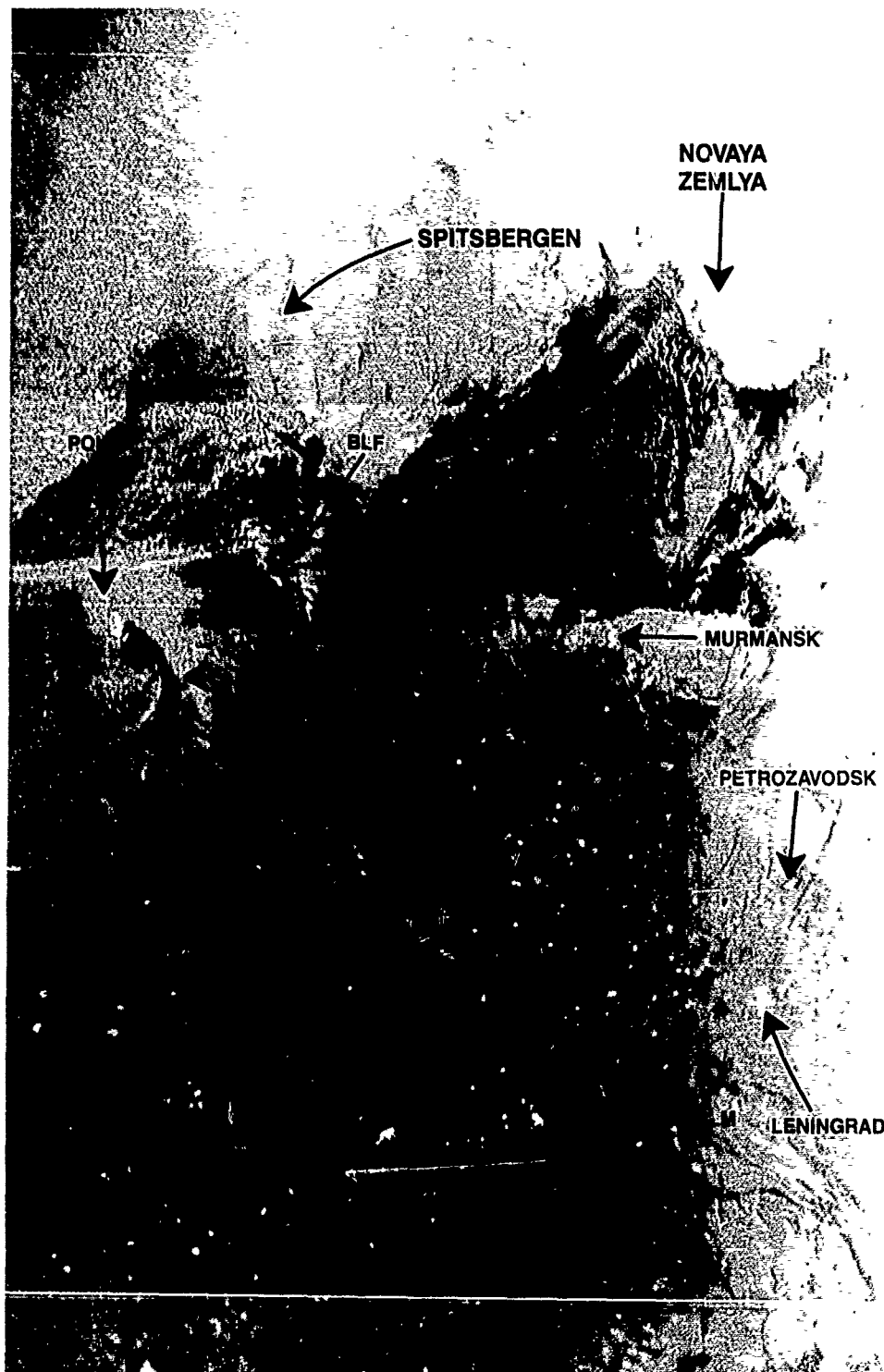




2A-163a. FNOC Surface Analysis. 0600 GMT 21 December 1983.



2A-164a. DMSP Infrared (TS) Mosaic Data. 1004 GMT 21 December 1983.



2A-165a. DMSP Nighttime Visual (LS) Data. 1732 GMT 21 December 1983.



2A-166a. DMSP Nighttime Visual (LS) Data. 1913 GMT 21 December 1983.

An interesting clear area extends between the polar low and the BLF to the east. A strong, southward dipping ridge would be anticipated in this region as northerly winds on the west side of the BLF veer to southeasterly further to the west, reflecting the circulation of the polar low.

A flare from the aurora borealis passes over the northern portion of the polar low, while to the southeast numerous city lights show the positions of major European cities. Lights can also be seen from some of the oil rigs of the North Sea.

The storm really intensifies during the next 2 hr, as shown by another DMSP nighttime visual (LS) view at 1913 GMT (Fig. 2A-166a). Strong winds are particularly suggested in the western semicircle of the storm where long and tightly spaced cloud lines are indicative of winds in the 40- to 50-kt range.

The FNOC surface analysis for 1800 GMT (Fig. 2A-167a) is grossly in error in indicating anticyclonic flow in the region  $70^{\circ}$  to  $75^{\circ}$ N, when, in fact, as the cloud lines show, flow was strongly cyclonic in that region. Both Jan Mayen's surface report and that of the ship UUOR are northwesterly, perpendicular to the incorrectly drawn isobars, reflecting the cyclonic flow in the outer circulation of the approaching low. Short-wave ridge lines are located north of  $70^{\circ}$ N and between Jan Mayen and Iceland, as shown on a gridded version of the DMSP data in Fig. 2A-168a. The cold off-ice flow is advected southward around the storm—a factor favorable for intensification, as the cold air sinks and the warmer air near the center of the storm rises in response.

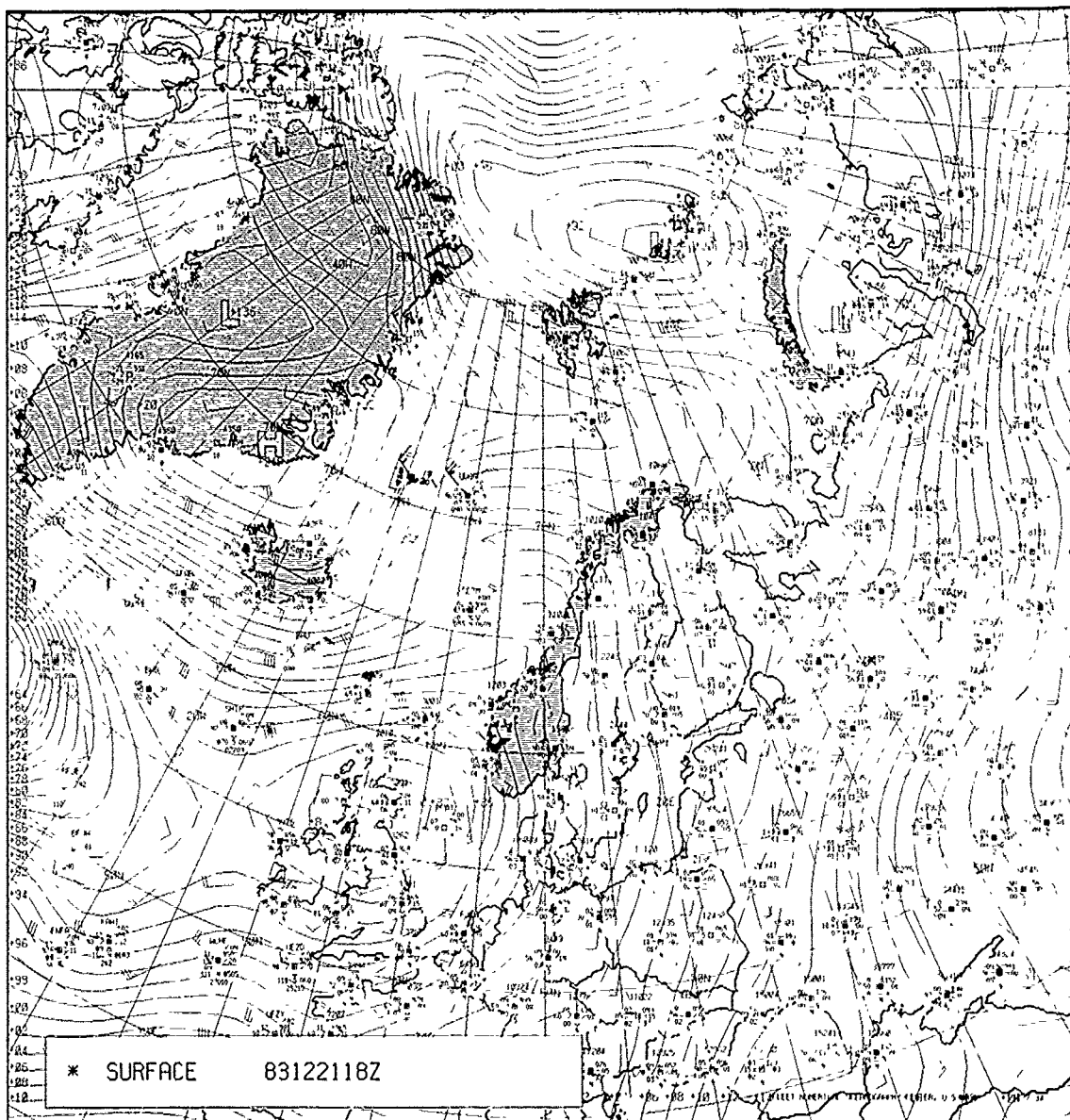
A DMSP infrared (TS) view of the storm slightly earlier at 1823 GMT (Fig. 2A-169a) shows the off-ice flow with somewhat better clarity. In this view high cloud plumes over Spitsbergen reveal northerly flow on the north side of the upper level cold trough over the region. Anticyclonically turning cirrus streamers in the northeast quadrant of the storm suggest outflow aloft in the manner seen over tropical disturbances, reflecting a warm core system.

A view of the storm late on 21 December, at 2236 GMT, is shown in enhanced DMSP infrared (TS) data (Fig. 2A-170a). Thin low-level cloud streets continue to define the very sharp ridge to the north of the storm. The secondary BLF, which had been quite prominent 5 hr earlier (Fig. 2A-165a), now seems to have largely dissipated, while the major vortex still appears moderately intense.

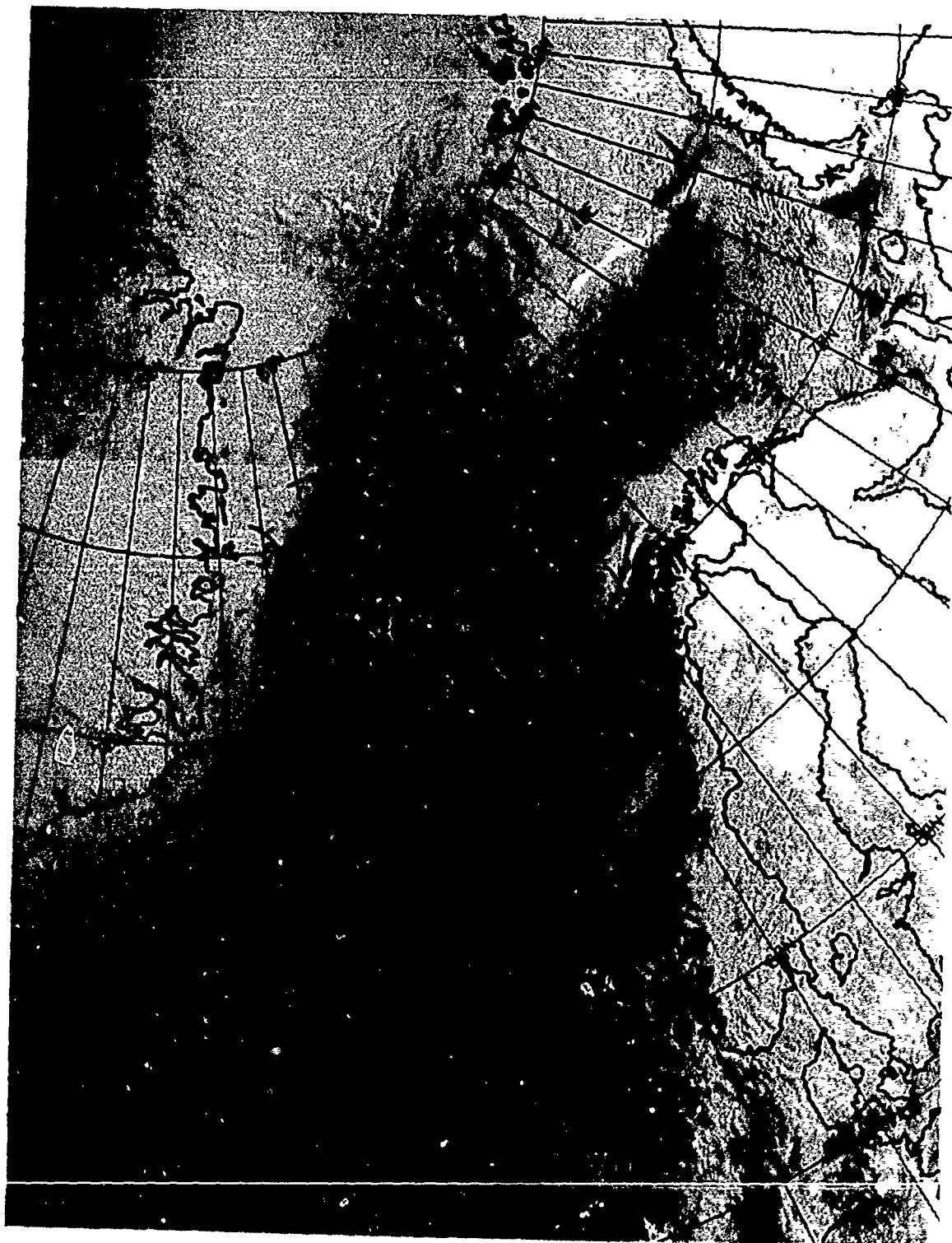
## 22 December 1983

The storm still had not been detected or analyzed on the FNOC surface analysis for 0000 GMT 22 December (Fig. 2A-171a). DMSP enhanced infrared (TS) data (Fig. 2A-172a) suggest a center very near  $71^{\circ}$ N  $4^{\circ}$ W. The surface observation together with a report (labeled BAD) from a nearby ship support low pressure near that location. The ship report indicates a pressure of 998.8 mb, which is probably not unreasonable. It was, however, disregarded in this analysis.

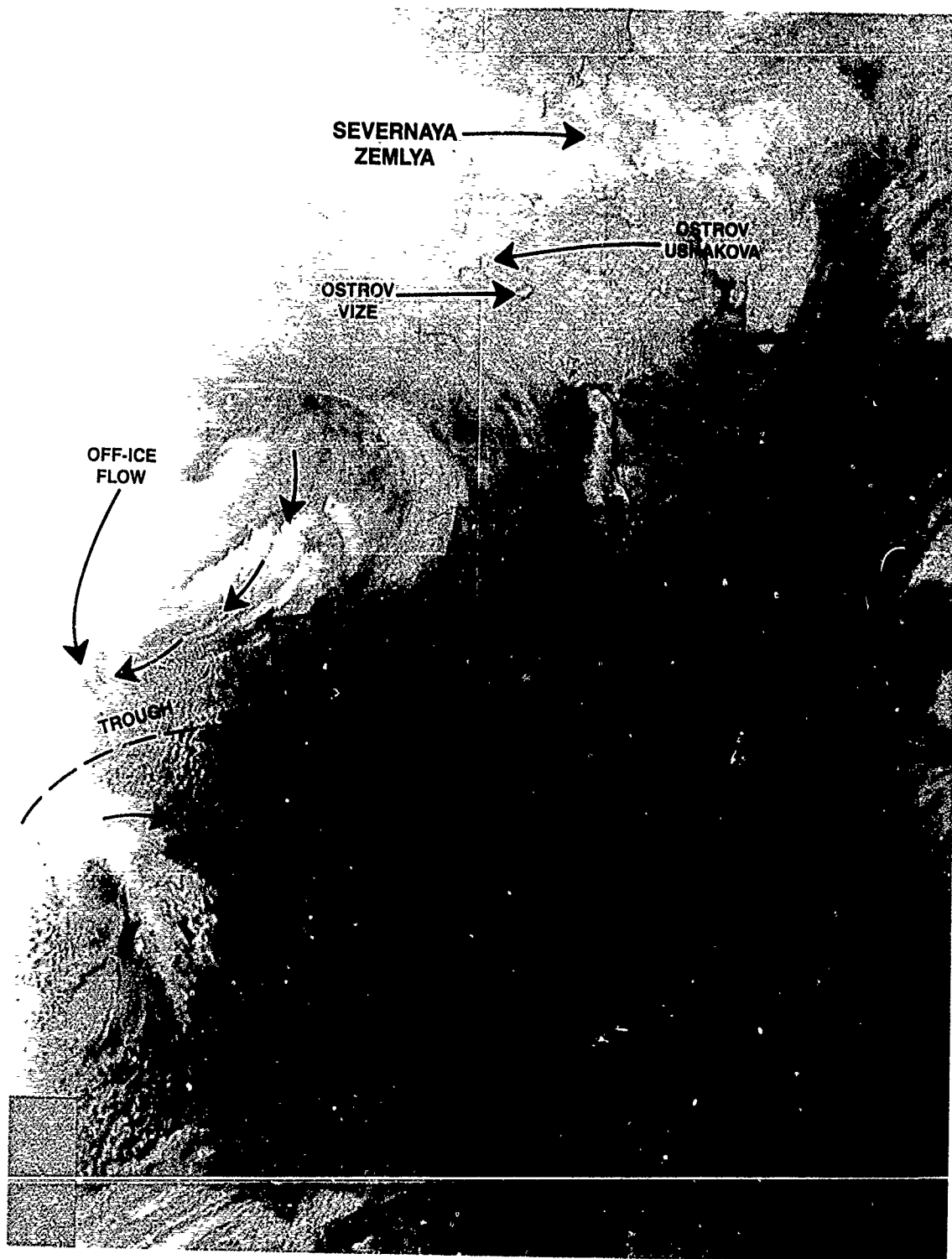
The FNOC 500-mb analysis for 0000 GMT (Fig. 2A-173a) continues to reveal the presence of a cold trough aloft. Its exact configuration of the 500-mb analysis in the storm region is unknown and would require a dense series of observations to define. However, one clue, commonly associated with polar low development suggests coldest temperatures and lowest pressures aloft immediately south of the vortex. The clue is the enhanced cumulonimbus development of cloud cells in that region, which form as a result of thermally-induced unstable conditions related to the cold air aloft.



2A-167a. FNOC Surface Analysis. 1800 GMT 21 December 1983.

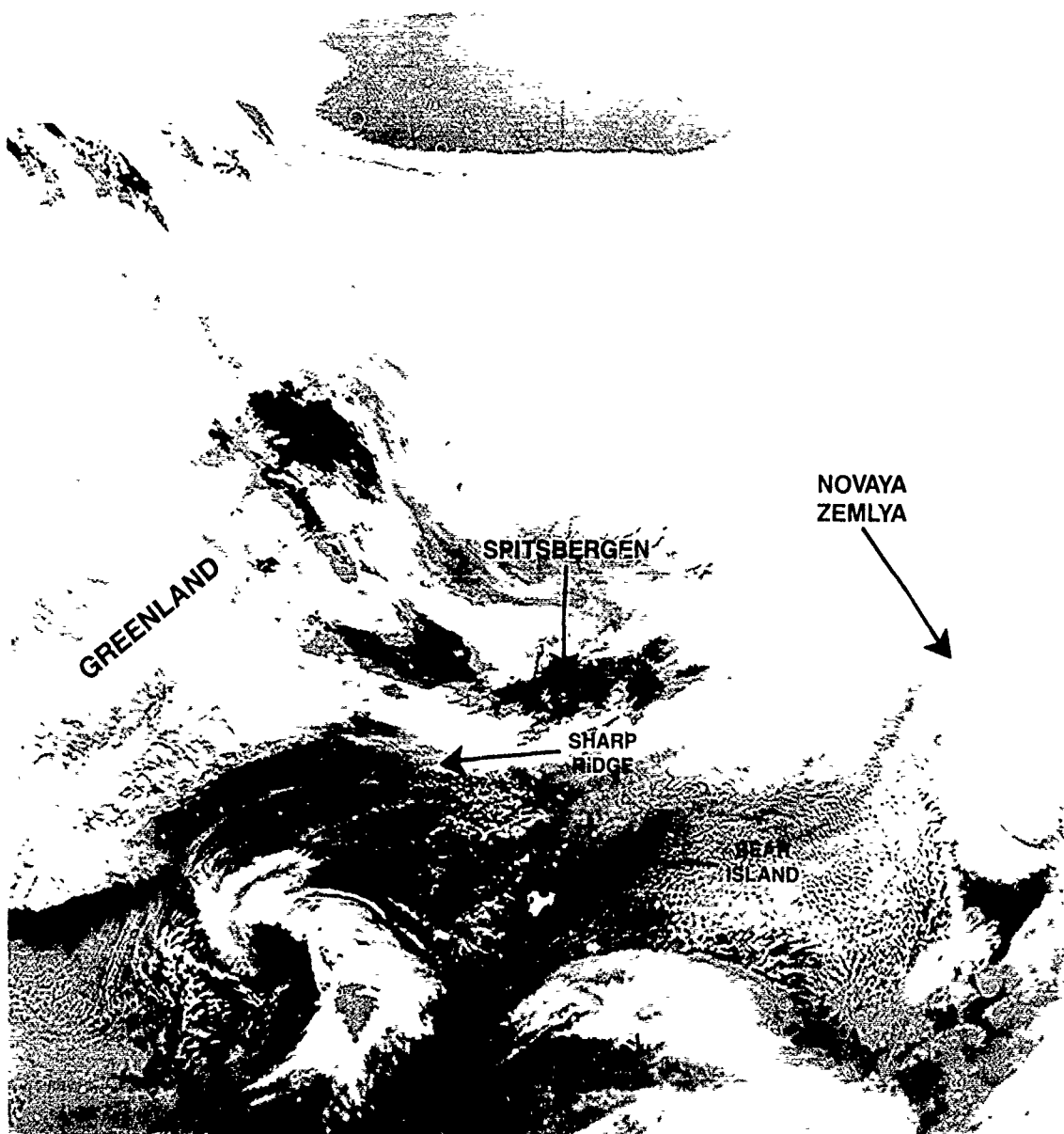


2A-168a. Gridded DMSP Nighttime Visual Data. 1913 GMT 21 December 1983.

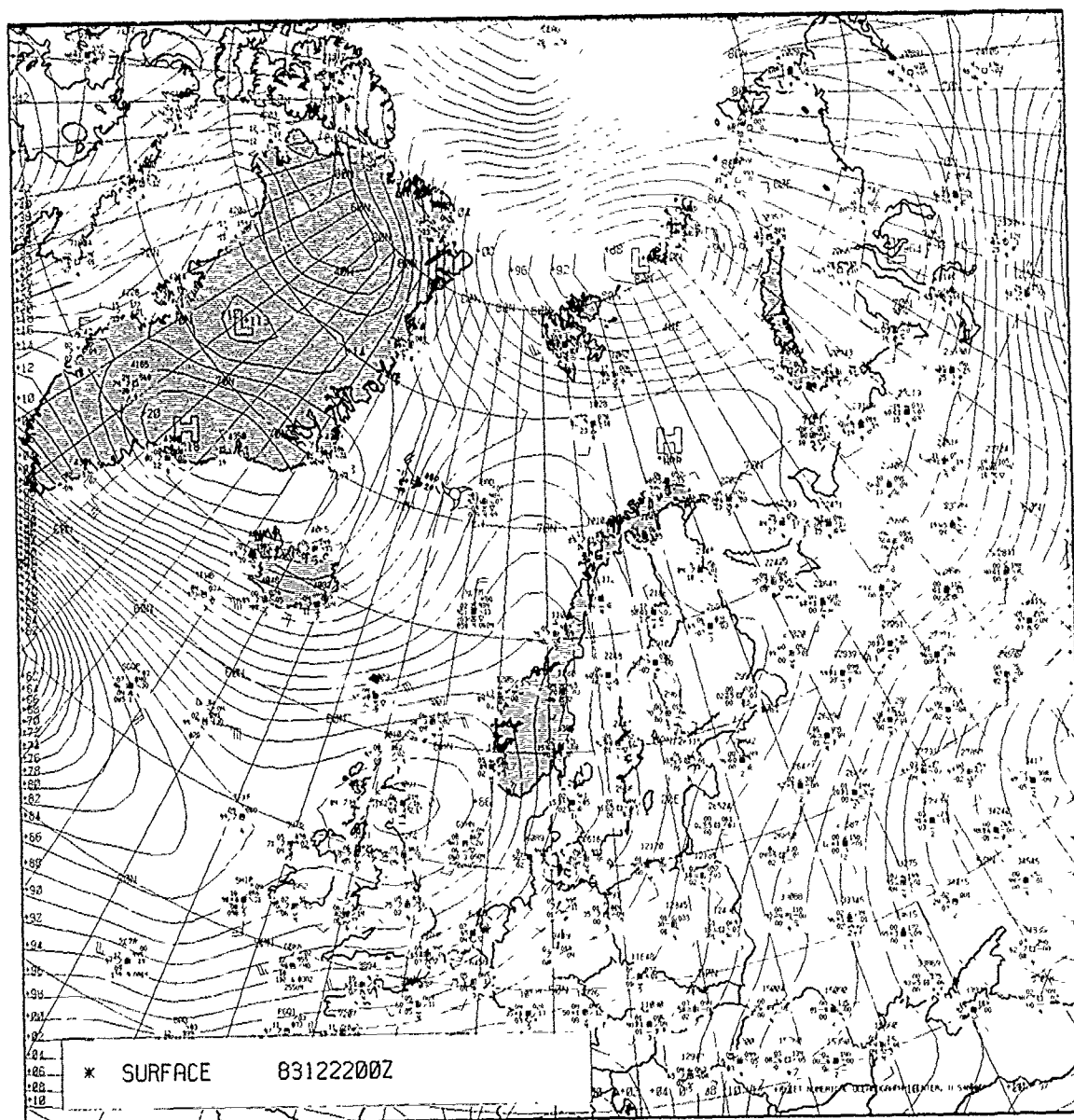


2A-169a DMSP Infrared (TS) Data. 1823 GMT 21 December 1983.

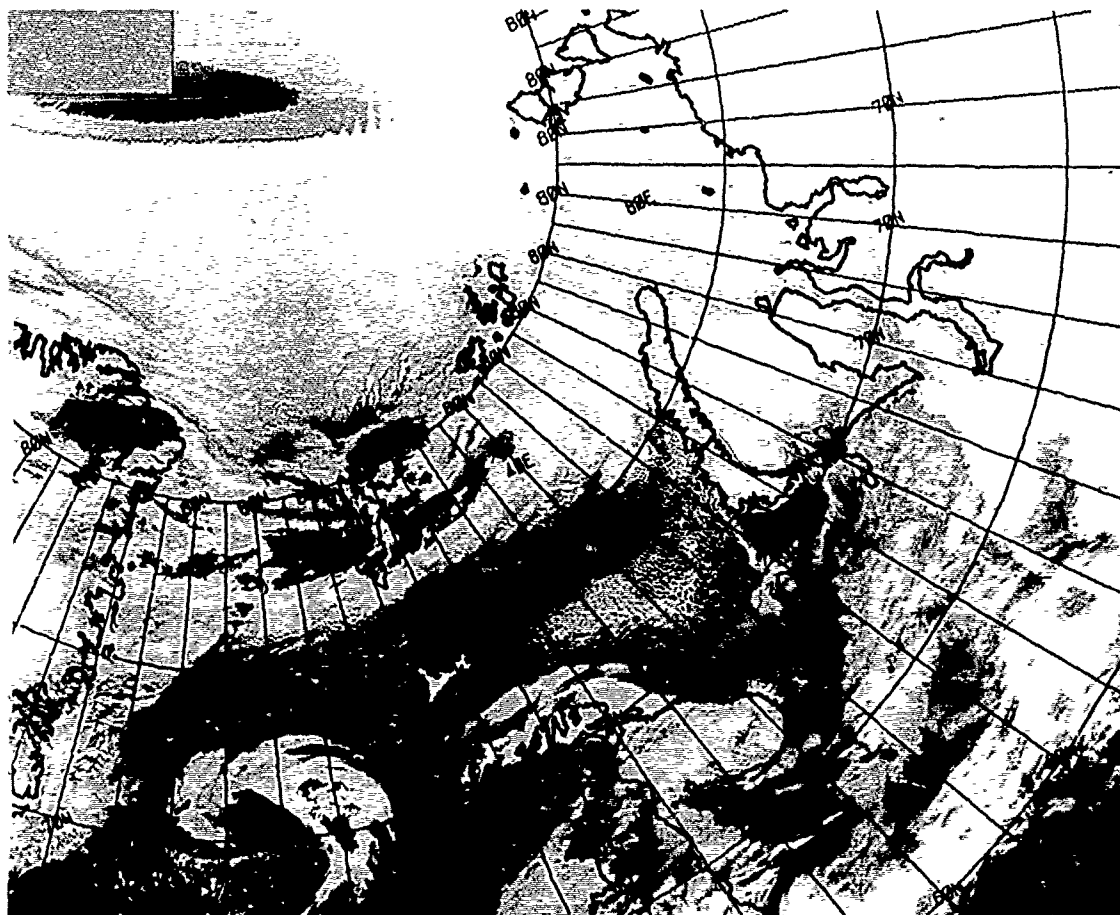




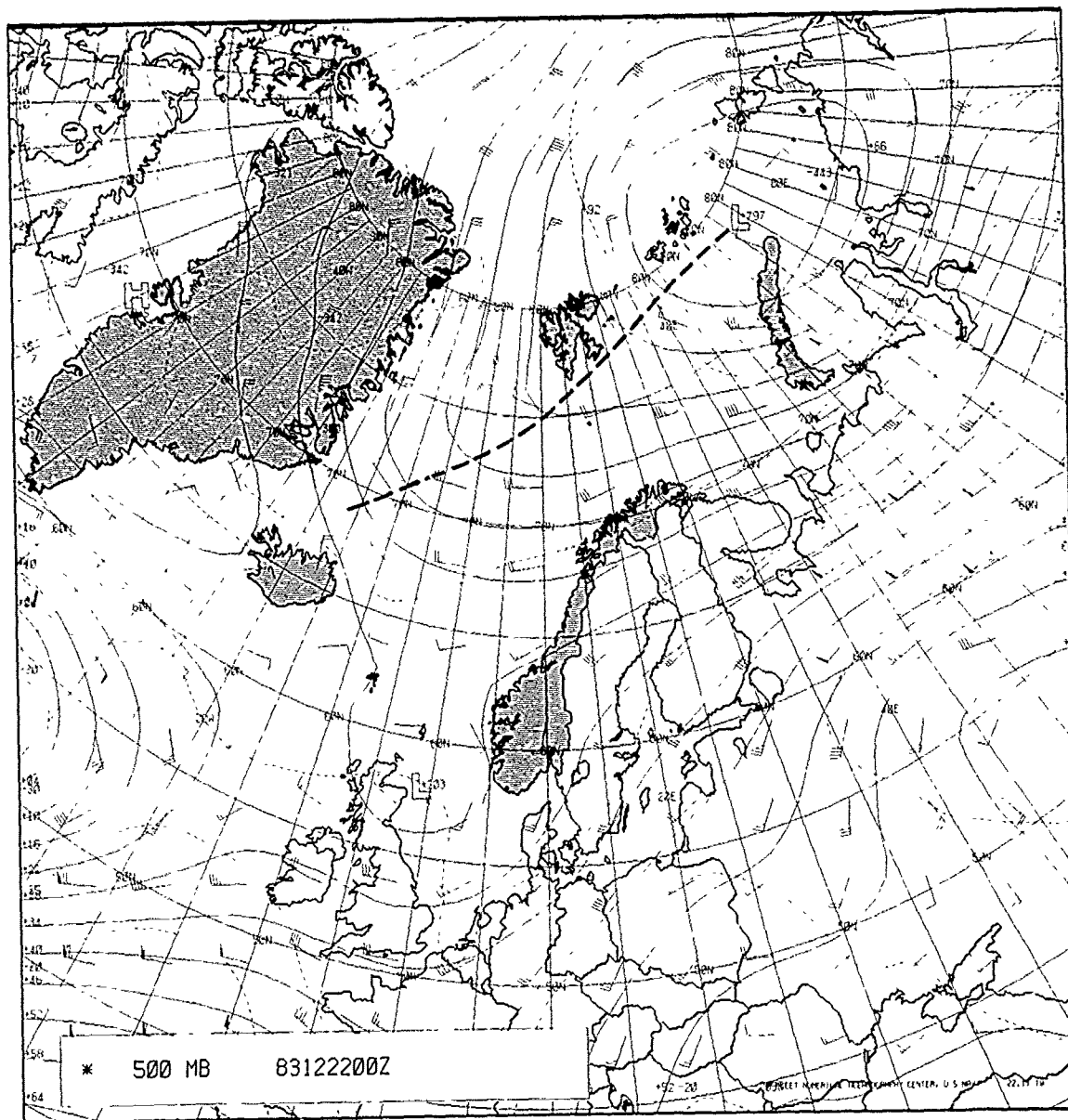
2A-170a DMSP Enhanced Infrared (TS) Data 2236 GMT 21 December 1983.



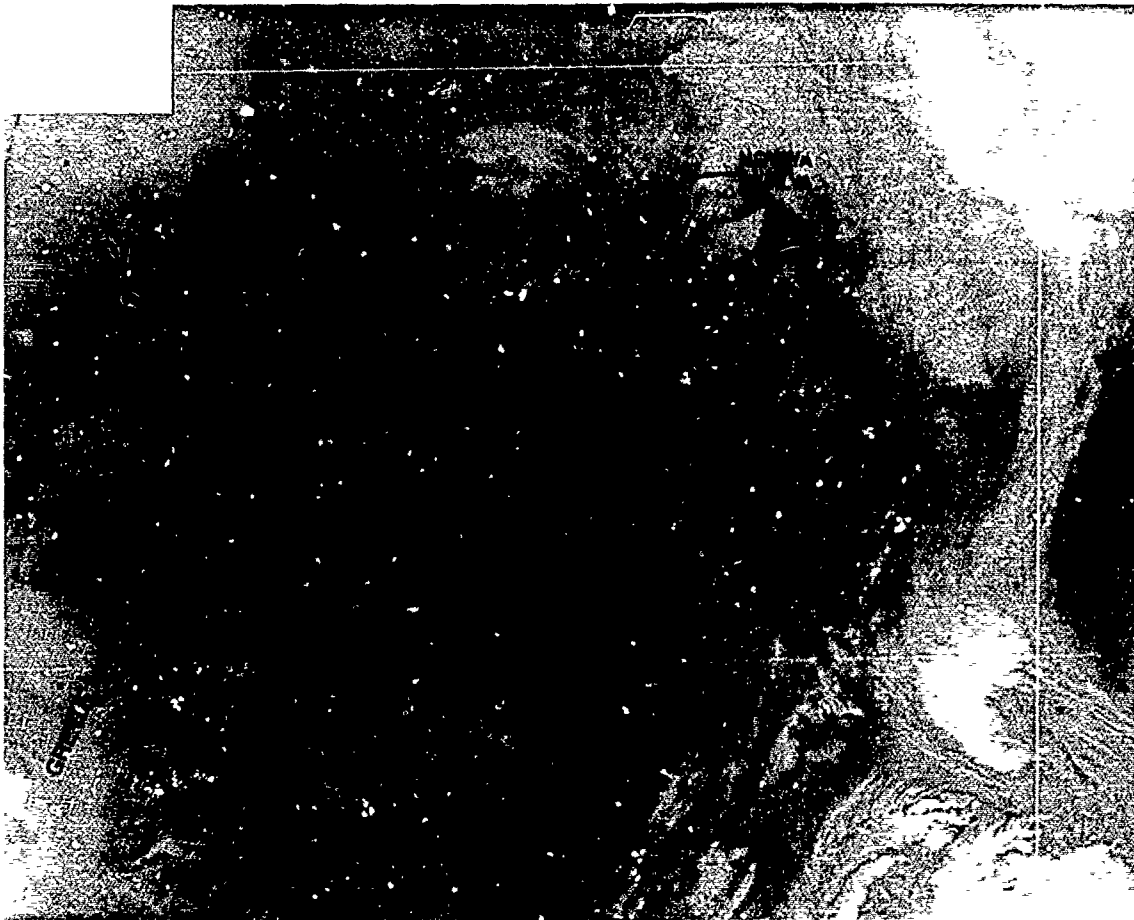
2A-171a. FNOC Surface Analysis. 0000 GMT 22 December 1983



2A-172a. DMSP Enhanced Infrared (TS) Data. 0017 GMT 22 December 1983.



2A-173a. FNOC 500-mb Analysis 0000 GMT 22 December 1983.



2A-174a DMSP Infrared (TS) Data 0200 GMT 22 December 1983.

The storm appeared to reach its maximum intensity near 0200 GMT, as revealed in DMSP infrared (TS) data (Fig. 2A-174a) at that time. The vortex is clearly ringed by spiral clouds and is the dominant feature of the Greenland/Norwegian Seas—its presence, however, apparently unknown to meteorologists of FNOC, or NMC (who also failed to detect the storm).

A DMSP nighttime visual (LS) view of the system at 0340 GMT (Fig. 2A-175a) and an infrared (TS) mosaic view at 1034 GMT (Fig. 2A-176a) show the gradual unwinding of the system.

The FNOC surface analysis for 1200 GMT (Fig. 2A-177a) still fails to resolve the storm feature. Observations in the region suggest that the diameter of closed circulation is rather small so detection really is only feasible when satellite data are utilized to assist in the analysis.

The FNOC 1200 GMT, 500-mb analysis (Fig. 2A-178a) shows a trough almost superimposed over the storm area. This configuration is not conducive to development and by 1943 GMT (Fig. 2A-179a) DMSP infrared data reveal the swirls of cumulonimbus typical of that underlying an upper level cold core low.

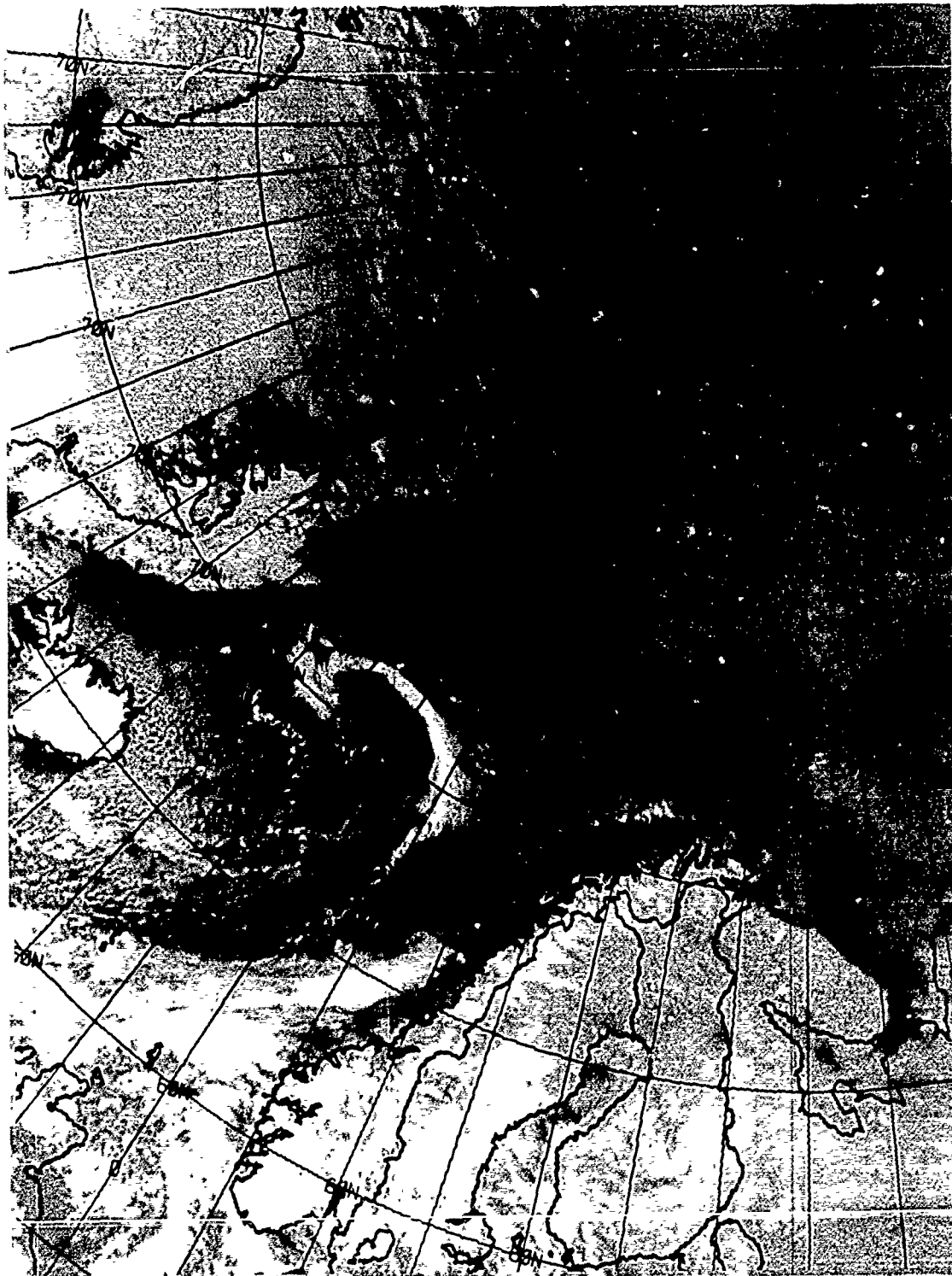
### *23 December 1983*

FNOC 500-mb data at 0000 GMT (Fig. 2A-180a) indicate a cold trough over that region. However, NMC's analysis (not shown) indicated a low center and this is shown in Fig. 2A-180a very near the location of the dissipating polar low.

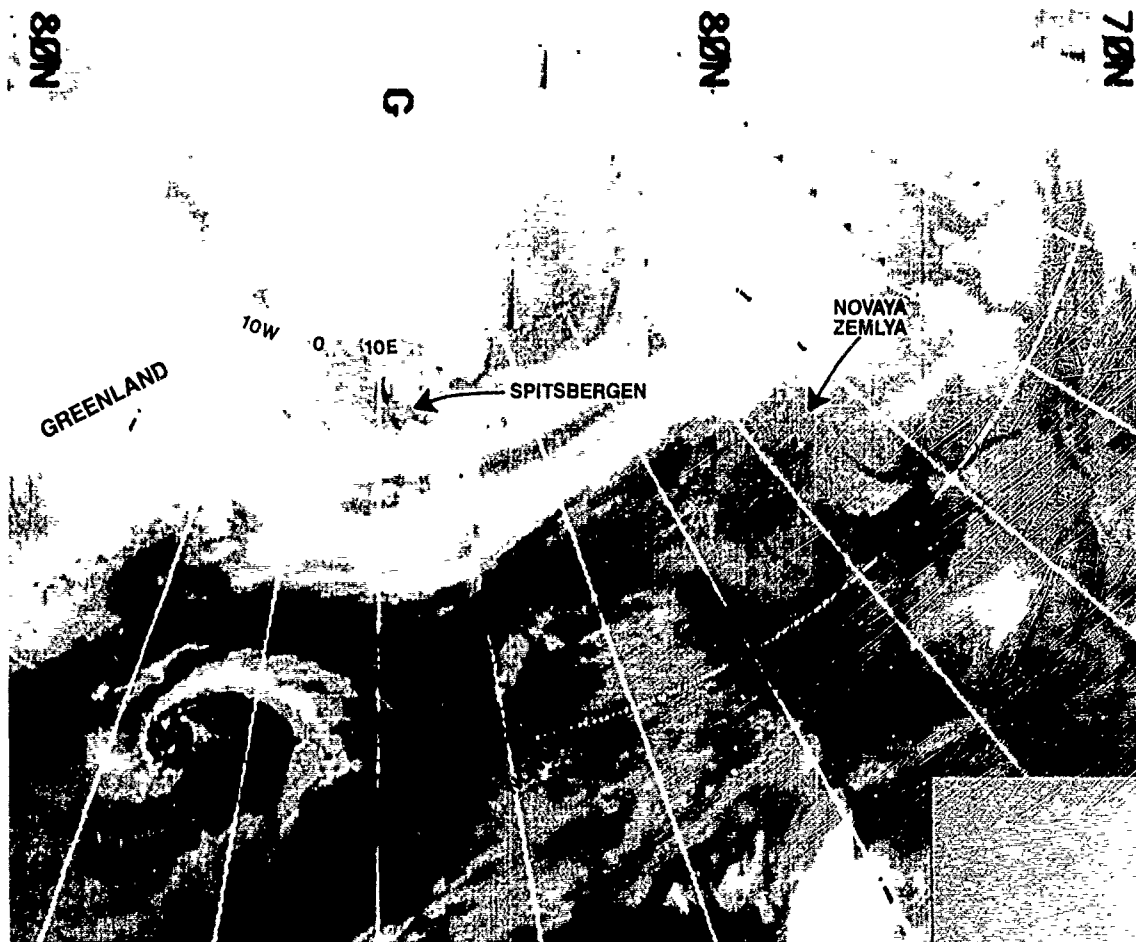
The FNOC surface analysis for 0000 GMT (Fig. 2A-181a) is consistent in still failing to detect this storm system, now located near 67°N 7°W.

A final DMSP nighttime visual (LS) view of the storm area at 0137 GMT (Fig. 2A-182a) shows the storm now near 67°N 2°W. The storm has a well-defined center and, apparently showing signs of some reintensification, still carries winds of considerable strength. The storm passed near ocean station "MIKE," (66°N 2°E) by 1800 GMT. The FNOC surface analysis for that time (Fig. 2A-183a) shows MIKE reporting 40-kt sustained winds in showers with a 3-hr rising pressure tendency of +4.3 mb—the type of pressure rise characteristic of wake effects experienced following the passage of a polar low.

At this stage of the analysis, the storm was conveniently merged with the low pressure center that had been moving northward from Great Britain, but coastal stations of Norway were later surprised by the unexpected intensity of winds striking that region as the storm moved onshore.

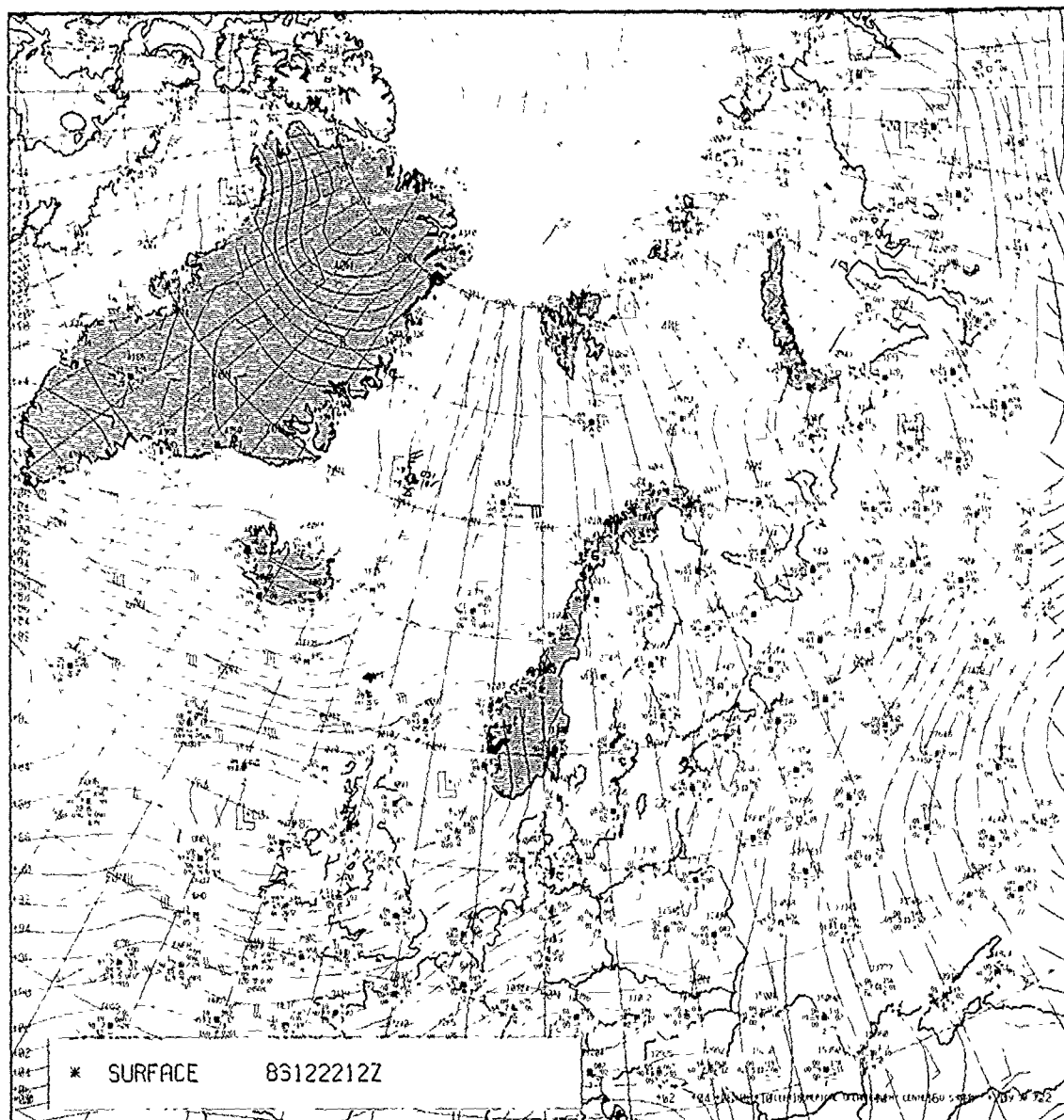


2A-175a DMSP Nighttime Visual (LS) Data 0340 GMT 22 December 1983

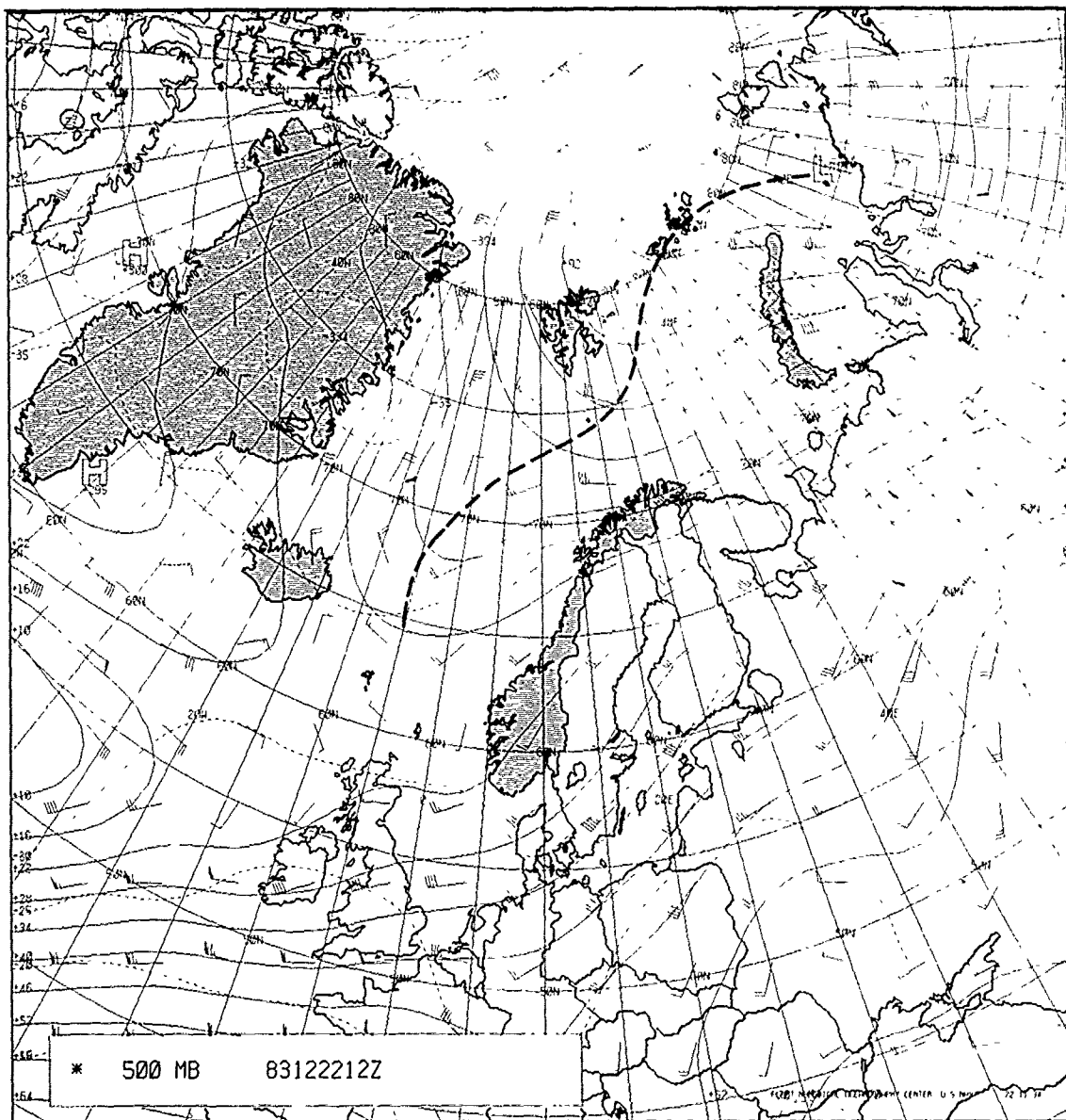


2A-176a DMSP Infrared (TS) Mosaic Data. 1034 GMT 22 December 1983

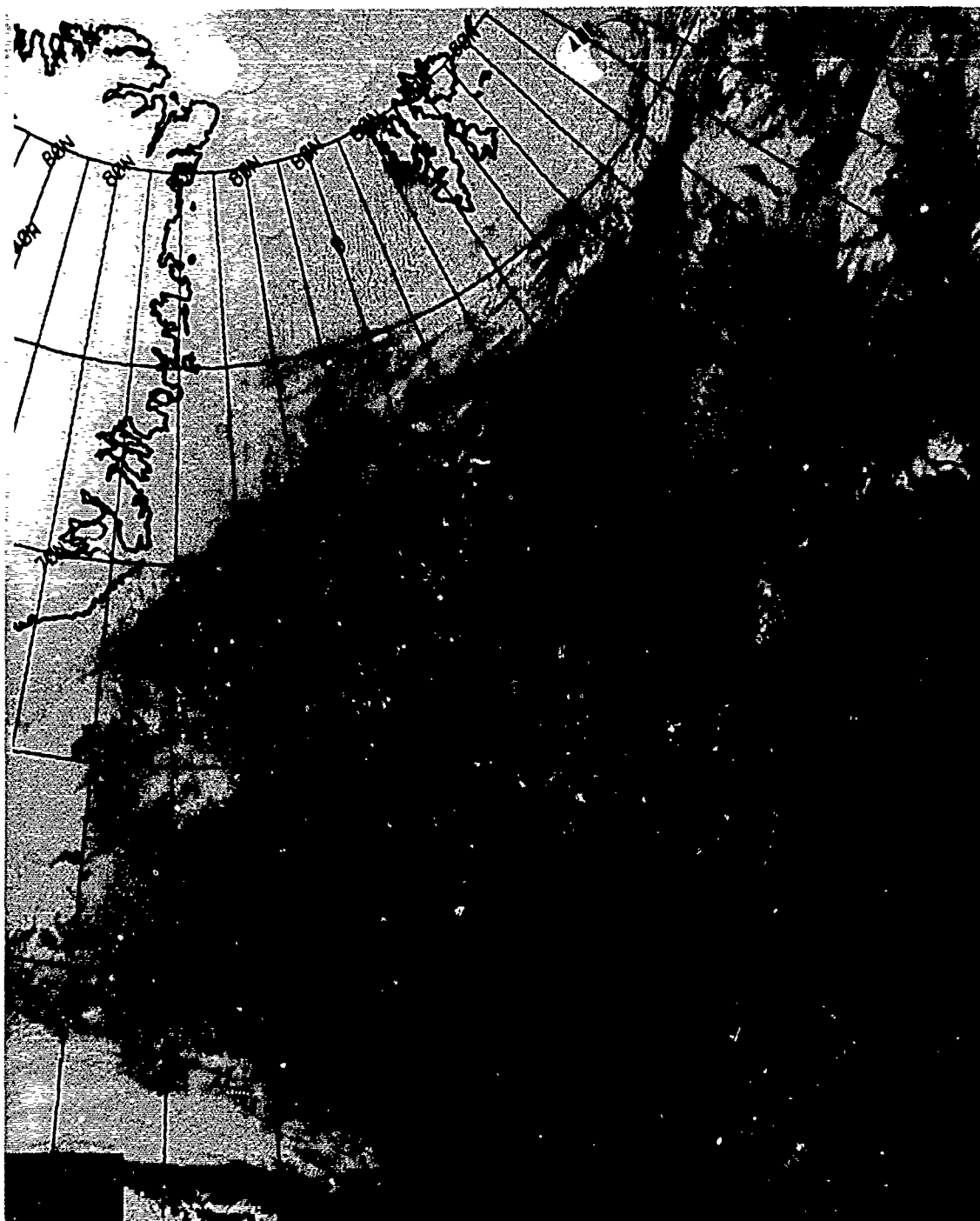




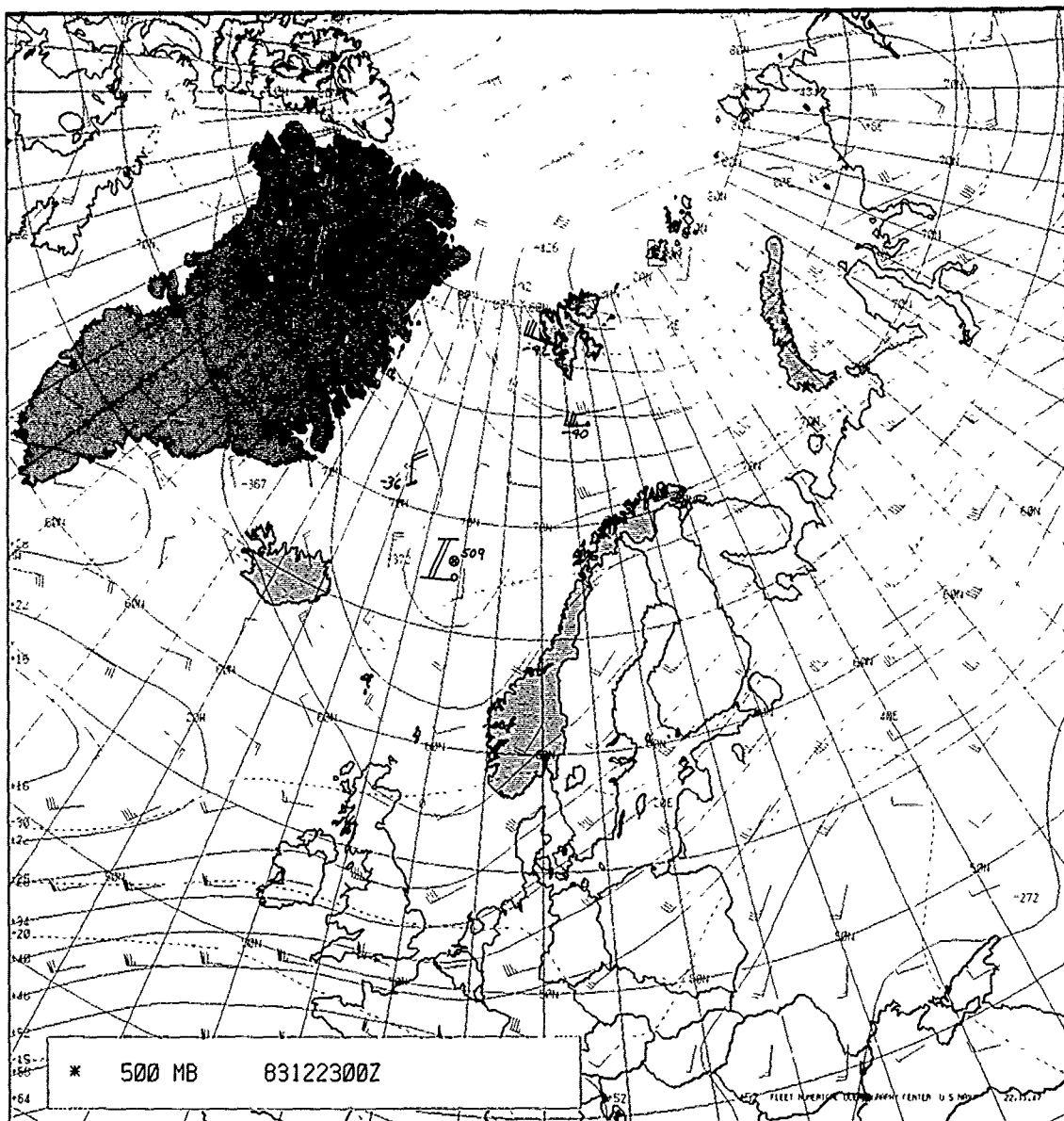
2A-177a FNOC Surface Analysis. 1200 GMT 22 December 1983



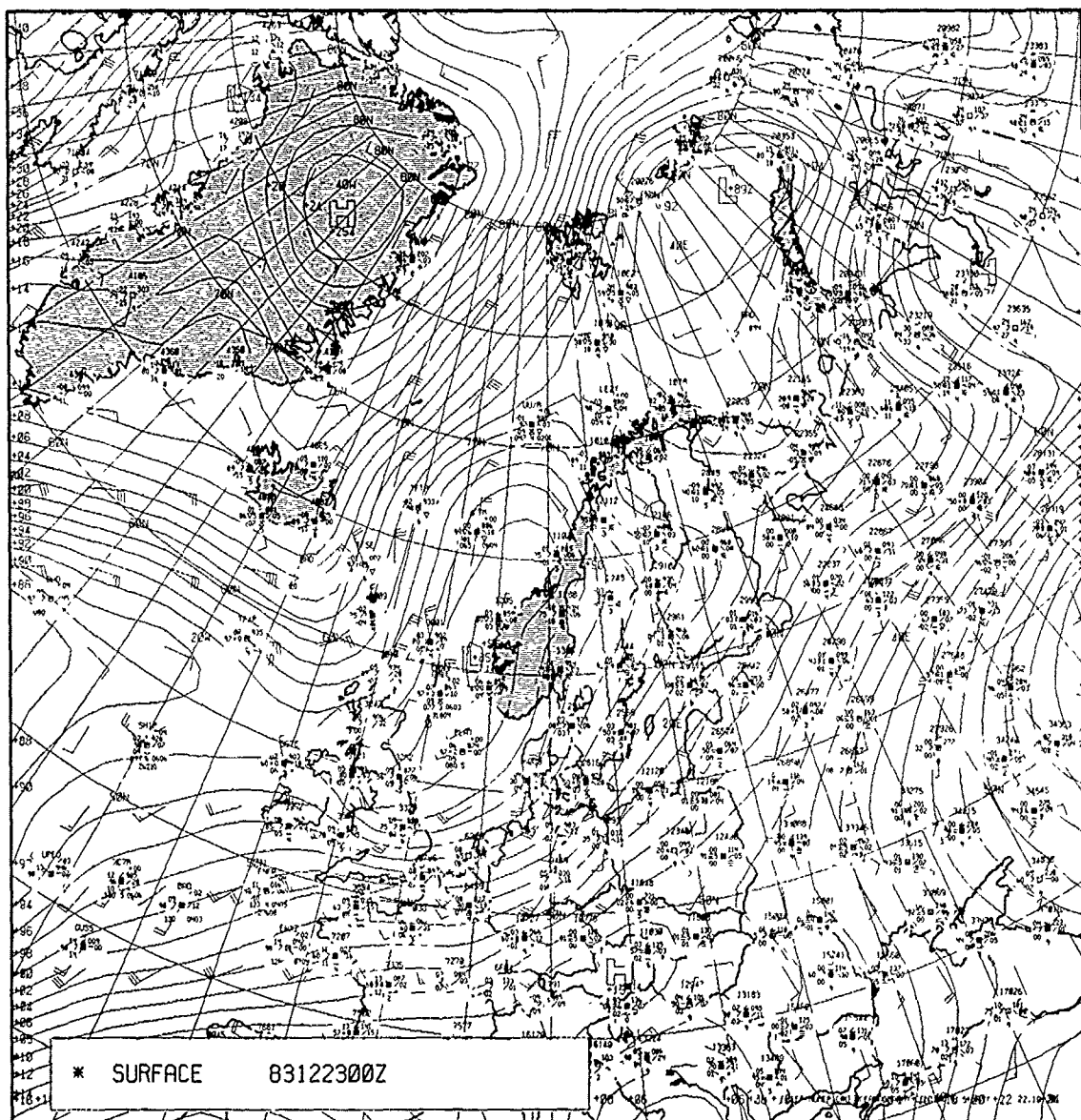
2A-178a. FNOC 500-mb Analysis. 1200 GMT 22 December 1983.



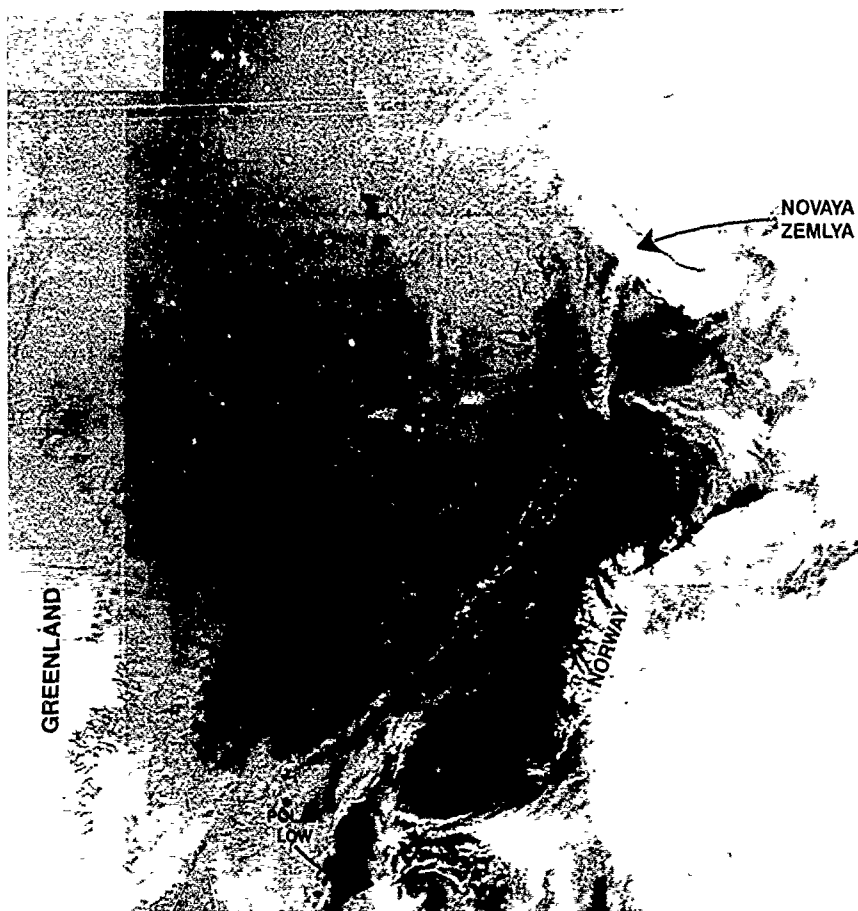
2A-179a. DMSP Infrared (TS) Data. 1943 GMT 22 December 1983.



2A-180a. FNOC 500-mb Analysis. 0000 GMT 23 December 1983.



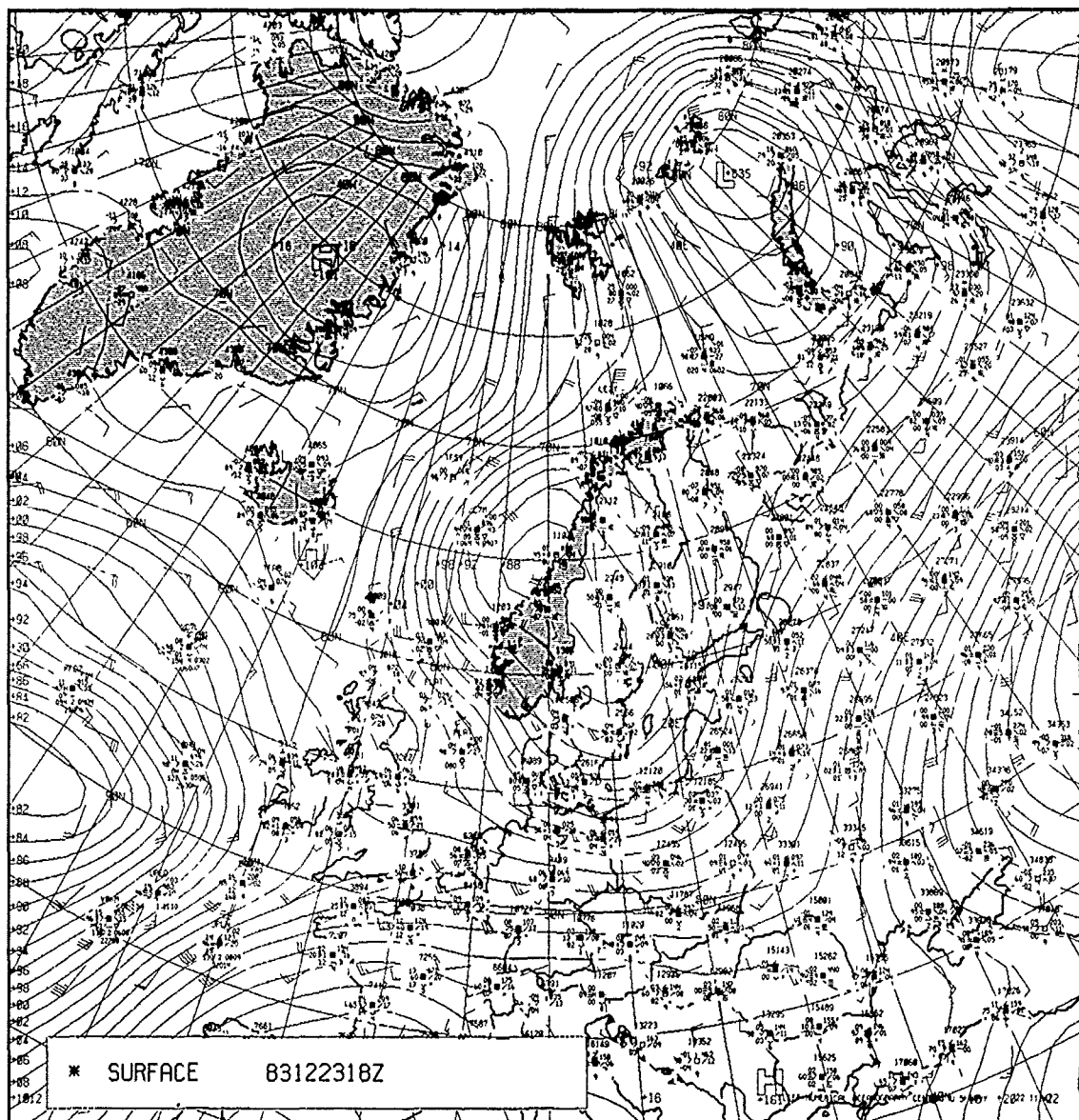
2A-181a. FNOC Surface Analysis. 0000 GMT 23 December 1983.



2A-182a DMSP Nighttime Visual (LS) Data 0137 GMT 23 December 1983

### **Important Conclusions**

1. Cold surge events and the progress of resulting boundary layer fronts are important to monitor because of their role in polar low development.
2. High quality satellite data are required at frequent intervals (every 2 to 3 hr) to successfully monitor evolutionary patterns of polar low development.
3. Ships and island locations in the Arctic should be closely monitored for unusually pronounced 3-hr pressure changes. These often signal the approach or passage of a polar low.
4. Before disregarding conventional observations showing unusually strong winds from odd directions or unusually low pressures, a check with satellite data should be made to ensure that there are no nearby unexpected storm developments.
5. Upper cold lows and upper cold troughs appear to be intimately involved in polar low development. During spring, fall, and winter, whenever such systems are forecast to move over the Greenland, Norwegian, or Barents Seas, the possibility of polar low development should be considered.



2A-183a. FNOC Surface Analysis. 1800 GMT 23 December 1983.



# Section 3

## *Local-Scale Atmospheric Phenomena and Effects*

### *3A Anomalous Cloud Lines*

Ship-Induced Effects ..... 3A-1

#### *Case Studies*

1 *An Anomalous Cloud Line in the Fram Strait* ..... 3A-2

### *3B Jet Streams and Mountain Waves*

Trapped Waves and Vertical Propagating Waves ..... 3B-1

#### *Case Studies*

1 *Detection of High Wind Speed Areas Over Mountainous Terrain in the Arctic (14-16 June 1984)* ..... 3B-2

2 *Use of Topographic and Polynya-Associated Cloud Plumes in Surface Wind Flow Determination and in Jet Stream/Arctic Front Detection (10-12 April 1987)* ..... 3B-22

### *3C Boundary Layer Fronts*

Characteristics of Boundary Layer Fronts ..... 3C-1

#### *Case Studies*

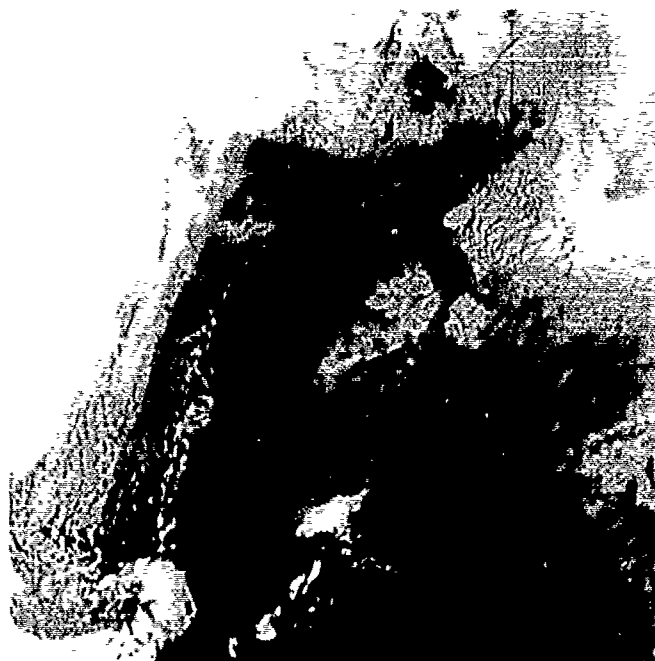
1 *Boundary Layer Frontal Movement Through the Fram Strait (23-27 March 1987)* ..... 3C-2

### 3A *Anomalous Cloud Lines*

#### *Ship-Induced Effects*

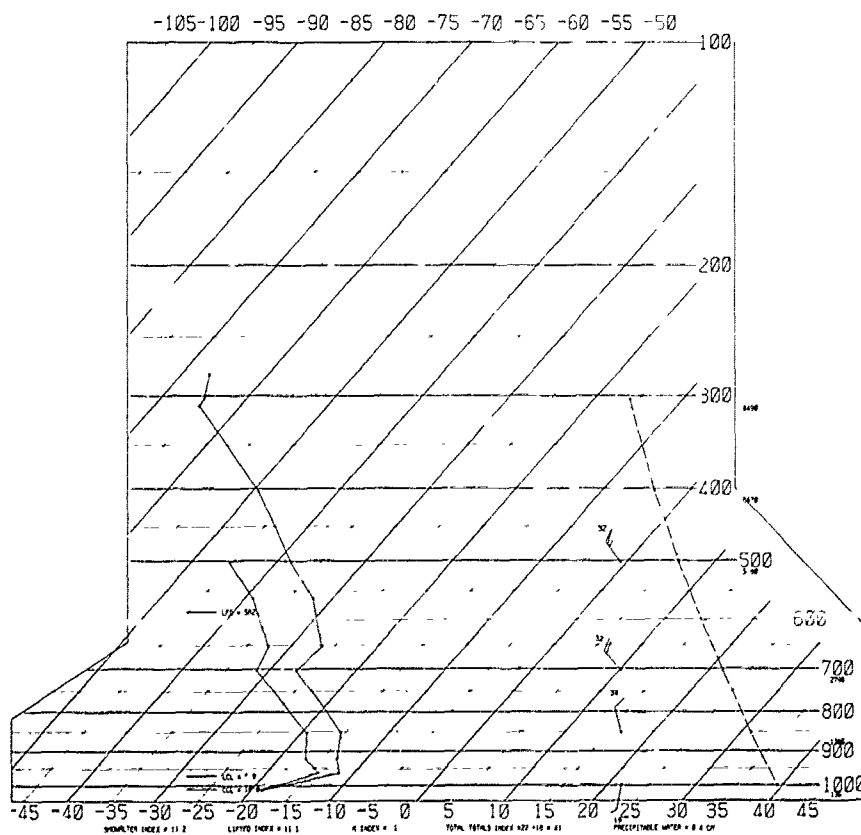
Ship-induced anomalous cloud lines are distinguished by being very narrow at the source and broadening downstream (see NTAG, Vol. 2, Sec. 1C). They tend to form in saturated or super-saturated conditions under a strong inversion. Under such conditions the stack exhaust provides condensation nuclei, which increase droplet formation. This activity releases latent heat of condensation and increases convective activity causing cloud line development followed by subsidence in a downdraft along the edges of the cloud.

3A-2a. DMSP Infrared (TS) Data.  
0443 GMT 21 January 1984.



SKEW T, LOG P DIAGRAM

840121  
1200Z  
20107



3A-2b. Radiosonde Analysis,  
Barentsburg, Spitsbergen.  
1200 GMT 21 January 1984.

## *Case 1 An Anomalous Cloud Line in the Fram Strait*

*21 January 1984*

DMSP infrared data at 0443 GMT (Fig. 3A-2a) reveal an anomalous cloud line in the Fram Strait with the plume advecting north-northeast over the marginal ice zone. The convective nature of the band, causing fairly intense compensating subsidence, is revealed by a clearing of adjacent cloudiness, especially along the northern edge of the band where the line first begins.

The line spreads out laterally over the MIZ. In this region increased surface roughness causes a turbulent dispersion laterally. That the band is in the boundary layer, capped by an inversion, is revealed in this infrared depiction by the warmer gray tone of the band, in comparison to the colder (whiter) ice over which it lies. Note that the temperature of the band is warmer over the ice than over the water. This change is undoubtedly related to the fact that boundary layer depth is greater over the water than over the ice. Assuming isentropic flow, the plume would dip to a lower elevation over the ice and, in the strong inversion conditions, radiate at warmer temperatures than over the water.

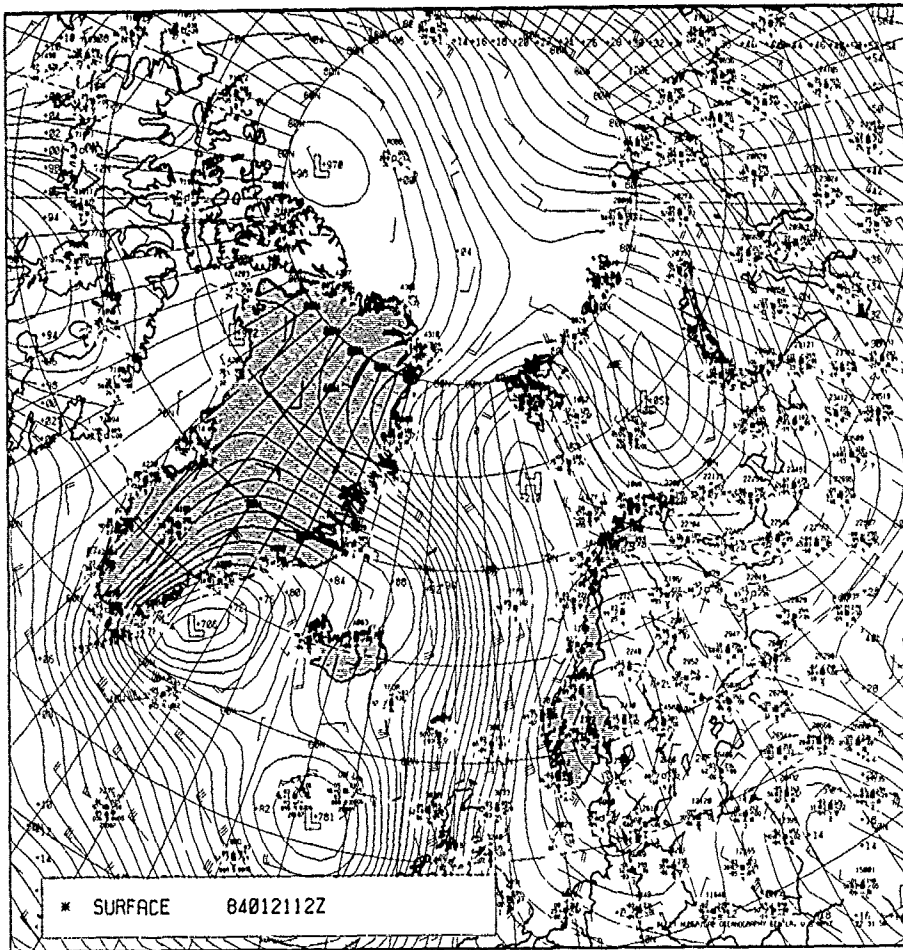
The 1200 GMT sounding from Barentsburg, Spitsbergen (Fig. 3A-2b) reveals a surface-based inversion and the very moist low-level conditions that existed under the inversion on this date. The surface relative humidity was 96.3% and was 96.7% at 1000 mb.

From this sounding it can be seen that the top of the plume could have been radiating at temperatures about 7°C warmer than the underlying surface. Hence the warm plume appearance in satellite infrared data.

An additional infrared view at 0625 GMT (Fig. 3A-3a) shows even better contrast in revealing the warm plume of the anomalous cloud line over the MIZ. The northern portion of the plume has advected slightly eastward but its source apparently is stationary and shows no movement.

An eastward drift of the northern portion of the plume continues in a final DMSP infrared view (Fig. 3A-3b) acquired at 0806 GMT. However, again the source position is unchanged.

A search was made for ship reports in the region. However, none were located. It is not unusual for Norwegian and other fishing vessels to be in the region and not provide weather reports to document their location. The FNOG 1200 GMT surface analysis (Fig. 3A-3c) shows the southerly on-ice flow that existed on this date—a fact that is implied by the anomalous cloud line orientation.



3A-3c. FNOG Surface Analysis. 1200 GMT 21 January 1984.



3A-3a. DMSP Infrared (TS) Data.  
0625 GMT 21 January 1984.



3A-3b. DMSP Infrared  
(TS) Data.  
0806 GMT 21 January 1984.

3A-3

### 3B Jet Streams and Mountain Waves

#### *Trapped Waves and Vertical Propagating Waves*

When winds of sufficient force blow nearly perpendicular to mountain ranges lee atmospheric waves or mountain waves result. Mountain waves have been described as consisting of two categories—the "trapped" wave and the vertically propagating wave (Durrant, 1986). Wavelengths of the trapped wave category are generally between 5 and 25 km. They are called trapped because they occur directly under an inversion, which limits their further extension to higher altitudes. When the air is moist clouds will develop parallel to the mountain range at each of the wave crests and extend downwind of the range for some distance—often several hundred kilometers. Vertically propagating waves have wavelengths exceeding 30 km and typically are revealed by only one pronounced wave crest with a long trailing tail. The length of the cloud from where it is formed to where it dissipates downstream will exceed its width. Trapped wave clouds are typified by an atmosphere in which wind speeds increase dramatically with height. The vertically propagating wave cloud also shows an increase in wind speed with height, but less dramatic. Stable layers also tend to be weaker in the vertically propagating wave.

The conditions described above are typically found in frontal zones. It is in such regions that heavy concentrations of moisture are found in conjunction with the requisite increase of wind speed with height. In arctic areas moisture is more scanty than in maritime, midlatitude regions. Quite frequently only scattered to broken amounts of midlevel and high-level clouds, striated in a band-like structure, are associated with arctic fronts.

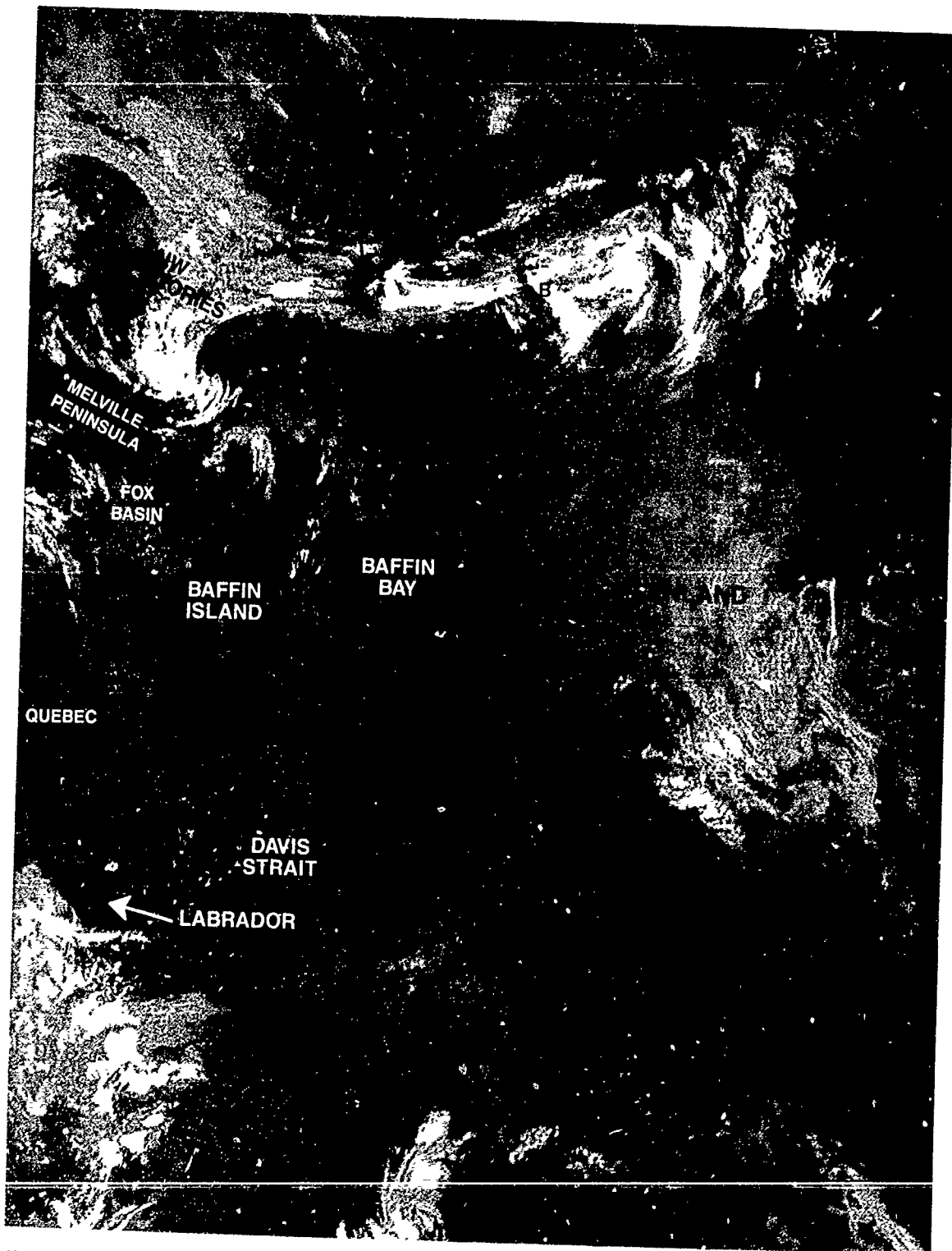
In such areas, where the front intersects hilly or mountainous terrain, wave cloud formations may dramatically appear due to orographic lifting in the high wind regime. Such formations facilitate identification of an arctic front location.

Operationally the vertically propagating wave is most dangerous, having the capacity to drive an aircraft, trying to maintain altitude, into the ground. Many aircraft accidents have resulted because of this effect. Clear air turbulence may also reach extreme values.

As indicated earlier, satellite data are very useful in locating areas where mountain waves are occurring and this helps in the identification of arctic fronts. Improved synoptic analysis and understanding of atmospheric structure is the final result, which leads to improved forecasts.

#### References

Durrant, D.R., 1986: Mountain waves. In *Mesoscale Meteorology and Forecasting*. P.S. Ray (Ed.), American Meteorological Society, Boston, 472-492.



3R-2a DMSP Infrared (TS) Data 1145 GMT 14 July 1984



## *Case 1 Detection of High Wind Speed Areas Over Mountainous Terrain in the Arctic (14-16 July 1984)*

*14 July 1984*

The 1145 GMT DMSP infrared depiction (Fig. 3B-2a) shows an interesting view of Greenland, Baffin Bay, the Davis Strait, Baffin Island, and other features of Labrador, Quebec, and the Northwest Territories.

Meteorologically, a small inverted wave appears near the Melville Peninsula and a series of bright, cold cloud plumes are evident over Devon Island and northern Greenland.

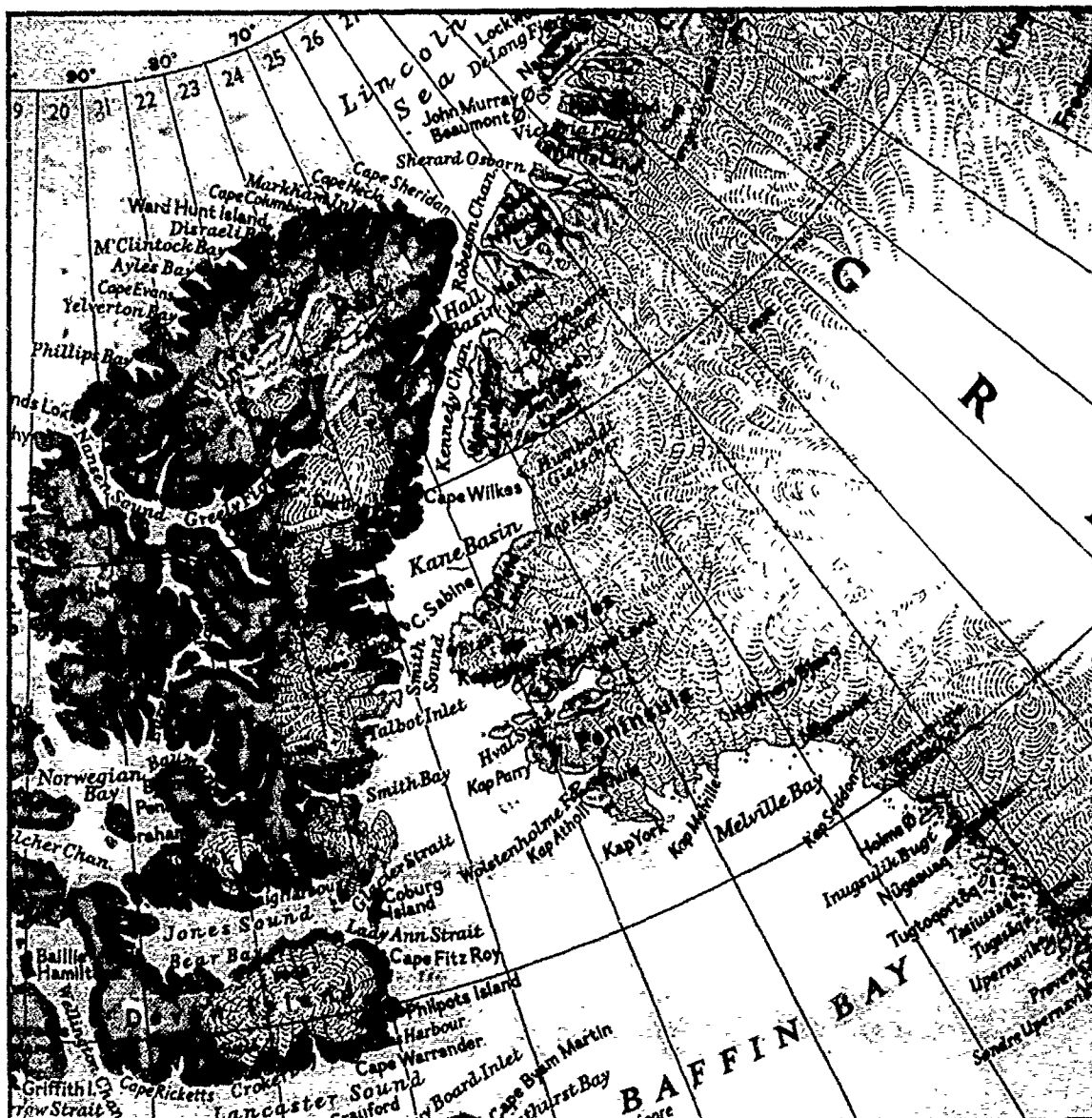
A map of the region (Fig. 3B-3a) shows that the cold cloud plumes are located over mountainous terrain. For example, plume "A" is in the lee of a 1908-ft ice cap on Devon Island and plume "B" is in the lee of a 4921-ft ice cap on the Hayes Peninsula of Greenland, near Kap Alexander. These clouds appear as a single crest with cirrus streamers forming an elongated tail, indicating advection by southwesterly winds aloft. The length of the cloud plume forming near Devon Island is much longer than its width. Hence it would be logical to assume that this is an example of a vertically propagating wave.

Note that the tail of the cloud plume flowing from Devon Island dissipates shortly before the crest of the second wave forming in the lee of a ridge with a peak of 4921 ft on the Hayes peninsula. Dissipation is in the downslope area of this ridge. Cloudiness from this tail again appears to be regenerated a little further downstream as a wispy feature superimposed over the second wave cloud.

Strong downslope winds in ranges with gentle windward and steep leeward slopes are associated with large amplitude mountain waves and can cause such dissipation or evaporation of cloudiness. Figure 3B-4a shows a cross section of the potential temperature field of a strong, large amplitude wave over Boulder, Colorado, which seems to fit the present example quite well. Clouds are preserved or generated up to the crest of the Continental Divide; a strong downdraft is implied to the lee over Boulder and then a second cloud generated in a strong updraft region still further to the lee. Note that the regions of turbulence extend from the clear slot at the base of the downslope area into the region of strong upward motion downstream. Other higher levels of clear air turbulence were also found tilting westward from the clear slot above the lee slope.

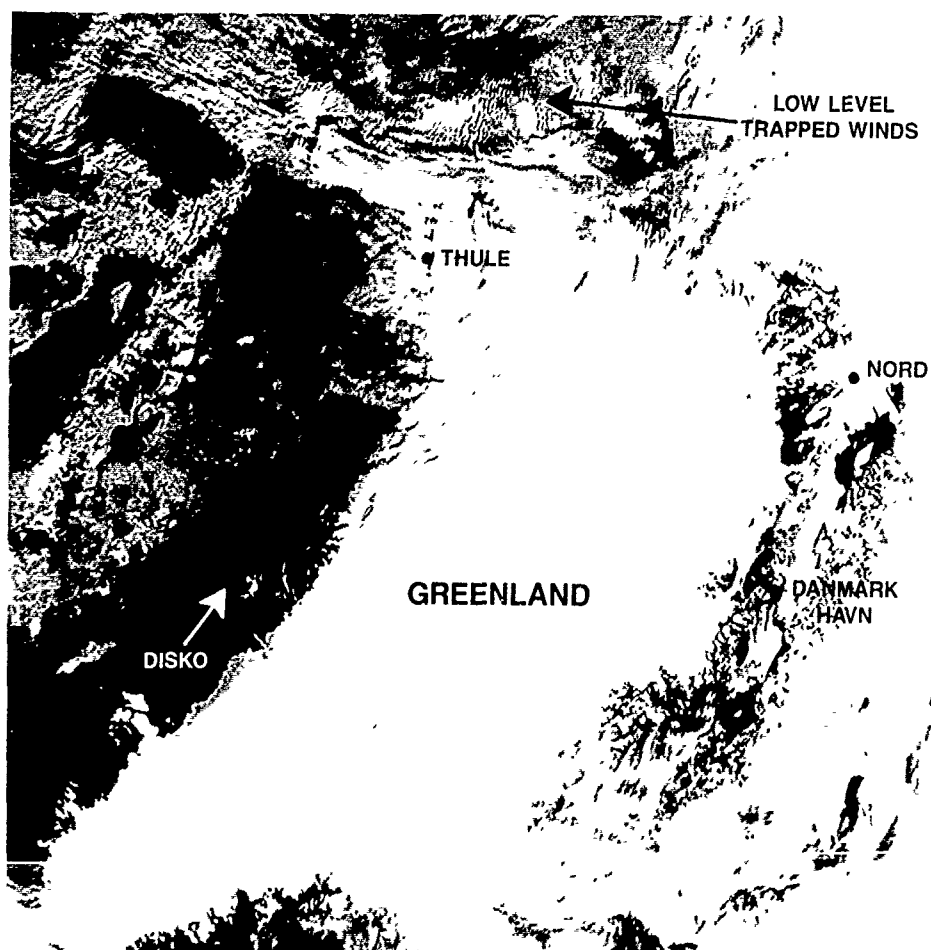
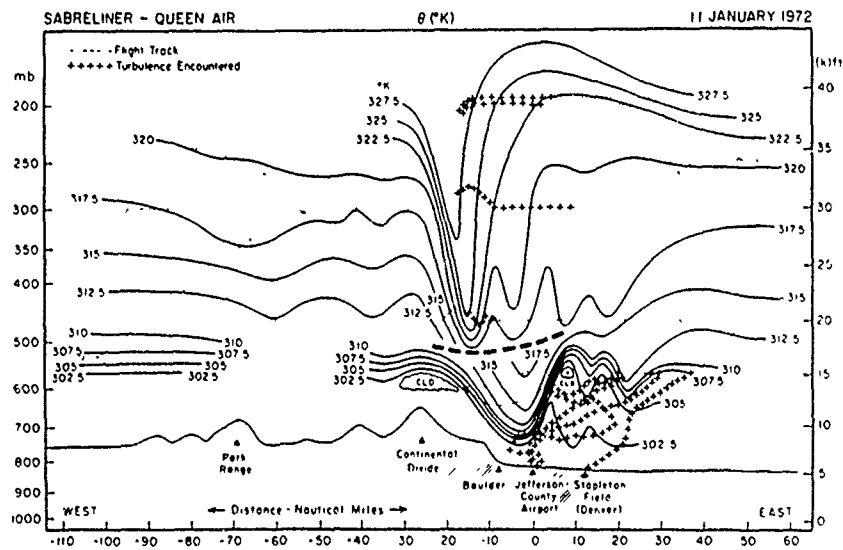
A careful view of the region to the north of the cold cloud plumes reveals a lower field of trapped wave clouds. These clouds are even more apparent in the visible DMSP view of the area taken a little earlier, at 1004 GMT (Fig. 3B-4b). The lower level trapped waves are also oriented northwest-southeast implying that they have formed in northwesterly flow.

A still earlier DMSP visible (LS) view of the region, at 0500 GMT (Fig. 3B-5a), reveals additional details of importance. First the low center position north of the mountain waves can be pinpointed by the clear-cut cloud vortex appearing in the upper left portion of the image. The position of the vortex agrees quite well with the FNOC surface analysis for 1200 GMT (Fig. 3B-6a), which shows a low center just northwest of Ellesmere Island. Using the wave clouds and adjoining banded cloudiness effects as indicators, early arctic frontogenesis can be positioned across northern Greenland, extending down to near the Melville Peninsula of the Northwest Territories. This is shown on the surface analysis in Fig. 3B-6a. The high shown on this computer-drawn analysis near 65°N 8°W is grossly exaggerated and was much de-emphasized on the corresponding NMC analysis for that time (not shown). The NMC charts showed a trough emanating from the low near Ellesmere Island until 15 July at 0000 GMT (Fig. 3B-7a) when arctic frontogenesis was first depicted. Using the DMSP satellite data, this occurrence was apparent more than 12 hr earlier.

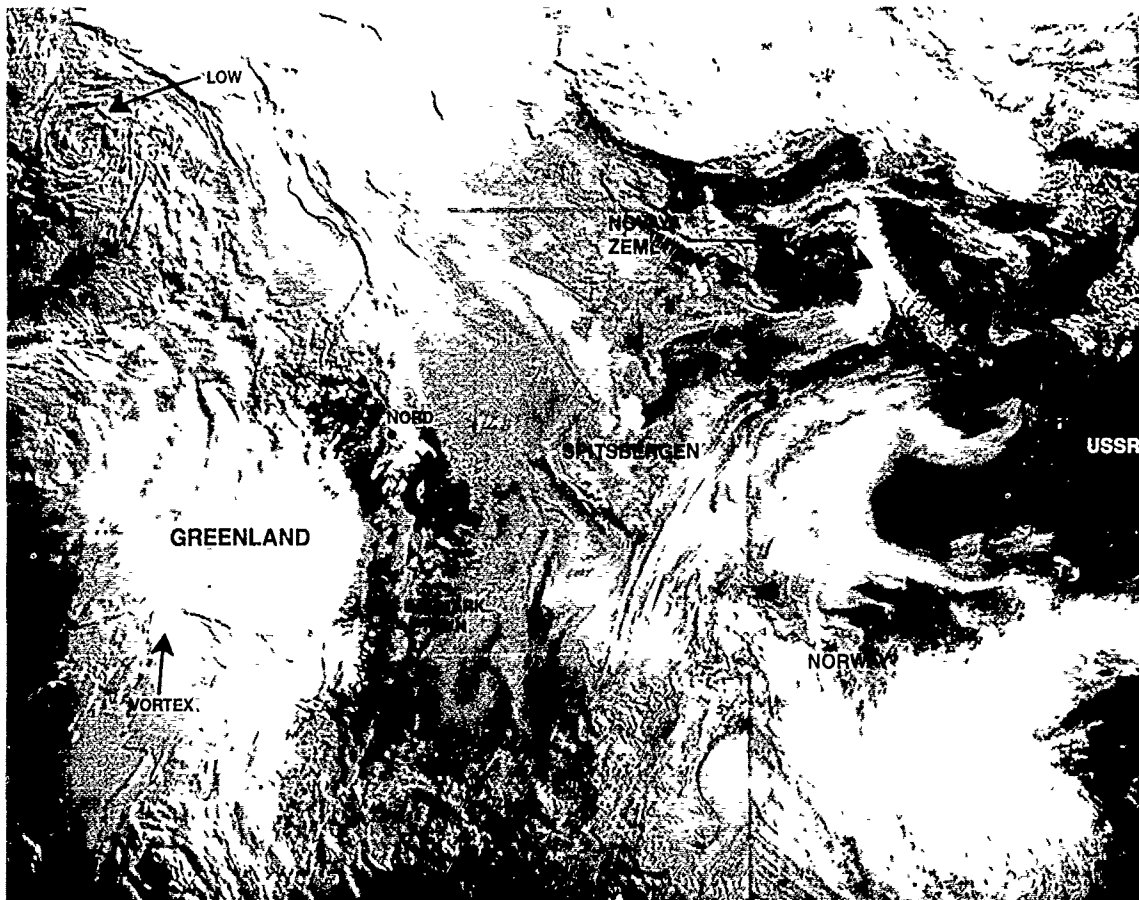


3B-3a Map of Canadian Archipelago

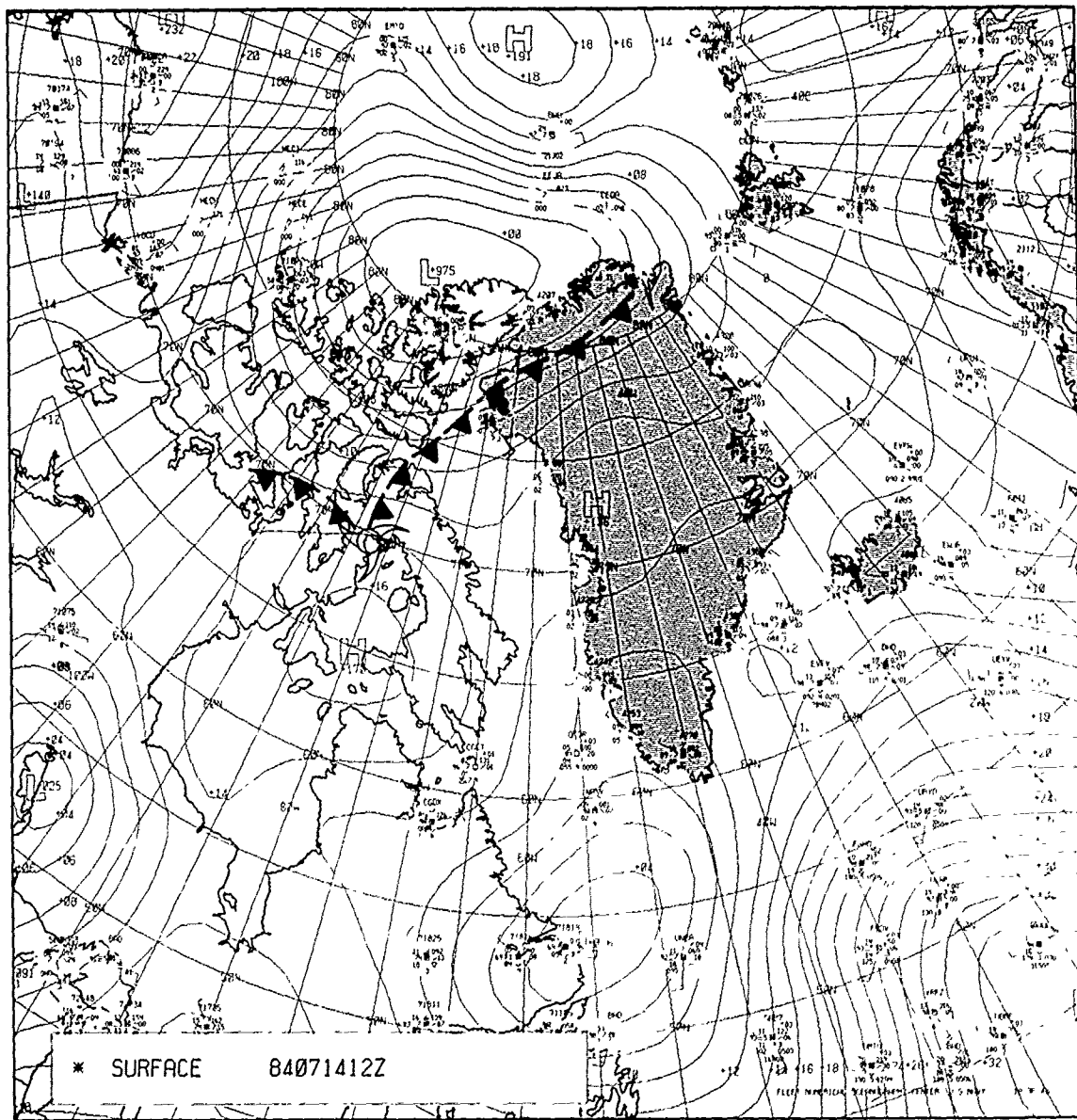
3B-4a Cross Section of Potential Temperature Over Boulder, Colorado (after Lilly and Zipser, 1972)



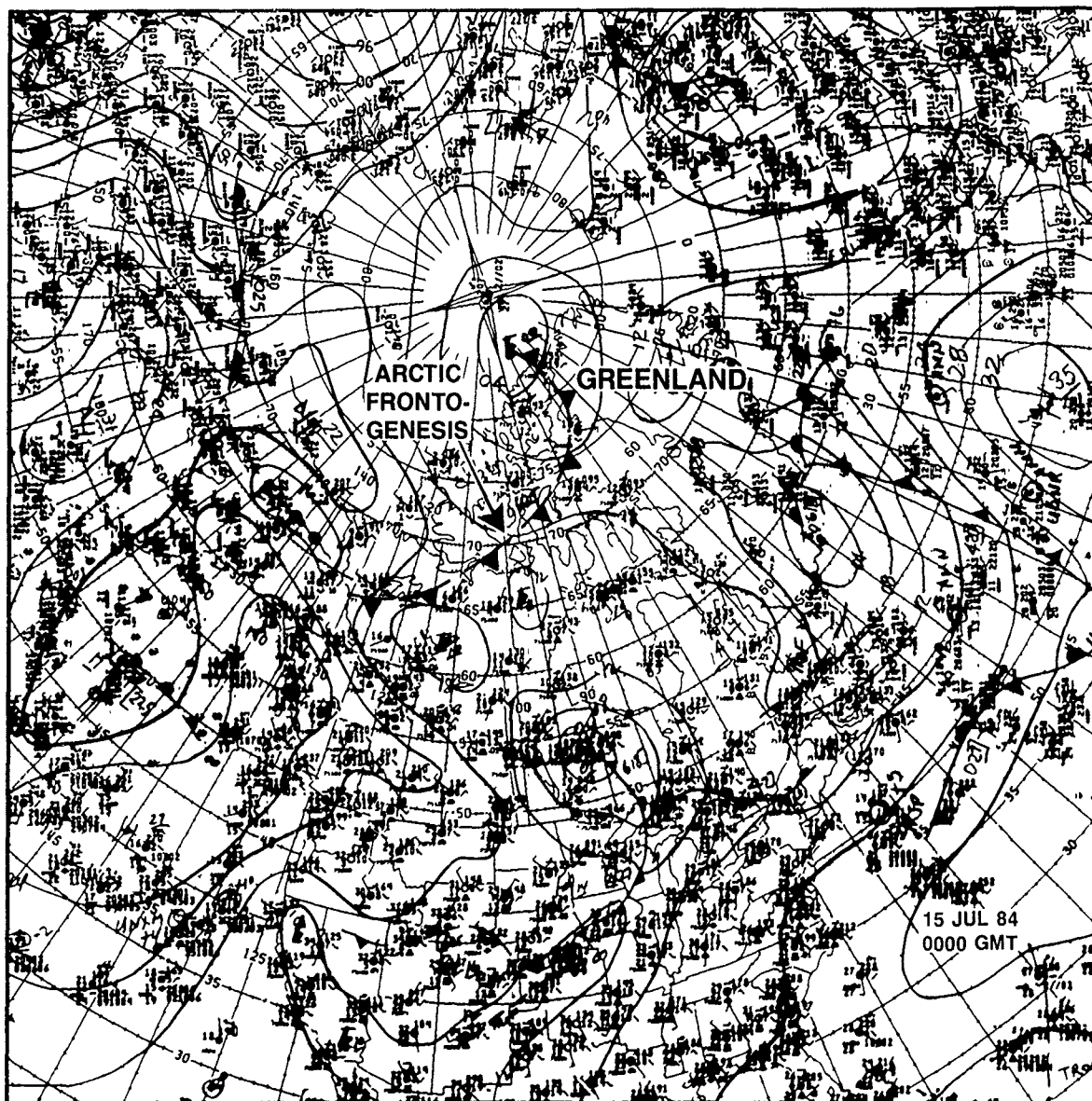
3B-4b. DMSP Visible (LS) data 1004 GMT 14 July 1984



3B-5a DMSP Visible (LS) Data 0500 GMT 14 July 1984



3B-6a. FNOC Surface Analysis 1200 GMT 14 July 1984



3B-7a NMC Surface Analysis 0000 GMT 15 July 1984



Returning again to Fig. 3B-5a, the anticyclonic turning of some of the cloud plumes southward over northern Greenland suggests that there is a divergence asymptote at upper levels with part of the southwesterly current turning northward around the low center and part southward toward a cloud vortex visible over the ice cap of central Greenland.

Conditions aloft at the 500-mb level are shown in Fig. 3B-8a. The analysis indicates that the 500-mb contours are vertically stacked over the surface low. This condition implies little change in wind direction with height, which is conducive for vertically propagating wave development. A 40-kt isotach maximum is shown to be approaching Devon Island where the first wave cloud occurred (Fig. 3B-2a). Crosses mark positions of peaks northwest of the large group of cloud plumes. These peaks show little evidence of major wave cloud formation (of the vertically propagating type), and this is in an area of reduced wind speed where direction is also shifting to more southerly.

A divergence asymptote is clearly revealed ahead of the wind maximum as suggested by the satellite data (Fig. 3B-5a). The low over central Greenland is also apparent on this analysis.

The situation shows little change at the 300-mb level (Fig. 3B-9a) except for slightly stronger wind speeds.

The example suggests that vertically propagating, high amplitude mountain waves are related to jet streaks of at least moderate strength blowing perpendicular to the ridge lines. Using reverse reasoning satellite detection of such cloud formations enables the satellite meteorologist to detect high wind speed areas over mountainous terrain in the Arctic and also reveal additional details concerning the operationally important location of the arctic front.

#### 15 July 1984

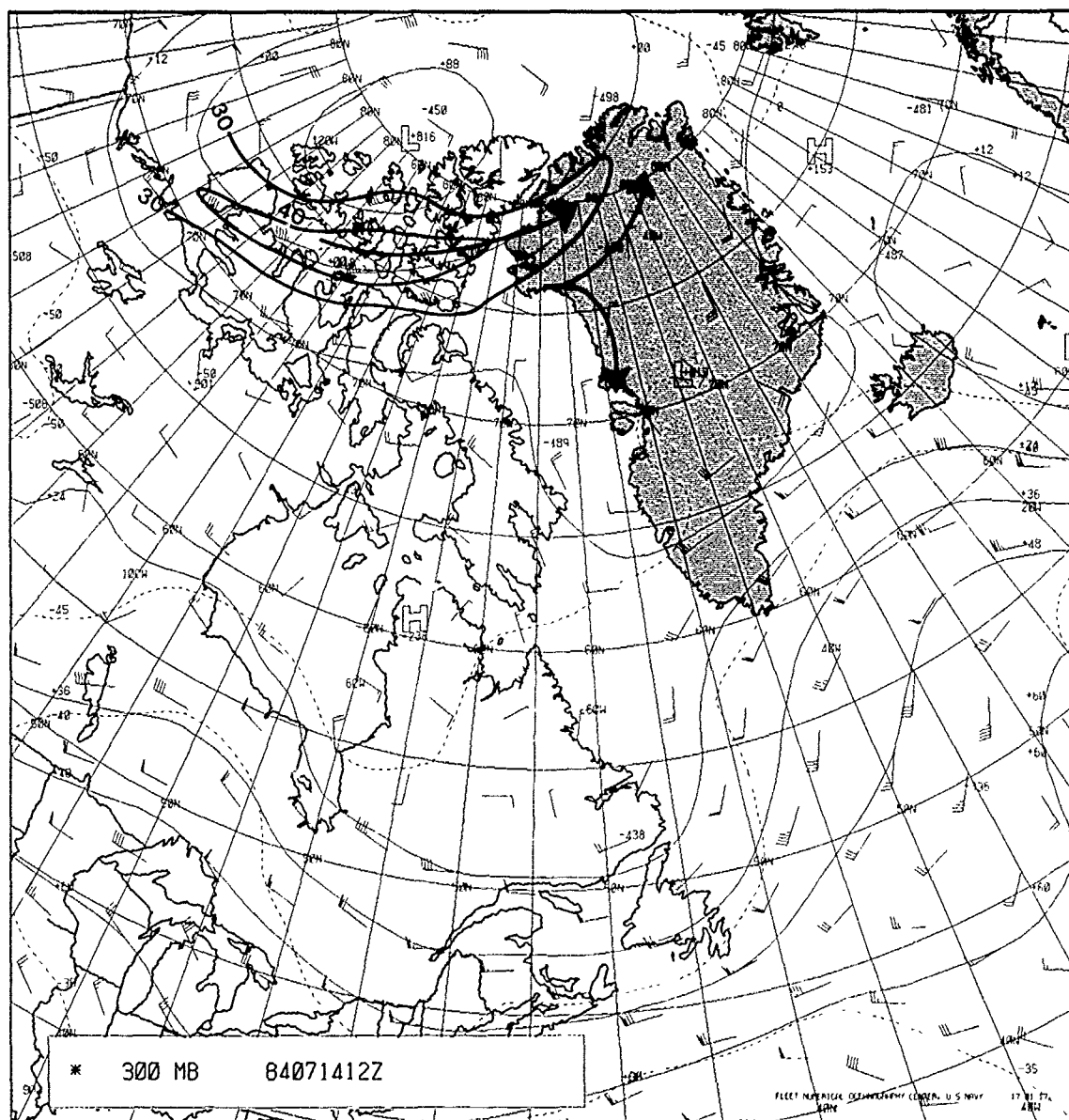
The DMSP infrared view at 0802 GMT on the following day (Fig. 3B-10a) shows persistence of mountain waves (and hence high wind speeds) over northern Greenland from a southwesterly to westerly direction. Interestingly, a large mountain wave is found close to the center of the northernmost cloud vortex. This cloud has formed in the lee of a ridge on Axel Heiberg Island, with one peak in the ridge reaching 8400 ft. The surface analysis (Fig. 3B-11a) shows the low positioned northwest of the island in reasonable agreement with the satellite data. A moderate pressure gradient extends from the low to the northern portion of Greenland. The position of the arctic front has been drawn on the analysis based on the satellite data. Fig. 3B-12a shows an independent surface analysis at the same time by NMC. NMC's position is in reasonably close agreement with the satellite-derived position.

At 1200 GMT 500-mb data (Fig. 3B-13a) and simultaneous 300-mb data (Fig. 3B-14a) confirm moderate 30- to 45-kt winds at those levels, associated with the arctic front. These winds, of course, are computer derived and one might expect some errors in a region of such sparse data. In particular the 15- to 20-kt winds indicated over Axel Heiberg Island seem too low to support the satellite-observed mountain wave cloud noted over the island.

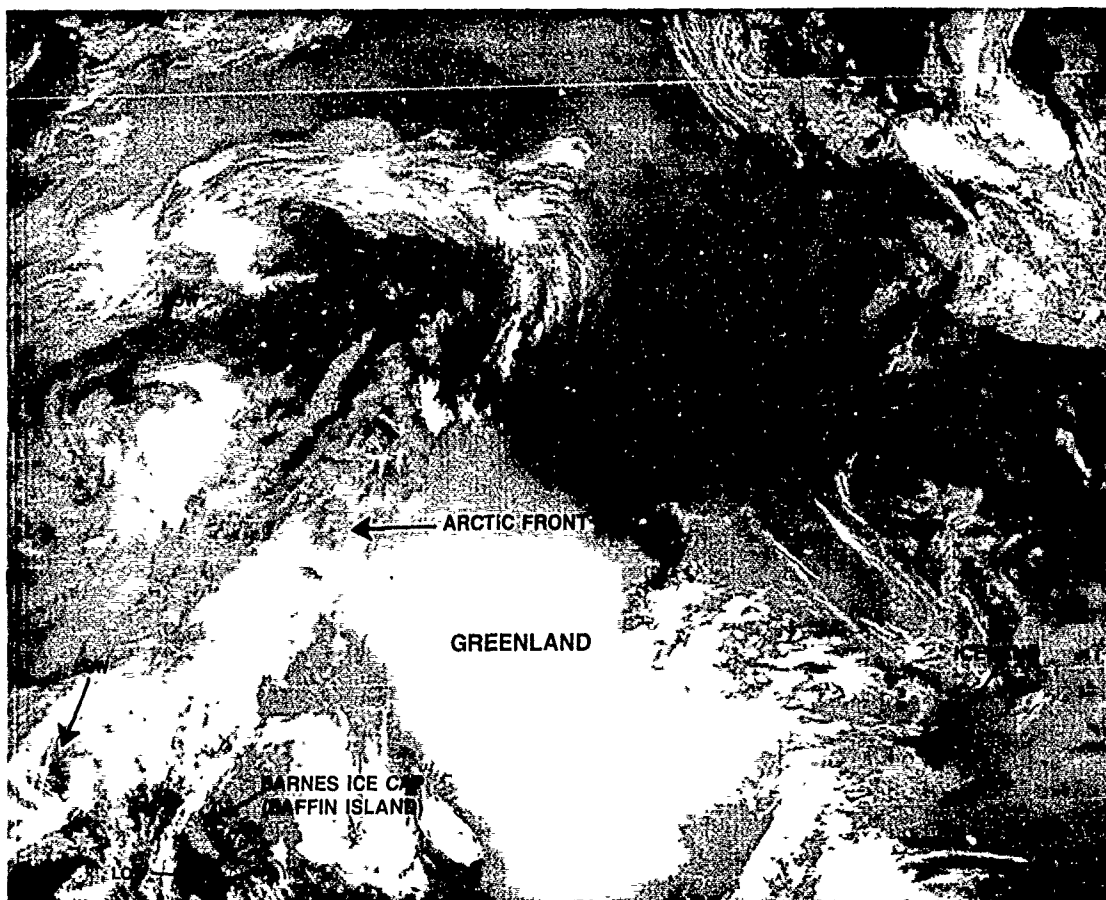
Probably mountain waves were induced over the mountains of Devon Island and Ellesmere, which according to the analyses were subject to similar winds. However, the arctic front and, hence, moisture was to the south of these islands. Mountain waves could therefore be induced, but these would occur in clear air as a result of lack of moisture. The hazard for aircraft remains the same.

The vortex, previously noted over central Greenland, is still suggested on the 500- and 300-mb analyses (Figs. 3B-13a and 3B-14a), but difficult to discern in the satellite image for 0802 GMT (Fig. 3B-10a). Two additional vortices can be detected in this image, one near Barnes Ice Cap on Baffin Island and another one to the west along 70°N.



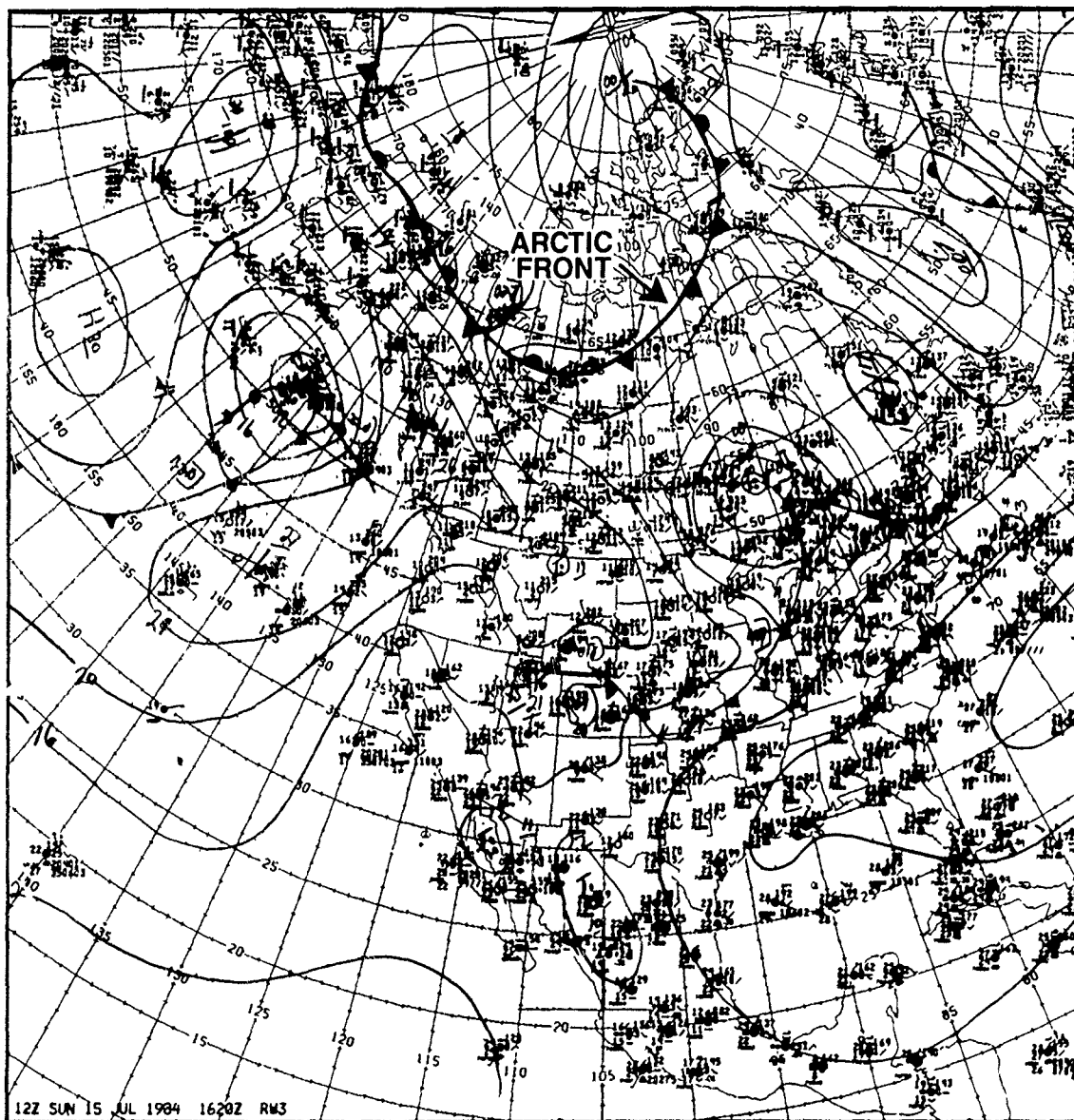


3B-9a. FNOC 300-mb Analysis. 1200 GMT 14 July 1984.

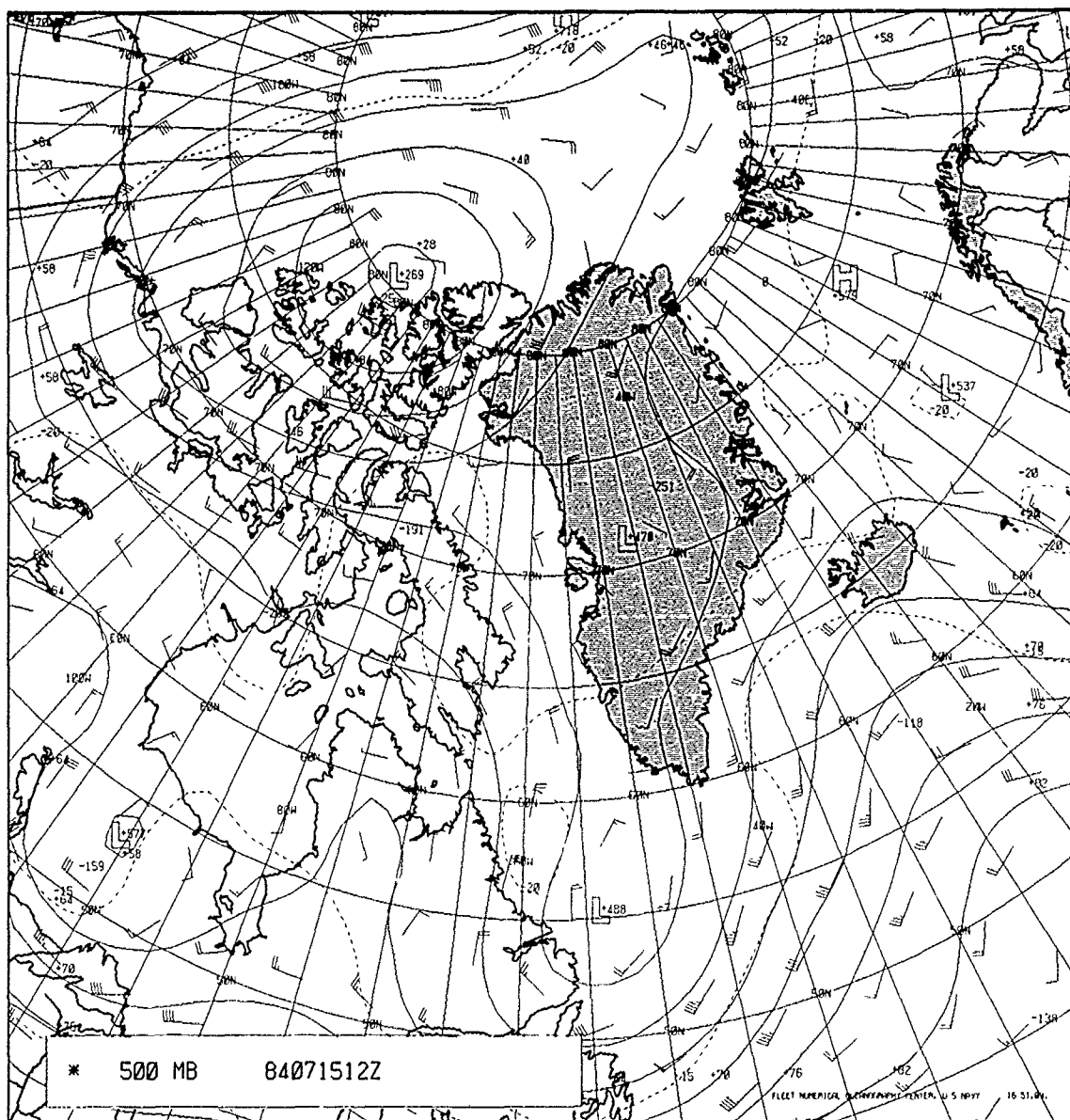


3B-10a DMSP Infrared (TS) Data 0802 GMT 15 July 1984

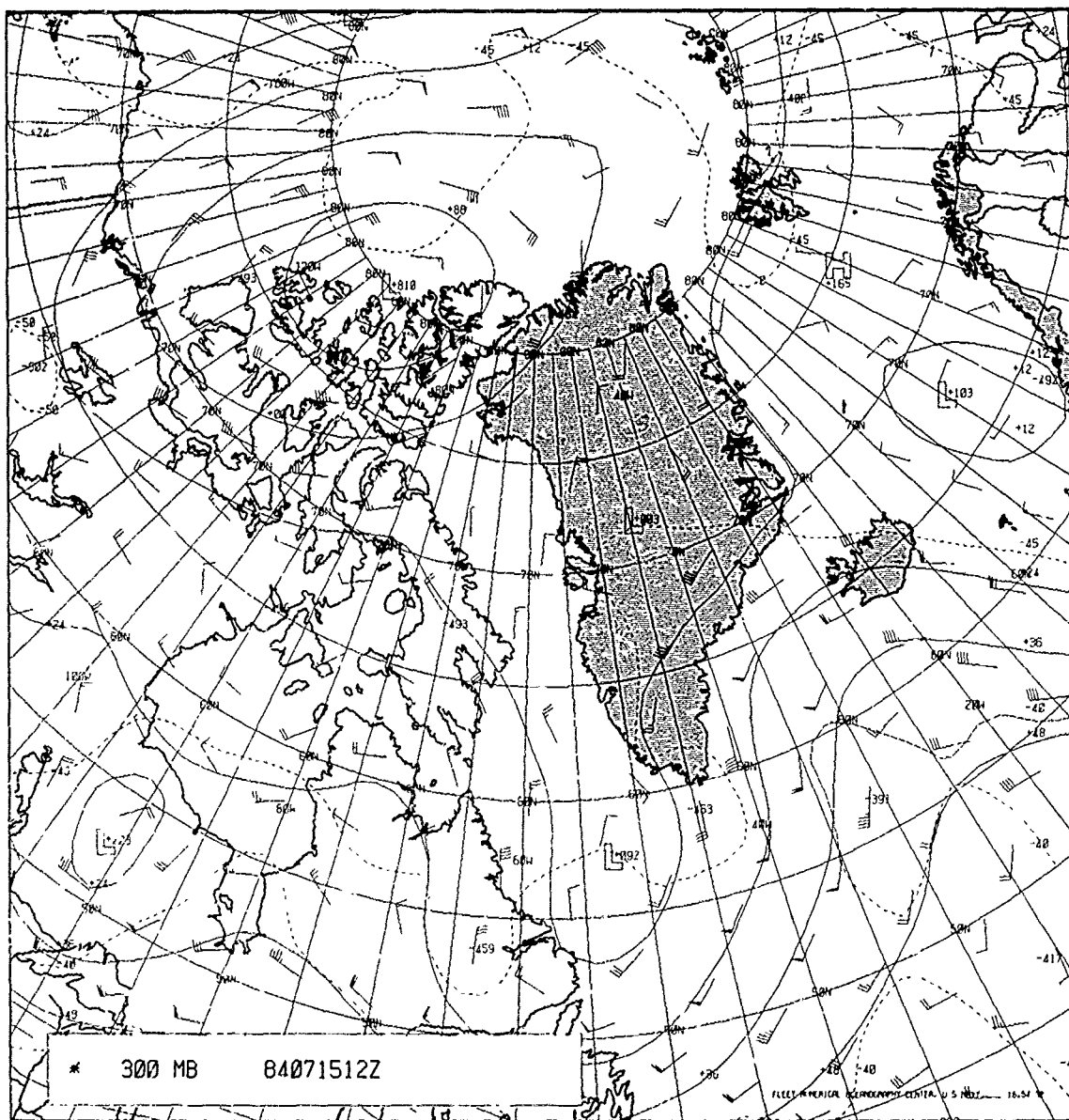




3B-12a NMC Surface Analysis. 1200 GMT 15 July 1984



3B-13a. FNOC 500-mb Analysis. 1200 GMT 15 July 1984



3B-14a FNOC 300-mb Analysis 1200 GMT 15 July 1984

These vortices can be seen again in DMSP infrared data for 0944 GMT (Fig. 3B-15a). This image shows some cloud striations along western Greenland suggesting the remnants of an upper level vortex over the central part of the island. Note that the wave cloud pattern seems to be abating at the time of this image suggesting a weakening of the air flow and arctic front over northern Greenland.



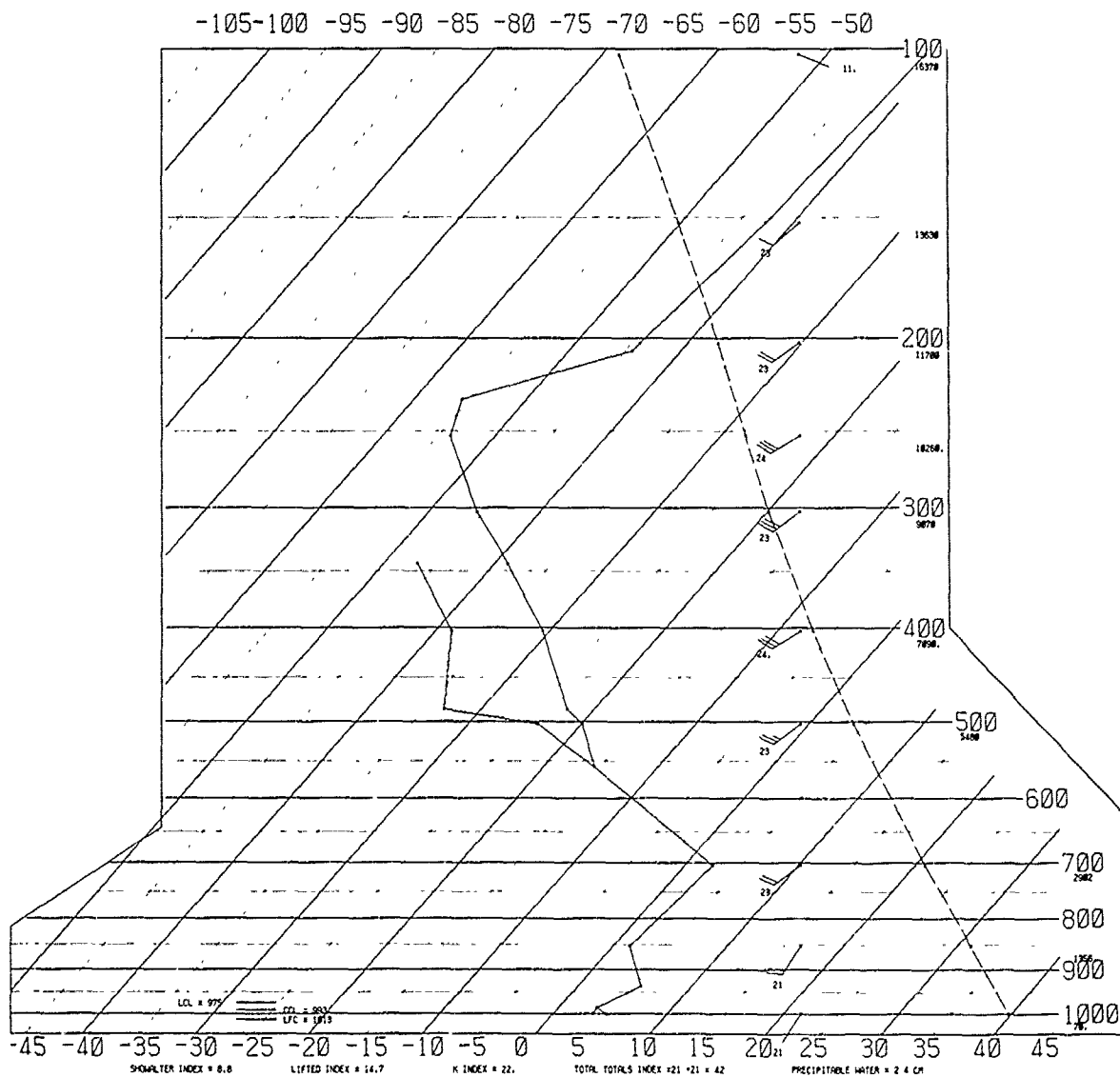
3B-15a. DMSP Infrared Data 0944 GMT 15 July 1984.

# SKREW T, LOG P DIAGRAM

840715

1200Z

4202



3B-16A Radiosonde Analysis, Thule, Greenland. 1200 GMT 15 July 1984.



Thule's sounding for 1200 GMT (Fig. 3B-16a) shows 25-kt winds at the 500-mb level and 30-kt winds at the 300-mb level, which are somewhat stronger than suggested in the computer analyses. The dew point depression was missing at lower levels, but the sounding does show pronounced stability to 700 mb of the type to be expected in mountain wave formation.

#### *16 July 1984*

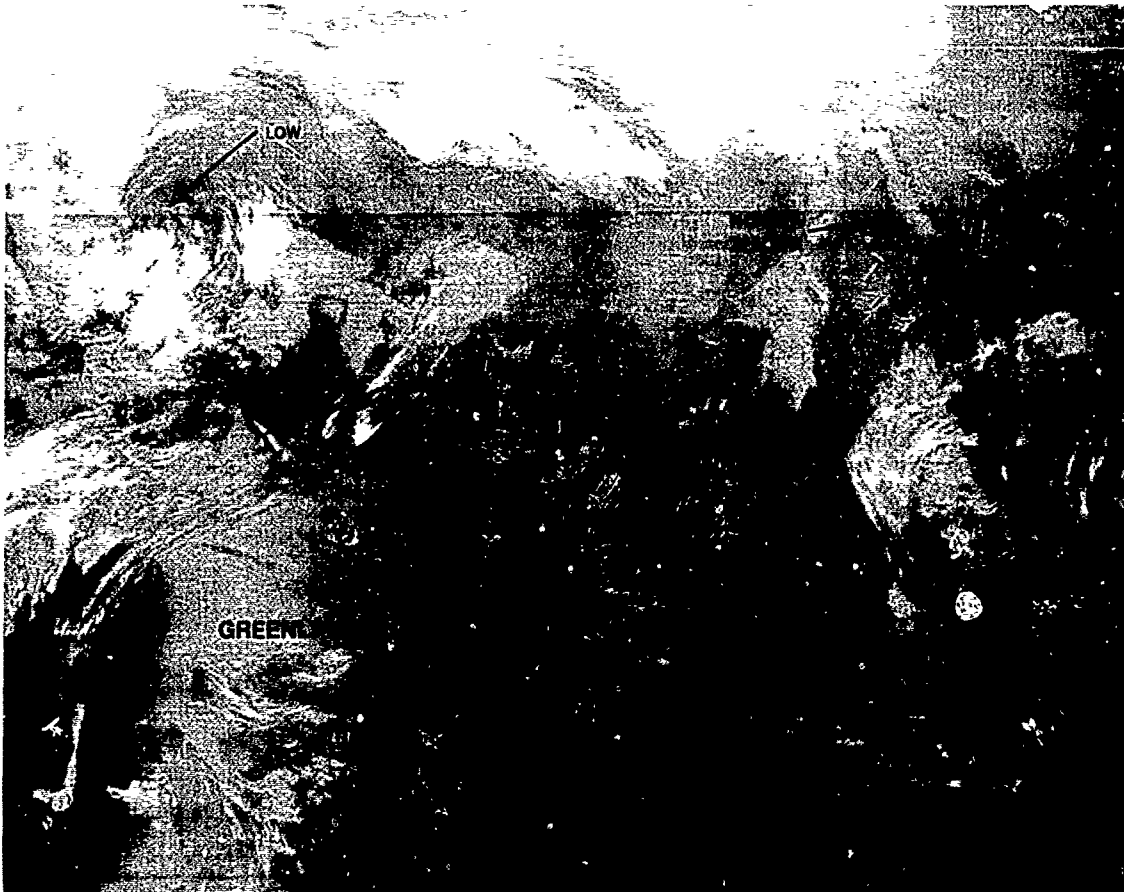
An early morning (0133 GMT) DMSP infrared view on this date (Fig. 3B-17a) shows the low still defined northwest of Greenland. Some wave cloud activity is evident over northern Greenland.

A few hours later at 0419 GMT DMSP visible data (Fig. 3B-18a) show the area in sunlight. Shadows of the wave clouds are clearly evident indicating their vertical development.

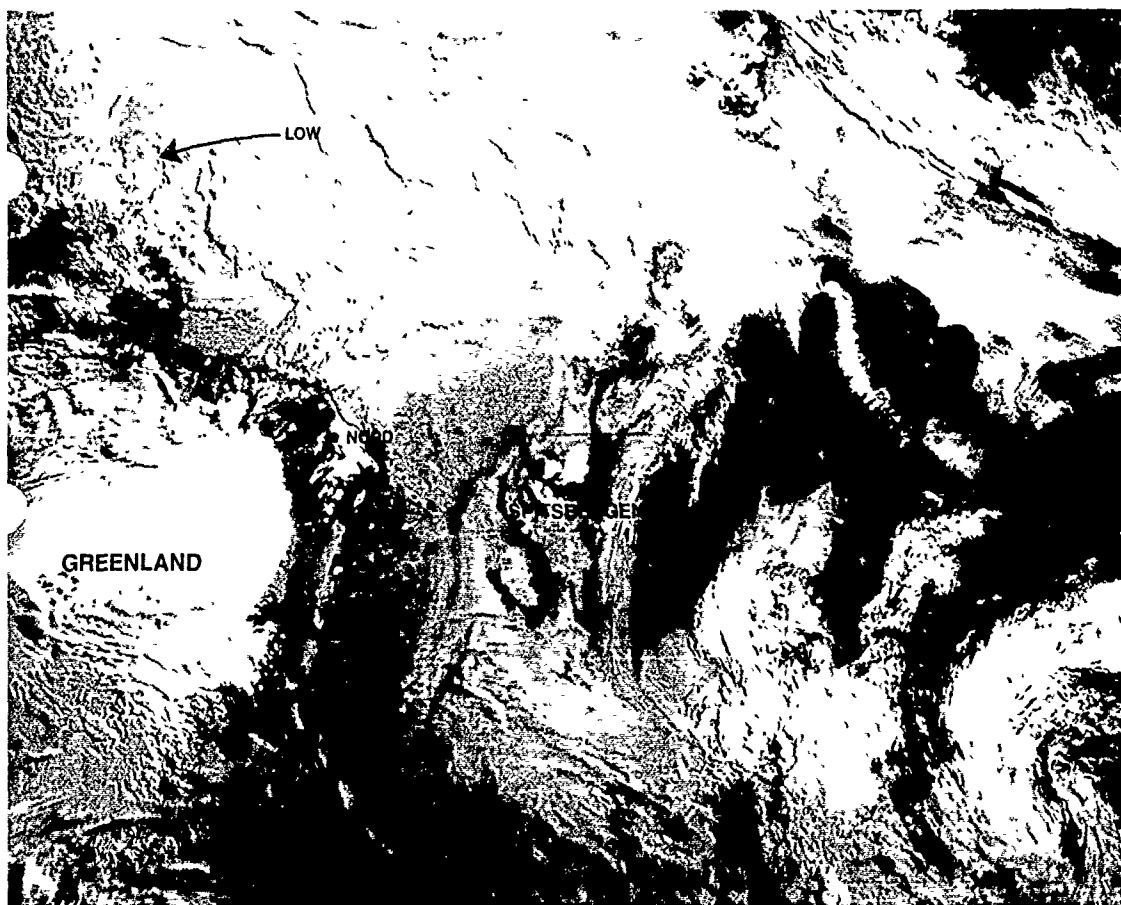
At 0637 GMT additional DMSP visible data (Fig. 3B-19a) seem to indicate the weak low previously noted over central Greenland, now with an apparent center near the central western coast. The vortex is low level as can be seen by simultaneous infrared data (Fig. 3B-20a), which reveal the warm clouds swirling around the center. The warm flat-appearing clouds are evidence that they have formed under a low-level inversion. Wave clouds still persist over northern Greenland, apparently generated by persisting moderate southwesterly flow. However, they do not exhibit the cold temperatures previously noted—an indication of weakening wind speeds aloft. Observations of the DMSP satellite views showed that the northern portion of the arctic front never passed Nord. The western portion, however, did penetrate slowly into central Canada. Its position had been followed quite well by NMC analysts. Figure 3B-21a shows the front still being maintained as it pushes into northern Hudson Bay.

#### **Important Conclusions**

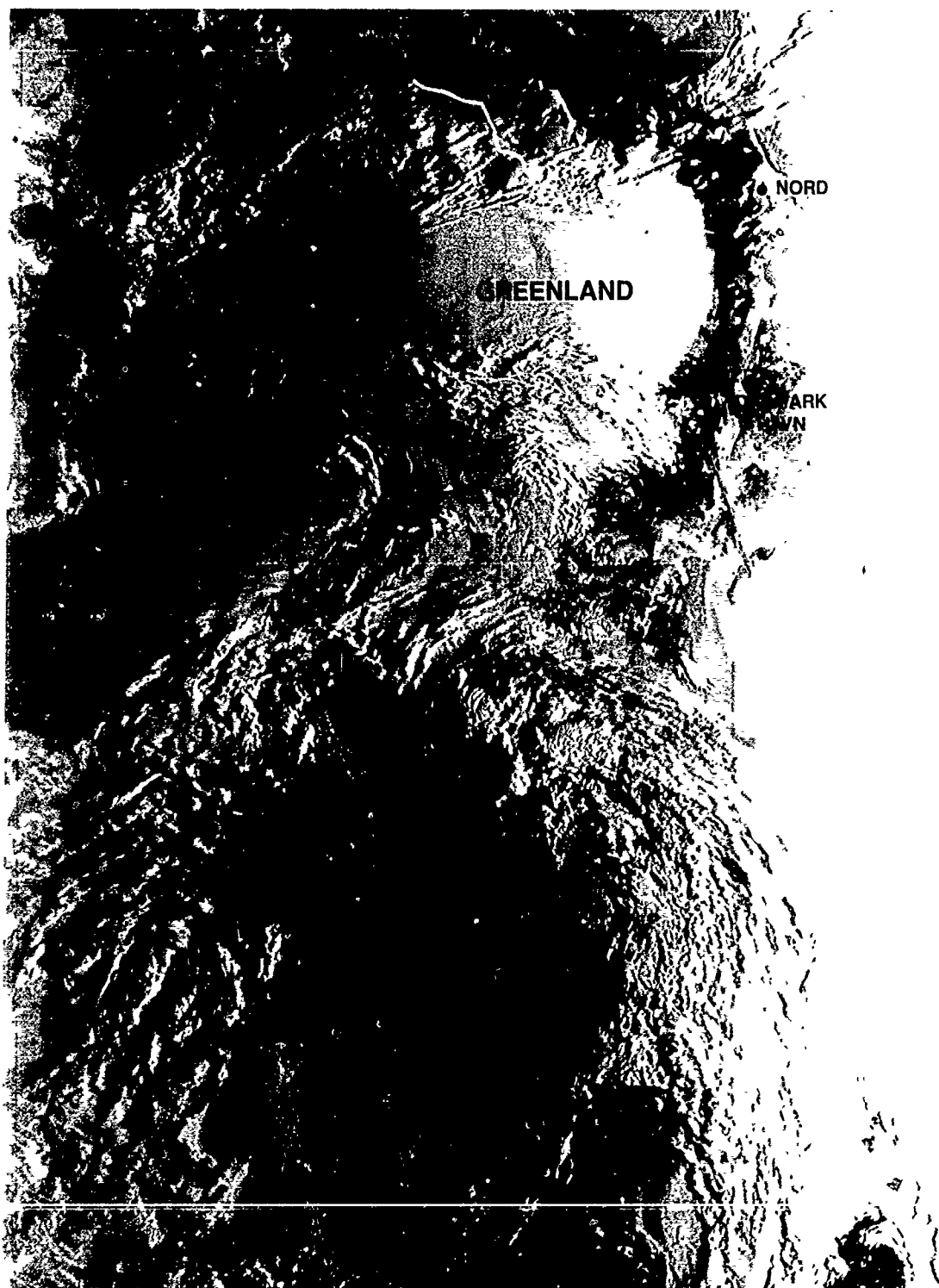
1. Two categories of mountain waves have been defined:
  - a. The trapped wave, a lower level phenomenon existing under an inversion; and
  - b. the vertically propagating, high amplitude wave that can have effects extending to high altitudes.
2. The high amplitude, vertically propagating wave is dangerous for aircraft operations because of associated strong and persistent downdrafts and heavy turbulence.
3. Satellite data are extremely useful in pinpointing areas and precise locations where mountain waves are occurring. This provides the clue to detection of arctic fronts with strong winds aloft.
4. Shifting synoptic patterns or erroneous analyses can often be detected by using mountain wave plumes as indicators of atmospheric conditions over a given area.



3B-17a. DMSP Infrared (TS) Data, 0133 GMT 16 July 1984.



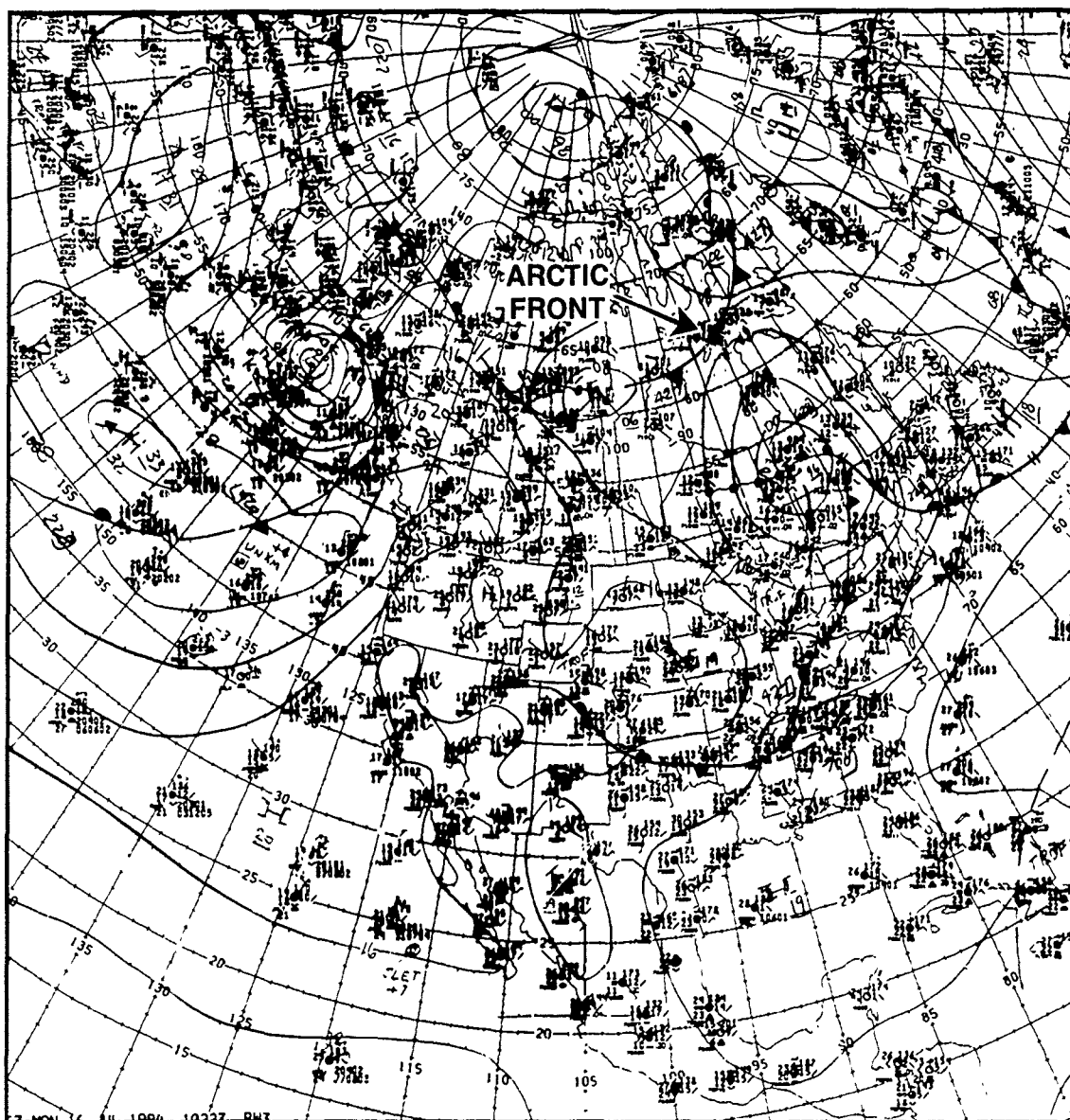
3B-18a DMSP Visible (LS) Data. 0419 GMT 16 July 1984



3B-19a DMSP Visible (LS) Data 0637 GMT 16 July 1984



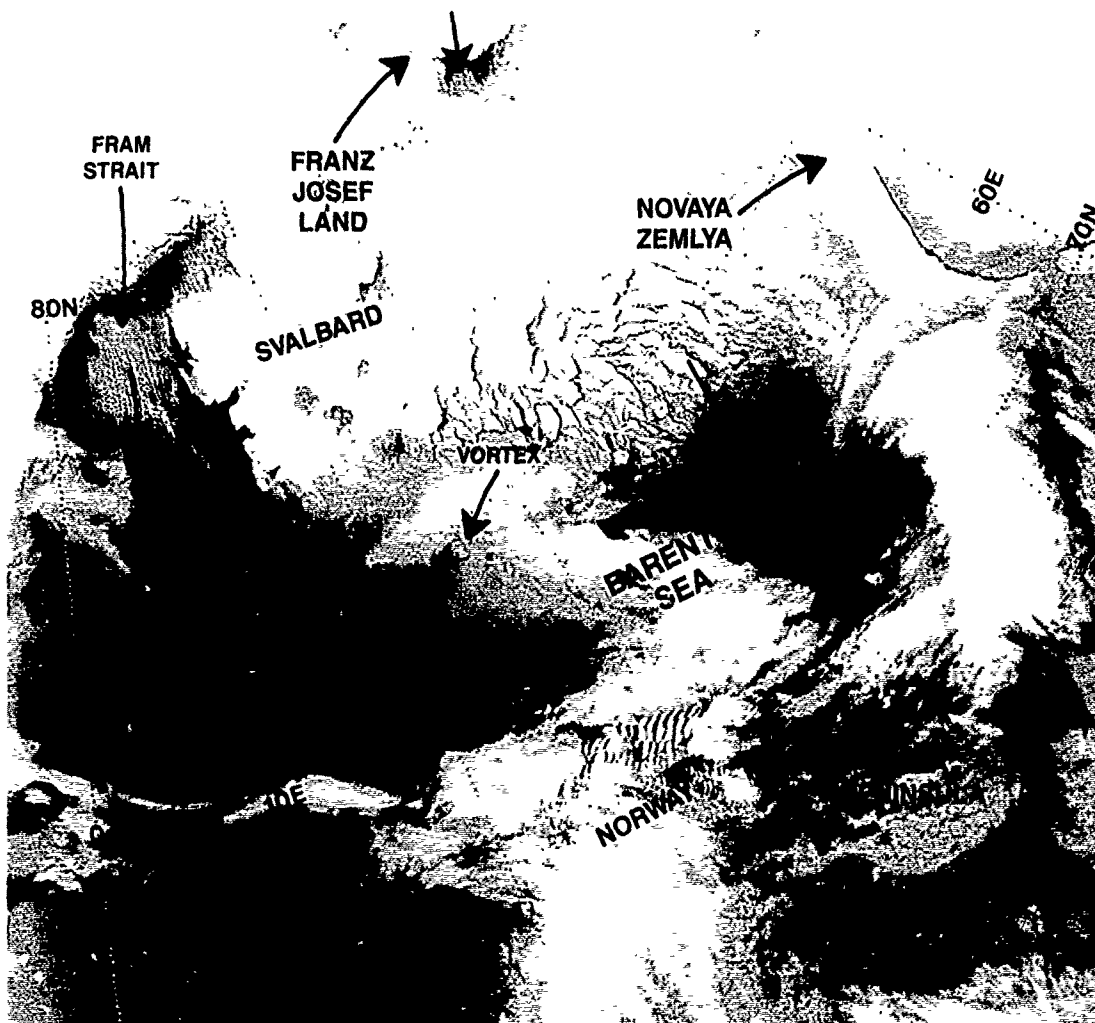
3B-20a. DMSP Infrared (TS) Data. 0637 GMT 16 July 1984.



3B-21a NMC Surface Analysis, 0600 GMT 16 July 1984.

#### References

Lilly, D.K., and E.J. Zipser. 1972 The front range windstorm of 11 January 1972—A meteorological narrative *Weatherwise*, 25, 56-63



3B-22a. NOAA-9 HRPT (Ch 4) Data. 0320 GMT 10 April 1987.

*Case 2 Use of Topographic and Polynya-Associated Cloud Plumes  
in Surface Wind Flow Determination and in Jet Stream/Arctic  
Front Detection (10-12 April 1987)*

*10 April 1987*

NOAA-9 HRPT infrared (Ch 4) data, which were acquired at 0320 GMT (Fig. 3B-22a) over the Norwegian and Barents Sea region, show a cold surge in progress in the Fram Strait and northerly flow entering the Barents Sea west of Novaya Zemlya. Northerly flow is also shown by cloud plume alignment emanating from a polynya south of Franz Josef Land.

Westerly flow has produced a region of trapped wave clouds over northern Norway along the remnants of an old arctic front with wave-like protuberances to the north of it, suggesting low pressure or vorticity centers, one near 74°N 23°E and the other near 72°N 47°E.

The FNOC surface analysis for 0000 GMT (Fig. 3b-23a) basically confirms these suggestions, except for the weak vorticity centers, and offers additional detail in revealing a low pressure center near 80°N 60°E, north of Novaya Zemlya. The surface observations show strong 30-kt westerly winds over northern Norway where the trapped wave cloud formations were noted. The development of such clouds is associated with a low-level inversion and a condition of increasing wind speeds with height.

The FNOC 500-mb analysis (Fig. 3B-24a) for the same time shows an upper cold low associated with the surface system near Franz Josef Land. The -35°C isotherm has been highlighted to emphasize the cold temperatures aloft. A northwesterly jet stream sweeps past southern Spitsbergen, over Bear Island, and southeastward into the Barents Sea. Jet-force winds exist over northern Norway where the trapped wave clouds were noted.

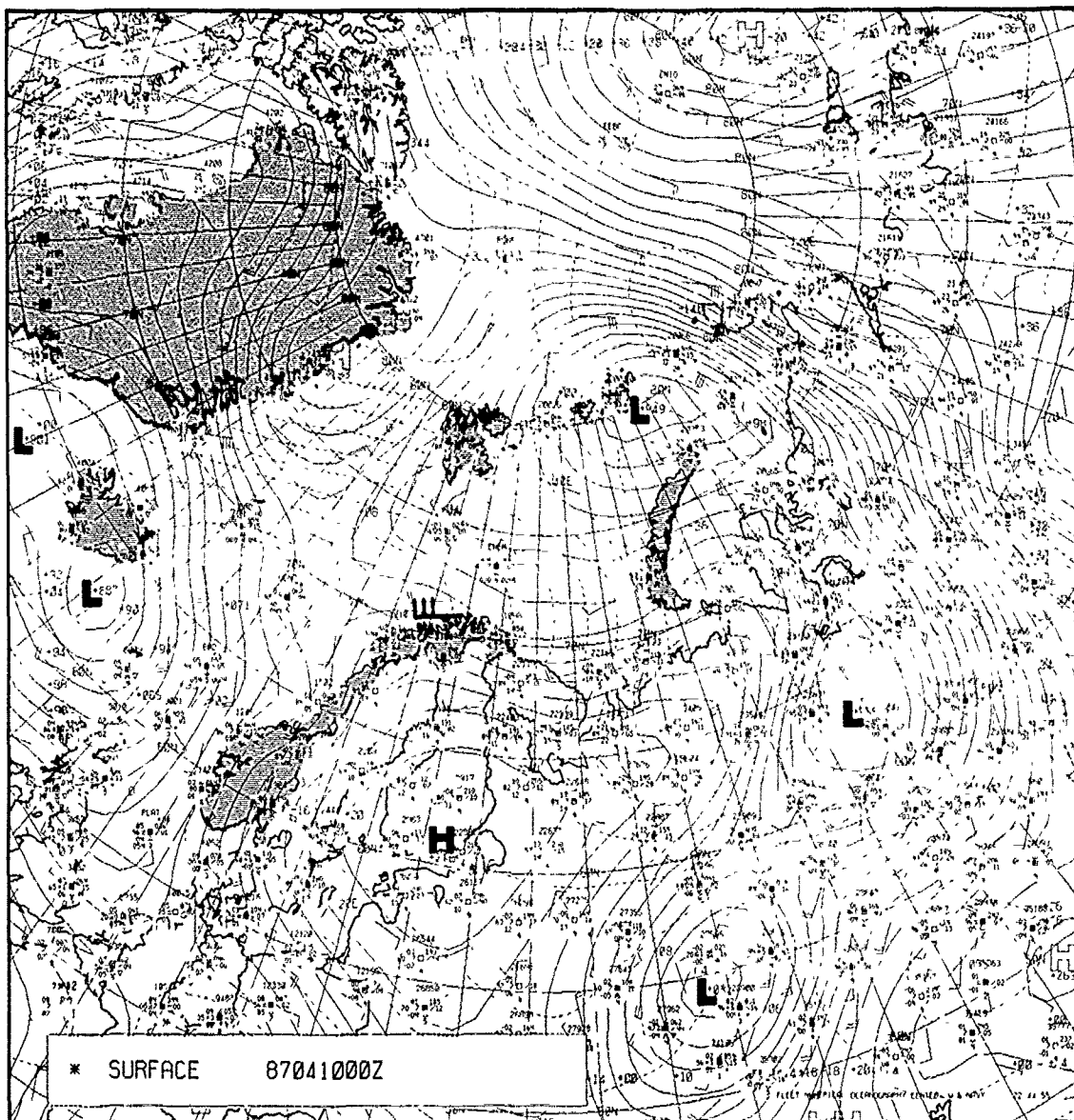
NOAA-10 HRPT infrared (Ch 4) data received at 0812 GMT (Fig. 3B-25a) show further evolution of features of flow. In particular a boundary layer front is apparent south of the Fram Strait. Divergence of flow from north-northwest to northeast, leading up to the BLF, is clearly revealed by alignment of cloud lines in the area. The BLF connects to the small vortex in the Barents Sea, also apparent in Fig. 3B-22a.

An orographically produced cloud plume over Kvitoya, generated by high speed winds aloft, suggests the position of a jet stream and new arctic front. Meanwhile, cloud plumes from the polynya south of Franz Josef Land continue to show northerly flow.

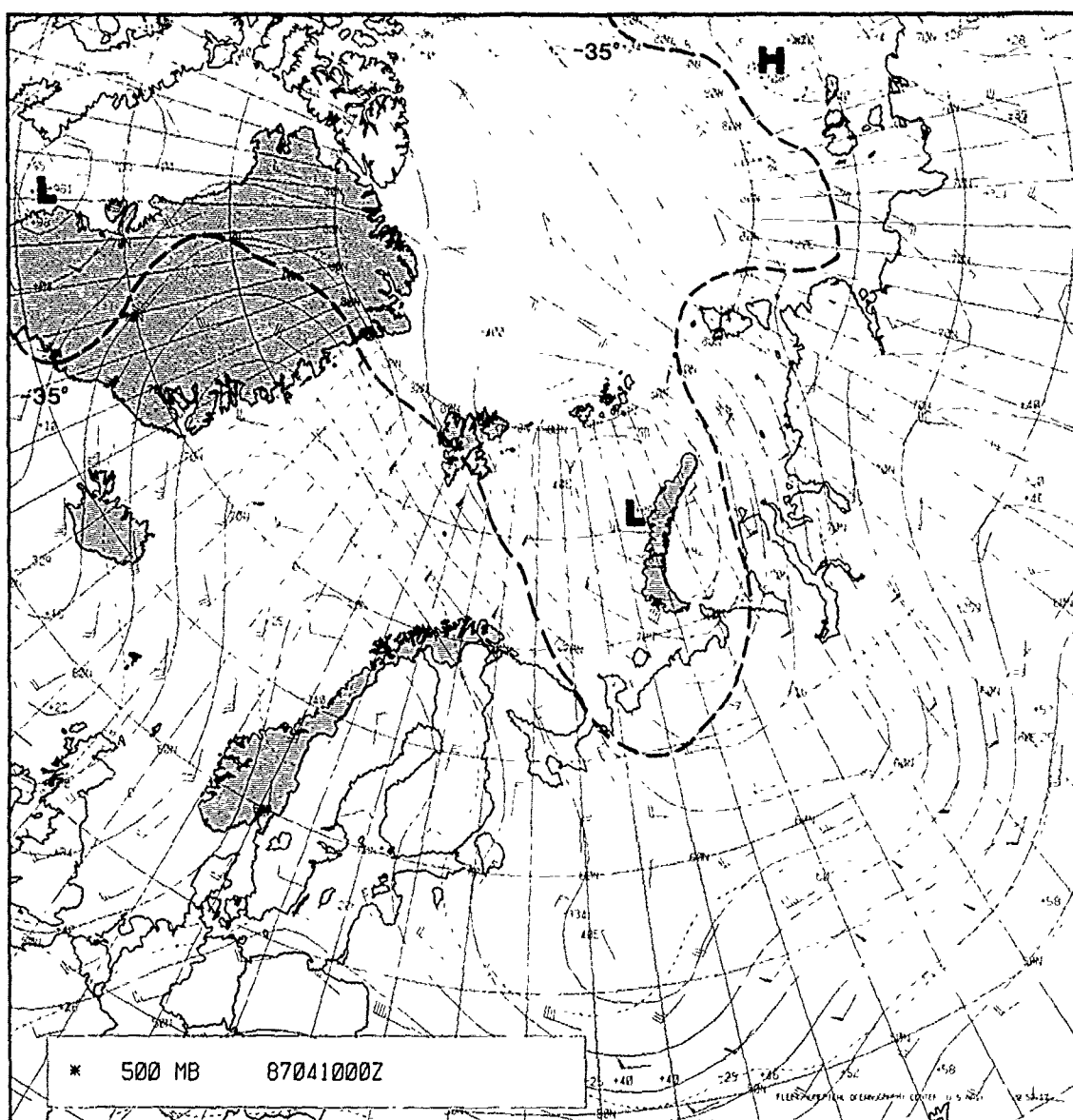
Finally, cloud plumes over southern Novaya Zemlya suggest southwesterly flow, reflecting the trough leading into the eastern-most system noted earlier over the Barents Sea southwest of Novaya Zemlya (Fig. 3B-22a).

NOAA-10 HRPT enhanced infrared (Ch 4) data at 0952 GMT (Fig. 3B-26a) show the very cold orographically produced cloud plume emanating from the island of Kvitoya. Note the implied difference in temperature between this orographically produced cloud plume and the cloud plume emanating from the polynya on the south side of Franz Josef Land. Kvitoya has an east-west-oriented topographic ridge line with average elevation of about 1350 ft over which the air, moving southward, must be lifted. The cloud plume top, however, apparently extends much higher. Measurement of the black-body temperature of this plume from satellite digital data yields a temperature of -36°C. This data implies an altitude of about 20,000 ft, near the 450-500-mb level, judging from soundings at Barentsburg, Spitsbergen, and Heyse, Franz Josef Land.

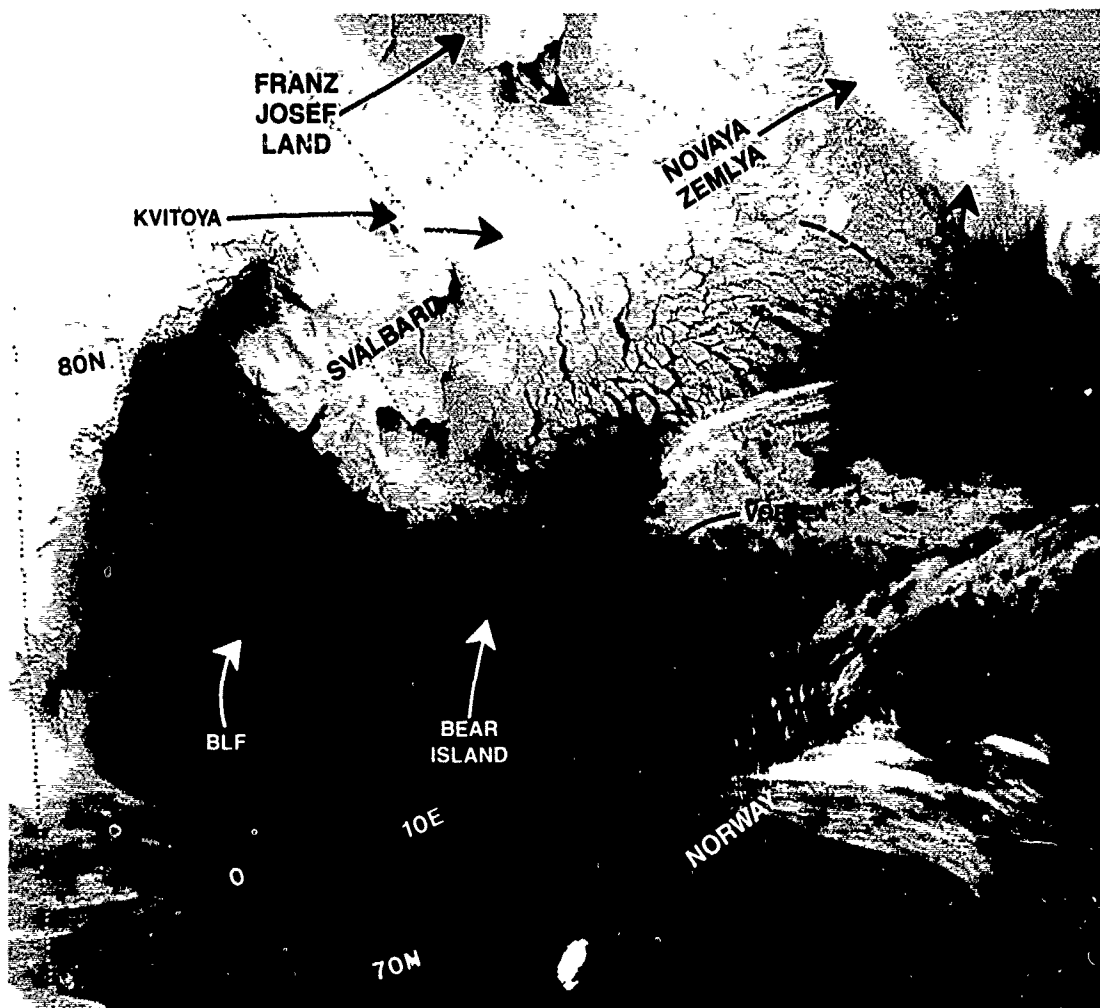




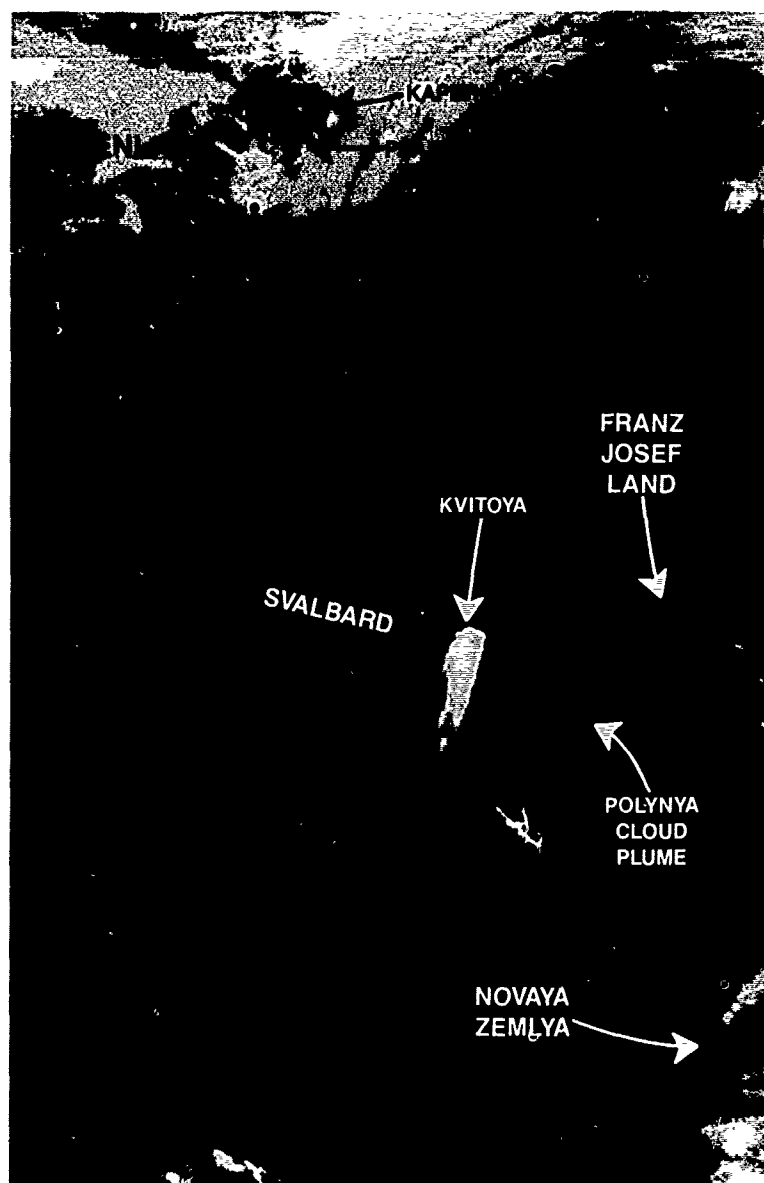
3B-23a FNOC Surface Analysis. 0000 GMT 10 April 1987.



3B-24a, FNOC 500-mb Analysis 0000 GMT 10 April 1987



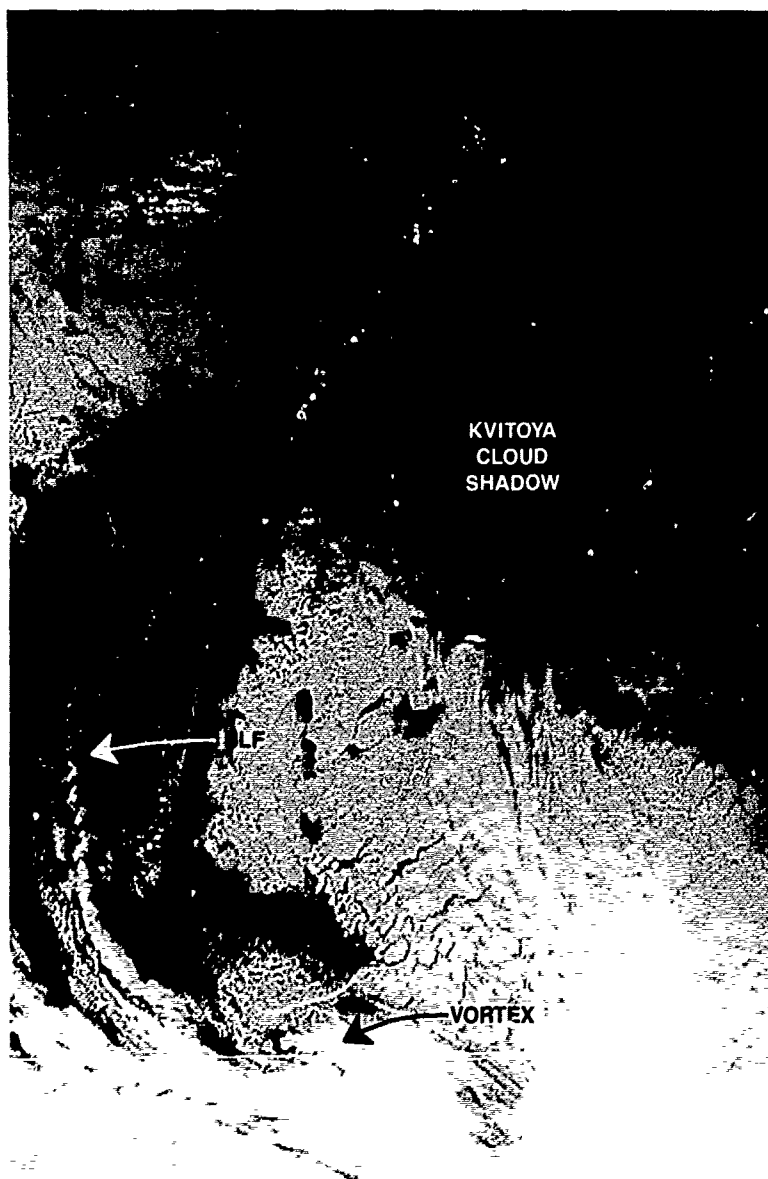
3B-25a. NOAA-10 HRPT (Ch 4) Data. 0812 GMT 10 April 1987.



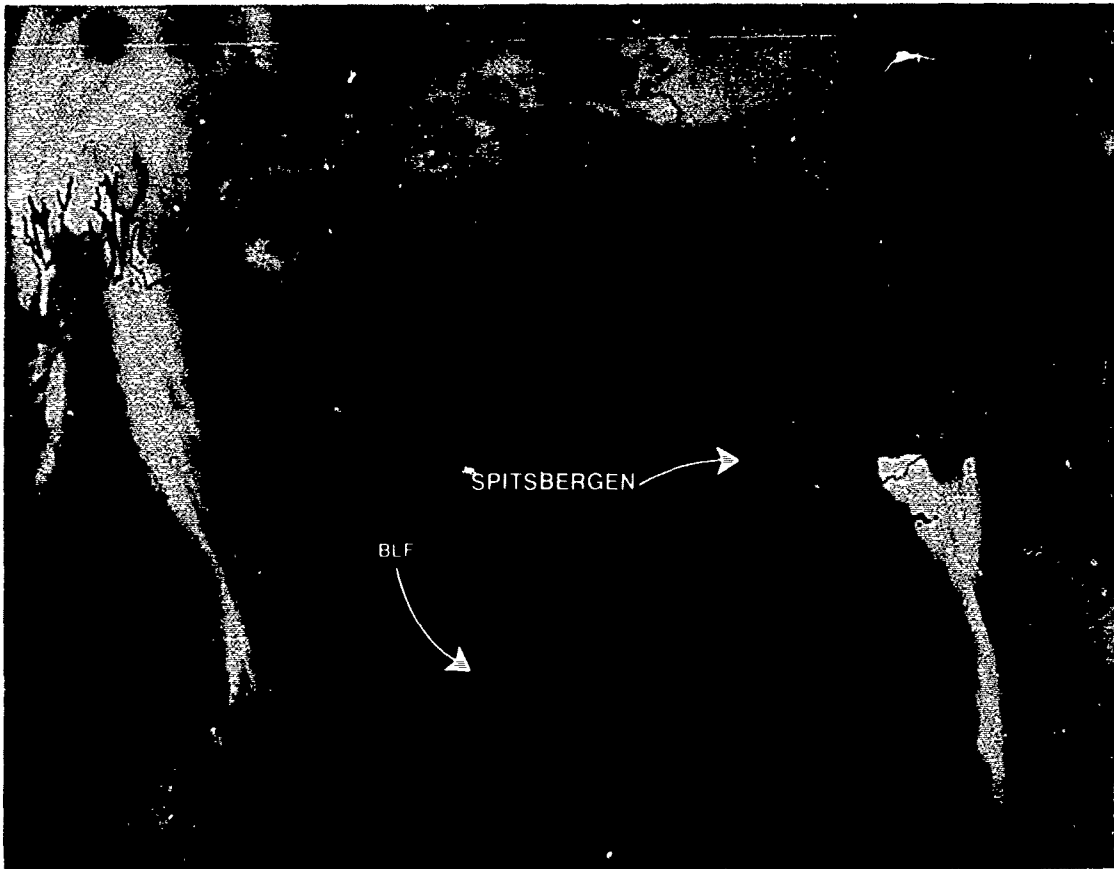
3B-26a. NOAA-10 HRPT (Ch 4) Data. 0952 GMT 10 April 1987.

Fortunately, an independent measurement can be made from simultaneous NOAA-10 visible (Ch 2) data (Fig. 3B-27a). A cloud shadow approximately 12-miles long extends from the north side of the cloud's edge. Using this distance and the Sun's zenith angle of  $71.7^\circ$  (valid for 10 April 1987, at 0952 GMT) a height of 20,954 ft is calculated, in excellent agreement with the inferred height based on the black-body temperature of the cloud mass.

Further development of the BLF, with small mesoscale vortices developing along its axis, and continued connection to the vortex in the Barents Sea is also apparent in this image.



3B-27a. NOAA-10 HRPT (Ch 2) Data. 0952 GMT 10 April 1987.



3B-28a. NOAA-10 HRPT (Ch 5) Data. 1633 GMT 10 April 1987.

Another NOAA-10 HRPT infrared (Ch 5) image, acquired at 1633 GMT (Fig. 3B-28a) provides additional detail concerning the nature of the orographic clouds, now apparent over Nordauslandet, as well as Kvitoya. An examination of the topography of Nordauslandet (Fig. 3B-29a) reveals that the beginning of the cloud plume has formed in the lee of a northeast-southeast-oriented topographic ridge line. Clouds that form in such a fashion are created by a vertically propagating mountain wave that gives rise to strong upward vertical motions at higher levels and equally strong downward motions at lower levels over the ridge line and on the lee slope of the mountain.

Fig. 3B-30a is a diagram showing theoretical results of a streamline configuration inflow over an isolated asymmetric ridge. Wave-induced cirrus clouds are produced most effectively in the lee of a ridge having a steep leeward slope (as is the case in this example). Strong downward motion also clears cloudiness along the ridge line. Vertically propagating waves are typified by a horizontal wavelength much longer than the width. The cloud plume effectively demonstrates this characteristic, thereby distinguishing this wave pattern from the trapped wave pattern apparent over northern Norway in the NOAA data shown in Figs. 3B-22a and 3B-25a.

An enlargement of the cloud plume region of Fig. 3B-28a is shown in Fig. 3B-30b. This image, produced on a system for digital processing of satellite data, was transected to determine variation of the infrared-sensed temperature along the red line drawn on the image. The printout of temperature variation again confirmed temperatures of  $-36^{\circ}\text{C}$  over the Kvitoya plume, which fell to  $-46^{\circ}\text{C}$  over the Nordauslandet plume—indicative of higher cloud top in the latter region.

#### *11 April 1987*

Continued presence of a jet stream over the region is shown by NOAA-9 HRPT infrared (Ch 4) data (Fig. 3B-31a) acquired at 0309 GMT on this date. The major change seems to be the direction of wind flow over Franz Josef Land, which shows a shift to easterly winds from previous northerly (Figs. 3B-25a, 3B-26a, and 3B-27a), judging from polynya-based cloud plume alignments. The shift, along with continued northwesterly flow over Kvitoya, suggests that a surface low center should be found just south of Franz Josef Land.

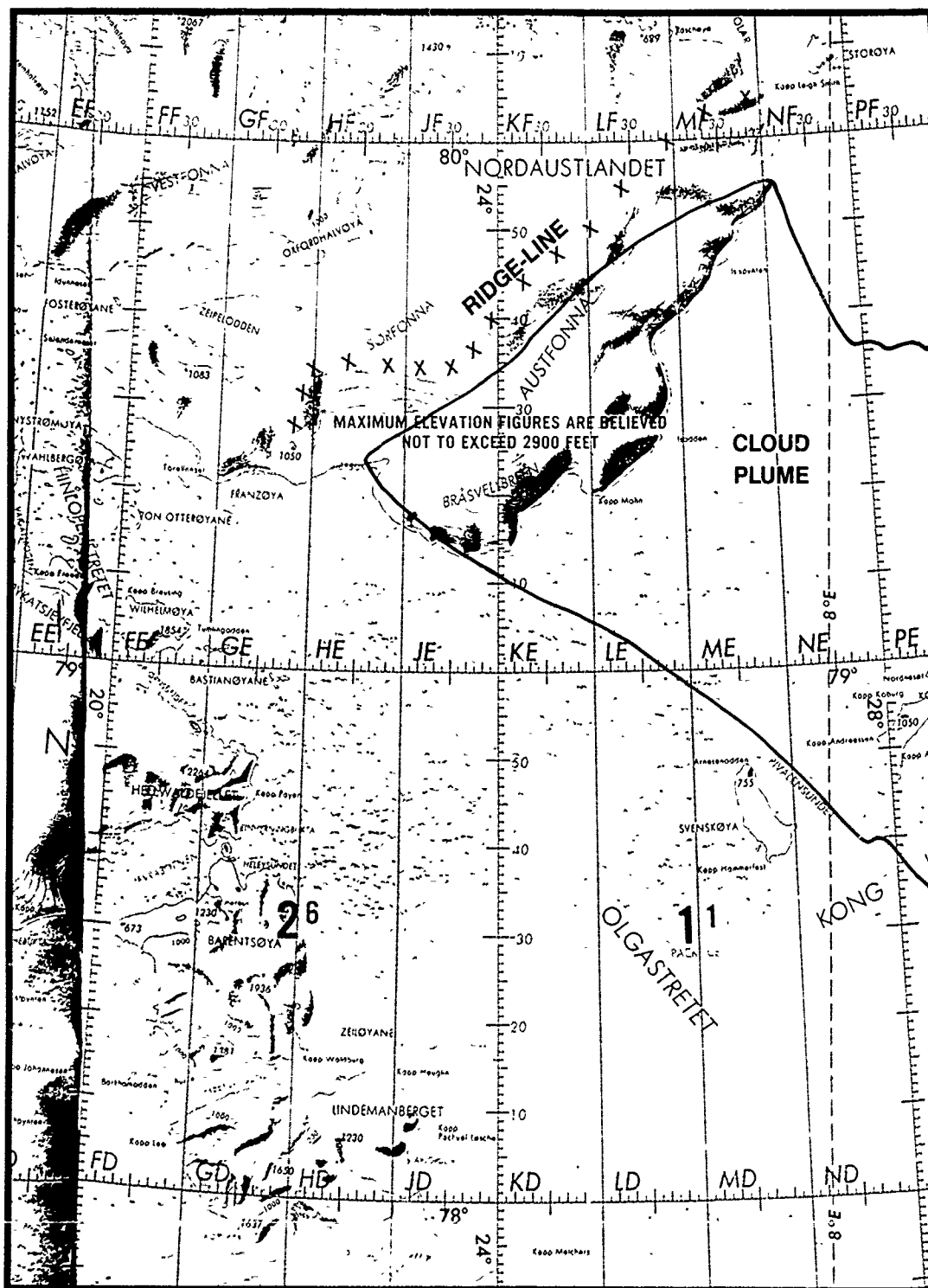
The FNOC surface analysis for 0000 GMT (Fig. 3B-32a), in fact, shows a low slightly northeast of Franz Josef Land, approaching Kvitoya.

Little evidence can be found in the NOAA data (Fig. 3B-31a) of the small vortex in the Barents Sea, which apparently has dissipated.

The FNOC 500-mb analysis for 0000 GMT (Fig. 3B-33a) shows continued evidence of the jet stream passing over Kvitoya into the Barents Sea. The upper cold low associated with the surface low continues to be displaced to the south in the region just south of Franz Josef Land.

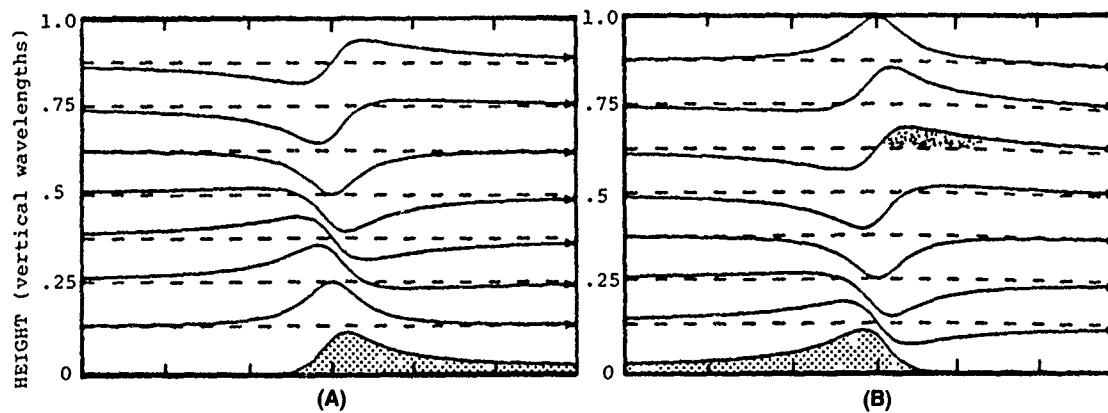
At 0930 GMT NOAA-10 HRPT infrared (Ch 4) data (Fig. 3B-34a) reveal polynya plume indications that a surface low exists in the region southwest of Franz Josef Land. The probable location has been marked on the overlay to the image. The FNOC surface analysis for 0600 GMT (Fig. 3B-35a) incorrectly shows a low not southwest, but northwest of Franz Josef Land. Winds in the Barents Sea have shifted from northwesterly to westerly.

A digital enhancement of the NOAA (Ch 4) image (Fig. 3B-36a) emphasizes the sweep of cloudiness associated with the jet that passes from the ice pack, over Nordauslandet, across the Barents Sea, and which finally passes over southern Novaya Zemlya. The FNOC 500-mb analysis for 1200 GMT (Fig. 3B-37a) verifies the basic positioning of the jet, following the satellite indications.

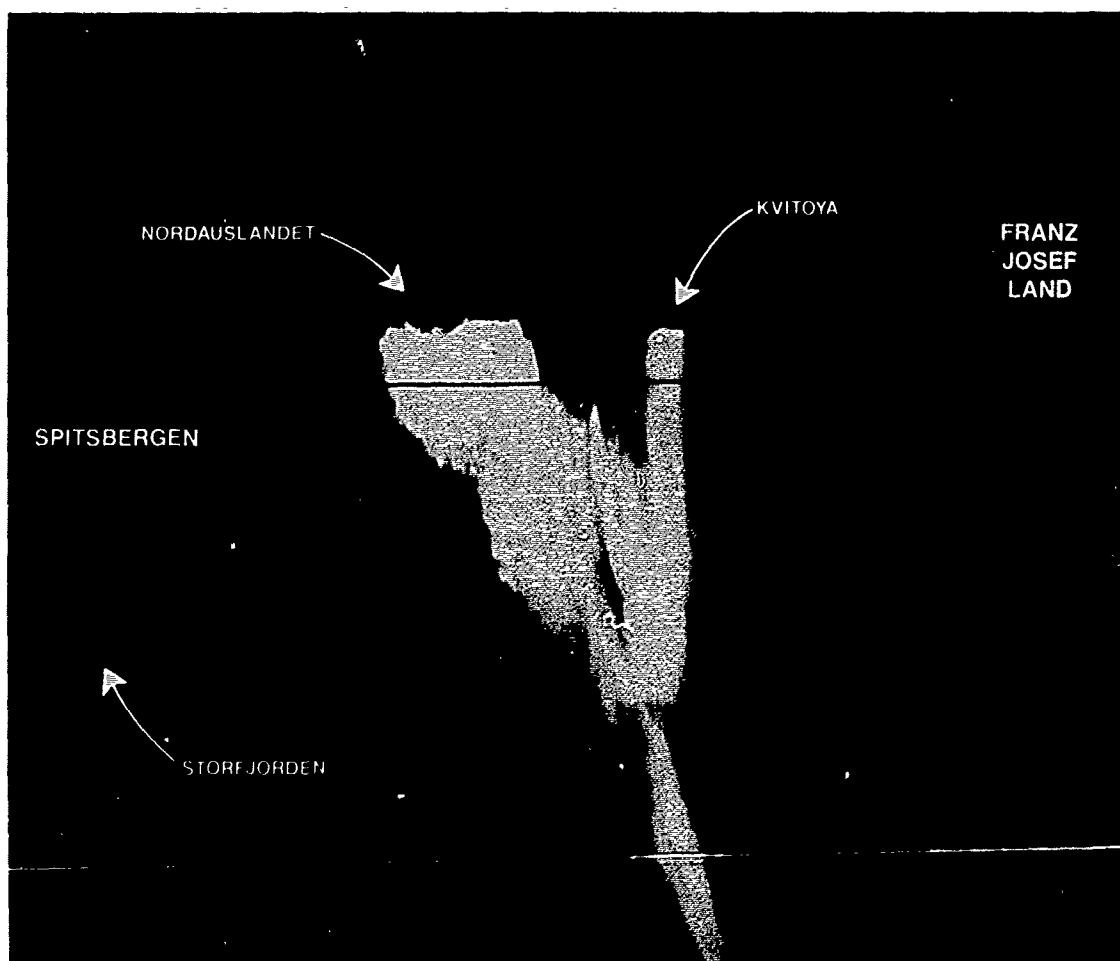


3B-29a. Topography of Nordauslandet (Svalbard) showing ridge-line position relative to cloud plume location from Fig. 3B-28a.

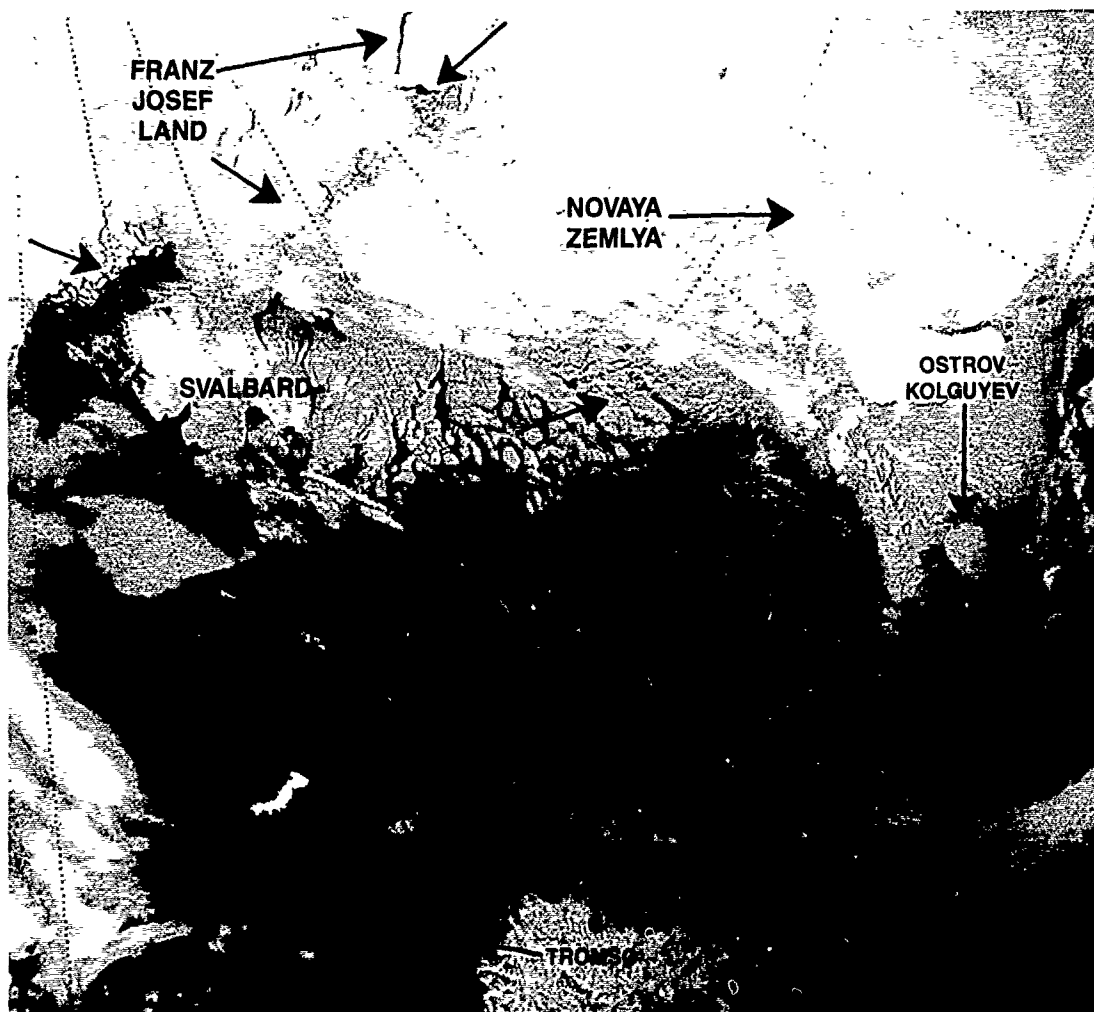




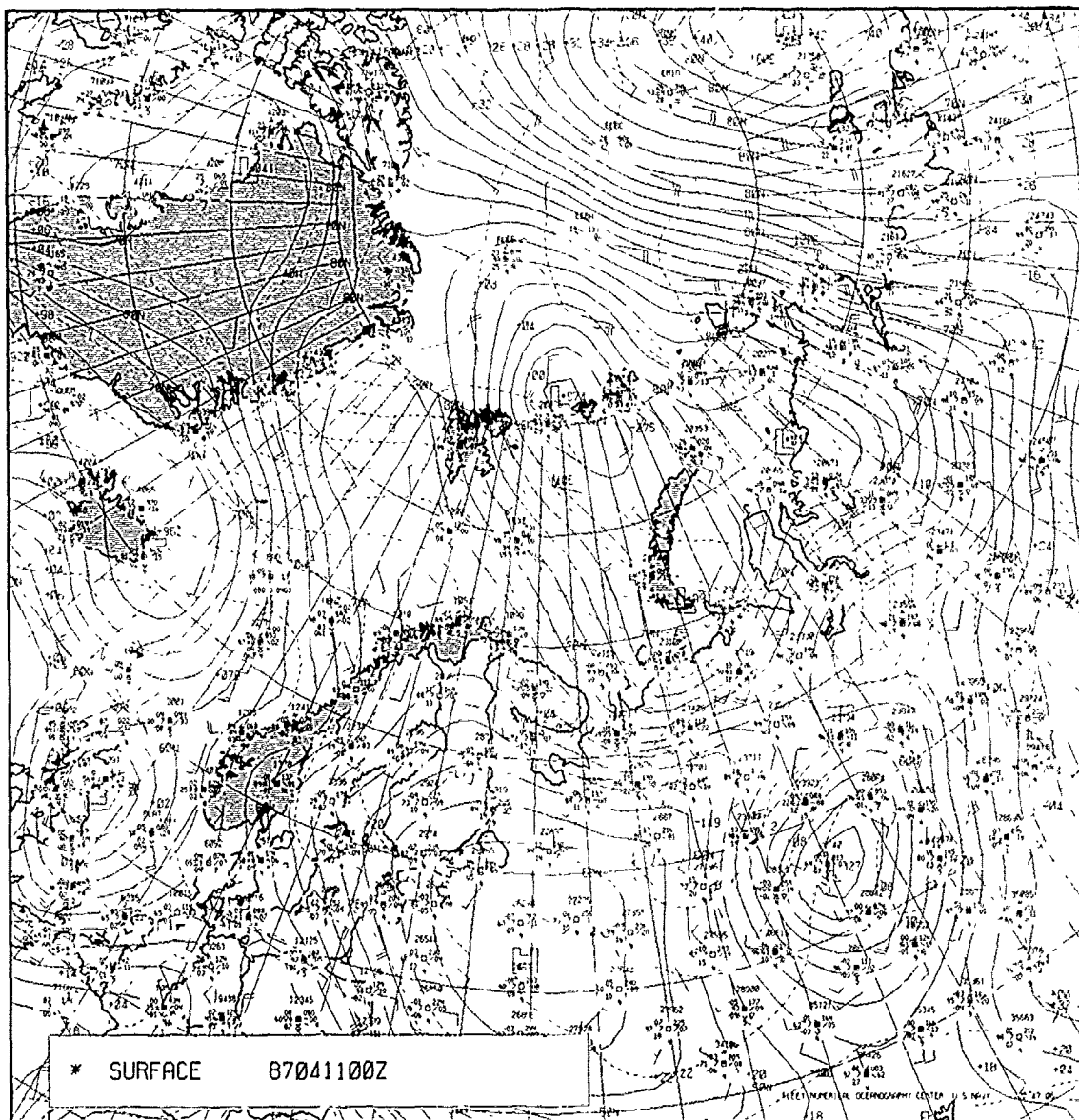
3B-30a. Streamlines in steady airflow over an isolated ridge: (A) steep windward slope, (B) steep leeward slope (Durrant, 1986).



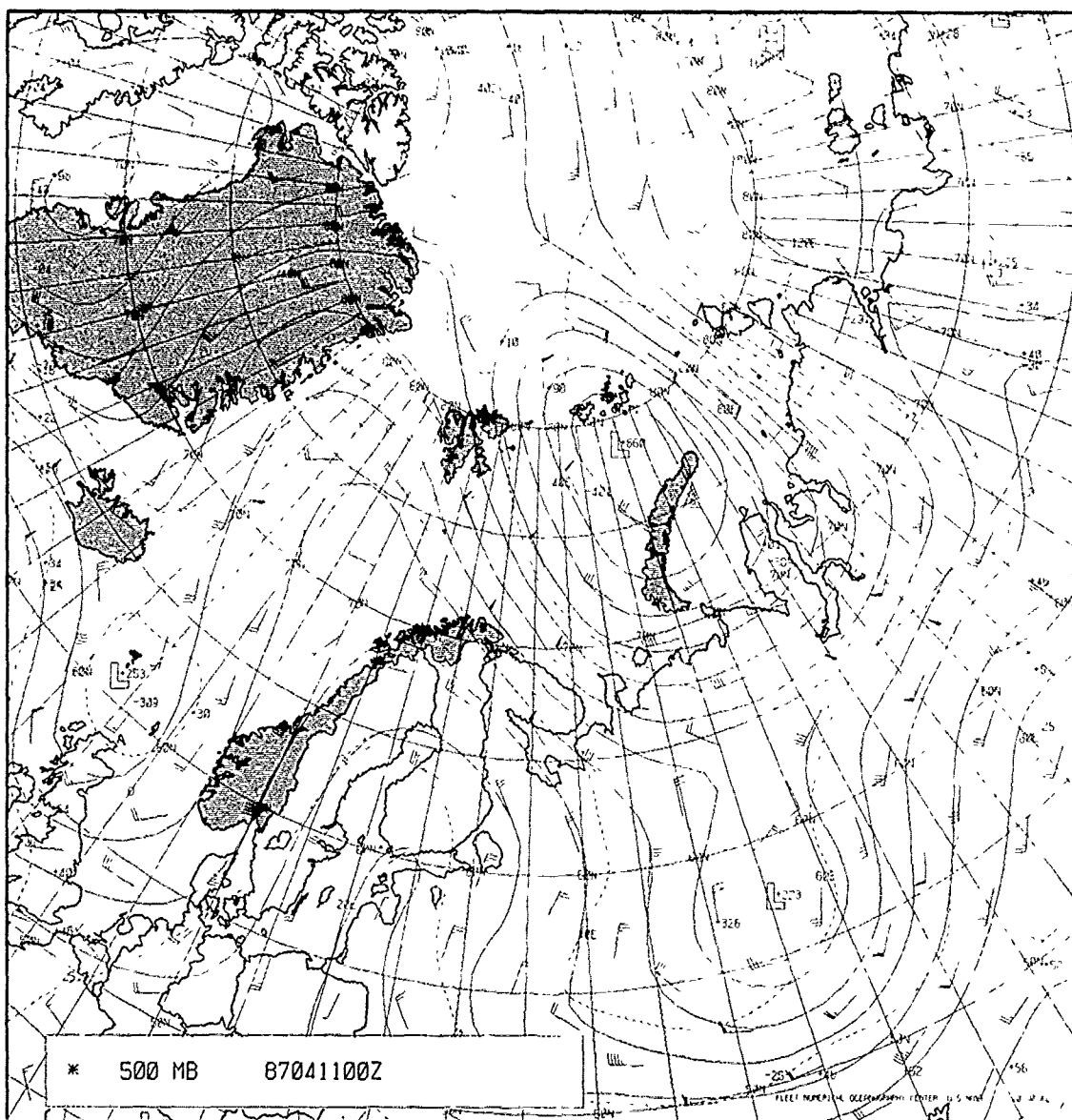
3B-30b. An enlargement of Fig. 3B-28a. 1633 GMT 10 April 1987.



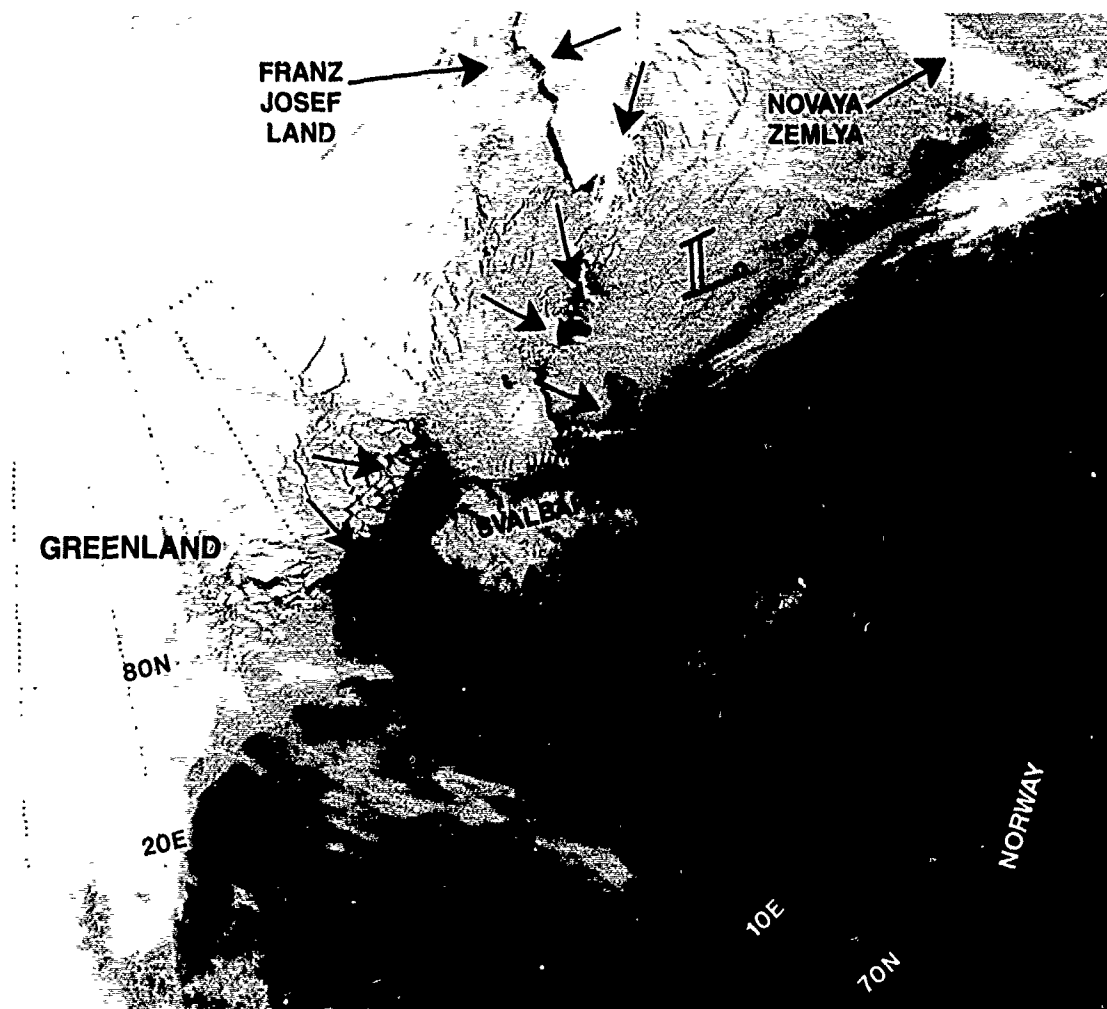
3B-31a NOAA-9 HRPT (Ch 4) Data. 0309 GMT 11 April 1987.



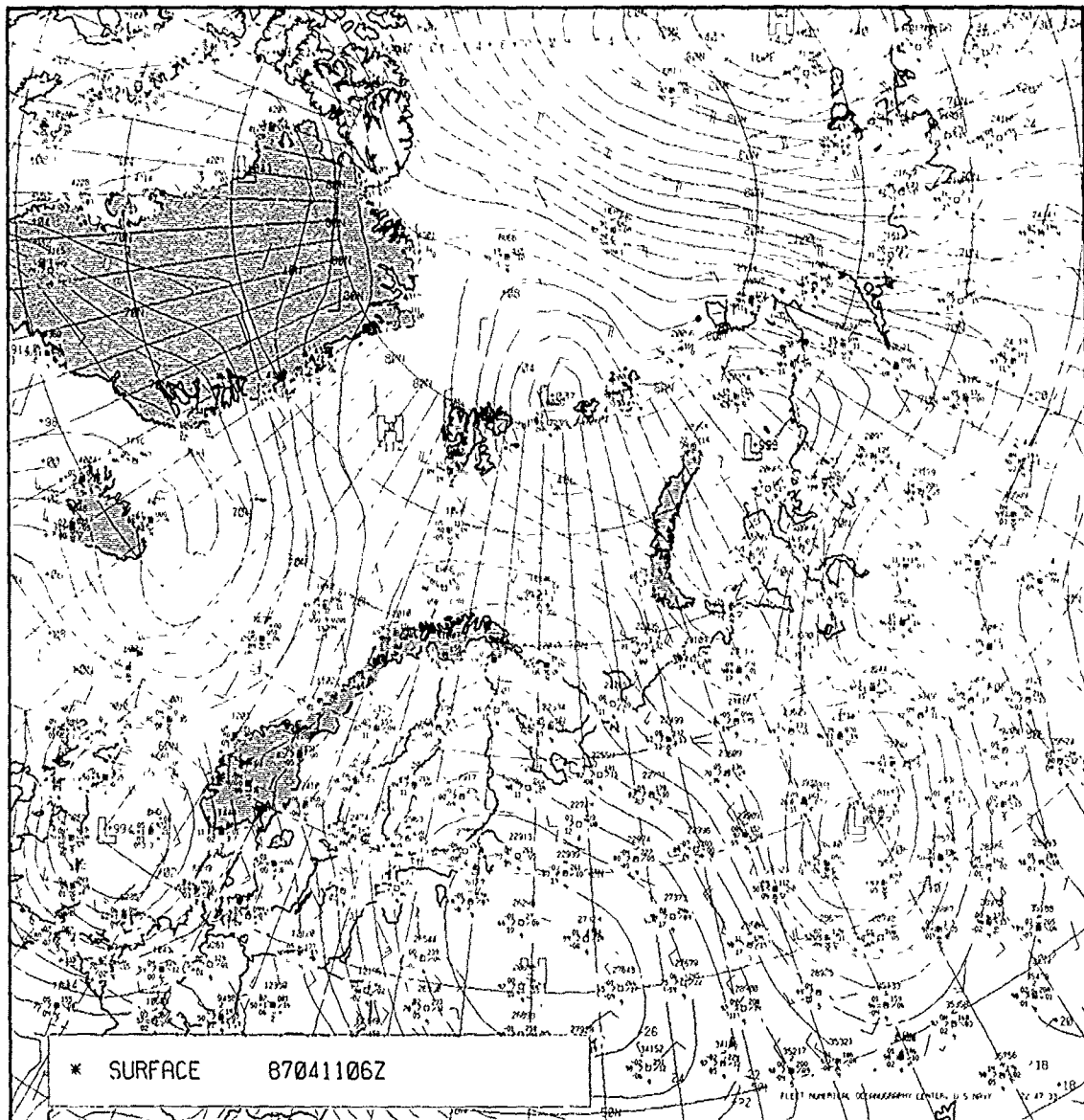
3B-32a. FNOC Surface Analysis. 0000 GMT 11 April 1987.



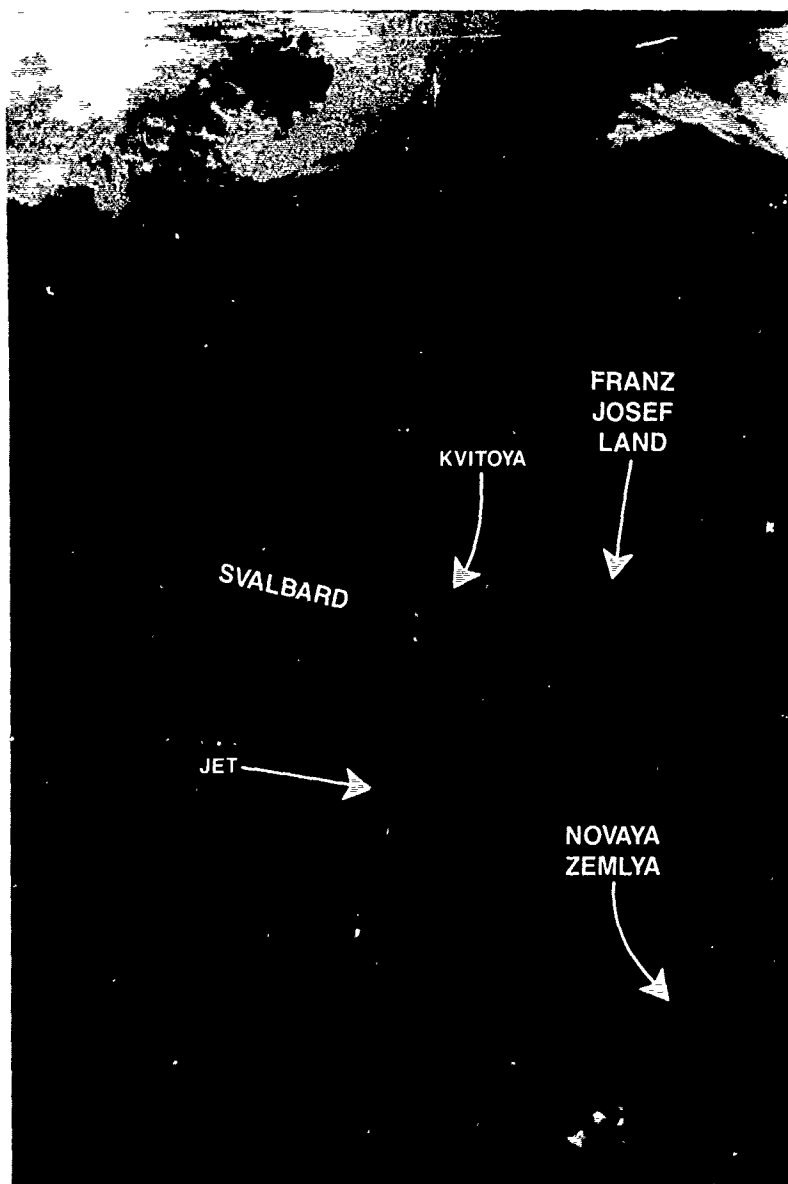
3B-33a. FNOC 500-mb Analysis. 0000 GMT 11 April 1987



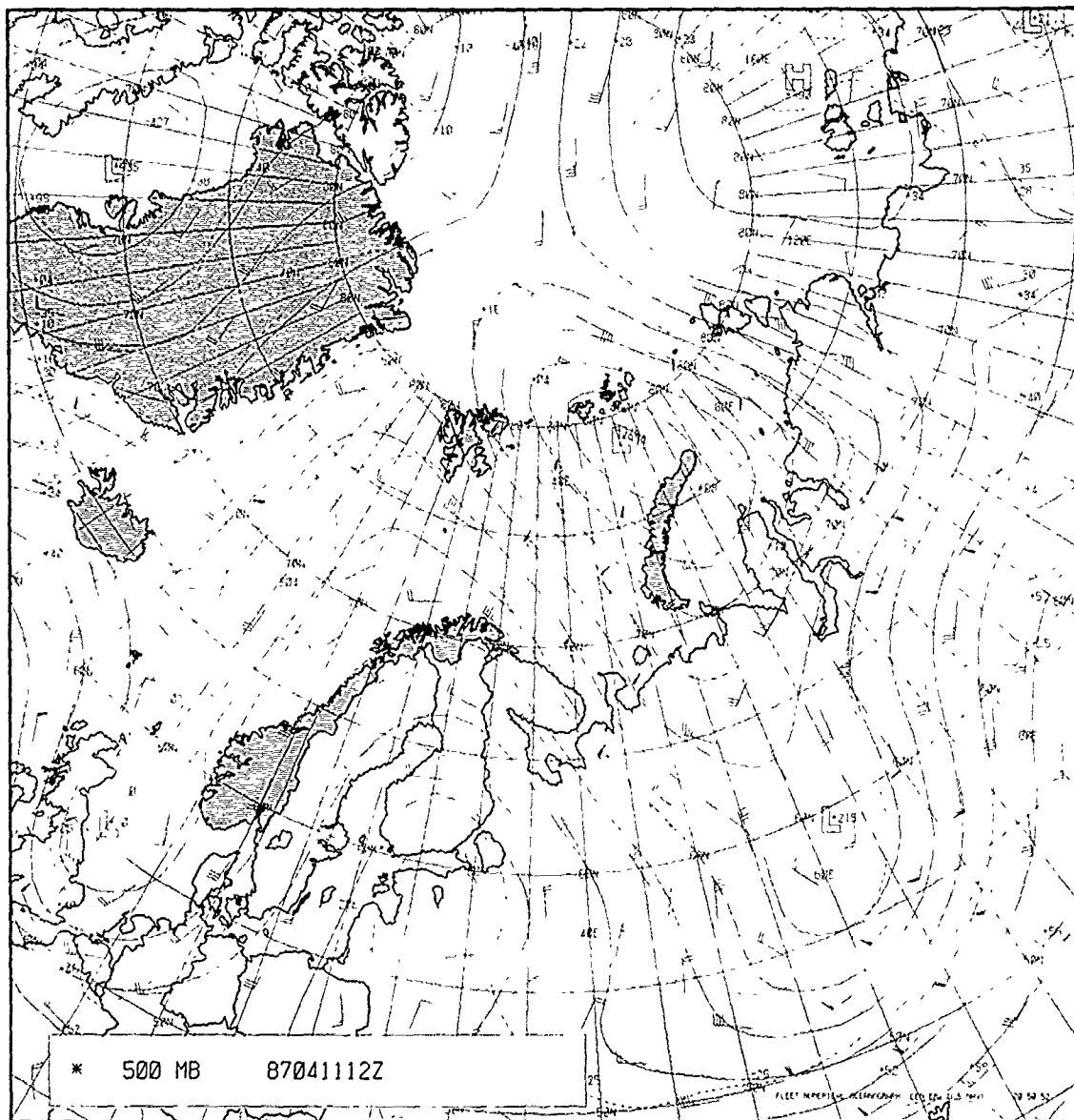
3B-34a. NOAA-10 HRPT (Ch 4) Data. 0930 GMT 11 April 1987.



3B-35a. FNOC Surface Analysis. 0600 GMT 11 April 1987

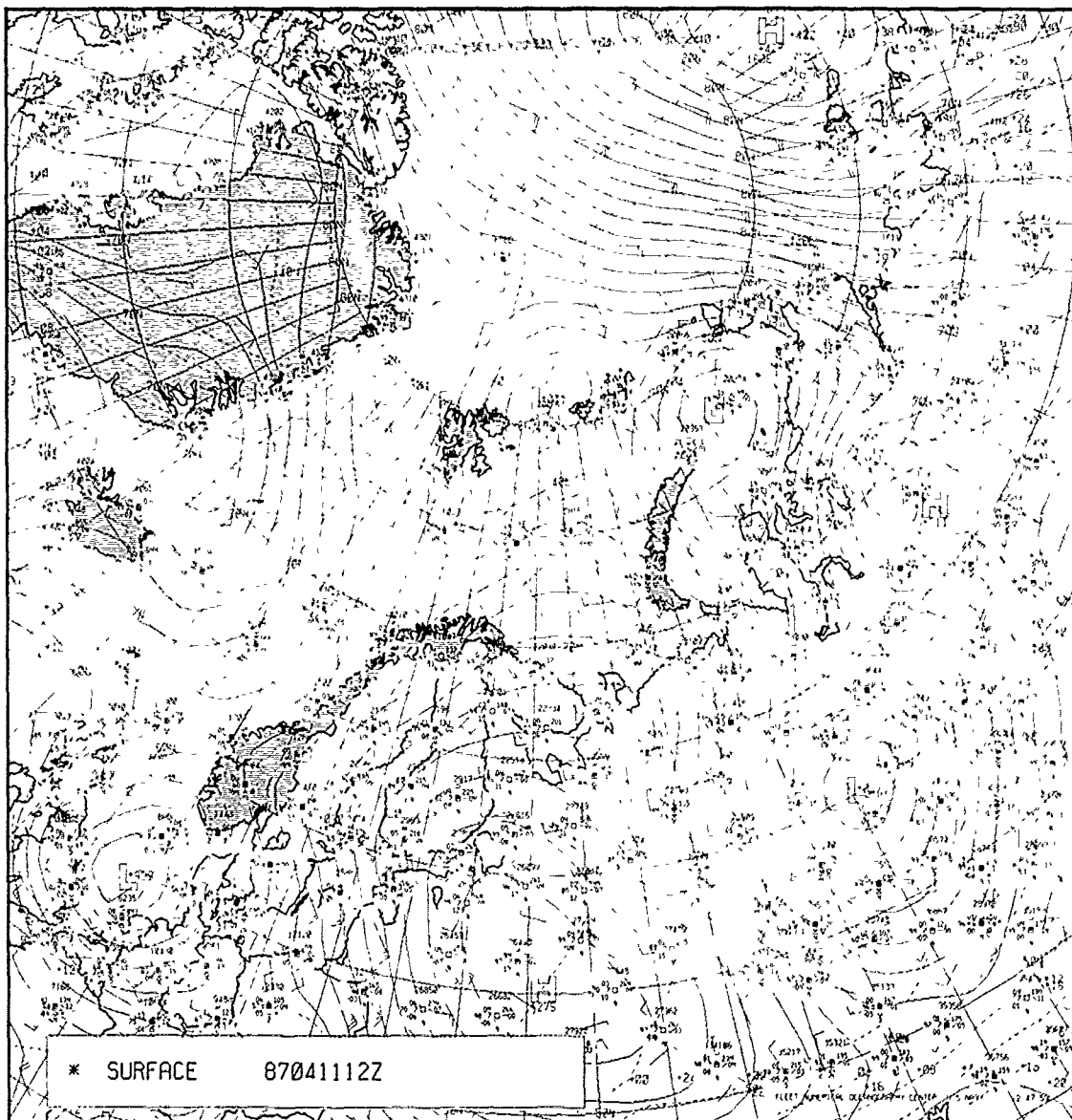


3B-36a. Digitally-Enhanced NOAA-10 HRPT (Ch 4) Data. 0930 GMT 11 April 1987.



3B-37a FNOC 500-mb Analysis. 1200 GMT 11 April 1987.





3B-38a. FNOC Surface Analysis 1200 GMT 11 April 1987.

The corresponding FNOC surface analysis (Fig. 3B-38a) retains the low positioned near Franz Josef Land but still northwest of the position suggested by the satellite data (Fig. 3B-34a). Winds over the Barents Sea remain generally westerly with ridging noticeable along 40°E.

A final NOAA-10 HRPT infrared (Ch 4) image on this date at 1606 GMT (Fig. 3B-39a) suggests that the jet stream and associated arctic front have moved south since orographic plumes are no longer apparent over Svalbard, and only polynya plumes are visible, which continue to define a cyclonic circulation south of Franz Josef Land. Wave clouds in the northern Barents Sea imply strong low-level winds from the east, increasing with height consistent with a jet over that area.

The FNOC surface analysis for 1800 GMT (Fig. 3B-40a) offers little except a weak trough to substantiate the satellite evidence of a low south of Franz Josef Land and shows a very weak gradient over the Barents Sea. The low that had consistently appeared near Franz Josef Land (Fig. 3B-38a) is dropped from the analysis. Two ship observations in the Barents Sea, however, are of special interest on this analysis. Ship "EKDH" (74.5°N 29°E) reports a light northwesterly wind and a -6°C temperature with a rising 3-hr pressure tendency of plus 0.9 mb. Ship "EWEM" (73.8°N 28°E) reports a west-northwesterly wind of 15 kt, a surface temperature of -2°C, and its 3-hr pressure tendency indicates a sharp fall of 3 mb. The observations are consistent with the existence of an arctic front between the two points.

#### *12 April 1987*

The trough over the Barents Sea sharpens radically on the FNOC surface analysis for 0000 GMT (Fig. 3B-41a). Ship "LLXE" near 74.5°N 30°E reports a northeasterly wind of 15 kt with a 3-hr pressure rise of 1 mb, as the temperature falls to -9°C. An arctic front has passed!

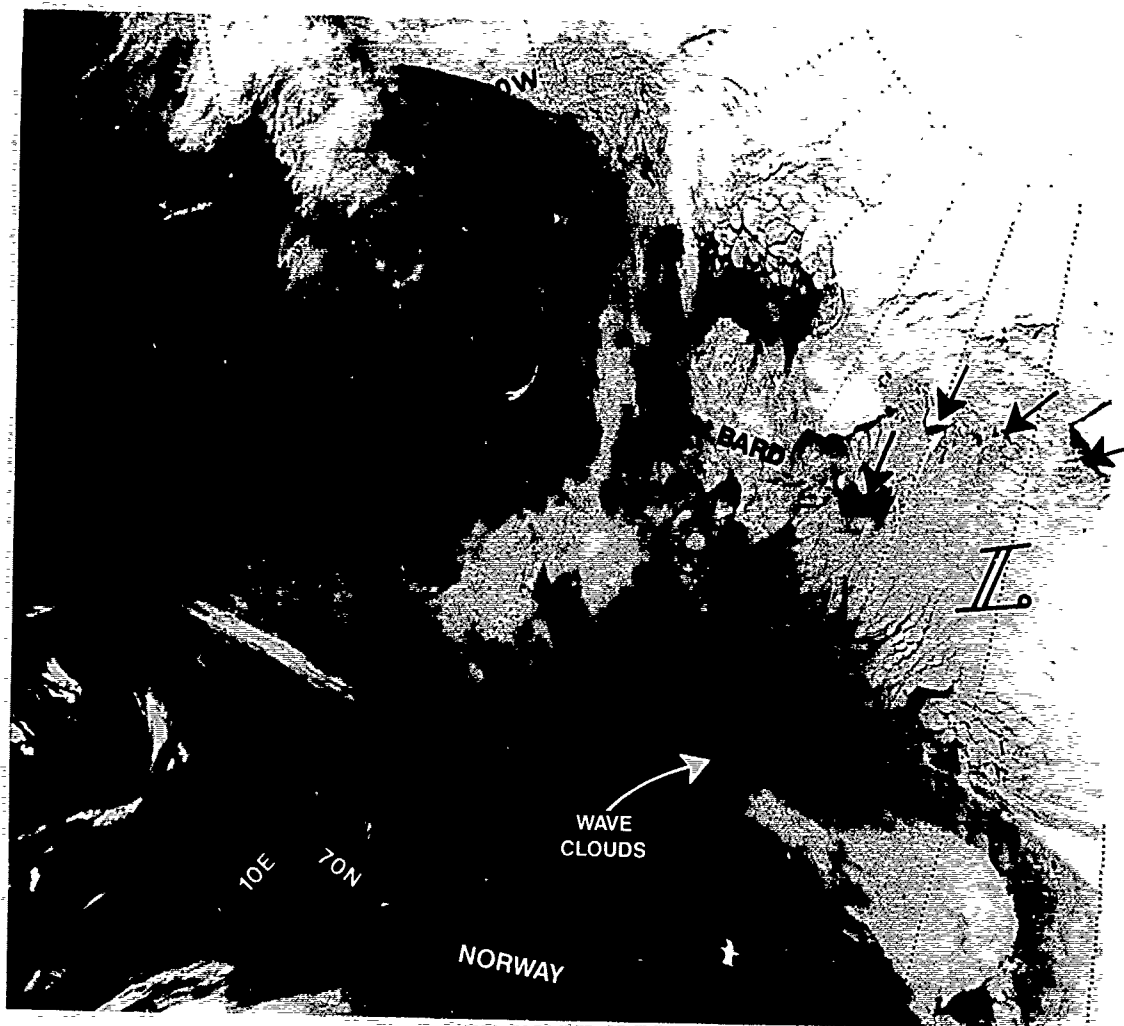
NOAA-9 HRPT infrared data about 3 hr later, at 0258 GMT (Fig. 3B-42a), reveal the dramatic change that occurred as an arctic frontal band becomes visible and cloud lines from off the Barents MIZ reveal the cold northerly surge of air behind the front.

#### **Important Conclusions**

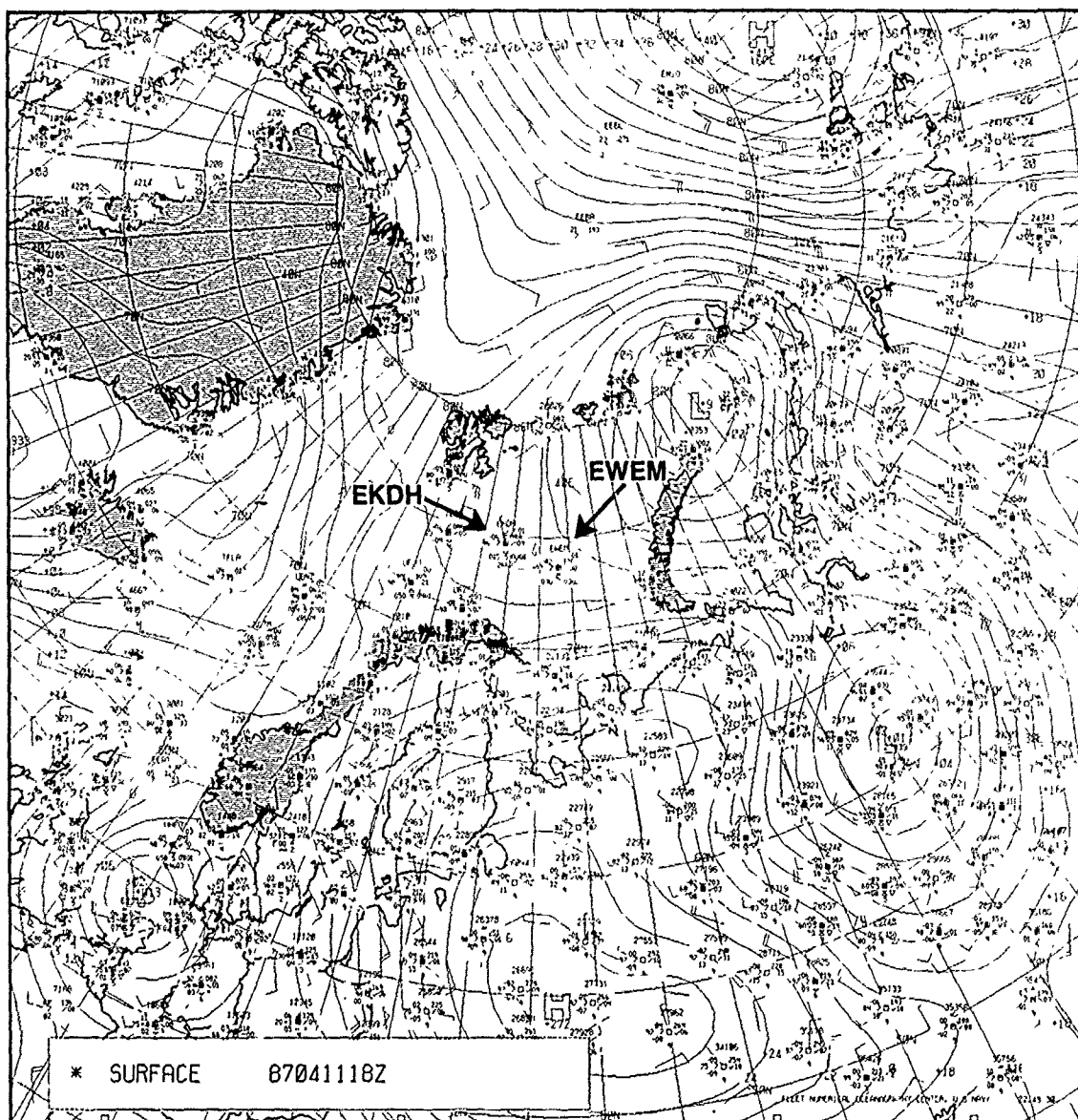
1. Polynya cloud plumes are excellent indicators of the direction of low-level wind flow and, in time series, of the approach and passage of low and high pressure centers over the ice pack.
2. Orographic cloud plumes appearing in the lee of orographic ridge lines indicate the presence of a jet stream aloft and a vertically propagating lee wave, which is indicative of strong upward vertical motions at mid and high levels at the leading portion of the plume and strong downward vertical motion at lower levels over the ridge line and lee slope.
3. An orographically produced cloud plume is normally associated with an Arctic front in polar regions, and an approaching low pressure center.
4. Prediction of arctic frontal movement over the Barents Sea can be aided by carefully monitoring polynya and orographically produced cloud plumes. Additional detail from available ship reports and their 3-hr pressure tendencies are useful in assessing an arctic frontal position.
5. Although not emphasized in the text, knowledge of impending arctic frontal passage is of great importance to ships operating in the region because of the sudden dramatic change in sea state, wind, temperature, and associated icing conditions. Ship captains like to be prepared for such changes.

#### **Reference**

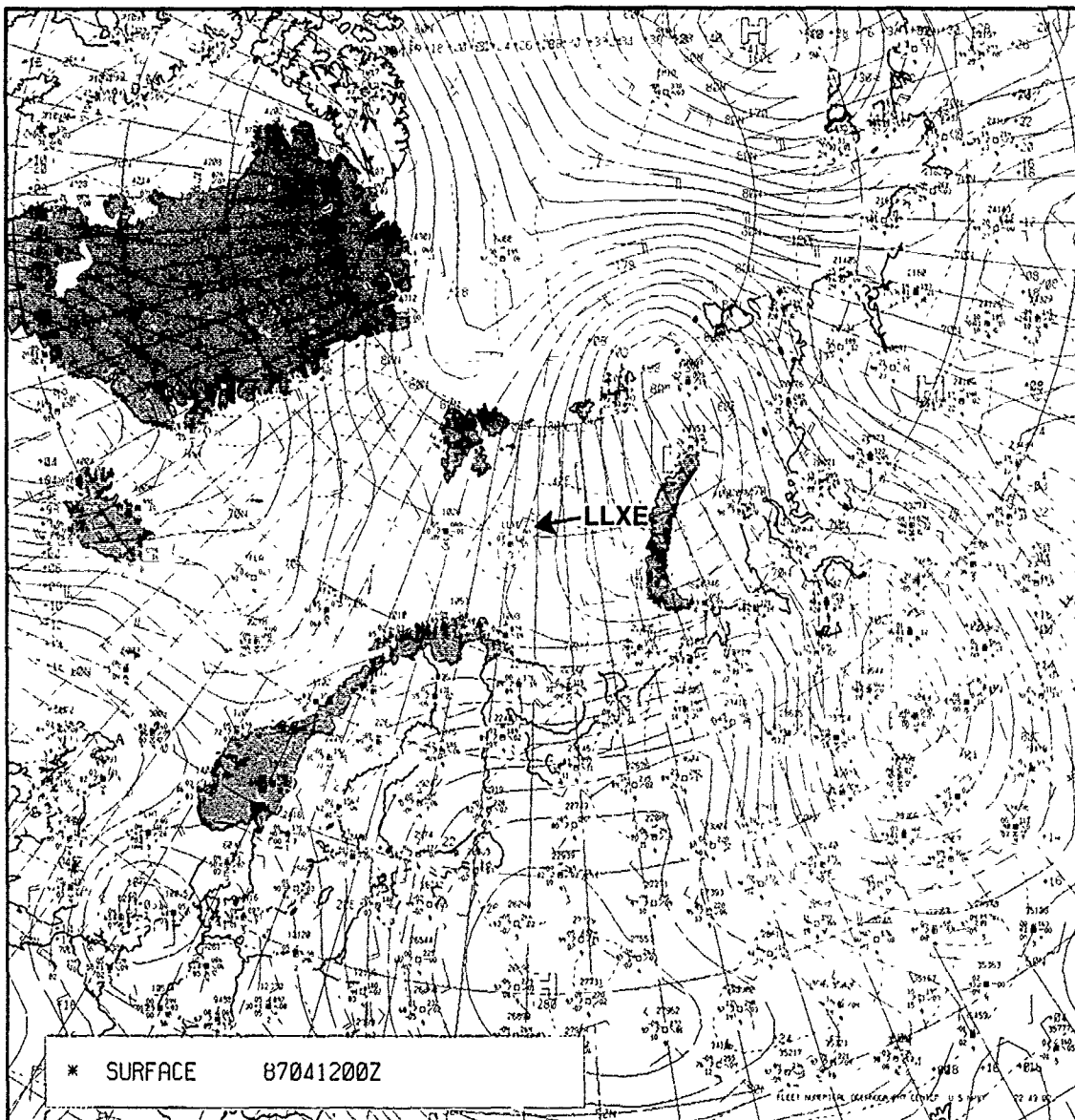
Durrant, D.R., 1986: Mountain waves. In *Mesoscale Meteorology and Forecasting*, P.S. Ray (Ed.), American Meteorological Society, Boston, 472-492.



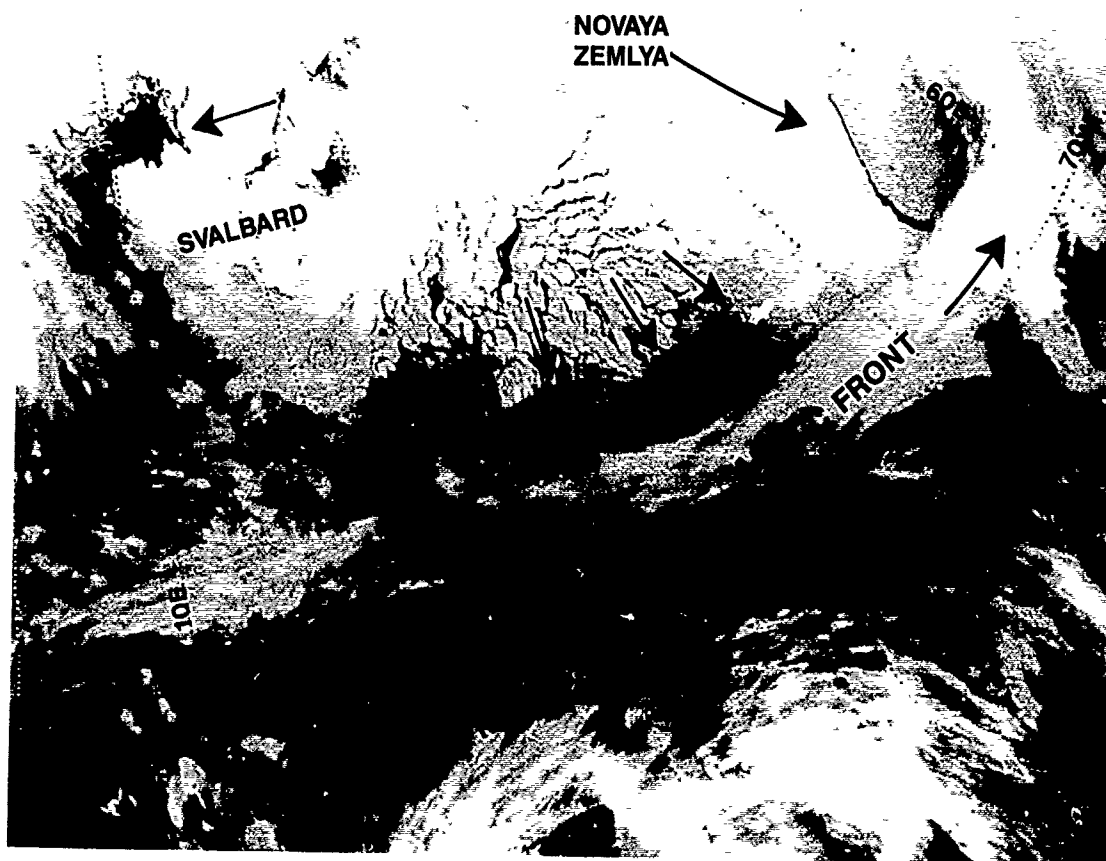
3B-39a. NOAA-10 HRPT (Ch 4) Data. 1606 GMT 11 April 1987.



3B-40a. FNOG Surface Analysis. 1800 GMT 11 April 1987.



3B-41a. FNOC Surface Analysis. 0000 GMT 12 April 1987.



3B-42a. NOAA-9 HRPT (Ch 4) Data. 0258 GMT 12 April 1987.

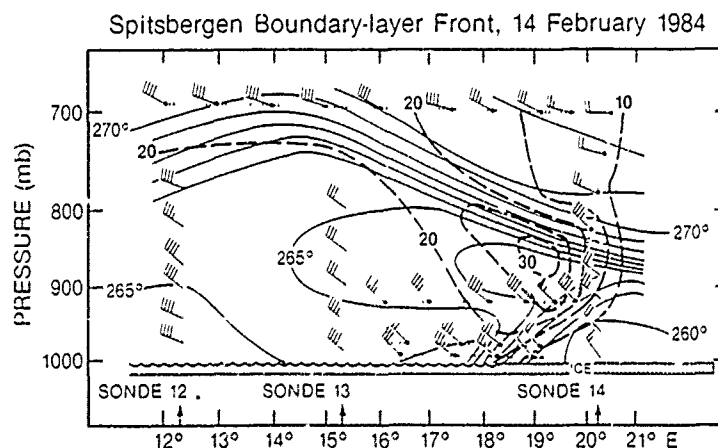
### 3C Boundary Layer Fronts

#### *Characteristics of Boundary Layer Fronts*

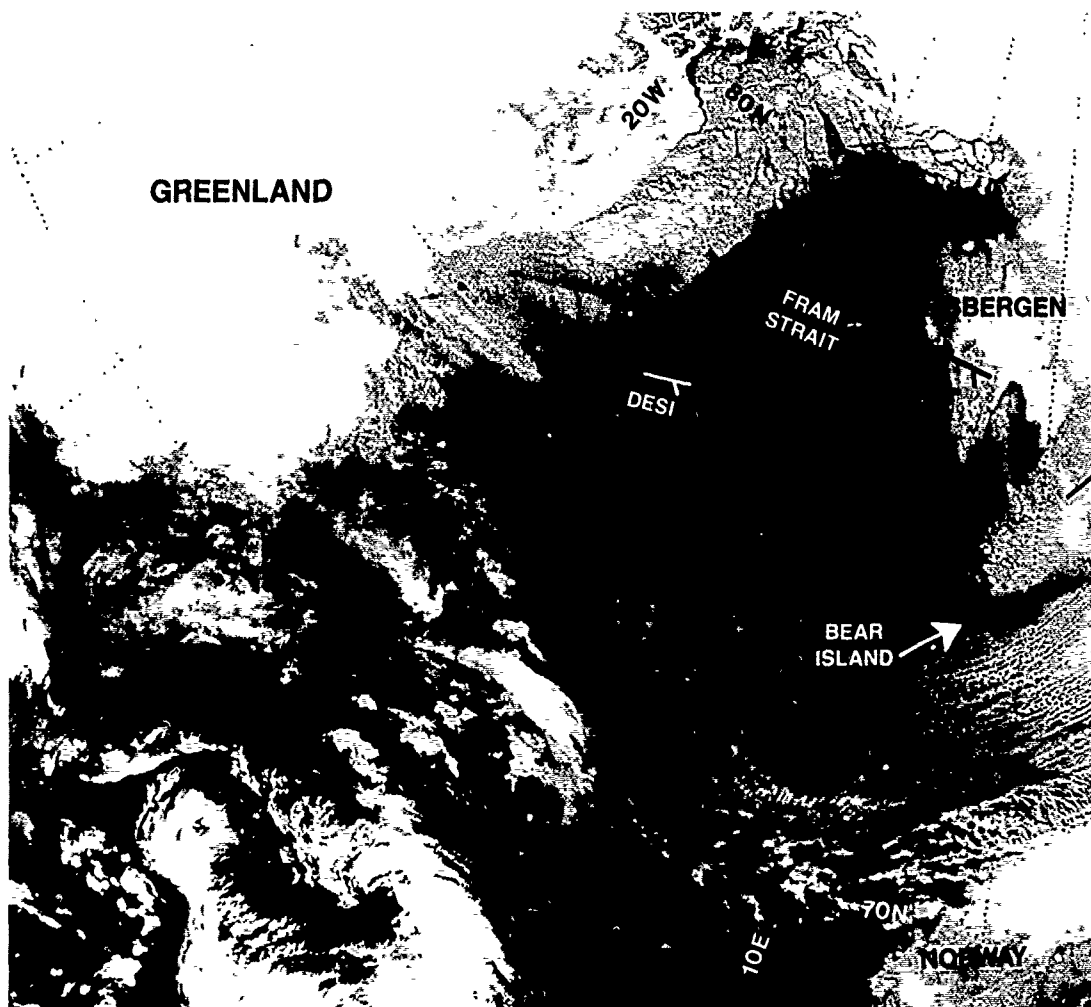
Boundary layer fronts in their initial stage separate cold, dry, arctic air over the ice pack, from modified arctic air that has spent resident time over adjacent, relatively warmer, water areas. The nature of the front varies, dependent upon direction of wind flow relative to the alignment of the ice edge.

Shapiro and Fedor (1986) provide documentation of a stationary BLF that developed parallel to the west coast of Spitsbergen on 14 February 1984. In this region, during winter, a natural baroclinic zone exists between the ice-covered island and the relatively warm open water of the Fram Strait, kept free of ice by a branch of the Gulf Stream. Under northerly flow conditions over both the Fram Strait and Spitsbergen, a shallow BLF is created, separating air being heated and moistened from below over the Fram Strait from the non-heated air over Spitsbergen. A narrow convective band denotes the position of the BLF and is hypothesized to result from "Diabatically-forced vertical circulations in the vicinity of the BLF. . ." (Shapiro and Fedor, 1986).

Dropsonde data released in an east-west transect through the front enabled the determination of frontal structure shown in Fig. 3C-1a. The figure represents an east-west cross-section analysis of potential temperature (solid lines) and wind speed (dashed lines). It can be seen that an inversion exists and is highest over the open water and lowest over land (ice). A  $30 \text{ ms}^{-1}$  low-level jet (LLJ) is centered just above the frontal boundary near 850 mb.



3C-1a. An east-west cross-section analysis of potential temperature (solid lines) and wind speed (dashed lines). Wind speed is indicated by barbs (1 barb=10 kt). Isotach analysis is in meters per second (Shapiro and Fedor, 1986).



3C-2a. NOAA-9 HRPT Infrared (Ch 4) Data. 1313 GMT 23 March 1987.



The example documented by Shapiro was used in a numerical model simulation (Langland, Tag, and Fett, 1989) in an attempt to isolate causes and determine sensitivities to changes in flow direction. The modes accurately simulated effects documented by Shapiro and produced a LLJ when wind flow paralleled the west coast of Spitsbergen.

It was determined that the LLJ was due to a thermal wind effect created by surface temperature gradients between the ice-covered island and the sea. The temperature contrast resulted in an ageostrophic circulation that could be termed an "ice breeze." This effect is a thermally-direct secondary circulation analogous to the well-known coastal land breeze circulation, where air flows from land to the water, rises off-shore, and then reverses direction in a return circulation.

The LLJ occurs in its fully developed form only when the wind flow parallels the ice edge (in this example in northerly flow). As might be expected wind flow from the east reinforced the ice breeze, but, since advection of cold off-ice flow occurred at all levels, it blocked the return circulation, and wind speeds aloft increased only slightly. In this case the BLF would be expected, under continued easterly flow, to propagate westward, away from the coastline and, unless invigorated by some process, gradually degenerate.

Shapiro, however, notes that when BLFs "are driven out to sea by synoptic wind flow, they maintain their identity. . . and can often be traced from their origin at the ice edge and propagate as far away as Norway and the United Kingdom."

The case study to follow shows an example of a propagating BLF that traveled from east to west across the Fram Strait. Research ships in the Fram Strait released RAOBS and took surface observations, which enabled documentation of its structure while over the water. Unlike the Shapiro example the BLF showed a higher inversion east of the front than to the west and there was no evidence of an associated LLJ. The reversed inversion effect may be the result of more vigorous heat and moisture fluxes occurring with off-shore flow (as opposed to flow parallel to the ice). Under such a circumstance turbulent interchange would increase the depth of the boundary layer east of the front.

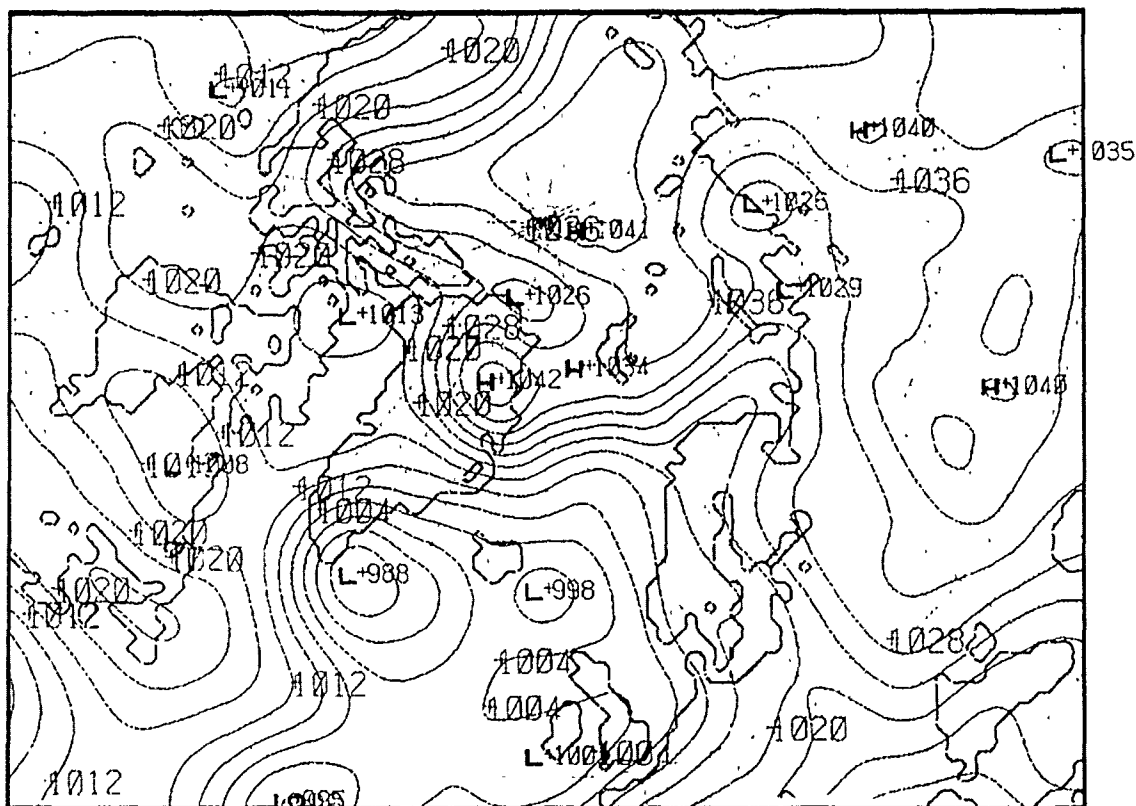
### *Case 1 Boundary Layer Frontal Movement Through the Fram Strait (23-27 March 1987)*

*23 March 1987*

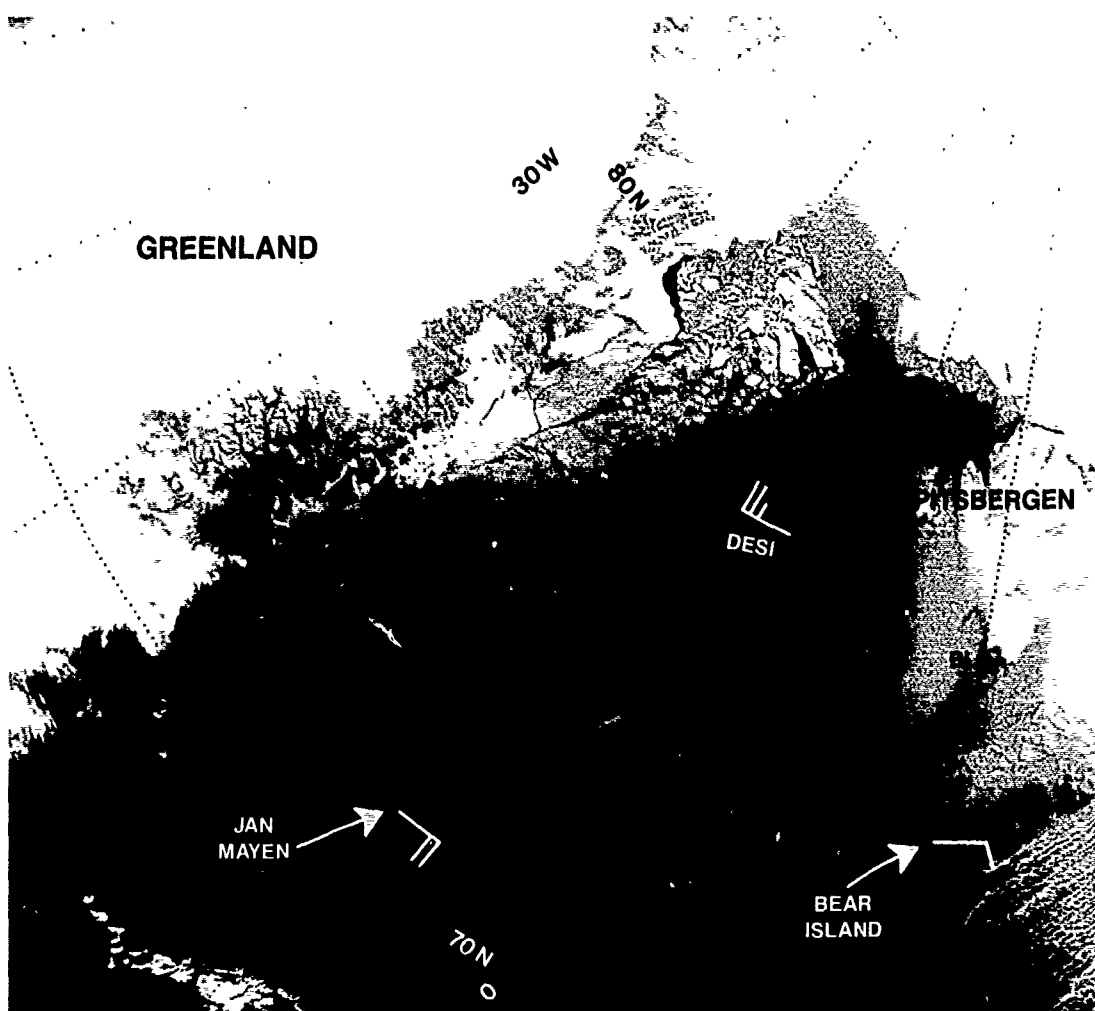
Fig. 3C-2a is a NOAA-9 HRPT infrared (Ch 4) image showing the Fram Strait region at 1313 GMT. Northeasterly flow, coming off the ice south of Spitsbergen, turns anticyclonically south of the Fram Strait, as delineated by the curvature of clouds in that region. A few wind observations superimposed on the figure substantiate flow direction and suggest the possibility of a high pressure center somewhere in the northern Fram Strait. (The westernmost observation is from the German research vessel Valdivia [DESI].)

A Navy Operational Regional Atmospheric Prediction System (NORAPS) analysis for 1200 GMT (Fig. 3C-3a) supports this latter hypothesis, showing a high pressure center in the middle of the Fram Strait.

NORAPS 109X 82X12 80K  
 1200 GMT 23 MAR 1987  
 ANAL SFC PRESSURE — TAU=0



3C-3a. A Navy Operational Regional Atmospheric Prediction System (NORAPS) Surface Analysis.  
 1200 GMT 23 March 1987.



3C-4a. NOAA-9 HRPT Infrared (Ch 4) Data. 1303 GMT 24 March 1987.

#### 24 March 1987

NOAA-9 HRPT infrared (Ch 4) data about 24 hr later, at 1303 GMT (Fig. 3C-4a), suggest that the high center has slipped to the south. Winds are off-ice from Greenland, to the north (supported by a superimposed Valdivia report of west winds at 25 kt), and cloud lines suggest anticyclonic turning, so that high pressure exists between Valdivia and Jan Mayen Island, which reports an easterly wind at 20 kt. From a satellite perspective the suppressed nature of the cloudiness and small stratocumulus cell size imply a high pressure center in that region.

The first appearance of a BLF is seen as an enhanced north-south-oriented cloud line that extends from close to the shore of Spitsbergen down to the latitude of Jan Mayen. A close inspection of clouds lines northwest of Bear Island suggests a veering of the wind to southeasterly up to the BLF, and then turning northerly in the flow beyond the front, as dictated by the high pressure center and shown by cloud lines in the region. This flow pattern creates an inverted streamline trough coincident with the frontal boundary.

None of these features have been captured very well on the Norwegian (Tromsø) surface analysis for 1200 GMT (Fig. 3C-5a), close to the time of the HRPT data. The observations do reveal light snow at Barentsburg, on Spitsbergen, in the overcast region behind the BLF—quite different from the weather being experienced west of the frontal boundary—and is a perceivable characteristic condition for the area immediately east of the BLF.

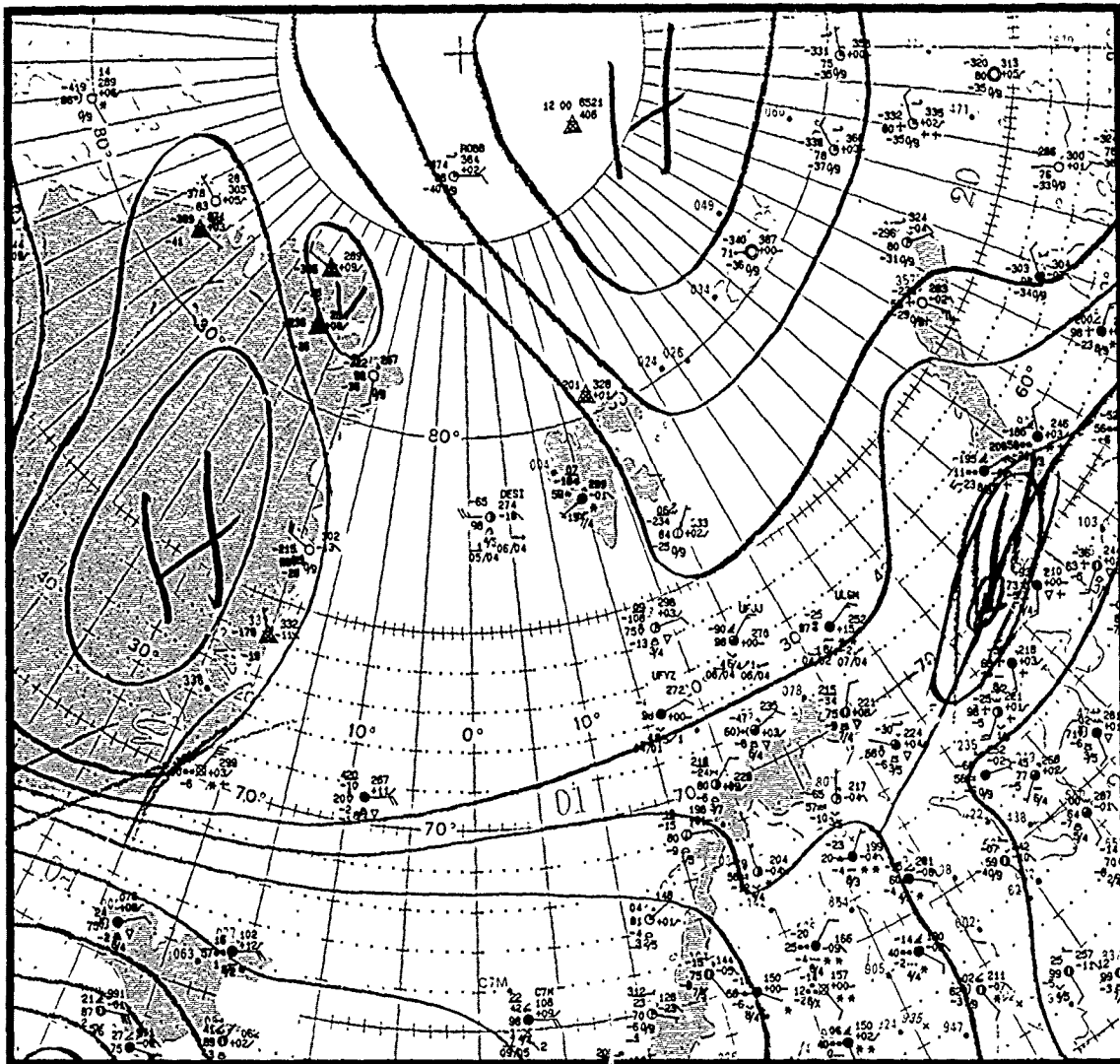
#### 25 March 1987

Valdivia passed through the BLF on 25 March between 0300 and 0600 GMT. Soundings from Valdivia on 24 March, in the high pressure region prior to frontal passage (Fig. 3C-6a), show a well mixed layer to about 600 or 700 m, the base of the inversion, and the apparent stratocumulus cloud top, shown by a moist layer just below that level.

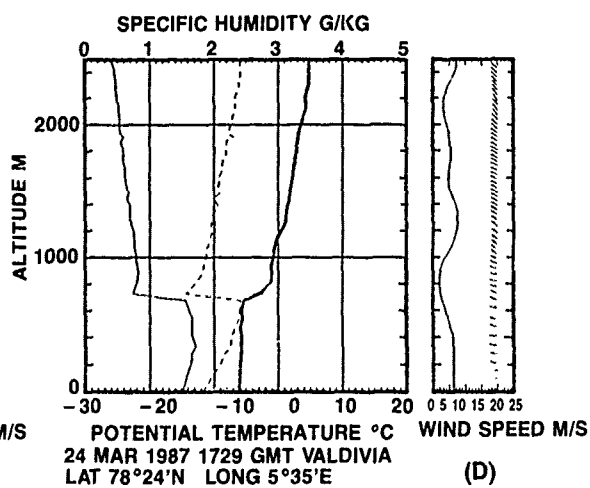
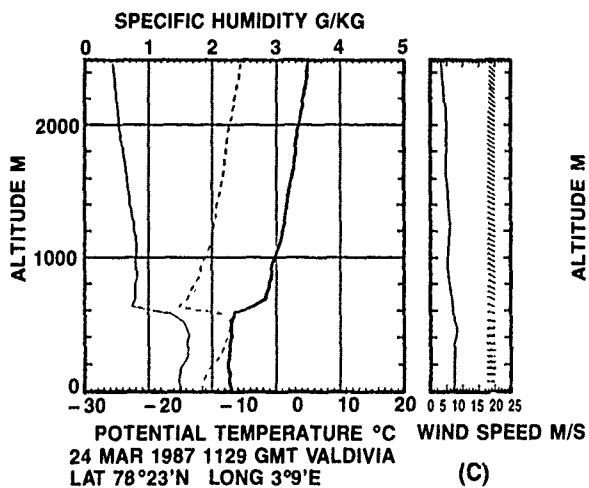
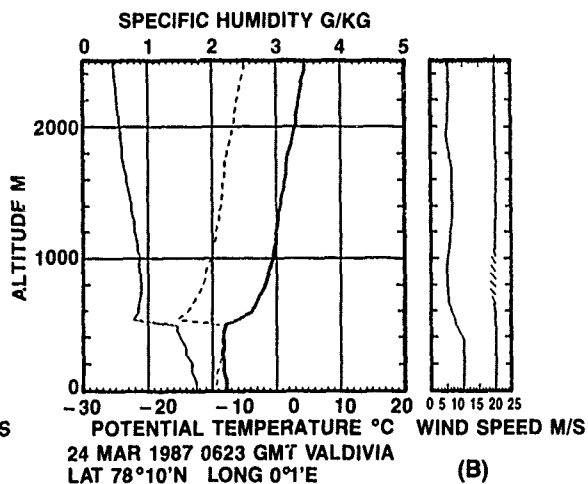
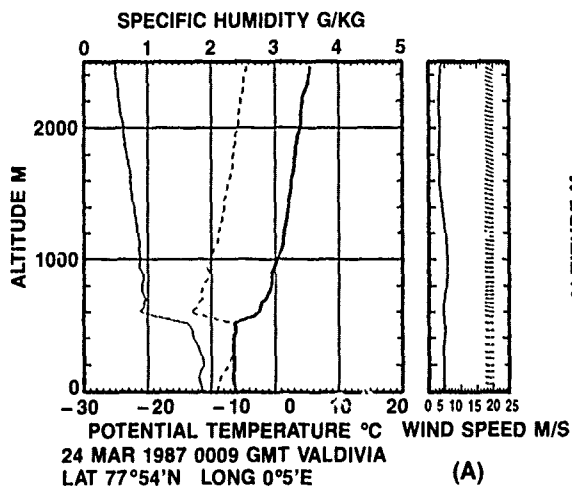
Soundings late on 24 March and later on 25 March (Fig. 3C-7a) show the mixed layer increasing in depth as Valdivia approached the BLF (2315 GMT, 24 March), and then lifting and becoming saturated up to about the 2000 m elevation, after passing the front from west to east. Surface temperature fell from  $-4.6^{\circ}\text{C}$  on 25 March at 0000 GMT, prior to frontal passage, to a low of  $-10.5^{\circ}\text{C}$  during 25 March, after frontal passage. The 0600 GMT observation from Valdivia indicated a change in sky conditions from four-eighths coverage to overcast as the ship entered an area of moderate continuous snow. Winds, at the same time, which had been blowing from the west, changed to east-southeasterly at 25 kt.

Fig. 3C-8a is a NOAA-9 HRPT infrared (Ch 4) depiction of the region on 25 March at 1100 GMT. By this time two other research vessels were in the area, Polar Circle (call sign "JXBT"), and Hakon Mosby (call sign "LJIT"). Wind observations from the three ships have been plotted at 1200 GMT (Fig. 3C-8a). An observation for Jan Mayen at 1200 GMT was missing; however 0600 and 1800 GMT data show easterly flow at 10 kt, and the 0600 GMT observation is shown. The observations continue to support the suggestion of an inverted streamline trough coincident with the BLF axis and indicate that the small high pressure center has slipped slightly southwestward from its previous position. Vorticity, increased by the sudden cyclonic shift of winds along the trough axis, has produced a series of mesoscale vortices on the BLF. Multiple vortex formations along the BLF appear common and were also noted in the Shapiro study.

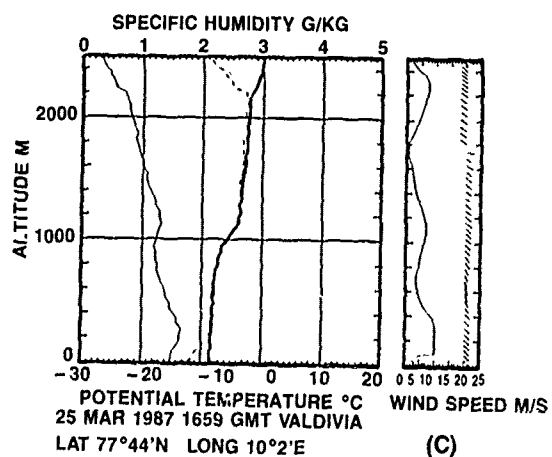
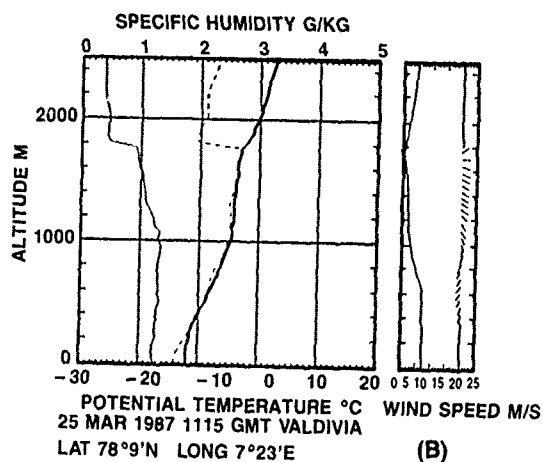
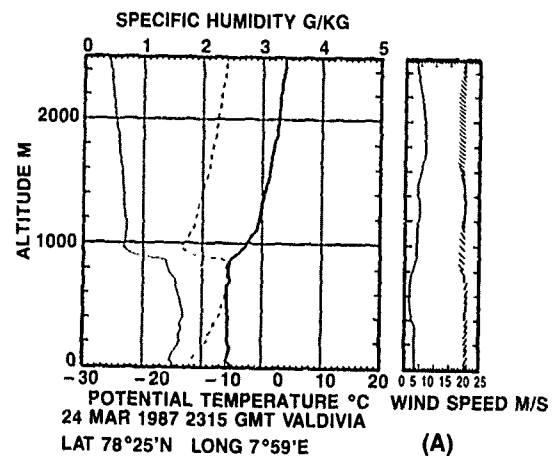
The Norwegian surface analysis for 25 March at 1200 GMT (Fig. 3C-9a) shows an inverted trough over the Fram Strait, but the analysis is gross since data from the three ships and Jan Mayen were apparently not available by analysis time.



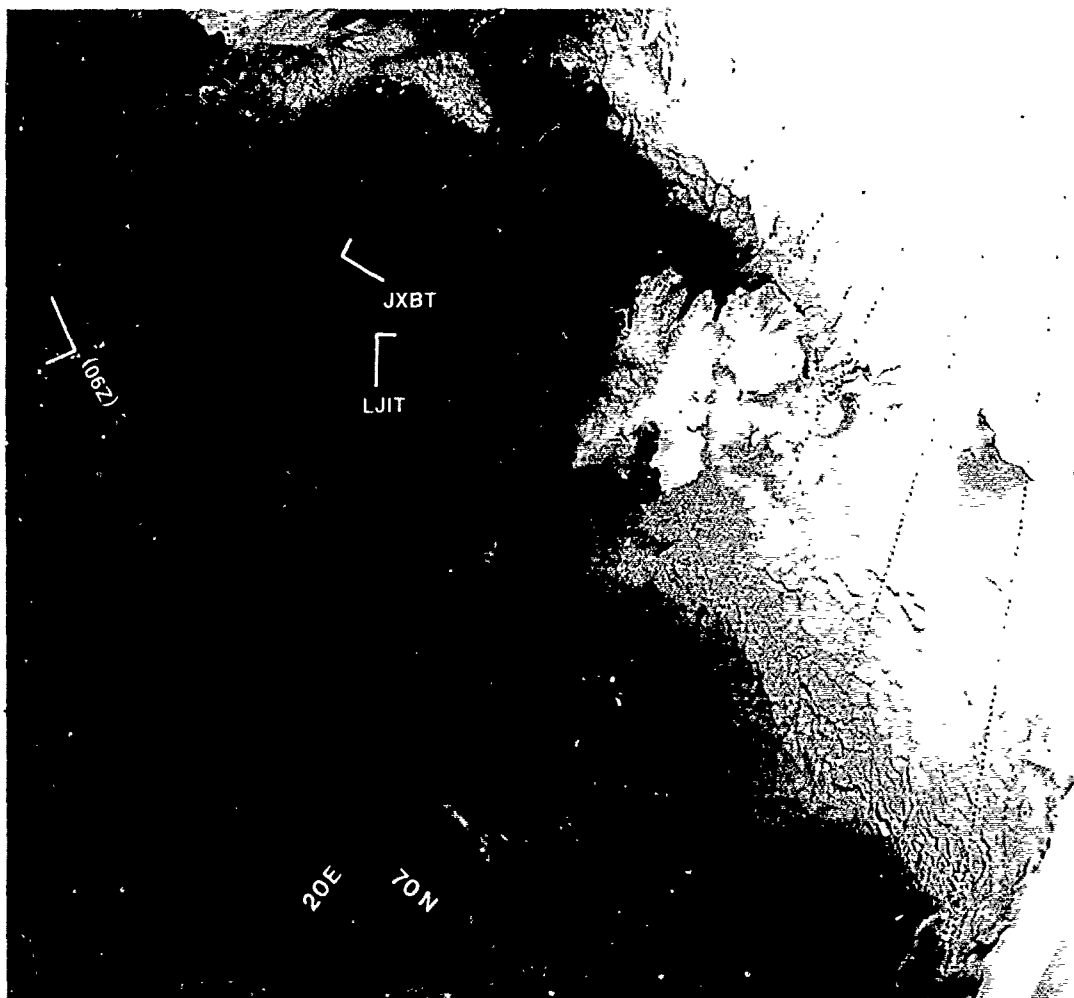
3C-5a. Northern Norway Forecast Center (Tromsø) Surface Analysis. 1200 24 March 1987.



3C-6a. Rawinsonde profiles for Valdivia on 24 March 1987. The figure shows potential temperature (thick solid line), potential dew point (dashed line) and specific humidity (thin solid line). The adjacent plot is wind direction and wind speed to the same height scale. Wind directions have barbs pointing into the wind and start along an imaginary vertical line above the 20  $\text{ms}^{-1}$  label. Vertical upward represents a north wind; to the right an east wind, etc.

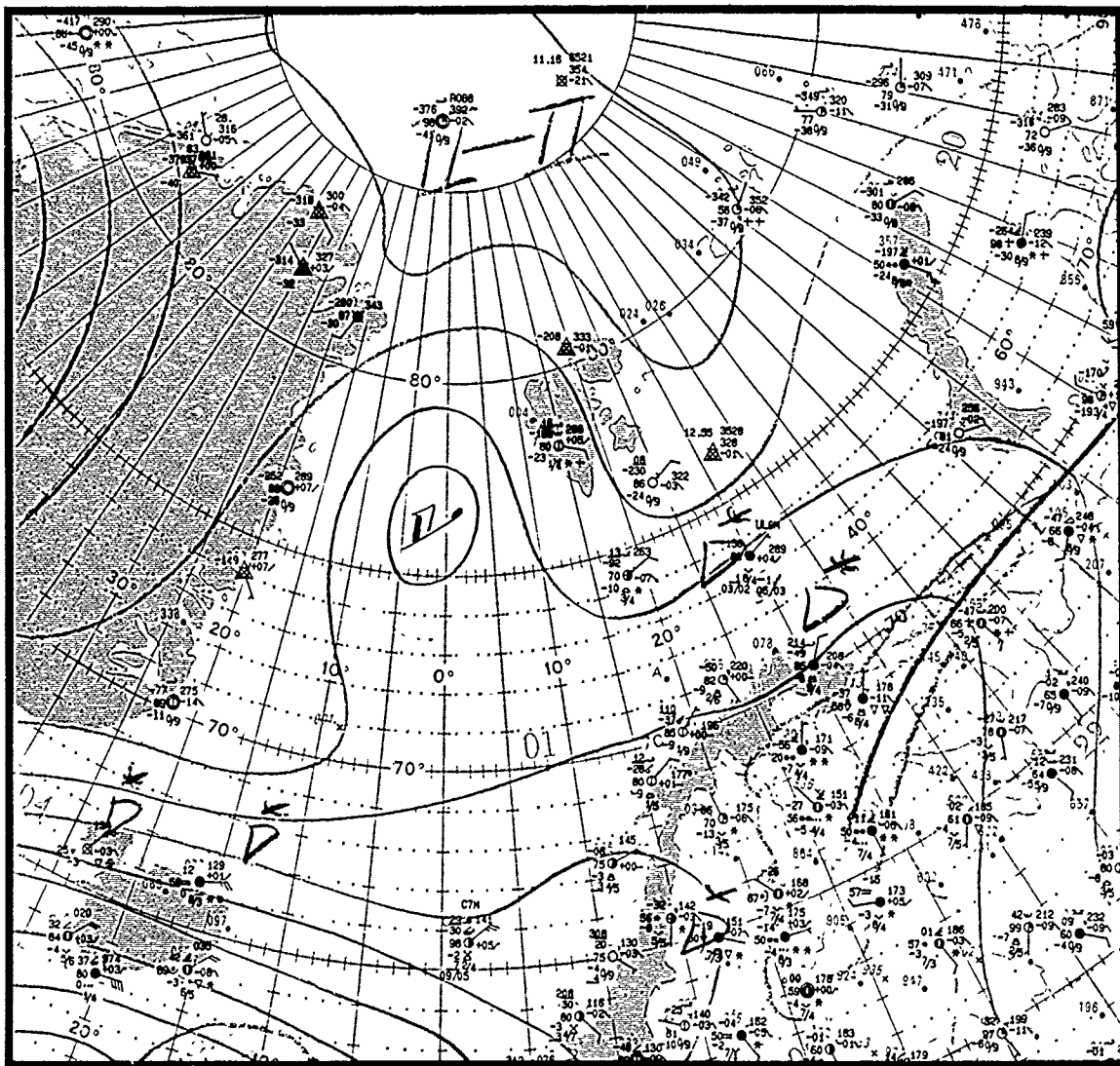


3C-7a. Rawinsonde Profiles for Valdivia. 24-25 March 1987 (same as Fig. 3C-6a).

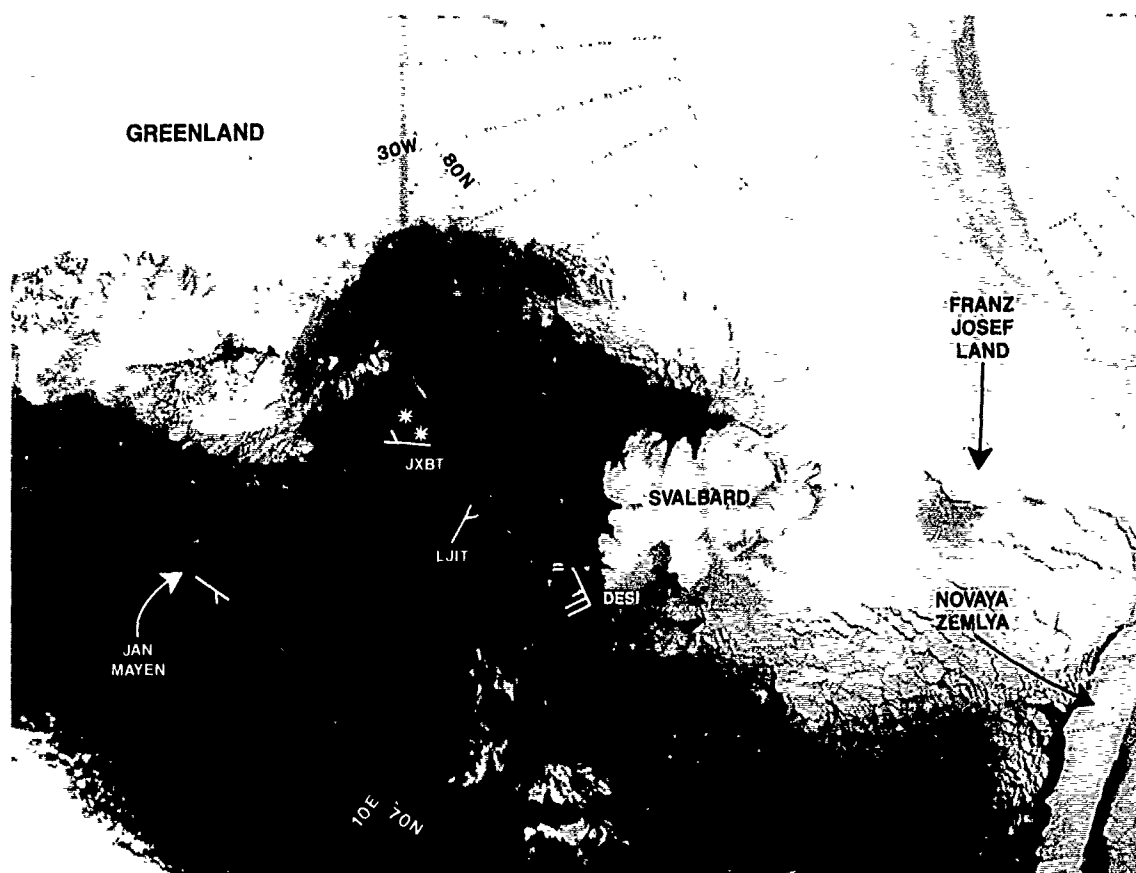


3C-8a. NOAA-9 HRPT Infrared (Ch 4) Data. 1100 GMT 25 March 1987.





3C-9a. Northern Norway Forecast Center (Tromsø) Surface Analysis. 1200 GMT 25 March 1987



3C-10a. NOAA-9 HRPT Infrared (Ch 4) Data. 0601 GMT 26 March 1987.

26 March 1987

NOAA-9 HRPT infrared (Ch 4) data acquired at 0601 GMT are shown in Fig. 3C-10a. Striking anticyclonic curvature of cloud lines in the Fram Strait coincide with moderate (25 kt) winds that extend up to the BLF axis.

Evidence of the small high or ridge is still suggested to the southwest, north of Jan Mayen Island, by the satellite data and ship and surface observations. High pressure also exists in the vicinity of Svalbard, as indicated by the anticyclonic curvature of cloud lines in the region.

Evidence of small vortices along the BLF appears greatest at the southern end, but intensity is obviously weak. The surface observations from Valdivia (DESI) and Polar Circle (JXBT) are interesting in that Valdivia (DESI) is reporting fog in 25 kt winds at the time of observation with a visibility of only 0.5 km (0.3 nm), while Polar Circle (JXBT) reports continuous snow in only 5 kt winds with 1 km (0.6 NM) visibility. Valdivia (DESI) is located very close to the edge of Spitsbergen where off-ice winds have just begun their fetch across the water. Another example of a ship very near the ice edge, under conditions of off-ice flow reporting heavy fog, was given in Section 1D, Case 1. The two reports are probably not a coincidence. The suggestion is that fog should be anticipated whenever ships are operating close to the ice edge and wind flow changes to off-ice. In this region, close to the ice edge, the inversion is very low and the cold air flowing over the warm water saturates very rapidly.

Polar Circle (JXBT) was operating in a region surrounded by ice. When flow changes to on-ice, fog or low stratus is also commonly observed but over a larger area than in the off-ice example. In the present case warm temperatures of the overcast, obscuring much of the MIZ up to the Greenland coastline, indicate that relatively warm, moist air has advected from the sea to the ice. In this region cooling and saturation of the air has occurred in sufficient quantity to permit fallout of continuous snow from the overcast, as indicated by the Polar Circle (JXBT) observation.

Fig. 3C-11a is a surface analysis for 26 March at 0600 GMT, which implies the flow pattern that would produce the observed effects. The pressure gradient on the east side of the trough is much stronger than on the west side, consistent with the Valdivia (DESI) ship report and wind flow implications of the satellite data.

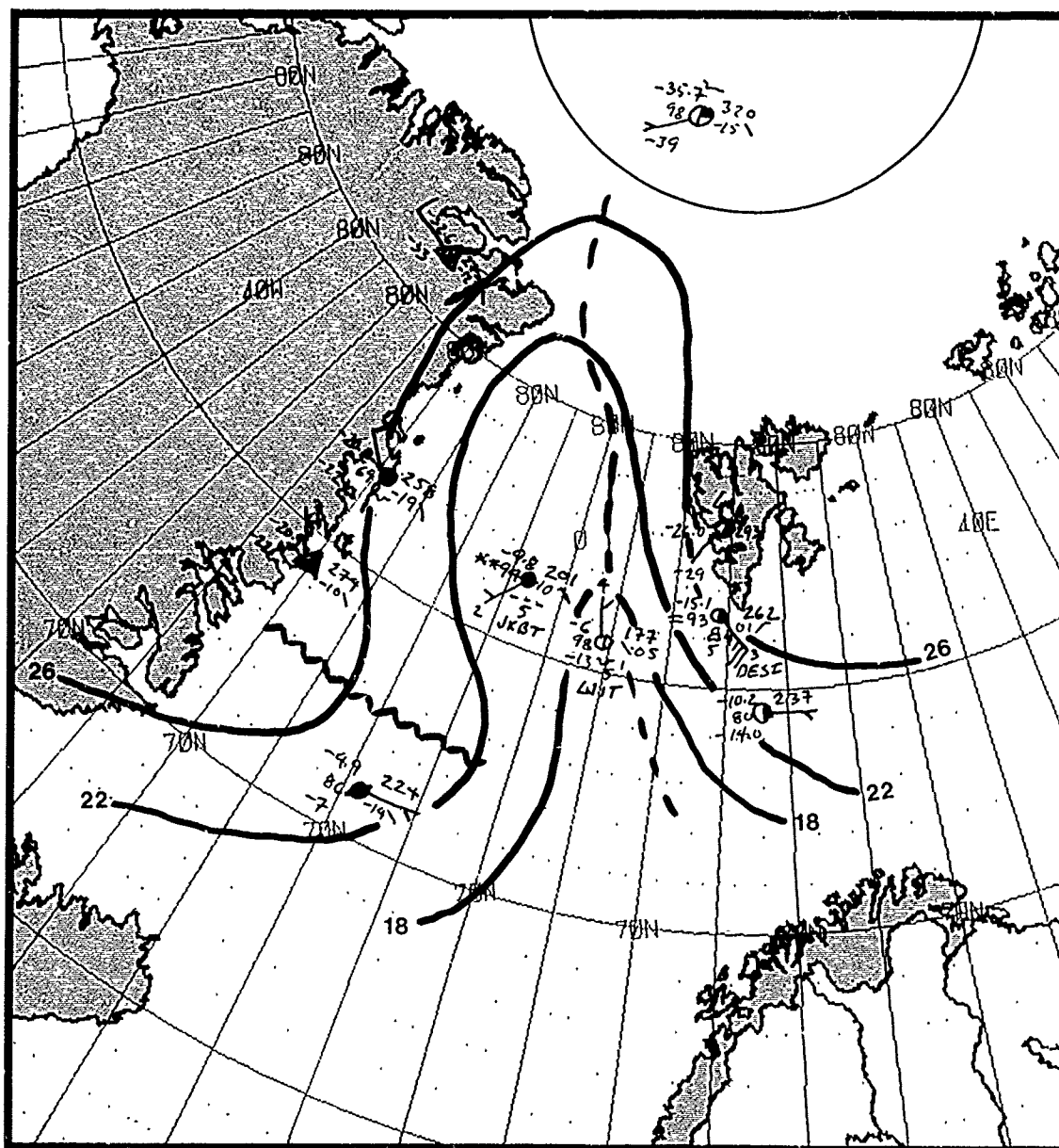
About 2 hr after the time of the NOAA data (Fig. 3C-10a) Hakon Mosby (LJIT) reported a clockwise shift in wind direction from northerly to southeasterly as the front moved by. Wind speed increased, at the same time, to in excess of 20 kt. Following frontal passage visibility dropped to a low of 2 km (1500 GMT 26 March), with overcast skies in intermittent moderate snowfall, quite similar to effects experienced by Valdivia (DESI).

Polar Circle (JXBT) was the last ship to experience frontal passage that occurred after 1800 GMT, 26 March, as winds shifted from westerly to southeasterly at 20 kt. As with the other ships Polar Circle (JXBT) experienced overcast skies with intermittent snowfall following frontal passage. Radiosonde data (not shown) reveal that the inversion rose from 800 to 1600 m on the east side of the front.

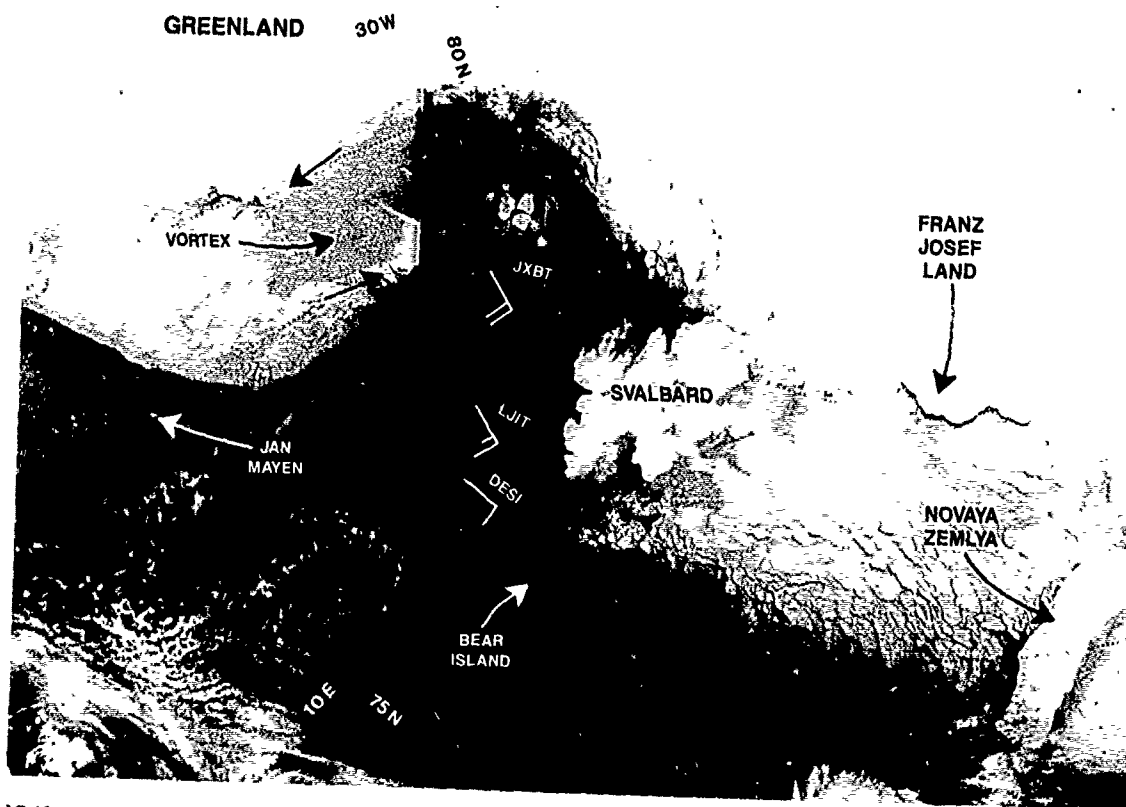
27 March 1987

Fig. 3C-12a is a NOAA-9 HRPT infrared (Ch 4) view of the area on this date at 0550 GMT. All ships are now located on the east side of the front, which is beginning to weaken as it moves over the ice edge. Low stratus cloudiness and/or fog are apparent over the MIZ as a dark (warm) gray shade, stretching to the coast of Greenland. The stratus, or fog development, is indicative of on-ice flow, which appears to encircle a small vortex at low levels over the position as shown on the image.

The Norwegian surface analysis for 0600 GMT 27 March is shown in Fig. 3C-13a. The analysis supports on-ice flow along the Greenland MIZ; however surface reports are inadequate to resolve the small low-level vortex.



3C-11a. Surface Analysis. 0600 GMT 26 March 1987.



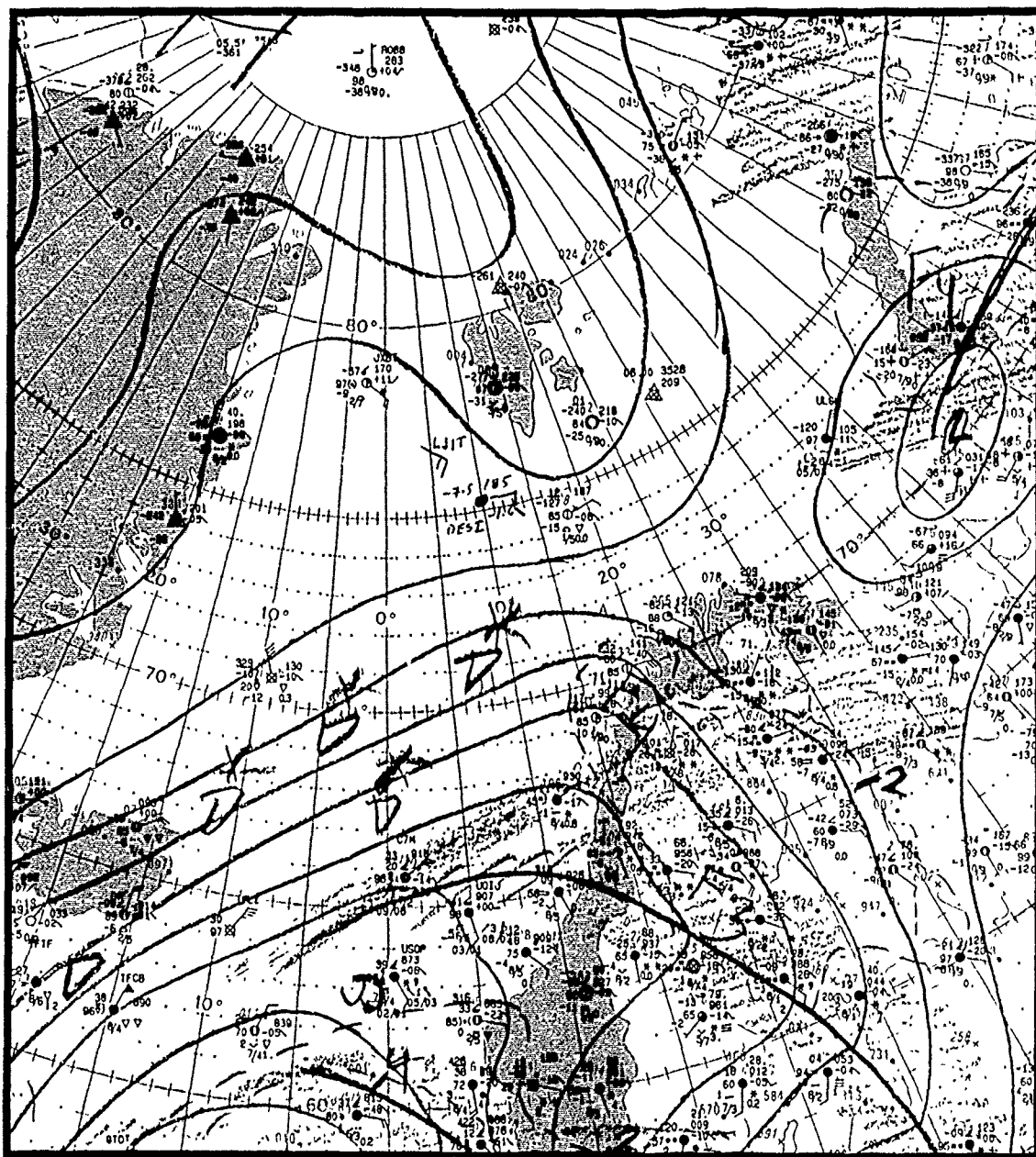
3C-12a NOAA-9 HRPT Infrared (Ch 4) Data. 0550 GMT 27 March 1987.

### Important Conclusions

1. BLF's are mesoscale systems found during the cold season over arctic waters, either stationary and parallel to the edge of arctic ice, or as propagating systems, that move in the prevailing direction of lower level wind flow.
2. BLF movement from east to west across the Fram Strait is well documented.
3. Winds are characteristically stronger on the east side of BLFs.
4. Intermittent moderate snow with poor visibilities are commonly observed in the region just east of the BLF axis. All ships in this study reported commencement of moderate continuous or at least intermittent snowfall following BLF passage.
5. Heavy fog should be anticipated in a restricted region close to the ice edge during strong off-ice flow.
6. The BLF is characterized by an enhanced cloud line where vorticity is large and mesoscale vortex development is common.
7. Fog and/or stratus development with occasional snow is commonly observed over the MIZ when flow is on-ice

### References:

- Langland, R.H., P.M. Tag, and R.W. Fett, 1989. An Ice Breeze Mechanism for Boundary Layer Jets. *Boundary Layer Meteorology* 48, 177-195.
- Shapiro, M.A., and L.S. Fedor, 1986. *The Arctic Cyclone Expedition, 1984: Research Aircraft Observations of Fronts and Polar Lows Over the Norwegian and Barents Sea, Part I. Polar Lows Project*, Technical Report No. 20, NOAA/ERL/Wave Propagation Laboratory, Boulder, CO 80303, 56 pp.



3C-13a Northern Norway Forecast Center (Tromsø) Surface Analysis. 0600 GMT 27 March 1937.

This section is  
under development  
and will be forwarded  
for inclusion in this volume.